DETERMINATION OF CAPACITY REDUCTION DUE TO OPENINGS IN MASONRY WALLS

YIĞMA YAPILARDA AÇIKLIKLARDAN DOLAYI KAPASİTEDE AZALMANIN BELİRLENMESİ

MUHAMMED ALANKUŞ

ASSOC. PROF. DR. ALPER ALDEMİR
Supervisor

Submitted to
Graduate School of Science and Engineering of Hacettepe University
as a Partial Fulfillment to the Requirements
for be Award of the Degree of Master of Science
in Civil Engineering

2021

ABSTRACT

DETERMINATION OF CAPACITY REDUCTION DUE TO OPENINGS IN MASONRY WALLS

Muhammed ALANKUŞ

Master of Science, Department of Civil Engineering
Supervisor: Assoc. Prof. Alper ALDEMİR
August 2021, 235 pages

Masonry structures have been used throughout human history, and they have an important place in the history of construction. The masonry structures are safe, sustainable, environment friendly, and they can be produced with minimum energy. These structures were built with various construction methods and materials in different communities or regions. Therefore, the materials used in masonry structures are very different, and masonry structures have many different mechanical properties due to various materials. In this case, the classification of masonry structures in modeling and analyzing is challenging. Developing technological devices and innovative ideas in the field of construction led to a more detailed investigation of the masonry walls. As a result, several models for assessing the performance of masonry buildings are developed.

In this study, masonry walls with the finite element method were analyzed to understand on the in-plane behavior of unreinforced masonry walls with different openings. The size and position of openings in unreinforced masonry walls can have an impact on failure mechanisms and capacities of walls. Therefore, the aim of this study is to determine the impact of openings in the capacities of masonry walls. First of all, the geometry of numerical models was created utilizing data from existing masonry structures. In ANSYS, the mechanical properties of the materials in unreinforced masonry walls are

defined, and the element used for modeling is determined. Then, the modeling techniques for masonry walls are selected. The macro modeling method is used in all of the numerical models. After determining the loading and boundary conditions, analyzes are performed. All numerical models are evaluated based on the boundary conditions of the walls in seismic design category 1 in TEC 2018. The length of openings and piers is evaluated based on the relationship between the location and percentage of openings and the wall capacity. The lengths or percentages were proposed to increase the safety of masonry structures under the effect of seismic loads.

Keywords: Unreinforced Masonry Walls, In-Plane Behavior, Finite Element Methods with Modelling, Masonry Walls with Openings, Failure Patterns

ÖZET

YIĞMA YAPILARDA AÇIKLIKLARDAN DOLAYI KAPASİTEDE AZALMANIN BELİRLENMESİ

Muhammed ALANKUŞ

Yüksek Lisans, İnşaat Mühendisliği Bölümü
Tez Danışmanı: Doç. Dr. Alper ALDEMİR
Ağustos 2021, 235 sayfa

İnsanlık tarihi boyunca kullanılan ve kullanılmaya devam edilen yığma yapılar, yapı tarihinde önemli bir yer tutmaktadırlar. Güvenli, sürdürülebilir, çevre dostu olmaları ve minimum enerjiyle üretilebilmeleri yığma yapıların önemini gün geçtikçe arttırmaktadır. Yığma yapılar tarih boyunca farklı topluluklarda ya da bölgelerde farklı inşa yöntemleriyle yapılmışlardır. Bundan dolayı, yığma yapıları oluşturan malzemeler çeşitlidir ve farklı mekanik özelliklere sahiplerdir. Gelişen teknolojik aygıtlar ve inşaat alanındaki yenilikçi fikirler yığma yapıların daha detaylı incelenebilmesine olanak sağlamıştır. Bunun sonucunda yığma yapıların performansını değerlendiren birçok model geliştirilmiştir.

Bu çalışma da mevcut yığma yapıların, taşıyıcı sistemi olan duvarları daha iyi analiz edebilmek ve yeni yapıların daha güvenli ve depreme karşı yüksek performanslı sisteme sahip olmaları için yapılarda mevcut olan çeşitli açıklıkların taşıyıcı sistem üzerindeki etkisi sonlu elemanlar yöntemiyle modellemesi yapılarak düzlem içi yüklemede davranışları incelenmiştir. Donatısız yığma duvarlarda, açıklıkların büyüklüğünün ve konumunun duvarların kapasitelerinde ve hasar modlarında önemli etkisisi vardır. Bu yüzden, bu çalışmanın hedefi yığma duvarların kapasitelerinde açıklık etkisini belirlemektir. İlk olarak, mevcut yığma yapılardan veriler elde edilmiş ve nümerik

modellerin geometrileri oluşturulmuştur. Ansys'te, donatısız yığma duvarlarda kullanılan malzemelerin mekanik özellikleri tanımlanmış ve modelleme de kullanılan eleman tipi belirlenmiştir. Modelleme tekniği seçilmiştir. Tüm modellemeler makro modelleme tekniği ile modellenmiştir. Yükleme ve sınır şartları belirlendikten sonra, modellerin analizi yapılmıştır. Türkiye Bina Deprem Yönetmeliği 2018'e göre tasarım deprem sınıfı 1' de yer alan duvarlarda belirtilen sınır şartları esas alınarak duvarlar değerlendirilmiştir. Duvar kapasitesiyle, açıklıkların konumu ve yüzdesi arasındaki ilişki esas alınarak açıklıkların ve sütunların uzunlukları değerlendirilmiştir. Sismik yüklerin etkisi altında yığma yapıların güvenliğini artırmak için sütun ve açıklıklarda uzunluk ve miktar önerilmiştir.

Anahtar Kelimeler: Donatısız Yığma Duvarlar, Düzlem içi Davranış, Sonlu Eleman Metoduyla Modelleme, Açıklıklı Yığma Duvarlar, Hasar Mekanizmaları

ACKNOWLEDGEMENT

First of all, I would like to thank my supervisor Assoc. Prof. Dr. Alper ALDEMİR for his patience and support throughout this thesis. I am also very grateful to him for his interest and ideas in my graduate study. In addition, I owe a debt of gratitude to Prof. Dr. Mustafa ŞAHMARAN for all his contributions and guidance during my graduate study.

Lastly, I am also thankful to my family for their patience with me and I would like to give a strong thanks to Bade BOSTAN that she always back up to me and made sacrifice.

TABLE OF CONTENTS

LIST OF TABLES

LIST OF FIGURES

SYMBOLS AND ABBREVIATIONS

Symbols

E	Modulus of Elasticity
E_w	Young's Modulus of Masonry Wall
f_m	Characteristic Compressive Strength of Masonry Wall
f_{mt}	The Tensile Strength of Masonry Wall
f_{vko}	The Initial Shear Strength of Masonry Wall
h_{ef}	Effective Wall Height
h	Greater Clear Height
ℓ_n	Unsupported Wall Length
Rss	Lateral Capacity of a Masonry Wall due to Sliding Shear Failure
t_{ef}	Effective Wall Thicknesses
V_{bo}	Shear Bond Strength
μ	Coefficient Of Friction
σ_y	Vertical Stress
ε	Strain

Abbreviations

AAC	Autoclave Aerated Concrete
IBC	International Building Code
MSJC	Masonry Standards Joint Committee
URM	Unreinforced Masonry
FRPs	Fiber Reinforced Polymers
TRM	Textile Reinforced Mortar
ECC	Engineered Cementitious Composite
CMU	Concrete Masonry Unit
AAC	Autoclaved Aerated Concrete
FEM	Finite Element Method
SDC	Seismic Design Category

1. INTRODUCTION

Masonry structure is one of the most commonly used and still existing in construction systems around the world and, it has a lot of advantages. There are significant structures in masonry as monuments, mosques, palaces, bridges. Many of them were built using traditional construction methods in the design and construction process, however some of them aren't still demolished at the present time.

Masonry structures have been built from past to present, and they are still built in many regions. Masonry structures usually consist of materials such as stone, briquette, brick, and mortar. The function of mortar layers is to provide interconnecting these masonry units together. The materials used in masonry structures are generally around the region where they were built. In this case, masonry structures with many different mechanical properties arise due to various masonry materials.

Although masonry structures are easy to construct, it is challenging to predict their structural performance and mechanical properties. Generally, they are non-engineered buildings, and they have some risks, because traditional methods is not taken into consideration behavior of materials and building systems. Analysis and design of masonry structures are very important to understand the behavior of masonry structures under effects of seismic loads; therefore, it is necessary to improve the traditional concepts of masonry buildings.

Nowadays, there are many studies for masonry structures to determine their behavior. In this way, masonry structures with developing technology and studies have new construction methods. Regulations and innovations for existing structures and to be built in the future are examined, and they are necessary to make safer structures.

1.1 Purpose of Thesis

The main goals of this thesis is to investigate the effect of openings on walls of masonry structures. These openings are created for various purposes such as windows and doors. Masonry wall, which is a continuous ambient, but openings in wall reduce the capacity

of the system; therefore locations, sizes, and percentages of openings in the wall are very vital.

In this study, masonry walls with the finite element method were analyzed to understand the in-plane behavior of unreinforced masonry (URM) walls with different openings. The materials that constitute the masonry wall and their mechanical properties were explored. The types of masonry structures were examined. Different design standards were used to assess the location and size of openings in the URM wall. The features of element type and the ANSYS program used in modeling are explained. The relationship between the size and location of the openings in the wall and the in-plane capacity of the wall was investigated.The variation of failure mechanisms due to the aspect ratios of the piers was investigated.

1.2 Literature Review

Masonry structures have been the preferred type of building in the past and today due to their many advantages. Its ease of construction, low cost and low engineering service in terms of design are the main reasons why it is still widely used [1].

Masonry structures, the oldest of the existing structural systems, have been the focus of numerous studies. Walls, which is load-bearing system of masonry buildings, especially are examined. Many researchers have investigated the behavior of masonry walls under the effect of seismic loads. The behavior of URM walls under seismic loading are examined by Priestley. This is comparison assessing performance of URM walls under seismic loadings based on elastic stress calculations and energy considerations [2].

The modeling of URM walls under shear and compression was examined by Chaimoon. Chaimoon suggested a procedure to determine the intersection between the compression cap and the Coulomb failure line because there is very important case that considering fracture in mortar joints and brick units to enhance its relevance with experimental results [3].

Abrams investigated the strength and deformation capability of URM walls in a number of investigations. [4]. The damages and crack patterns of specimens with different aspect

ratios are observed and redistribution of stresses are actualized after first crack on wall and also, force-deflections relations is proven to energy dissipation of URM wall in ductile manner.

The effect of spandrel types is evaluated on the basis of force-drift curves and observed damages. There were three types of spandrels used: one with a wooden lintel, one with just masonry arch, and one with both masonry arch and RC bond beam. Seismic response of URM wall is reasonably affected by spandrels between the piers [5].

They are performed on concrete and masonry walls with fiber reinforced polymers (FRPs), there is a significant increase in the ductility and load-carrying capacity of the wall components [6]. Albert examined effects in increasing capacity of unreinforced masonry walls using fiber-reinforced polymers as externally. The type and amount of fiber reinforcement, the layout of the fiber reinforcement and axial loads on masonry walls reinforced FRPs are investigated that these affect overall stiffness and ductility of walls [7]. On the other hand, there are some drawbacks of using FRPs as high cost and poor fire resistance. Researchers have proposed strengthened by natural fibers to minimize drawbacks. A study was develop to enchance capacity of URM walls which strengthened by natural hemp fibers and research results indicate that the flexural capacity of the walls improves as the hemp reinforcement ratio rises [8]. An investigation carried out to study the effectiveness of using polymer textile reinforced mortar(TRM) for enhancing the structural performance of URM walls. The deformation capability of TRM strengthened URM walls increased significantly [9]. The usage of the engineered cementitious composite (ECC) shotcrete and steel reinforcing bars for URM are investigated and it was observed that the strength of the wall increased [10]. Matsumura investigated shear strength and behaviors of reinforced masonry walls subjected to in-plane loadings [11]. Matsumura observed that many parameters affect the ultimate shear strength in reinforced masonry walls such as grouting, shear-span ratio, shear reinforcement ratio. Formulas were developed to predict ultimate shear load.

A finite element method is improved to model strengthened URM walls. Experimental and numerical results were compared for load bearing capacity and demonstrate a good

match. Moreover, the ductility and lateral capacity of panel increases with using fiber [12].

Openings of masonry walls are necessary for architectural aesthetics and needs but irregularity of openings that changing size and amount of openings per story can cause non-uniform distribution of gravity loads and local collapse. Parisi examined effects of irregular cases to capacity in URM walls [13]. In URM walls, a non-uniform distribution of gravity loads can cause demand of strength and displacement in local areas of walls and this situation leads to local failure. Different sizes and openings in masonry walls affect strength and stiffness of masonry walls. Relationship between the sizes and locations of openings on the in-plane behavior of URM walls are examined by Liu et al. The failure mechanism of URM walls is affected by the effect of openings, and the in-plane capacity of walls decreases as the opening size increases [14]. The location of openings in URM walls under extreme out-of-plane loads can result in different failure modes and Ghobarah investigated in this case. The lateral load capacity and failure types of the unstrengthened URM walls and strengthened using carbon fiber-reinforced polymer laminate strips URM masonry walls were examined and the ductility and lateral load capacity of strengthened URM walls with openings were found to be greater than those of unstrengthened URM walls with openings [15]. The behavior of confined masonry shear walls with openings are also investigated by Yáñez. The diagonal failure mechanism and deformation capacity in URM walls with openings are changed depending on the masonry unit type and size of the openings [16]. Allen, et al. investigated force-displacement relationships of the URM wall with opening that wall geometry and pre-compression levels changed failure modes and crack patterns of spandrels and piers [17].

2. MASONRY STRUCTURES

2.1. History of Masonry Structures

Masonry structures have been one of the most popular structure types throughout construction history. In the earliest samples of masonry structures, it was created by using sun-baked clay bricks and overlapping stones. Masonry walls date back to the use of sunbaked clay brick, marble, stone. There are many important monumental structures like the Egyptian Pyramids, the Roman Colosseum, the Taj Mahal, and the Great Wall of China that were built with production techniques of masonry structures [18].

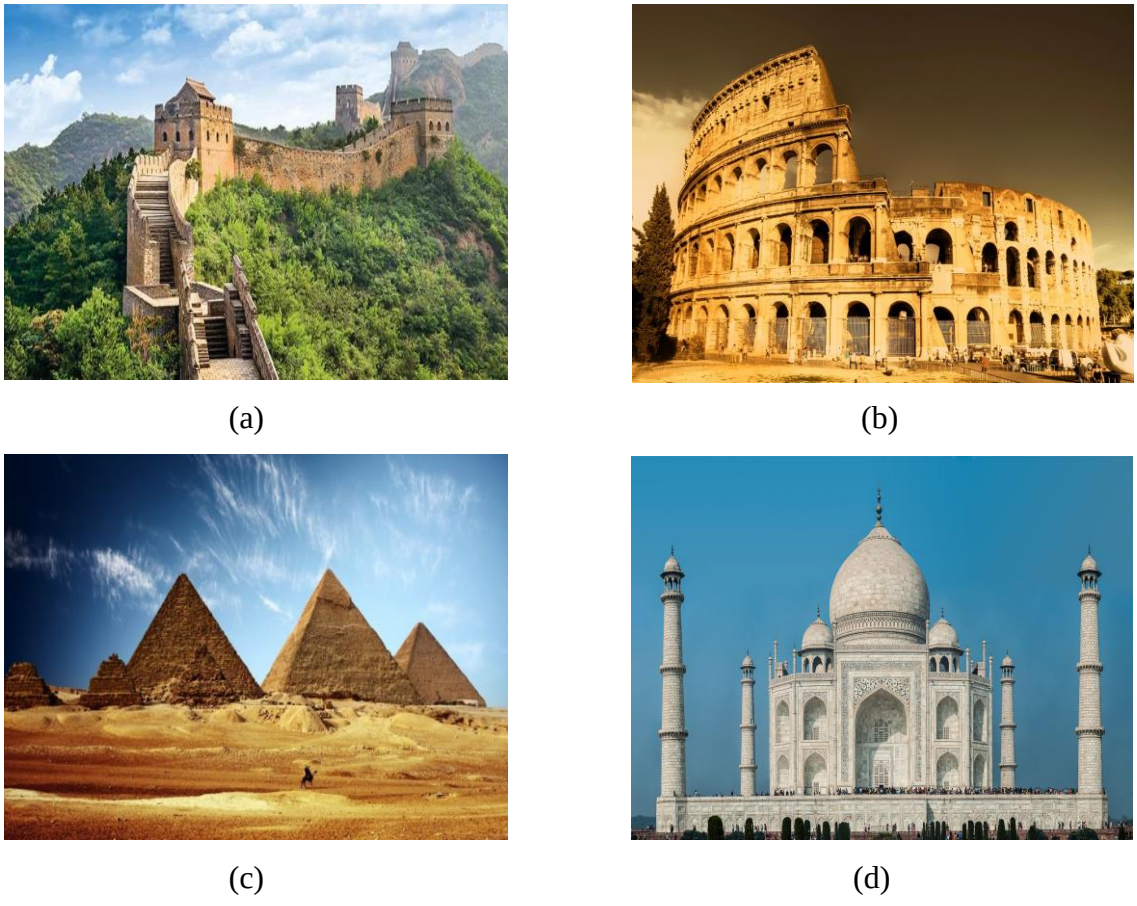

(a) (b)

(c) (d)

Figure 2.1. Masonry Structures: (a) Great Wall of China; (b) Roman Colosseum; (c) Egyptian Pyramids; (d) Taj Mahal

For many reasons, masonry constructions have been favoured throughout history. For instance, they have resistant to earthquakes, fires and masonry materials and are durable to other environmental effects [19]. When developing common mortars and masonry units over time, a variety of materials were used to construct masonry structures.The

usage of masonry structures has been gradually decreasing in recent years. The main reason is that reinforced concrete structures and steel structures have better mechanical characteristics, and allowing structures to perform better against external factors. However, its numerous advantages, such as being cheap, long lasting, environmentally friendly and its ease of construction, masonry structures are generally utilized in rural regions. Although, masonry structures are used today for office buildings, schools, residential, and fireplaces in urban regions.

URM walls are made up of brick units and mortars. Masonry units can be made of a variety of materials, including brick, stone, concrete blocks, etc. The usage of these units is typically determined by the region in which they are found. Mortars are adhesives that hold masonry units together, resulting in a composite wall. It is critical to have a better understanding of the behavior of masonry walls when subjected to seismic forces because, masonry structures have been shown to have low seismic capability. The in-plane lateral capacity of the wall is affected by the openings and mechanical characteristics of the materials therefore, it is critical for the design and analysis of the URM walls in seismic zones.

2.2. Materials used in Masonry Structures

Masonry buildings are made of a wide range of materials. Brick, stone, concrete blocks, and mortars are samples of these materials. Although some masonry materials, such as adobe, can be utilized in specific areas, the resistance of the wall against seismic effects is insufficient therefore, they are not suitable for use in masonry walls.

The materials of masonry walls are durable, brittle and non-combustible and they possess a resistance against weather, pests, decomposition so, these materials have a long lifespan [20]. Types of materials used in masonry structures can be identified by TEC2018. The materials to be utilized in the masonry walls are shown in the Table 2.1 [21].

Table 2.1. Types of Masonry Materials in Standards

Types of Materials	Standards
Brick Masonry Units	TS EN 771-1
Concrete Block Masonry	TS EN 771-3
Autoclaved Aerated Concrete Units	TS EN 771-4
Artificial Stone Masonry Units	TS EN 771-5
Natural Stone Masonry Units	TS EN 771-6

To prevent compromising wall strength, the hollow ratio in masonry materials must be controlled within specific limitations; these ratios are listed in Table 2.2 [21]. Infill wall materials such as adobe, stone, and concrete briquettes should not be utilized as load-bearing wall materials.

Table 2.2. Hollow Ratio for Masonry Materials

Type of Material for Masonry	Group I	Group II
Brick	$\alpha \leq \%35$	$\%35 < \alpha \leq \%50$
Concrete	$\alpha \leq \%35$	$\%35 < \alpha \leq \%50$

2.2.1. Brick Masonry

Bricks used in masonry constructions appear in a range of types, sizes depending on the location or production facility. Ingredients of brick materials are silica, alumina, lime, iron oxide and magnesia [22]. Sun-dried bricks, burnt clay bricks, fly ash bricks, concrete bricks, engineering bricks, sand lime bricks, and fire bricks are only a few examples. Some of them are given in Figure 2.2. Bricks have several advantages, like being long-lasting, resistant to high temperatures, and less expensive when compared to other materials.

Figure 2.2. Masonry Bricks Types

The brick masonry units have several drawbacks, since bricks have a poor resistance to tension and torsion. Moreover it has a poor tensile strength relative to its compressive strength, and it takes a long time to build structures..

2.2.2. Stone Masonry

These materials are extremely durable, weather resistant, and have an appealing appearance. It exists in a range of forms and is one of the most often used materials units. Low tensile and flexural strength are drawbacks of stone masonry. The mechanical properties of the stones vary depending on their type are listed in the Table 2.3.

Table 2.3. Mechanical Properties on Types of Stone

Types of Stone	Density (g/cm^3)	Compression strength (MPa)	Modulus of Elasticity(MPa)x10^4
Granite	2.6-2.8	160-240	5
Basalt Stone	2.9-3.0	200-400	9-12
Marble	2.7-2.8	100-180	4-7
Quartz	2.6-2.8	180-300	5-7

2.2.3. Concrete Block Masonry

Concrete blocks masonry, also known as concrete masonry unit (CMU), has a number of advantages, including fire resistance, weather resistance, and pest resistance. They may also be utilized as an excellent sound and moisture insulation system. CMU can be solid or hollow blocks. There are differences regarding porosity and amount of aggregate between solid and hollow blocks. Solid concrete blocks have a density of 1500-2000 kg/m^3, whereas hollow concrete blocks have a density of 1000 to 1500 kg/m^3, and solid concrete blocks have a higher compressive strength than hollow concrete blocks.

2.2.4. Mortars

Mortars are used to bind masonry units together in wall or to fill irregular or regular gaps. The lime or cement, sand, and water are some of the components of binding materials.. Mortars can be used for decoration. Although Portland cement has been the most well-known binder since the twentieth century, the lime is still utilized in the construction of new buildings and the restoration of existing structures. When masonry constructions are erected, all horizontal and vertical joints in URM walls must be filled with binding mortar [21].

Figure 2.3. Mortar

2.2.5. Wooden

Wooden is a material that is used to improve the tensile and flexural strength of masonry walls. The usage of wooden increase wall strength to reduce slenderness of wall. It has the drawback of absorbing water over time.

2.3. Types of Masonry Walls

There are four distinct types of masonry walls for TEC2018. URM walls, reinforced masonry walls, confined masonry walls and reinforced autoclaved aerated concrete panel systems walls are all variations of masonry walls [21].

2.3.1. Unreinforced Masonry Walls

URM walls consist of masonry units and mortars without any reinforcing bars. The ductility level of walls is low, the materials utilized on walls are brittle. The mechanical characteristics and behavior of materials are critical in determining the seismic performance of unreinforced masonry walls. The length of load bearing walls, the size and amount of openings, the aspect ratio, the type of materials, and the wall geometry can all impact the failure mode and seismic capacity of the spandrel and piers.

2.3.2. Reinforced Masonry Walls

These walls include reinforcements, in addition to masonry units and mortars. The primary reason for using reinforcing bars in masonry walls is to increase ductility, because masonry units are brittle and cannot demonstrate ductile behavior under ground motions. Reinforcements must be placed in the proper region of walls or between masonry units to behave as composite materials. This will provide the much higher strength and ductility. A reinforced masonry wall is shown in Figure 2.4.

Figure 2.4. Reinforced Masonry Wall

2.3.3. Confined Masonry Structures

Wall systems of confined masonry structures consist of masonry unit, mortars, reinforced and girder in vertical and horizontal directions. Despite their low ductility, confined masonry walls have a higher strength than URM walls. The quality of the wood or concrete used in girders is critical for effective load distribution. There is an example in Figure 2.5 [23].

Figure 2.5. Confined Masonry Structures

2.3.4. Reinforced AAC Panel Systems Structures

These ductile walls consist of autoclaved aerated concrete (AAC) units and reinforcing bars. Autoclaved aerated concrete; it is a lightweight building material formed by a mixture of siliceous sand, lime, cement, aluminum powder and water. Despite its low density, AAC unit has excellent heat and sound insulation, fire resistance, and carrying capacity.

2.3.5. Other Types of Walls

Masonry wall behavior under horizontal and vertical loads is influenced by the geometry of the walls, the strength of the materials. Furthermore, the behavior of masonry structures is influenced by the solid or cavity wall of one or more leaves. [24]. These cavity walls are usually exterior walls that are comprised of two separate walls interconnected by metal ties or mortars. A cavity wall is seen in Figure 2.6 [25].

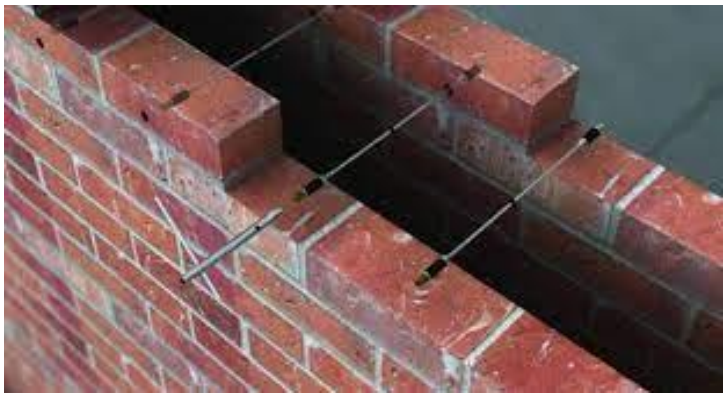

Figure 2.6. Cavity Wall

3. MODELLING TYPES AND DESIGN STANDARDS OF MASONRY WALL

3.1. Modelling Types in Masonry Walls

Finite element modeling is required for masonry walls because it eliminates some of the drawbacks of experimentation. Experimental approaches can be highly expensive, time-consuming, and have size and measurement limits, as well as being hazardous to existing structures. It's much more advantageous to combine experimental and numerical approaches. The finite element method (FEM) can be used to simulate masonry systems under the combined impacts of vertical and horizontal loads. FEM is an effective approach for accurately representing complicated geometry. Walls can be represented in FEM using a variety of techniques. The different modelling types are listed in Table 3.1 [21].

Table 3.1. Modelling Techniques for Masonry Structures

Heterogeneous Modelling	**Homogeneous Modelling**
Simplified micro modelling	Macro modelling
Detailed micro modelling	

These modeling approaches are also shown in Figure 3.1 [26].

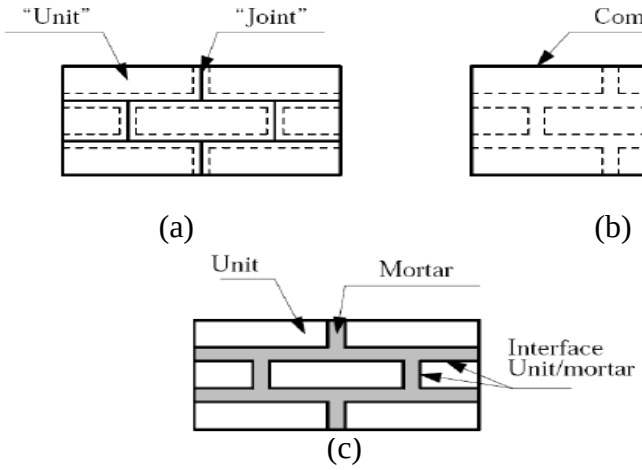

Figure 3.1. Modeling techniques for masonry structures: (a) simplified micro-modeling; (b) macro-modeling; (c) detailed micro-modeling.

3.1.1. Heterogeneous Modelling

Heterogeneous modelling is a discrete modelling of masonry wall that all components of materials are modeled separately. Heterogeneous modeling is divided into two categories for TEC2018. The detailed micro modeling and simplified micro modeling are the two types of heterogeneous modeling.

3.1.1.1. Simplified micro modelling

Masonry units and contact surfaces are modeled, but mortar layers, which are a separate component of walls, are not included in this method of modeling. This simplification is required for structural analysis approaches to obtain faster results. These types of modeling are suitable for thin-layer mortar. The thickness of mortar affects the size of masonry units.

3.1.1.2. Detailed micro modelling

All wall components are modeled such as masonry units, mortars, and contact surfaces. The analysis step of this form of modeling is relatively slow, but the data obtained is more accurate and detailed.

3.1.2. Homogeneous Modelling

Walls are modeled as a composite structure with all of its components. The composite structure is determined by a periodically repeated part of the wall. The type of modeling is determined by the research to be carried.

3.2. Material Models in Masonry Walls

The defined material models are one of the most important factors affecting the behavior of masonry walls under seismic loadings. Since elastic and inelastic materials behave differently, the material models used in FEM must be appropriate in order to obtain accurate results.

3.2.1. Linear Material Models

Masonry units and mortars are usually non-ductile materials that can crack and crush when suddenly loaded. There are three types of material models in linear material models. These are anisotropic materials, orthotropic materials and isotropic materials. These

materials in masonry walls are convenient for elastic region. Since the anisotropic materials used in masonry walls have variable mechanical characteristics in all directions, structural analysis is complex. Isotropic material model, which assumes that wall materials are solid and have the same properties in all directions. This approach simplify structural analysis of walls.

3.2.2. Non-linear Material Models

Non-linear material models can be used to represent materials in masonry buildings. This material modeling allows for a better understanding of material behavior under loads since materials in the inelastic zone can crack, crush, and collapse.

3.3. Design Standards for Masonry Walls

3.3.1. Minimum Thickness of Load-Bearing Walls

The walls must fulfill certain requirements in order to be designed a load-bearing system. TEC2018 determines the minimum wall thicknesses to be applied in masonry walls under shear stress, which are described in Table 3.2.

Table 3.2. Geometric Conditions for Masonry Wall Types in TEC 2018

Types of Masonry	**$(t_{ef})_{min}$ (mm)**	**$(h_{ef} / t_{ef})_{max}$**
Unreinforced masonry with naturel stone	350	9
Unreinforced masonry with other units	240	12
Confined masonry	240	15
Reinforced masonry	240	15
Reinforced AAC Panel Systems	200	15

In Eurocode 6, minimum effective wall thickness should be only 100 mm. According to Eurocode 8, the recommended geometric conditions for load-bearing walls are given in the Table 3.3 [27]. In parameters, t_{ef} and h_{ef} are minimum effective wall thicknesses and height.

Table 3.3. Geometric Conditions for Masonry Wall Types in Eurocode 8.

Masonry Types	**$(t_{ef})_{min}$ (mm)**	$(h_{ef} / t_{ef})_{max}$
Unreinforced, with natural stone units	350	9
Unreinforced, with any other type of units	240	12
Unreinforced, with any other type of units, in cases of low seismicity	170	15
Confined masonry	240	15
Reinforced masonry	240	15

The thickness of load-bearing walls in multi-storey masonry structures should be larger than 203 mm in each level, according to IBC2006 and MSJC2005. In one-storey masonry constructions, the thickness of load-bearing walls shall not be less than 152 mm. The minimum thickness of rough, coursed rubble stone walls shall not be less than 152 mm. The minimum thickness of masonry shear walls shall not be less than 203mm thick [28, 29].

3.3.2. Openings and Maximum Unsupported Length of Load Bearing Walls

Openings in masonry walls are required for architectural aesthetics and needs, however they reduce wall strength and vary the failure mechanism. These unsupported wall lengths can be different in reinforced masonry walls and reinforced AAC systems because of using reinforcing bars. According to TEC2018, the unsupported length in URM walls shall not exceed 5.5 m for seismic design category (SDC) 1, 1a, 2 and 2a, and 7.5 m for SDC 3, 3a, 4 and 4a, as shown in Figure 3.2. The distances between vertical girders in masonry structures should not exceed 4 m. These values can be increased by 20% for reinforced masonry buildings and AAC panel systems structures. For door and window openings, there are some particular limitations. The limits between the distances are represented in Figure 3.3.

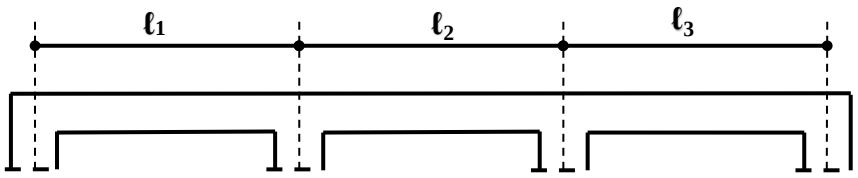

Unsupported wall length: ℓ1, ℓ2, ℓ3 ≤ 5.5m (SDC 1, 1a, 2 and 2a)

≤ 7.5m (SDC 3, 3a, 4 and 4a)

Figure 3.2. Unsupported Wall Length for Masonry Structures

In TEC2018, the boundary conditions for length of pier between openings are shown in the Figure 3.3. In Eurocode 8, the maximum unsupported length of a load-bearing wall should not be more than 7 m and proper $(l/h)_{min}$. The values of $(l/h)_{min}$ are given in the Table 3.4. The ratio of the length of the wall, l, to the greater clear height, h, of the openings adjacent to the wall.

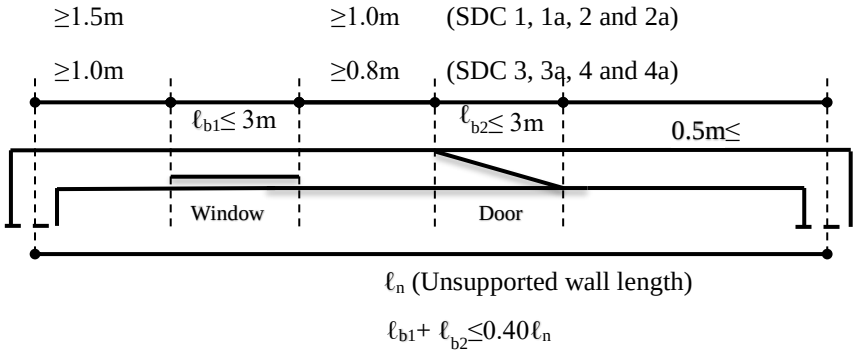

Figure 3.3. Boundary Conditions for Openings in Masonry Walls

Table 3.4. Recommended Geometric Conditions for Masonry Walls in Eurocode 8

Masonry Type	**(l/h)min**
Unreinforced, with natural stone units	0.5
Unreinforced, with any other type of units	0.4
Unreinforced, with any other type of units, in cases of low seismicity	0.35
Confined masonry	0.3
Reinforced masonry	No Restriction

In addition, the door or window openings is supported by a lintel or stone block. In TEC 2018, the height of lintel must be least 150 mm and the length of the parts of the lintel on the wall must be at least 200 mm.

3.4. Failure Patterns for Masonry Walls

Three types of failure mechanisms can be observed in piers when URM walls are subjected to in-plane loads. These are sliding mechanism, rocking mechanism, diagonal tension mechanism. The mechanism is determined by the wall geometry, material characteristics, boundary conditions, and loads acting on the wall [30]. In addition, irregular walls or different size of openings cause a non-uniform distribution of gravity loads in wall and in this way, concentration of strength and displacement take place in local areas of walls. This leads to a local failure [5].

Although structural stability is preserved for cracks on walls subjected to in-plane loads, these cracks cause irreversible structural damage when external forces act in the plane. When URM walls are subject to in-plane loadings, shear stress cause damage or cracks around the openings. These cracks usually appears as diagonal cracks or vertical cracks. Wall stability under out-of-plane loads is critical, and wall thickness and slenderness have an impact on the in-plane capacity of URM walls.

3.4.1. Sliding Mechanism

A sliding mechanism occurs when the upper part of the wall slides over the lower part of the wall. This mechanism is mostly caused by low axial load and inadequate mortar quality. This mechanism cause crack paths in the bed joints under seismic loads [31].

Mohr-Coulomb formulation can be used to predict shear strength associated with sliding.

$$Rss = L * t * fv$$

where

$$fv = Vbo + \mu * \sigma y$$

Rss is capacity because of sliding shear failure, t is the wall thickness, L is the wall length, Vbo is the shear bond strength at zero compression (in MPa), μ is the coefficient of friction, σy is the vertical stress (in MPa).

3.4.2. Rocking Mechanism

The rocking mechanism is based on aspect ratios, which result in overturning of the wall and crushing of the corners. The rocking mechanism is more ductile, although it can cause significant wall displacements. The displacement capacity can be up to 10% of the whole wall height [31].

3.4.3. Diagonal Tension Mechanism

This type of mechanism occurs, when a solid wall or a wall with opening has diagonal cracks that propagate along the wall. In the URM walls, decrasing aspect ratio cause this type of failure mechanism.

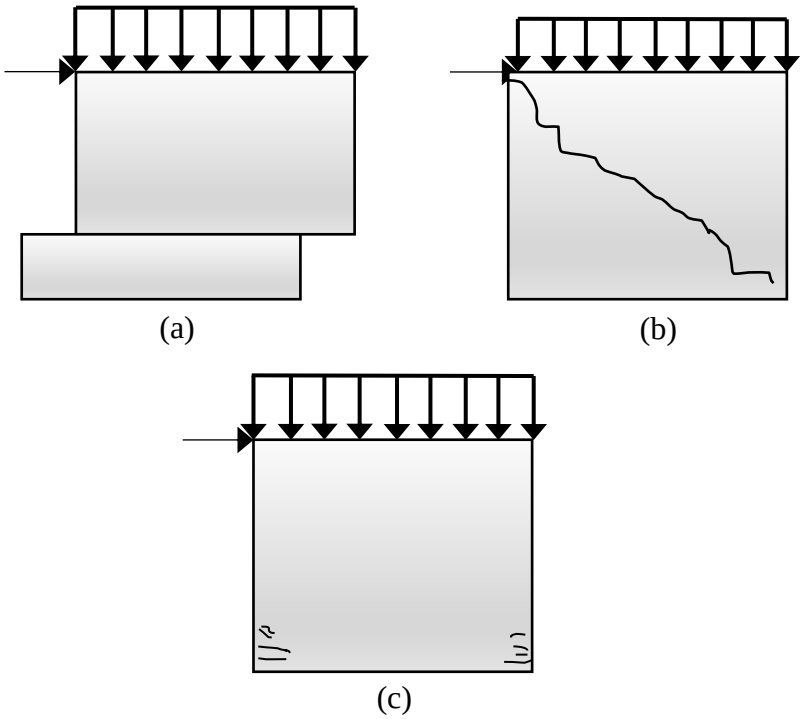

Figure 3.4. Failure Modes for Walls: (a) Sliding; (b) Diagonal-tension; (c) Rocking

4. FINITE ELEMENT MODELING OF MASONRY WALL ELEMENTS

This section firstly introduces ANSYS, which is used to provide the analysis in URM walls. The solid65 element and input parameters are then presented. The input paramaters and element types of the models were selected in accordance with the analysis. In models, the Solid65 element has the properties of cracking and crashing. Besides, the qualification of this model is determined by comparing its estimations with the experimental results of URM wall tests.

4.1. ANSYS Software

The FEM is a numerical method that has many advantages in solving the problems. This method chooses the suitable elements and materials to solve different types of problems. A finite element meshing is created. Sets of equation come out and these sets of equations are solved by computers. ANSYS, which is a computer program, uses the finite element method to solve difficulties that arise in numerical methods. In ANSYS, it is critical to define the unit system, material properties, elements properties, geometry of models, finite element mesh, boundary conditions, loads and proper methods of analysis. The accuracy of the observed results improves as the number of analyses increases.

4.2. SOLID65 Element Description

The Solid65 element has many properties. The Solid65 element is used to perform nonlinear or linear analysis in URM wall models. The Solid65 element is designed for modeling with or without rebars. Solid65 element can be used to model brittle materials such as geological materials (sand, rock). This element has eight nodes and all of them have three degrees of freedom. The Solid65 element is given in Figure 4.1 [28].

Since it can exhibit properties of cracking, crushing, and plastic deformations, the Solid65 element in URM walls is a suitable finite element for depicting crack pattern and collapse mechanisms.

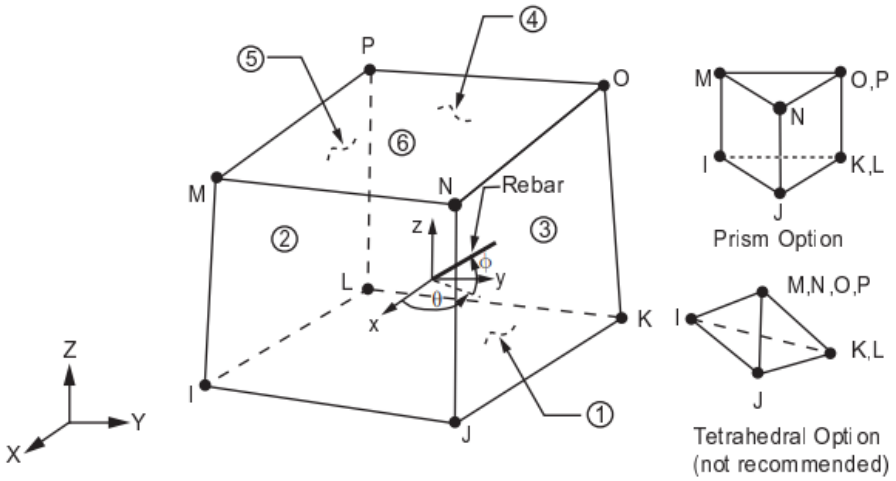

Figure 4.1. Solid65 Element (3D)

There are some rules and restrictions given in ANSYS Element Reference and ANSYS Theoretical Reference are listed below.

- All Solid65 elements should have eight nodes.
- There are three degrees of freedom at each nodes.
- Zero volume element is not allowed.
- The sum of the volume ratios for all rebar must be less than 1.0.
- Brittle materials can be modeled with Solid65 elements.
- Elements can perform cracking in tension and crushing in compression.
- It has isotropic material acceptance in elastic analysis.

Concrete material model in Solid65 element is used to identify behavior of brittle materials as stone, bricks. This material is defined as an isotropic material. In ANSYS, failure modes are described using a combination of the William-Warnke failure theory and multilinear isotropic hardening.

4.3. Input Parameters of Elements and Materials for Modelling Masonry Walls

In this study, while modeling URM walls, the Solid65 element was used. The stress relaxation after cracking is neglected. The open shear transfer coefficient and closed shear transfer coefficient are taken as 0 and 1, respectively. The compressive and tensile strengths of concrete are used to define the material. Multilinear isotropic hardening is used to determine the plasticity, and the model is shown in Figure 4.2.

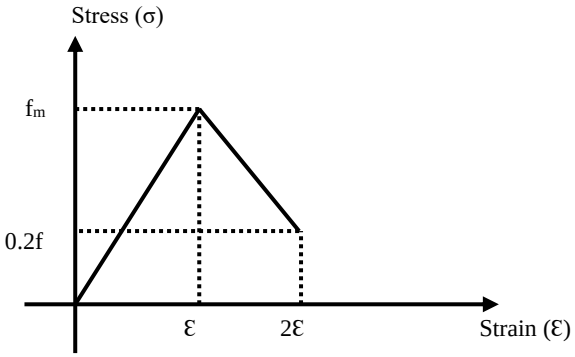

Figure 4.2. Multilinear Isotropic Plasticity Model used in Analytical Models

4.4. Verification of Modelings by Experimental Datas

The experimental datas and the nonlinear analytical model created with ANSYS for in-plane behavior of URM walls are compared. Three types of walls and failure mechanisms are found in this study, all of which are dependent on aspect ratios. As a result, the proposed models should be compared and verified using the experimental datas.

4.4.1. Verification of Diagonal Failure Pattern for URM Walls

The experiments on URM walls at ETH Zurich were considered the most suitable test for verifying the diagonal tension mechanism of analytic models. This tested wall consists of hollow clay bricks. A reinforced concrete slab and foundation are also placed on the wall. The dimensions of tested wall are shown in Figure 4.3 [33]. The mechanical properties of the tested wall are given in Table 4.1. The loading was carried out in two parts. The wall is monotically pushed from the side after a uniform load is supplied vertically. Diagonal shear cracks appear on the wall at the ultimate stage.

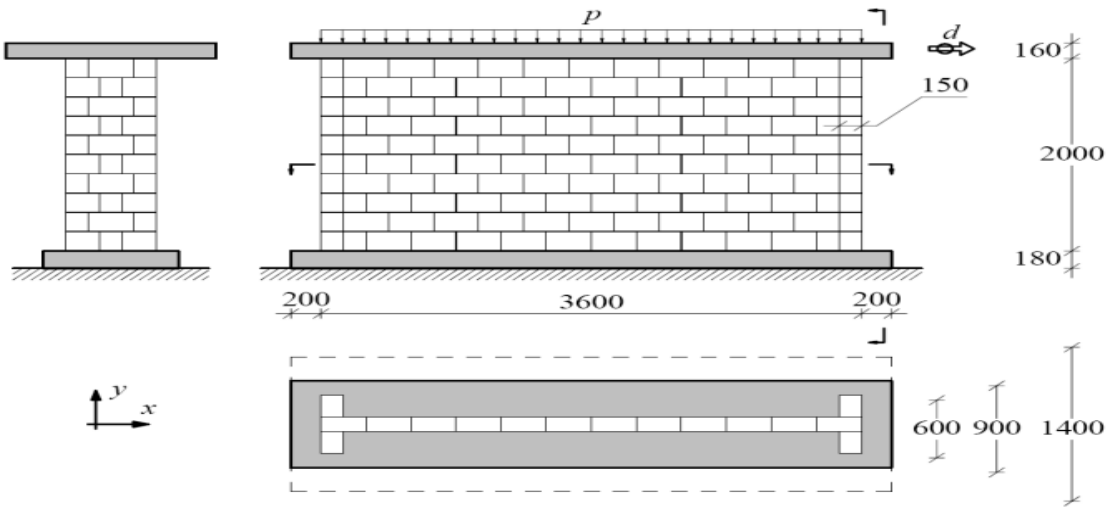

Figure 4.3. The Dimensions of Wall tested in ETH Zurich (All dimensions are in mm and p=0.61 N/mm^2)

Table 4.1. The Mechanical Properties of Tested Wall

E(Mpa)	ν	G (MPa)	f_m (MPa)	f_{mt} (MPa)
2460	0.18	1130	7.61	0.28

In the finite element model, the bottom of the wall is supposed to be fixed to the base. Solid 65 elements are used with only Willam-Warnke plasticity for slabs. The loading was carried out in two parts. The wall is monotically pushed from the side until failure after a uniform load is supplied vertically. Both analytic and experimental analyses show that crack types and propagation are similar that is given in Figure 4.4.

The capacity curve obtained from the analysis and the experiment is given in Figure 4.5. It is shown that the analytical model effectively simulates behavior of wall. In the analytic model and experiment, the maximum lateral load was 265 kN and 272.8 kN, respectively. Moreover, the model determines the displacement capacity as 14.2 mm, whereas the experiment determines it as 14 mm. The in-plane behavior of the analytical model is similar to the behavior of the experiment. These results indicates that this model can be used for the assessment of tested walls.

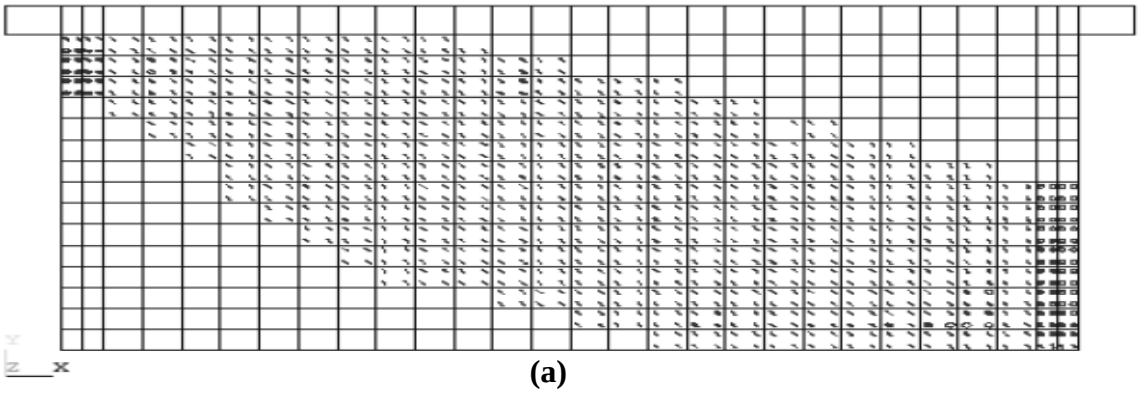

(a)

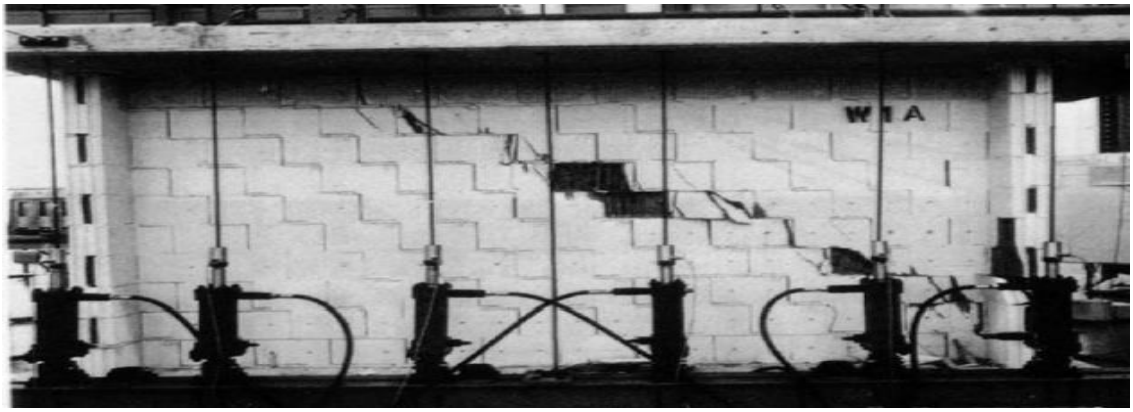

(b)

Figure 4.4. a) The Crack Pattern from the FE Analysis, b) The Damage Observed at the End of the Test in ETH Zurich.

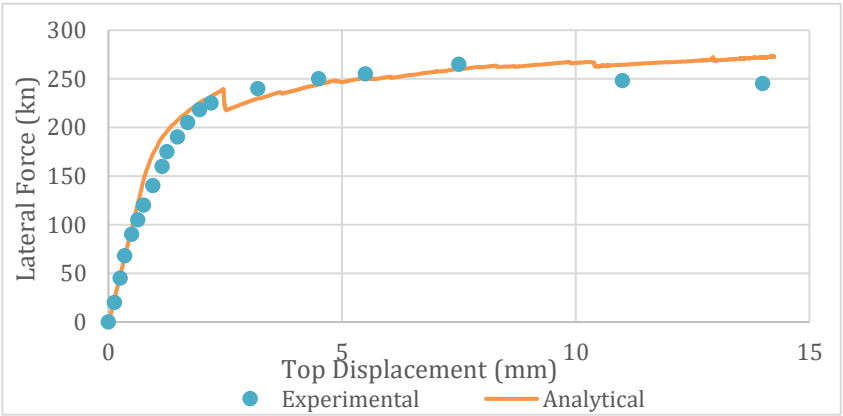

Figure 4.5. The Comparison of Capacity Curves of the Wall Specimen from the FE Analysis and the Experiment

4.4.2. Verification of Base Sliding and Rocking Failure Patterns for URM

In this part, the experiments on URM walls carried out by Franklin were considered the most suitable test for verifying the base sliding and rocking mechanisms of analytic

models [34]. These masonry wall units consists of clay masonry units. The geometry in wall test is given in Figure 4.6 [34].

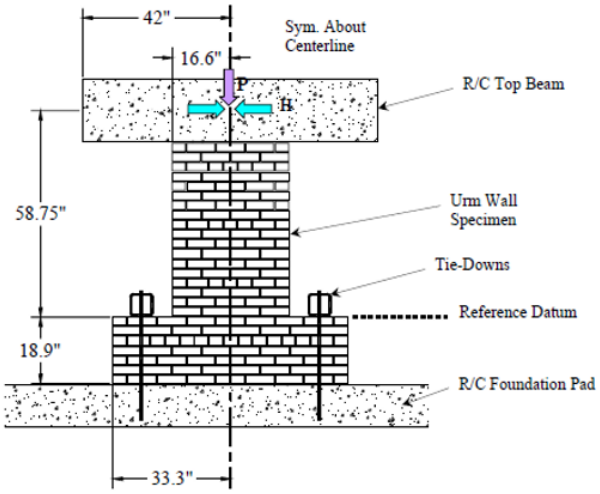

Figure 4.6. Specimen Dimension

The bottom of piers was constrained for any rotation or translation, but the top of walls are free for rotation or translation in all directions. There are R/C loading beam used to provide accurately loading situations. In analytic models, Solid 65 element is used and the modulus of elasticity and poisson ratios of the materials are 4275 MPa and 0.2, respectively. Capacity curves of analytic and experimental studies are similar to each other. These curves is given in Figure 4.7 and 4.8. It is shown that the analytical model effectively simulates behavior of wall.

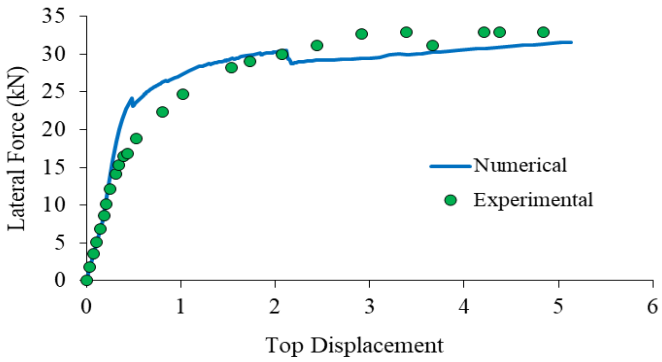

Figure 4.7. The Comparison of Capacity Curves of Squat Specimens from the Experiment with the Ones Obtained Through FE Analysis.

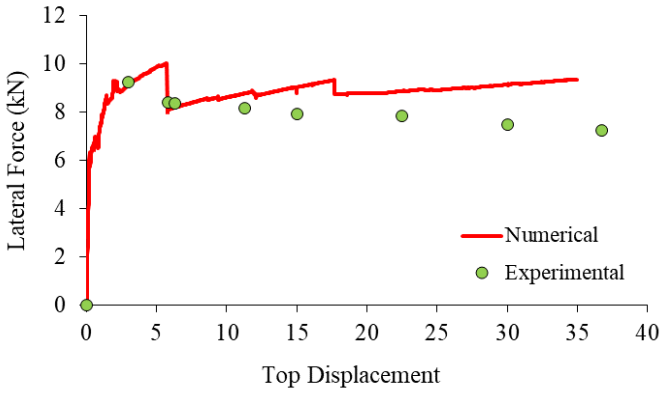

Figure 4.8. The Comparison of Capacity Curves of Slender Specimens from the Experiment with the Ones Obtained Through FE Analysis.

In the Figure 4.7 and 4.8, the capacity curves of squat and slender specimens were obtained, respectively. The in-plane behavior of the analytical model is similar to the behavior of the experiment for base sliding mechanism and rocking mechanism. These results indicates that this model can be used for the assessment of tested walls.

5. MODELS FOR DETERMINING IN-PLANE BEHAVIORS OF UNREINFORCED MASONRY WALLS WITH OPENINGS

5.1. Introduction

Analytical modelling in URM walls require to determine capacity of URM walls with openings under seismic loads. In this part, a procedure has been executed to determine the reduction of capacity and failure modes in URM walls with openings. The main purpose of this procedure is to determine the failure patterns and capacities of URM walls affected by the location, percentage and size of the openings. The different wall models were analyzed and the limit states for openings were tried to be determined.

There are some proposed assumptions in this method that only URM wall with opening is used for modelling. 21 different types of wall with openings were used. One of the walls is solid wall and the others have openings for various purposes. The total number of models is 334 and the characteristic compressive strength of the walls is taken as 3 MPa and 8 MPa. The lintels have elastic material model and masonry units have inelastic material models. In all models, there are a restriction for out-of-plane failure of URM walls.

5.2. Characteristics of Material used in Masonry Walls

The components of an URM wall are masonry units and mortars. The mechanical characteristics and structural behavior of an URM wall are defined by the materials used. Therefore, it is necessary to understand the mechanical characteristics of the materials. Many research have been conducted in order to determine compressive strength of the wall in terms of mortar and masonry units. In TEC2018, the characteristic compressive strength (f_m) of a masonry wall can be determined in two ways. The first is the tests in TS EN 1052-1 to be carried out on the wall samples. Secondly, the compressive strength of masonry walls can be obtained using Table 5.1. Hence, it should be determined the compressive strength of the mortar and masonry units.

Table 5.1. The Compressive Strength of Masonry Wall, f_m (MPa)

Masonry Units	Mortar Classes	Compressive Strength of Mortar (MPa)	Compressive Strength of Masonry Units (MPa)					
			5	10	15	20	25	30
Grup I	General Mortar	M10-M20	3.4-4.2	5.5-6.8	7.3-9.0	8.9-11.0	10.4-12.9	11.9-14.6
		M2.5-M.9	2.2-3.3	3.6-5.3	4.8-7.1	5.9-8.7	6.9-10.1	7.8-11.5
		M1-M2	1.7-2.1	2.8-3.4	3.7-4.5	4.5-5.5	5.2-6.4	5.9-7.3
Grup II		M10-M20	2.8-3.4	4.5-5.5	6.0-7.4	7.3-9.0	8.5-10.5	9.7-12.0
		M2.5-M9	1.8-2.7	3.0-4.4	3.9-5.8	4.8-7.1	5.6-8.3	6.4-9.4
		M1-M9	1.4-1.7	2.3-2.8	3.0-3.7	3.7-4.5	4.3-5.3	4.9-6.0

In addition, there are limits for masonry materials in TEC2018. The compressive strength of masonry units should be greater than $f_{m,min}$ =5.0 MPa in case of perpendicular to the horizontal joints of masonry units and greater than $f_{mh,min}$ = 2.0 MPa in the parallel direction. These values can be determined according to TS EN 772-1. The cube compressive strength of the mortar to be used for unreinforced and confined masonry should be greater than $f_{m,min}$ =5.0 MPa. In addition, it should be greater than $f_{m,min}$ =10.0 MPa for reinforced masonry structures. These values can be determined according to TS EN 1015-11.

The compressive strength of masonry walls was investigated with regard to the compressive strength of the materials used [35]. In equation of 5.1.a and 5.1.b is appropriate for bricks with 1:3 lime mortar and bricks with 1:2:8 mortar, respectively.

$$fm = 0.27fb \qquad (5.1.a)$$

$$fm = 0.22fb \qquad (5.2.b)$$

In this study, two groups were formed based on the compressive strength of the masonry walls. In terms of mean values, these classes are 3 MPa and 8 MPa. These values are taken from the Table 5.1. Since brick and M2 or M2.5 mortar are used, the compressive strength of the wall are taken as 3 and 8 MPa, respectively.

Tension manner in masonry walls are generally insignificant, because tensile strength of masonry units and mortars are low. Strength of masonry walls under shear forces can be designed in equation of 5.2.

$$f_{vk} = f_{vko} + 0.4\sigma_d \leq 0.10\ f_b \qquad (5.2)$$

Characteristic initial shear strength (f_{vko}) is determined with testings or in Table 5.2.

Table 5.2. The Initial Shear Strength of Masonry Wall, (f_{vko})

Masonry Units	**General Mortar**		**Thin Layer Mortar**
Brick	M10-M20	0.3	0.3
	M2.5-M.9	0.2	
	M1-M2	0.1	
Concrete	M10-M20	0.2	0.3
Aerated Concrete	M2.5-M9	0.15	0.3
Stones	M1-M9	0.1	cannot be used

The tensile strength of masonry walls (f_{mt}) may be calculated using the $1.5f_{vko}$ formula. In this study, the tensile strengths of the URM walls are taken as 0.15 MPa and 0.30 MPa ,since brick and M2 or M2.5 mortar classes are used.

The rate of stress and strain of a material in elastic region is a constant value. This ratio gives the modulus of elasticity and this behavior is referred to as hook law.

$$\sigma = \varepsilon.E \qquad (5.3)$$

In the equation of 5.3, σ and ε are stress and strain, respectively. E is the Modulus of Elasticity. There are many empirical formulas to calculate Modulus of Elasticity of

masonry structures. The Modulus of Elasticity of masonry walls can be found using its compressive strength. It is known as a general formula in equation of 5.4.

$$E_w = \alpha f_m \quad (5.4)$$

In this equation, E_w is the Modulus of Elasticity of masonry wall, f_m is characteristics compressive strength of walls and α is a constant that varies depending on the earthquake codes. There are different values for α coefficient in various regulations. The Modulus of Elasticity and shear modulus for load-bearing walls in TEC2018 are 750fm and 750fm*0.4, respectively. In Eurocode 6 and FEMA 356, the Modulus of Elasticity are 1000fm and 550fm, respectively [36, 37].

In this study, the Modulus of Elasticity is taken as 550f_m MPa for all models.

5.3. Classification and Analysis of Masonry Walls

In this study, parameters including compressive strength, aspect ratio, opening effect were taken into account while assessing the masonry walls' capability. All modelling were done with ANSYS software. Material properties of the finite element models are determined as stated above. The method of modeling all of the components of a wall as a composite structure is known as macro modeling.

5.3.1 Classifications of Masonry Walls

In this study, the compressive strength of masonry walls was the primary criterion for classifying them. Walls with a compressive strength of 3 MPa are classified as low-strength, while those with a compressive strength of 8 MPa are classified as high-strength.

The second classification of walls was carried out, according to aspect ratio. The aspect ratio is the ratio of the wall height to wall length in horizontal direction. In models, many various aspect ratio values were found, and aspect ratio has a direct impact on the failure mechanisms and in-plane lateral capacity of wall.

The last classification of walls was carried out to identify for opening effect, including opening size ,opening position and numbers of openings in walls. 167 walls with different

geometries were evaluated using all of these parameters. The Solid65 elements are used in all models, the modulus of elasticity and poisson's ratio are $550f_m$ and 0.2, respectively. The f_m value was taken as 3 MPa and 8 MPa for all models. In material modeling, these bilinear curves are used as multilinear isotropic plasticity models and the stress-strain characteristics of subclasses in terms of compressive strength are shown in Figure 5.1. Nonlinear static analysis are used to obtain capacity curves of walls.

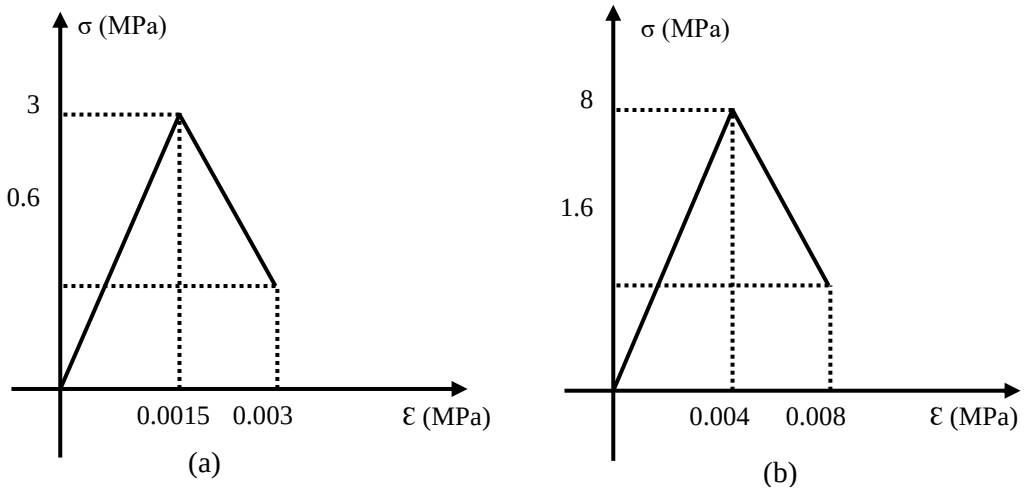

Figure 5.1. Stress-Strain Characteristics for Subclasses According to Compressive Strength Values of (a) 3 MPa, (b) 8 MPa

5.3.2 Loading and Restriction Situations in Wall Models

There are some assumptions for loading and restriction cases in all models as stated below:

- The bottom of walls is assumed to be fixed.
- The top of wall is assumed to be a free end.
- Firstly, the vertical loads as pressure loads are applied to the top of wall, then horizontal loads are applied to wall until failure.

Figure 5.2 presents the pressure loads and restriction situations in wall models with openings.

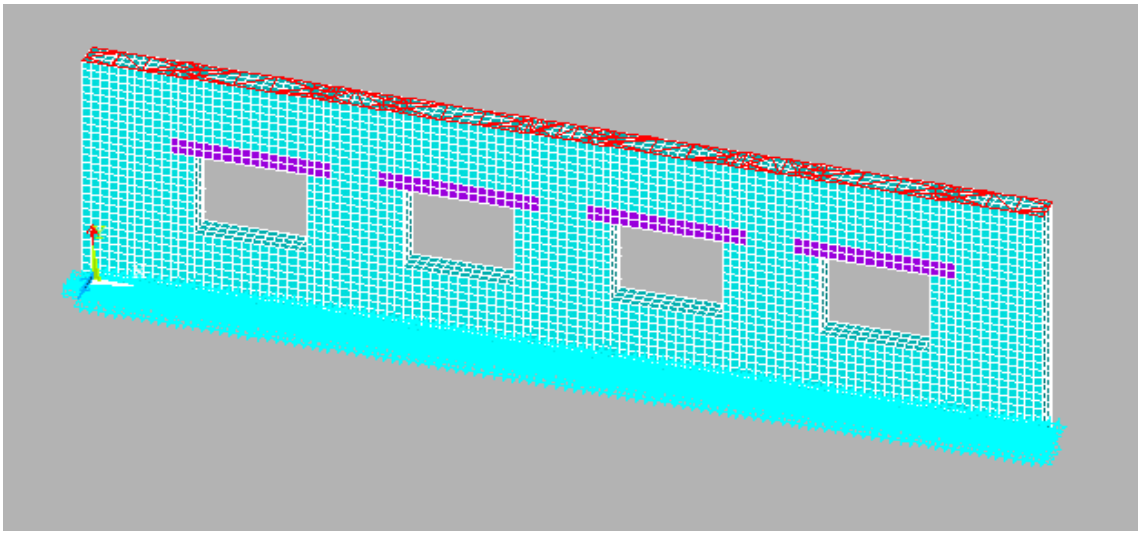

Figure 5.2. Loading and Restriction Situations for a Masonry Wall with Openings

5.4 Analysis of Masonry Walls with Openings

The URM walls with openings in this study are masonry buildings that can be found in the province of Düzce. The geometry of walls are taken from the 'Kamu Binaları Envanteri için Yöntem Geliştirme Çalışmaları' study. Therefore, the mechanical and geometric properties of walls were chosen to be suited for this region in all models. The walls are then divided into groups based on the types of openings. There are 21 different types of URM walls. The classifications of walls depend on types of opening as stated below:

- Single door opening
- Solid wall
- Single window opening
- Two-windows openings
- Three-windows openings
- Four-windows openings
- Five-windows openings
- Six-windows openings
- Seven-windows openings
- Eight-windows openings
- Nine-windows openings
- Door and windows openings
- Single door and two windows openings

- Single door and three windows openings
- Single door and four windows openings
- Single door and five windows openings
- Single door and six windows openings
- Single door and eight windows openings
- Two door and four windows openings
- Two door and six windows openings
- Two door and seven windows openings

The URM walls are divided into piers and spandrels by various types of openings. The representation of these structural components in all models is shown in Figure 5.3. All models and analysis were done with ANSYS. The element and material properties were assigned to the model after the geometry of the walls were created. Also, concrete lintels are used to support spandrels. The behavior of lintels is defined as linear elastic and the dimensions of the lintel were determined according to TEC2018. The modulus of elasticity and poisson ratio of lintels are taken as 30 000 MPa and 0.2 for all model, respectively. Masonry piers and spanderls are modelled according to the aforementioned structural parameters. The compressive strength of URM walls is taken as 3 MPa and 8 MPa. The analytical process started, after the support and loading conditions were determined. The crack patterns, collapse mechanisms and capacity of URM walls are evaluated as a consequence of the analyses.

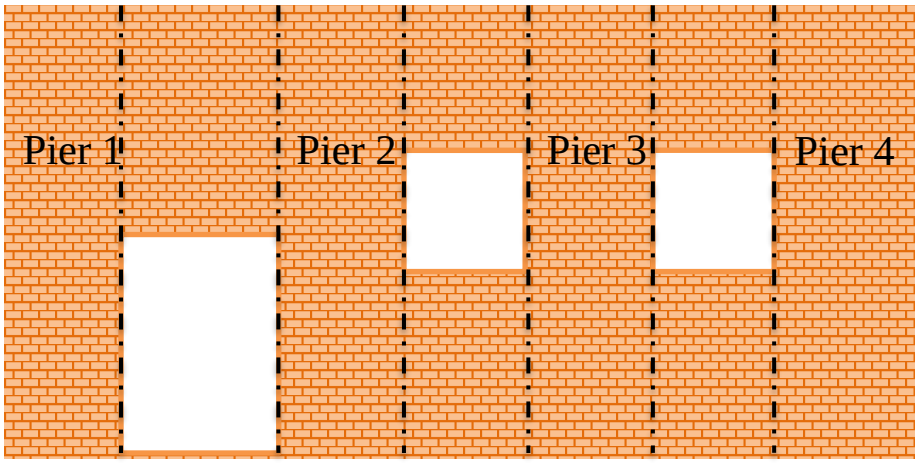

Figure 5.3. Representation of Piers in Masonry Models

5.4.1 Failure Modes of URM Walls

In this study, URM walls are divided into categories depending on different types of openings. Masonry walls can be grouped into 21 different types. Since compressive strength of the masonry walls are assumed to be 3 MPa and 8 MPa for each wall and two analyses for each wall have carried out. These walls, whose dimensions are given in Appendix A, are modelled and analyzed using Ansys. The crack patterns and collapse mechanisms of URM walls are investigated after the analytical progress. Furthermore, the impact of parameters including openings, aspect ratio, and compressive strength of walls on the in-plane performance of masonry wall was evaluated.

5.4.1.1 Failure Modes of Wall 1

In the wall 1, there are 15 different wall models. The impact of a single door opening was studied in these models of wall 1. Table A.1 shows the lengths of the walls. As seen in Figure 5.3, each pier is designated from left to right. The crack patterns obtained from the analysis of wall models corresponding to 15 different wall models are described in this section.

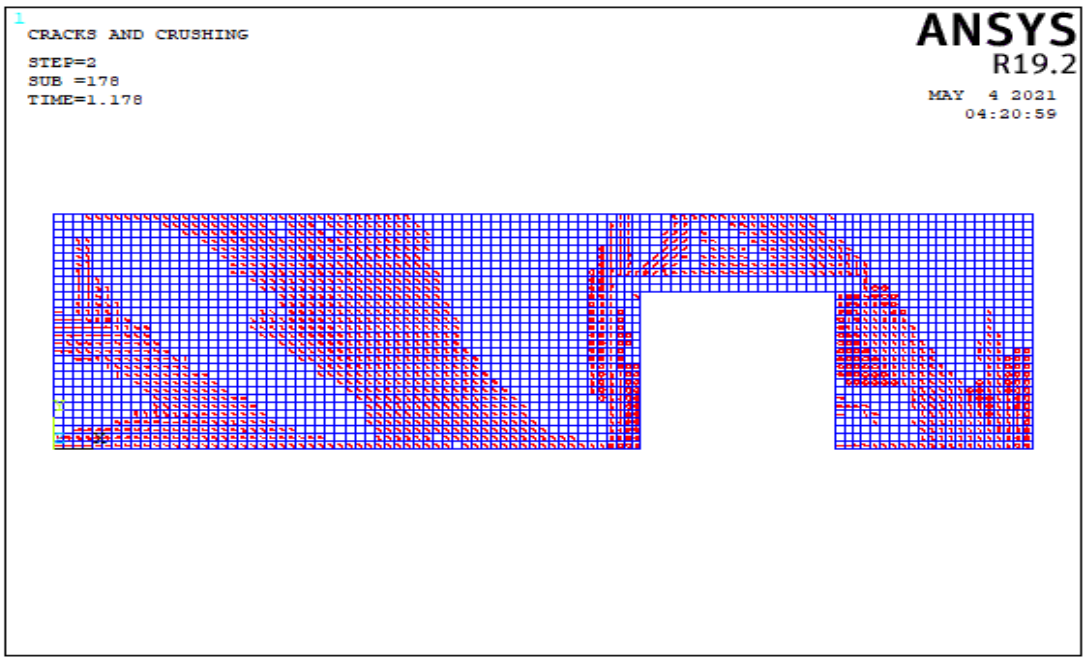

(a)

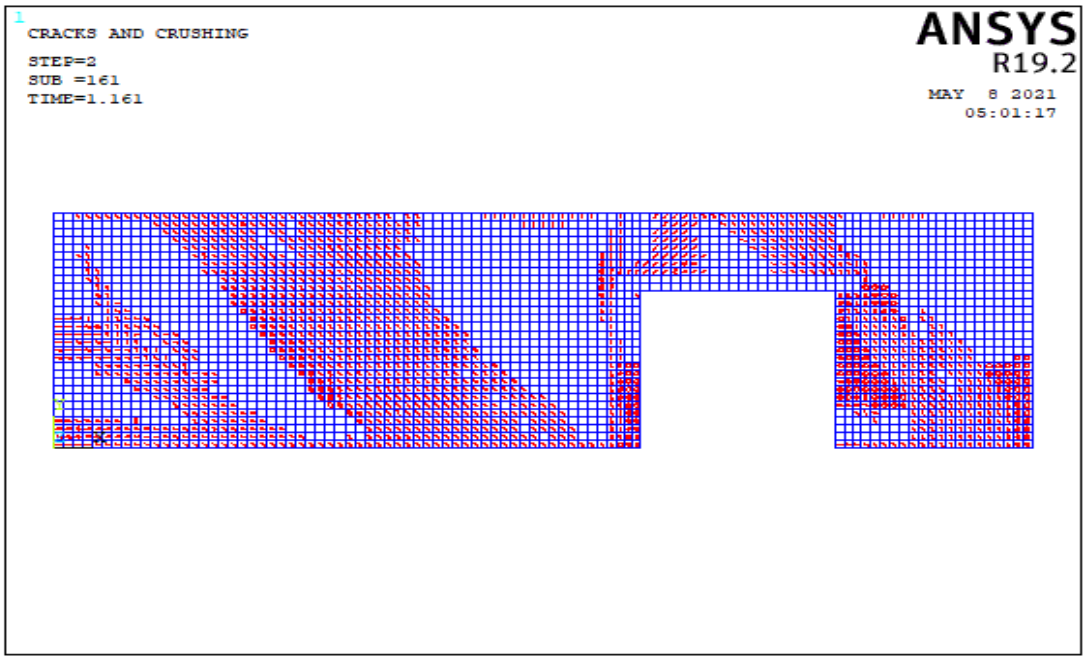

(b)

Figure 5.4. The Crack Pattern of Wall 1 Model 1 According to Compressive Strength Values of (a) 3 MPa, (b) 8 MPa

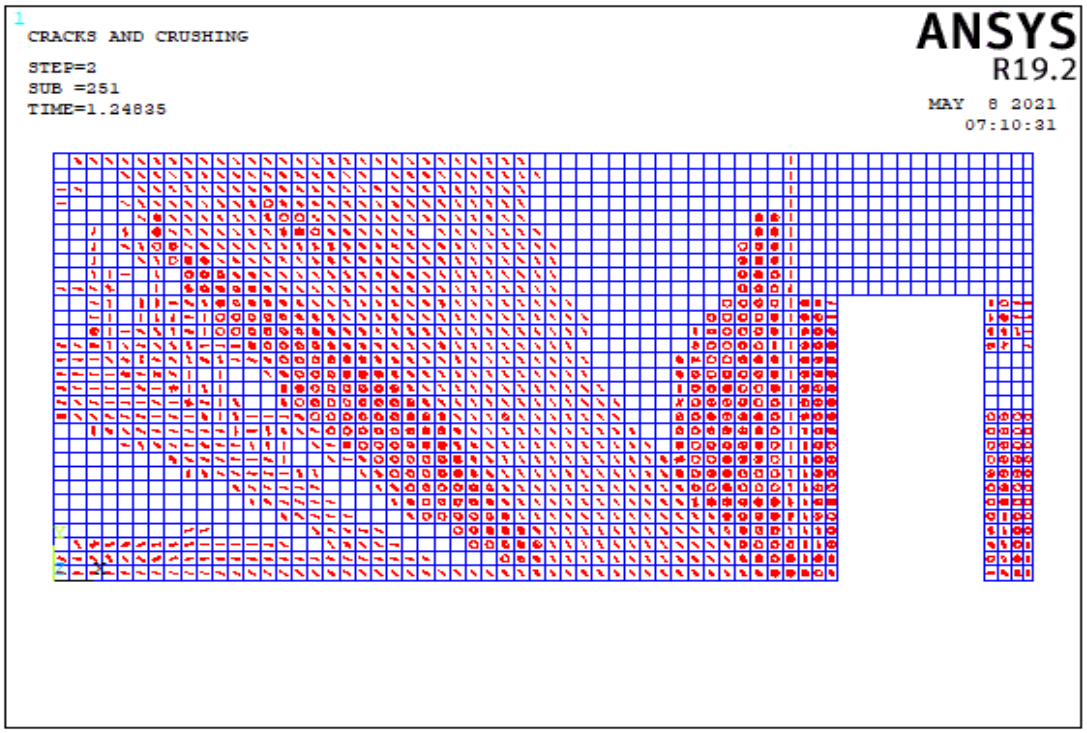

(a)

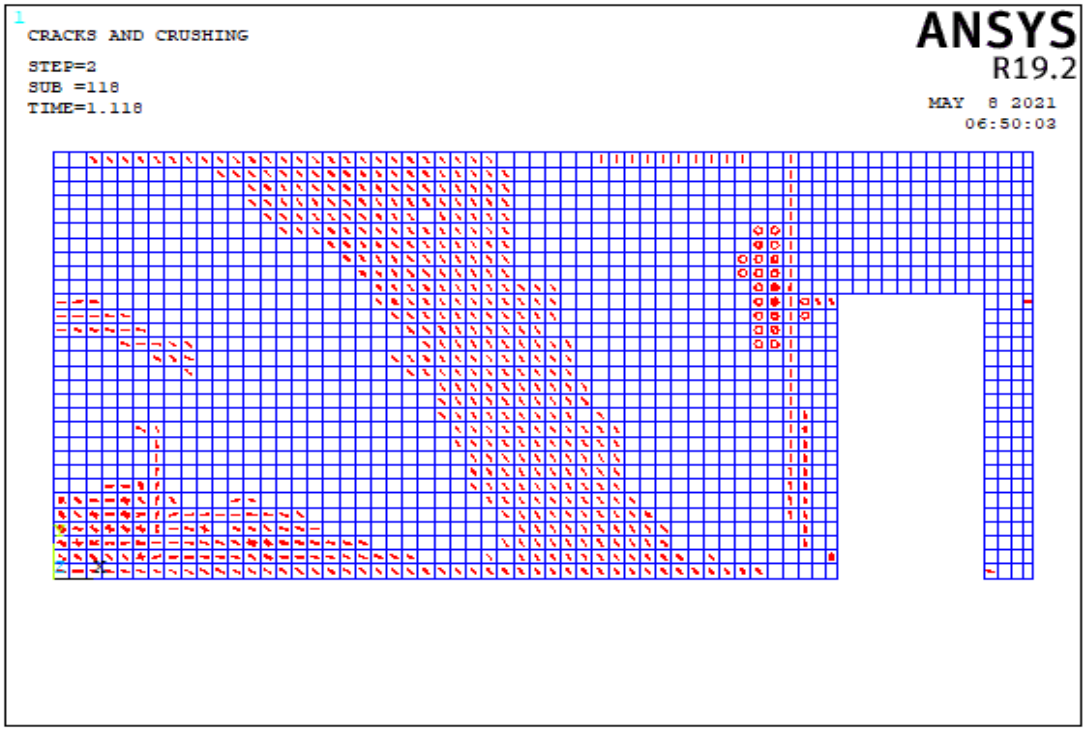

(b)

Figure 5.5. The Crack Pattern of Wall 1 Model 2 According to Compressive Strength Values of (a) 3 MPa, (b) 8 MPa

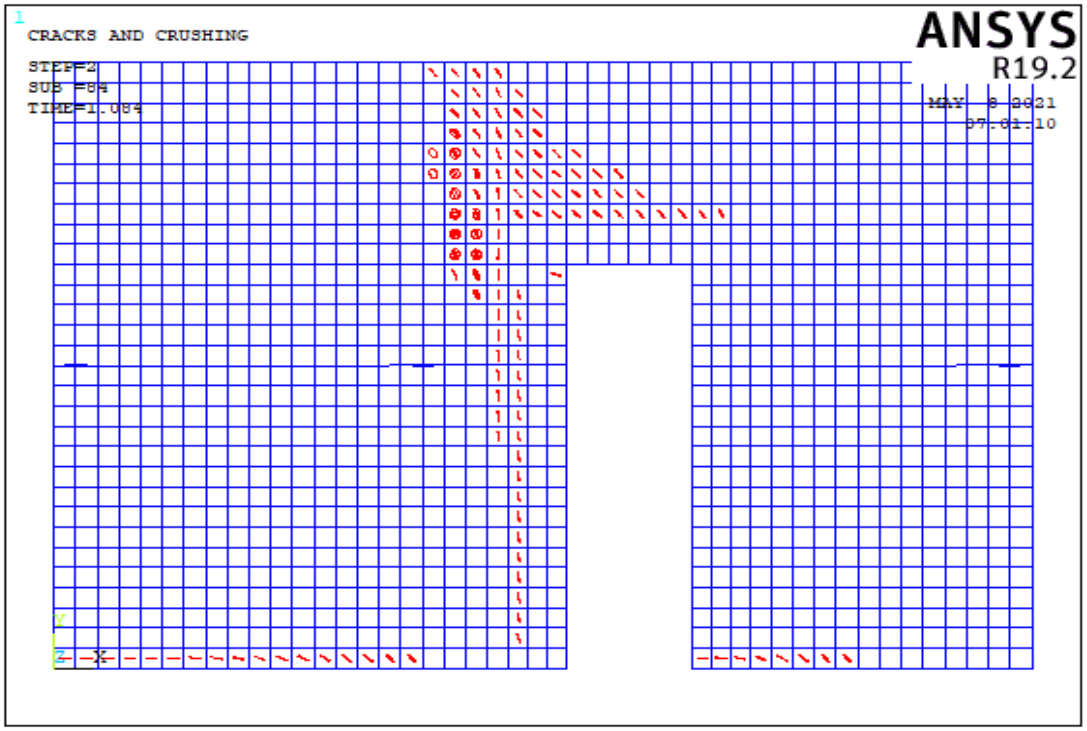

(a)

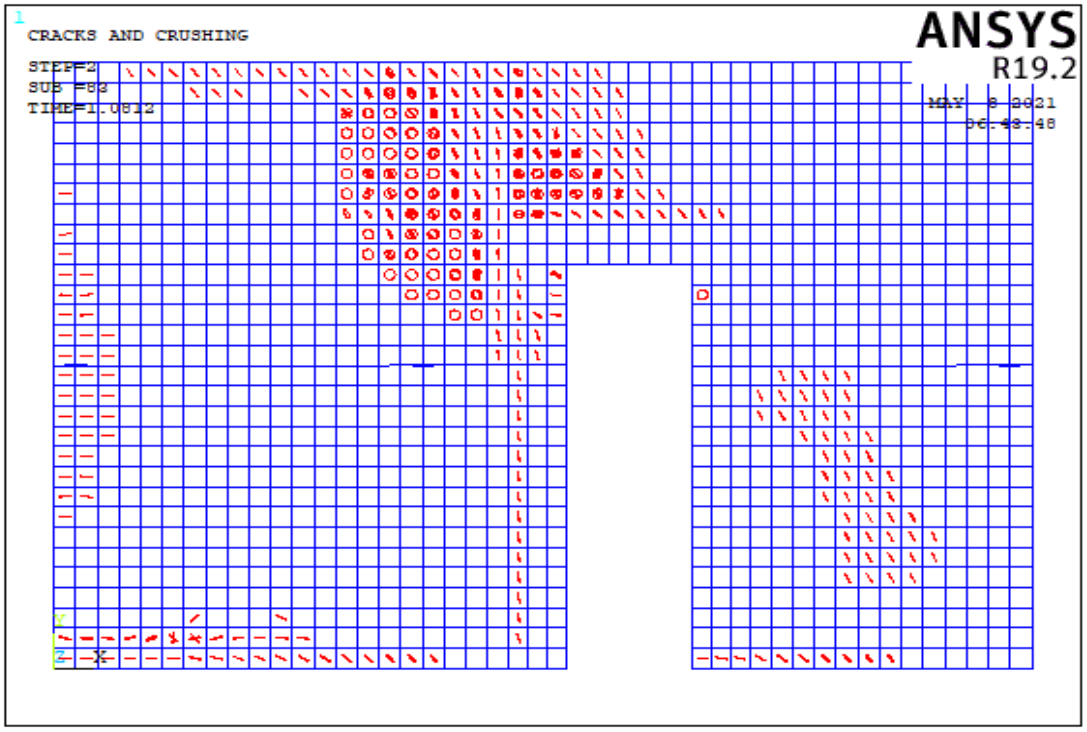

(b)

Figure 5.6. The Crack Pattern of Wall 1 Model 3 According to Compressive Strength Values of (a) 3 MPa, (b) 8 MPa

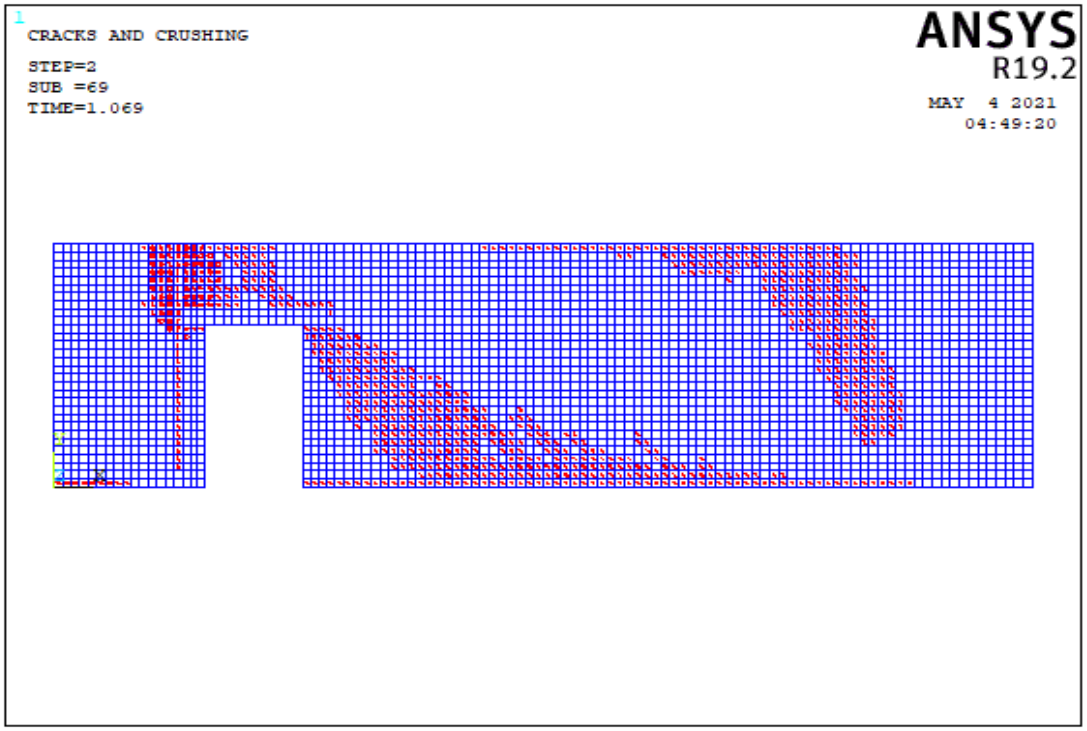

(a)

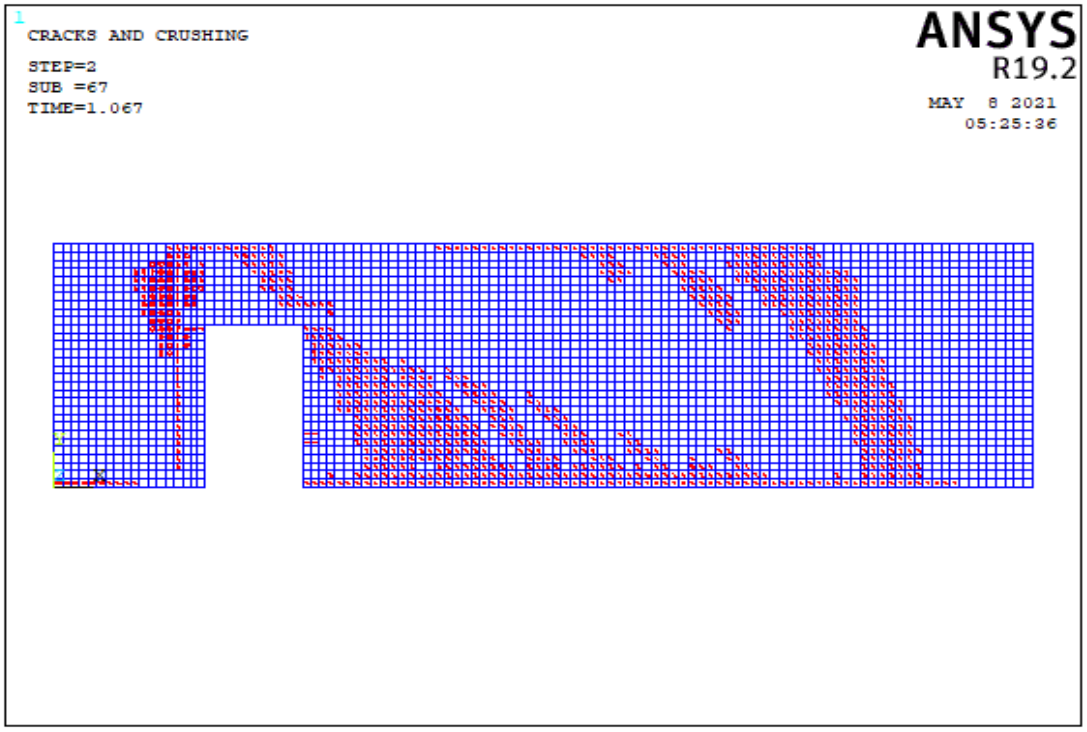

(b)

Figure 5.7. The Crack Pattern of Wall 1 Model 4 According to Compressive Strength Values of (a) 3 MPa, (b) 8 MPa

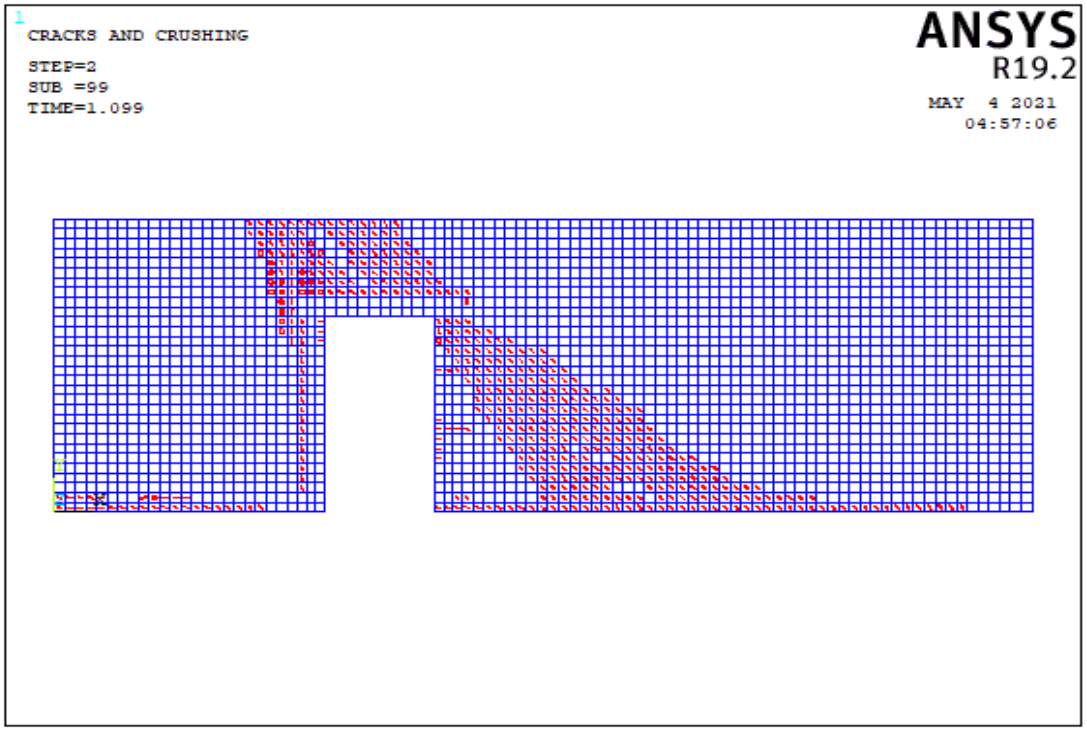

(a)

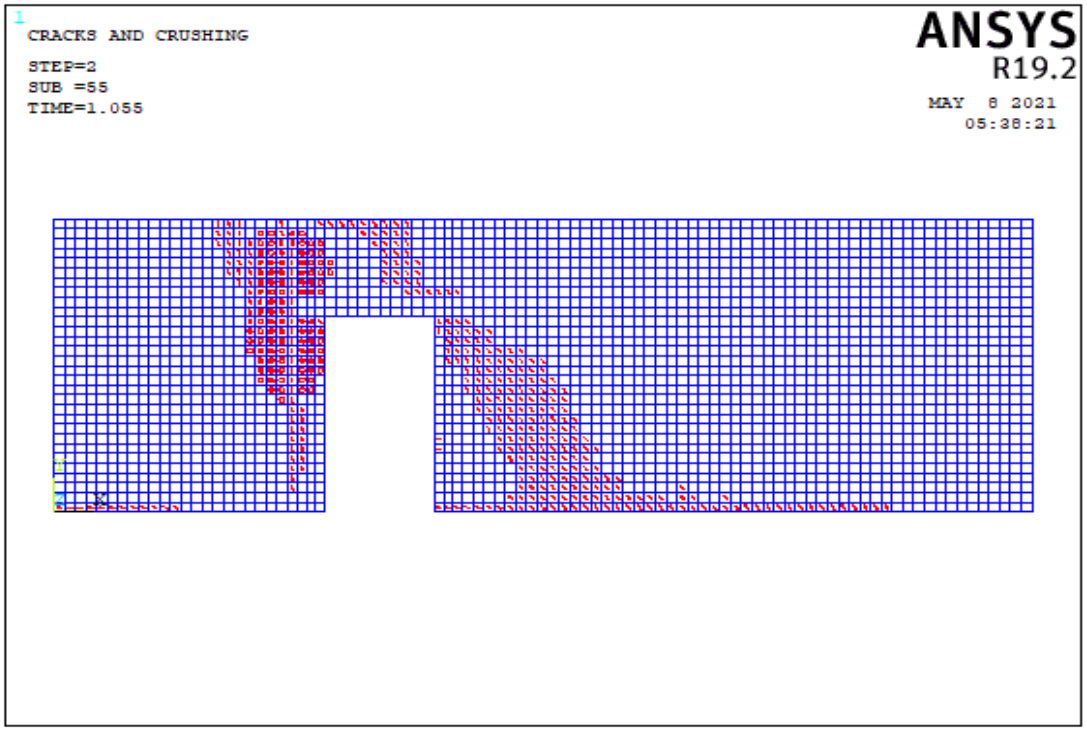

(b)

Figure 5.8. The Crack Pattern of Wall 1 Model 5 According to Compressive Strength Values of (a) 3 MPa, (b) 8 MPa

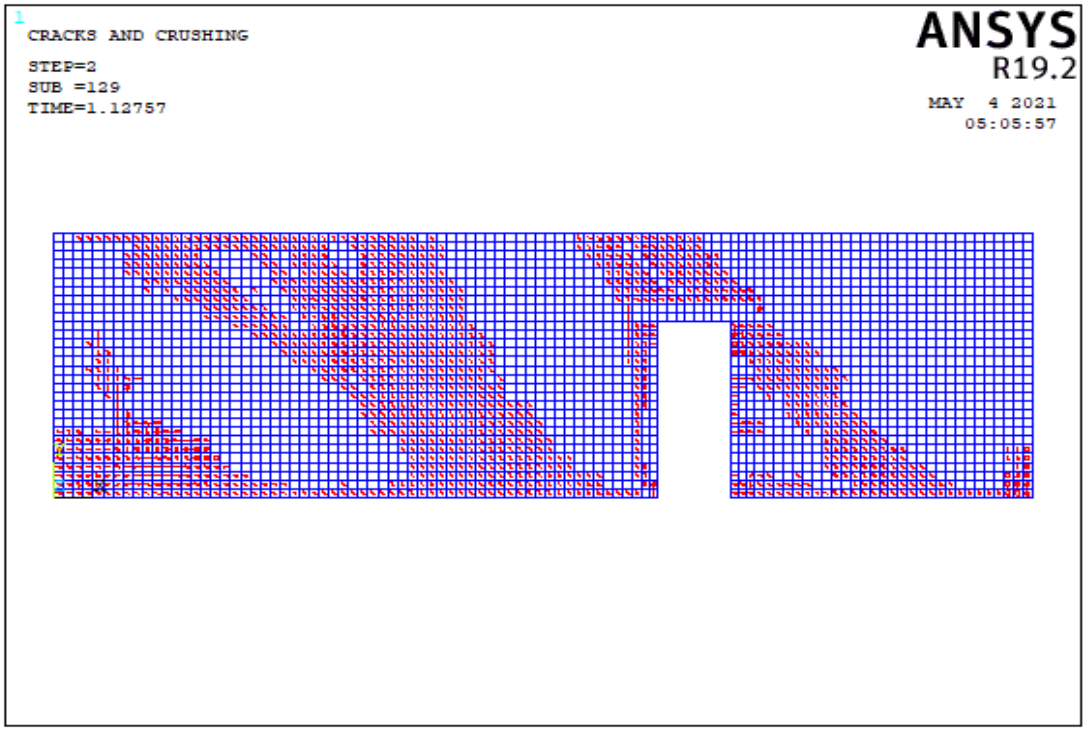

(a)

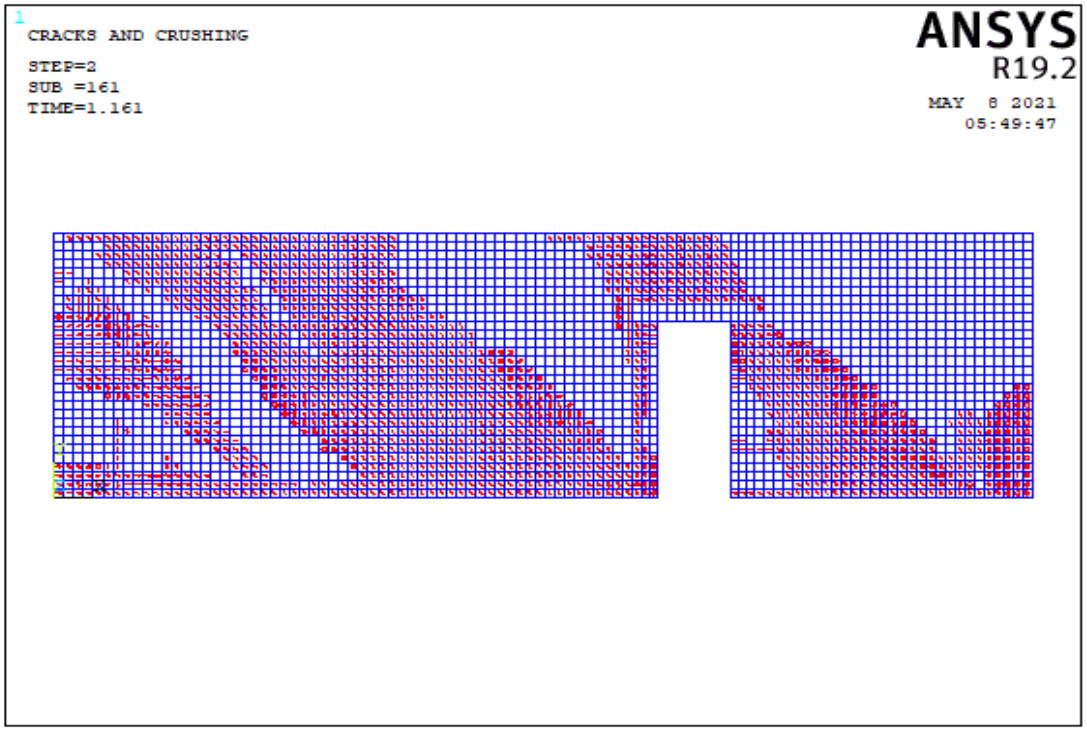

(b)

Figure 5.9. The Crack Pattern of Wall 1 Model 6 According to Compressive Strength Values of (a) 3 MPa, (b) 8 MPa

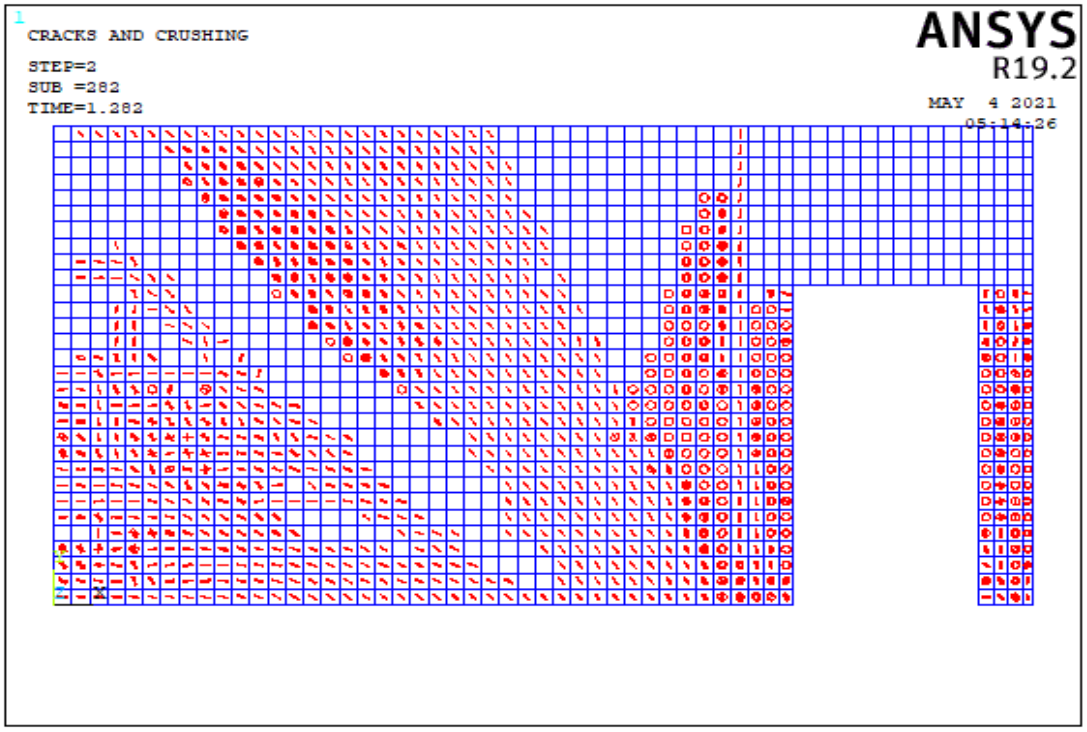

(a)

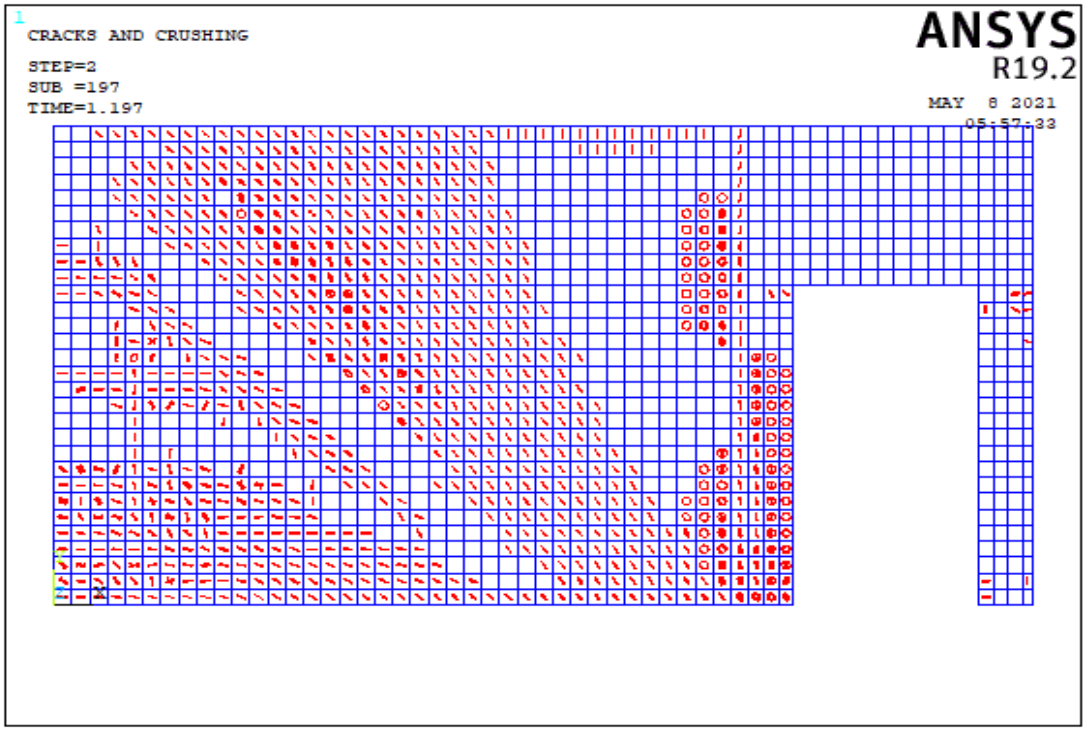

(b)

Figure 5.10. The Crack Pattern of Wall 1 Model 7 According to Compressive Strength Values of (a) 3 MPa, (b) 8 MPa

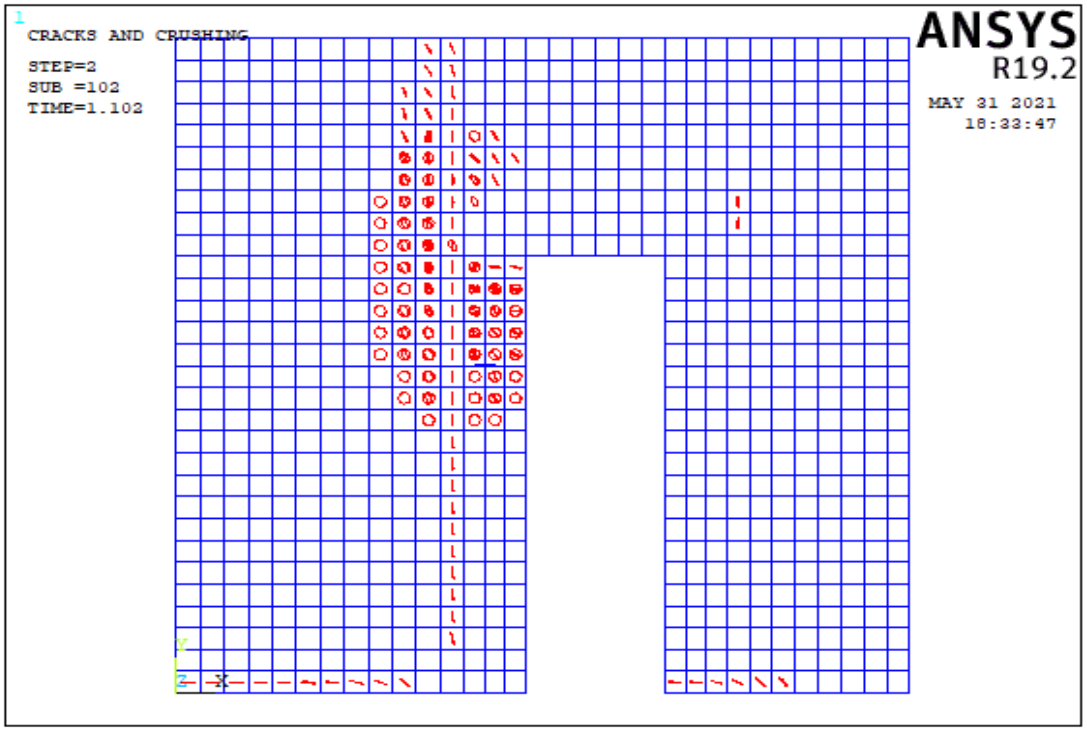

(a)

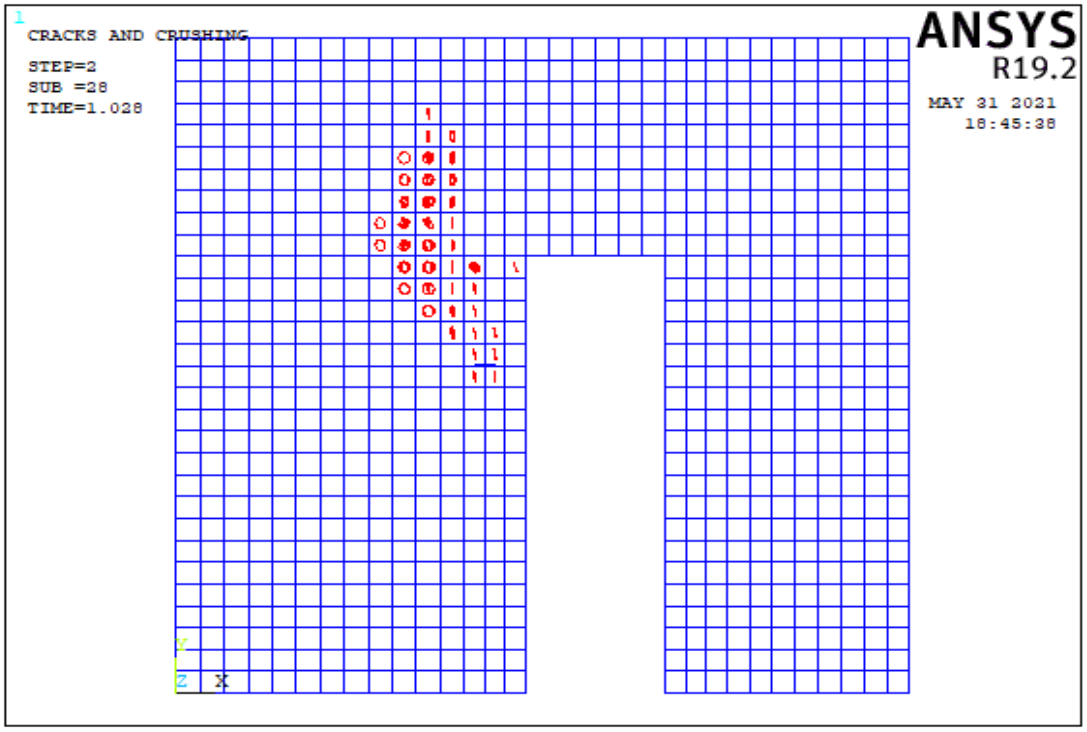

(b)

Figure 5.11. The Crack Pattern of Wall 1 Model 8 According to Compressive Strength Values of (a) 3 MPa, (b) 8 MPa

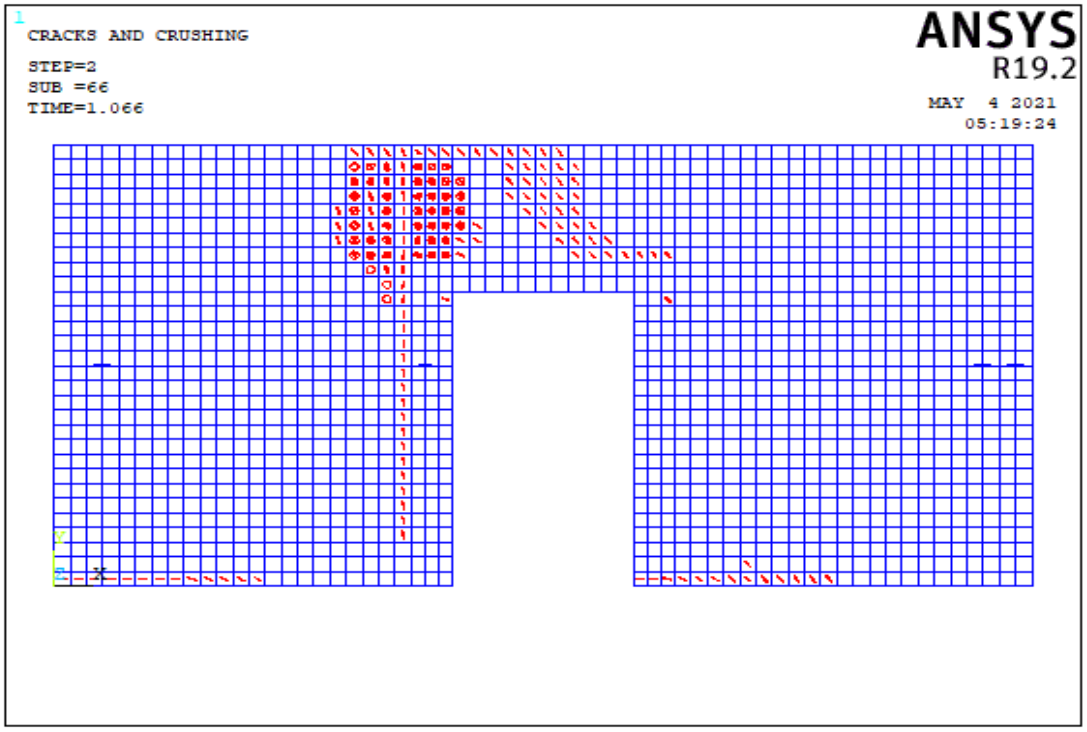

(a)

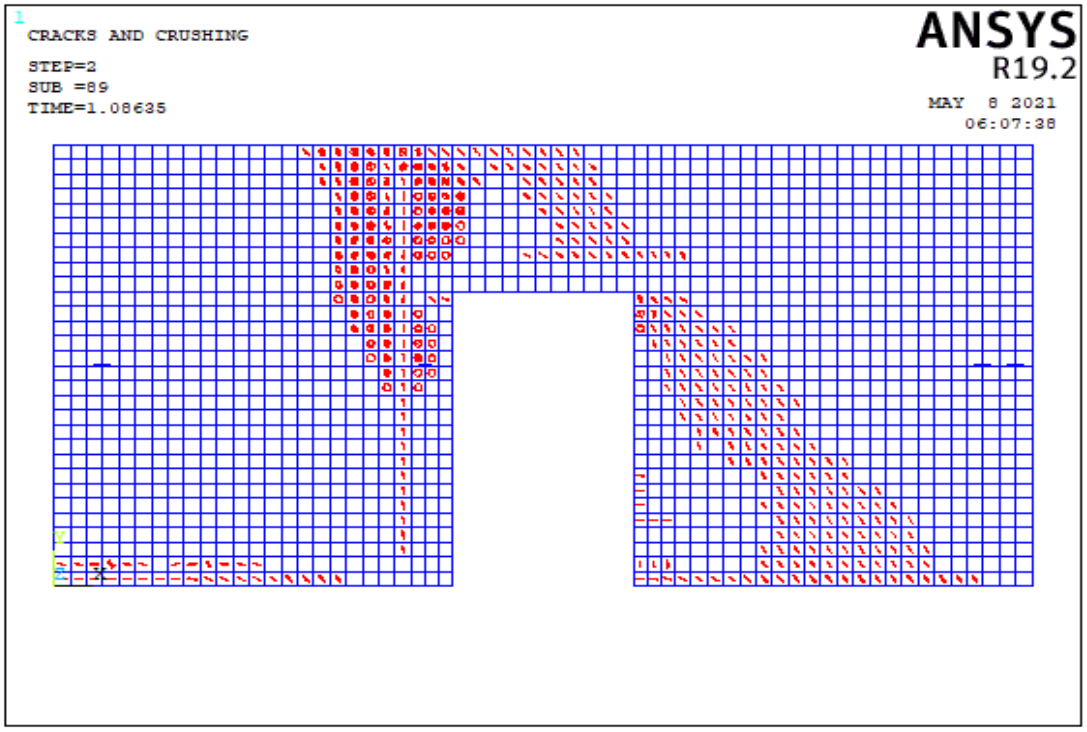

(b)

Figure 5.12. The Crack Pattern of Wall 1 Model 9 According to Compressive Strength Values of (a) 3 MPa, (b) 8 MPa

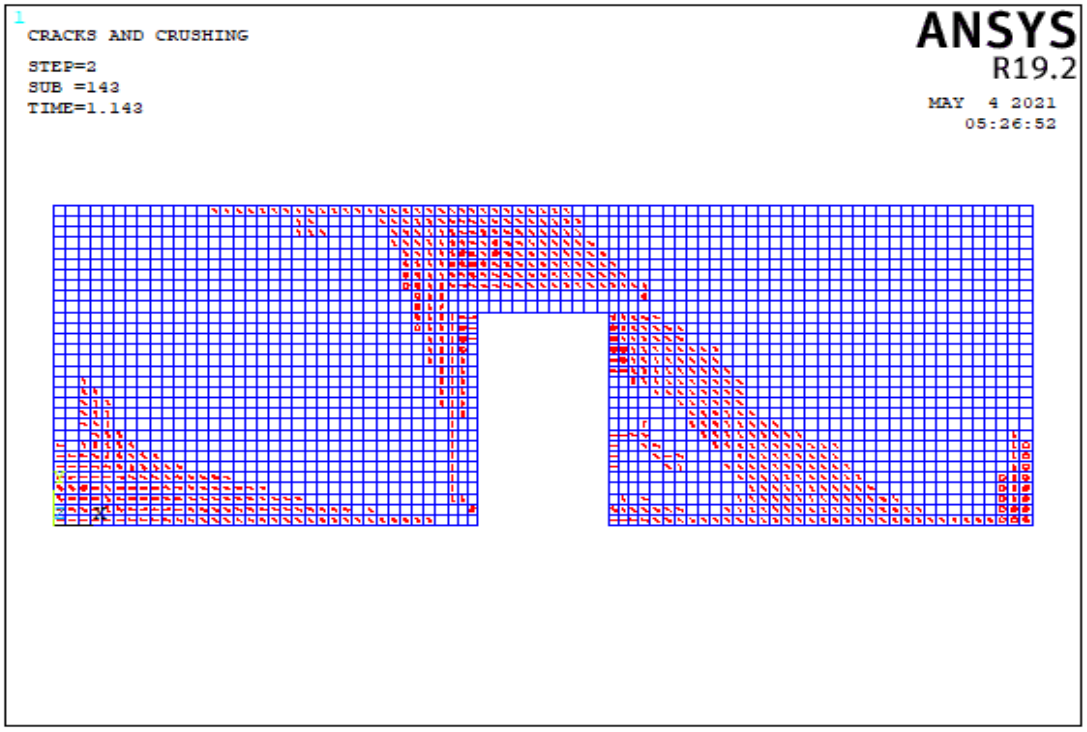

(a)

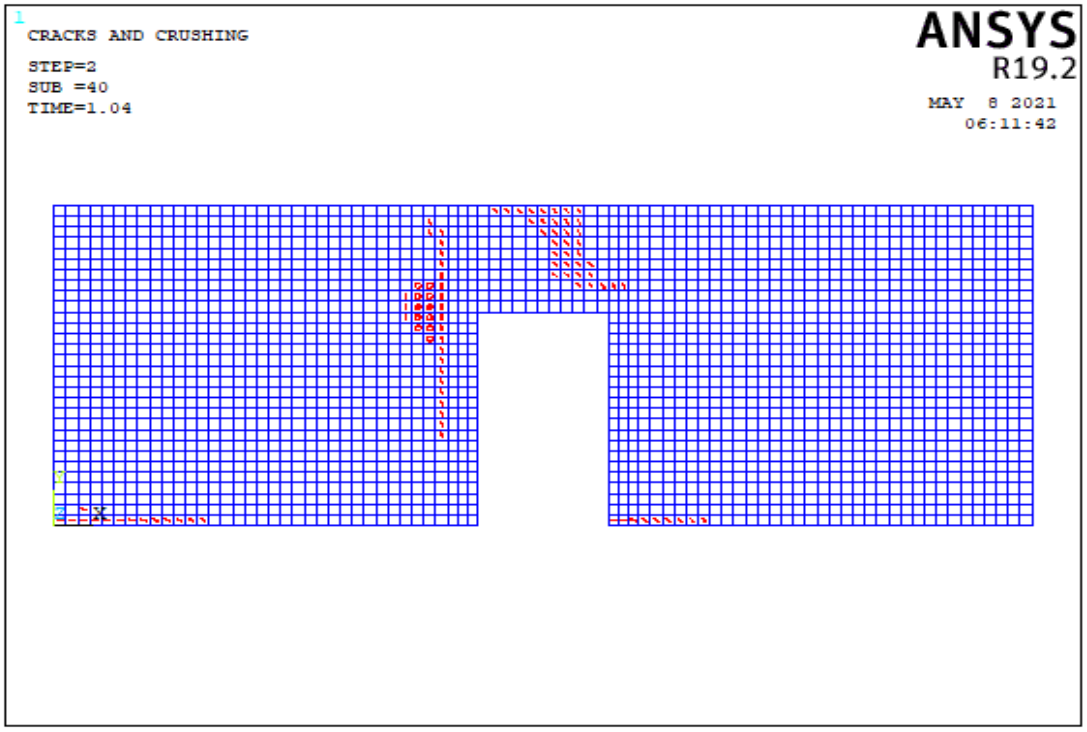

(b)

Figure 5.13. The Crack Pattern of Wall 1 Model 10 According to Compressive Strength Values of (a) 3 MPa, (b) 8 MPa

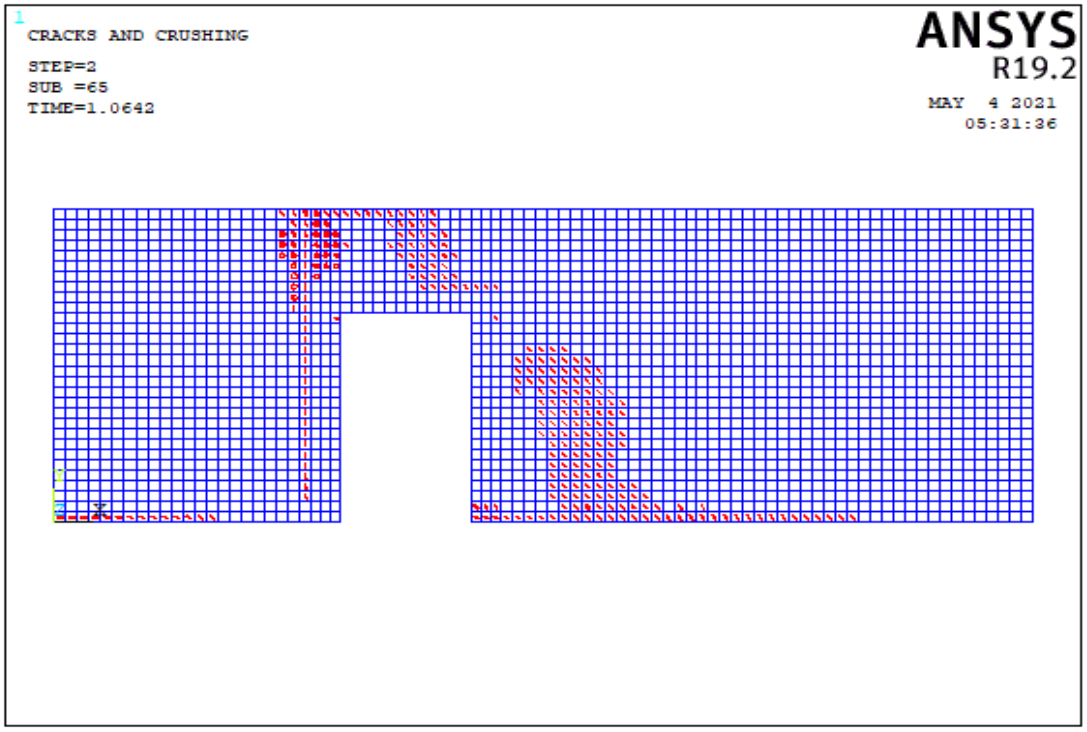

(a)

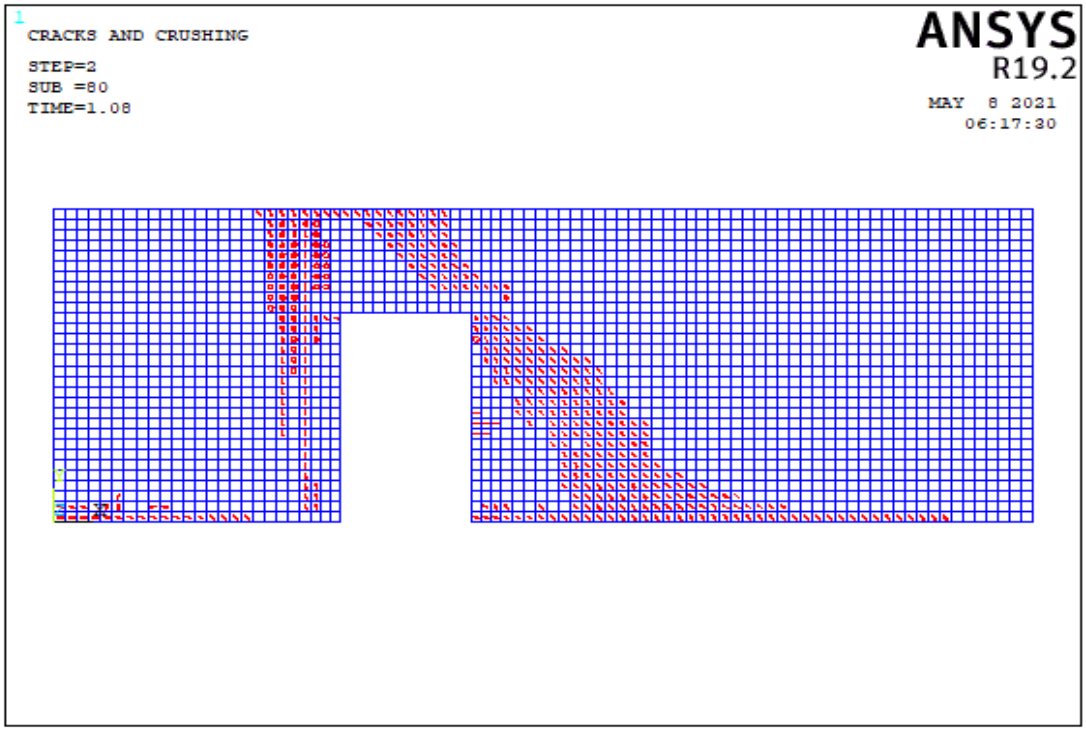

(b)

Figure 5.14. The Crack Pattern of Wall 1 Model 11 According to Compressive Strength Values of (a) 3 MPa, (b) 8 MPa

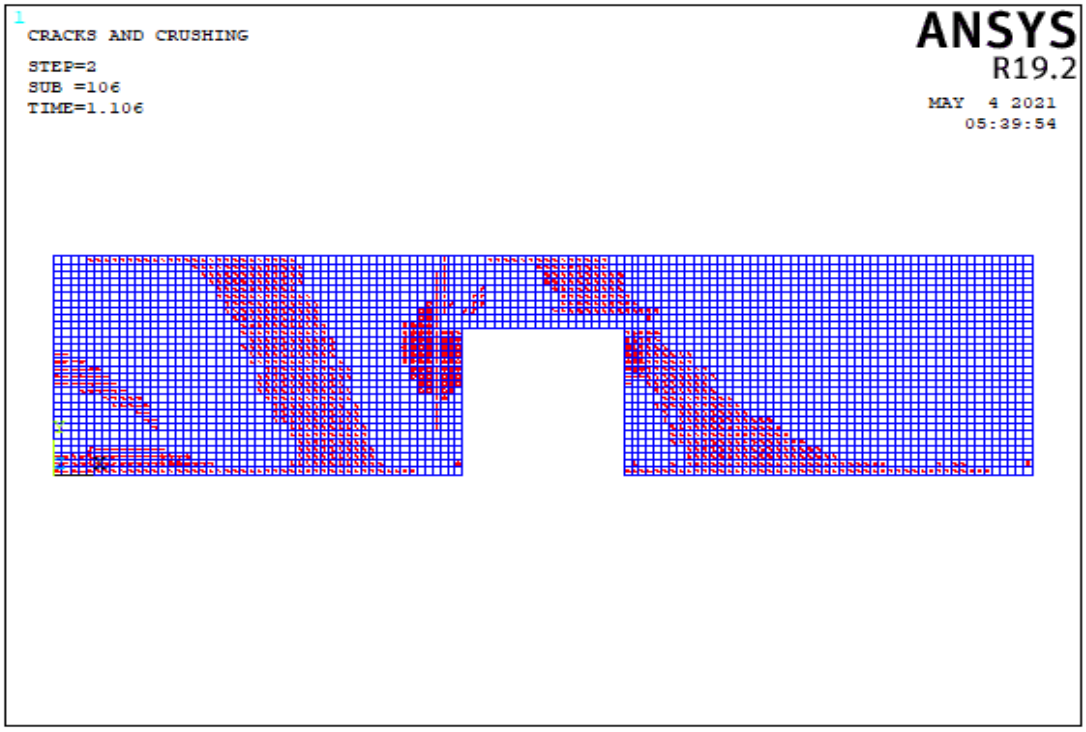

(a)

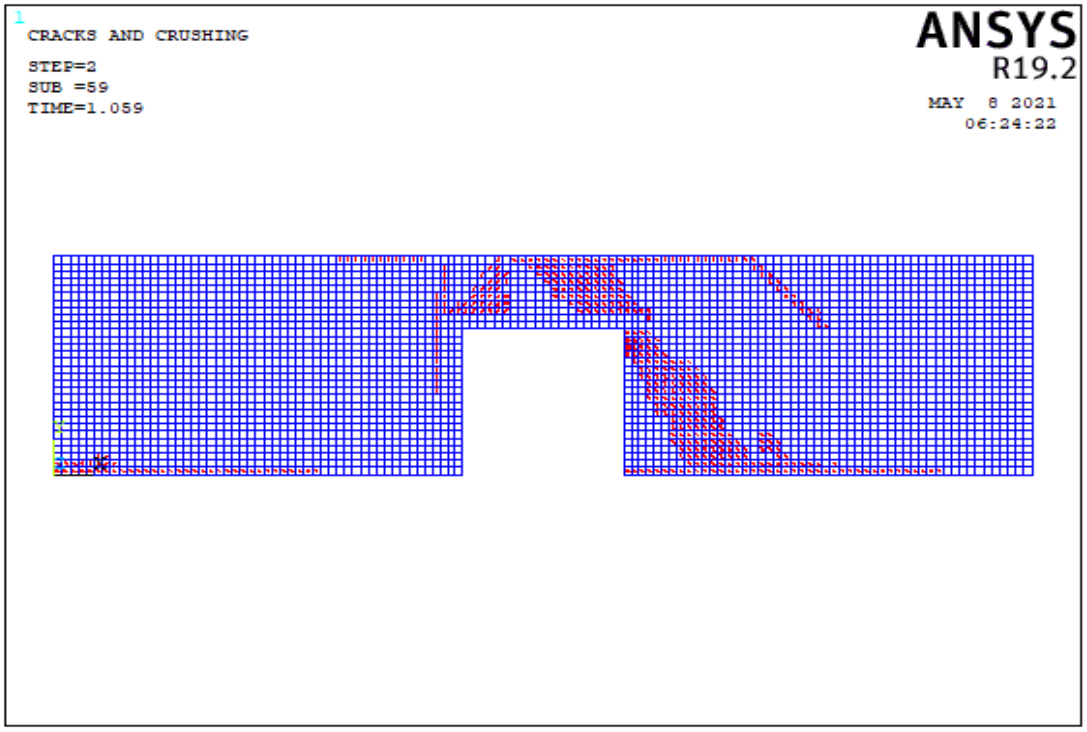

(b)

Figure 5.15. The Crack Pattern of Wall 1 Model 12 According to Compressive Strength Values of (a) 3 MPa, (b) 8 MPa

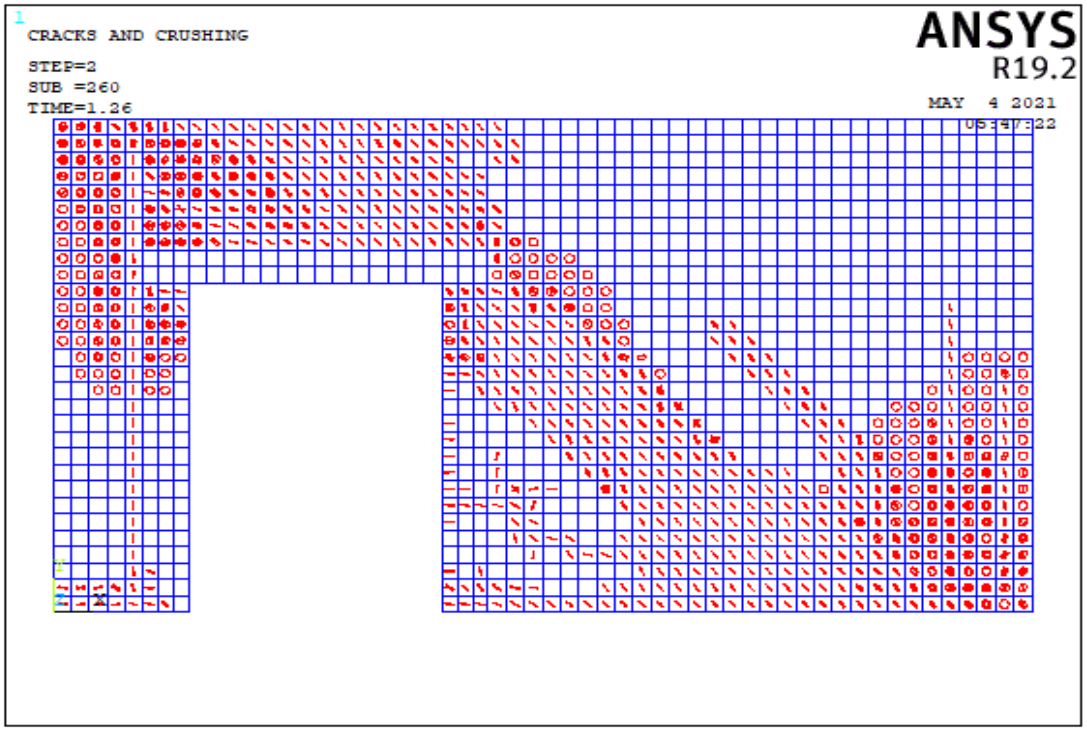

(a)

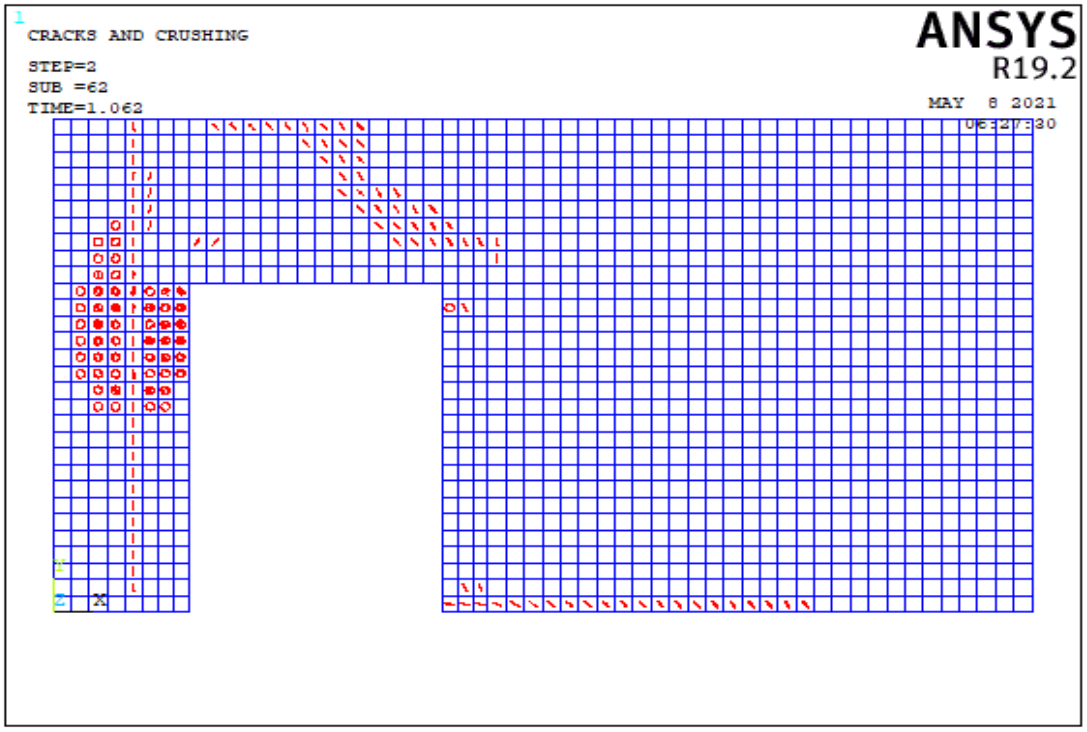

(b)

Figure 5.16. The Crack Pattern of Wall 1 Model 13 According to Compressive Strength Values of (a) 3 MPa, (b) 8 MPa

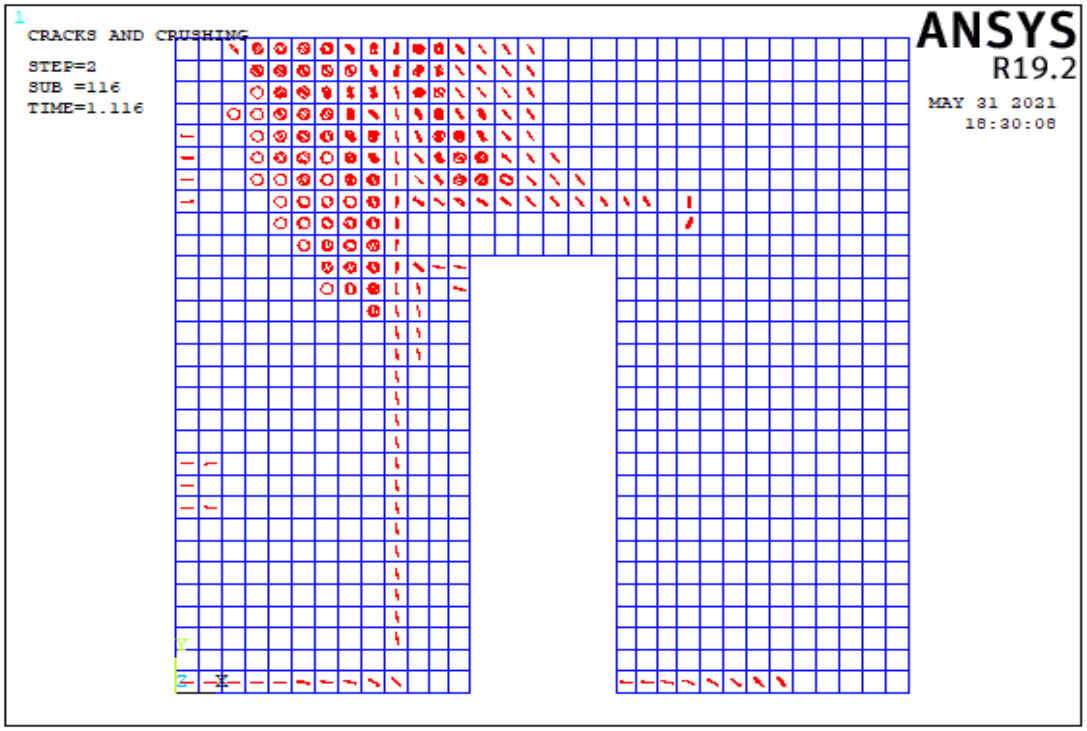

(a)

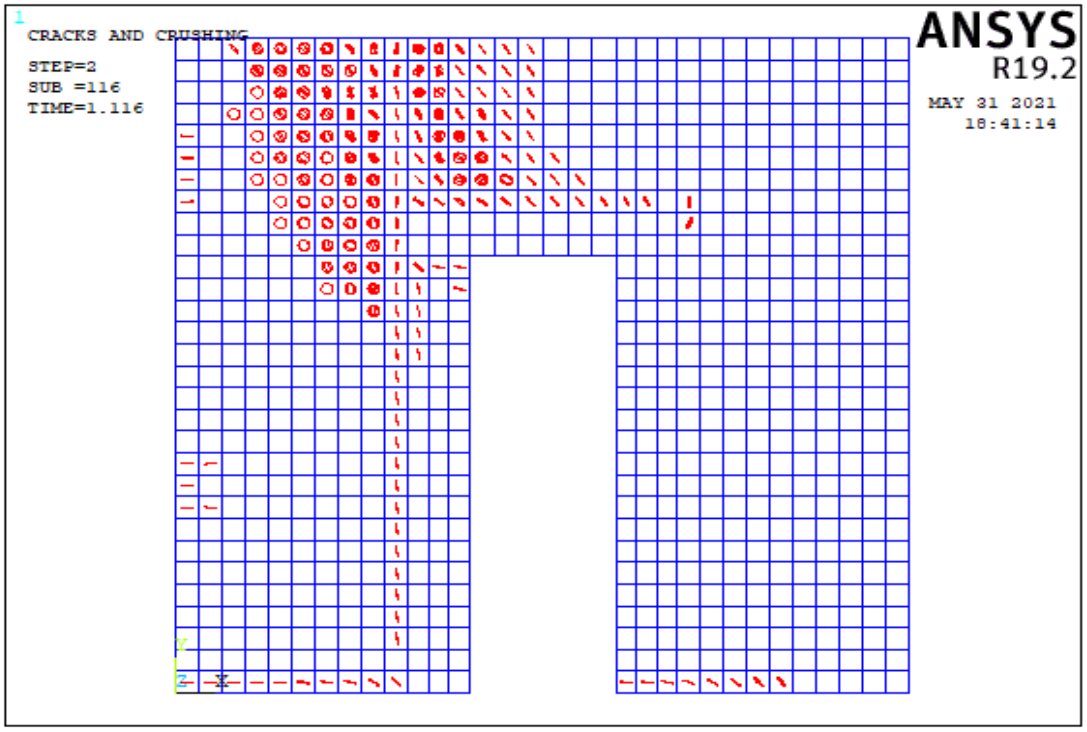

(b)

Figure 5.17. The Crack Pattern of Wall 1 Model 14 According to Compressive Strength Values of (a) 3 MPa, (b) 8 MPa

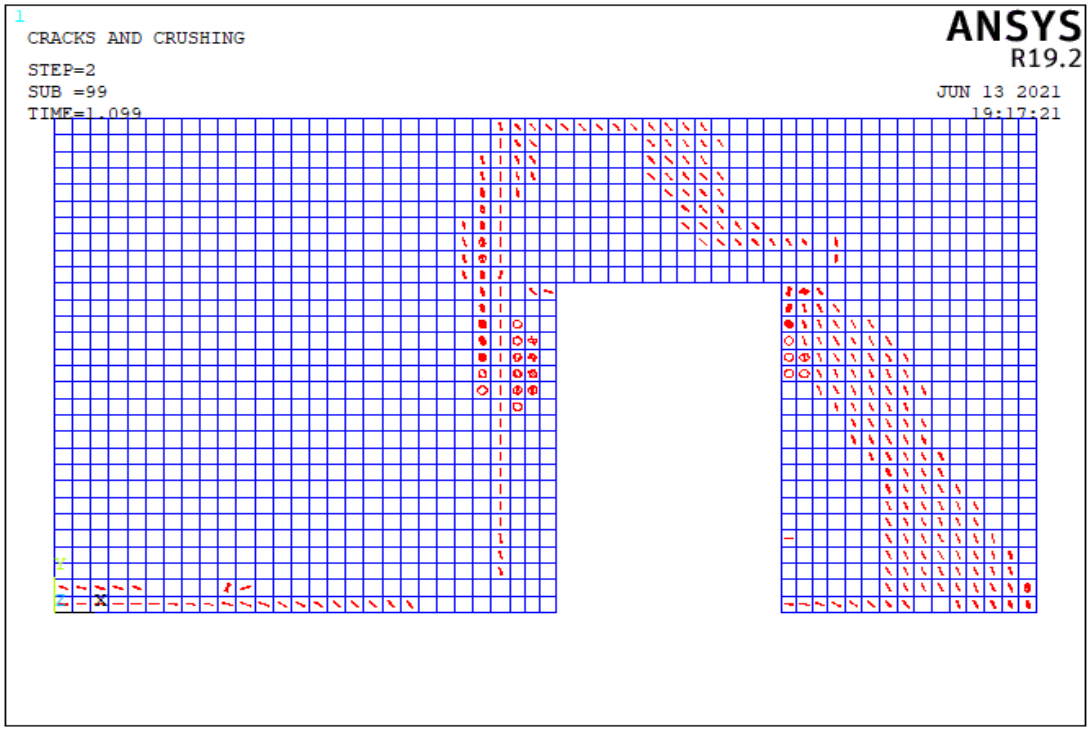

(a)

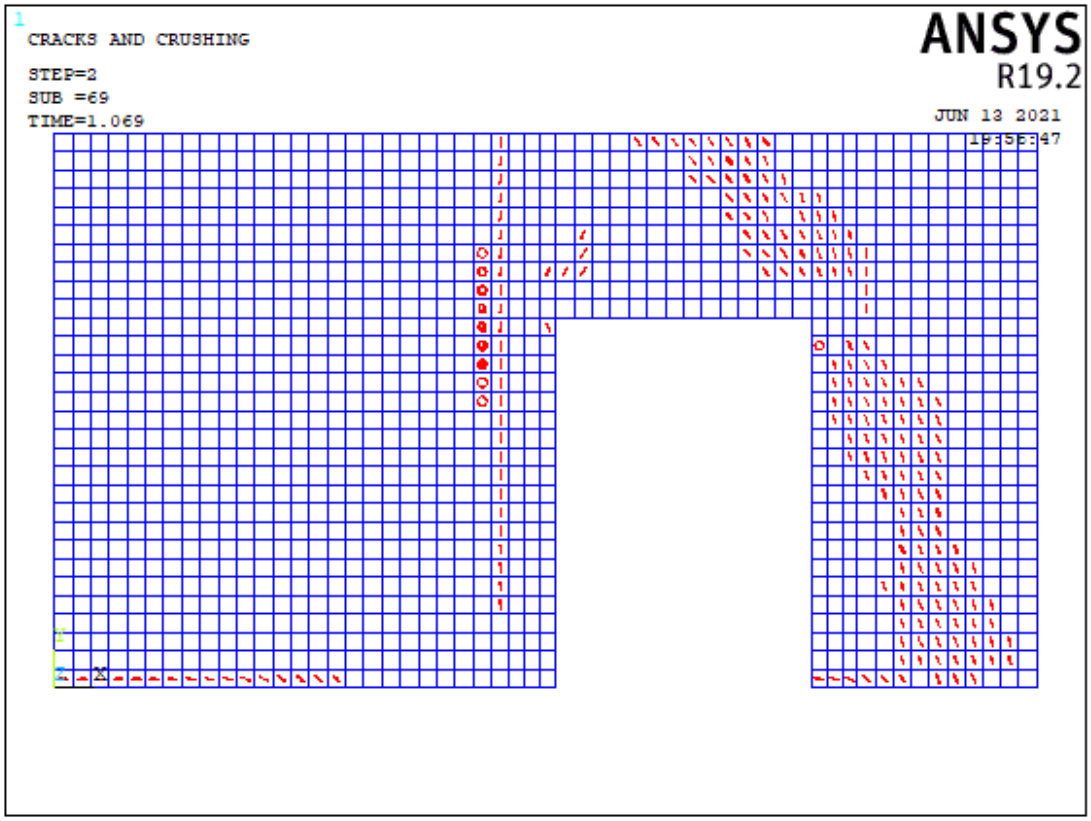

(b)

Figure 5.18. The Crack Pattern of Wall 1 Model 15 According to Compressive Strength Values of (a) 3 MPa, (b) 8 MPa

Table 5.3. Failure Patterns of Wall 1

Number of Model	Aspect ratio	fm=3 Mpa			fm=8 Mpa		
		Failure Pattern			Failure Pattern		
		Base Sliding	Rocking	Diagonal Tension	Base Sliding	Rocking	Diagonal Tension
Model 1	0.50			X			X
	1.50			X			X
Model 2	0.61			X			X
	10.00		X			X	
Model 3	1.33	X			X		
	2.00	X			X		
Model 4	1.79	X			X		
	0.37			X			X
Model 5	1.22	X			X		
	0.55			X			X
Model 6	0.49			X			X
	0.98			X			X
Model 7	0.72			X			X
	10.00		X			X	
Model 8	2.08	X			X		
	3.03	X			X		
Model 9	1.23	X			X		
	1.23	X					X
Model 10	0.85	X			X		
	0.85			X	X		
Model 11	1.23	X			X		
	0.63			X			X
Model 12	0.60			X	X		
	0.60			X			X
Model 13	4.12		X			X	
	0.93			X	X		
Model 14	2.50	X			X		
	2.50	X			X		
Model 15	1.11	X			X		
	2.46			X			X

In the TEC 2018, there are four important design cases in load-bearing walls for seismic design category 1.

- The lengths of each door or window opening should not exceed 3 meters.
- The distances between window and door openings should be greater than 1 meter.
- The distances between openings and corners of wall should not be less than 1.5 meters.
- The total opening lengths should not be greater than 40 percent of the total wall lengths.

In Table A.1, all length of doors is less than 3 m for all models and total opening percentage of walls is appropriate for TEC 2018. In models 2, 7, 8, 13, 14 and 15, the length of one of the piers is less than 1.5 m. The capacity of the wall in model 12 is much higher than the others due to length of wall. When models 1 and 6 were examined, it was observed that the in-plane capacity of URM walls increase, as the opening percentage of walls decrease. The different locations of openings can cause significantly lower capacity on walls or local failures. The pier length in model 7 is inadequate, and there are flexural cracks due to increased aspect ratio. But, model 7 has a compression diagonal strut due to the position of the opening at the corner of the wall. Although the model 9 has a similar opening percentage, its capacity is less. Because, the position of the opening in the model 9 prevent the strut action. The location and percentage of openings influence the wall failure mechanisms. Table 5.3 shows that, the diagonal tension mechanism dominates in low aspect ratio of wall. On the other hand, the rocking mechanism is predominant in high aspect ratio of wall.

5.4.1.2 Failure Modes of Wall 2

In the wall 2, there are 10 different wall models. Table A.2 shows the lengths of the walls. The crack patterns obtained from the analysis of wall models corresponding to 10 different wall models are described in this section.

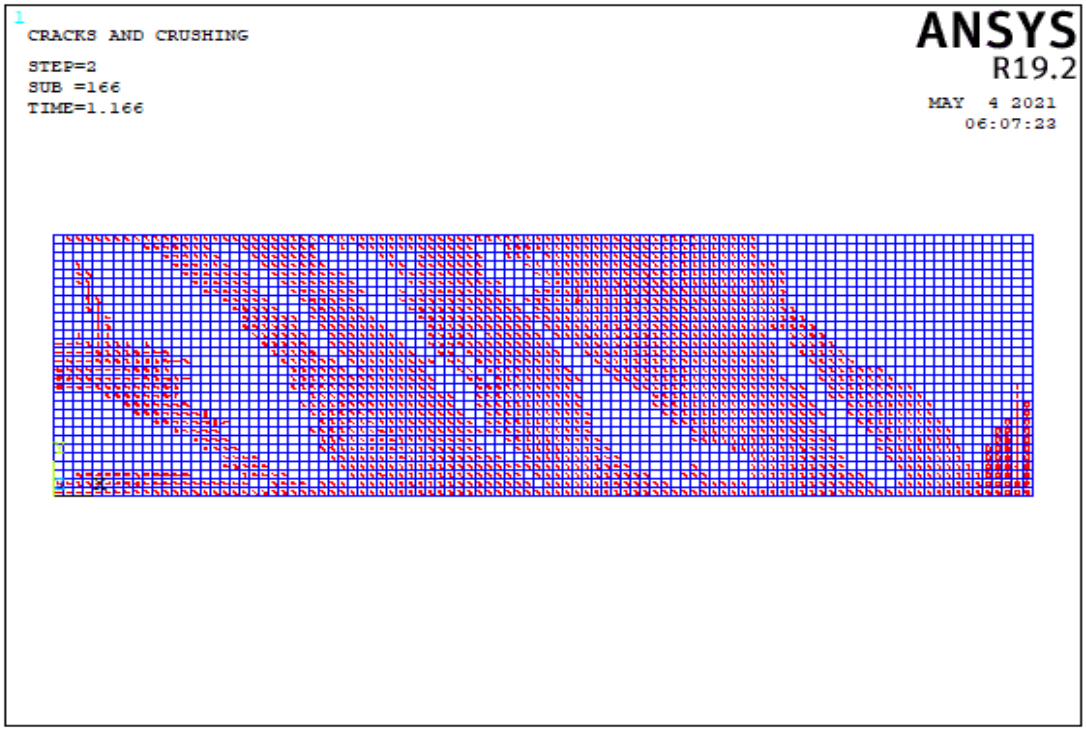

(a)

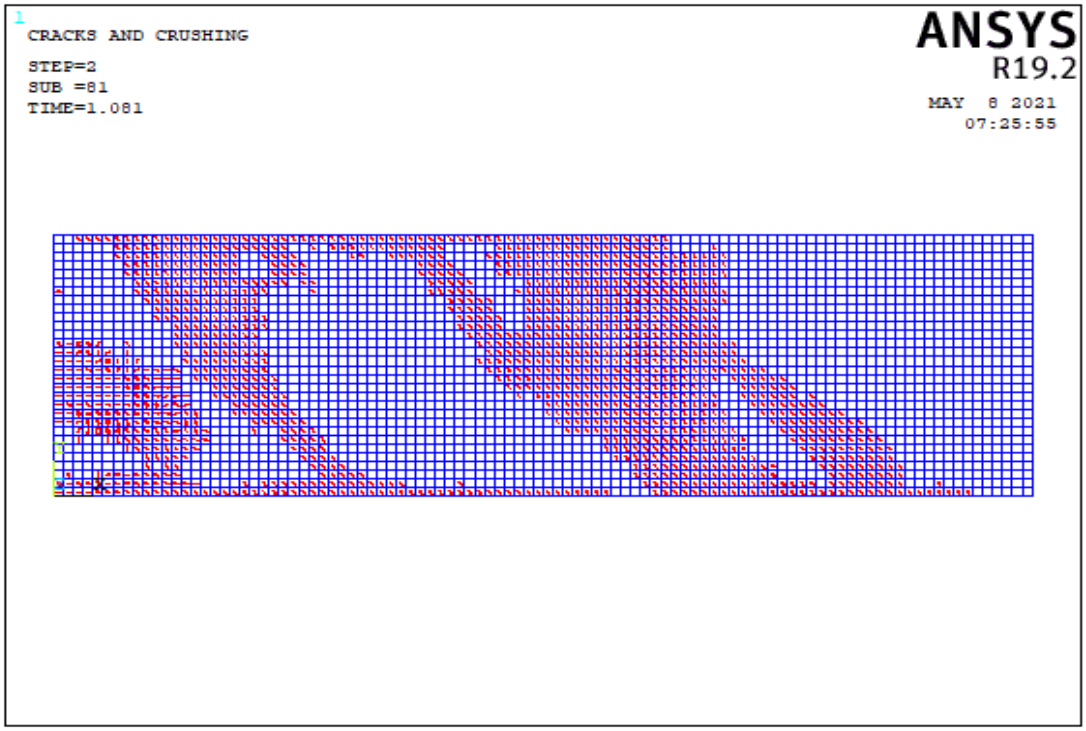

(b)

Figure 5.19. The Crack Pattern of Wall 2 Model 1 According to Compressive Strength Values of (a) 3 MPa, (b) 8 MPa

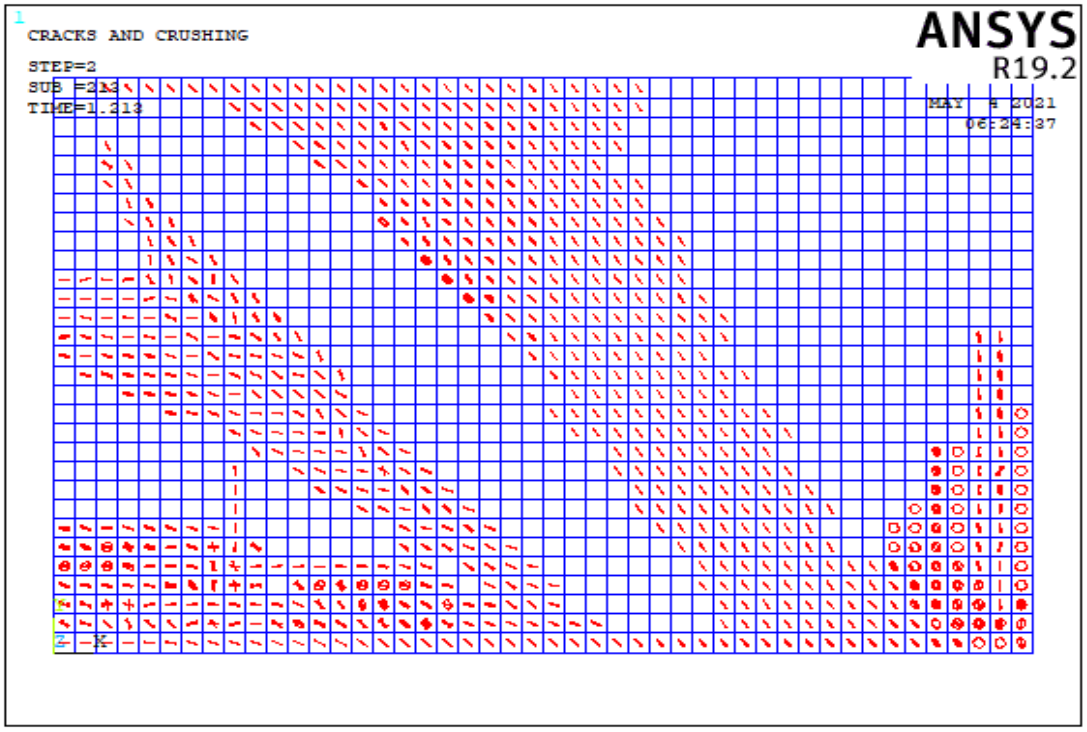

(a)

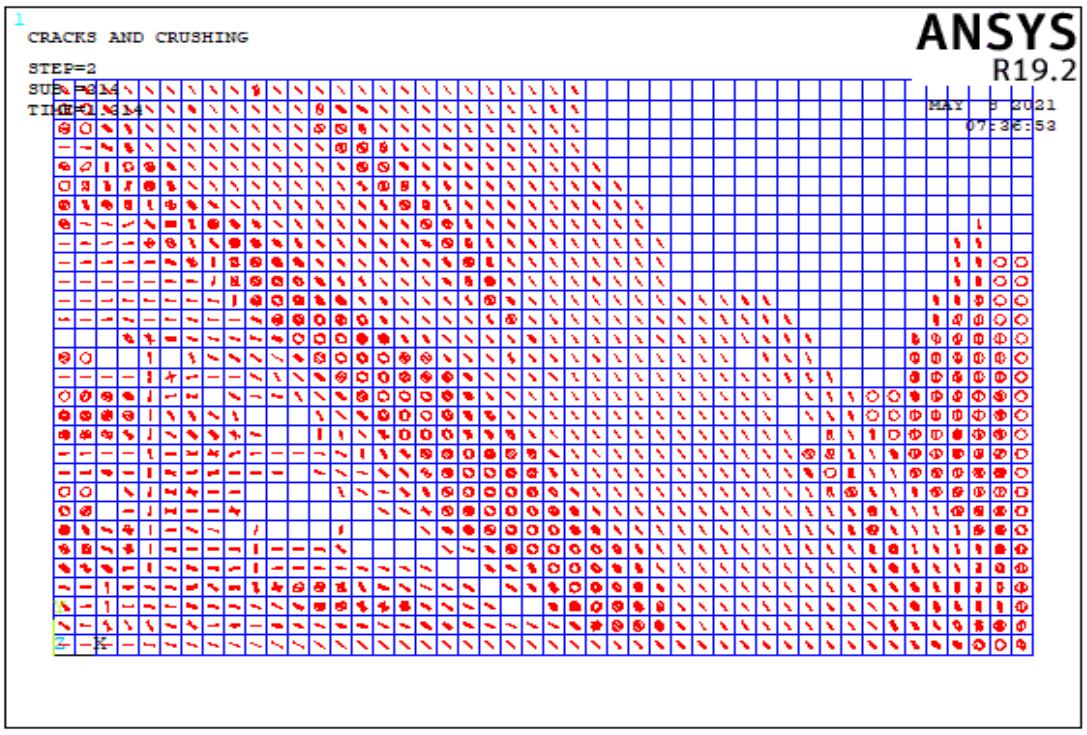

(b)

Figure 5.20. The Crack Pattern of Wall 2 Model 2 According to Compressive Strength Values of (a) 3 MPa, (b) 8 MPa

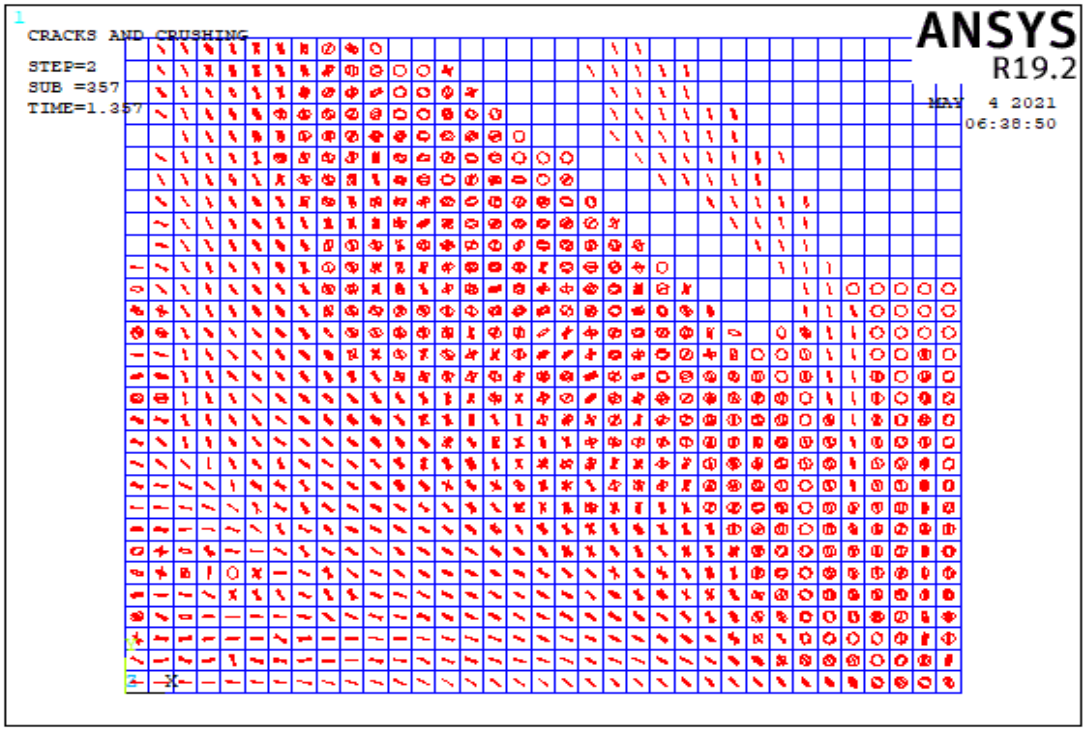

(a)

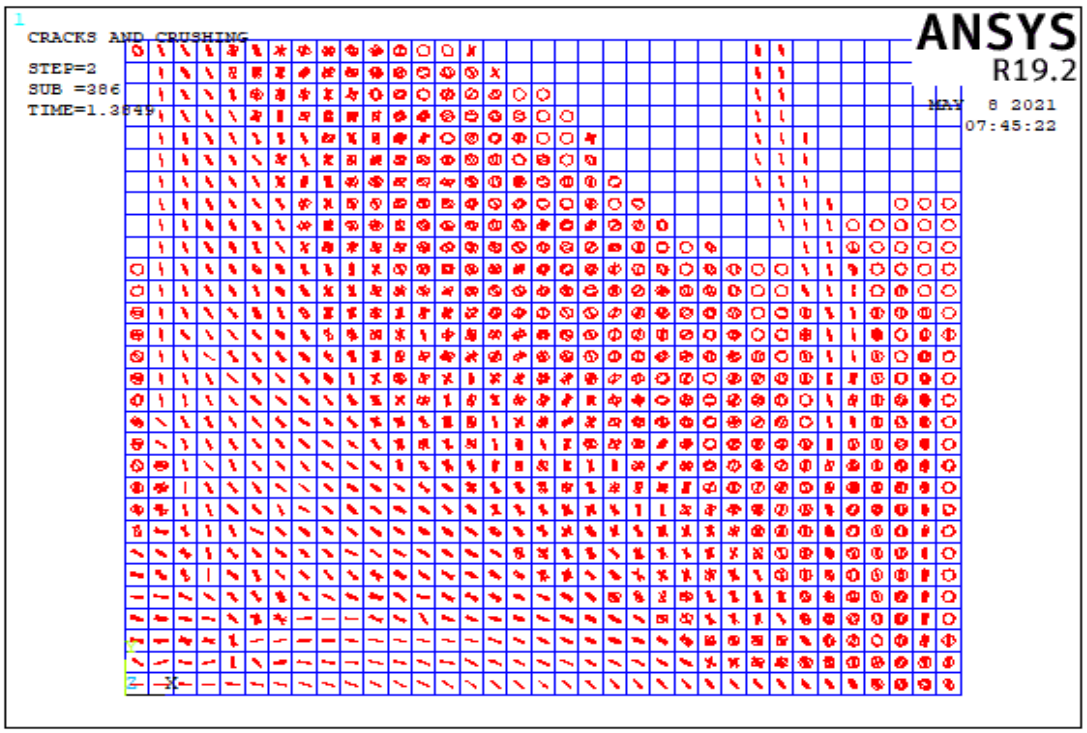

(b)

Figure 5.21. The Crack Pattern of Wall 2 Model 3 According to Compressive Strength Values of (a) 3 MPa, (b) 8 MPa

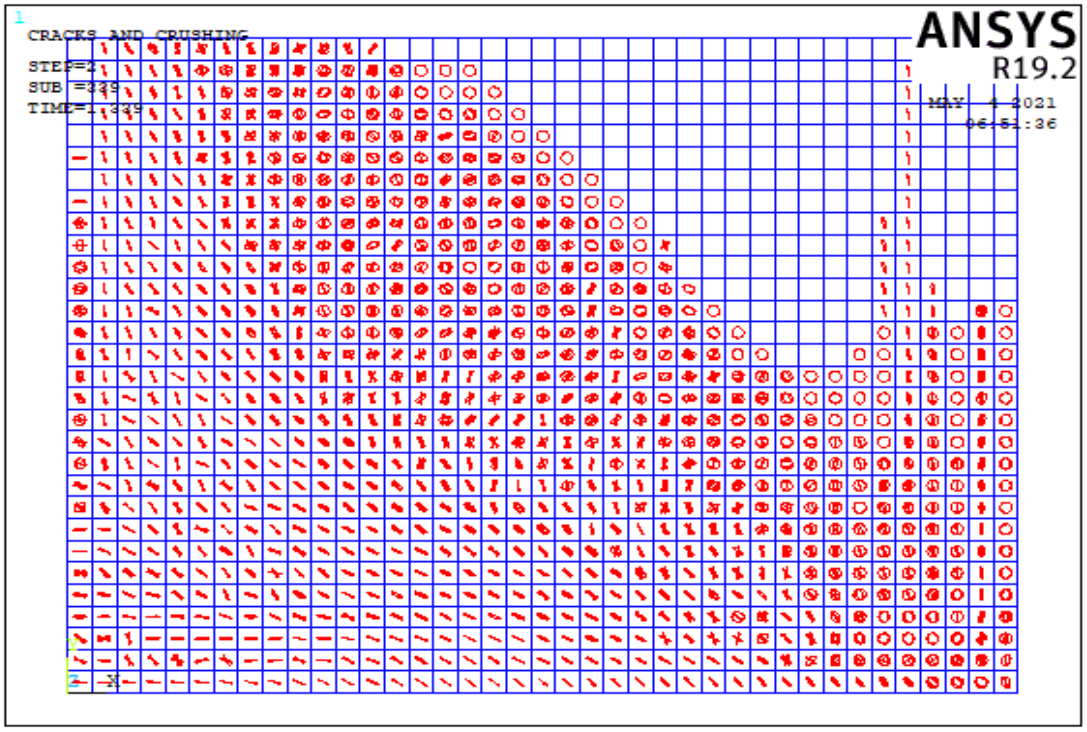

(a)

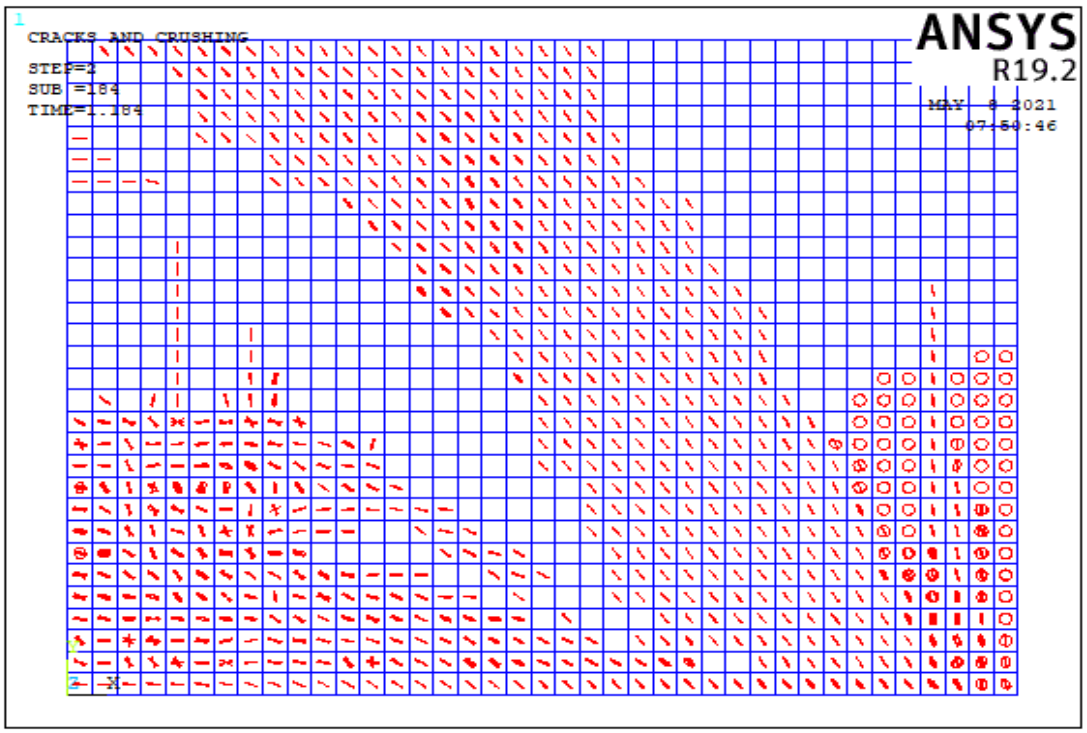

(b)

Figure 5.22. The Crack Pattern of Wall 2 Model 4 According to Compressive Strength Values of (a) 3 MPa, (b) 8 MPa

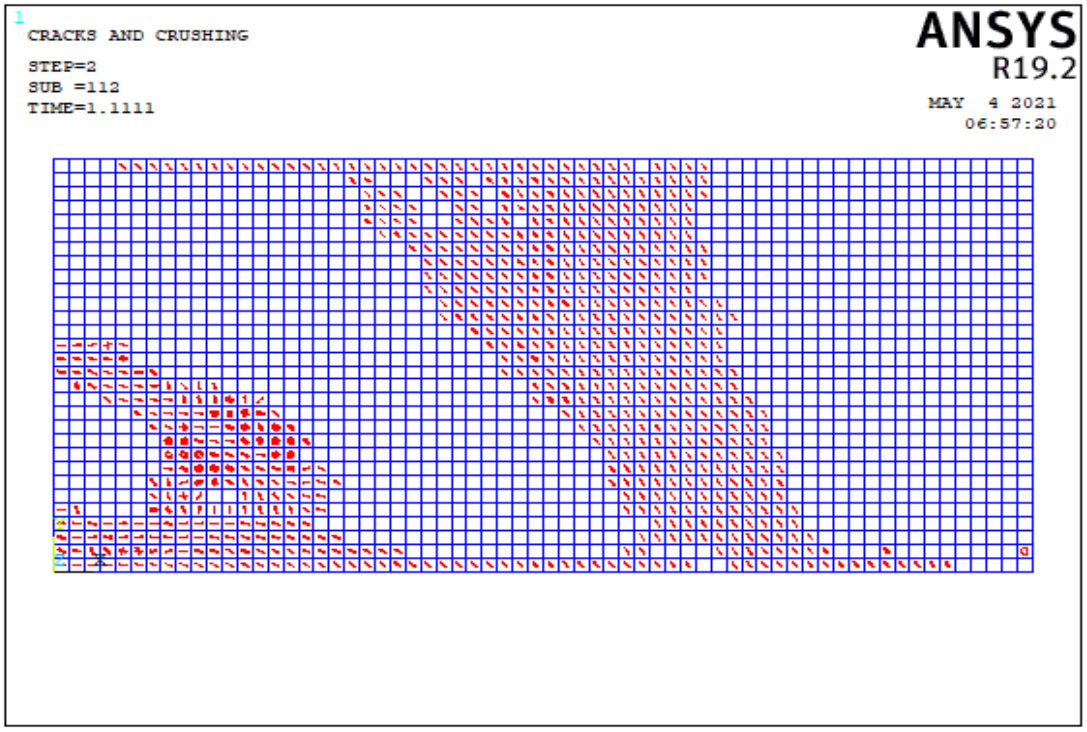

(a)

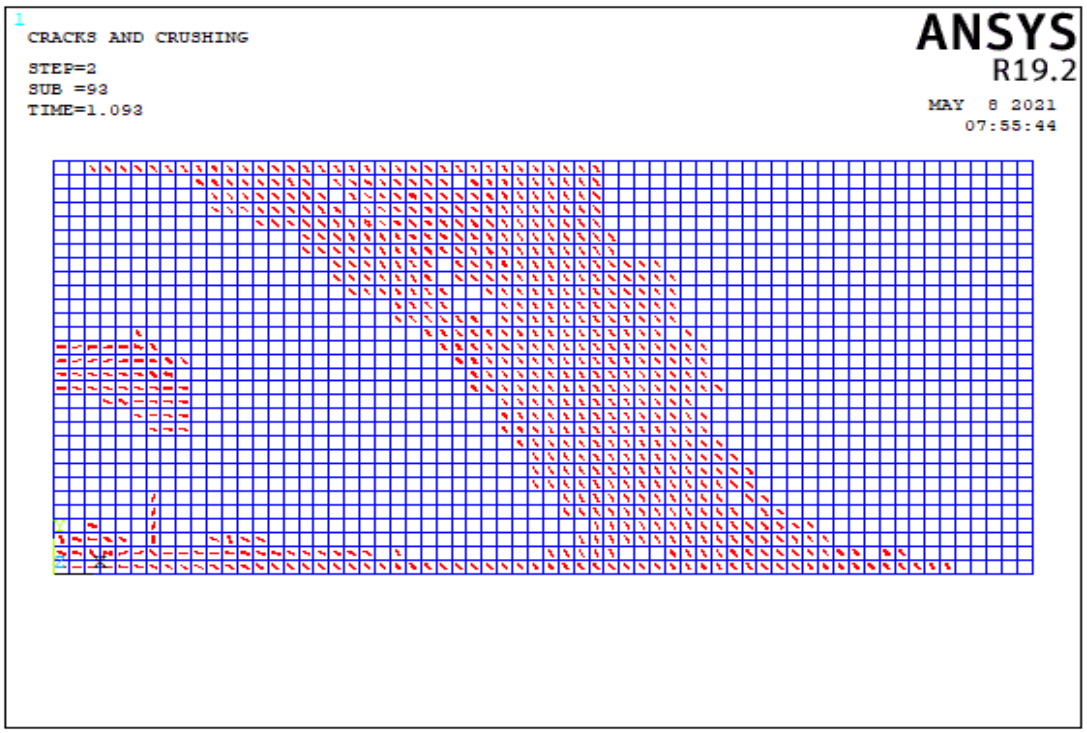

(b)

Figure 5.23. The Crack Pattern of Wall 2 Model 5 According to Compressive Strength Values of (a) 3 MPa, (b) 8 MPa

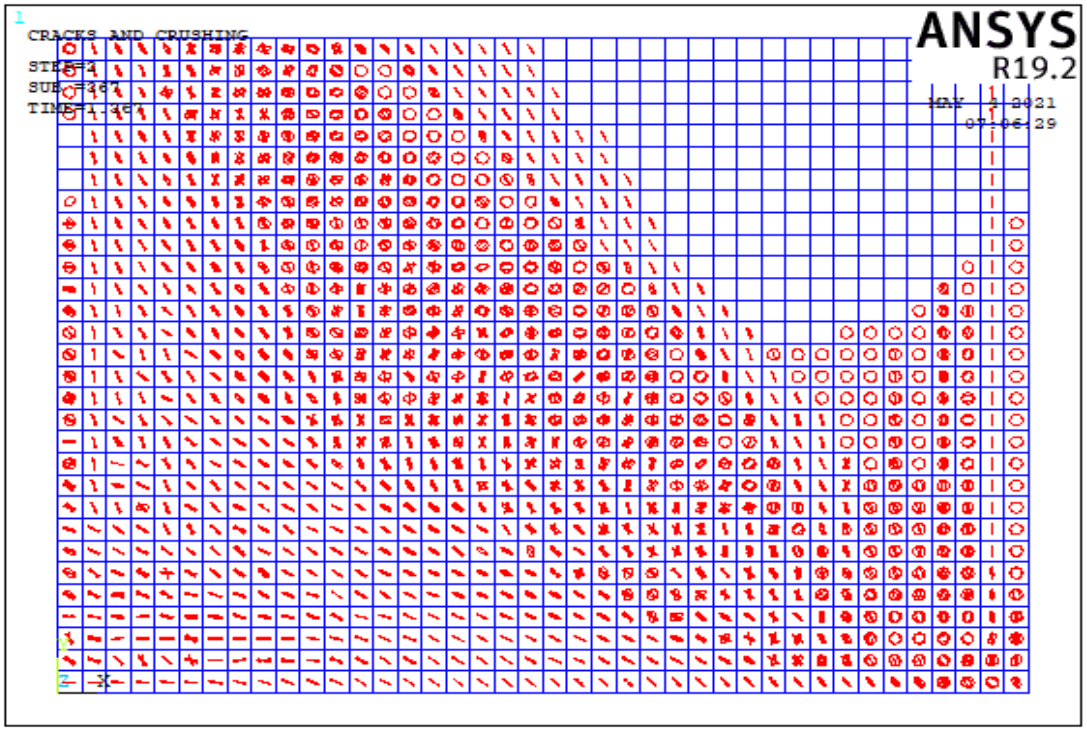

(a)

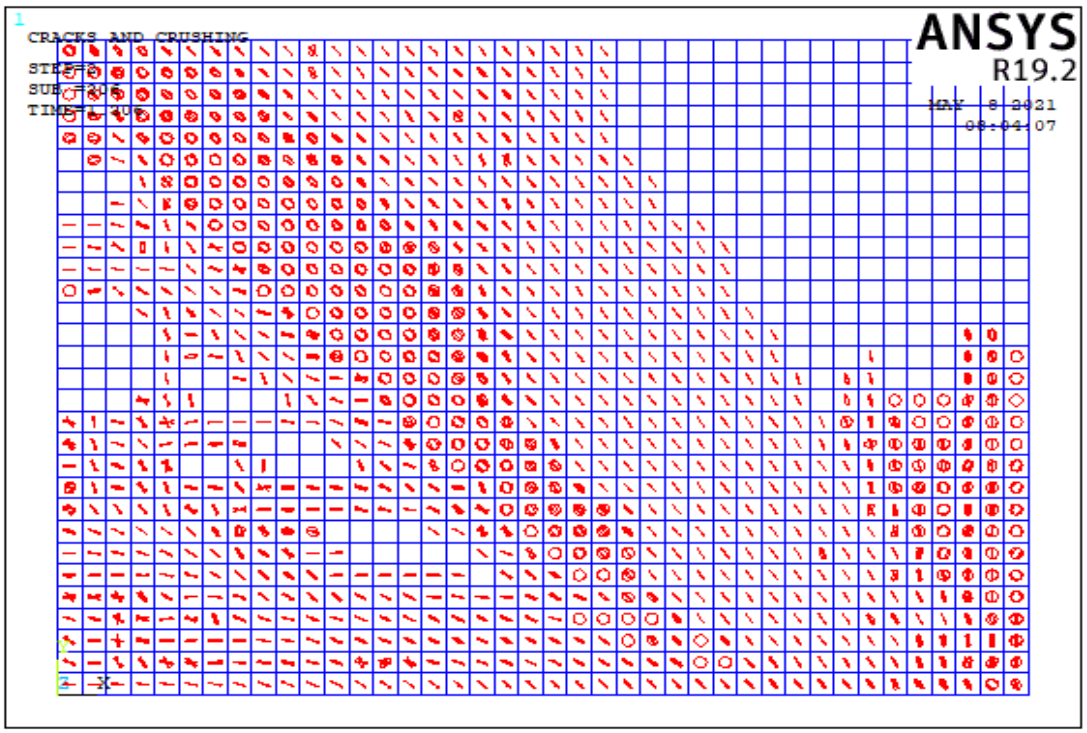

(b)

Figure 5.24. The Crack Pattern of Wall 2 Model 6 According to Compressive Strength Values of (a) 3 MPa, (b) 8 MPa

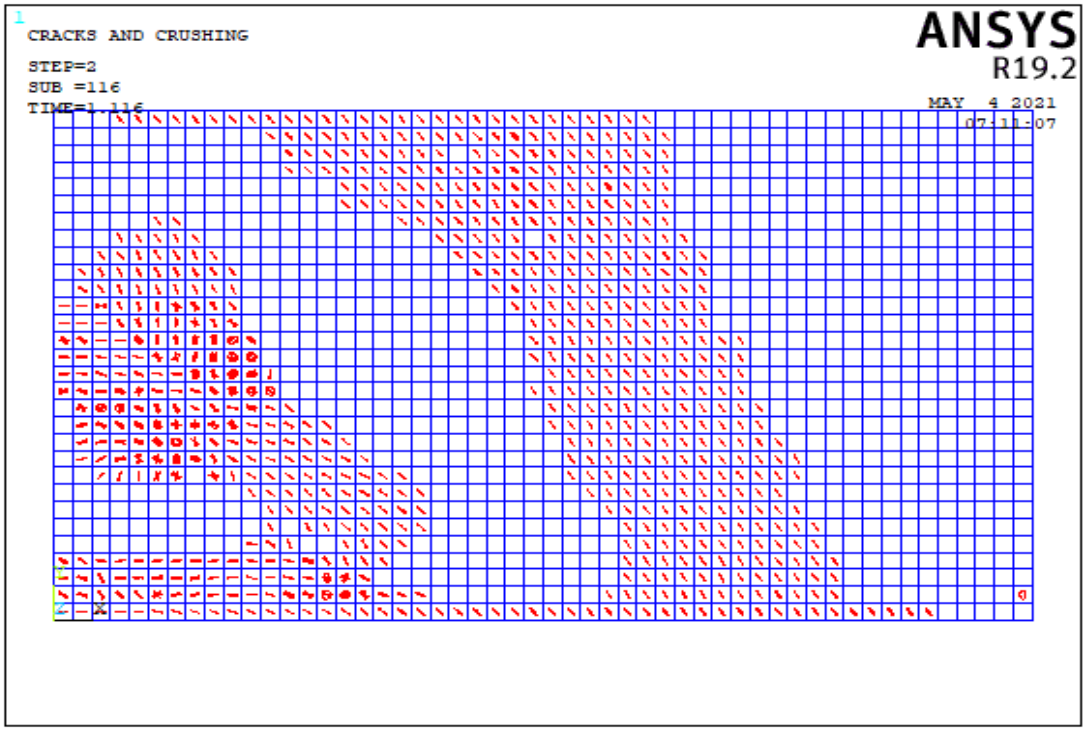

(a)

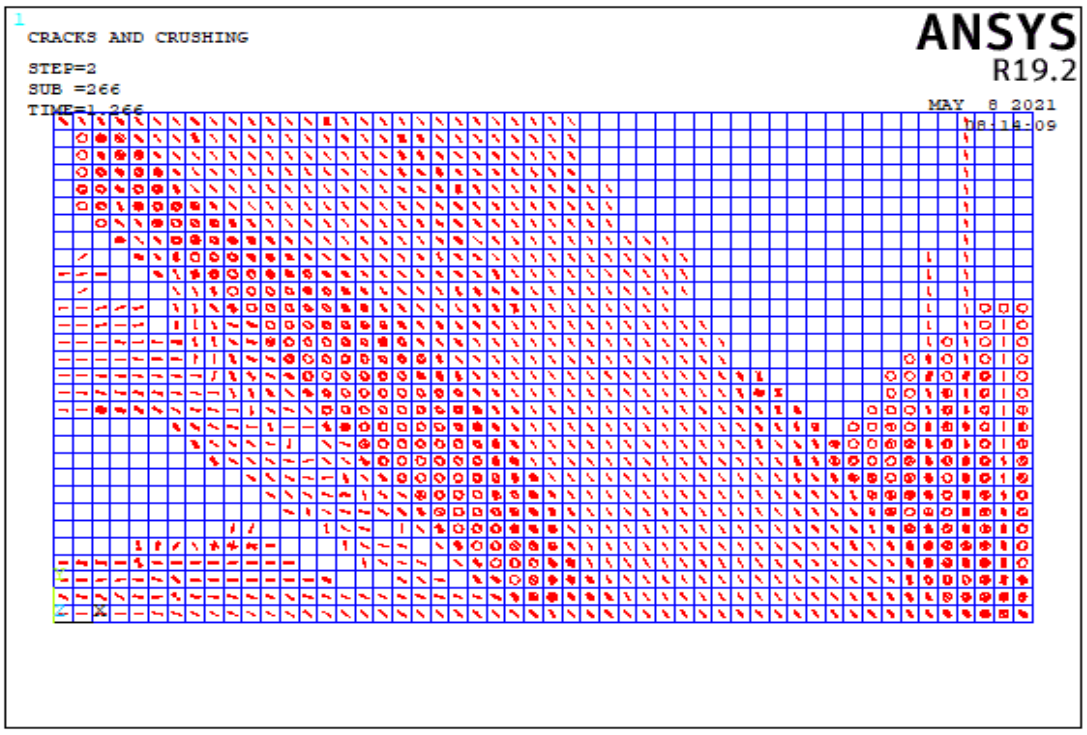

(b)

Figure 5.25. The Crack Pattern of Wall 2 Model 7 According to Compressive Strength Values of (a) 3 MPa, (b) 8 MPa

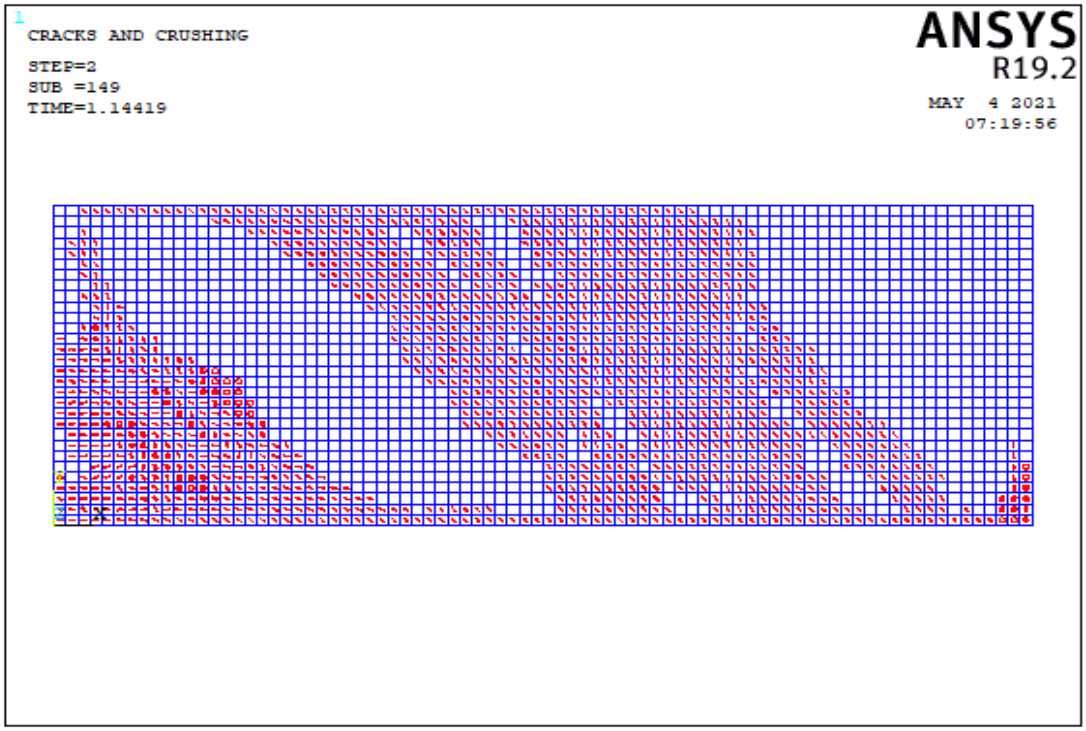

(a)

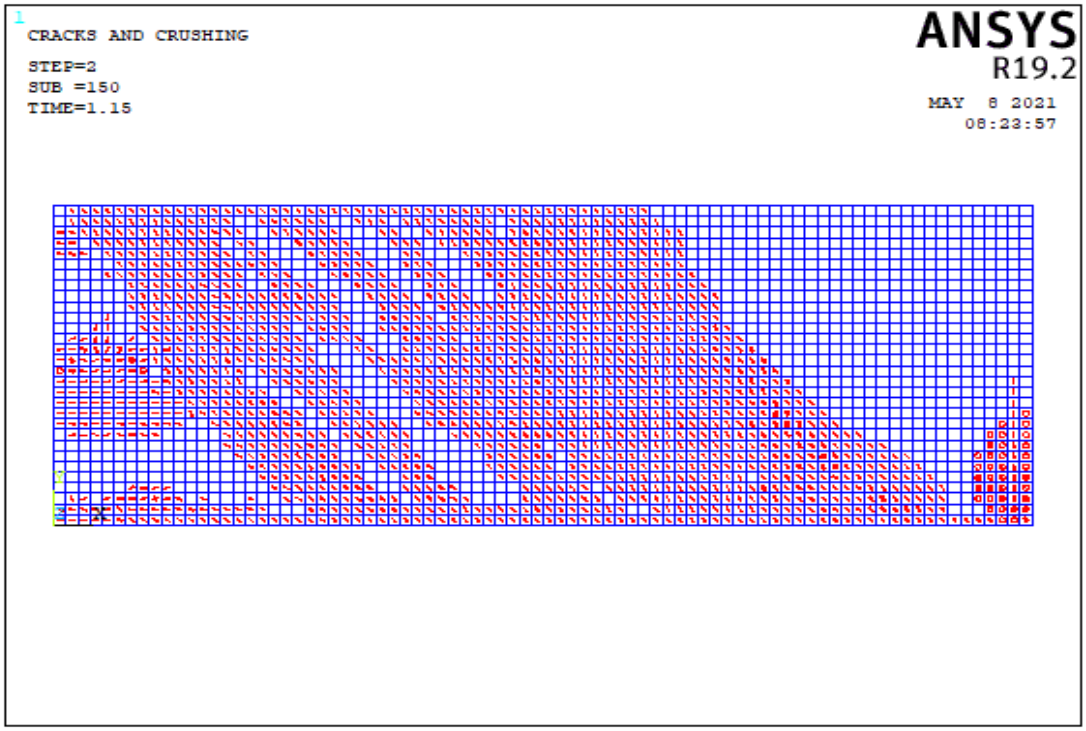

(b)

Figure 5.26. The Crack Pattern of Wall 2 Model 8 According to Compressive Strength Values of (a) 3 MPa, (b) 8 MPa

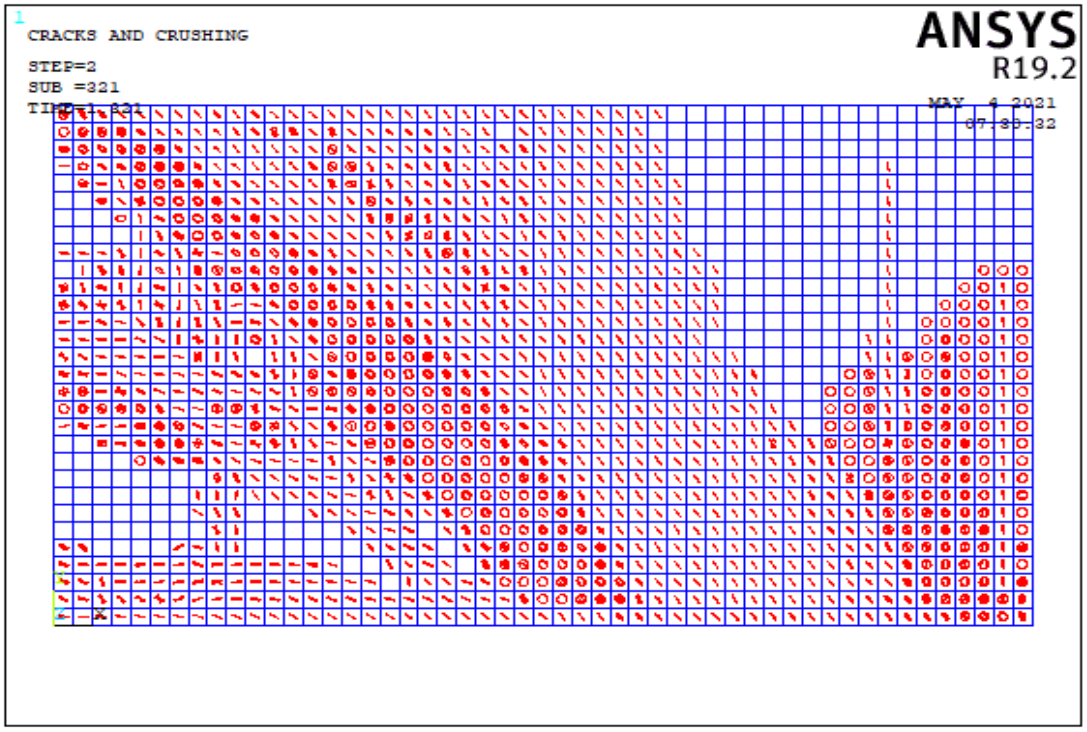

(a)

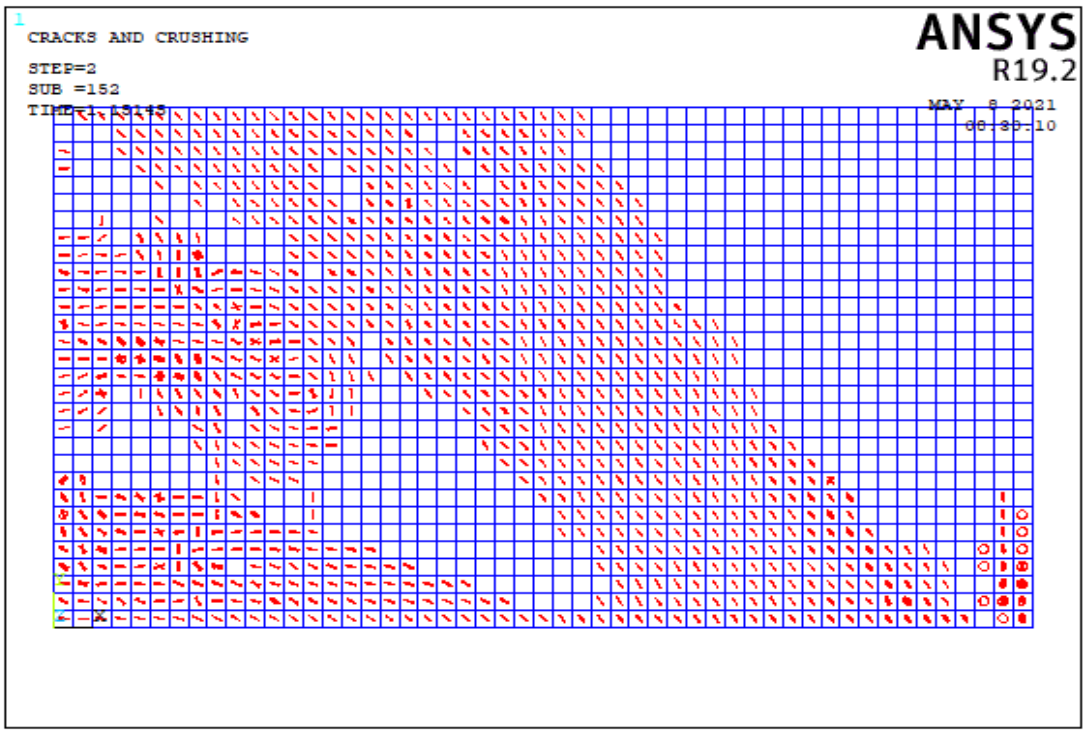

(b)

Figure 5.27. The Crack Pattern of Wall 2 Model 9 According to Compressive Strength Values of (a) 3 MPa, (b) 8 MPa

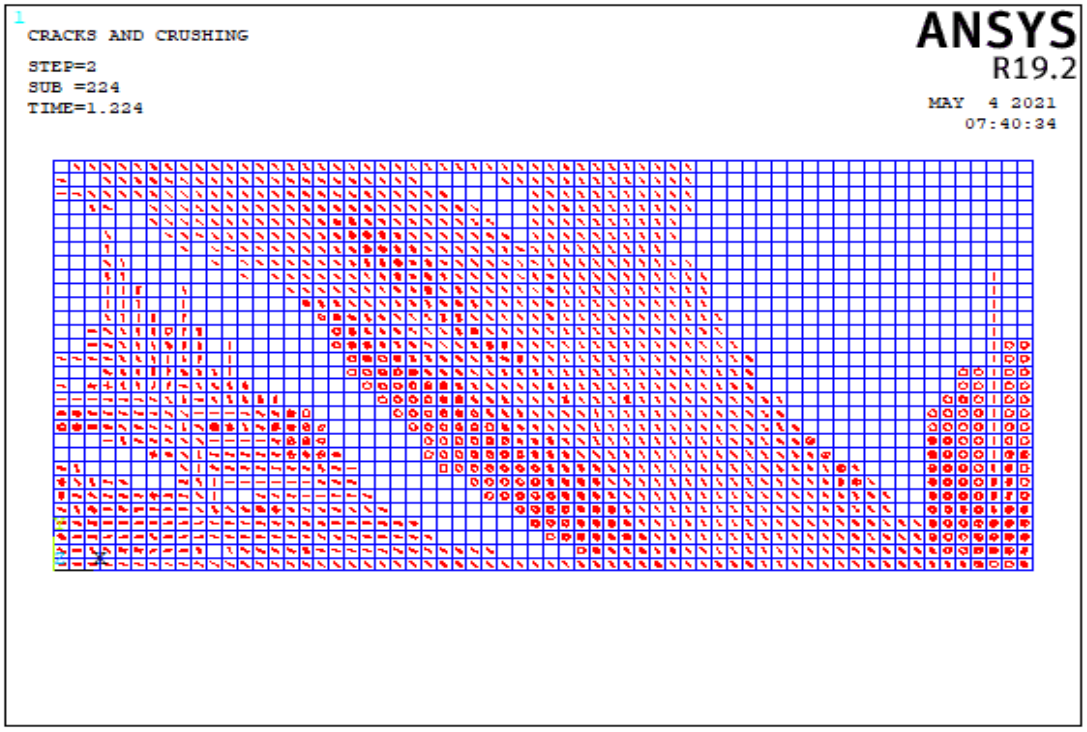

(a)

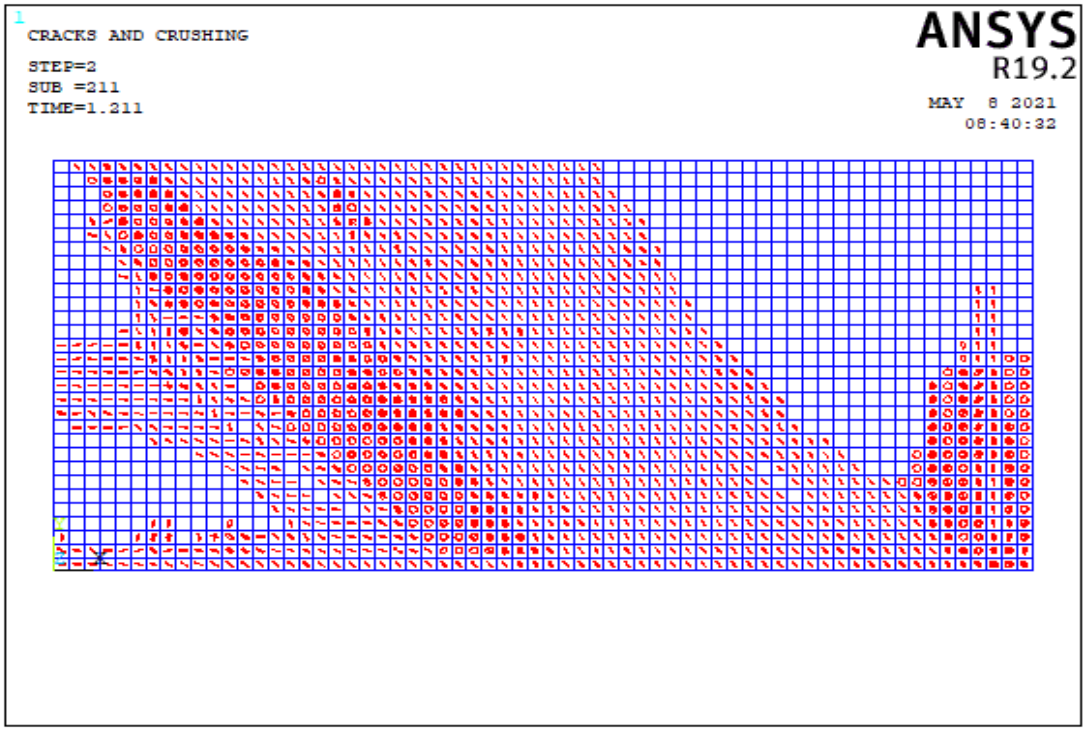

(b)

Figure 5.28. The Crack Pattern of Wall 2 Model 10 According to Compressive Strength Values of (a) 3 MPa, (b) 8 MPa

Table 5.4. Failure Patterns of Wall 2

Number of Model	Aspect ratio	fm=3 Mpa			fm=8 Mpa		
		Failure Pattern			Failure Pattern		
		Base Sliding	Rocking	Diagonal Tension	Base Sliding	Rocking	Diagonal Tension
Model 1	0.30			X			X
Model 2	0.66			X			X
Model 3	0.88			X			X
Model 4	0.77			X			X
Model 5	0.47			X			X
Model 6	0.76			X			X
Model 7	0.58			X			X
Model 8	0.37			X			X
Model 9	0.59			X			X
Model 10	0.47			X			X

In these models, the failure type of all piers is predominantly diagonal tension mechanism, but there are other types of failure modes. As the length of the solid walls increase, the strength of walls improve, although their ductility decrease. Several tension struts may be included in longer walls, such as model 1. Table 5.4 shows that, the diagonal tension mechanism dominates in walls with low aspect ratio.

5.4.1.3 Failure Modes of Wall 3

In the wall 3, there are 10 different wall models. The impact of a single window opening was studied in these models of wall 3. Table A.3 shows the lengths of the walls. As seen in Figure 5.3, each pier is designated from left to right. The crack patterns obtained from the analysis of wall models corresponding to 10 different wall models are described in this section.

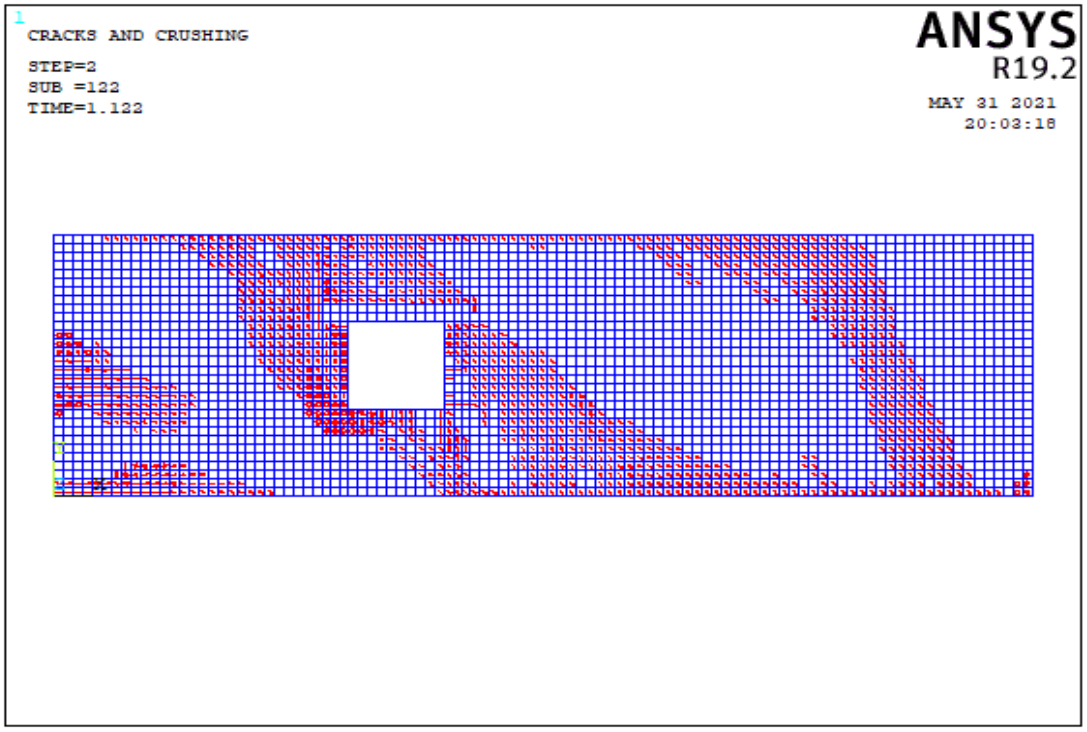

(a)

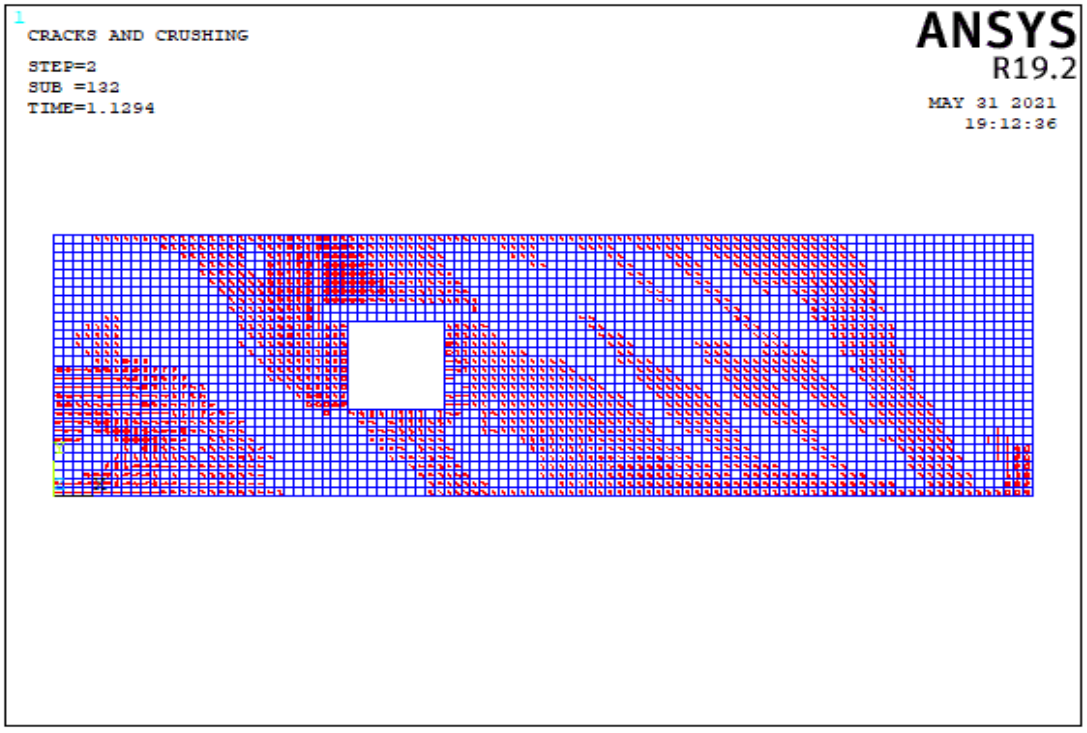

(b)

Figure 5.29. The Crack Pattern of Wall 3 Model 1 According to Compressive Strength Values of (a) 3 MPa, (b) 8 MPa

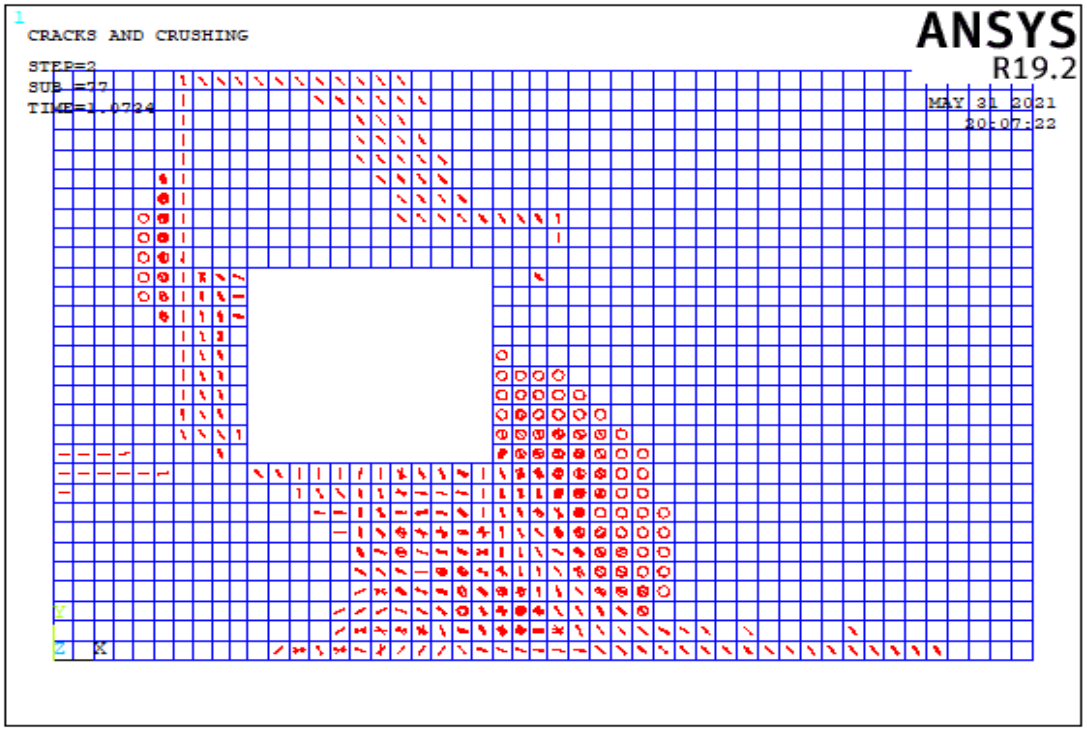

(a)

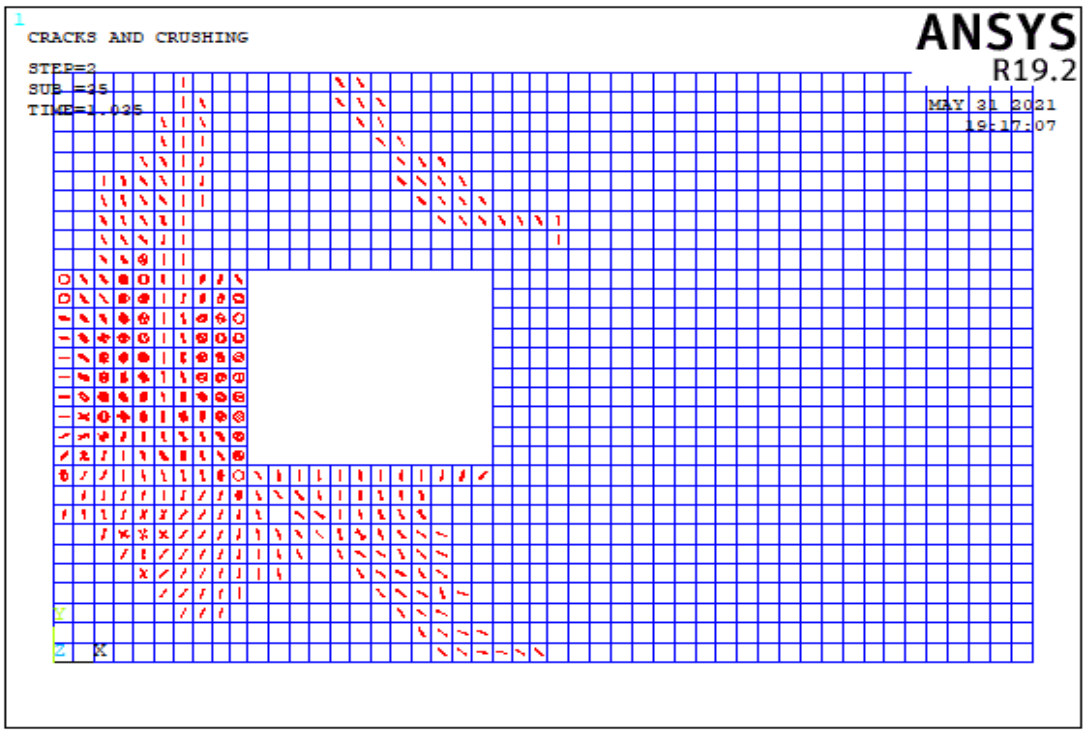

(b)

Figure 5.30. The Crack Pattern of Wall 3 Model 2 According to Compressive Strength Values of (a) 3 MPa, (b) 8 MPa

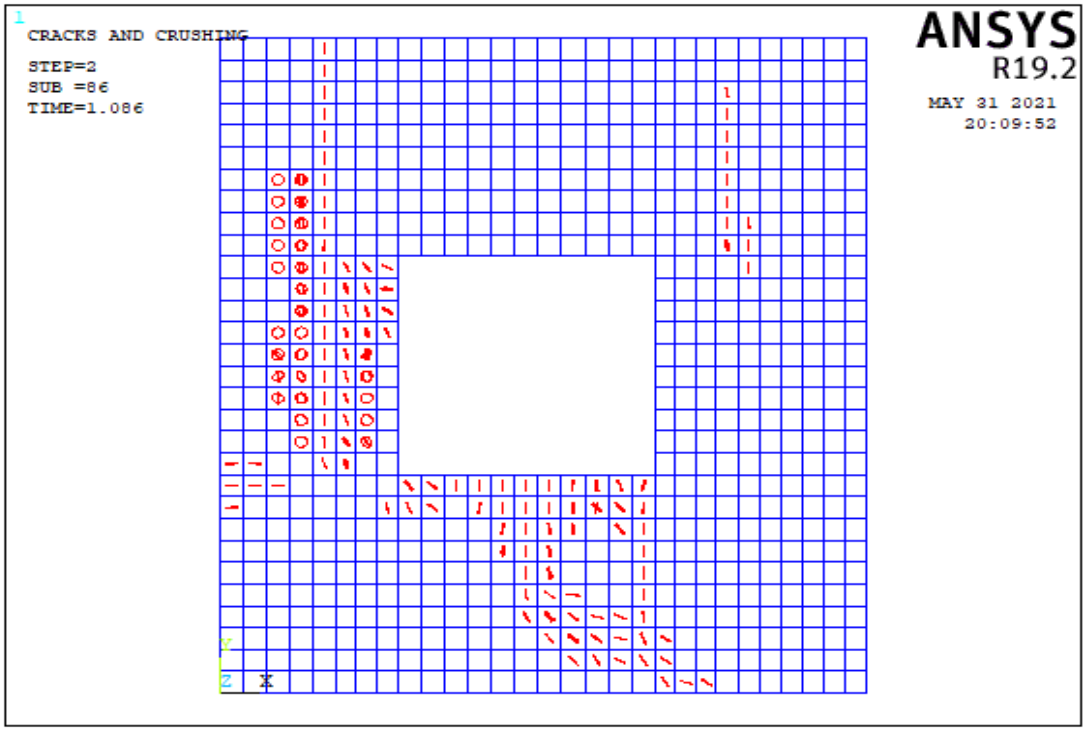

(a)

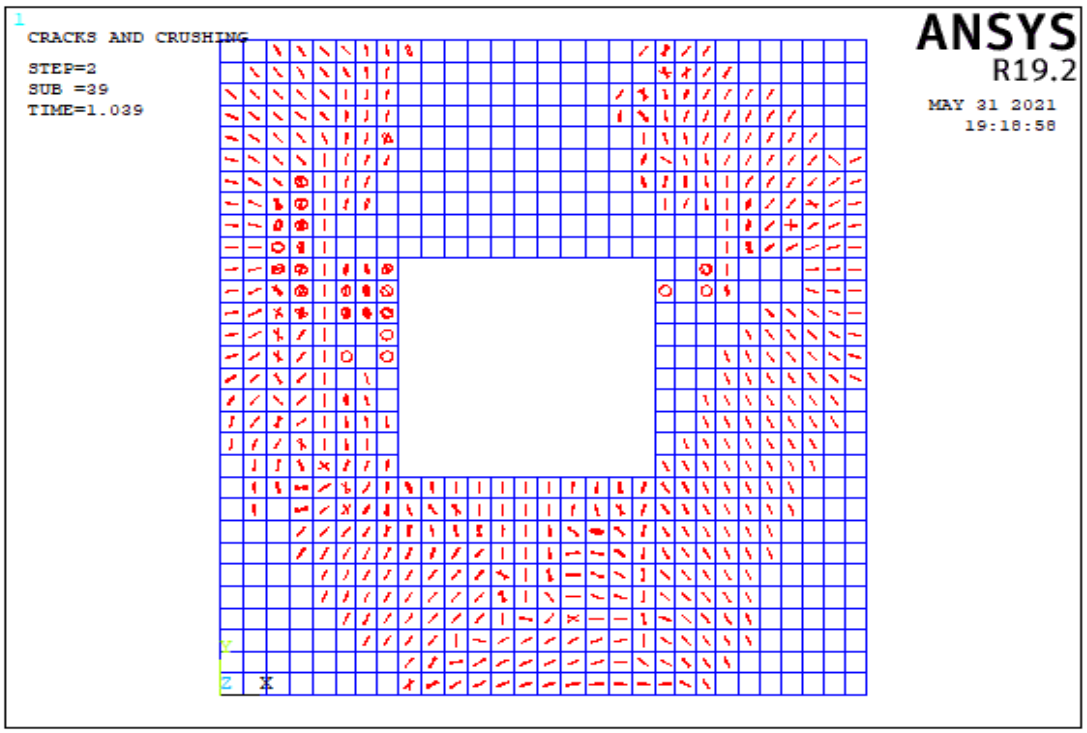

(b)

Figure 5.31. The Crack Pattern of Wall 3 Model 3 According to Compressive Strength Values of (a) 3 MPa, (b) 8 MPa

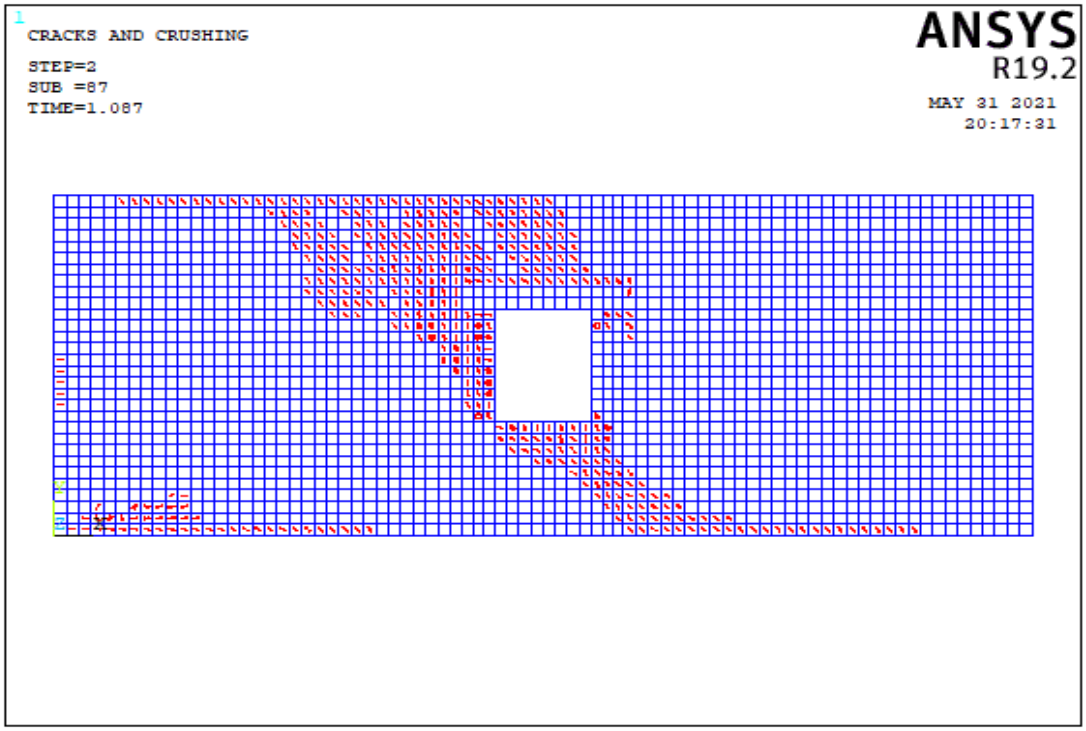

(a)

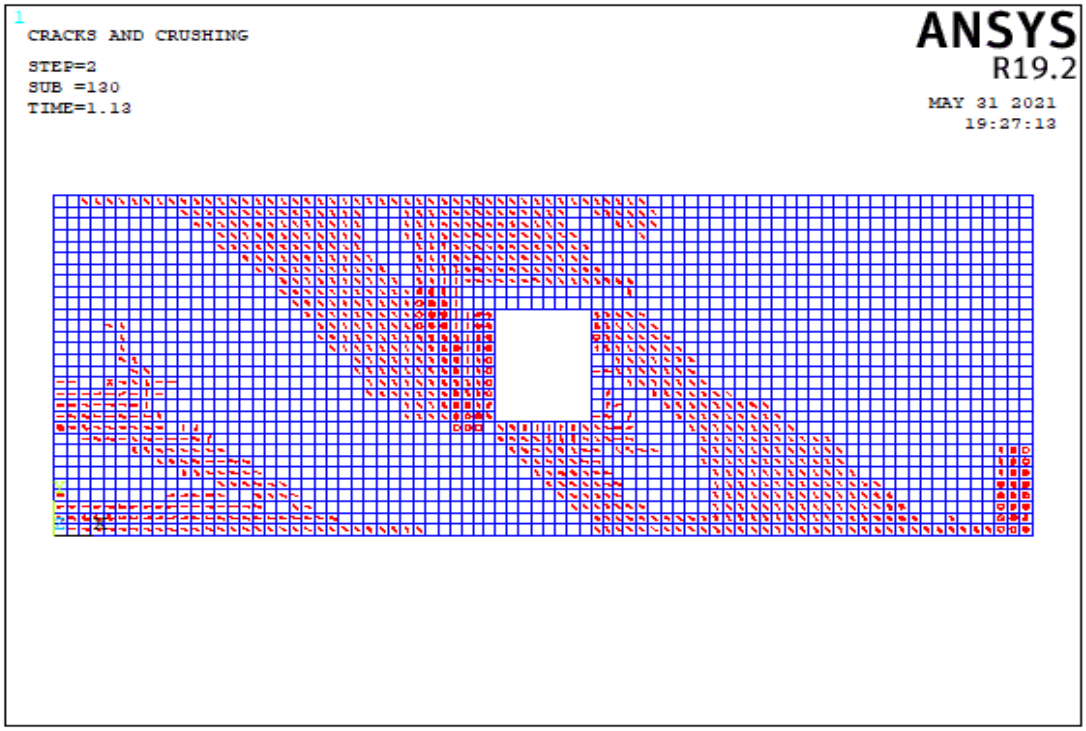

(b)

Figure 5.32. The Crack Pattern of Wall 3 Model 4 According to Compressive Strength Values of (a) 3 MPa, (b) 8 MPa

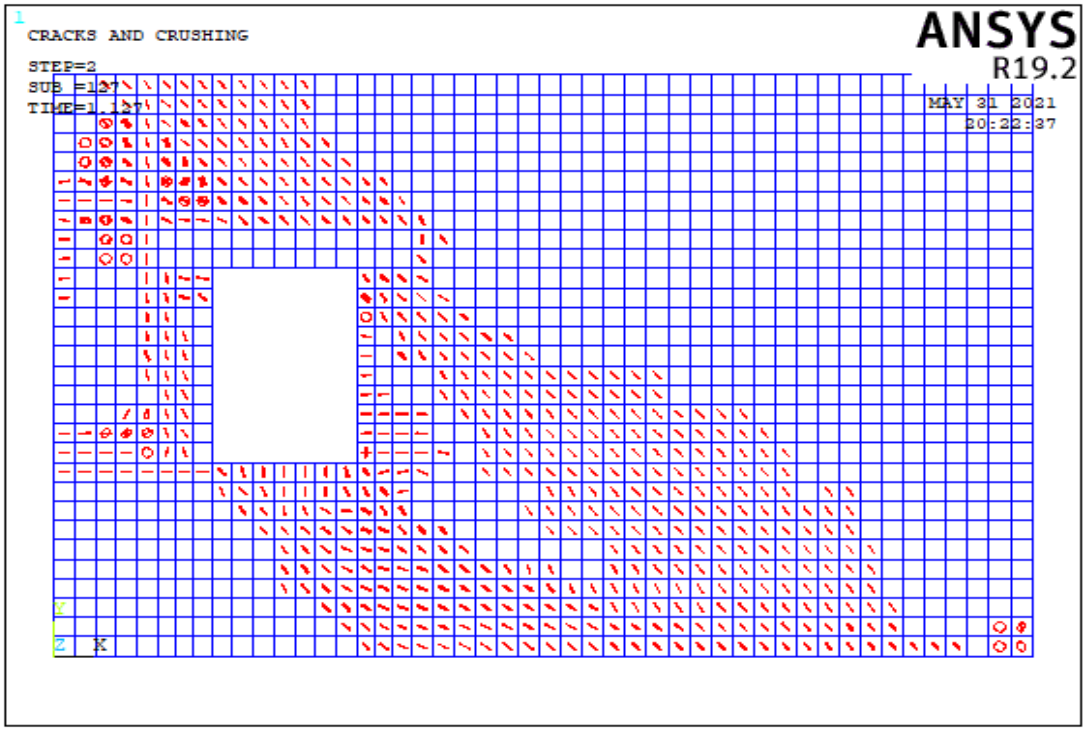

(a)

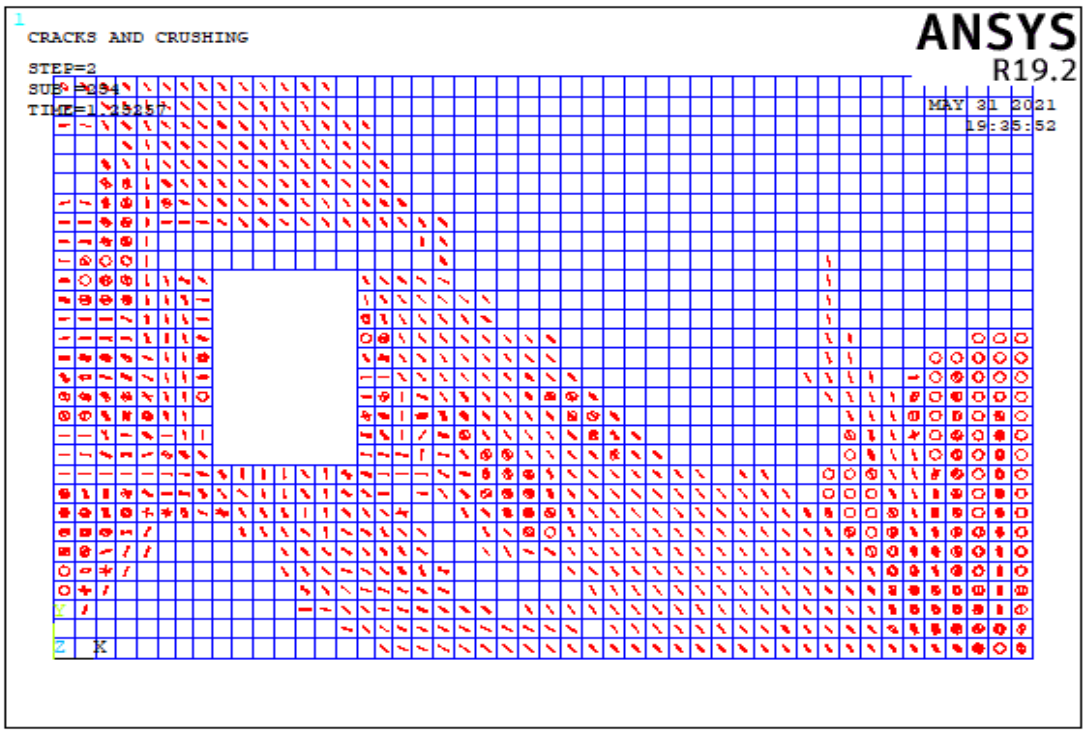

(b)

Figure 5.33. The Crack Pattern of Wall 3 Model 5 According to Compressive Strength Values of (a) 3 MPa, (b) 8 MPa

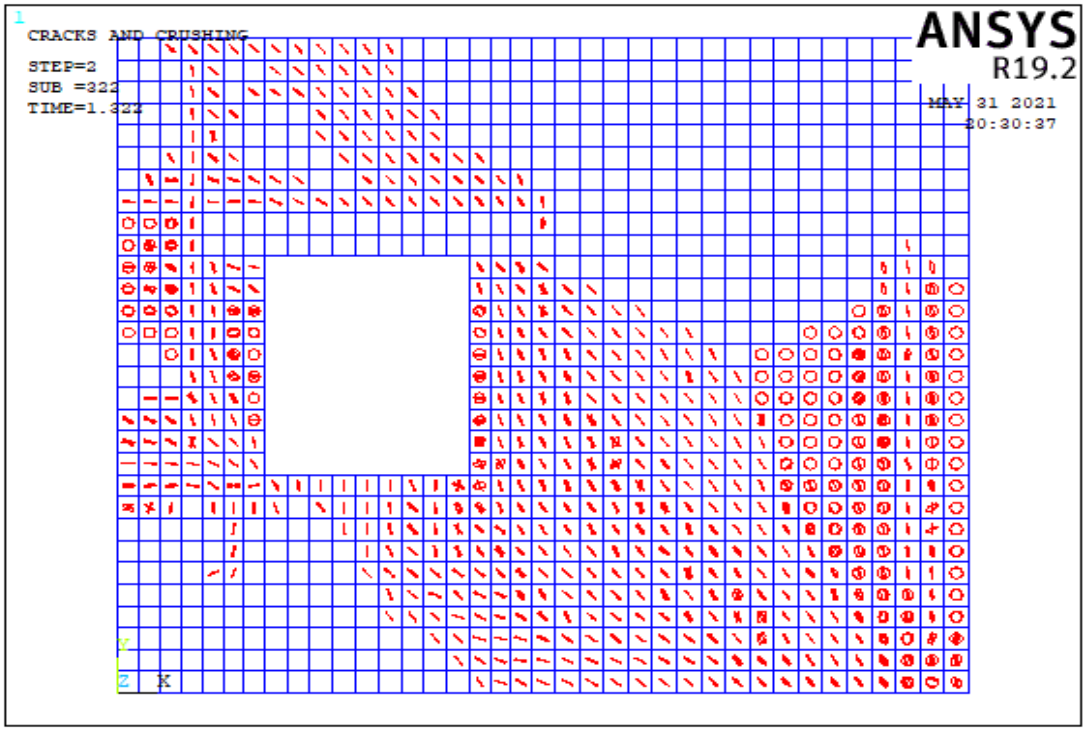

(a)

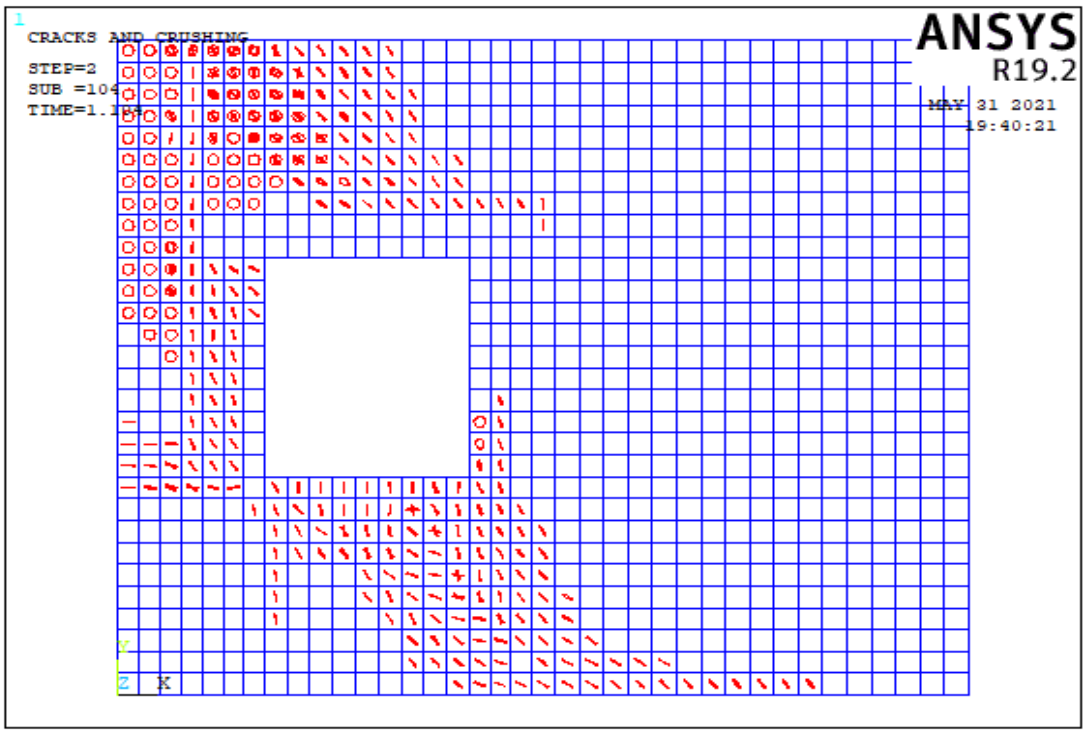

(b)

Figure 5.34. The Crack Pattern of Wall 3 Model 6 According to Compressive Strength Values of (a) 3 MPa, (b) 8 MPa

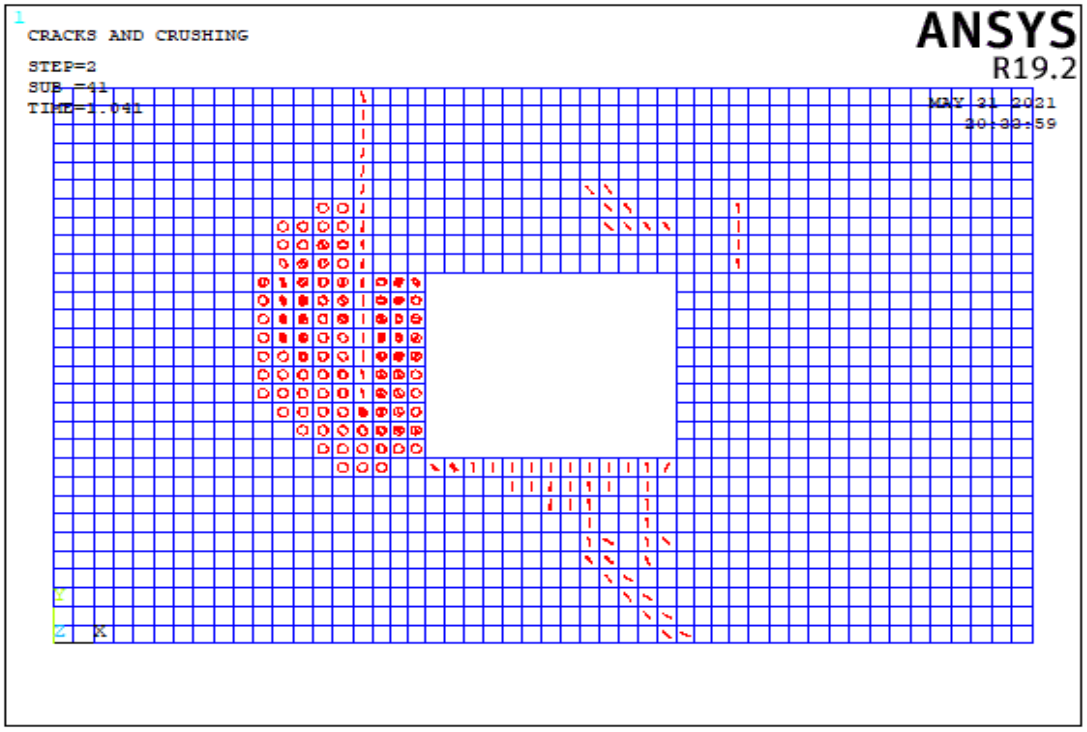

(a)

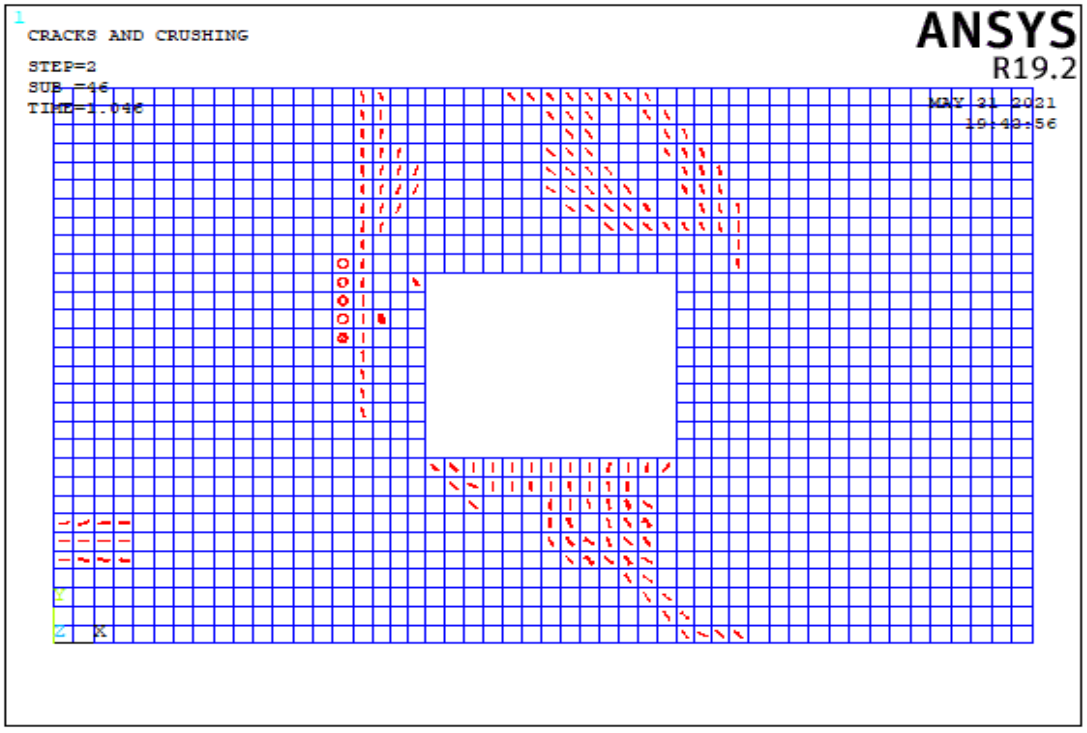

(b)

Figure 5.35. The Crack Pattern of Wall 3 Model 7 According to Compressive Strength Values of (a) 3 MPa, (b) 8 MPa

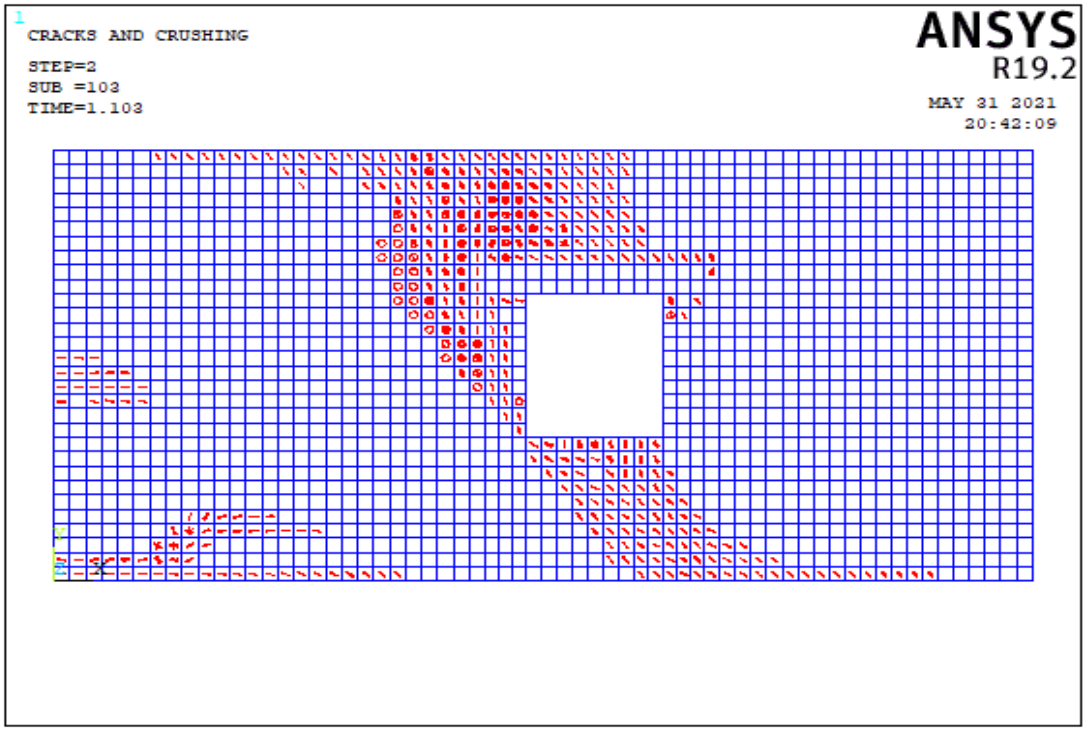

(a)

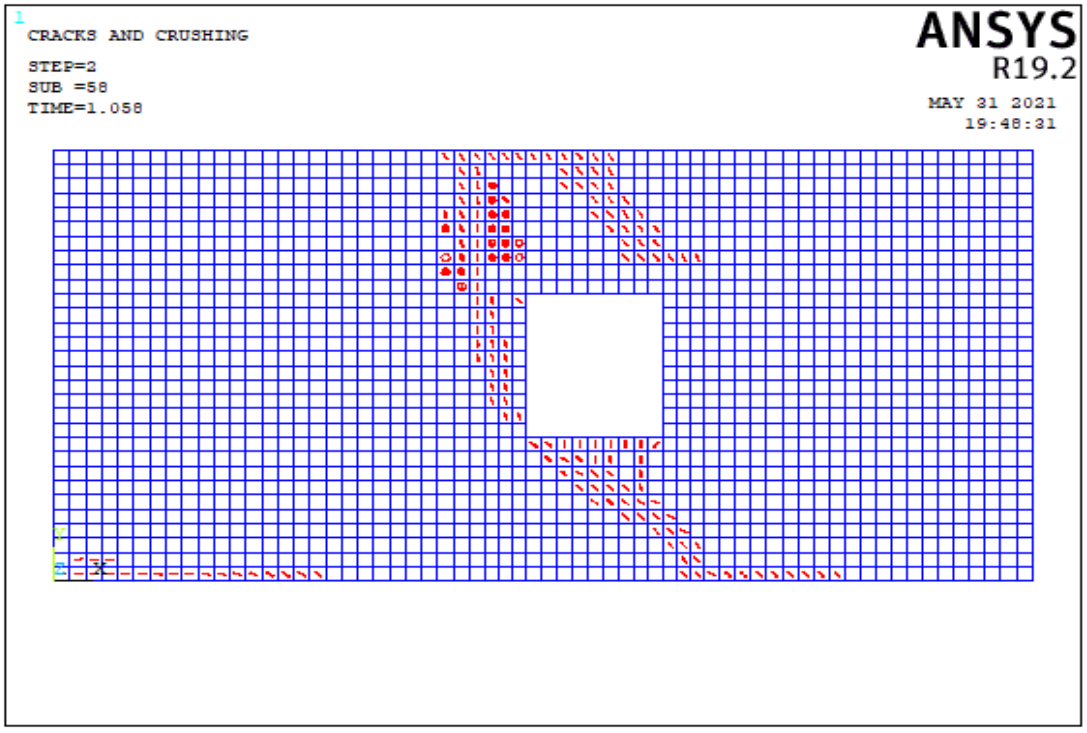

(b)

Figure 5.36. The Crack Pattern of Wall 3 Model 8 According to Compressive Strength Values of (a) 3 MPa, (b) 8 MPa

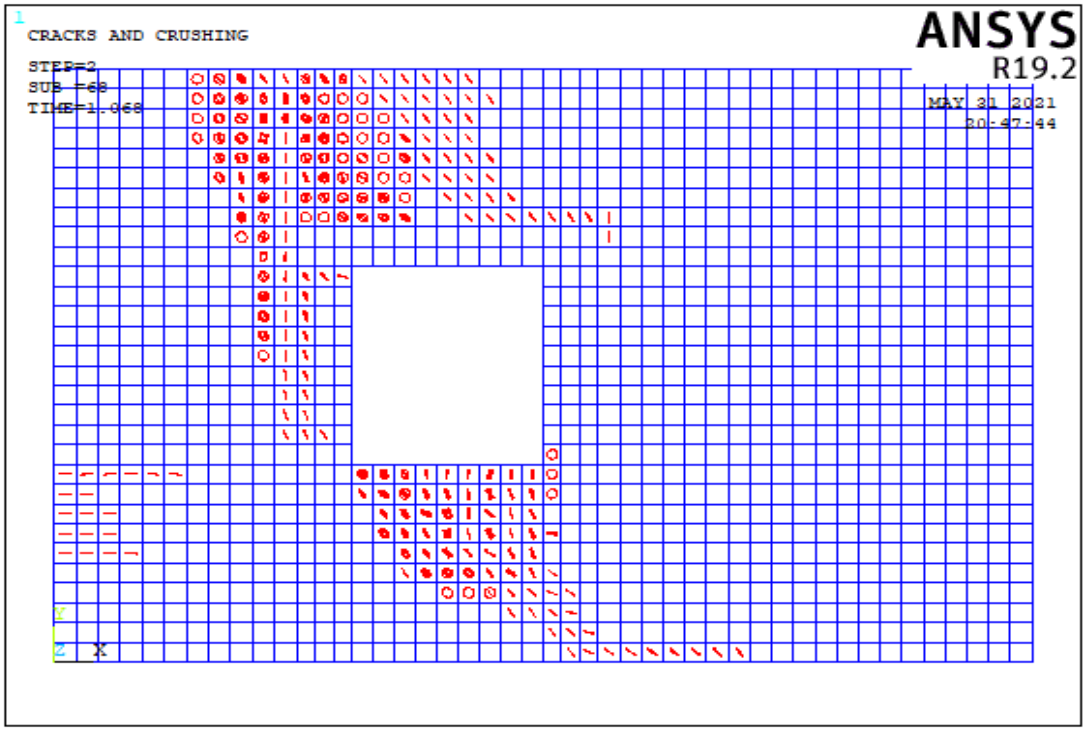

(a)

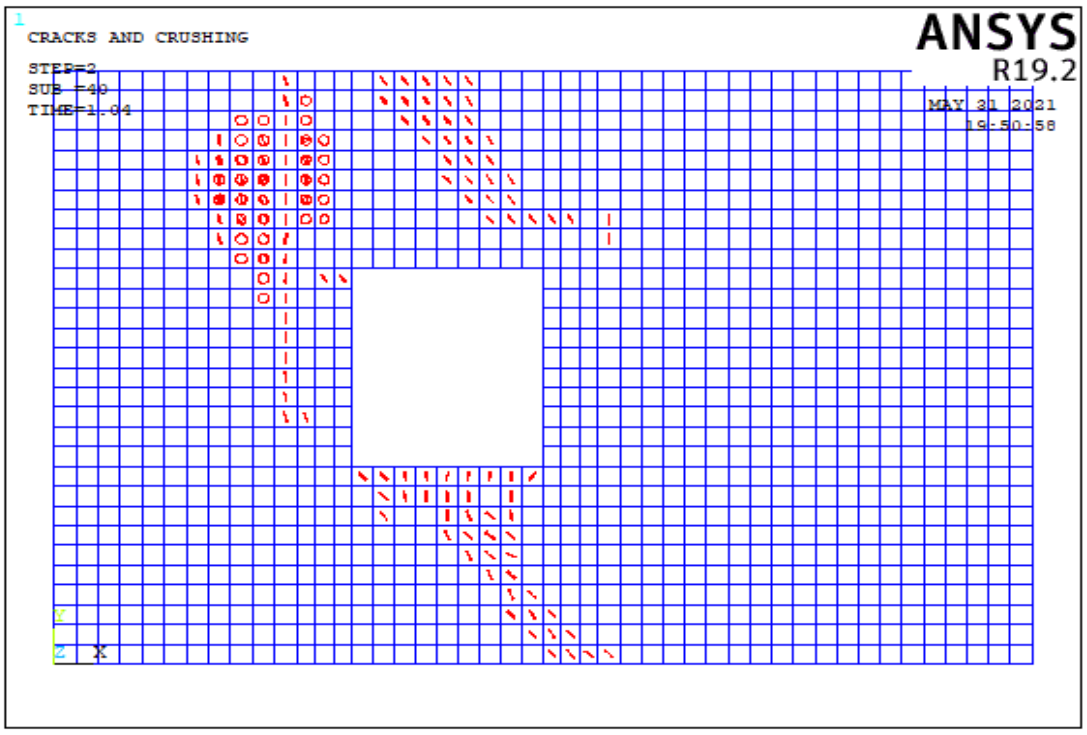

(b)

Figure 5.37. The Crack Pattern of Wall 3 Model 9 According to Compressive Strength Values of (a) 3 MPa, (b) 8 MPa

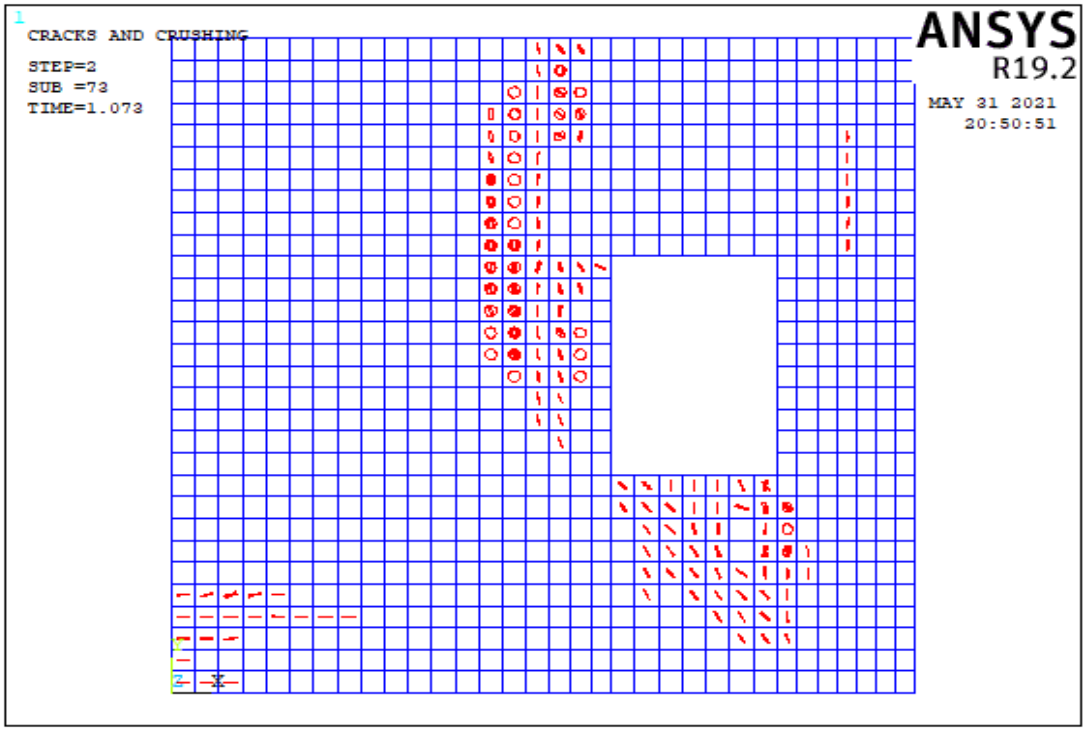

(a)

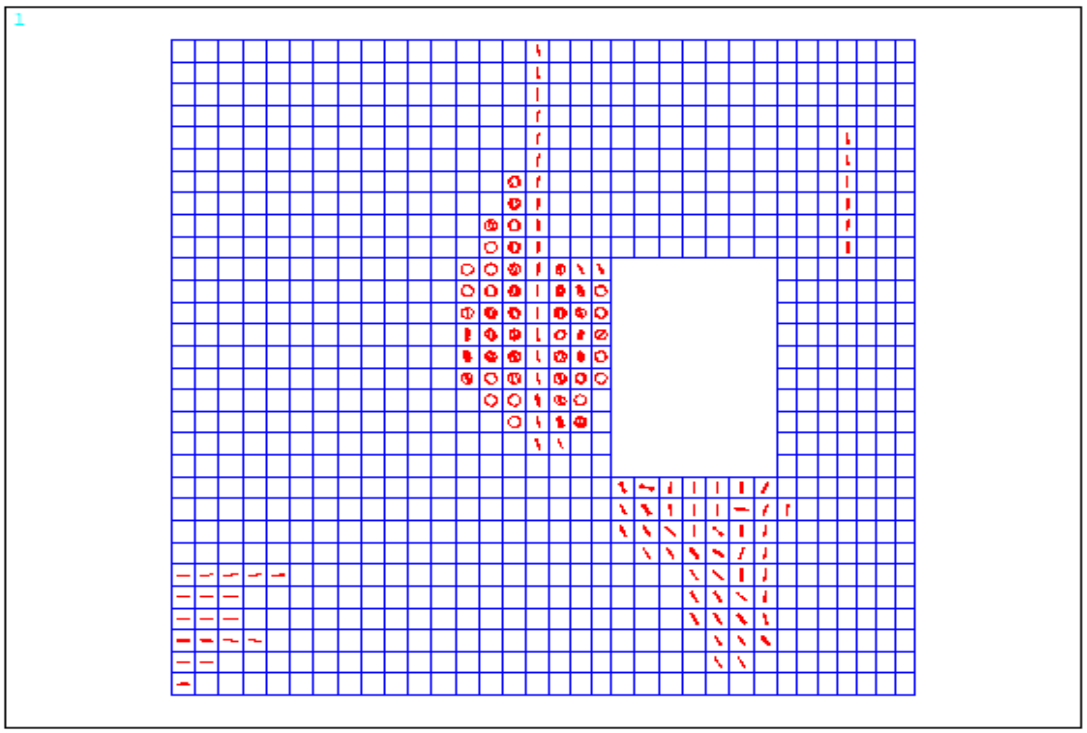

(b)

Figure 5.38. The Crack Pattern of Wall 3 Model 10 According to Compressive Strength Values of (a) 3 MPa, (b) 8 MPa

Table 5.5. Failure Patterns of Wall 3

Number of Model	Aspect ratio	fm=3 Mpa			fm=8 Mpa		
		Failure Pattern			Failure Pattern		
		Base Sliding	Rocking	Diagonal Tension	Base Sliding	Rocking	Diagonal Tension
Model 1	1.00			X			X
	0.50			X			X
Model 2	3.45		X			X	
	1.22			X			
Model 3	4.13		X			X	
	3.48		X			X	
Model 4	0.86			X			X
	0.86			X			X
Model 5	4.13		X			X	
	0.96			X			X
Model 6	5.00		X			X	
	1.47			X			X
Model 7	1.68		X			X	
	1.75						
Model 8	1.02			X	X		
	1.31	X					X
Model 9	2.23		X			X	
	1.36						
Model 10	1.67		X			X	
	5.35		X			X	

In Table A.3, all length of openings is less than 3 m for all models and total opening percentage of walls is appropriate for TEC 2018. In models 2, 3, 5, 6, 9 and 10, the length of corner piers is less than 1.5 m. In Model 1, the total length of the wall is 10 m and the percentage of opening is 3%. Therefore, the capacity of model 1 is higher than the others. When considering the capacity of models 2 and 5, the capacity of model 5 is greater due to its lower opening percentage. Table 5.5 shows that, the rocking mechanism is predominant in piers, when the aspect ratio of the piers is larger than 1.47. On the other hand, shear is predominant, when the aspect ratio of the piers is less than 1.47.

5.4.1.4 Failure Modes of Wall 4

In the wall 4 type, there are 10 different wall models. The impact of two window opening was studied in these models of wall 4. Table A.4 shows the lengths of the walls. As seen in Figure 5.3, each pier is designated from left to right. The crack patterns obtained from the analysis of wall models corresponding to 10 different wall models are described in this section.

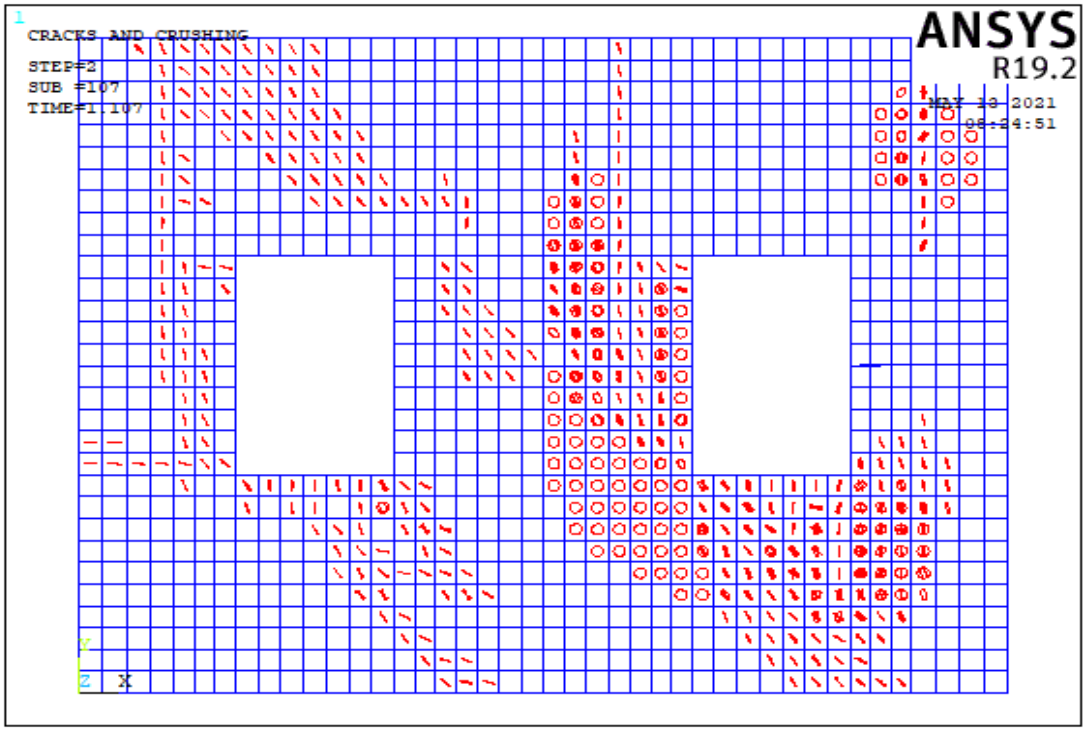

(a)

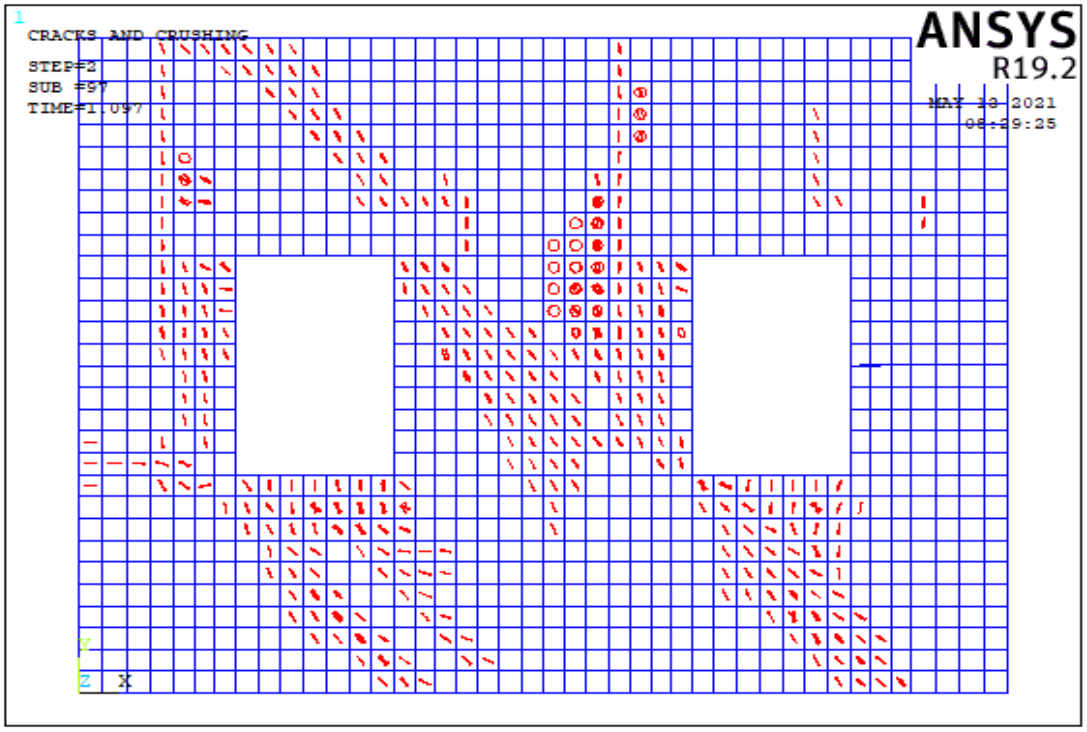

(b)

Figure 5.39. The Crack Pattern of Wall 4 Model 1 According to Compressive Strength Values of (a) 3 MPa, (b) 8 MPa

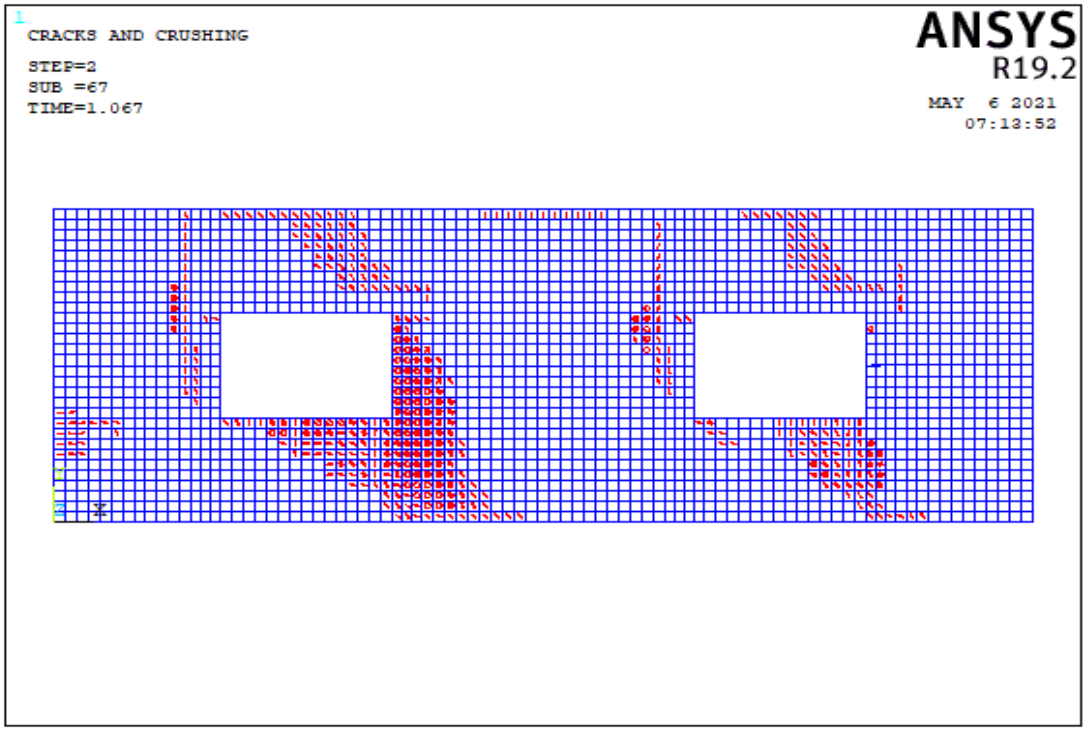

(a)

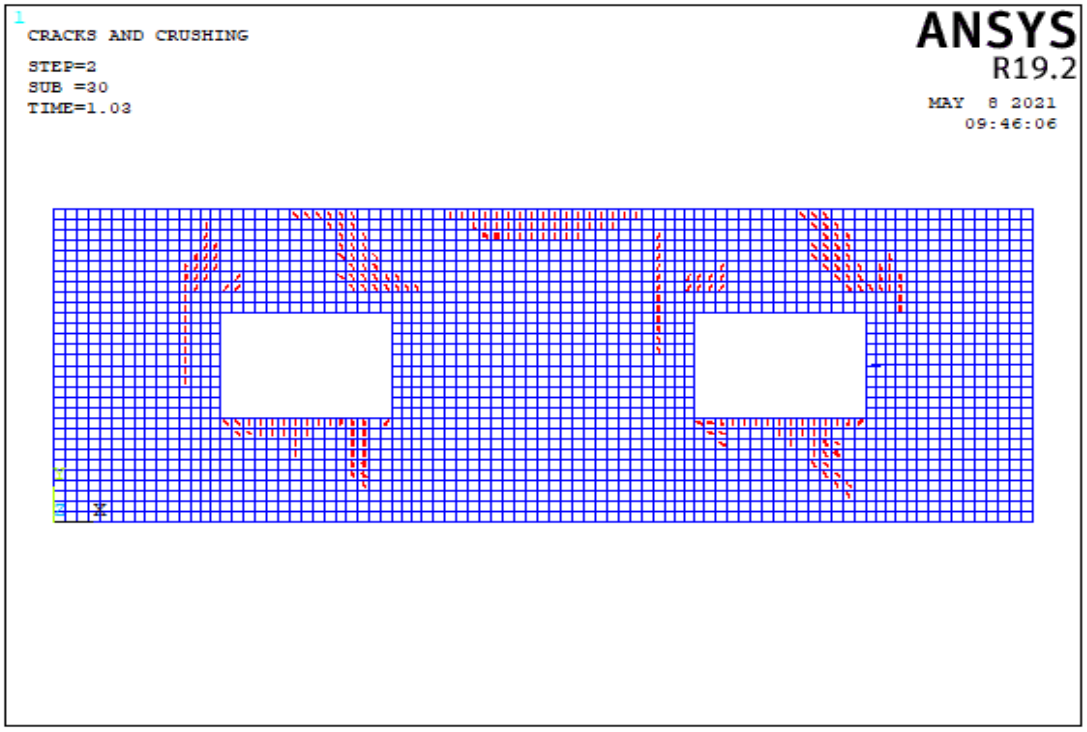

(b)

Figure 5.40. The Crack Pattern of Wall 4 Model 2 According to Compressive Strength Values of (a) 3 MPa, (b) 8 MPa

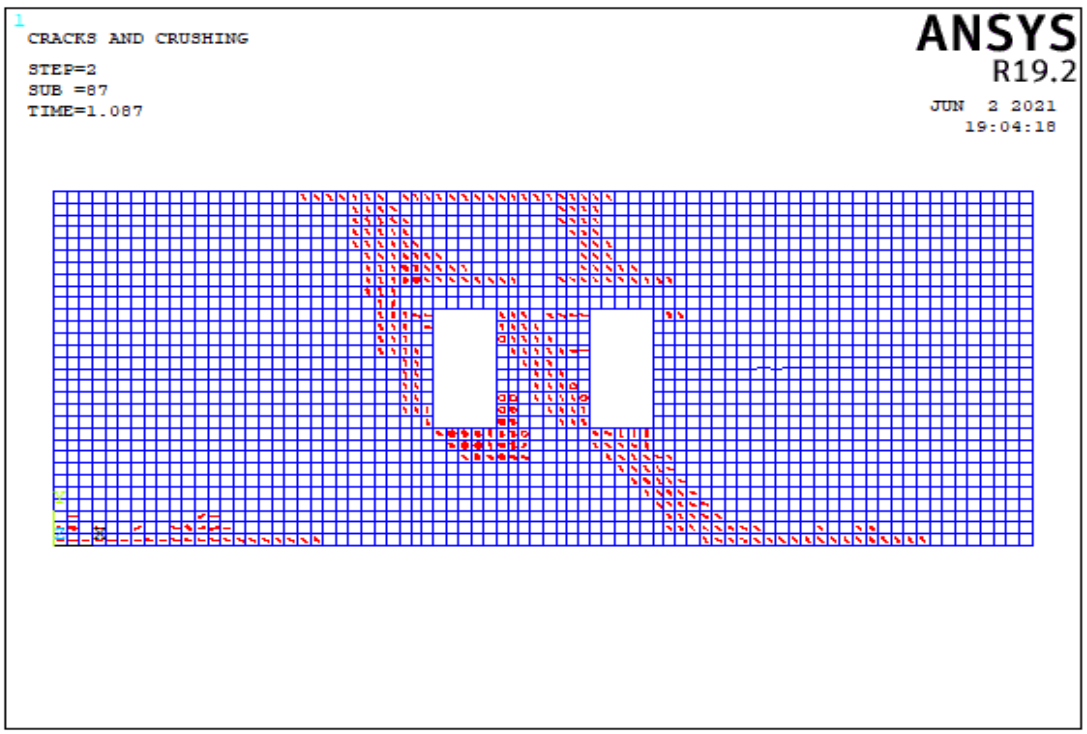

(a)

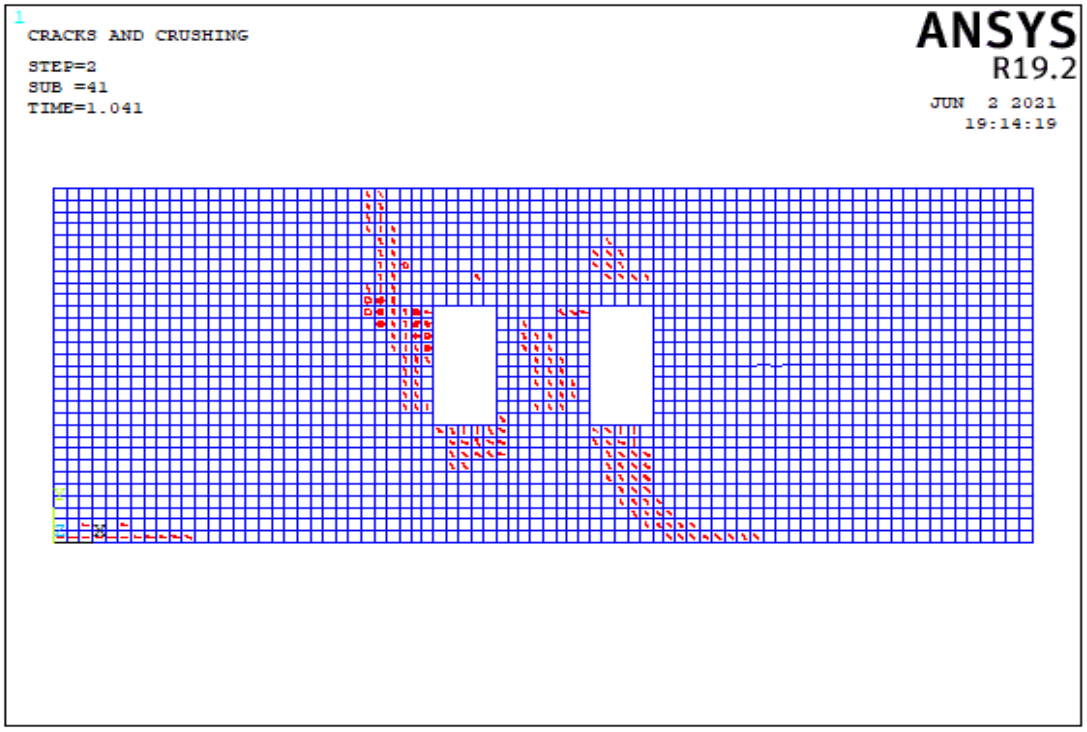

(b)

Figure 5.41. The Crack Pattern of Wall 4 Model 3 According to Compressive Strength Values of (a) 3 MPa, (b) 8 MPa

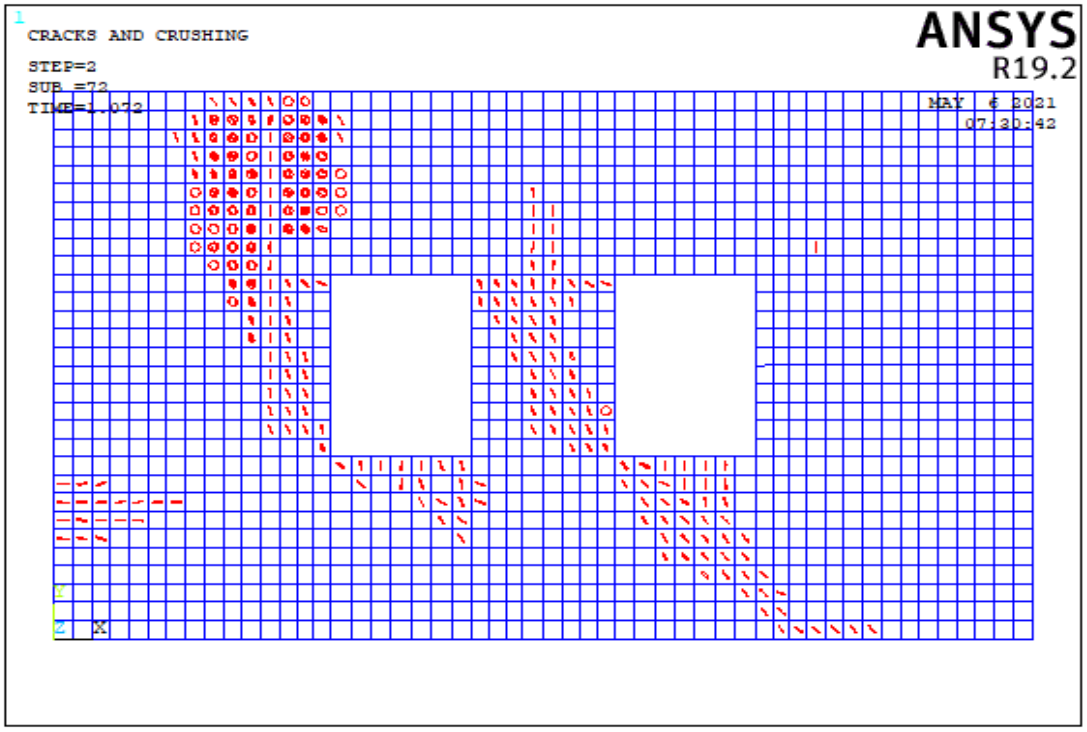

(a)

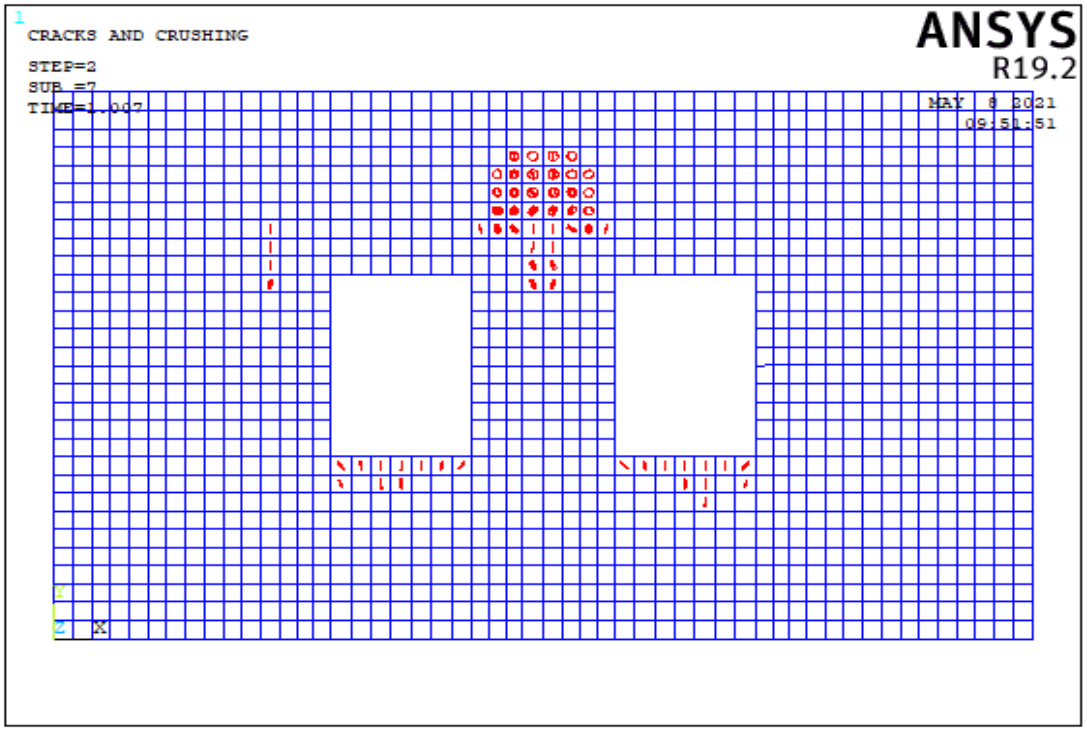

(b)

Figure 5.42. The Crack Pattern of Wall 4 Model 4 According to Compressive Strength Values of (a) 3 MPa, (b) 8 MPa

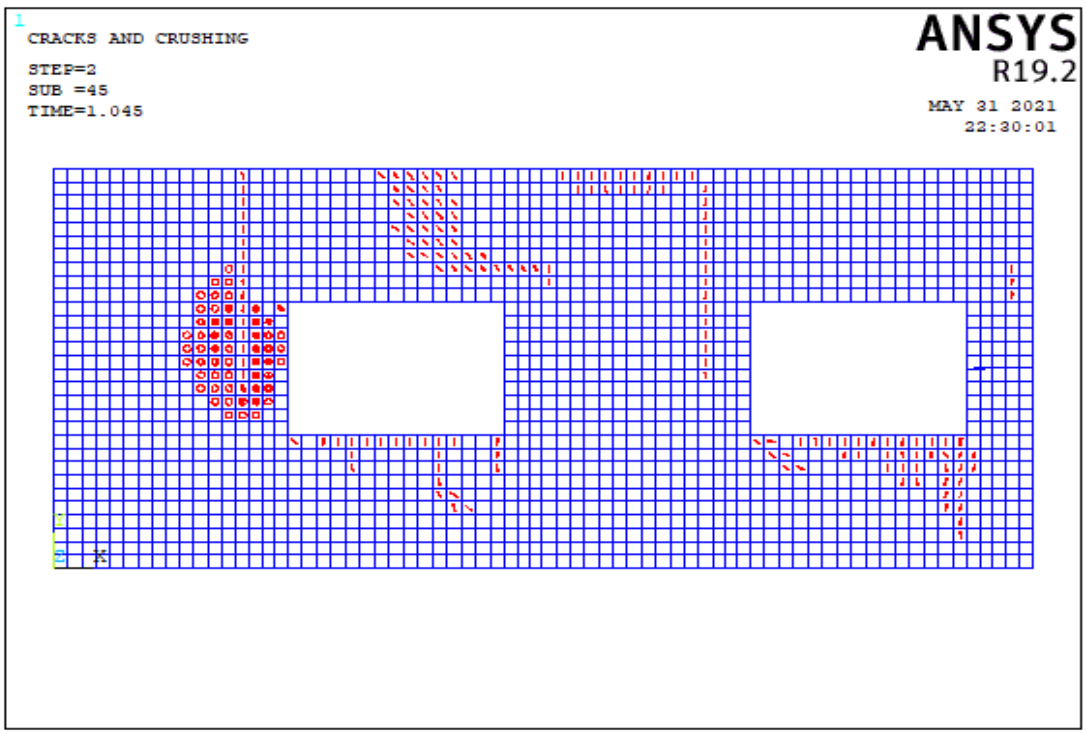

(a)

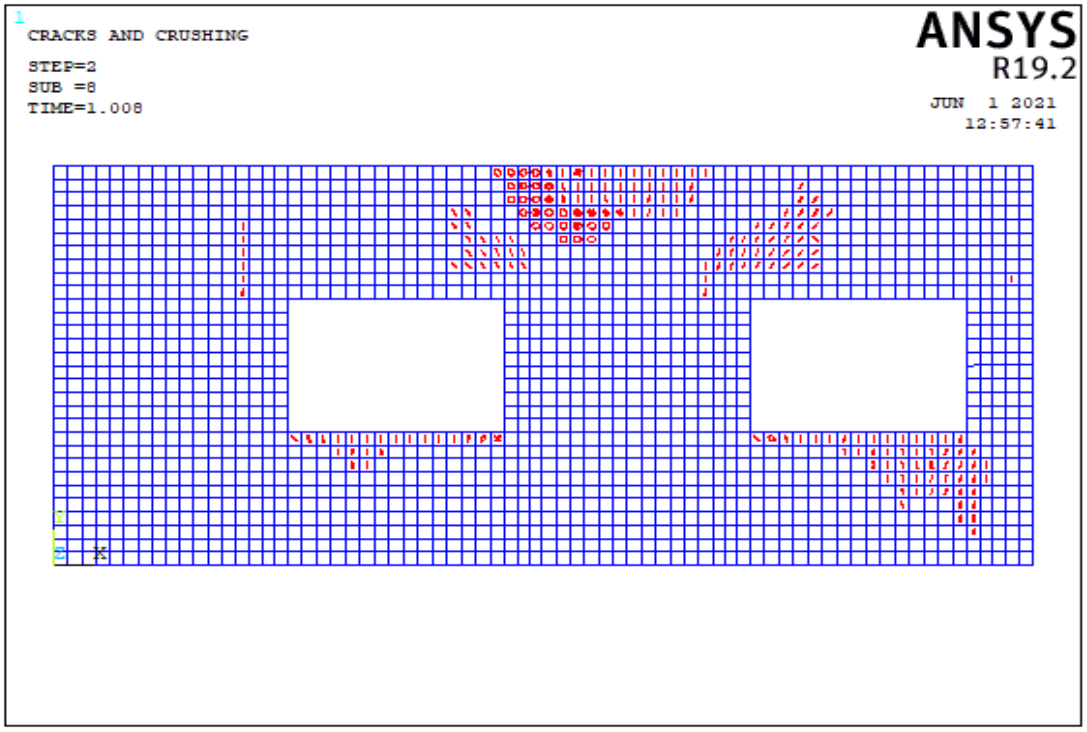

(b)

Figure 5.43. The Crack Pattern of Wall 4 Model 5 According to Compressive Strength Values of (a) 3 MPa, (b) 8 MPa

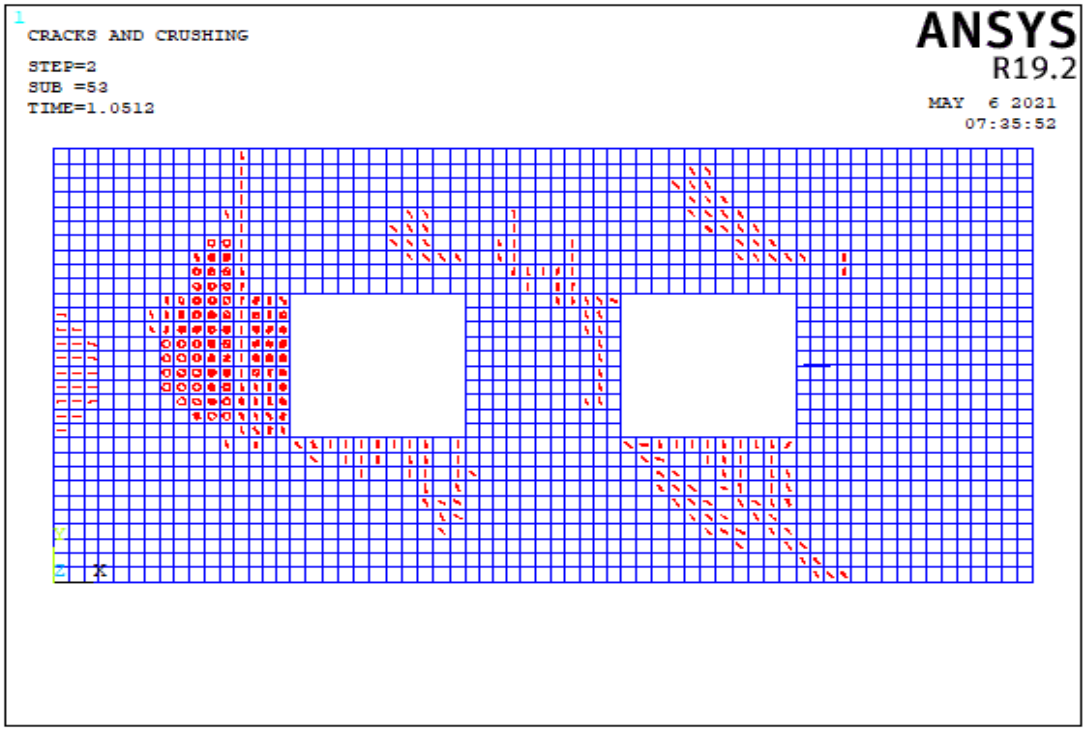

(a)

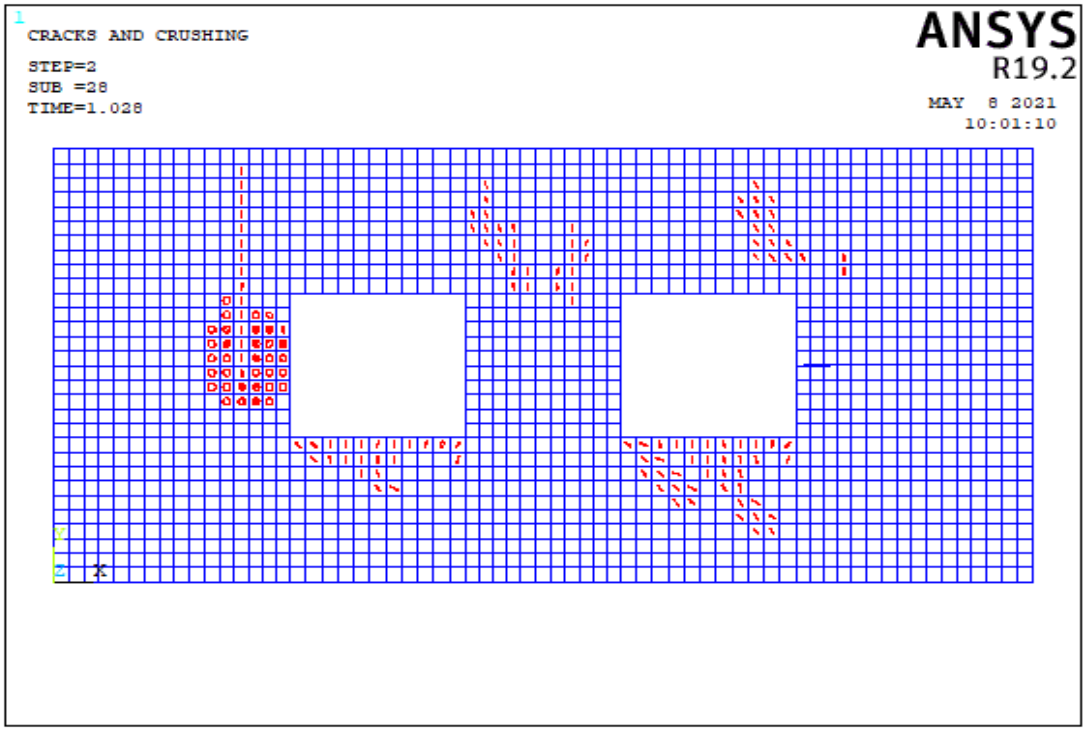

(b)

Figure 5.44. The Crack Pattern of Wall 4 Model 6 According to Compressive Strength Values of (a) 3 MPa, (b) 8 MPa

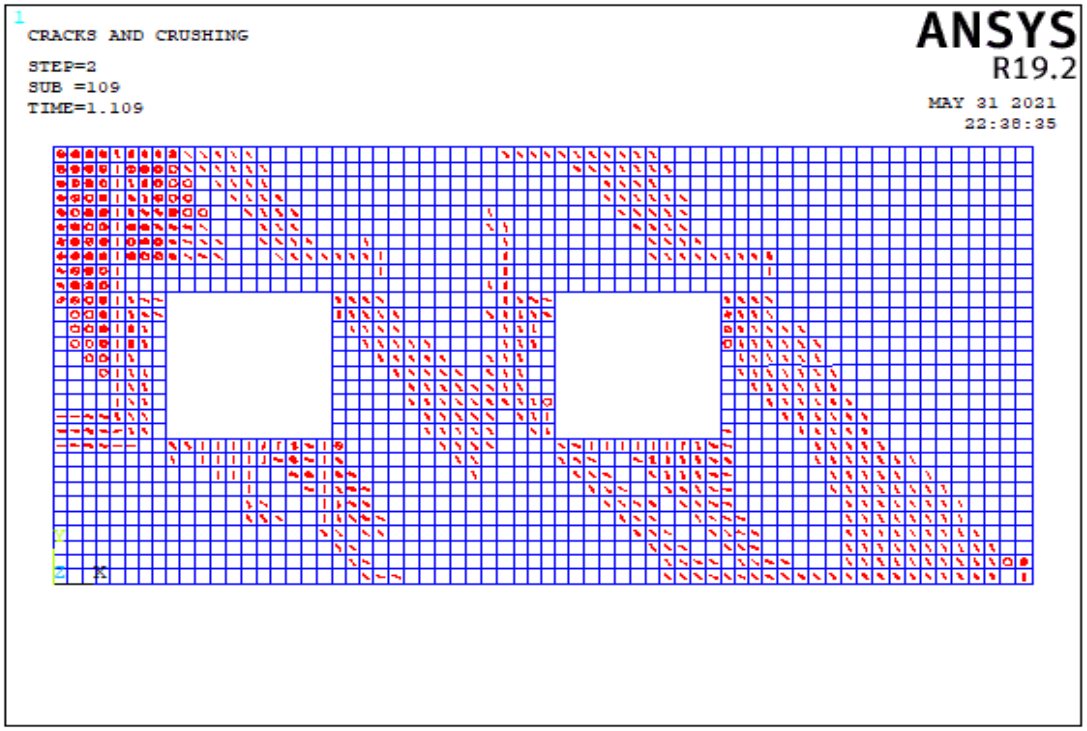

(a)

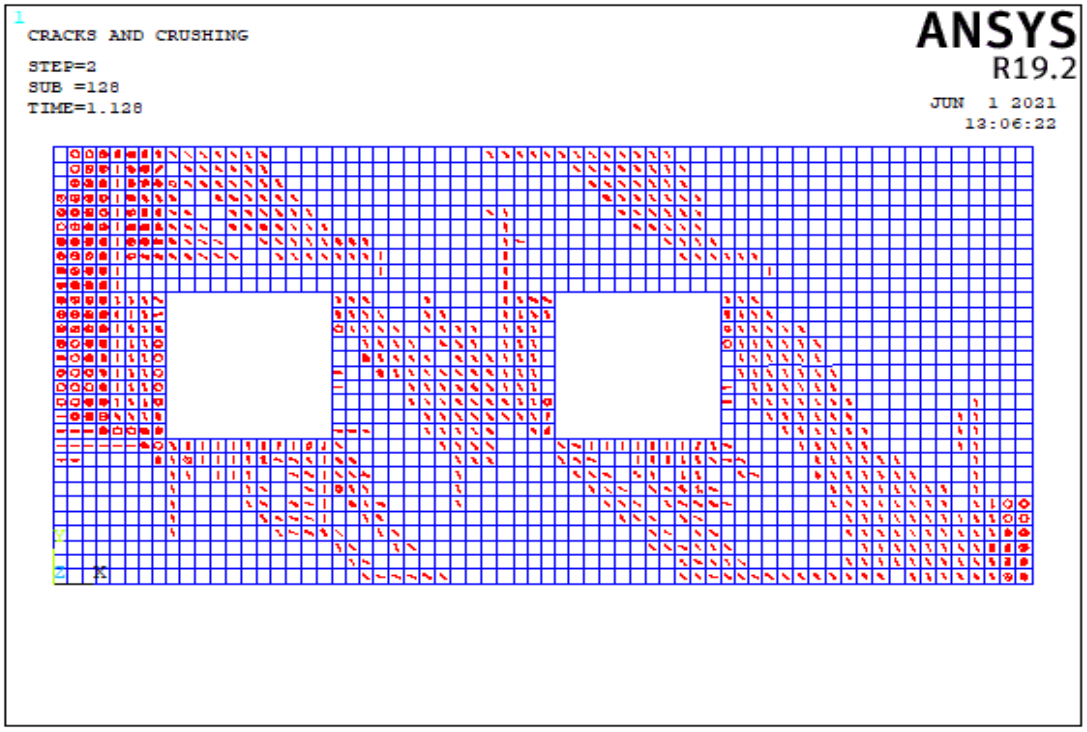

(b)

Figure 5.45. The Crack Pattern of Wall 4 Model 7 According to Compressive Strength Values of (a) 3 MPa, (b) 8 MPa

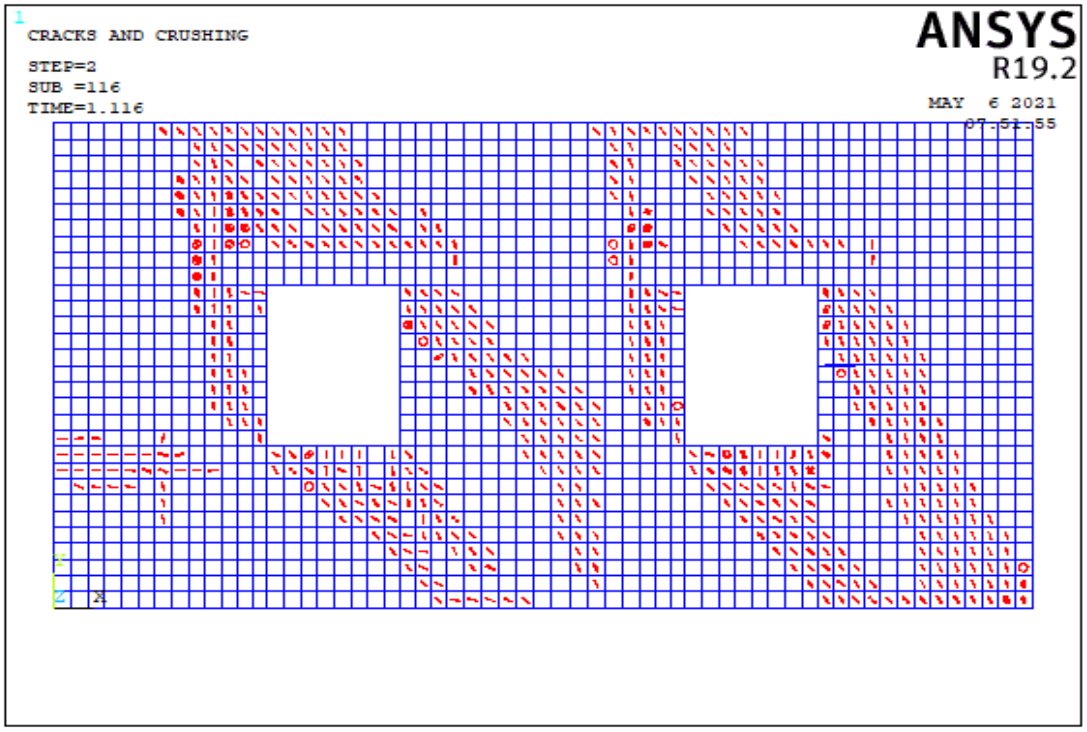

(a)

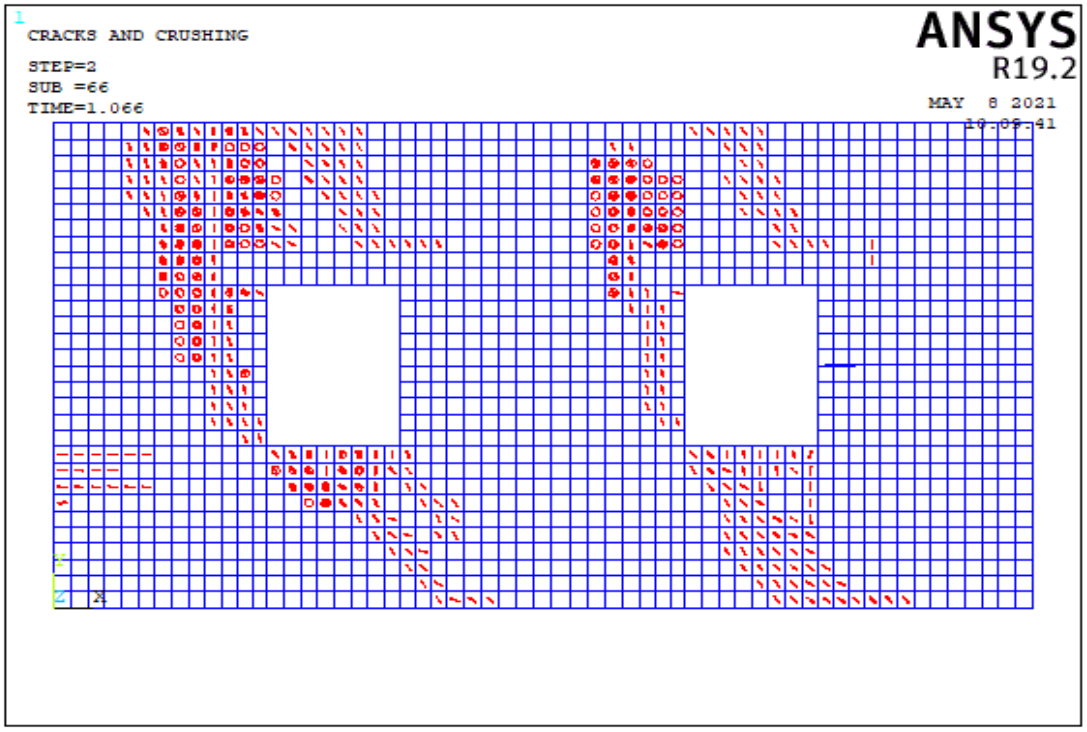

(b)

Figure 5.46. The Crack Pattern of Wall 4 Model 8 According to Compressive Strength Values of (a) 3 MPa, (b) 8 MPa

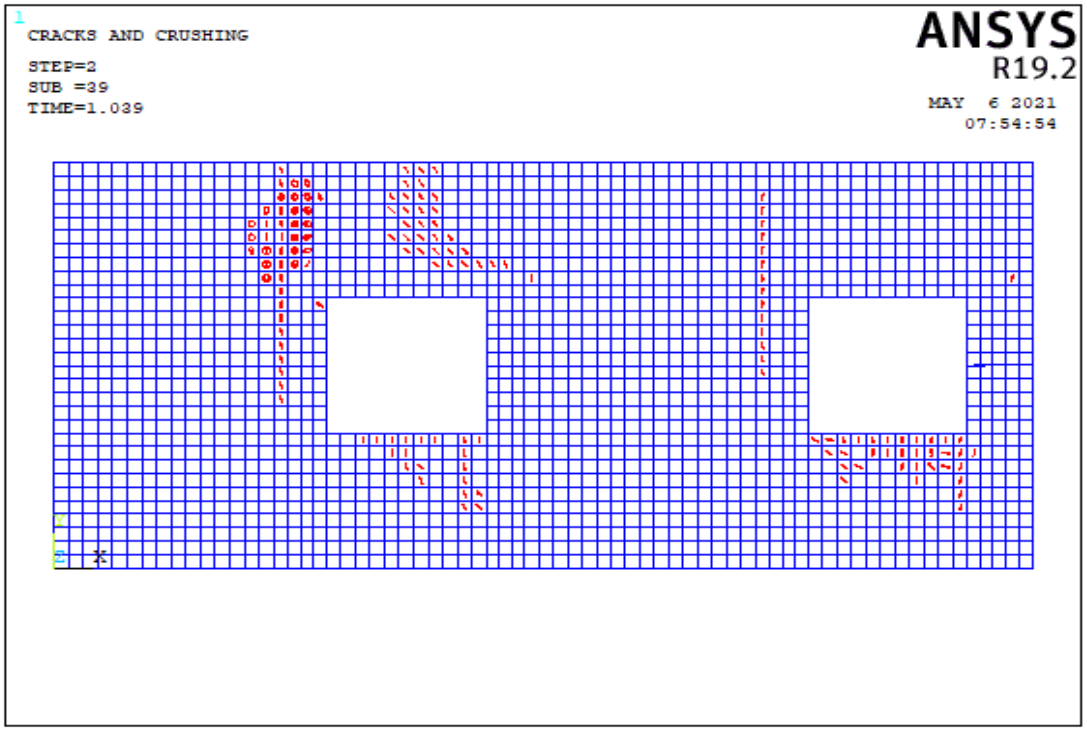

(a)

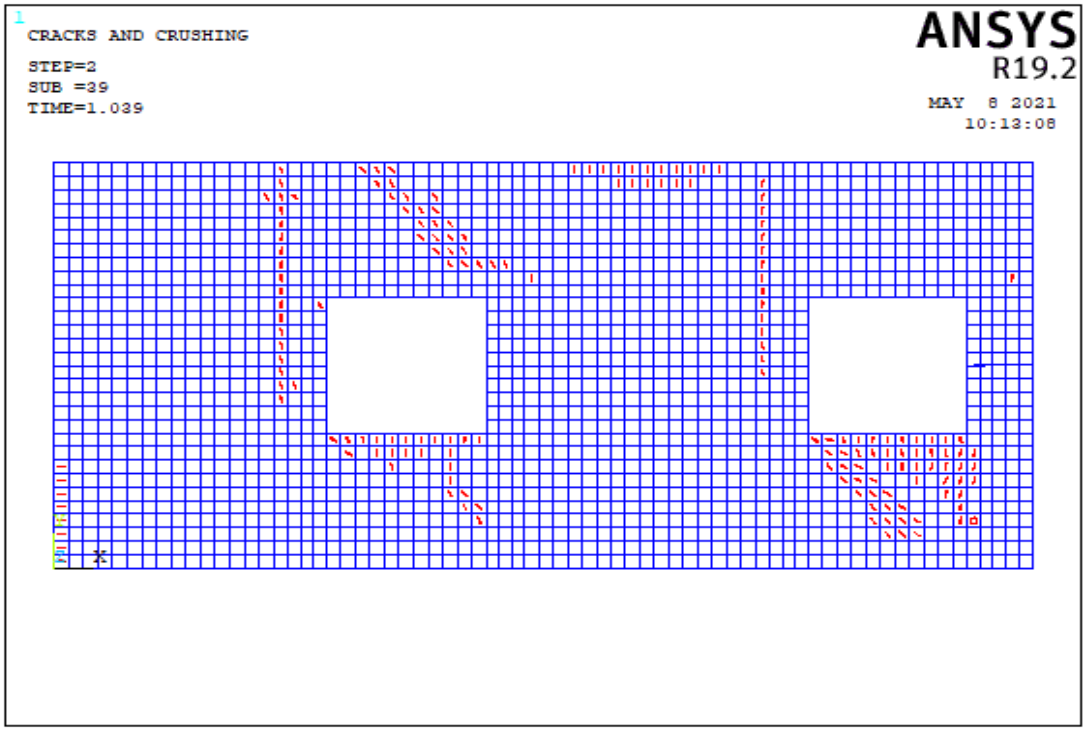

(b)

Figure 5.47. The Crack Pattern of Wall 4 Model 9 According to Compressive Strength Values of (a) 3 MPa, (b) 8 MPa

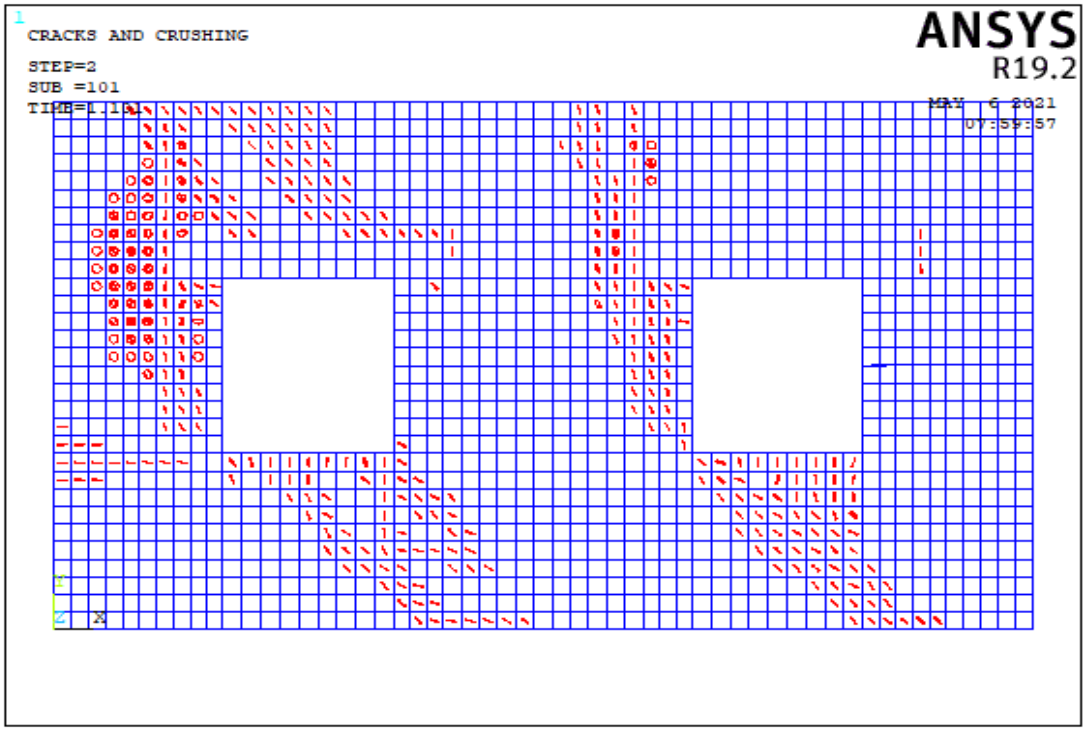

(a)

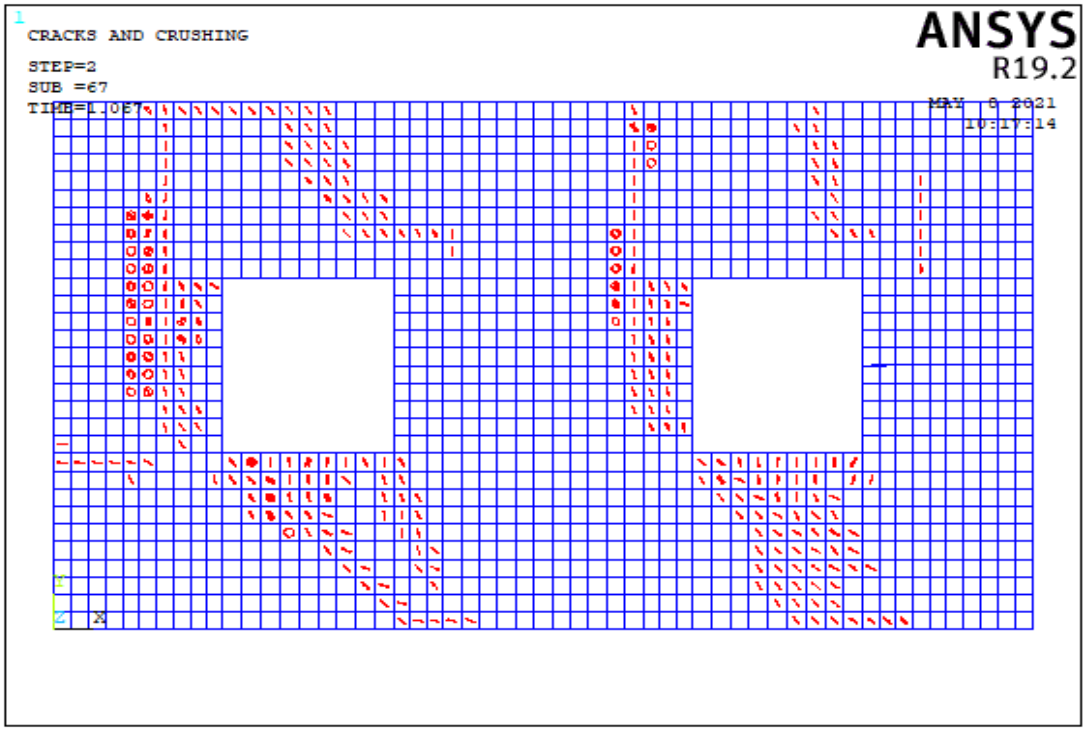

(b)

Figure 5.48. The Crack Pattern of Wall 4 Model 10 According to Compressive Strength Values of (a) 3 MPa, (b) 8 MPa

Table 5.6. Failure Patterns of Wall 4

Number of Model	Aspect ratio	fm=3 Mpa			fm=8 Mpa		
		Failure Pattern			Failure Pattern		
		Base Sliding	Rocking	Diagonal Tension	Base Sliding	Rocking	Diagonal Tension
Model 1	4.76		X			X	
	2.44			X			X
	4.76		X			X	
Model 2	2.09		X			X	
	1.16			X			
	2.10		X			X	
Model 3	1.05	X			X		
	4.29			X			X
	1.05	X			X		
Model 4	1.03	X					
	16.00			X			
	1.03						
Model 5	1.92		X				
	1.82		X				
	6.95		X				
Model 6	2.06		X			X	
	3.14		X			X	
	2.06		X			X	
Model 7	4.40		X			X	
	2.20			X			X
	1.57			X			X
Model 8	2.55		X			X	
	1.91			X			X
	2.55			X			X
Model 9	1.67		X			X	
	1.41						
	7.06		X			X	
Model 10	3.50		X			X	
	1.98						
	3.50		X			X	

In Table A.4, all length of windows are less than 3 m for all models and total opening percentage of walls for model 5 is not appropriate for TEC 2018. In model 3 and 4 for wall 4, the length of corner piers is more than 1.5 m. In models 3, 4 and 6, the length of the piers between the windows are more than 1 m. Models 1 and 10 display ductile behavior because of high aspect ratio of their walls. In Model 2, although the length of windows is 1.48 m, the wall capacity increased due to the effect of the location of the openings and sufficient length of piers. In model 3, capacity of wall is enhanced by 4% opening percentage. When models 6 and 7 are examined, it is observed that the wall capacity is higher as the opening position is located in the left corner of wall. This models show that, the aspect ratios of the piers influence their failure patterns. Table 5.6 shows that rocking mechanism emerges in corner piers ,as the aspect ratio of piers at corners increases,. However, diagonal tension failure is characterized by diagonal cracks between the windows and this type of failure occurs due to decreased aspect ratio of piers.

5.4.1.5 Failure Modes of Wall 5

In the wall 5 type, there are 10 different wall models. The impact of three windows openings was studied in these models of wall 5. Table A.5 shows the lengths of the walls. As seen in Figure 5.3, each pier is designated from left to right. The crack patterns obtained from the analysis of wall models corresponding to 10 different wall models are described in this section.

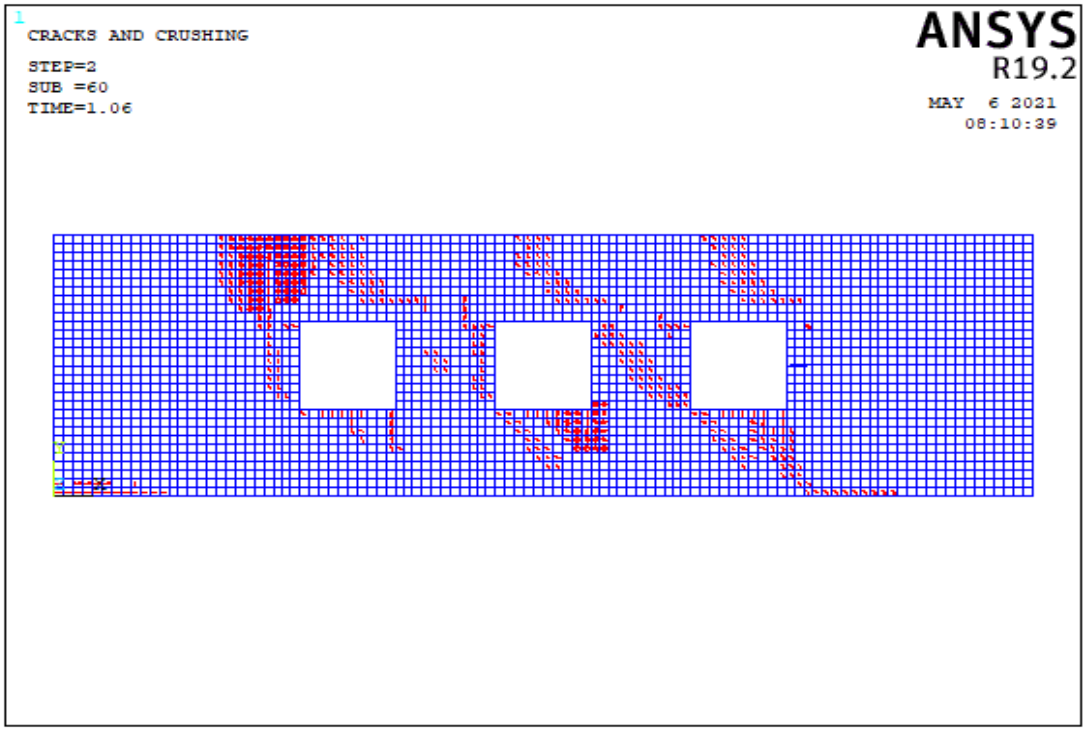

(a)

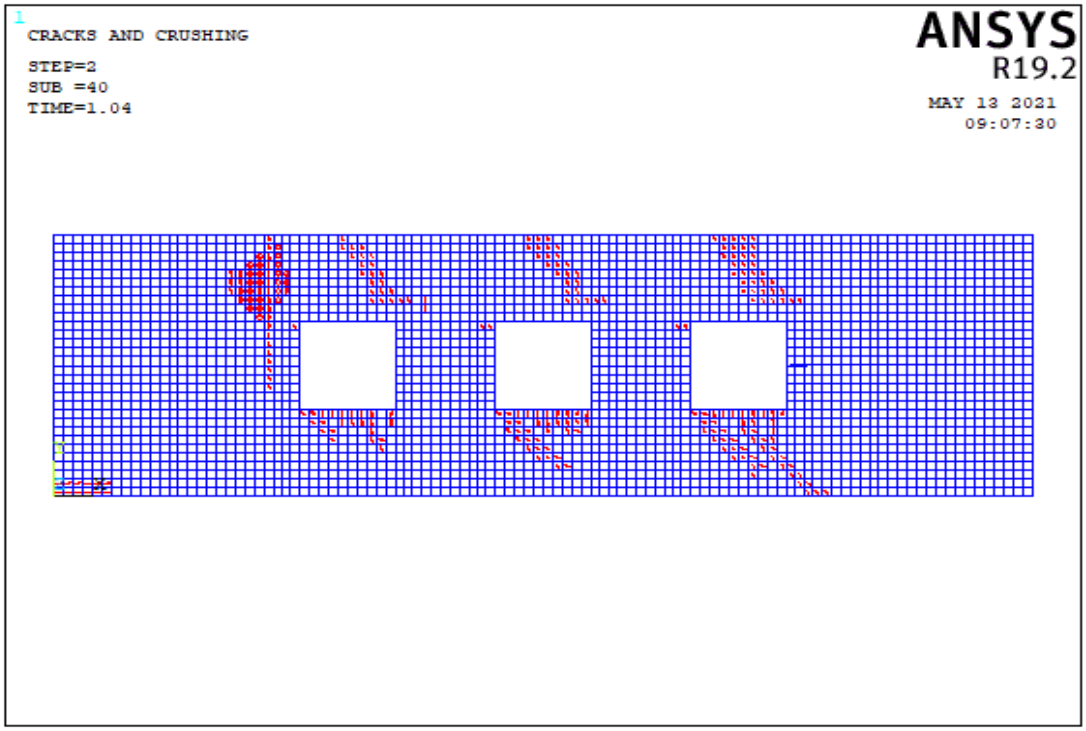

(b)

Figure 5.49. The Crack Pattern of Wall 5 Model 1 According to Compressive Strength Values of (a) 3 MPa, (b) 8 MPa

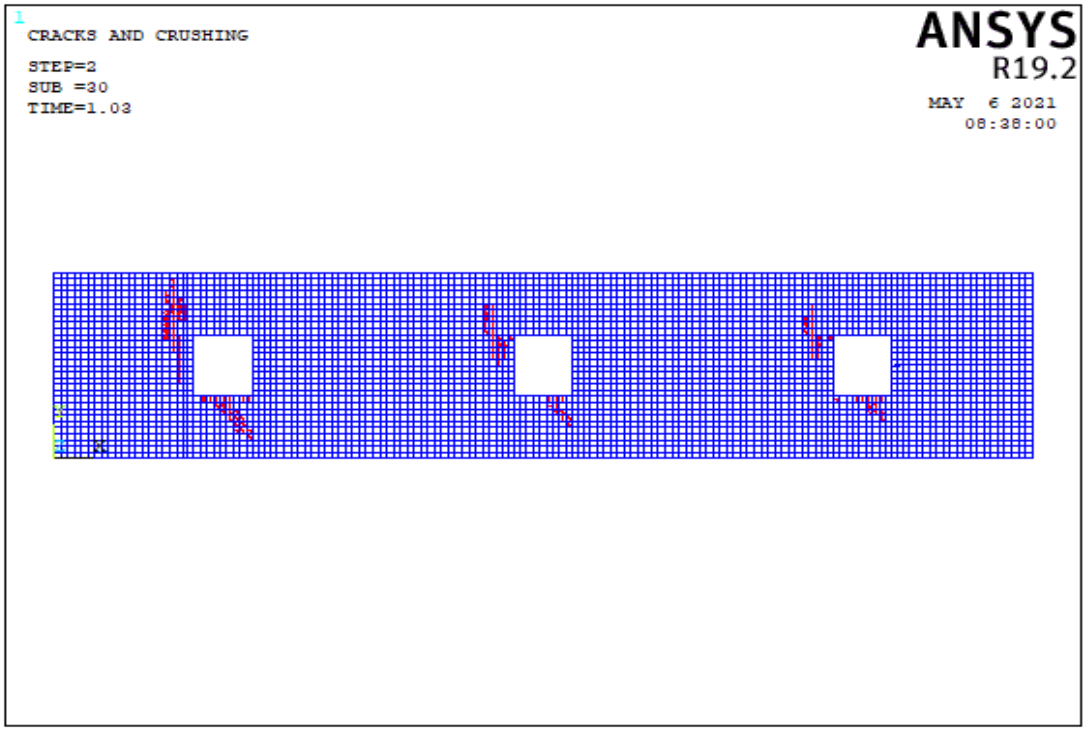

(a)

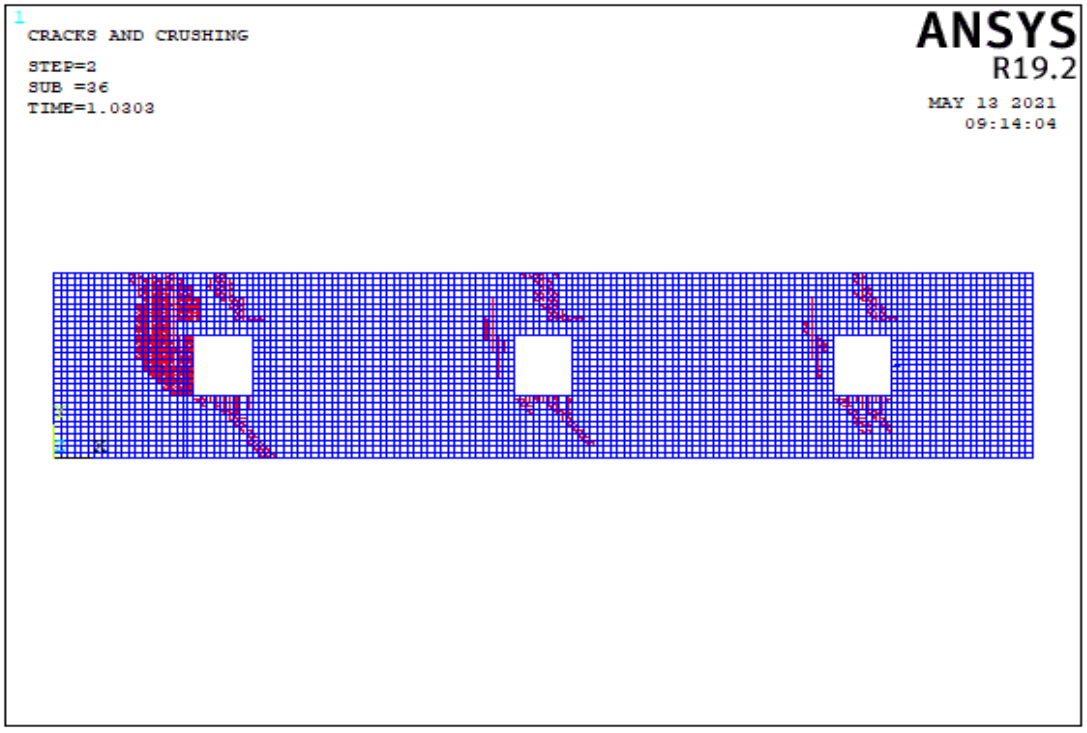

(b)

Figure 5.50. The Crack Pattern of Wall 5 Model 2 According to Compressive Strength Values of (a) 3 MPa, (b) 8 MPa

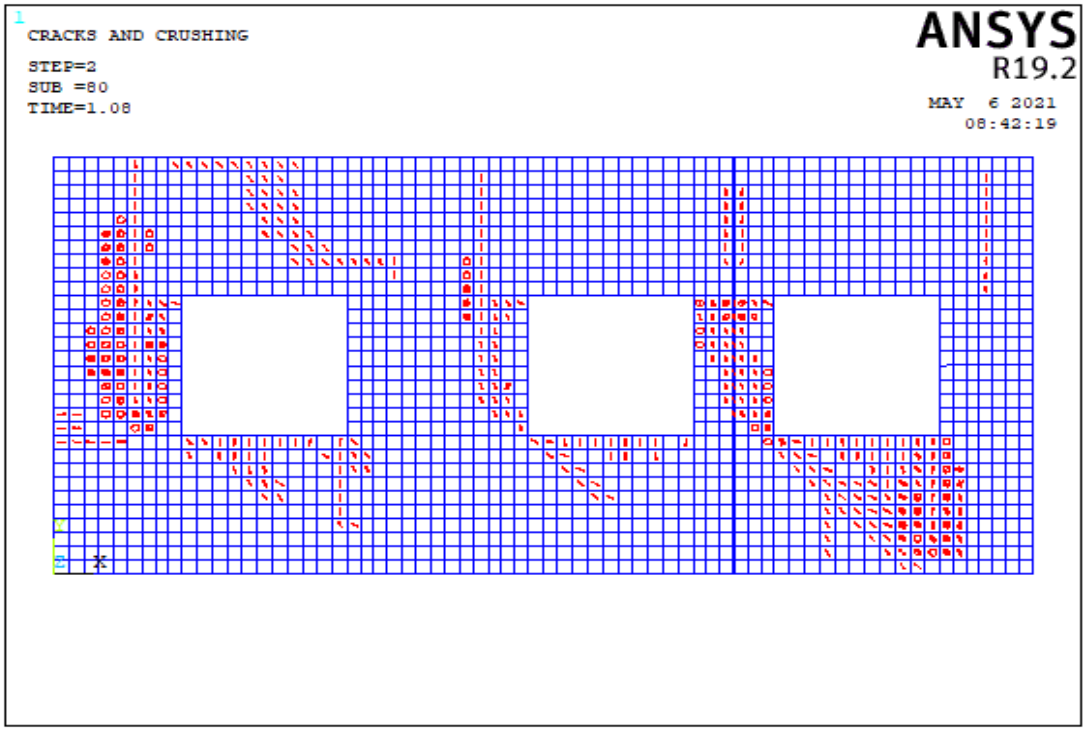

(a)

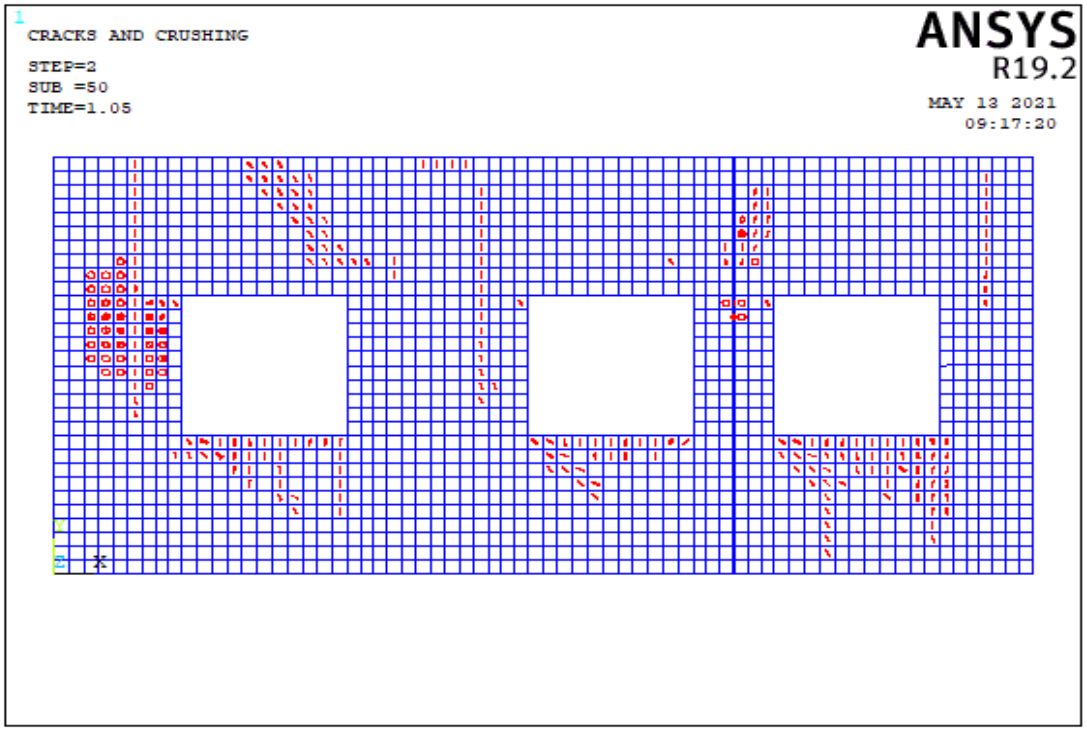

(b)

Figure 5.51. The Crack Pattern of Wall 5 Model 3 According to Compressive Strength Values of (a) 3 MPa, (b) 8 MPa

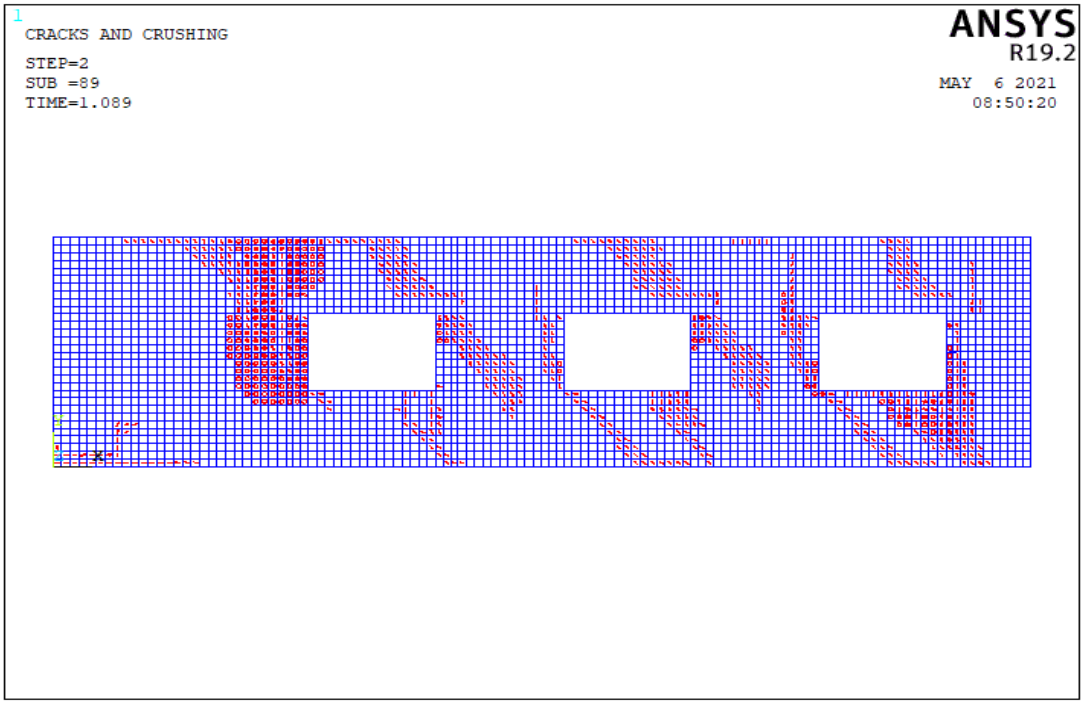

(a)

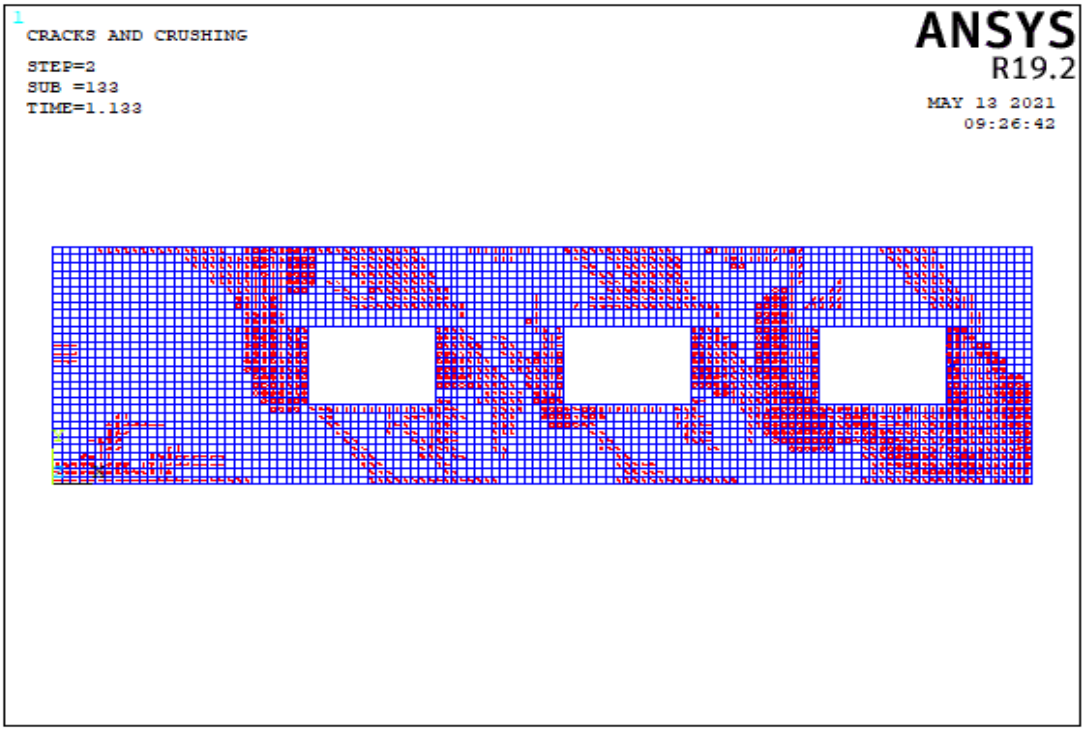

(b)

Figure 5.52. The Crack Pattern of Wall 5 Model 4 According to Compressive Strength Values of (a) 3 MPa, (b) 8 MPa

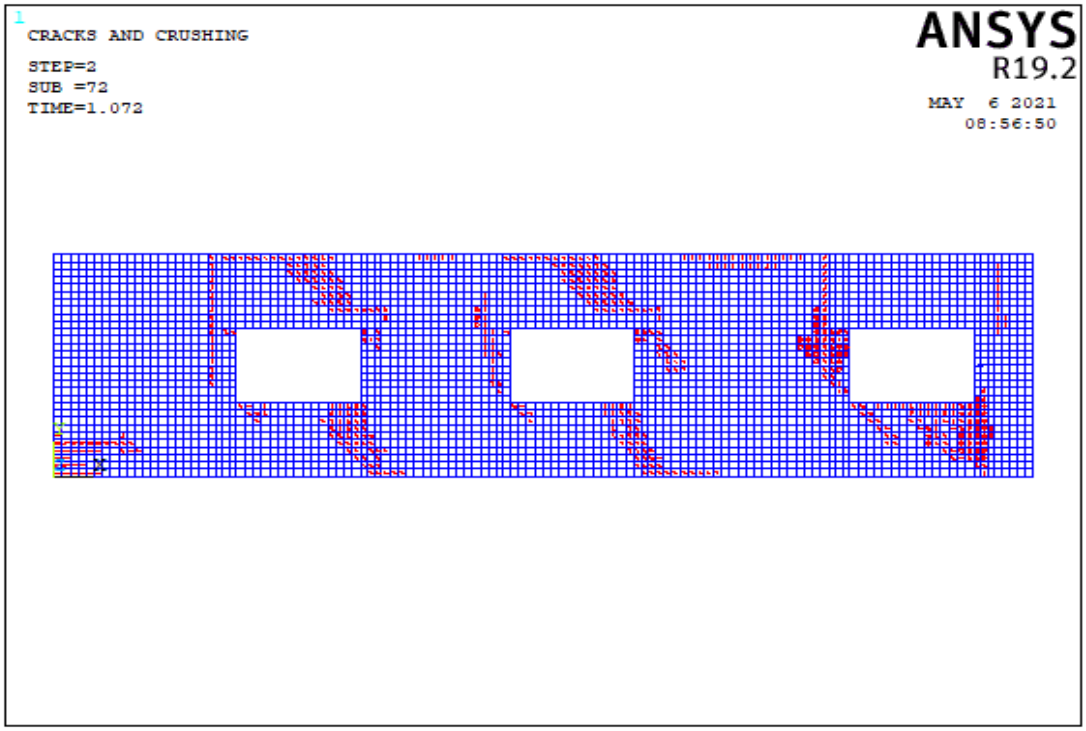

(a)

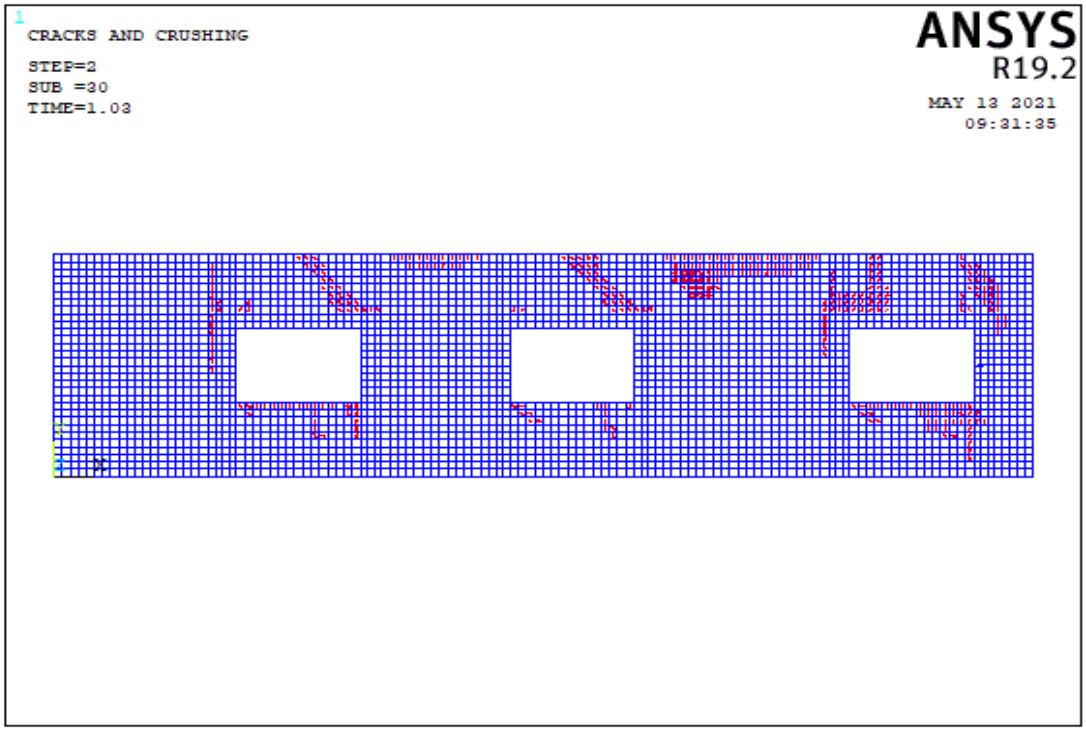

(b)

Figure 5.53. The Crack Pattern of Wall 5 Model 5 According to Compressive Strength Values of (a) 3 MPa, (b) 8 MPa

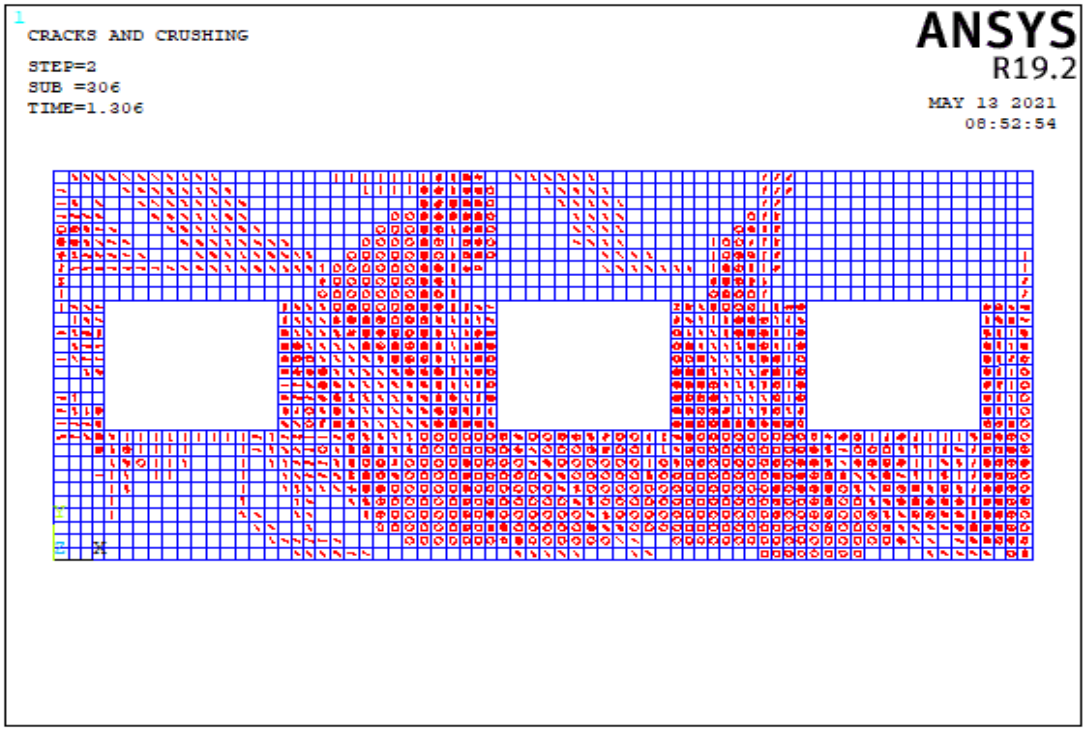

(a)

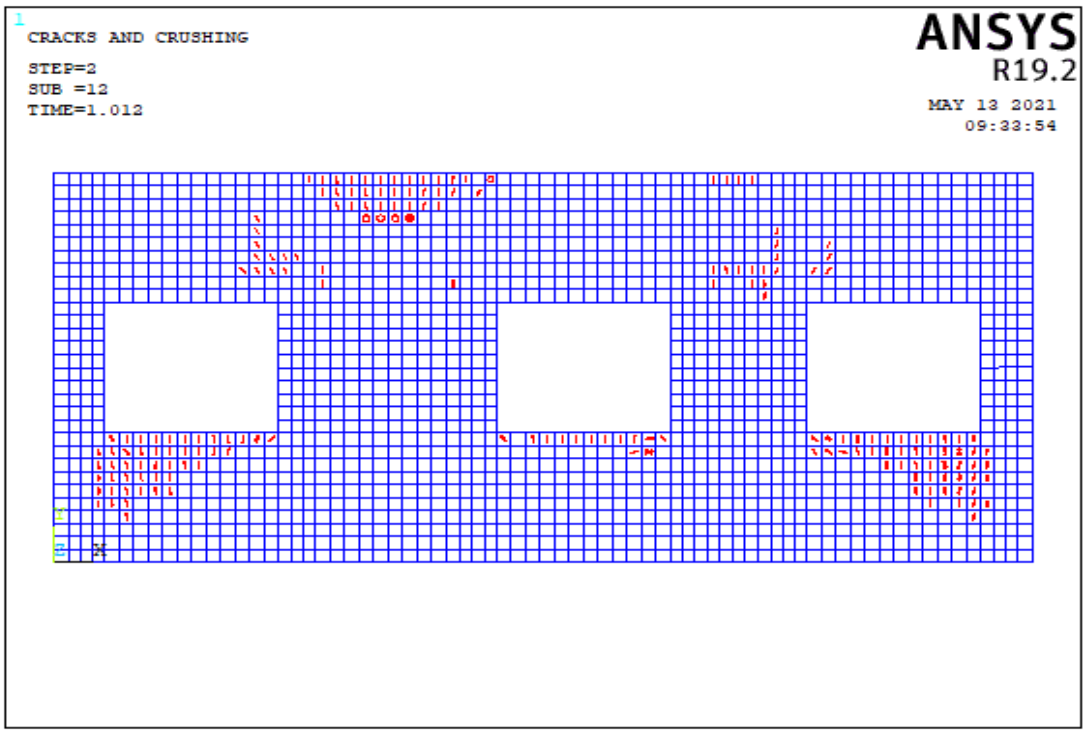

(b)

Figure 5.54. The Crack Pattern of Wall 5 Model 6 According to Compressive Strength Values of (a) 3 MPa, (b) 8 MPa

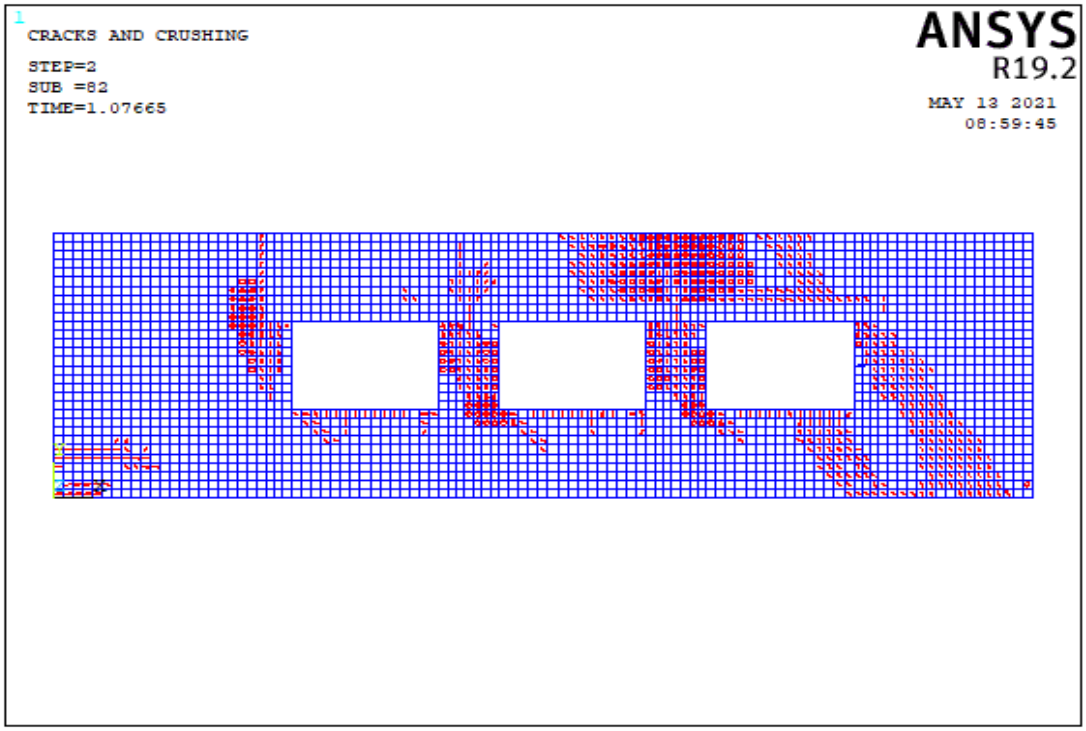

(a)

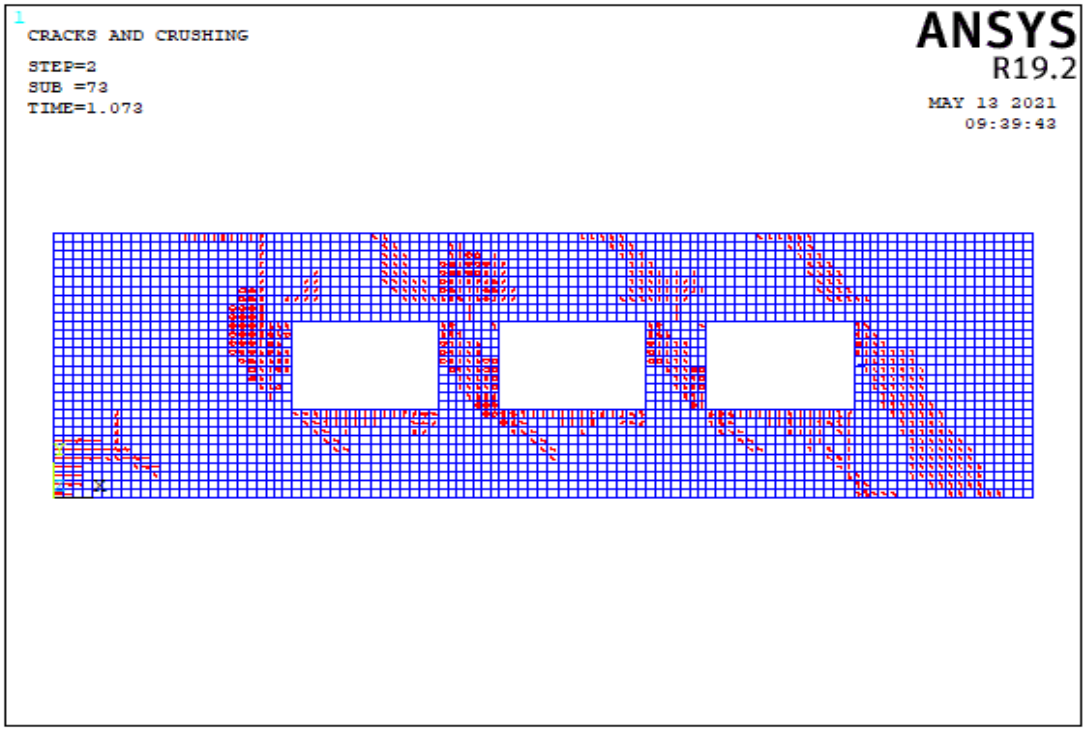

(b)

Figure 5.55. The Crack Pattern of Wall 5 Model 7 According to Compressive Strength Values of (a) 3 MPa, (b) 8 MPa

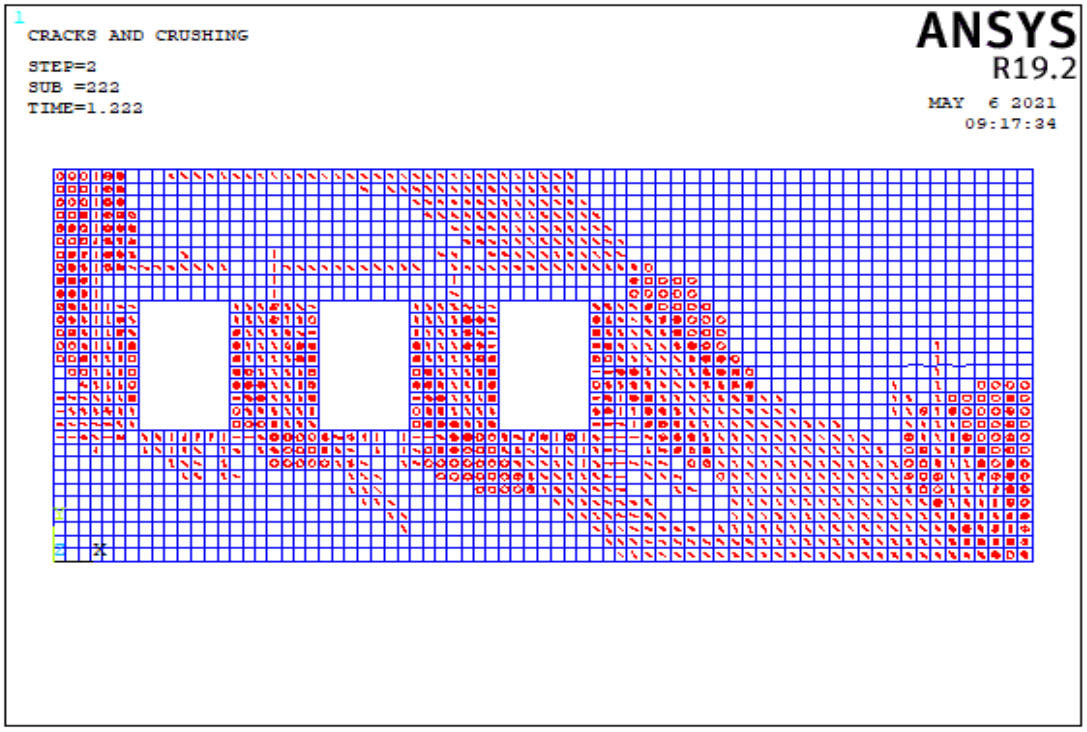

(a)

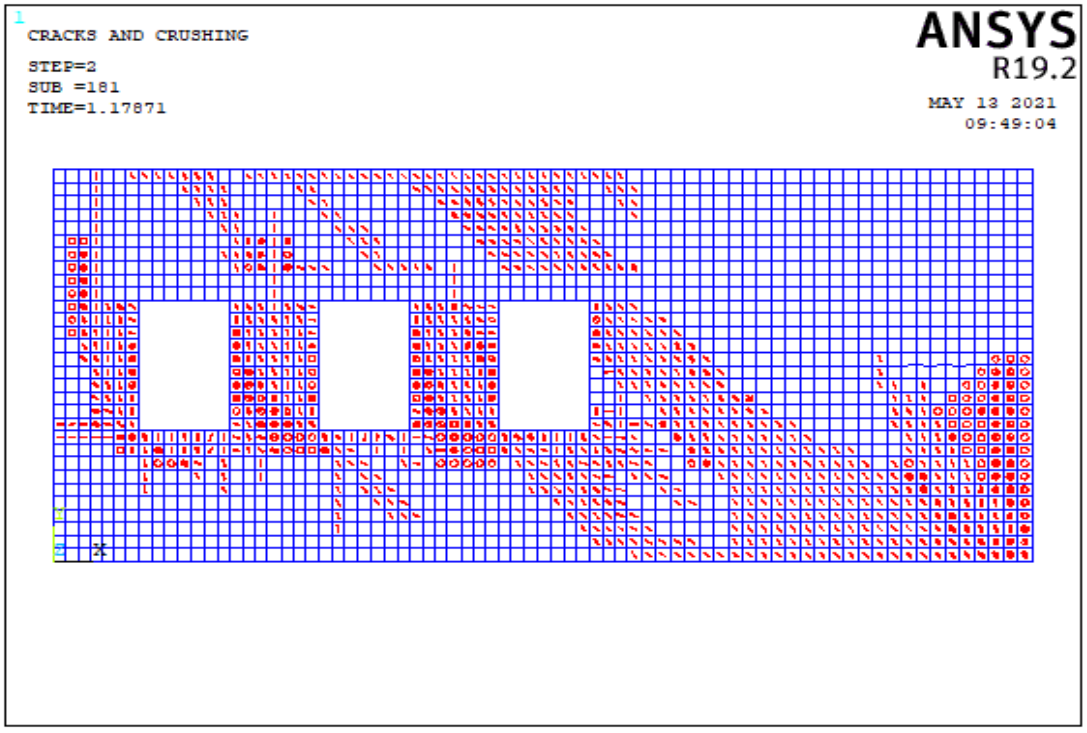

(b)

Figure 5.56. The Crack Pattern of Wall 5 Model 8 According to Compressive Strength Values of (a) 3 MPa, (b) 8 MPa

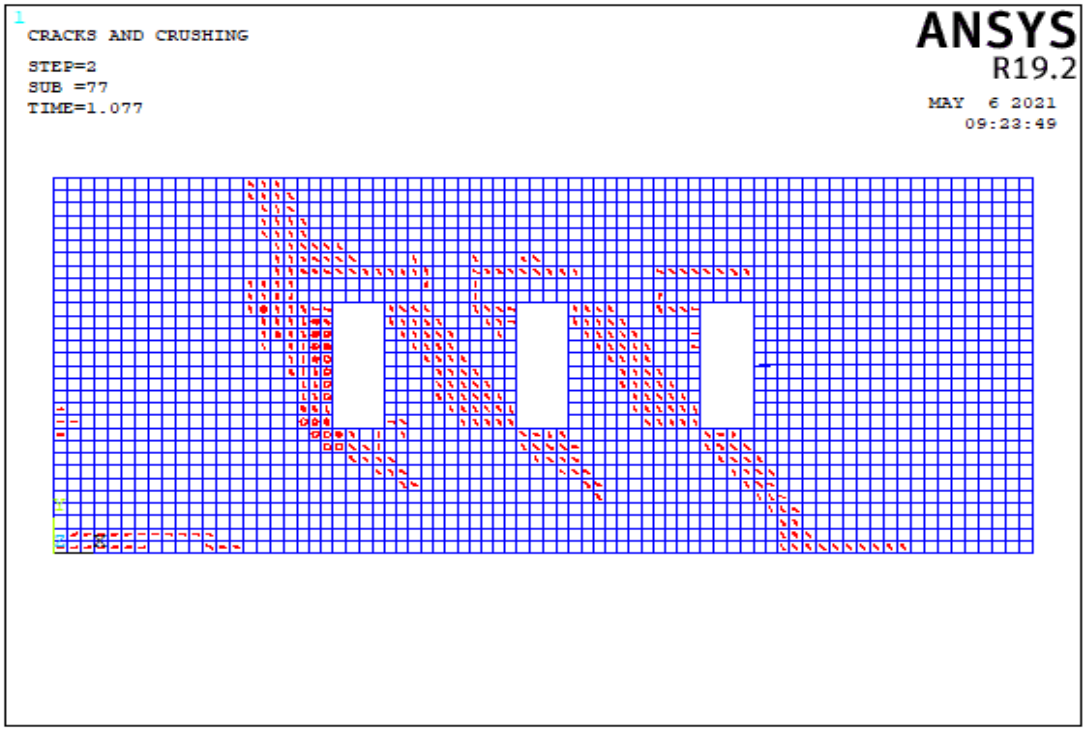

(a)

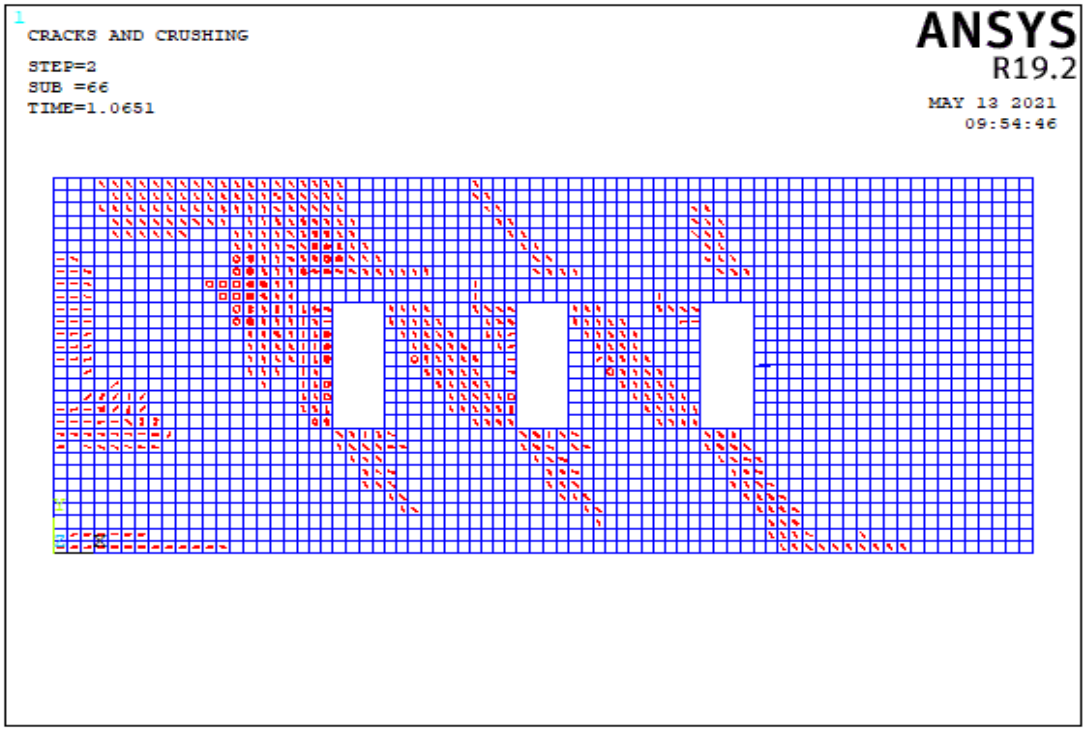

(b)

Figure 5.57. The Crack Pattern of Wall 5 Model 9 According to Compressive Strength Values of (a) 3 MPa, (b) 8 MPa

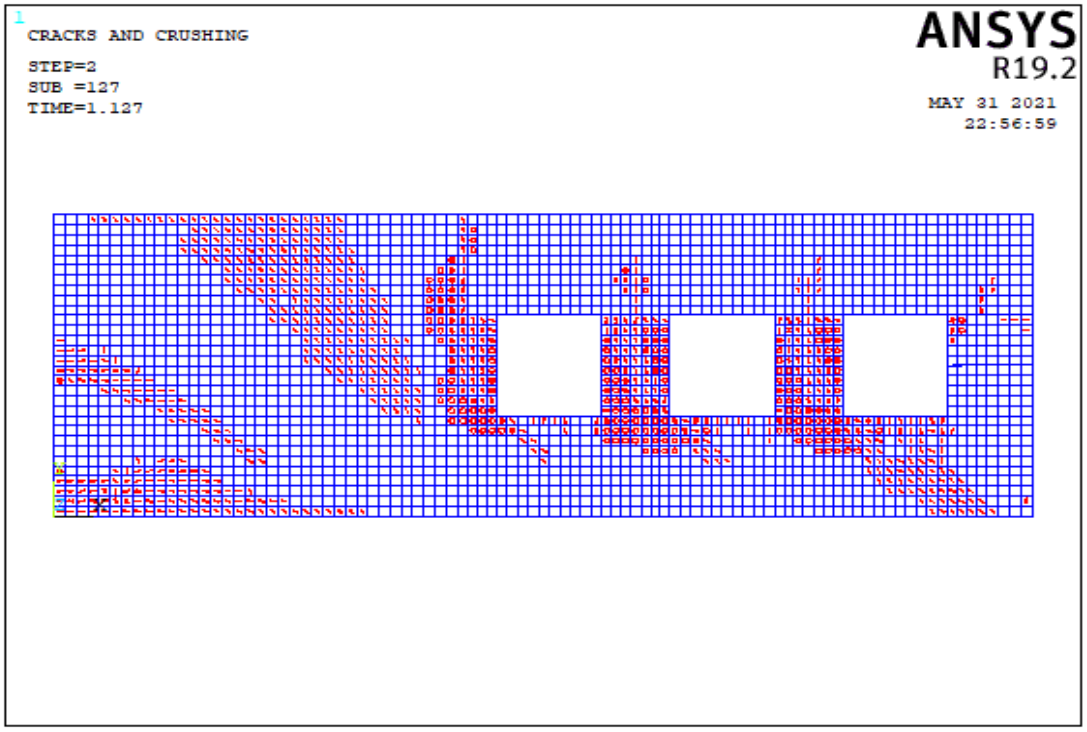

(a)

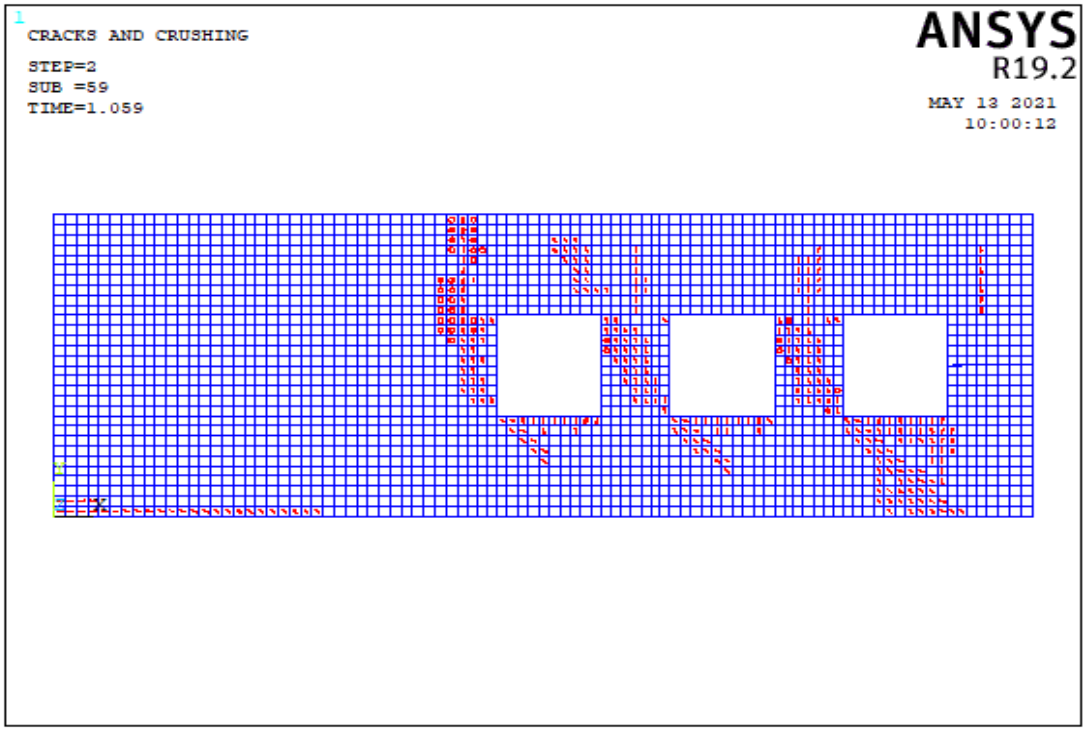

(b)

Figure 5.58. The Crack Pattern of Wall 5 Model 10 According to Compressive Strength Values of (a) 3 MPa, (b) 8 MPa

Table 5.7. Failure Patterns of Wall 5

Number of Model	Aspect ratio	fm=3 Mpa			fm=8 Mpa		
		Failure Pattern			Failure Pattern		
		Base Sliding	Rocking	Diagonal Tension	Base Sliding	Rocking	Diagonal Tension
Model 1	1.20	X			X		
	3.00			X			X
	3.00			X			X
	1.20	X			X		
Model 2	1.49						
	0.80			X			X
	0.80			X			X
	1.49						
Model 3	3.65		X			X	
	2.59						
	5.76		X			X	
	5.08		X			X	
Model 4	1.04	X					
	2.08			X			X
	2.08			X			X
	3.13			X			X
Model 5	1.36		X			X	
	1.67						
	1.15			X			
	4.28		X			X	
Model 6	8.57		X			X	
	2.00			X			
	3.20			X			
	8.57		X			X	
Model 7	1.25		X			X	
	12.50			X			X
	12.50			X			X
	1.66			X			X
Model 8	5.20		X			X	
	5.00			X			X
	5.00			X			X
	0.99			X			X
Model 9	1.51	X			X		
	3.20			X			X
	3.20			X			X
	1.51	X			X		
Model 10	0.76			X	X		
	5.00		X			X	
	5.00		X			X	
	4.00		X			X	

In Table A.5, all the length of openings is less than 3 m for all models and total opening percentage of walls in models 3, 6, and 7 are not appropriate for TEC 2018. In model 3, 4, 5, 6, 8 and 10 for wall 5, the length of corner piers is less than 1.5 m. In models 2, 4 and 5, the length of piers between the windows is more than 1 m. The length of the piers between the openings in models 1 and 7 is insufficient, which can lead to local collapse. When model 2 is compared other models, the aspect ratio of the its piers decrease and the strength of the wall increase, although its ductility decrease. In model 3, the capacity is reduced due to the 17% opening percantage and the higher aspect ratio of the pier. In model 4 and 5, the length and percentage of piers between are more than 1,44 m and 13%, respectively. Thus, the wall capacity has improved from the higher pier percentage. In model 8, as the percentage of one of the corner piers is %45, in-plane capacity of wall increase, although the length of piers between the windows decrease. Table 5.7 shows that, the diagonal tension mechanism dominates in low aspect ratio of wall. On the other hand, the rocking mechanism is predominant in high aspect ratio of wall.

5.4.1.6 Failure Modes of Wall 6

In the wall 6 type, there are 11 different wall models. The impact of four windows openings was studied in these models of wall 6. Table A.6 shows the lengths of the walls. As seen in Figure 5.3, each pier is designated from left to right. The crack patterns obtained from the analysis of wall models corresponding to 11 different wall models are described in this section.

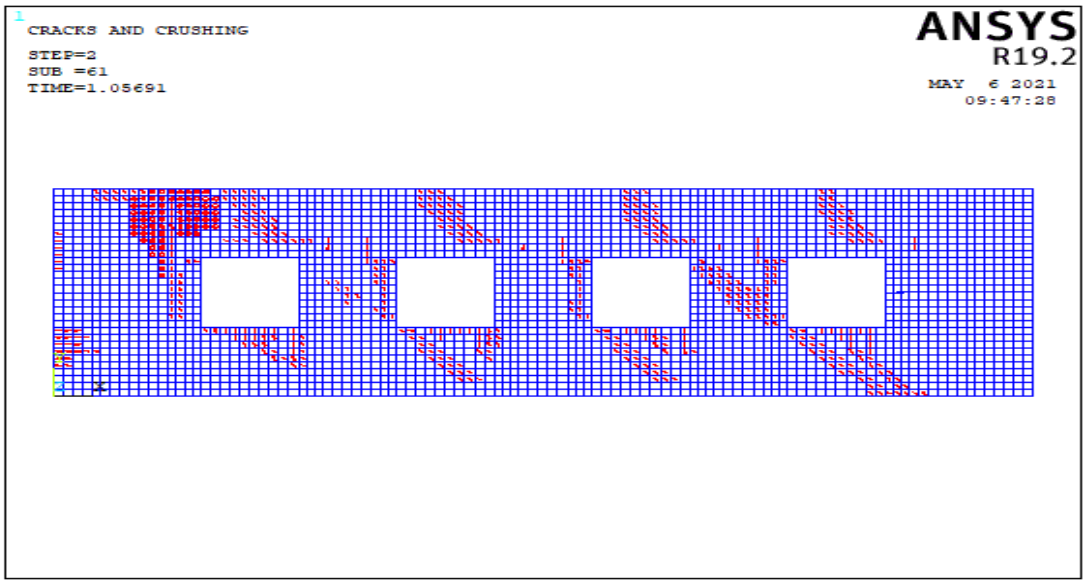

(a)

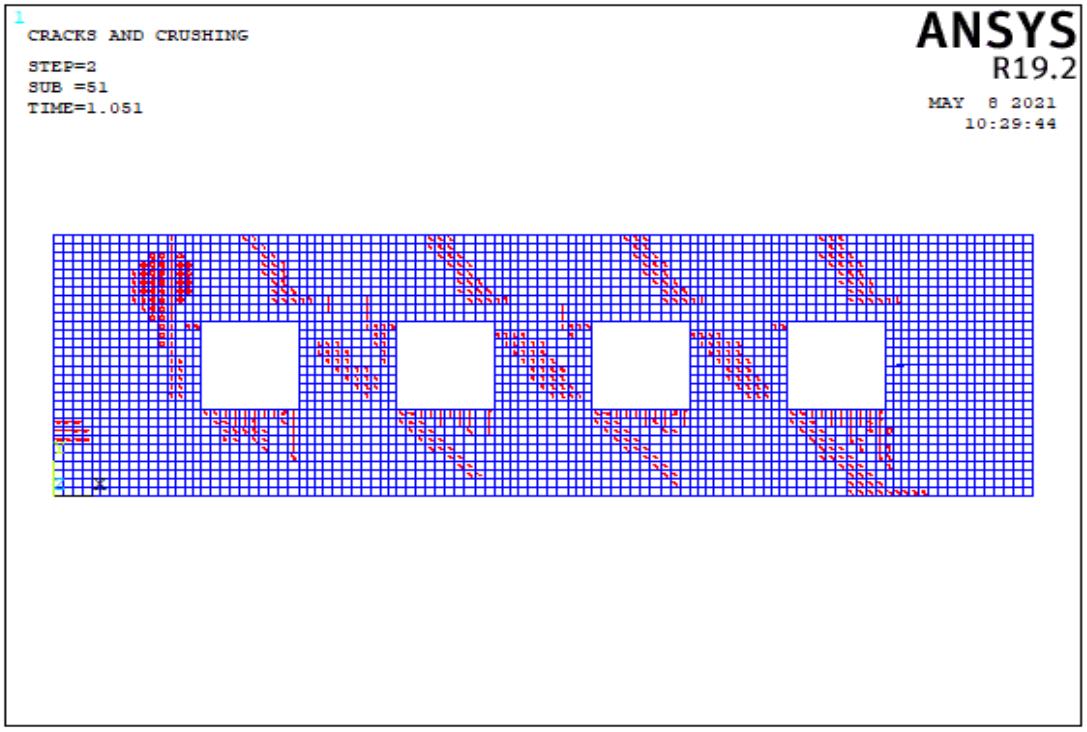

(b)

Figure 5.59. The Crack Pattern of Wall 6 Model 1 According to Compressive Strength Values of (a) 3 MPa, (b) 8 MPa

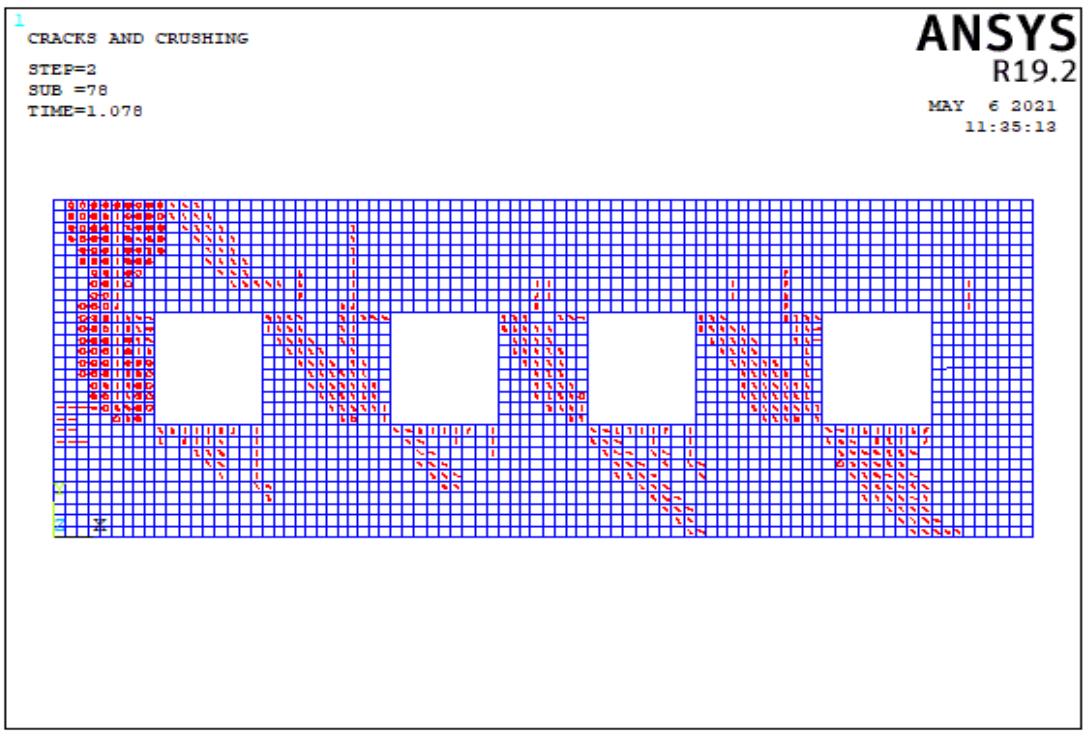

(a)

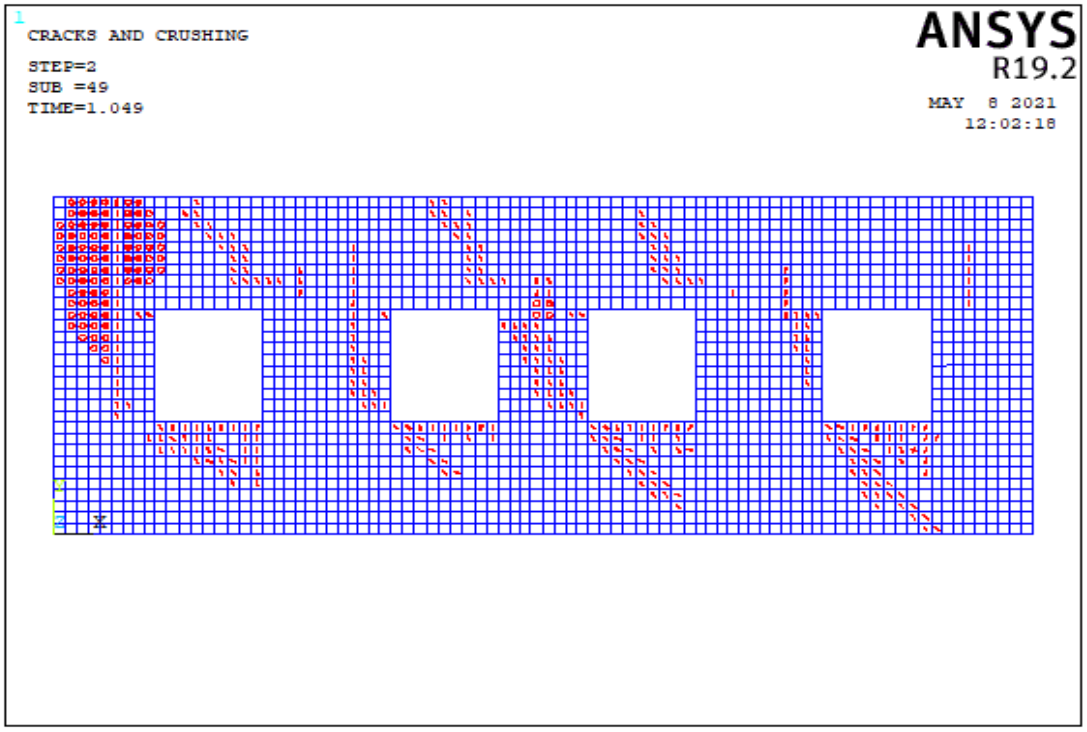

(b)

Figure 5.60. The Crack Pattern of Wall 6 Model 2 According to Compressive Strength Values of (a) 3 MPa, (b) 8 MPa

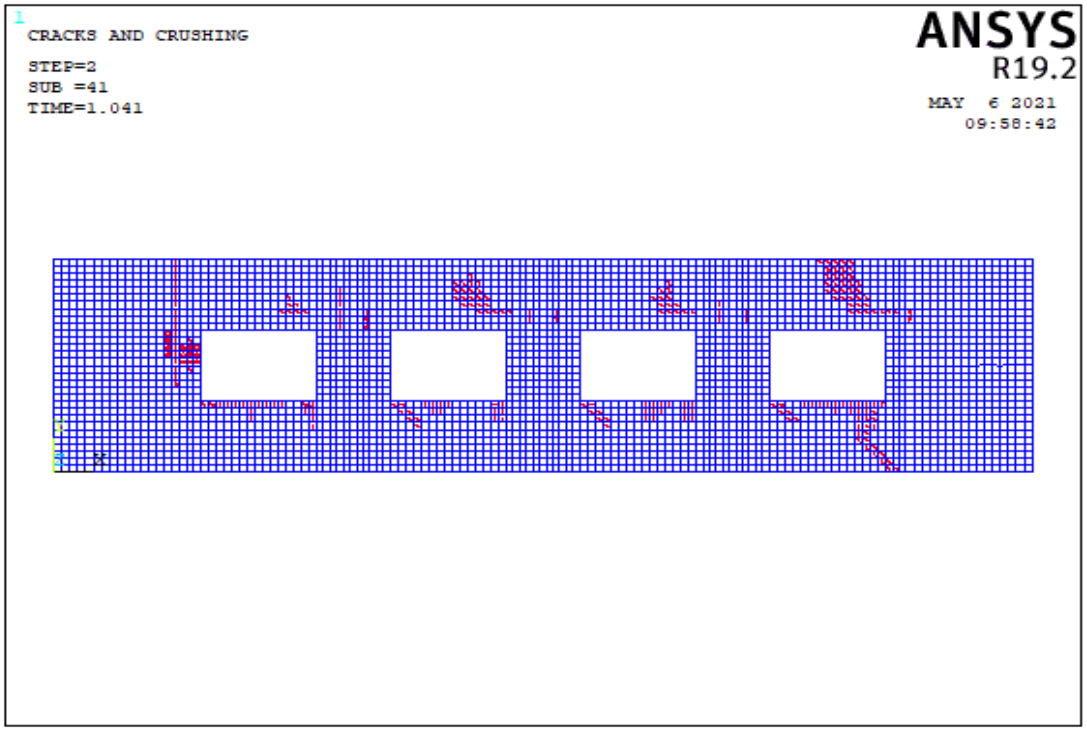

(a)

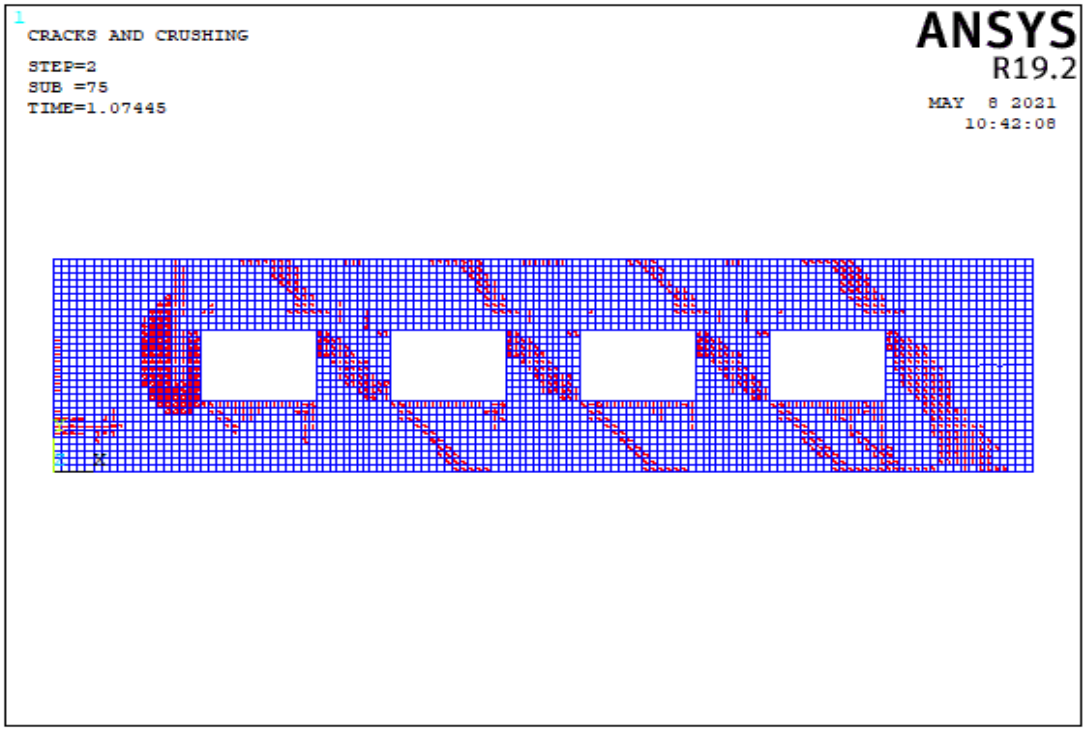

(b)

Figure 5.61. The Crack Pattern of Wall 6 Model 3 According to Compressive Strength Values of (a) 3 MPa, (b) 8 MPa

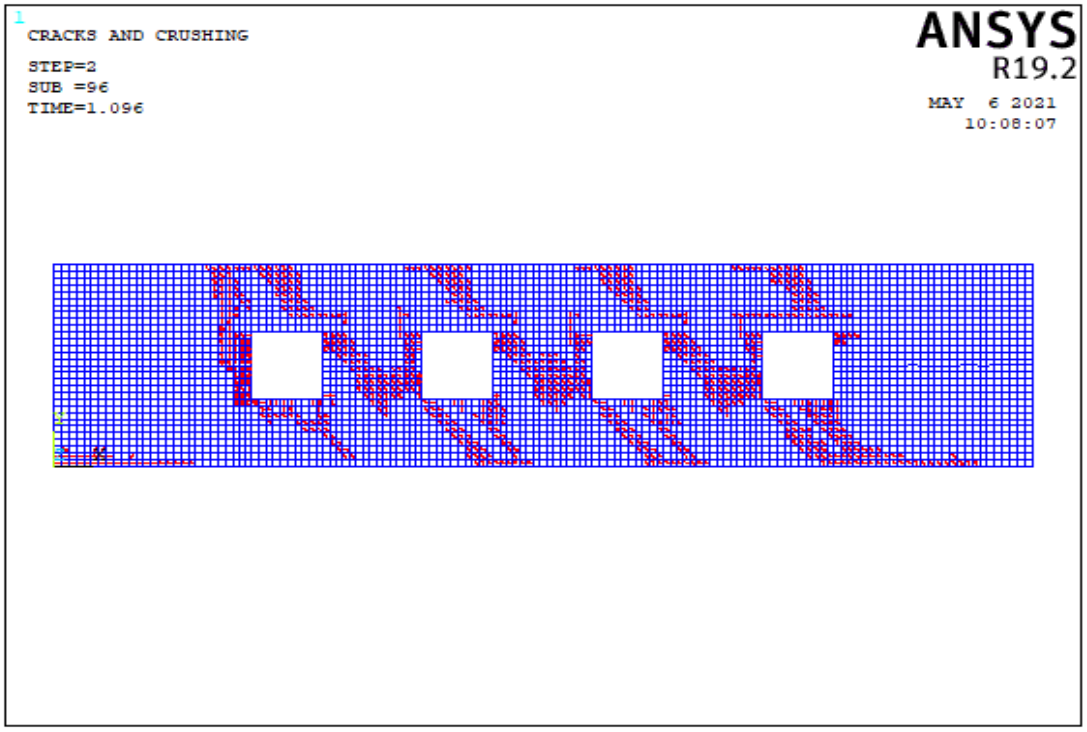

(a)

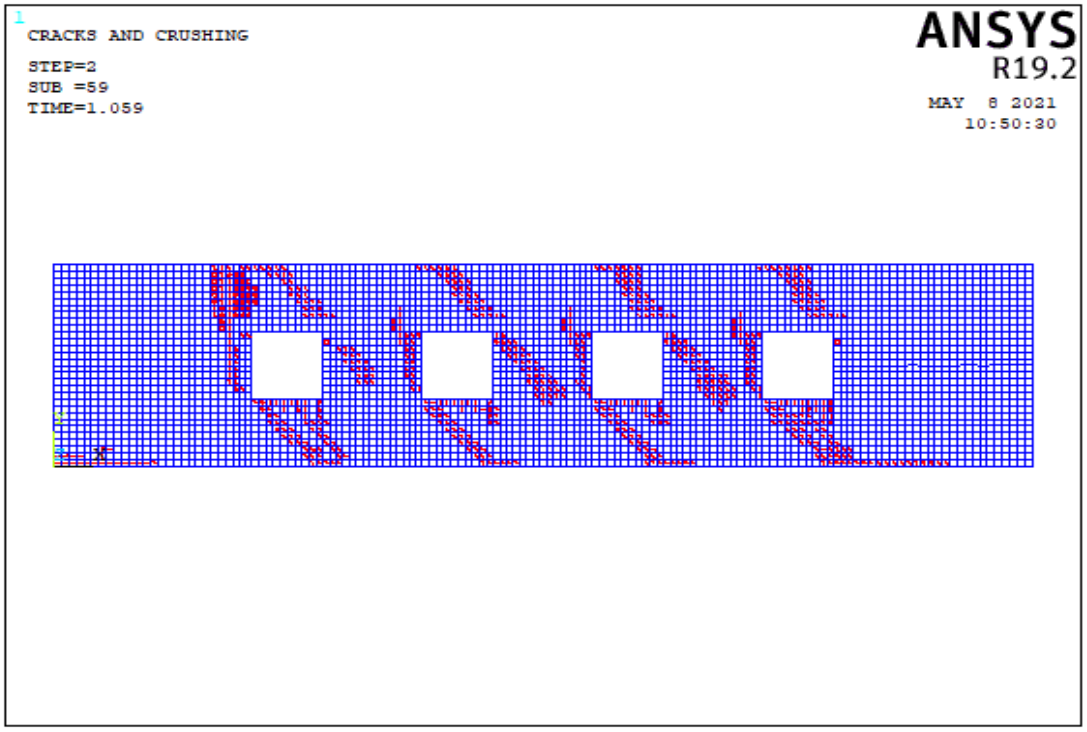

(b)

Figure 5.62. The Crack Pattern of Wall 6 Model 4 According to Compressive Strength Values of (a) 3 MPa, (b) 8 MPa

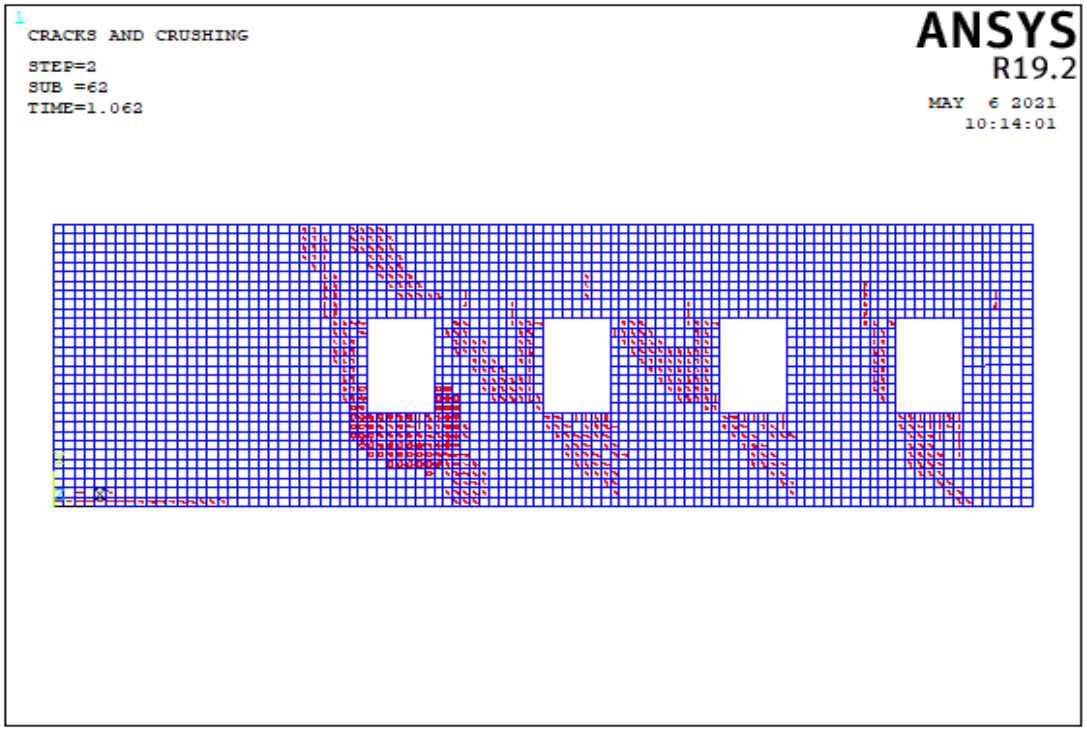

(a)

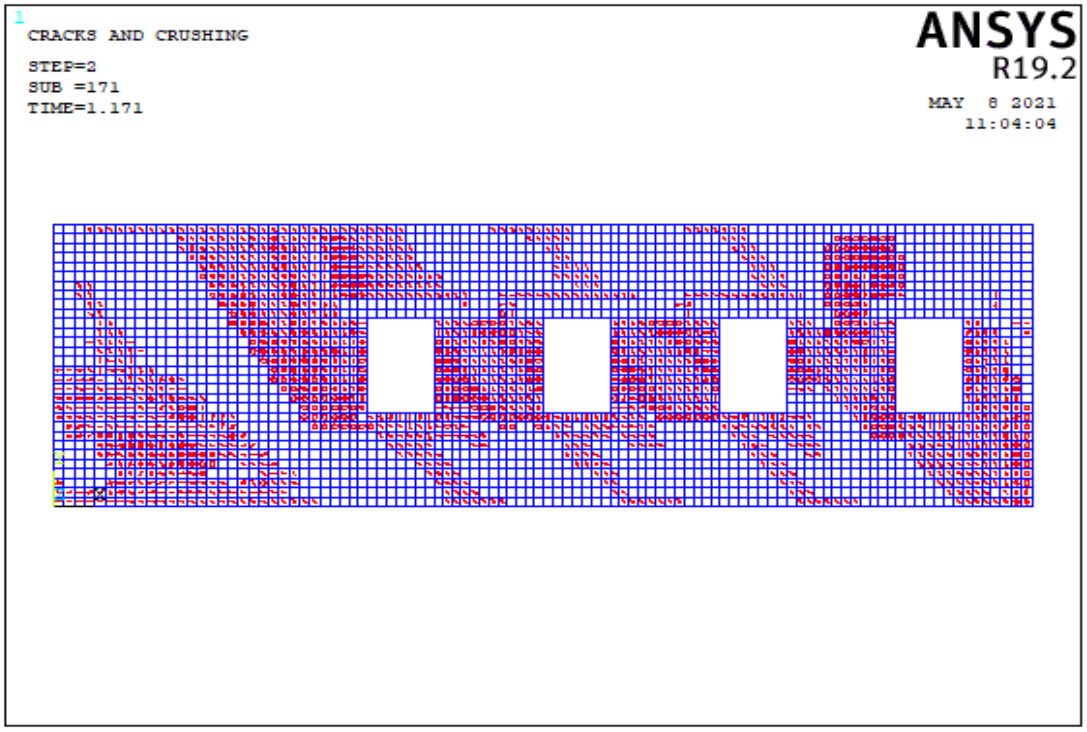

(b)

Figure 5.63. The Crack Pattern of Wall 6 Model 5 According to Compressive Strength Values of (a) 3 MPa, (b) 8 MPa

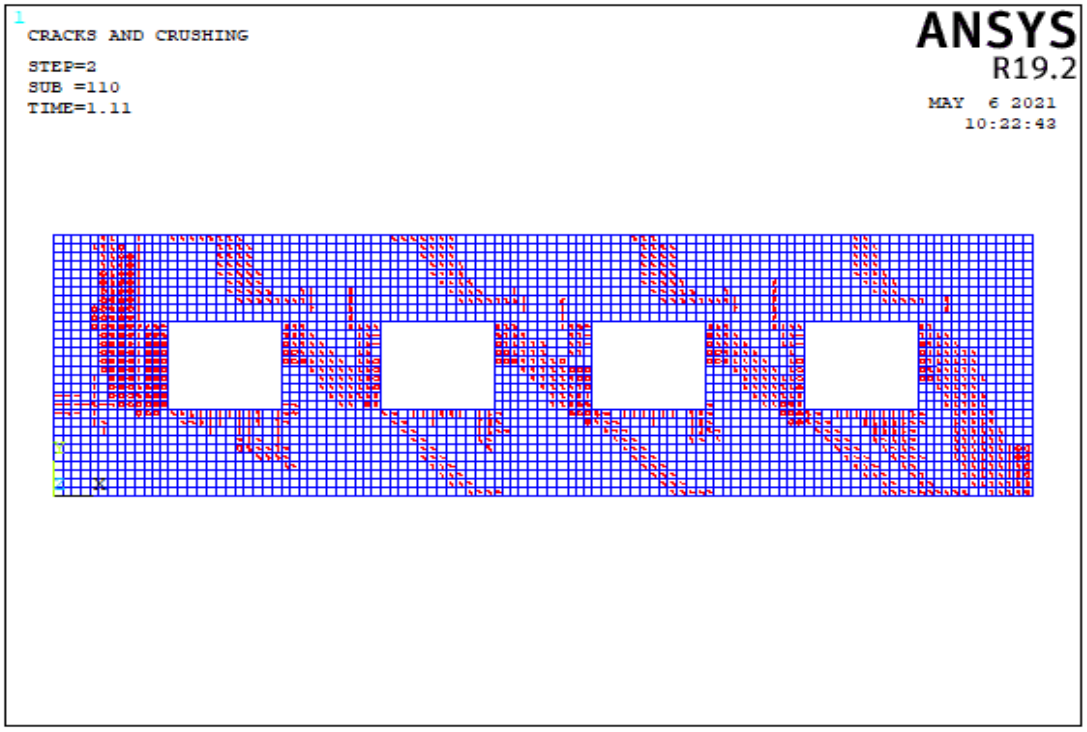

(a)

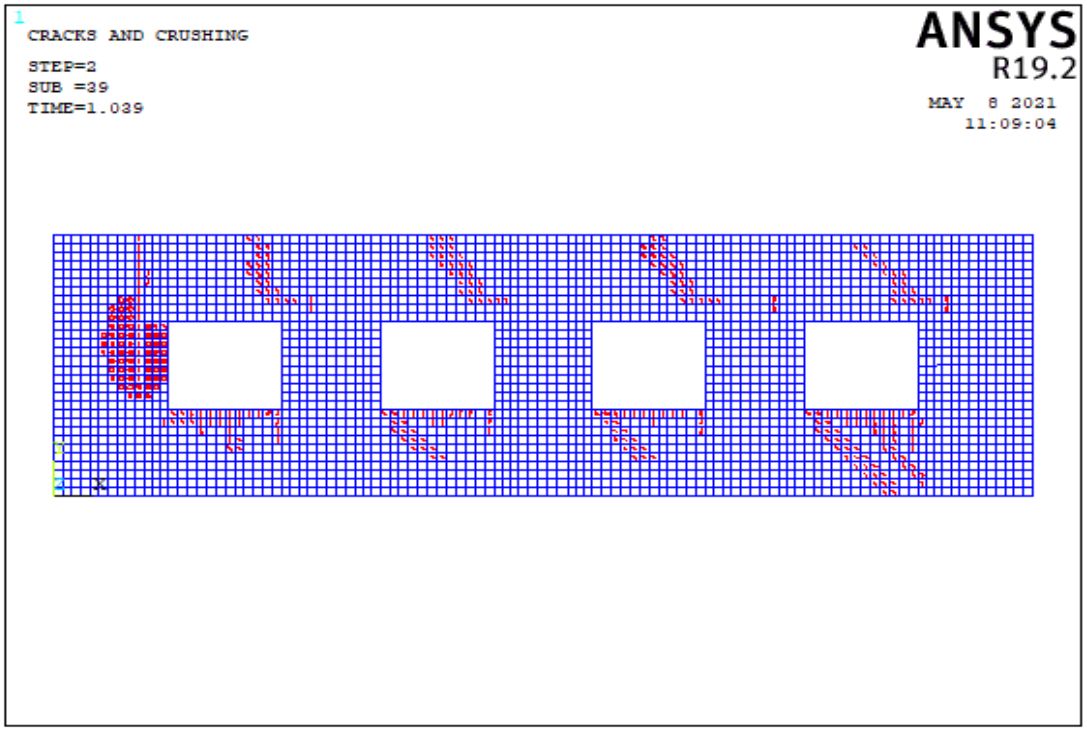

(b)

Figure 5.64. The Crack Pattern of Wall 6 Model 6 According to Compressive Strength Values of (a) 3 MPa, (b) 8 MPa

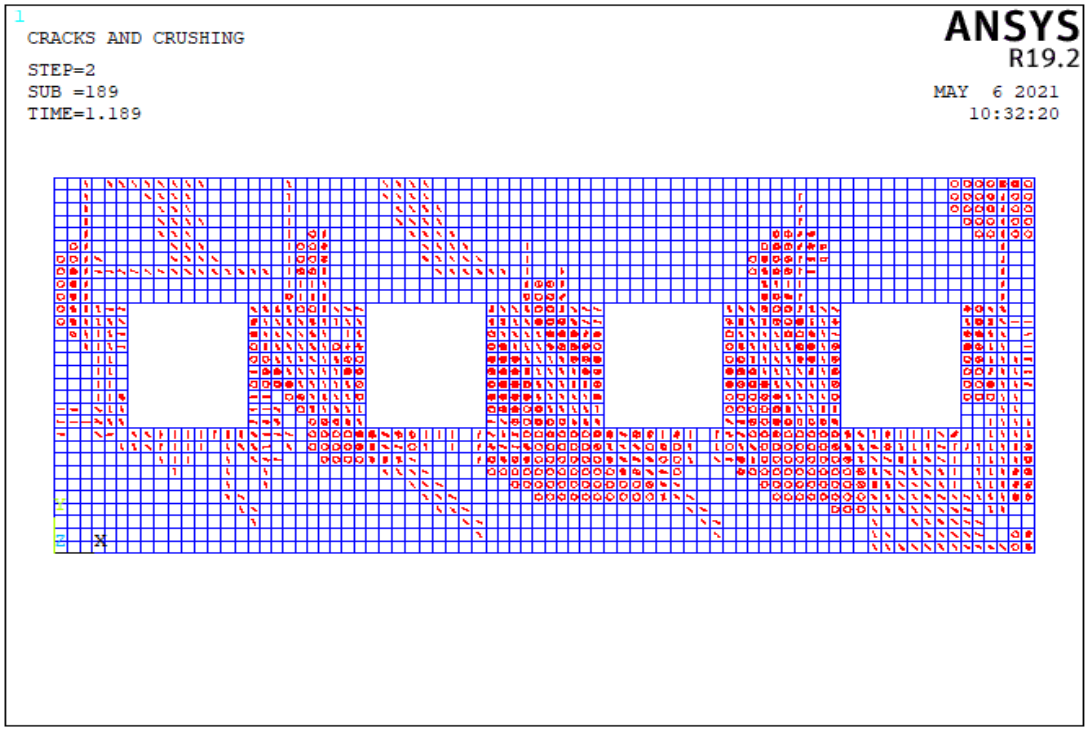

(a)

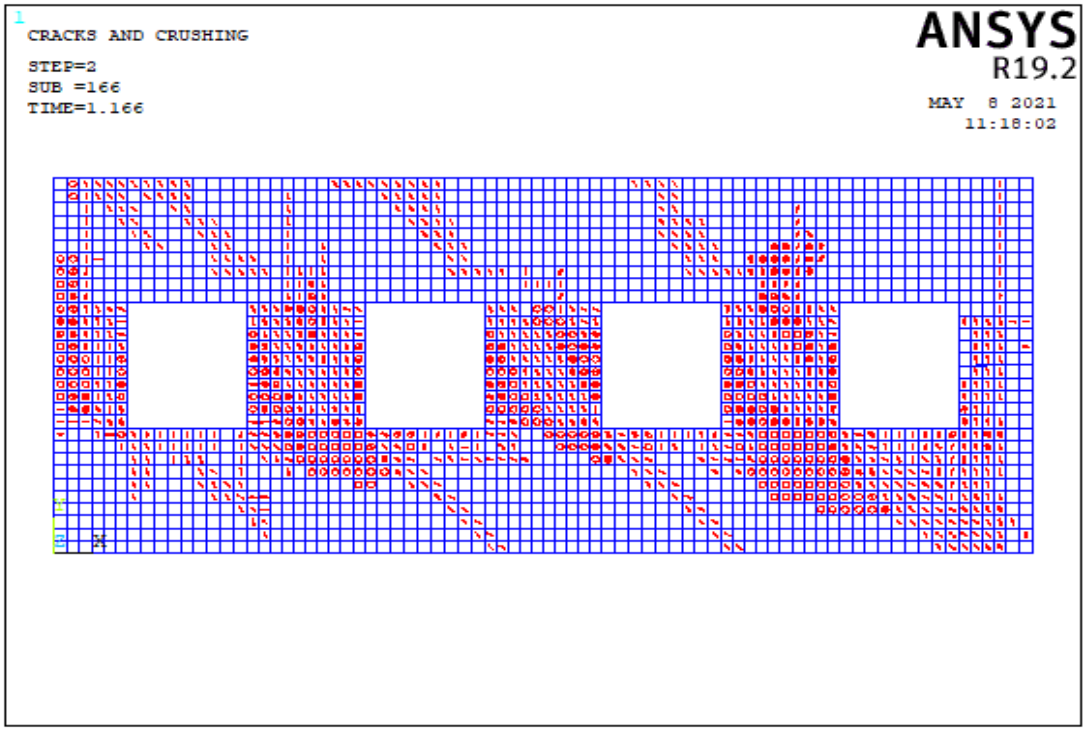

(b)

Figure 5.65. The Crack Pattern of Wall 6 Model 7 According to Compressive Strength Values of (a) 3 MPa, (b) 8 MPa

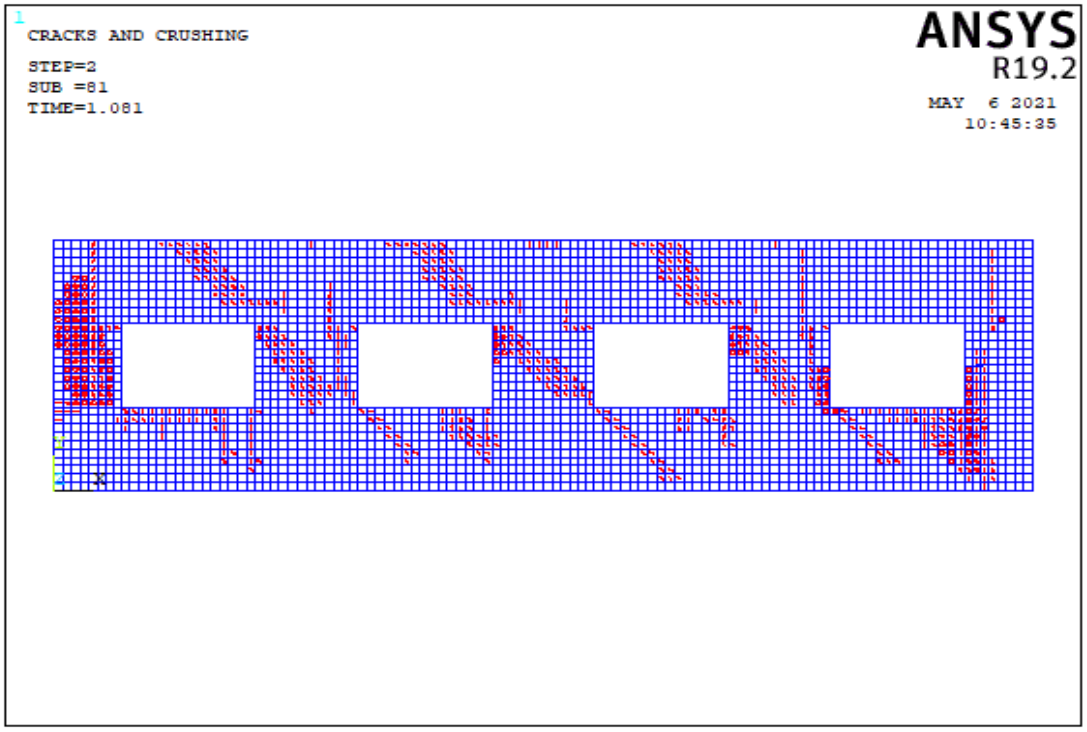

(a)

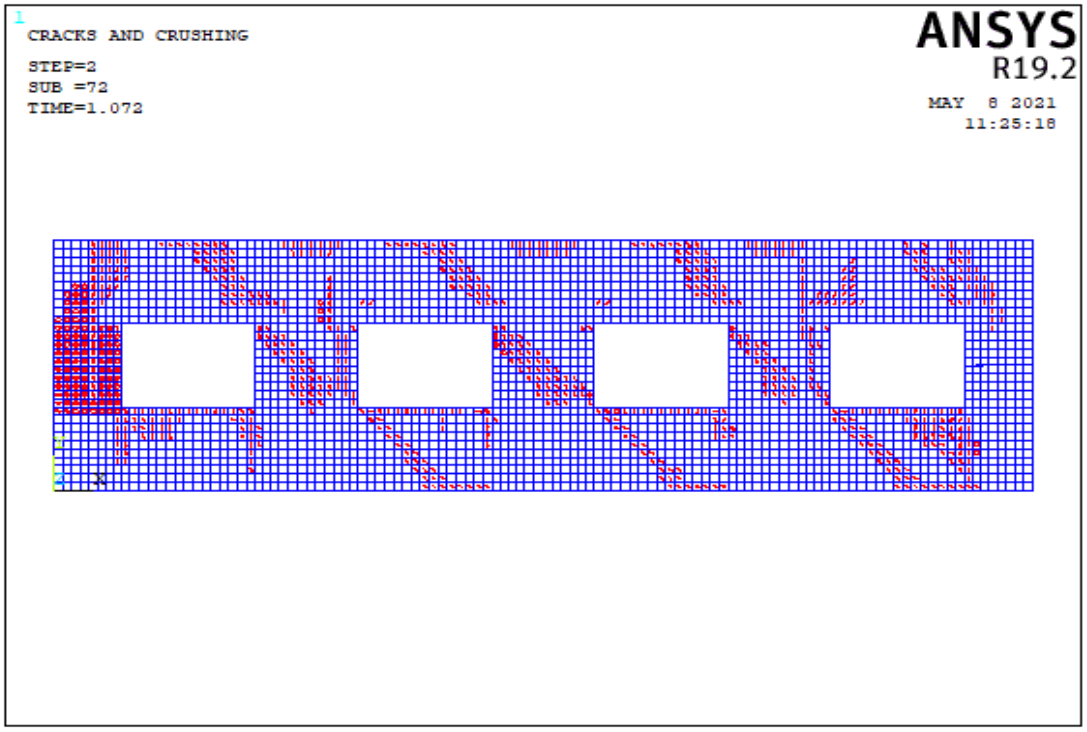

(b)

Figure 5.66. The Crack Pattern of Wall 6 Model 8 According to Compressive Strength Values of (a) 3 MPa, (b) 8 MPa

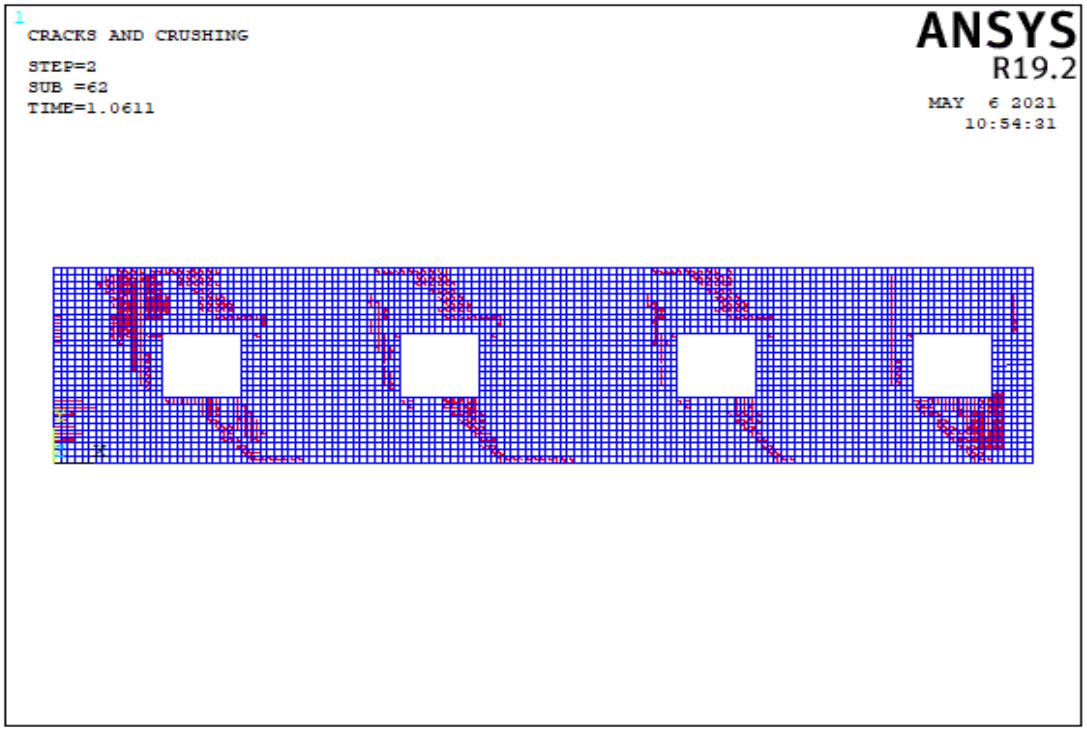

(a)

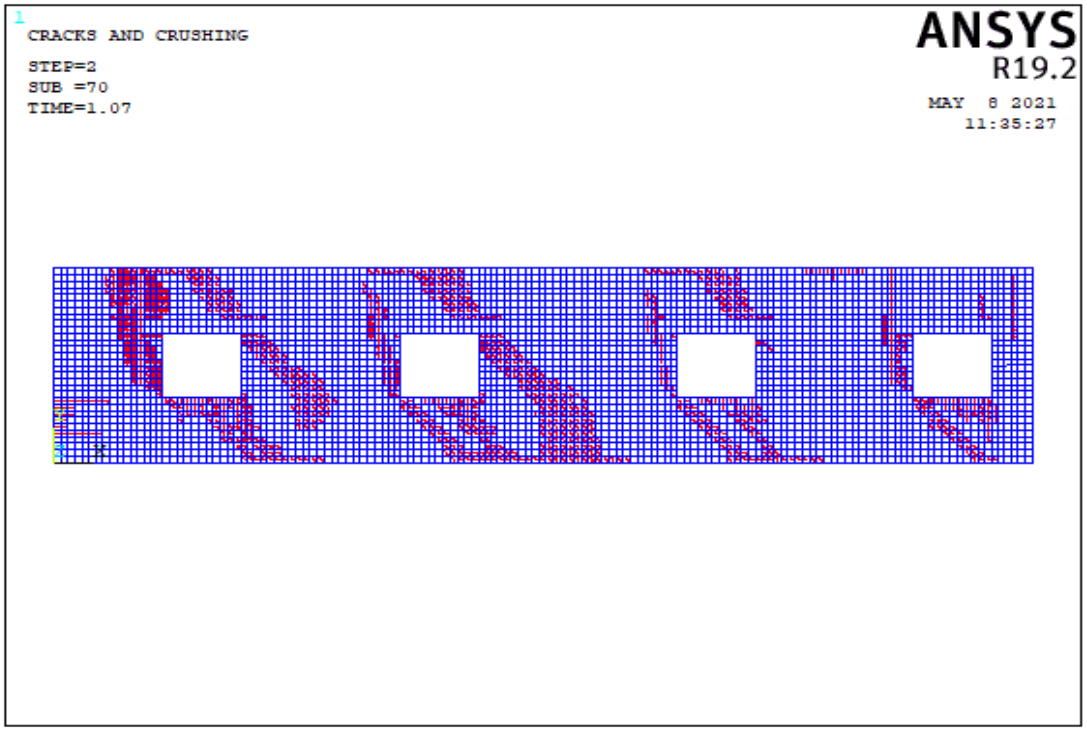

(b)

Figure 5.67. The Crack Pattern of Wall 6 Model 9 According to Compressive Strength Values of (a) 3 MPa, (b) 8 MPa

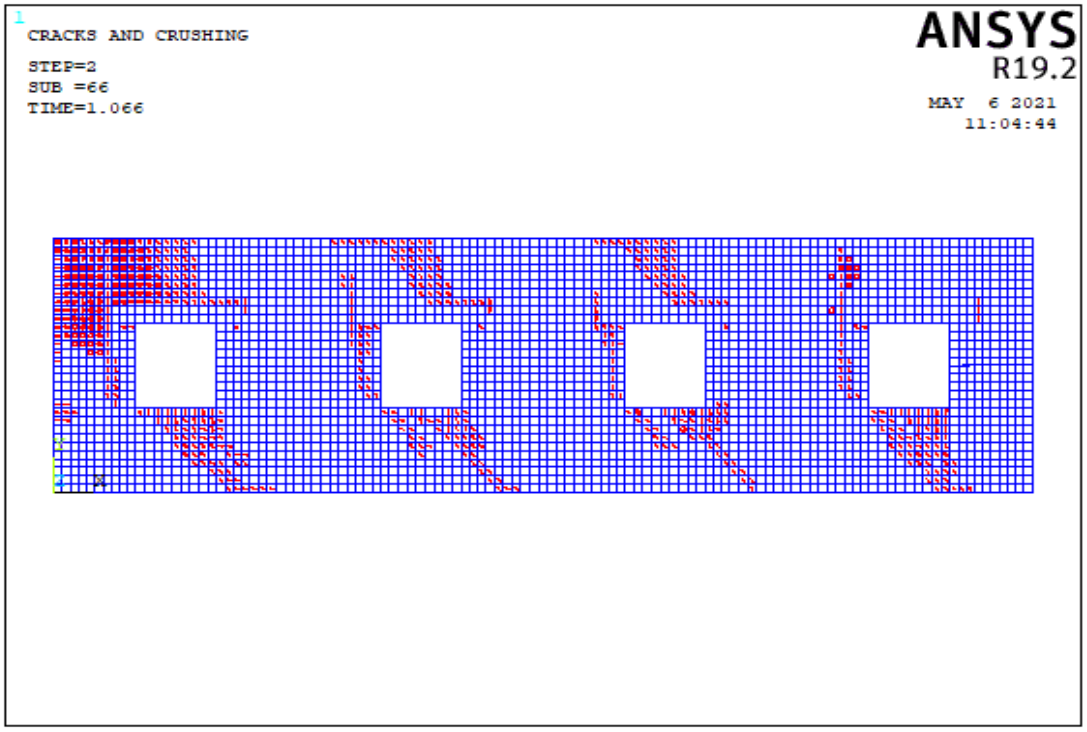

(a)

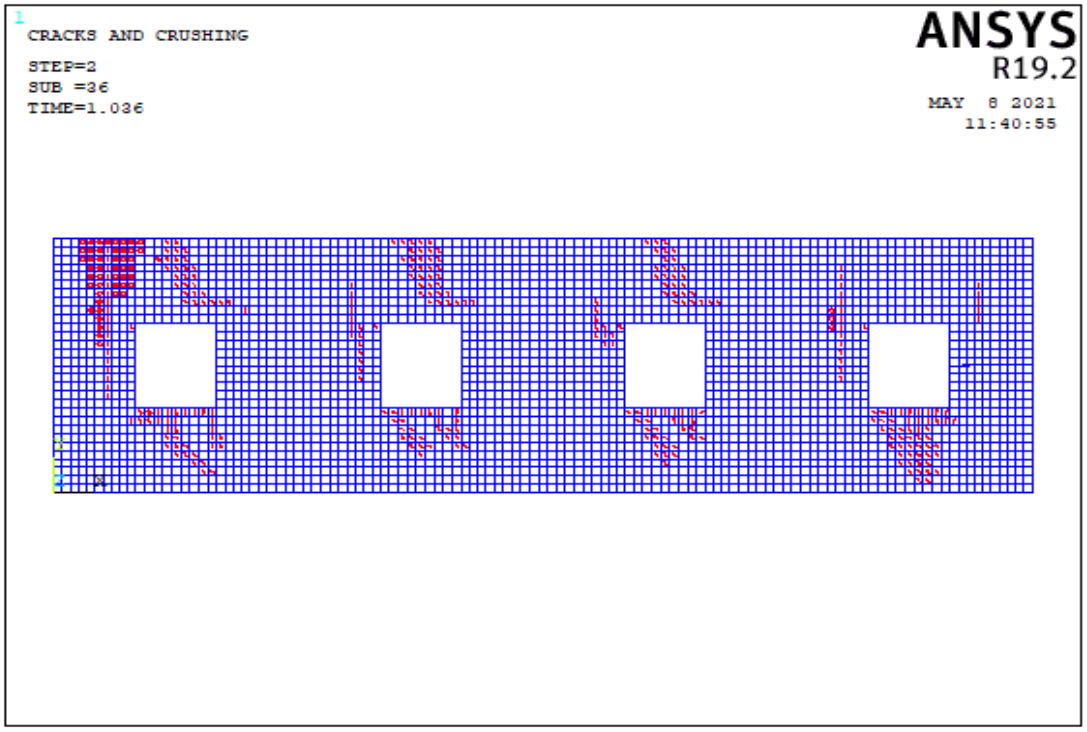

(b)

Figure 5.68. The Crack Pattern of Wall 6 Model 10 According to Compressive Strength Values of (a) 3 MPa, (b) 8 MPa

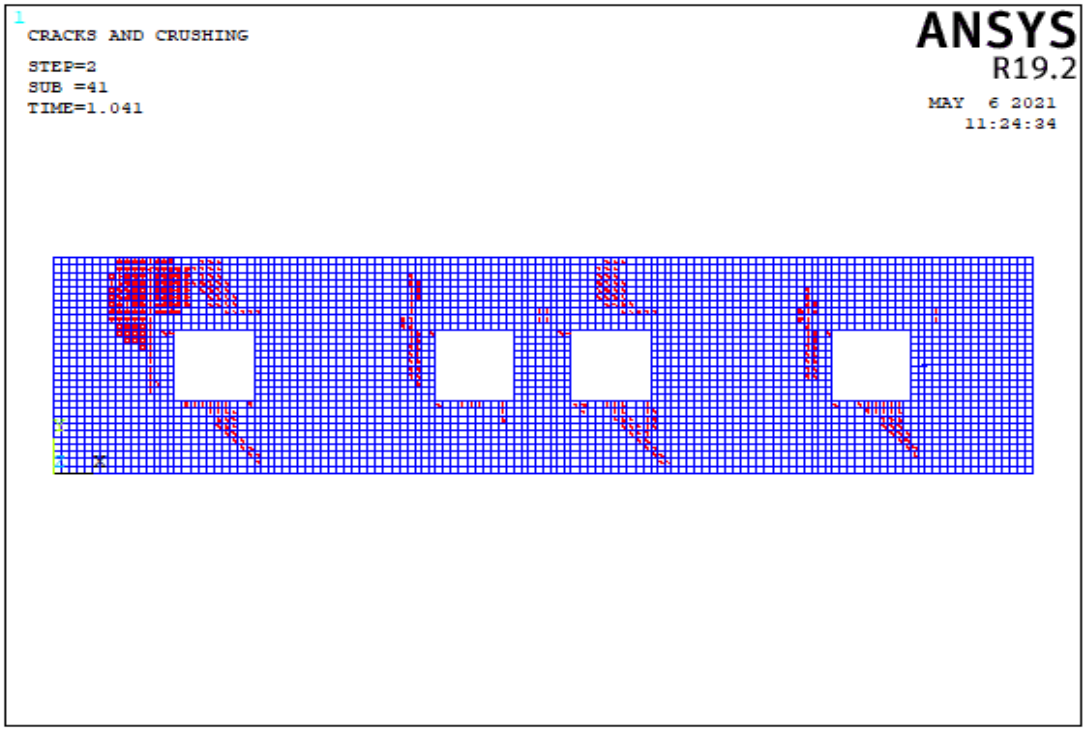

(a)

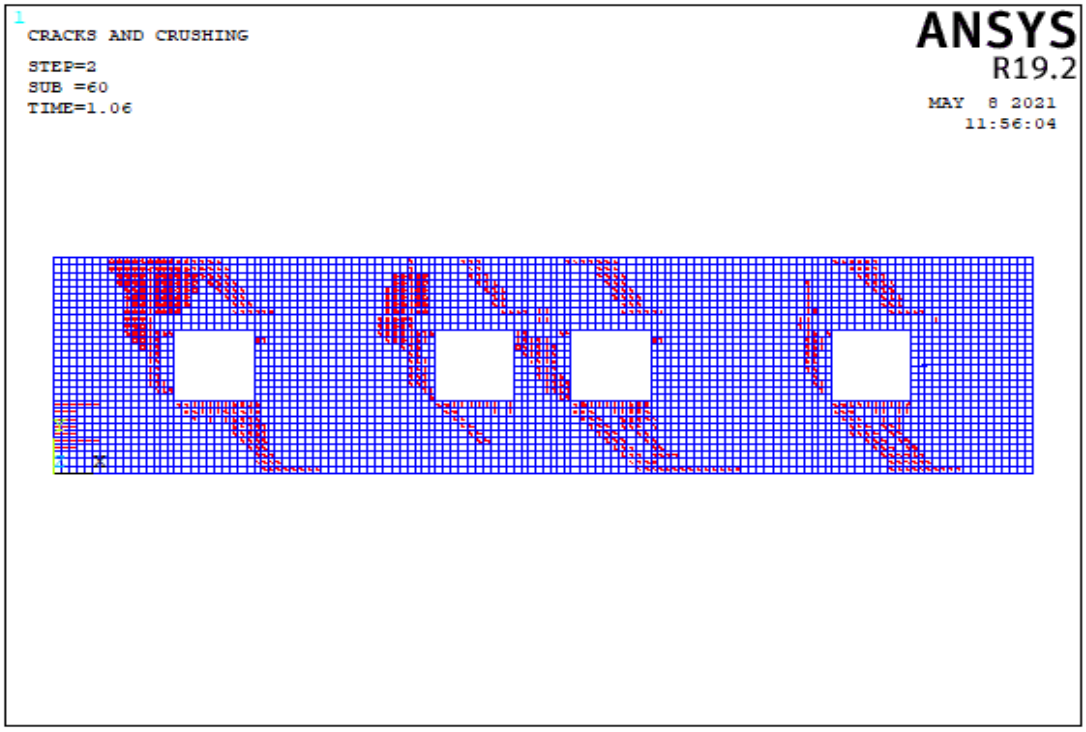

(b)

Figure 5.69. The Crack Pattern of Wall 6 Model 11 According to Compressive Strength Values of (a) 3 MPa, (b) 8 MPa

Table 5.8. Failure Patterns of Wall 6

Number of Model	Aspect ratio	fm=3 Mpa			fm=8 Mpa		
		Failure Pattern			Failure Pattern		
		Base	Rocki	Diagonal	Base	Rocki	Diagonal
Model 1	2.00		X			X	
	3.00			X			X
	3.00			X			X
	3.00			X			X
	2.00						
Model 2	3.77		X			X	
	2.99			X			X
	4.29			X			X
	2.99			X			X
	3.77						
Model 3	1.64					X	
	3.28						X
	3.28						X
	3.28						X
	1.64						X
Model 4	1.14	X			X		
	2.28			X			X
	2.28			X			X
	2.28			X			X
	1.14	X			X		
Model 5	1.01	X			X		
	2.90			X			X
	2.90			X			X
	2.90			X			X
	4.64		X			X	
Model 6	2.57		X			X	
	3.00			X			
	3.00			X			
	3.00			X			
	2.57		X			X	
Model 7	5.75		X			X	
	3.59			X			X
	3.59			X			X
	3.59			X			X
	5.75		X			X	
Model 8	4.18		X			X	
	2.75			X			X
	2.75			X			X
	2.75			X			X
	4.18		X			X	
Model 9	2.00		X			X	
	1.38						X
	1.10						X
	1.38						
	5.50		X			X	
Model 10	3.50		X			X	
	1.75						
	1.75						
	1.75						
	3.50		X			X	
Model 11	2.00		X			X	
	1.33		X			X	
	0.93						X
	1.33						
	2.00						

In Table A.6, all length of openings is less than 3 m for all models and total opening percentage of walls in models 2, 3, 6, 7 and 8 are not appropriate for TEC 2018. In models 1, 3, 4 and 11, the length of corner piers is more than 1.5 m. In models 2, 3 and 7, the length of piers between the windows are less than 1 meter. When considering models 1 and 6, the lengths of the walls are similar, but the percentages of openings are different. The strength of model 6 reduces as the opening percentage or aspect ratio of the corner piers increase. The model 4 and 9 show that the strength of models rise as aspect ratio of piers decrease. When the length and percentage of piers between windows are 1,32 and 10%, strength of wall increase significantly. In addition, the localized failure of corner piers does not occur when piers are larger than 1.5 m. Model 7 shows that wall has more ductility, as the aspect ratio of the wall increases, although its strength decreases.

5.4.1.7 Failure Modes of Wall 7

In the wall 7 type, there are 10 different wall models. The impact of five windows openings was studied in these models of wall 7. Table A.7 shows the lengths of the walls. As seen in Figure 5.3, each pier is designated from left to right. The crack patterns obtained from the analysis of wall models corresponding to 10 different wall models are described in this section.

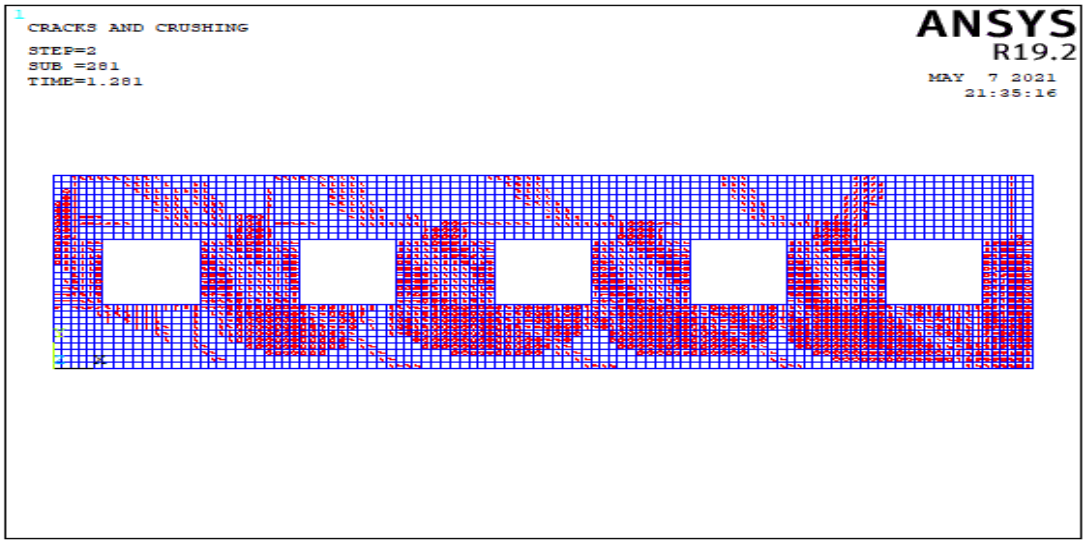

(a)

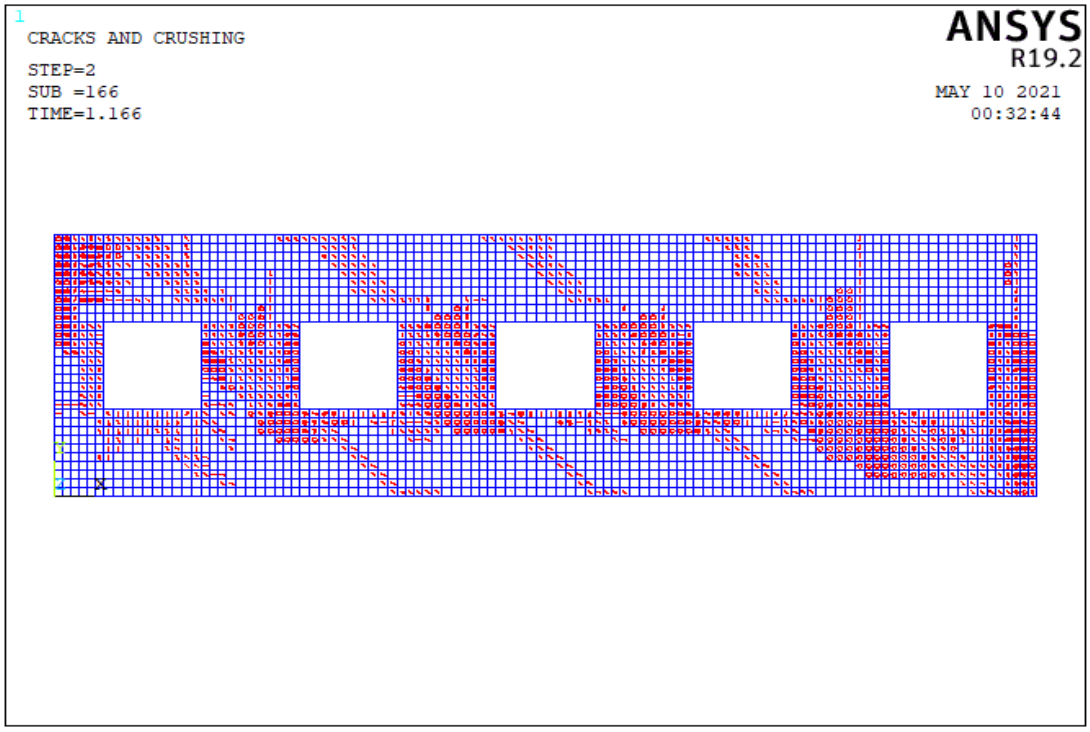

(b)

Figure 5.70. The Crack Pattern of Wall 7 Model 1 According to Compressive Strength Values of (a) 3 MPa, (b) 8 MPa

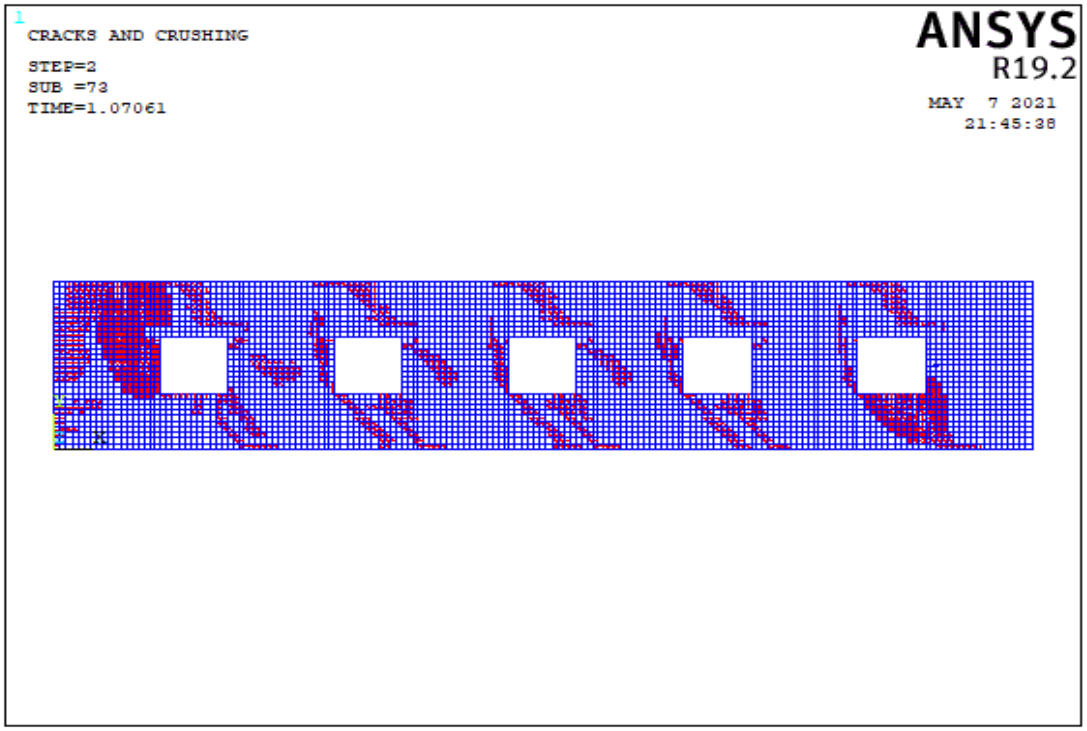

(a)

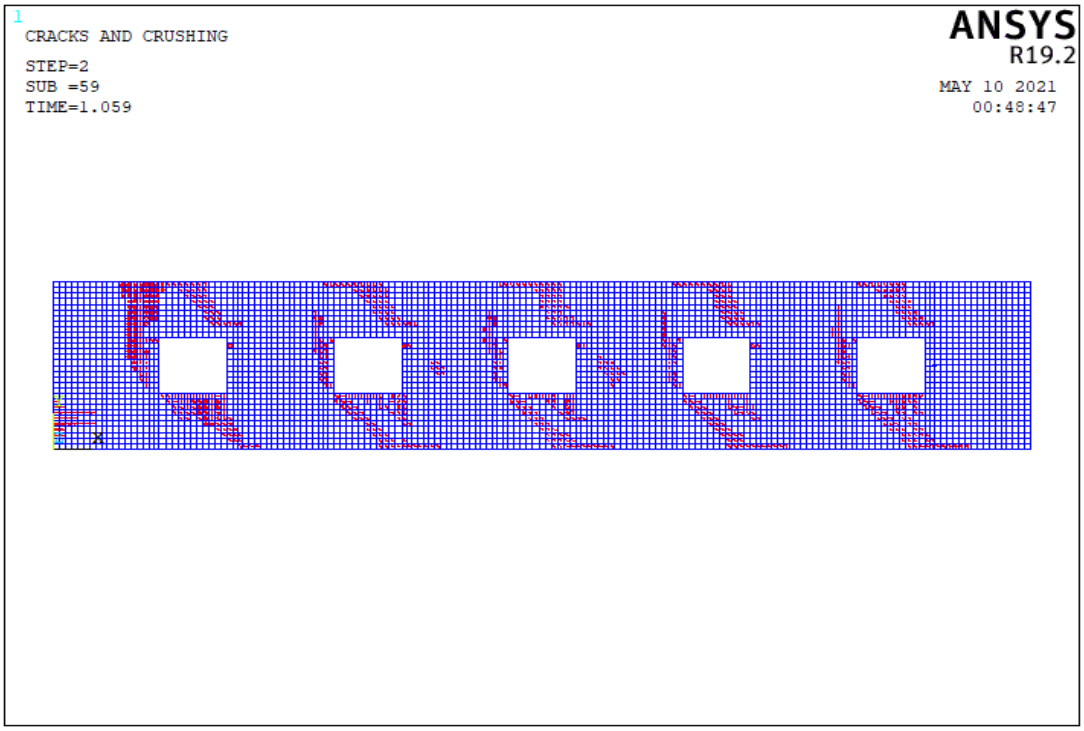

(b)

Figure 5.71. The Crack Pattern of Wall 7 Model 2 According to Compressive Strength Values of (a) 3 MPa, (b) 8 MPa

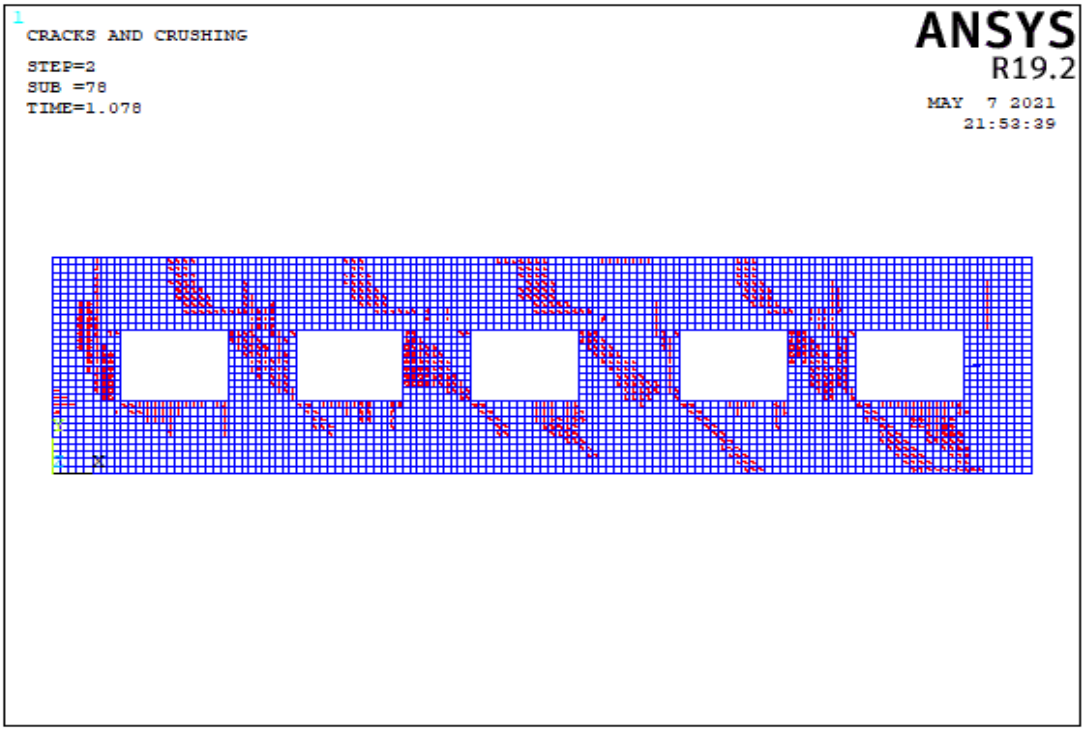

(a)

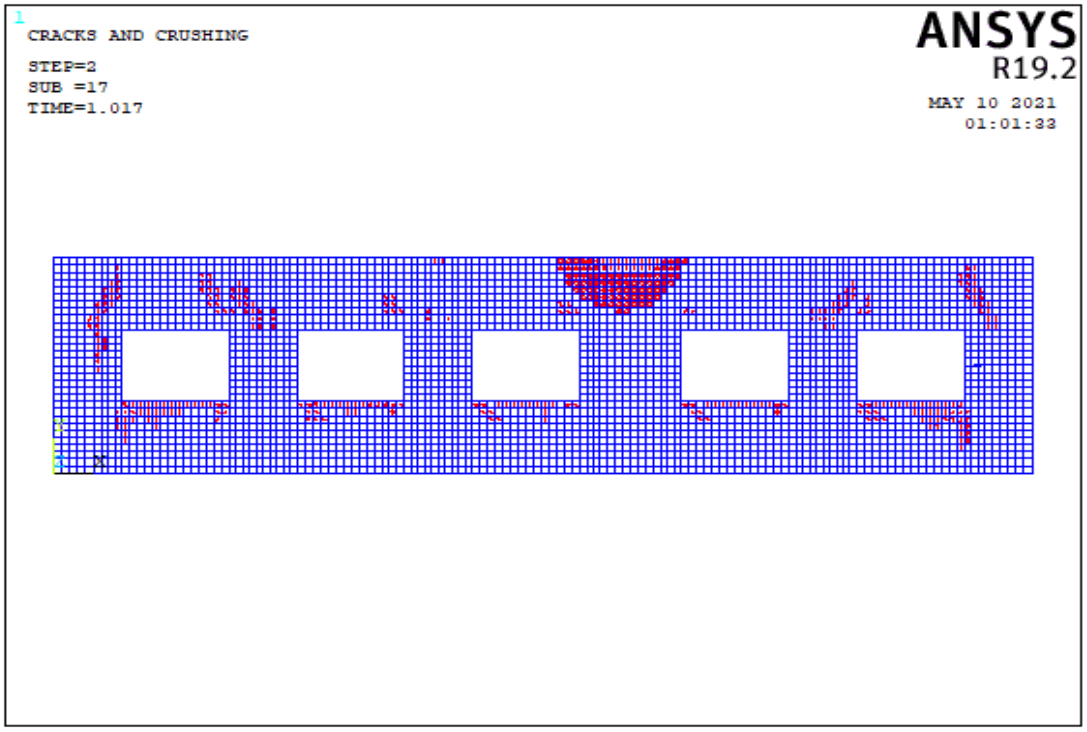

(b)

Figure 5.72. The Crack Pattern of Wall 7 Model 3 According to Compressive Strength Values of (a) 3 MPa, (b) 8 MPa

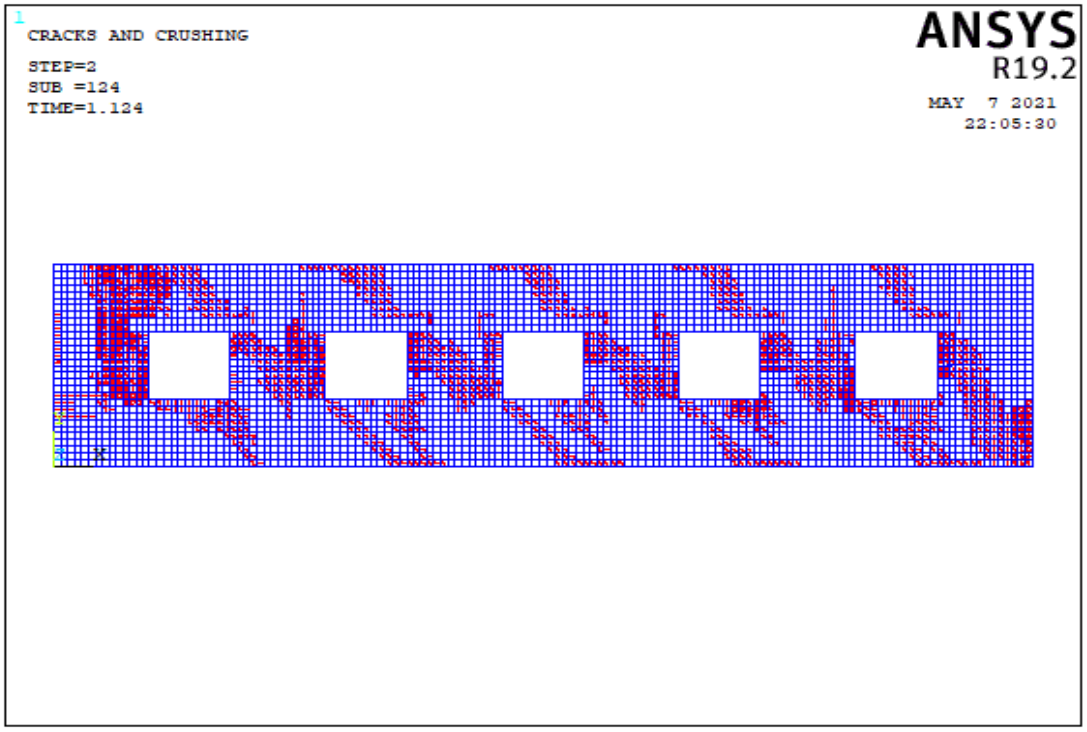

(a)

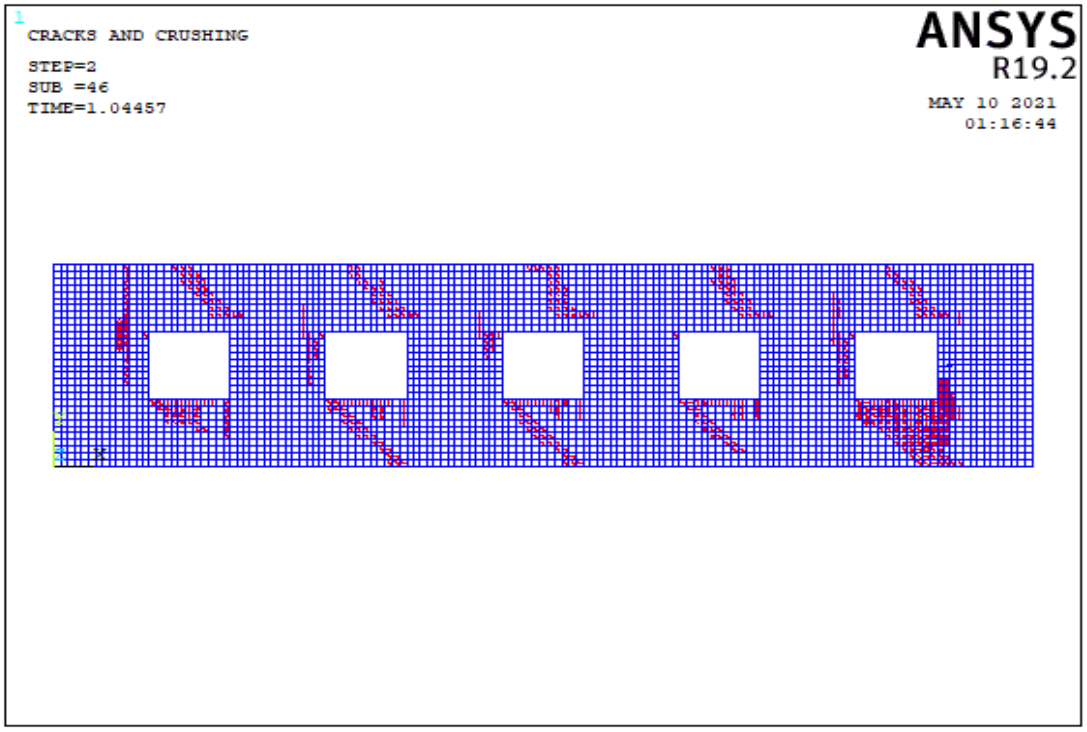

(b)

Figure 5.73. The Crack Pattern of Wall 7 Model 4 According to Compressive Strength Values of (a) 3 MPa, (b) 8 MPa

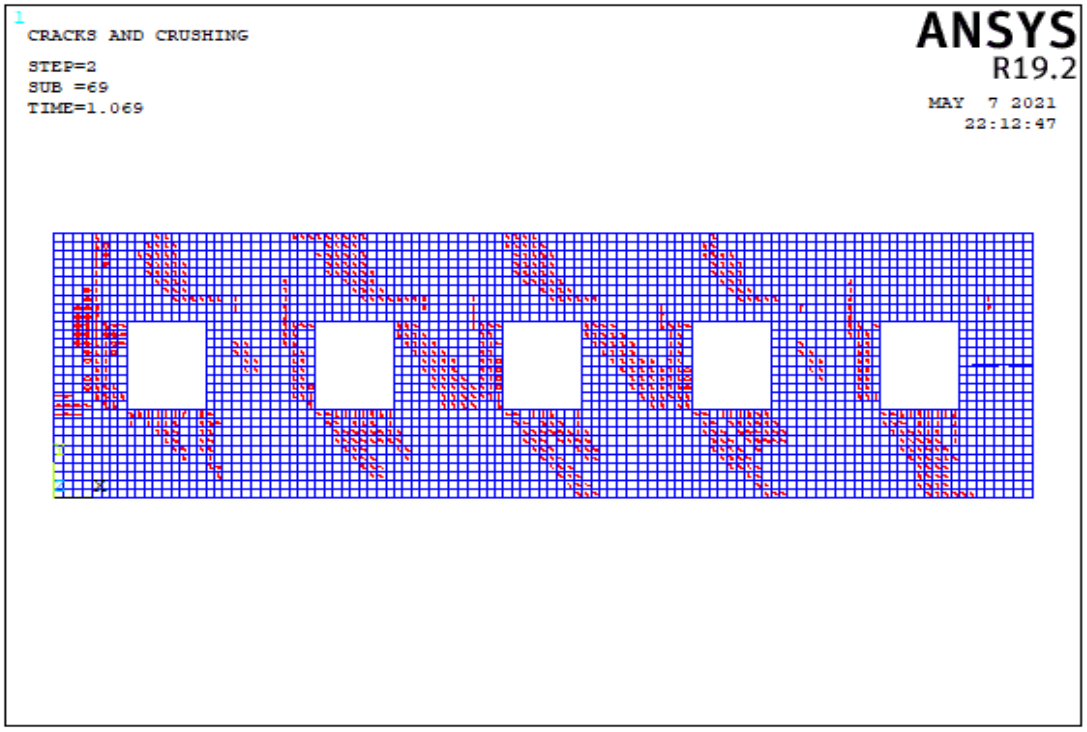

(a)

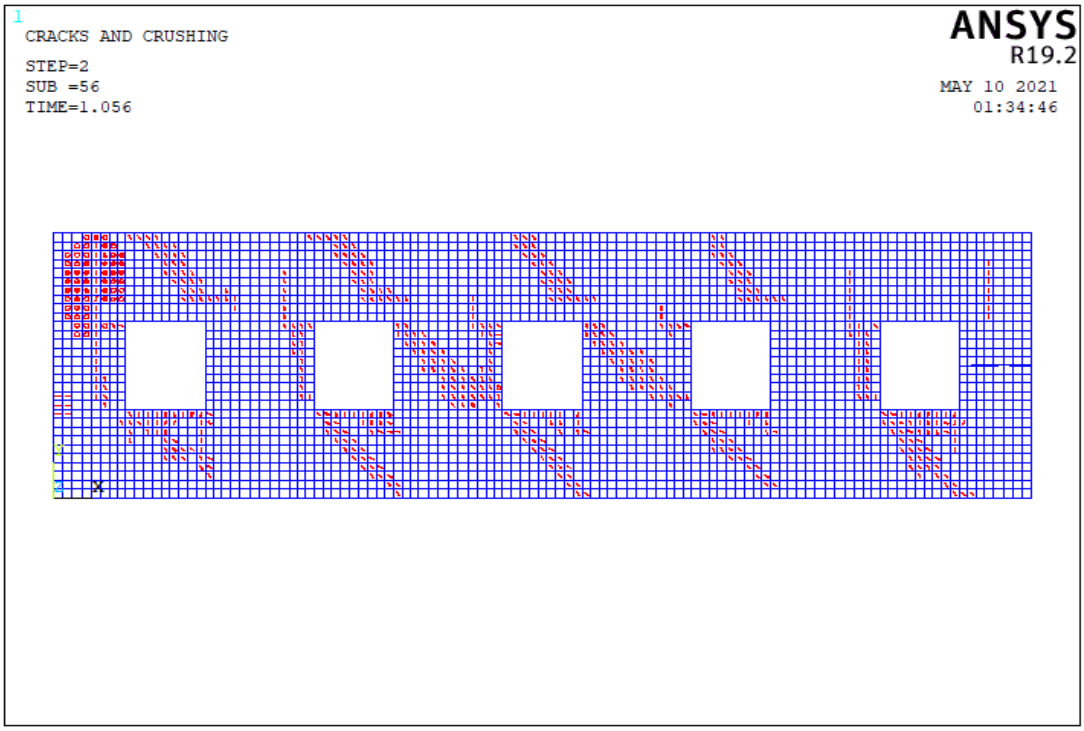

(b)

Figure 5.74. The Crack Pattern of Wall 7 Model 5 According to Compressive Strength Values of (a) 3 MPa, (b) 8 MPa

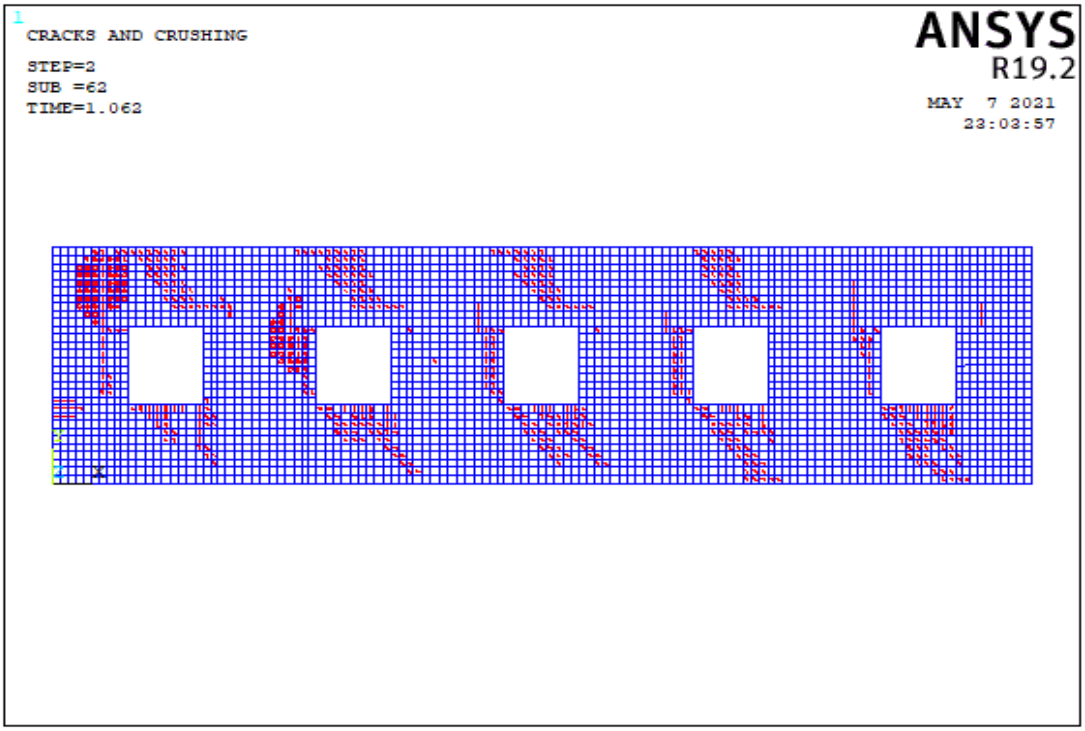

(a)

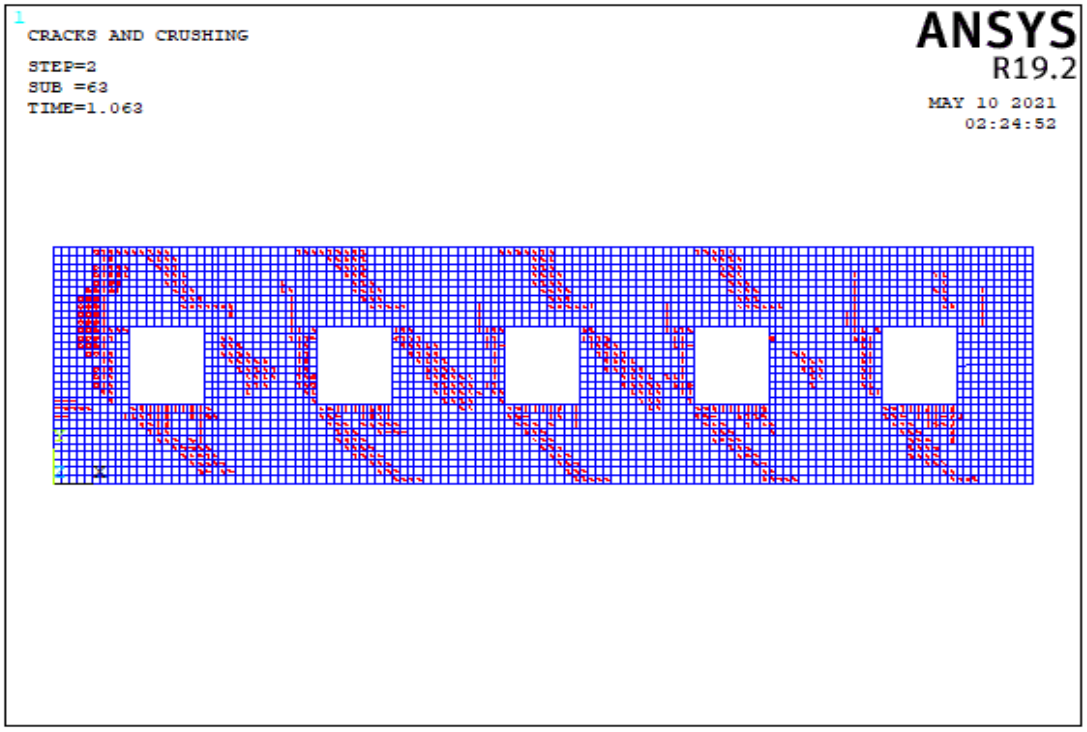

(b)

Figure 5.75. The Crack Pattern of Wall 7 Model 6 According to Compressive Strength Values of (a) 3 MPa, (b) 8 MPa

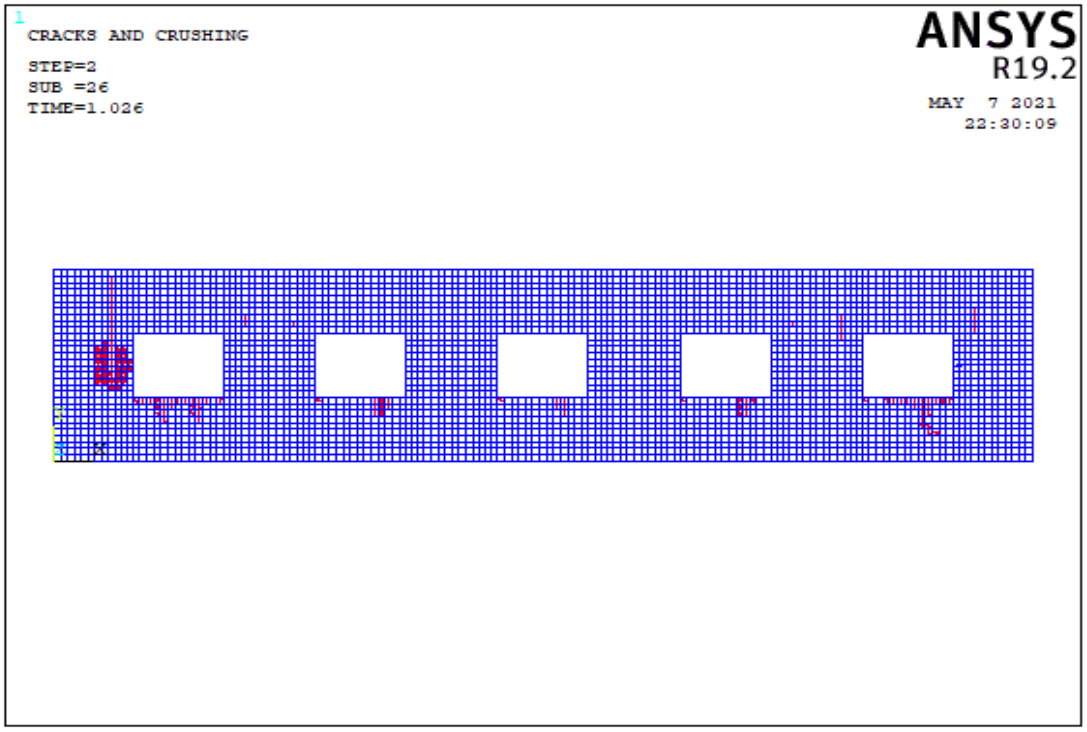

(a)

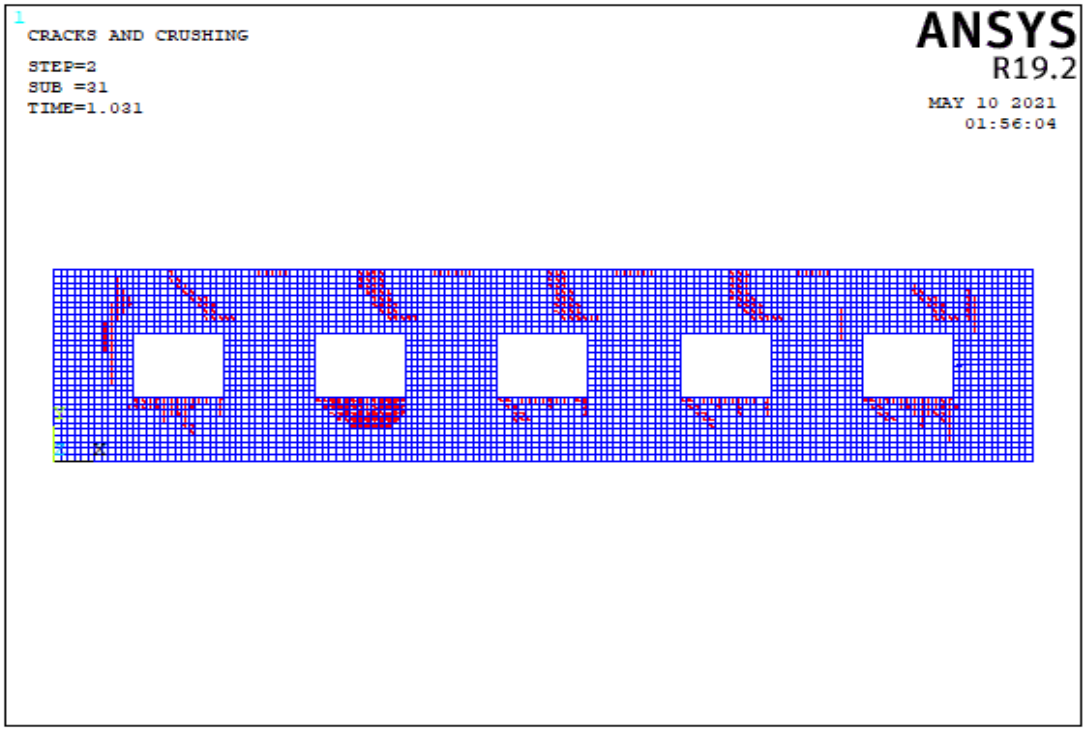

(b)

Figure 5.76. The Crack Pattern of Wall 7 Model 7 According to Compressive Strength Values of (a) 3 MPa, (b) 8 MPa

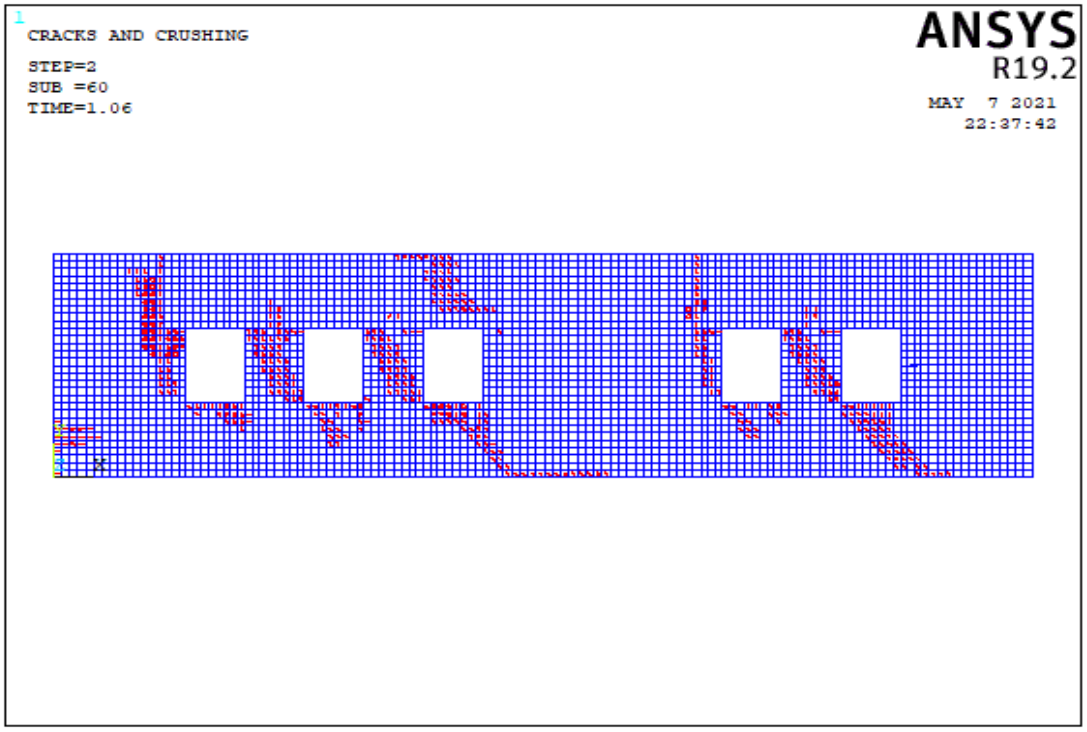

(a)

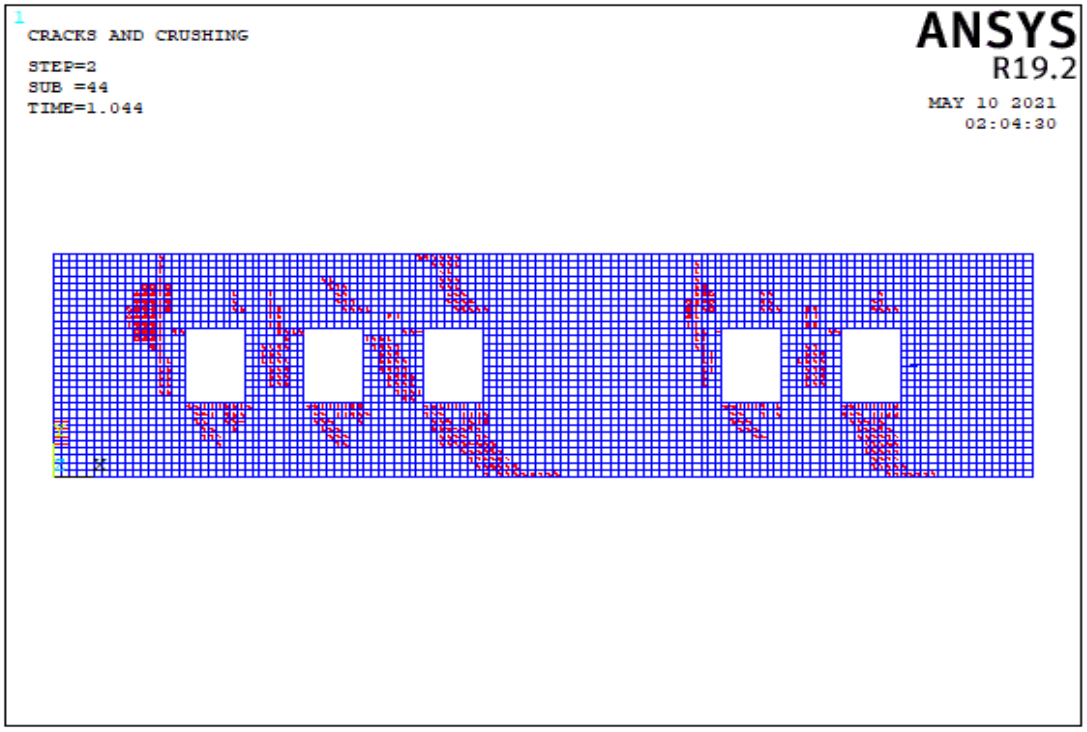

(b)

Figure 5.77. The Crack Pattern of Wall 7 Model 8 According to Compressive Strength Values of (a) 3 MPa, (b) 8 MPa

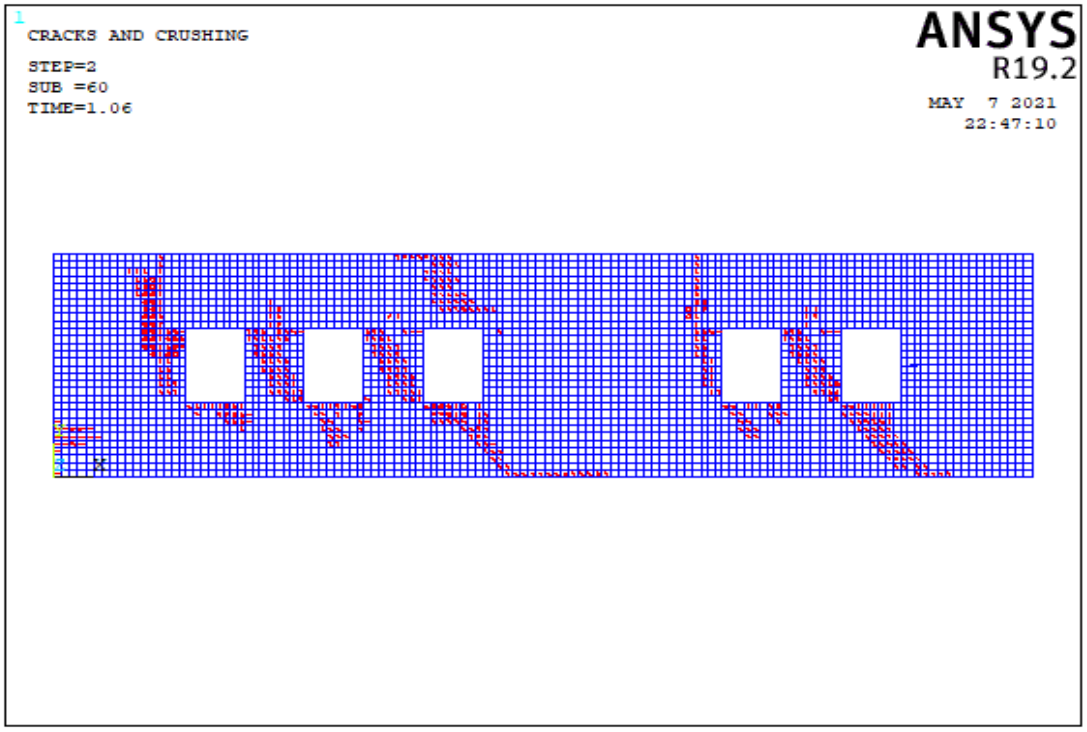

(a)

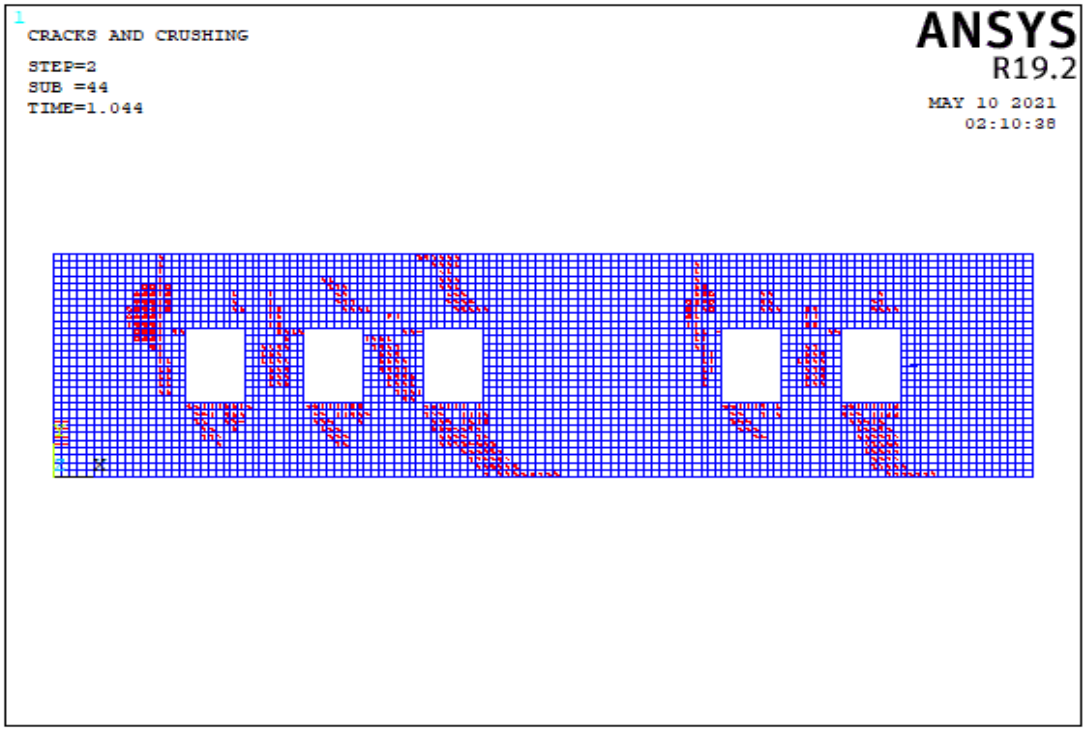

(b)

Figure 5.78. The Crack Pattern of Wall 7 Model 9 According to Compressive Strength Values of (a) 3 MPa, (b) 8 MPa

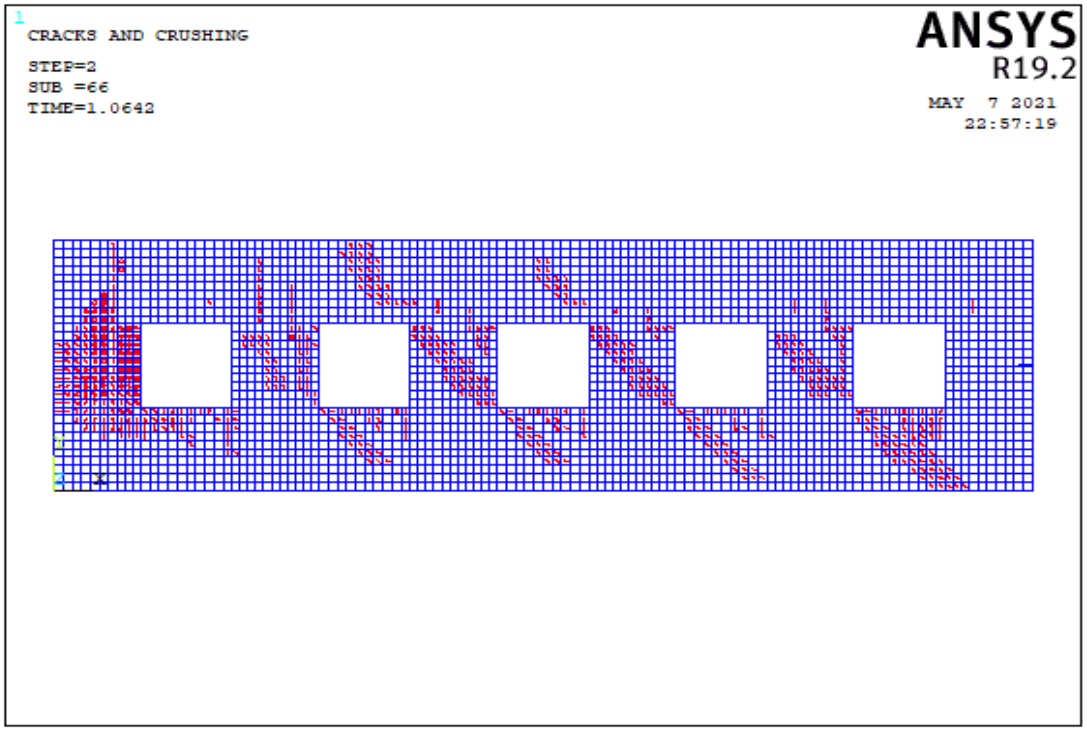

(a)

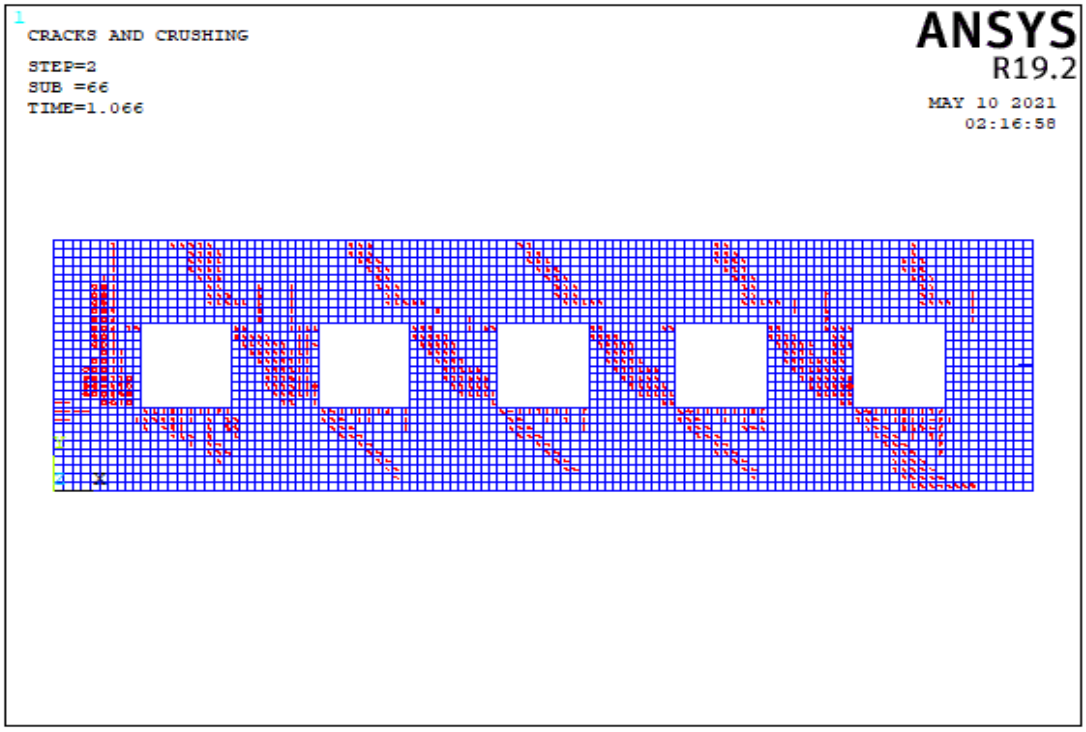

(b)

Figure 5.79. The Crack Pattern of Wall 7 Model 10 According to Compressive Strength Values of (a) 3 MPa, (b) 8 MPa

Table 5.9. Failure Patterns of Wall 7

Number of Model	Aspect ratio	fm=3 Mpa Failure Pattern			fm=8 Mpa Failure Pattern		
		Base Sliding	Rocking	Diagonal Tension	Base Sliding	Rocking	Diagonal Tension
Model 1	6.00		X			X	
	3.00			X			X
	3.00			X			X
	3.00			X			X
	3.00			X			X
	6.00		X			X	
Model 2	1.76		X			X	
	1.76			X			X
	1.76			X			X
	1.76			X			X
	1.76						
	1.76						
Model 3	3.58		X				
	3.58			X			
	3.58			X			
	2.38			X			
	3.58			X			
	3.58						
Model 4	2.39		X				
	2.39			X			
	2.39			X			
	2.39			X			
	2.39			X			
	2.39		X			X	
Model 5	4.10		X			X	
	2.73			X			X
	2.73			X			X
	2.73			X			X
	2.73			X			X
	4.10						
Model 6	3.50		X			X	
	2.33			X			X
	2.33			X			X
	2.33			X			X
	2.33			X			X
	3.50						
Model 7	2.72						
	2.34						
	2.34						
	2.34						
	2.34						
	2.72						
Model 8	1.91		X			X	
	4.29			X			X
	4.29			X			X
	1.05	X			X		
	4.29			X			X
	1.91		X			X	
Model 9	1.91		X			X	
	4.29			X		X	
	4.29			X			X
	1.05	X			X		
	4.29			X		X	
	1.91						
Model 10	3.22		X			X	
	3.22			X			X
	3.22			X			X
	3.22			X			X
	3.22			X			X
	3.22						

In Table A.7, all length of openings are less than 3 m for all models and total opening percentages of walls for models 1, 3, 4, 5, 7 and 10 are not appropriate for TEC 2018. In models 2, 8 and 9, the length of corner piers is more than 1.5 m. In models 3, 8, 9 and 10, the length of piers between the windows are less than 1 meter. This insufficient length of piers cause local failure on wall. The main reason for local collapses is that the size of opening is much or near the corners. In other words, excessive aspect ratios of piers can cause local failures. The strength of model 2 is much higher due to increased length of piers, but piers of model 2 do not behave ductile. Table 5.9 shows that the diagonal tension cracks usually appear in the piers between the openings. In addition, there are flexural cracks in the corner piers depending on the aspect ratio.

5.4.1.8 Failure Modes of Wall 8

In the wall 8 type, there are 4 different wall models. The impact of six windows openings was studied in these models of wall 8. Table A.8 shows the lengths of the walls. As seen in Figure 5.3, each pier is designated from left to right. The crack patterns obtained from the analysis of wall models corresponding to 4 different wall models are described in this section.

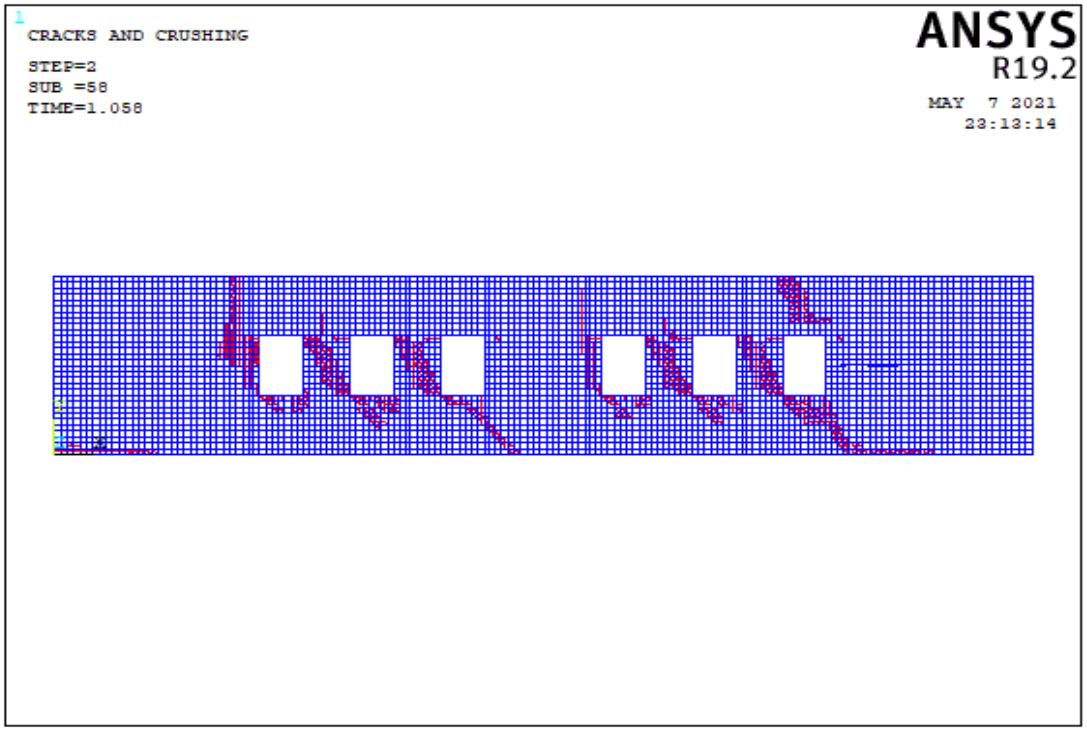

(a)

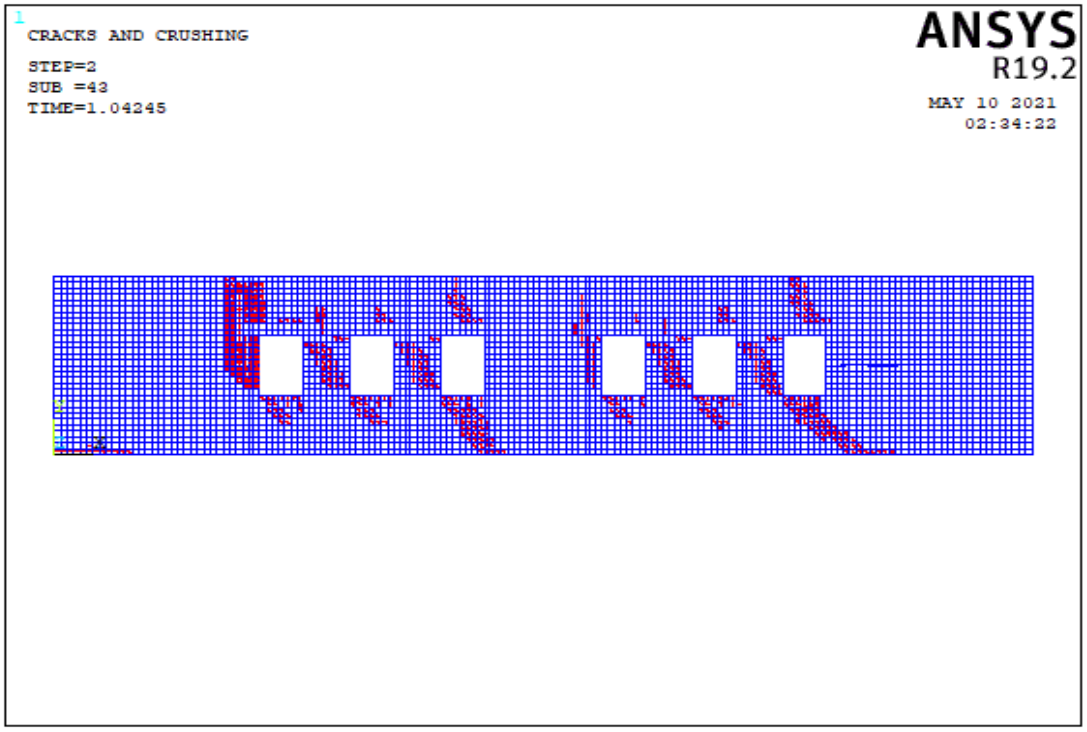

(b)

Figure 5.80. The Crack Pattern of Wall 8 Model 1 According to Compressive Strength Values of (a) 3 MPa, (b) 8 MPa

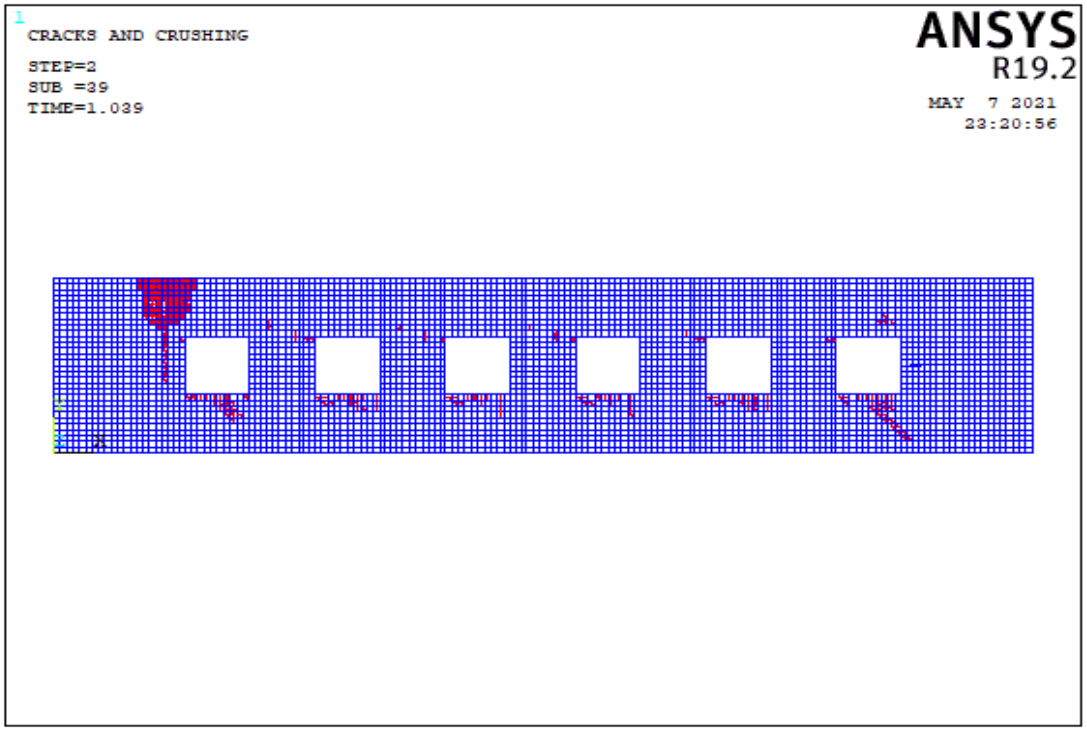

(a)

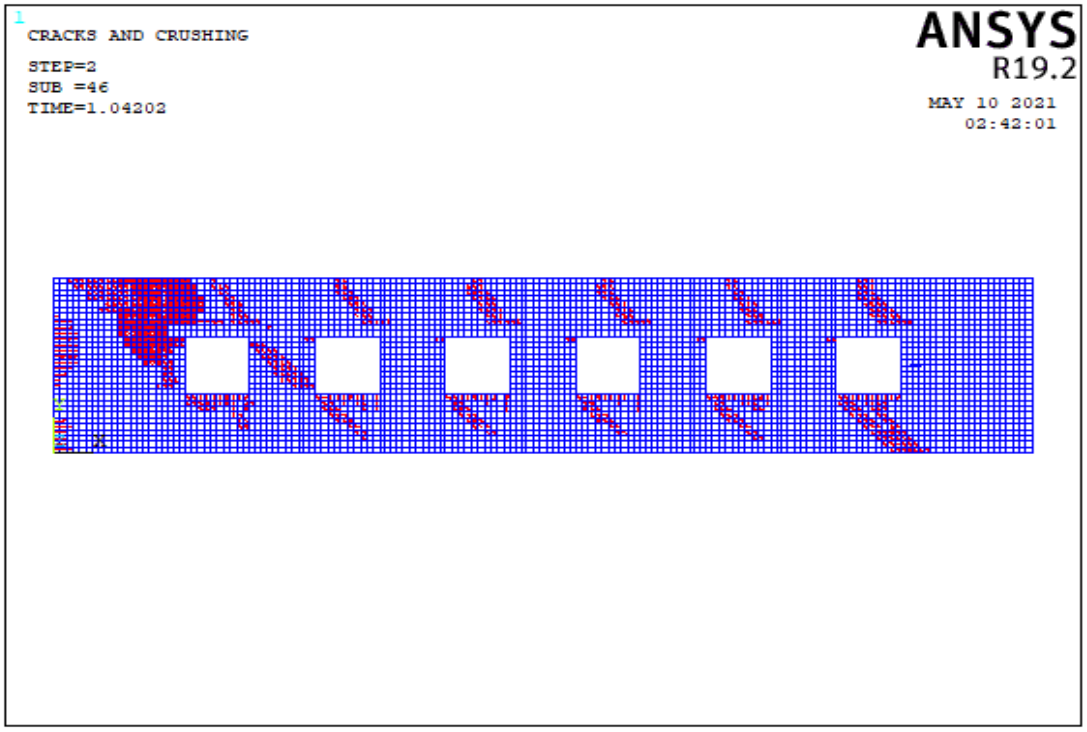

(b)

Figure 5.81. The Crack Pattern of Wall 8 Model 2 According to Compressive Strength Values of (a) 3 MPa, (b) 8 MPa

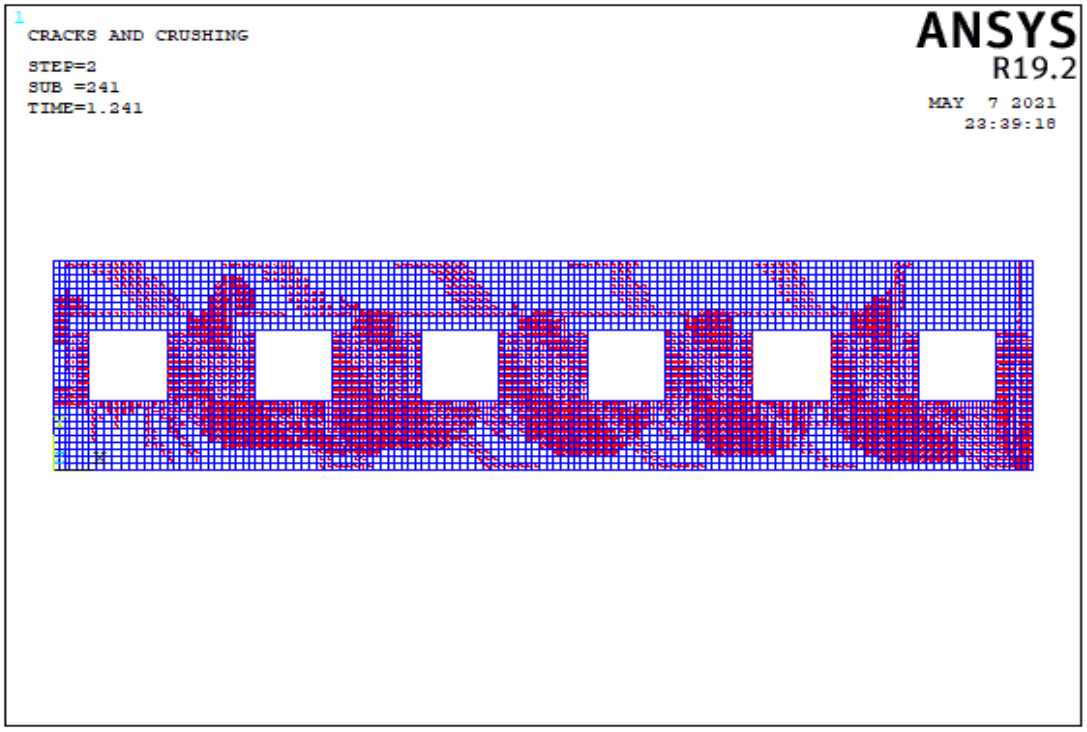

(a)

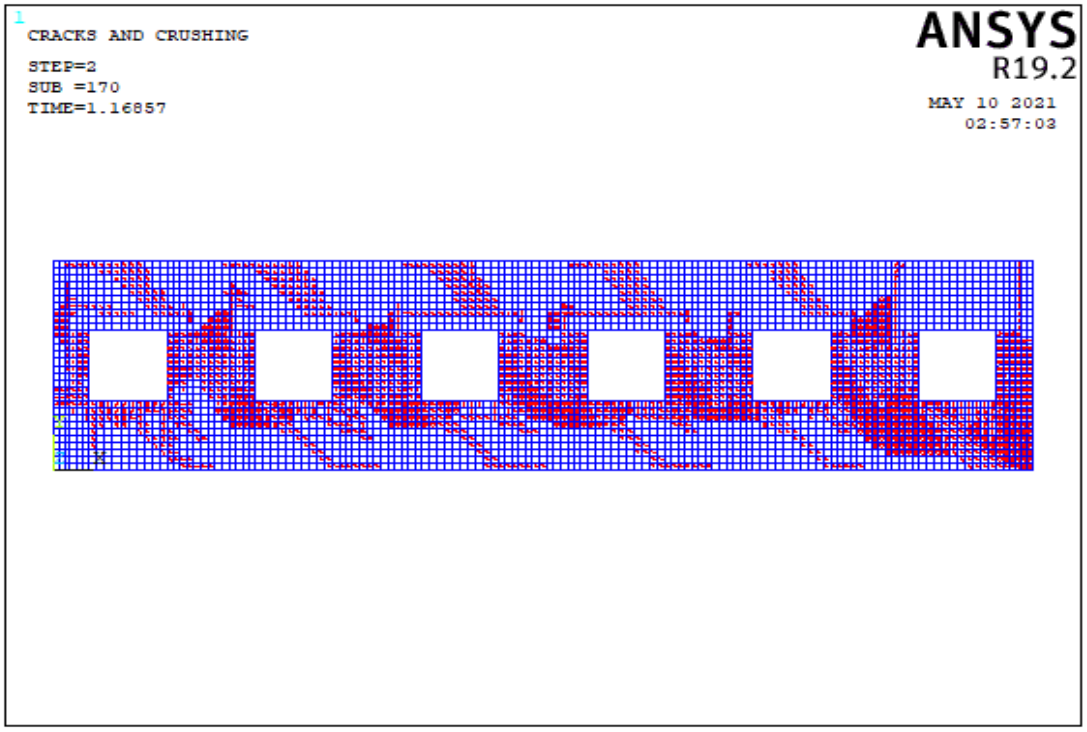

(b)

Figure 5.82. The Crack Pattern of Wall 8 Model 3 According to Compressive Strength Values of (a) 3 MPa, (b) 8 MPa

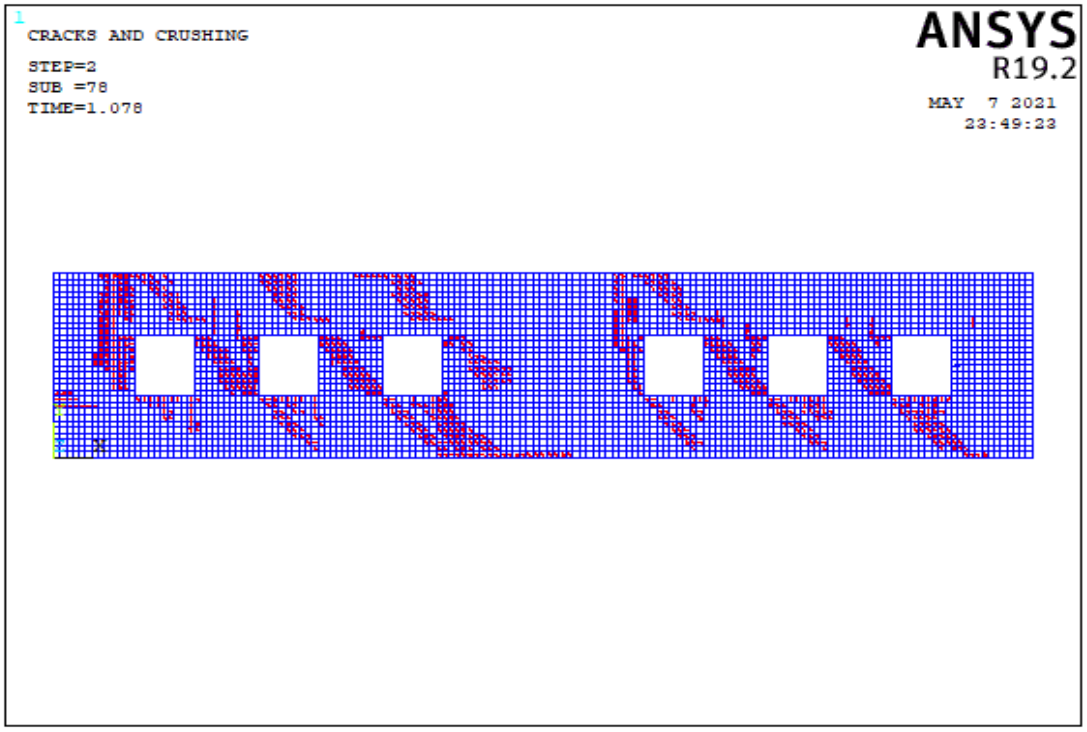

(a)

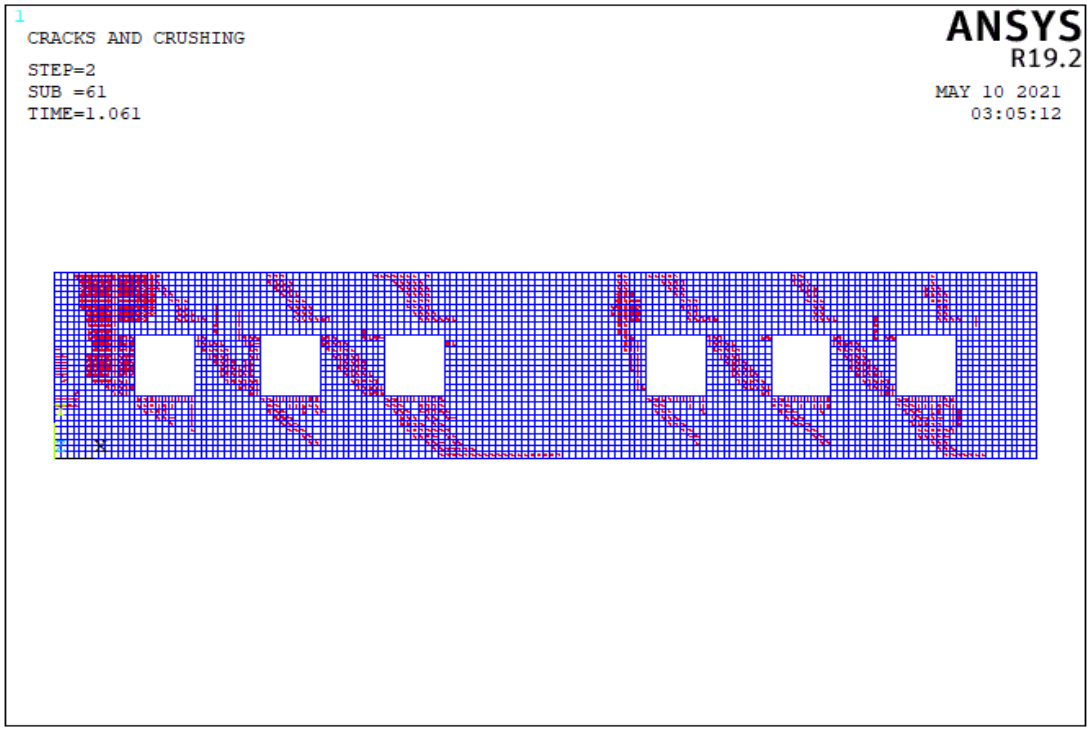

(b)

Figure 5.83. The Crack Pattern of Wall 8 Model 4 According to Compressive Strength Values of (a) 3 MPa, (b) 8 MPa

Table 5.10. Failure Patterns of Wall 8

Number of Model	Aspect ratio	fm=3 Mpa			fm=8 Mpa		
		Failure Pattern			Failure Pattern		
		Base Sliding	Rocking	Diagonal Tension	Base Sliding	Rocking	Diagonal Tension
Model 1	0.97	X			X		
	4.29			X			X
	4.29			X			X
	1.70						
	4.29			X			X
	4.29			X			X
	0.97	X			X		
Model 2	1.50					X	
	3.00						X
	3.00						
	3.00						
	3.00						
	3.00						
	1.50						
Model 3	6.60		X			X	
	2.64			X			X
	2.64			X			X
	2.64			X			X
	2.64			X			X
	2.64			X			X
	6.60		X			X	
Model 4	2.58		X			X	
	3.23			X			X
	3.23			X			X
	1.03	X			X		
	3.23			X			X
	3.23			X			X
	2.58						

In Table A.8, all length of the openings is less than 3 m for all models of wall 8 and total opening percentage of walls for model 3 is not appropriate for TEC2018. In model 3 and 4 for wall 8, the length of corner piers is less than 1.5 m. In models 1 and 4, the piers between windows is less than 1 meter. In model 3, the in-plane capacity of wall increase,

as the length or percentage of piers between the windows increase or aspect ratio of piers between the windows decrease. In model 4, base sliding mechanism emerged due to increased length of pier between windows. There are also diagonal tension cracks in the piers between the openings. Diagonal cracks and local cracks appeared in the spandrels. In addition, flexural mechanism is eventuated depending on aspect ratio in model 3. When the length of corner pier is 0.45 m, this slender pier has bending mechanism and local failure. Table 5.10 shows that, the diagonal tension mechanism dominates in low aspect ratio of wall. On the other hand, the rocking mechanism is predominant in high aspect ratio of wall.

5.4.1.9 Failure Modes of Wall 9

In the wall 9 type, there are 3 different wall models. The impact of seven windows openings was studied in these models of wall 9. Table A.9 shows the lengths of the walls. As seen in Figure 5.3, each pier is designated from left to right. The crack patterns obtained from the analysis of wall models corresponding to 3 different wall models are described in this section.

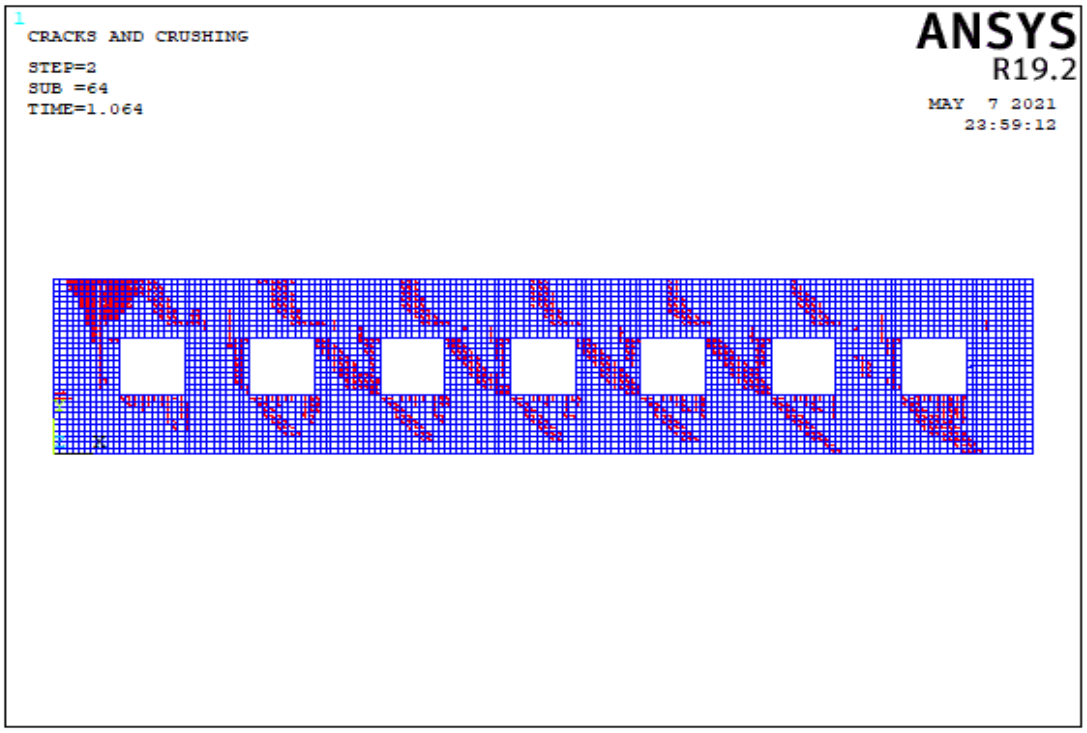

(a)

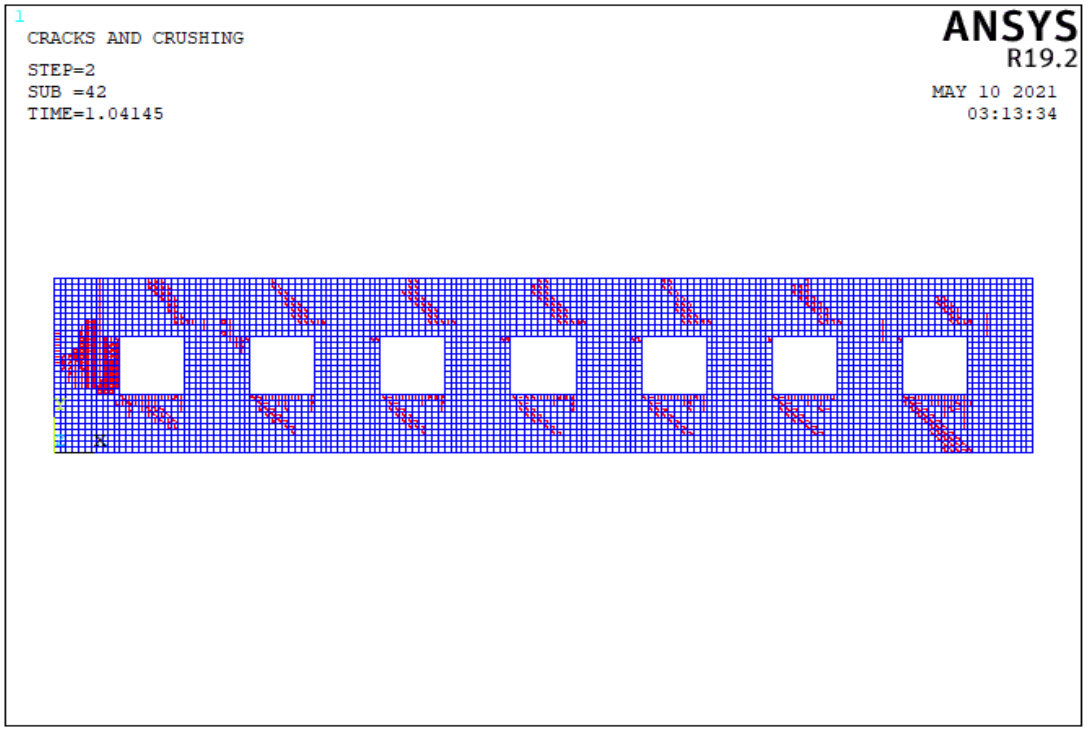

(b)

Figure 5.84. The Crack Pattern of Wall 9 Model 1 According to Compressive Strength Values of (a) 3 MPa, (b) 8 MPa

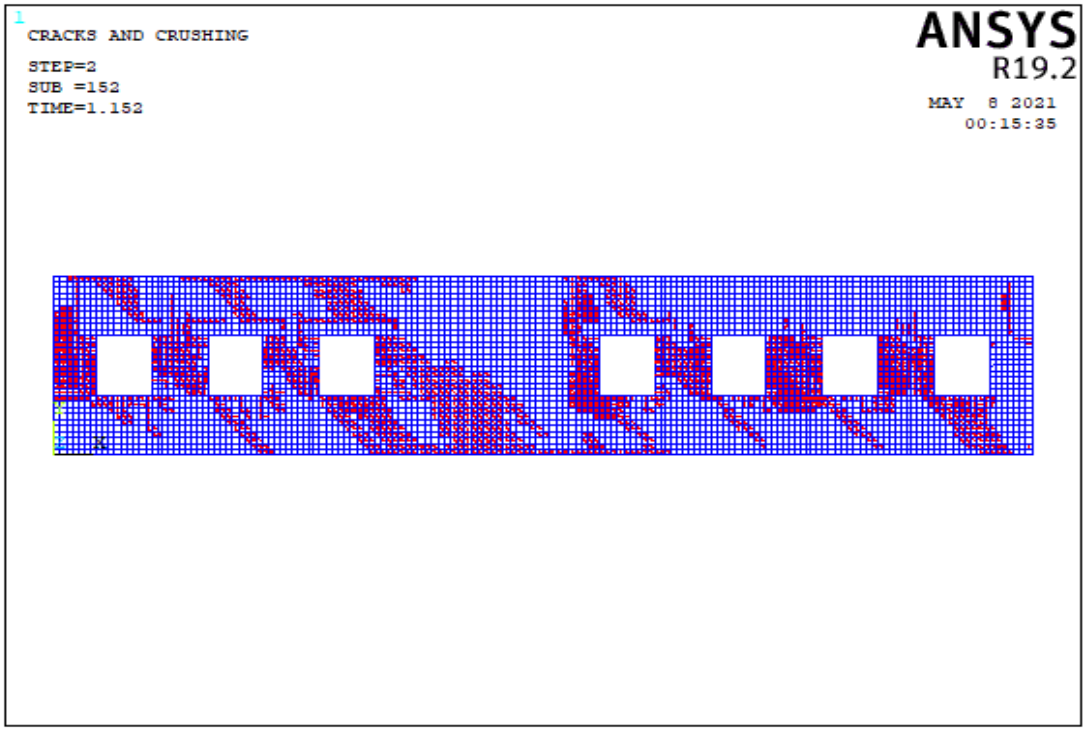

(a)

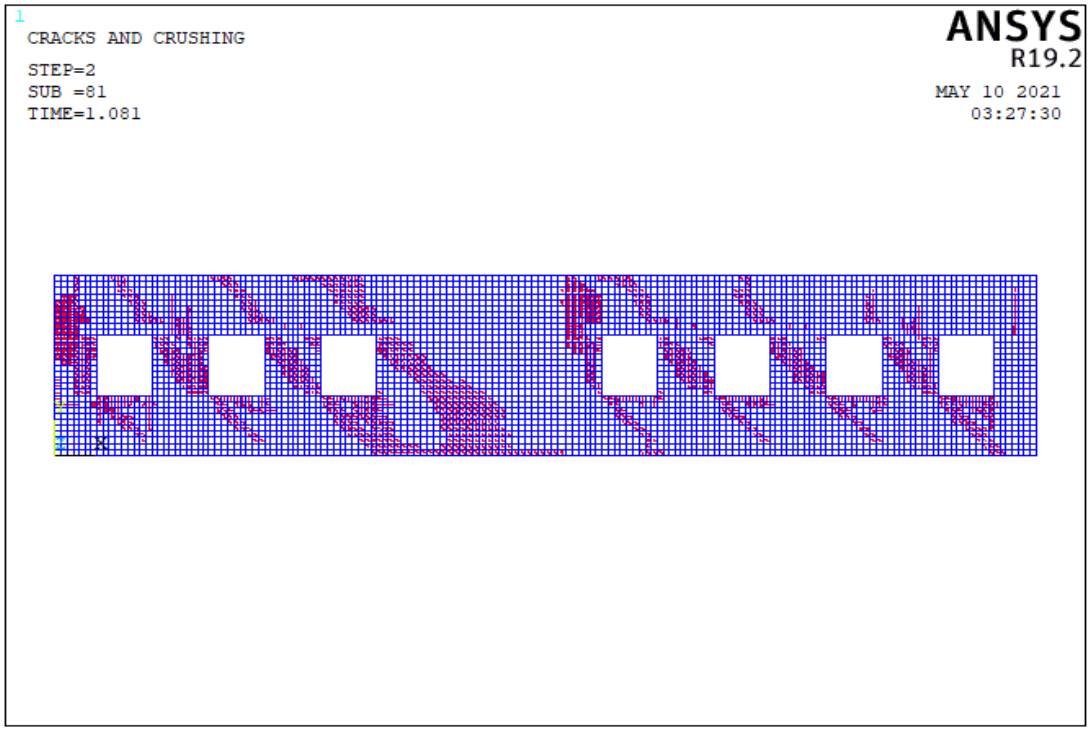

(b)

Figure 5.85. The Crack Pattern of Wall 9 Model 2 According to Compressive Strength Values of (a) 3 MPa, (b) 8 MPa

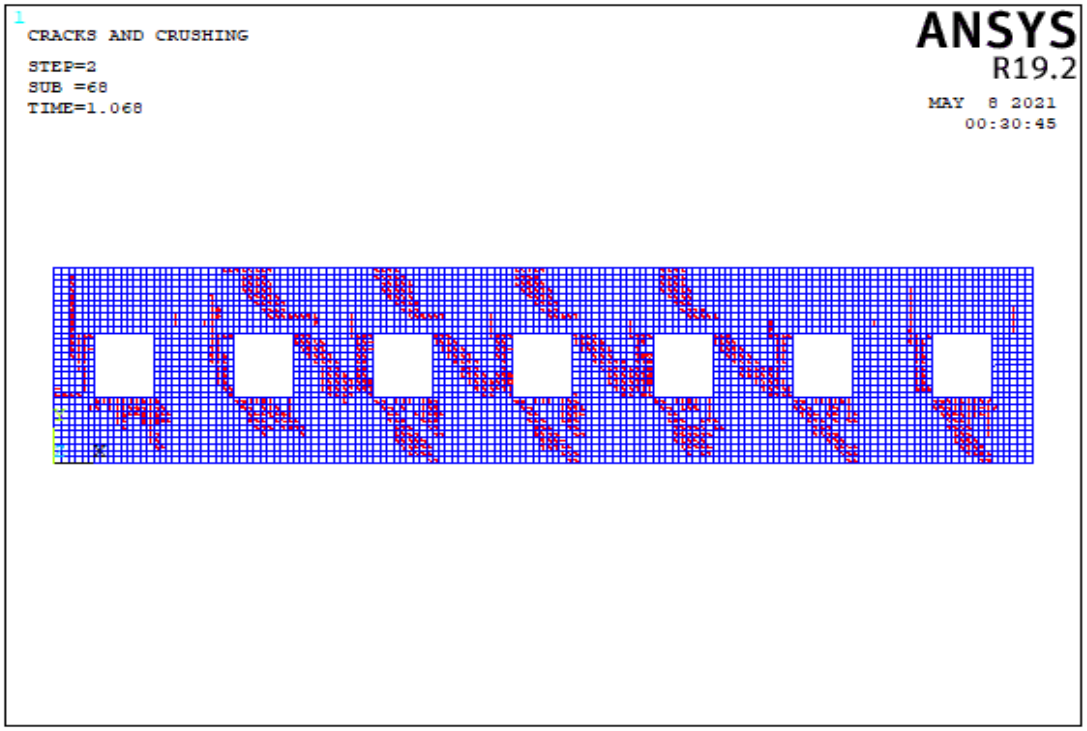

(a)

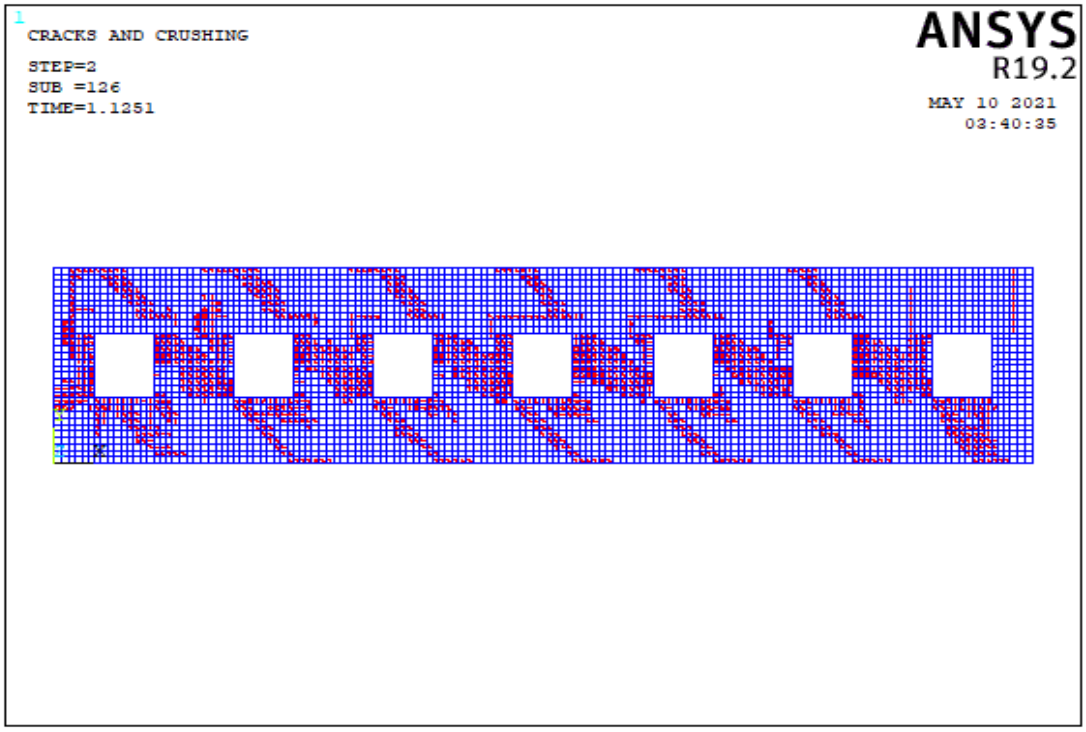

(b)

Figure 5.86. The Crack Pattern of Wall 9 Model 3 According to Compressive Strength Values of (a) 3 MPa, (b) 8 MPa

Table 5.11. Failure Patterns of Wall 9

Number of Model	Aspect ratio	fm=3 Mpa			fm=8 Mpa		
		Failure Pattern			Failure Pattern		
		Base Sliding	Rocking	Diagonal Tension	Base Sliding	Rocking	Diagonal Tension
Model 1	3.00		X			X	
	3.00			X			X
	3.00			X			
	3.00			X			
	3.00			X			
	3.00			X			
	3.00			X			
	3.00						
Model 2	4.80		X			X	
	3.60			X			X
	3.60			X			X
	0.90			X			X
	3.60			X			X
	3.60			X			X
	3.60			X			X
	4.80		X			X	
Model 3	5.50		X			X	
	2.75			X			X
	2.75			X			X
	2.75			X			X
	2.75			X			X
	2.75			X			X
	2.75			X			X
	5.50		X			X	

In Table A.9, all length of openings is less than 3 m for all models and total opening percentage of all models is appropriate for TEC 2018. In model 2 and 3, the length of corner piers is less than 1.5 m. In model 2, the length of piers between windows is less than 1 meter. This insufficient length of piers cause local failure on wall. The main reason for local collapses is that the size of opening is much or near the corners. In other words, excessive aspect ratios of piers can cause local failures. Table 5.11 shows that, the

diagonal tension mechanism dominates in low aspect ratio of wall. On the other hand, the rocking mechanism is predominant in high aspect ratio of wall.

5.4.1.10 Failure Modes of Wall 10

In the wall 10 type, there are 3 different wall models. The impact of eight windows openings was studied in these models of wall 10. Table A.10 shows the lengths of the walls. As seen in Figure 5.3, each pier is designated from left to right. The crack patterns obtained from the analysis of wall models corresponding to 3 different wall models are described in this section.

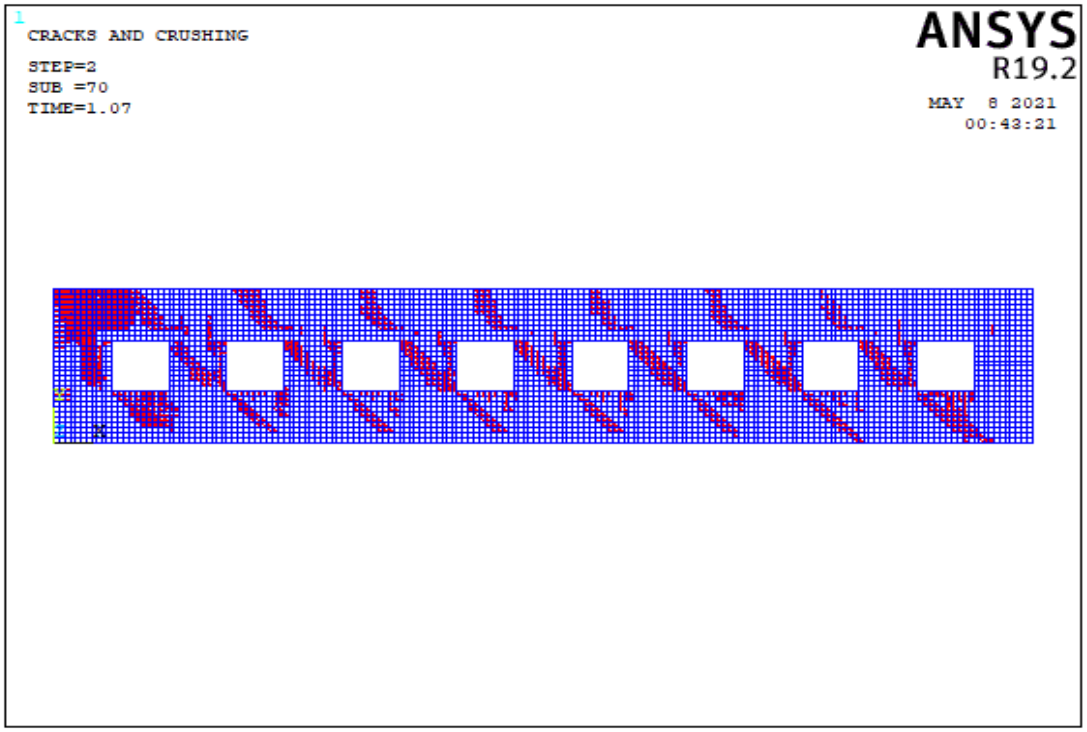

(a)

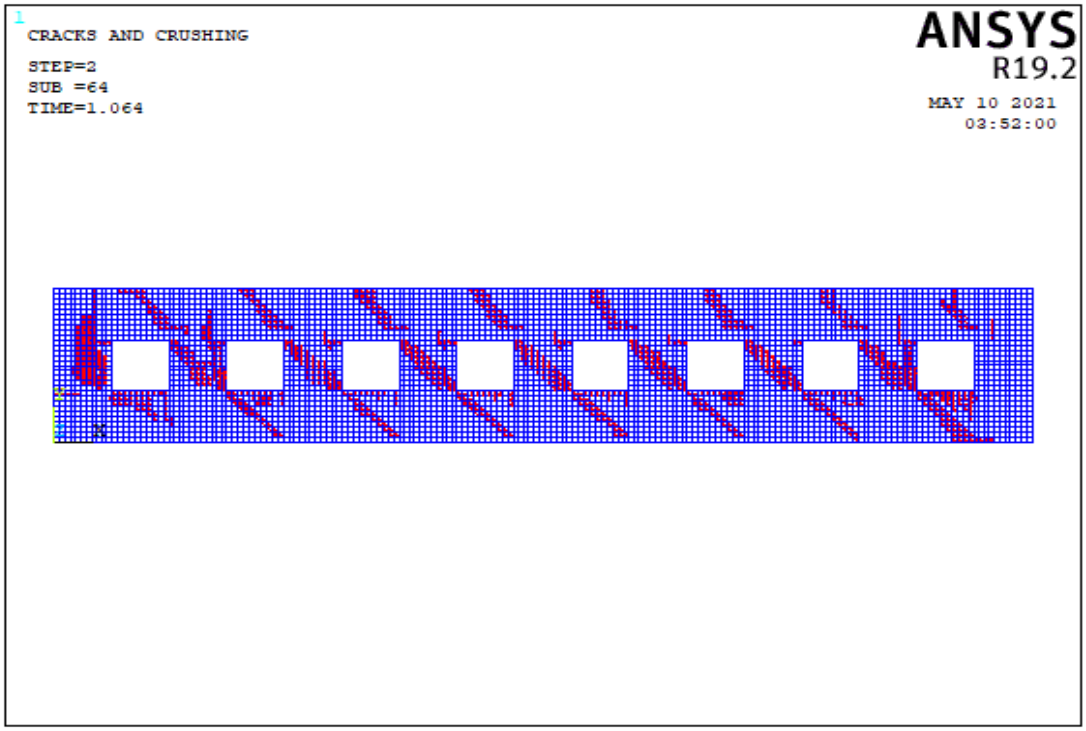

(b)

Figure 5.87. The Crack Pattern of Wall 10 Model 1 According to Compressive Strength Values of (a) 3 MPa, (b) 8 MPa

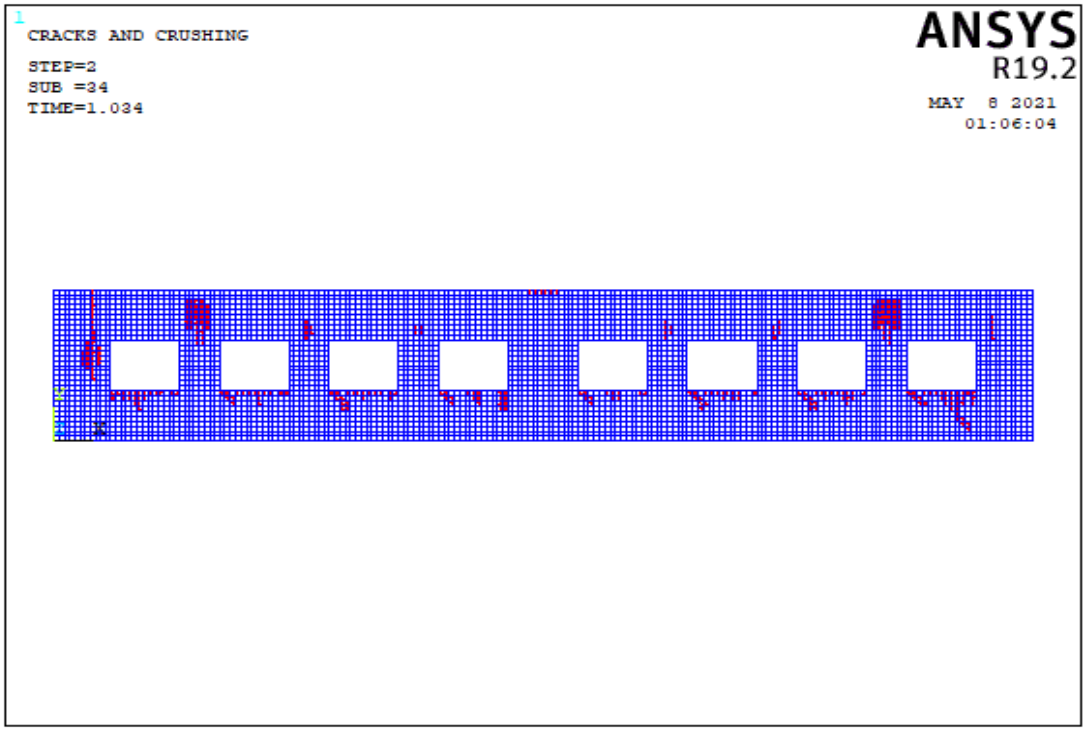

(a)

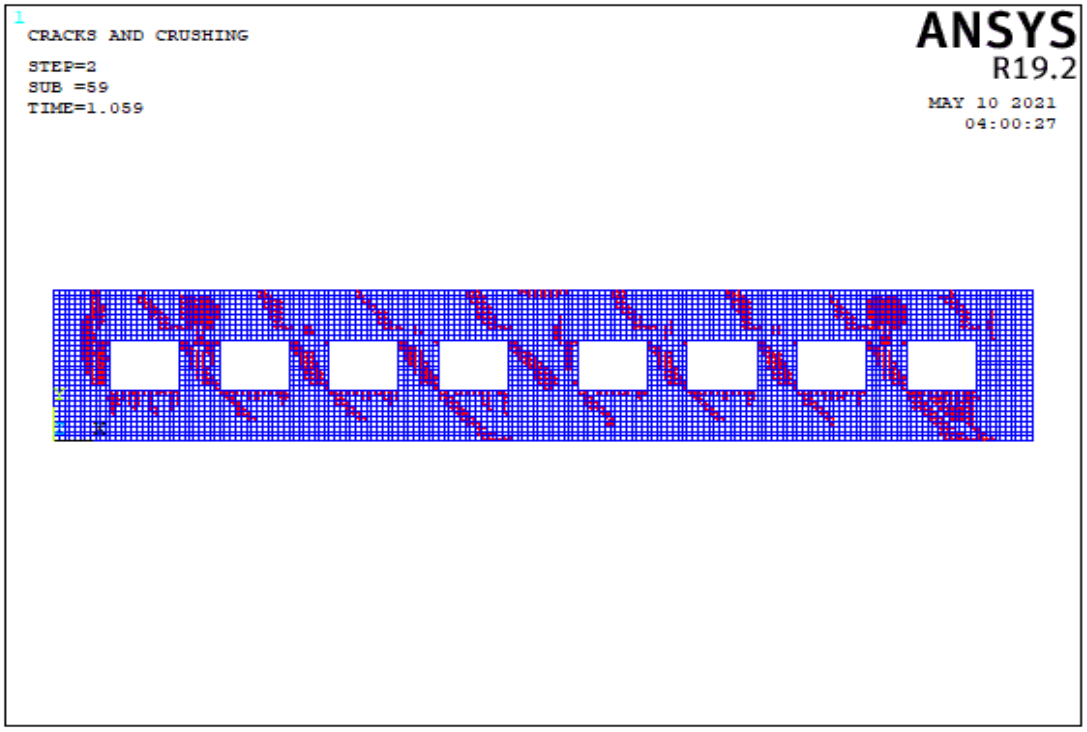

(b)

Figure 5.88. The Crack Pattern of Wall 10 Model 2 According to Compressive Strength Values of (a) 3 MPa, (b) 8 MPa

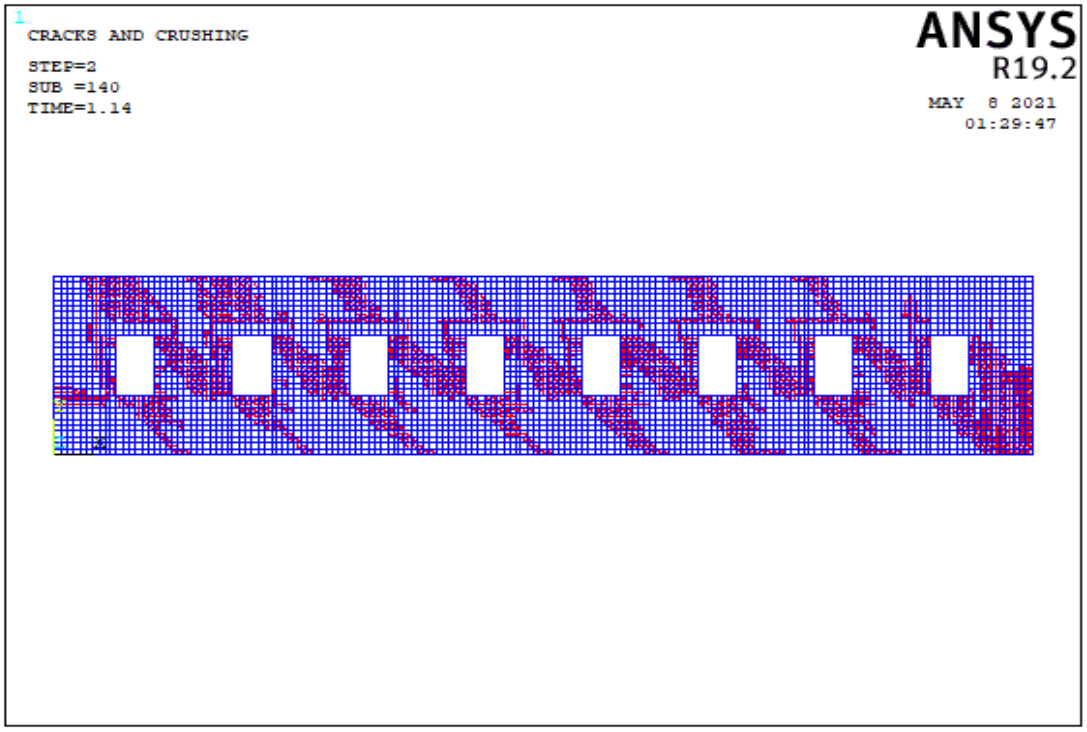

(a)

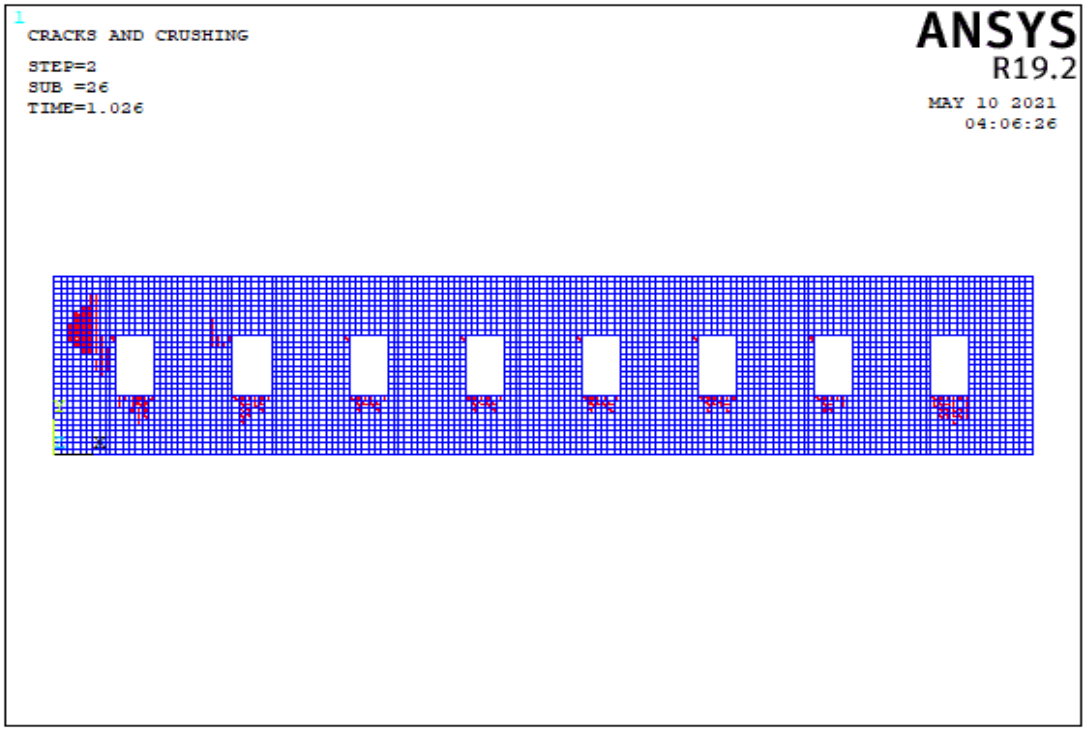

(b)

Figure 5.89. The Crack Pattern of Wall 10 Model 3 According to Compressive Strength Values of (a) 3 MPa, (b) 8 MPa

Table 5.12. Failure Patterns of Wall 10

Number of Model	Aspect ratio	fm=3 Mpa			fm=8 Mpa		
		Failure Pattern			Failure Pattern		
		Base Sliding	Rocking	Diagonal Tension	Base Sliding	Rocking	Diagonal Tension
Model 1	3.00		X			X	
	3.00			X			X
	3.00			X			X
	3.00			X			X
	3.00			X			X
	3.00			X			X
	3.00			X			X
	3.00			X			X
	3.00						
Model 2	3.04		X			X	
	4.29		X				X
	4.29						X
	4.29						X
	2.43						X
	4.29						X
	4.29						X
	4.29		X				X
	3.04		X				
Model 3	3.23		X			X	
	2.58			X			
	2.58			X			
	2.58			X			
	2.58			X			
	2.58			X			
	2.58			X			
	2.58			X			
	3.23		X				

In the Table A.10, all length of openings is less than 3 m for all models of wall 10 and total opening percentage of walls is appropriate for TEC 2018. In all models, the length of all piers is less than 1.5 m. Local failures are seen in all models due to the size of openings. These models show that piers between openings have diagonal tension mechanism, although the aspect ratios are high. The capacity of the pier changed depend on aspect ratio.

5.4.1.11 Failure Modes of Wall 11

In the wall 11 type, there are 4 different wall models. The impact of nine windows openings was studied in these models of wall 11. Table A.11 shows the lengths of the walls. As seen in Figure 5.3, each pier is designated from left to right. The crack patterns obtained from the analysis of wall models corresponding to 4 different wall models are described in this section.

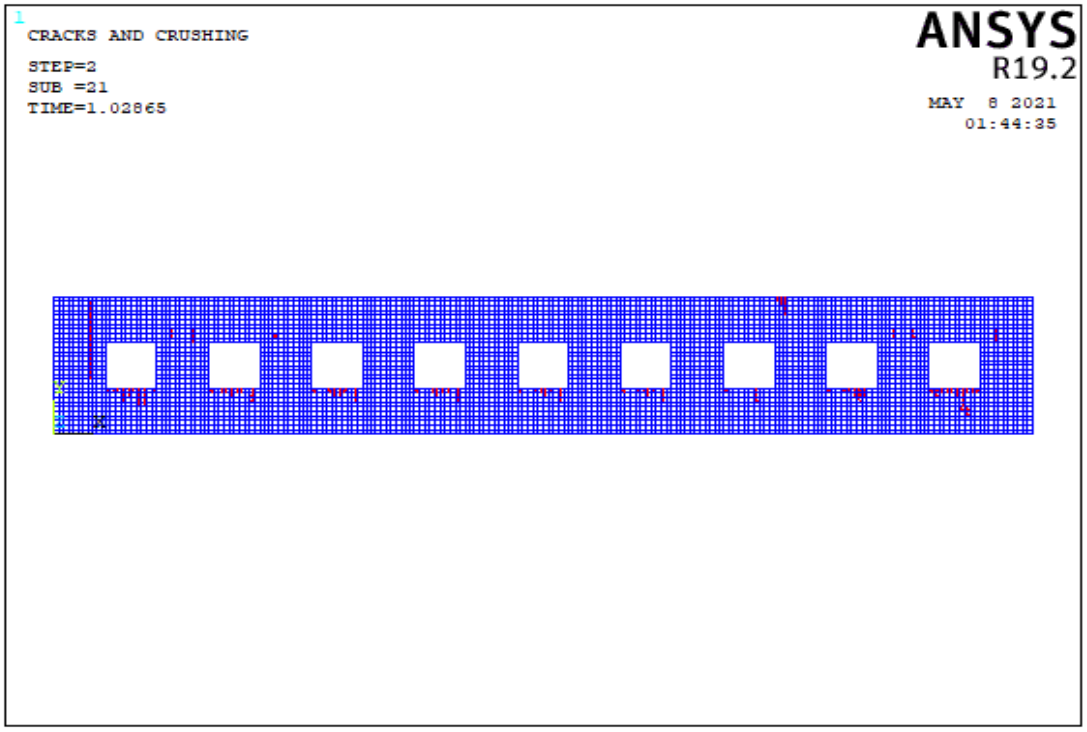

(a)

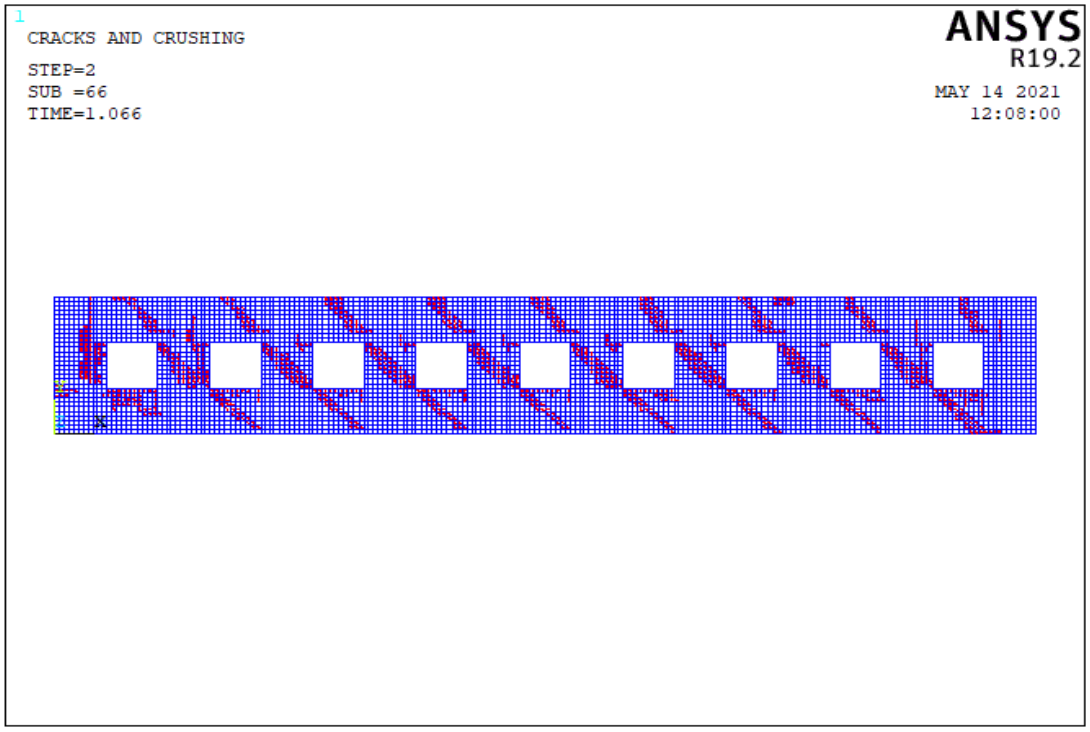

(b)

Figure 5.90. The Crack Pattern of Wall 11 Model 1 According to Compressive Strength Values of (a) 3 MPa, (b) 8 MPa

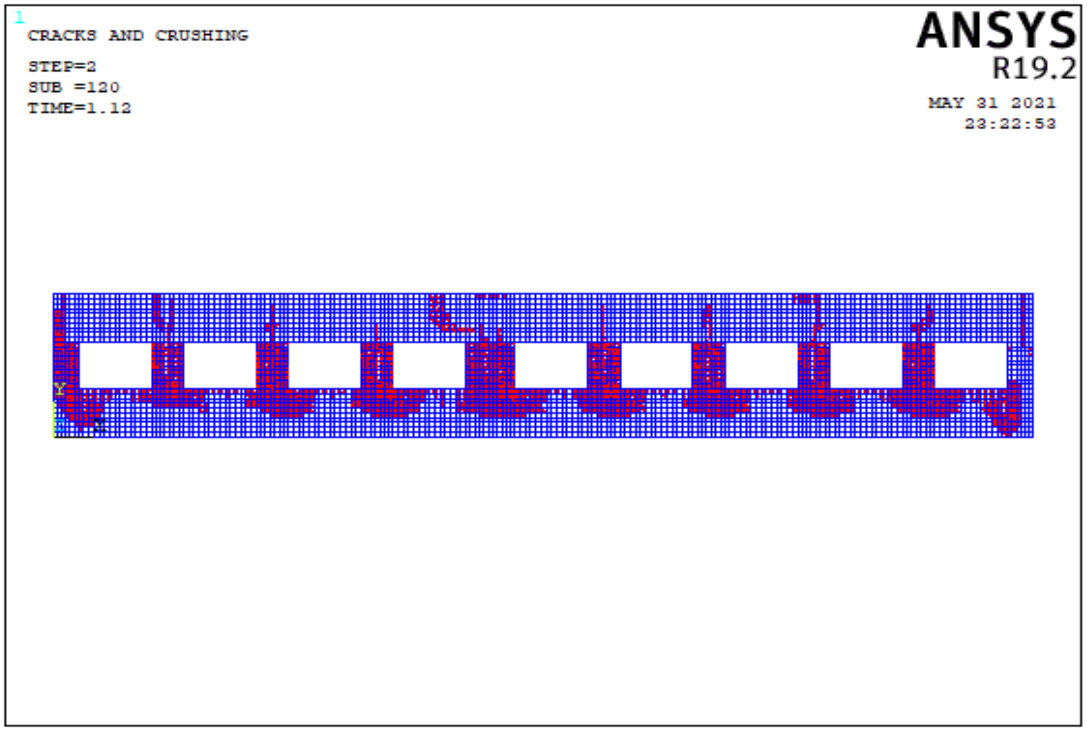

(a)

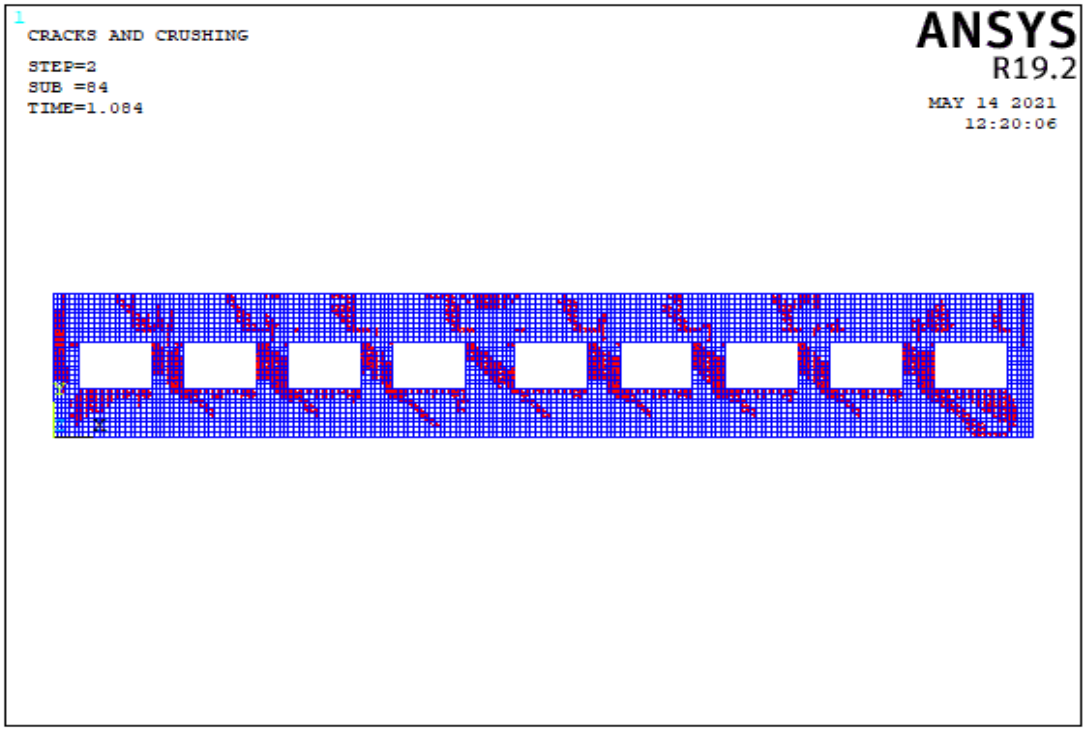

(b)

Figure 5.91. The Crack Pattern of Wall 11 Model 2 According to Compressive Strength Values of (a) 3 MPa, (b) 8 MPa

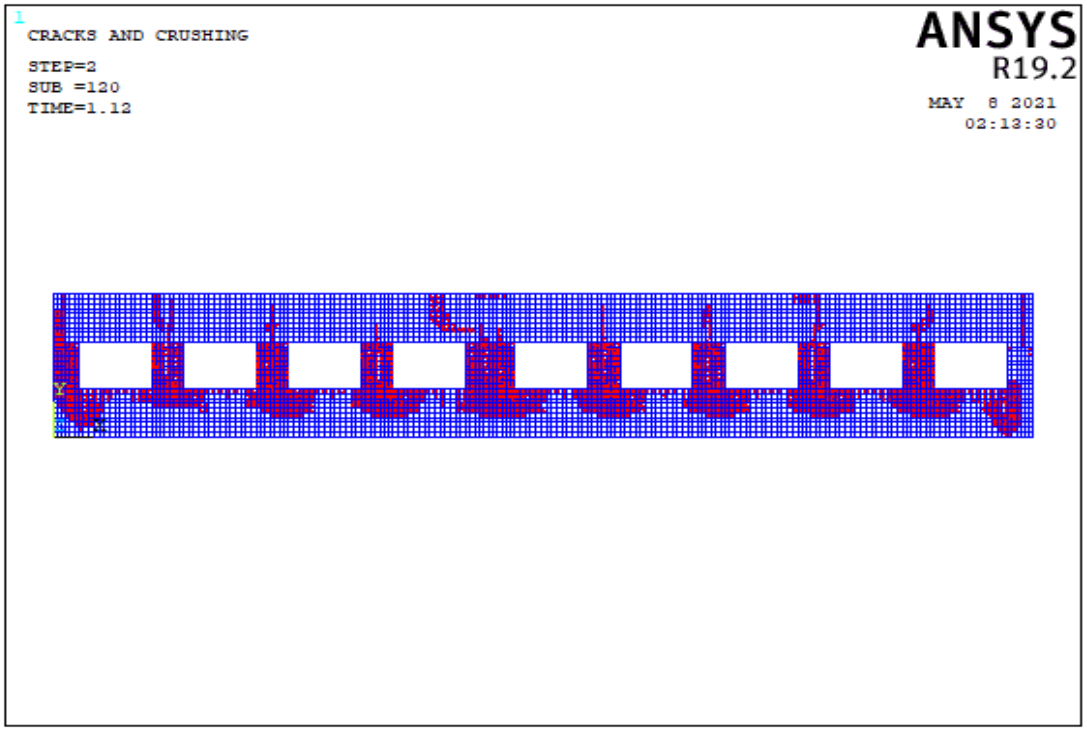

(a)

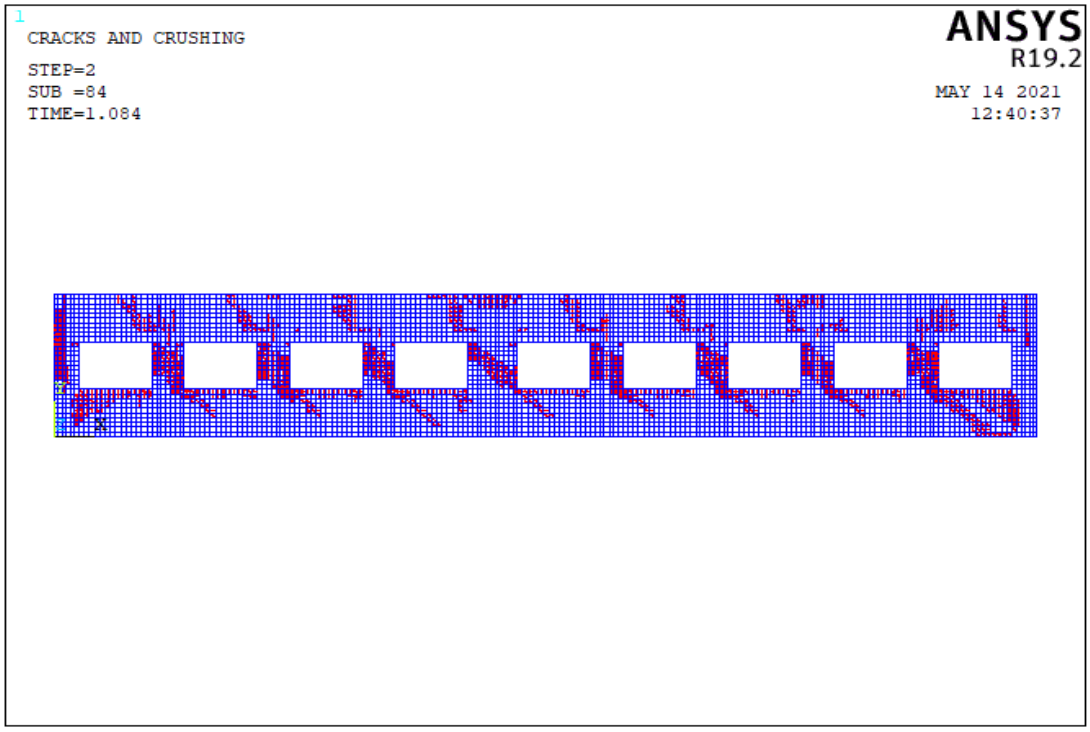

(b)

Figure 5.92. The Crack Pattern of Wall 11 Model 3 According to Compressive Strength Values of (a) 3 MPa, (b) 8 MPa

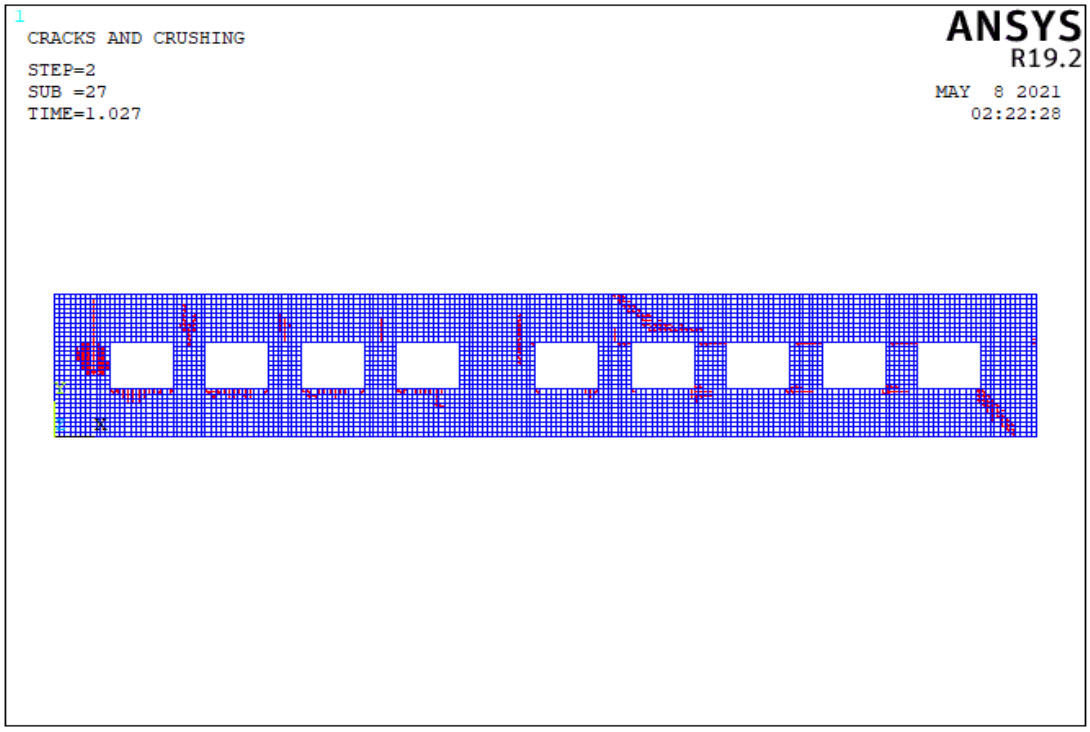

(a)

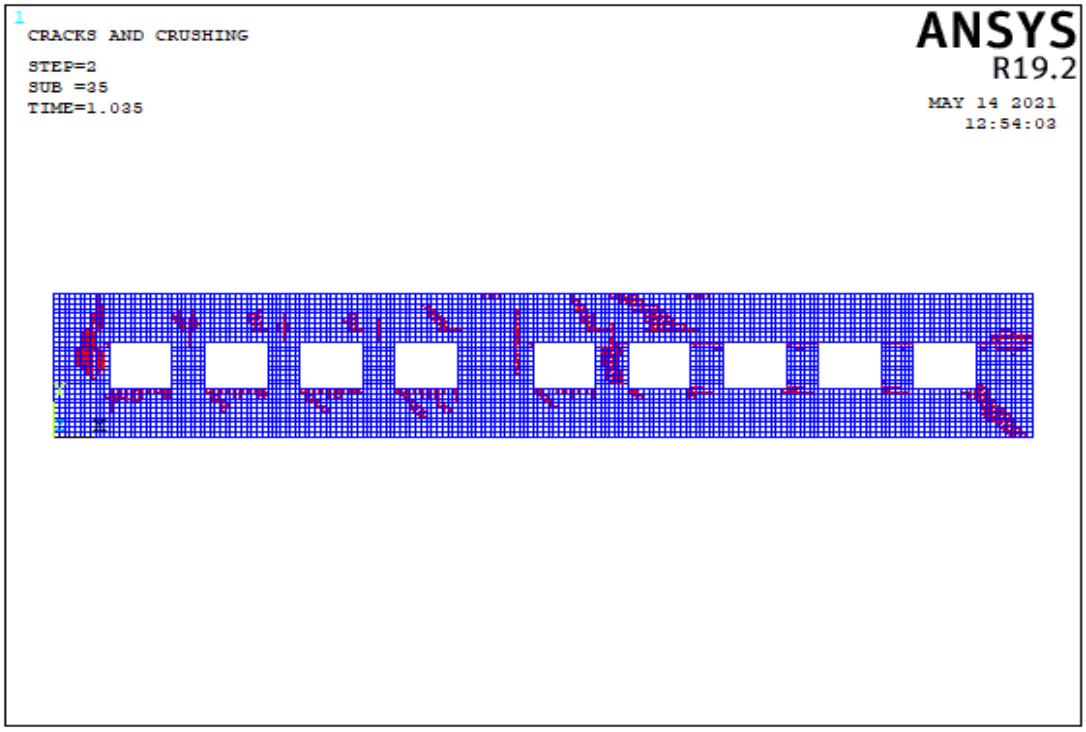

(b)

Figure 5.93. The Crack Pattern of Wall 11 Model 4 According to Compressive Strength Values of (a) 3 MPa, (b) 8 MPa

Table 5.13. Failure Patterns of Wall 11

Number of Model	Aspect ratio	fm=3 Mpa			fm=8 Mpa		
		Failure Pattern			Failure Pattern		
		Base Sliding	Rocking	Diagonal Tension	Base Sliding	Rocking	Diagonal Tension
Model 1	3.00		X			X	
	3.00						X
	3.00						X
	3.00						X
	3.00						X
	3.00						X
	3.00						X
	3.00						X
	3.00						X
	3.00					X	
Model 2	6.52		X			X	
	5.00						X
	5.00						X
	5.00						X
	3.26						X
	5.00						X
	5.00						X
	5.00						X
	5.00						X
	6.52		X			X	
Model 3	6.52		X			X	
	5.00			X			X
	5.00			X			X
	5.00			X			X
	3.26			X			X
	5.00			X			X
	5.00			X			X
	5.00			X			X
	5.00			X			X
	6.52		X			X	
Model 4	2.90		X			X	
	8.55						
	8.55						
	8.55						
	2.14						
	8.55			X			X
	8.55						
	8.55						
	8.55						
	2.90			X			X

In model 2, 3 and 4 , length of corner piers is less than 1 m, this insufficient length of piers cause local failure on wall. The main reason for local collapses is that the size of opening is much or near the corners. In other words, excessive aspect ratios of piers can cause local failures. Model 1 shows that it has more capacity due to reduced opening percentage and proper locations of openings. Table 5.13 shows that, the diagonal tension mechanism dominates in low aspect ratio of wall. On the other hand, the rocking mechanism is predominant in high aspect ratio of wall.

5.4.1.12 Failure Modes of Wall 12

In the wall 12 type, there are 10 different wall models. The impact of single door and window openings was studied in these models of wall 12. Table A.12 shows the lengths of the walls. As seen in Figure 5.3, each pier is designated from left to right. The crack patterns obtained from the analysis of wall models corresponding to 10 different wall models are described in this section.

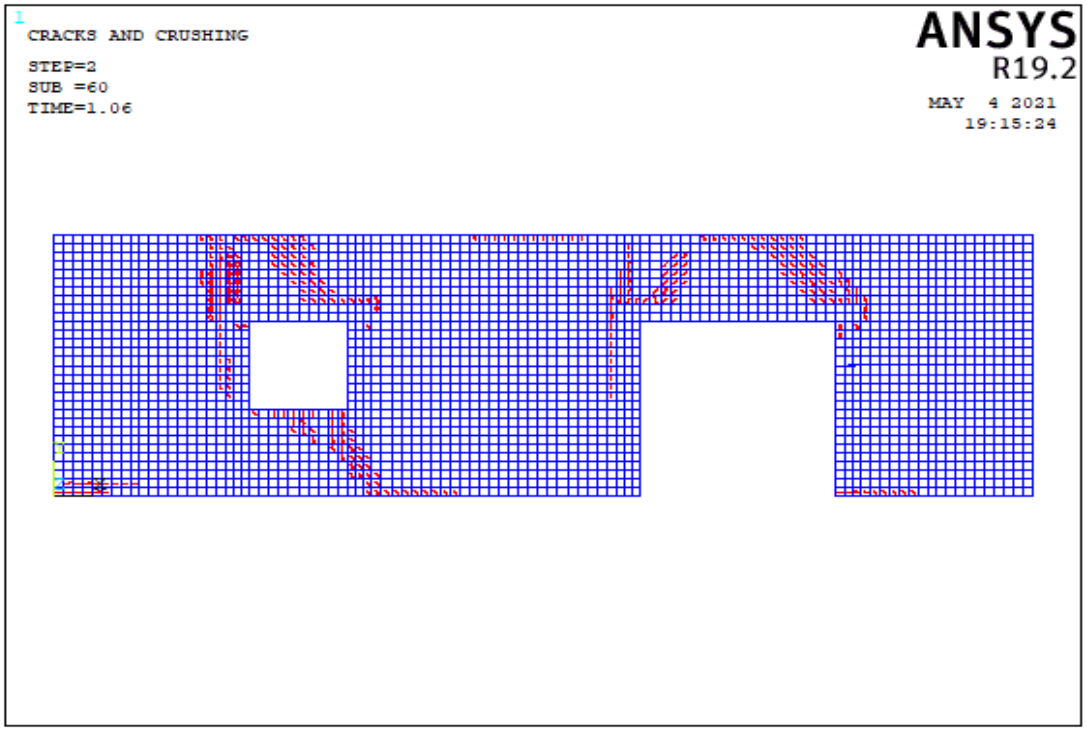

(a)

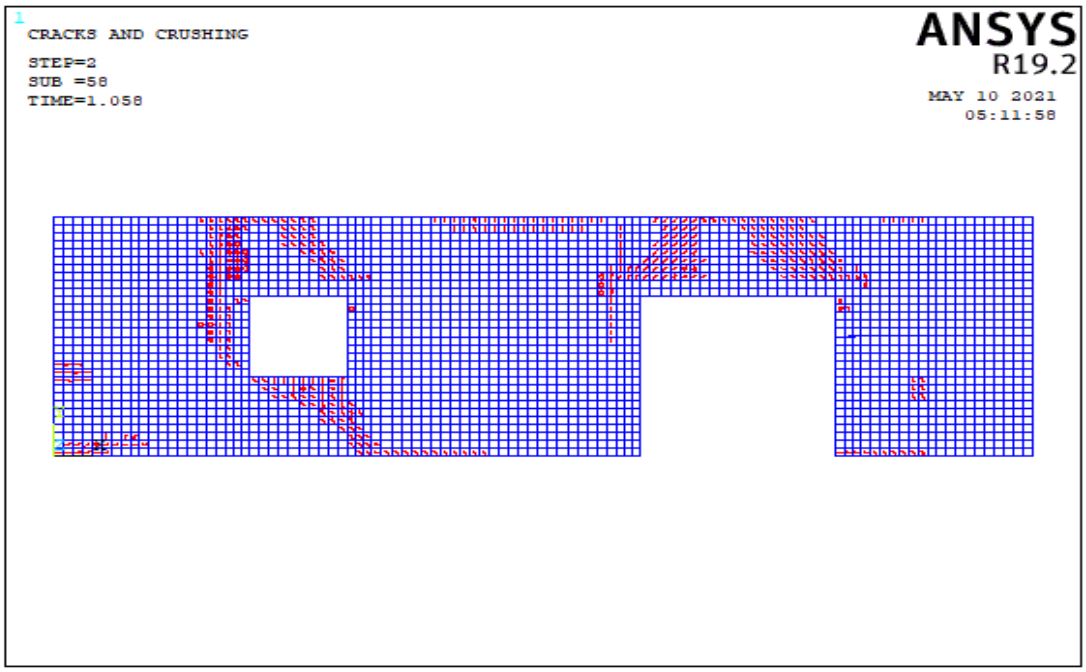

(b)

Figure 5.96. The Crack Pattern of Wall 12 Model 1 According to Compressive Strength Values of (a) 3 MPa, (b) 8 MPa

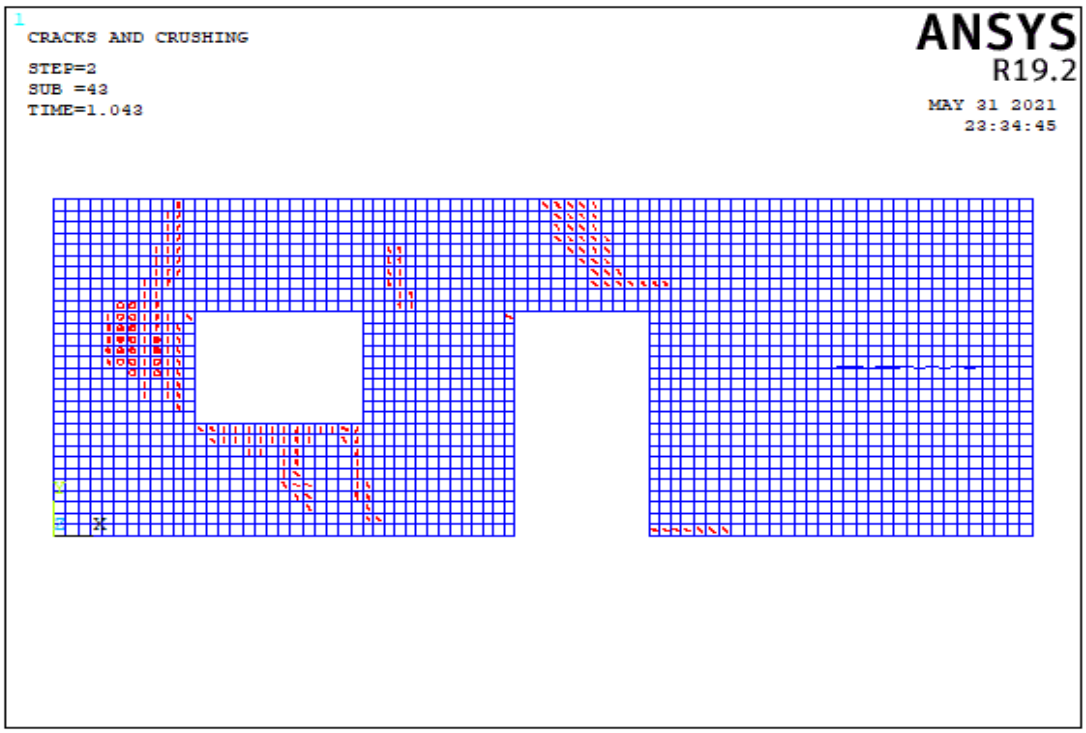

(a)

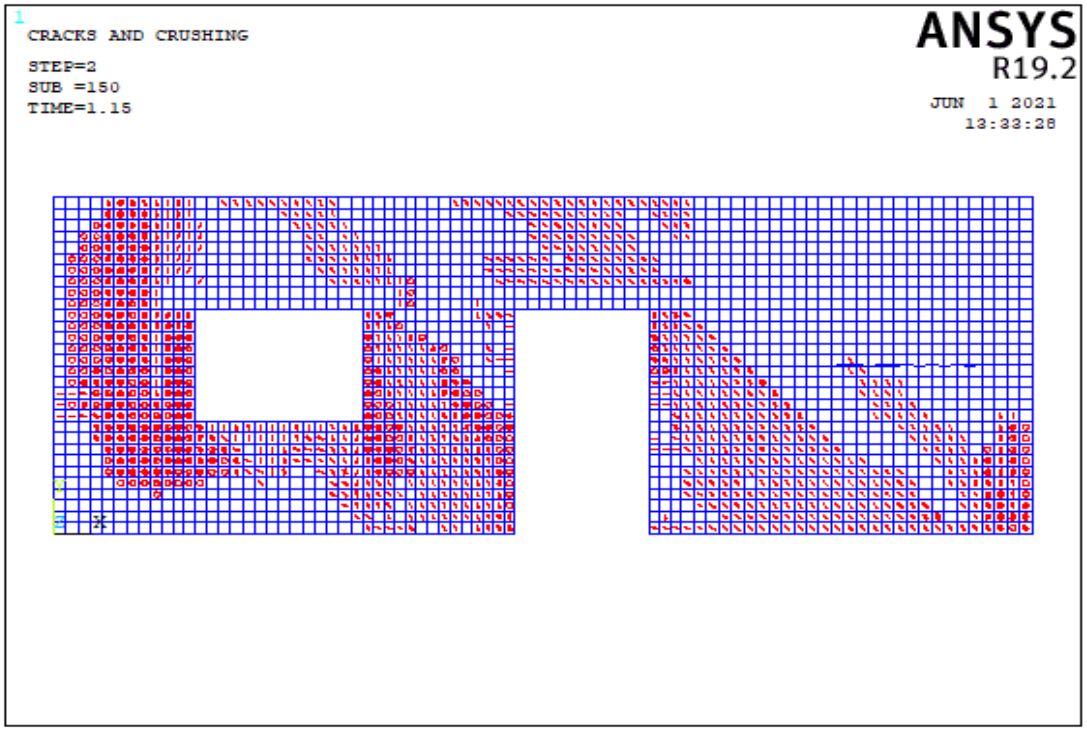

(b)

Figure 5.97. The Crack Pattern of Wall 12 Model 2 According to Compressive Strength Values of (a) 3 MPa, (b) 8 MPa

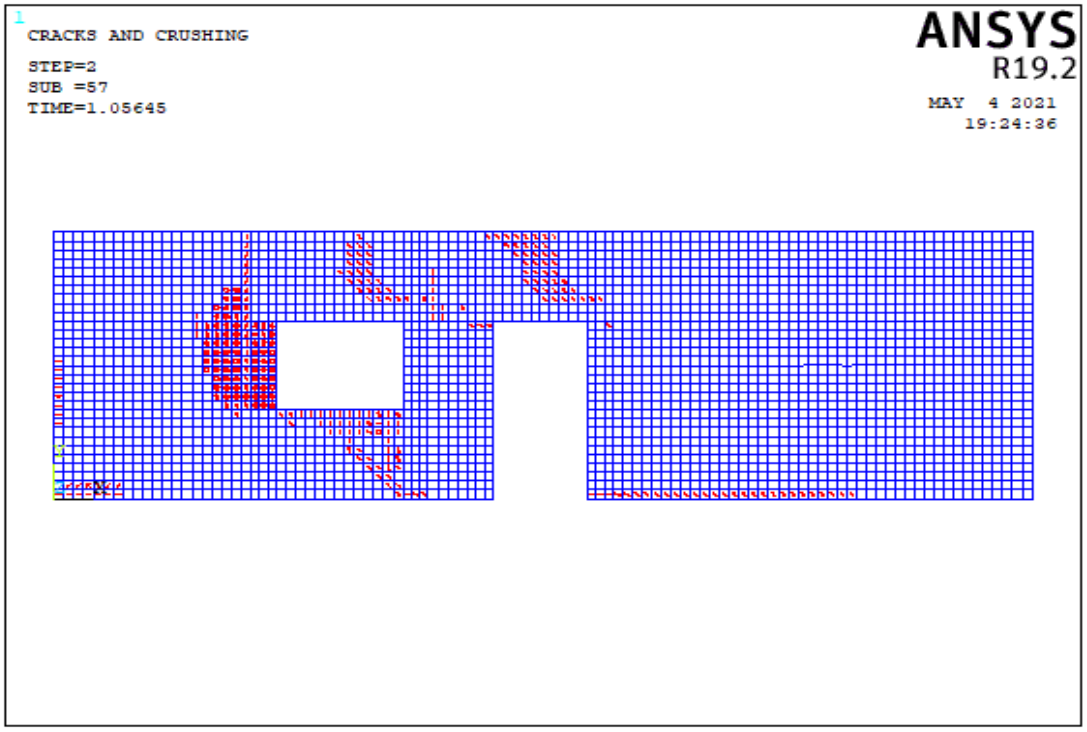

(a)

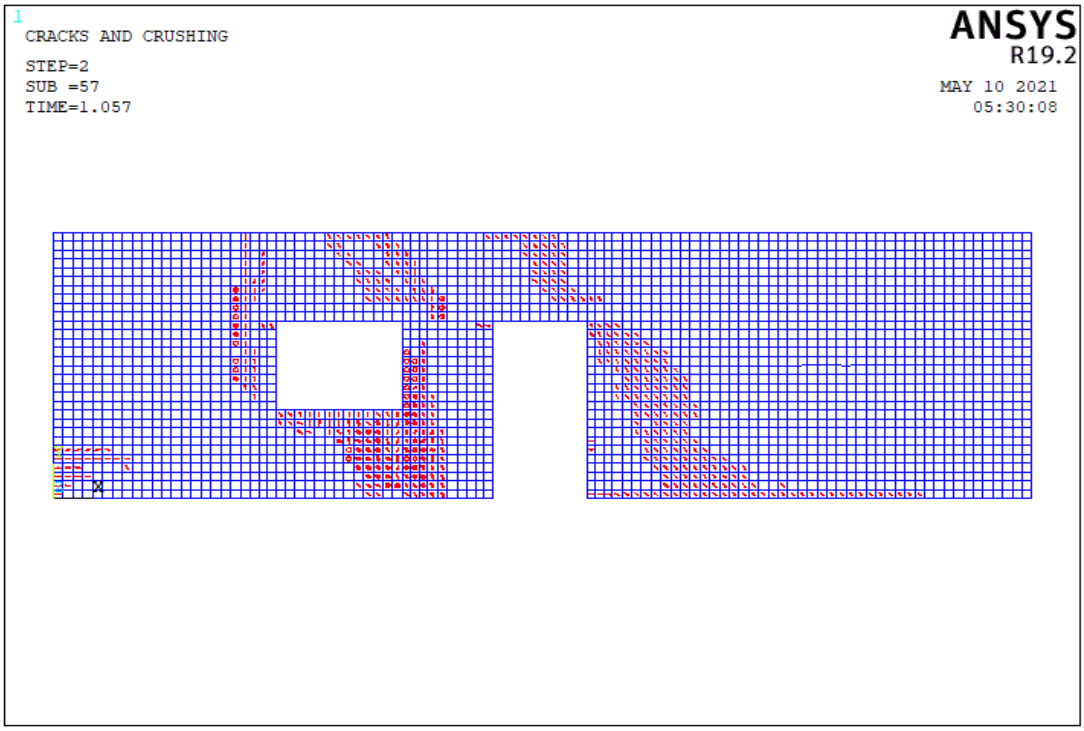

(b)

Figure 5.98. The Crack Pattern of Wall 12 Model 3 According to Compressive Strength Values of (a) 3 MPa, (b) 8 MPa

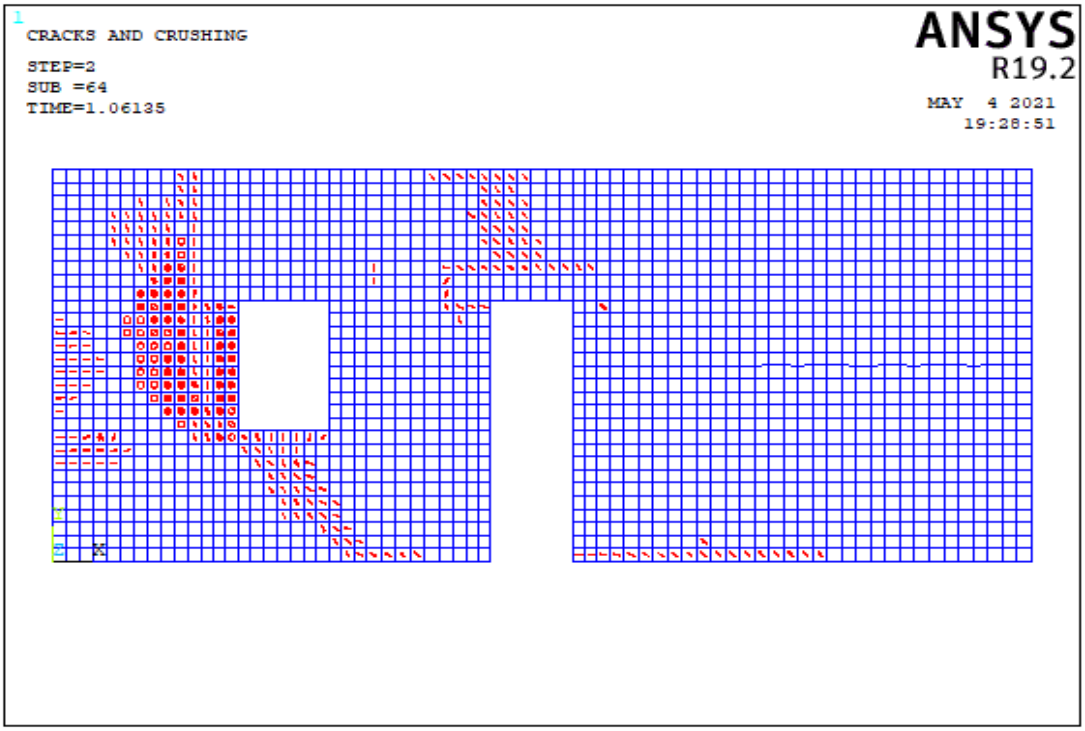

(a)

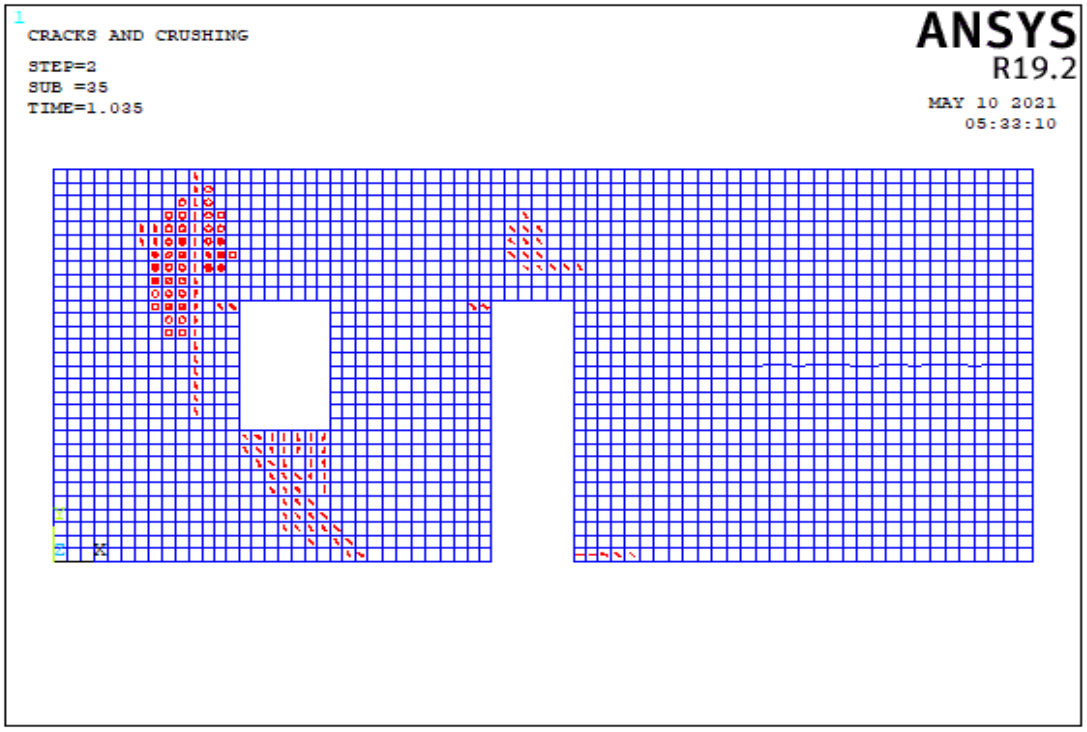

(b)

Figure 5.99. The Crack Pattern of Wall 12 Model 4 According to Compressive Strength Values of (a) 3 MPa, (b) 8 MPa

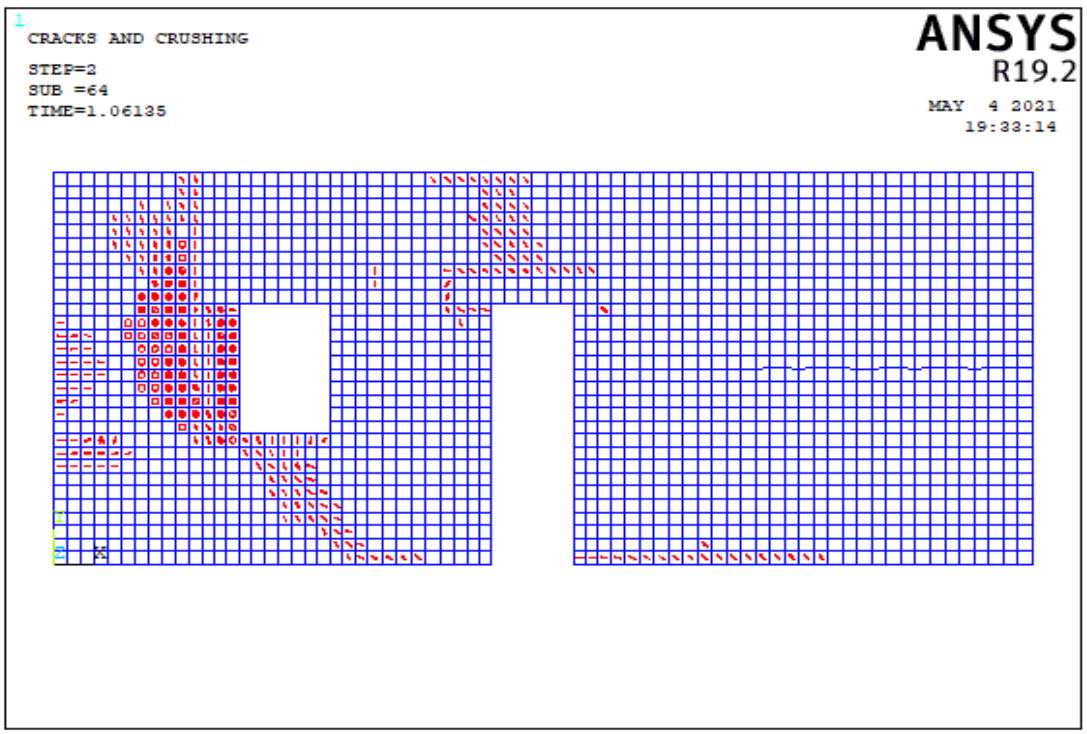

(a)

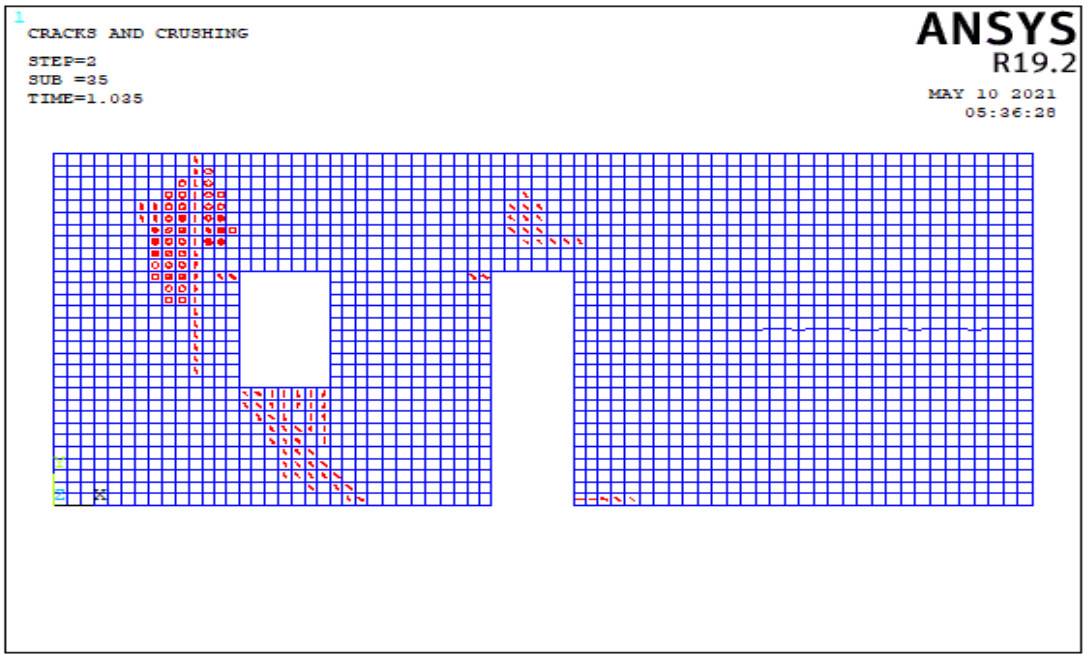

(b)

Figure 5.100. The Crack Pattern of Wall 12 Model 5 According to Compressive Strength Values of (a) 3 MPa, (b) 8 MPa

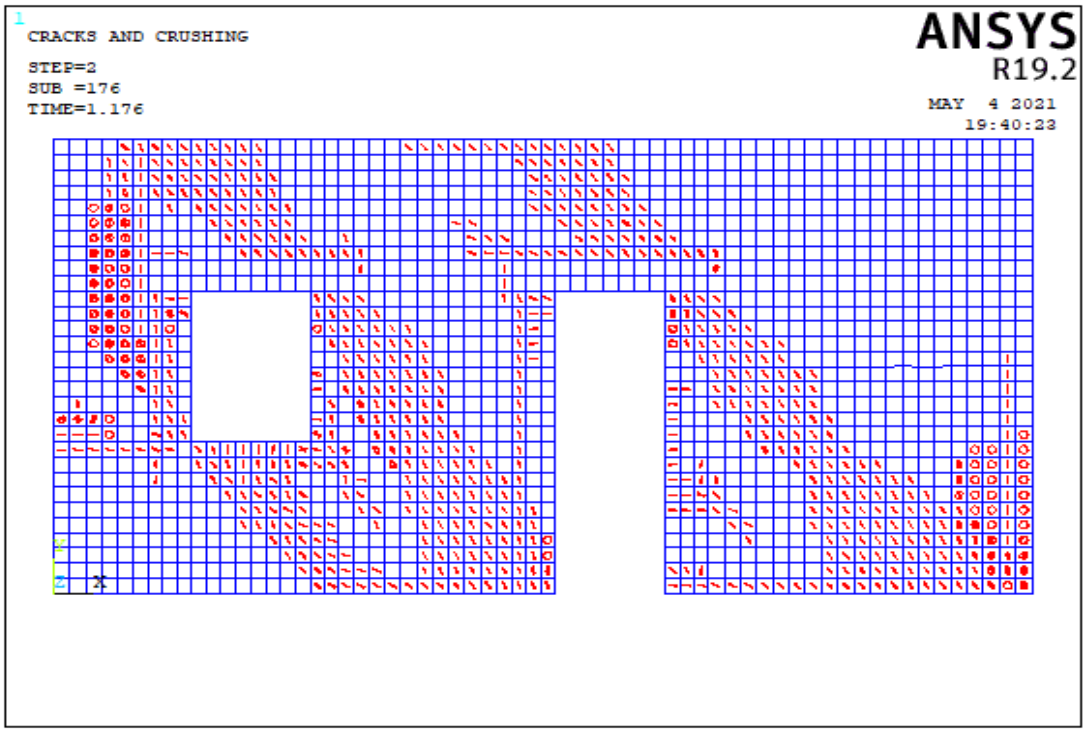

(a)

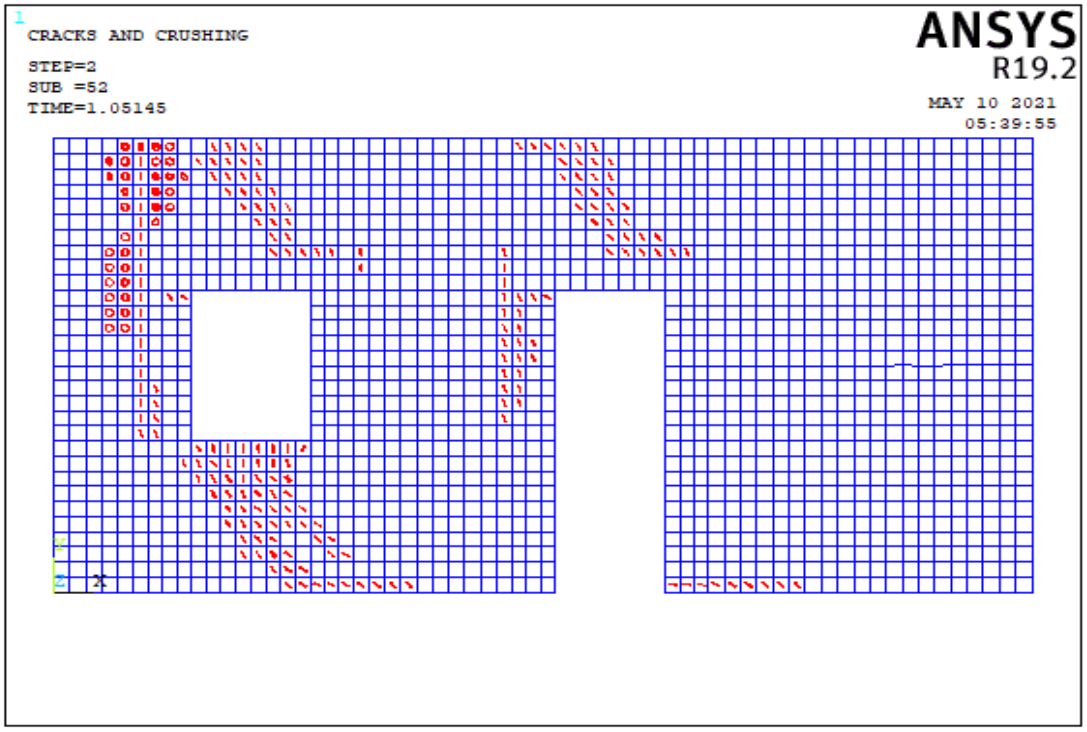

(b)

Figure 5.101. The Crack Pattern of Wall 12 Model 6 According to Compressive Strength Values of (a) 3 MPa, (b) 8 MPa

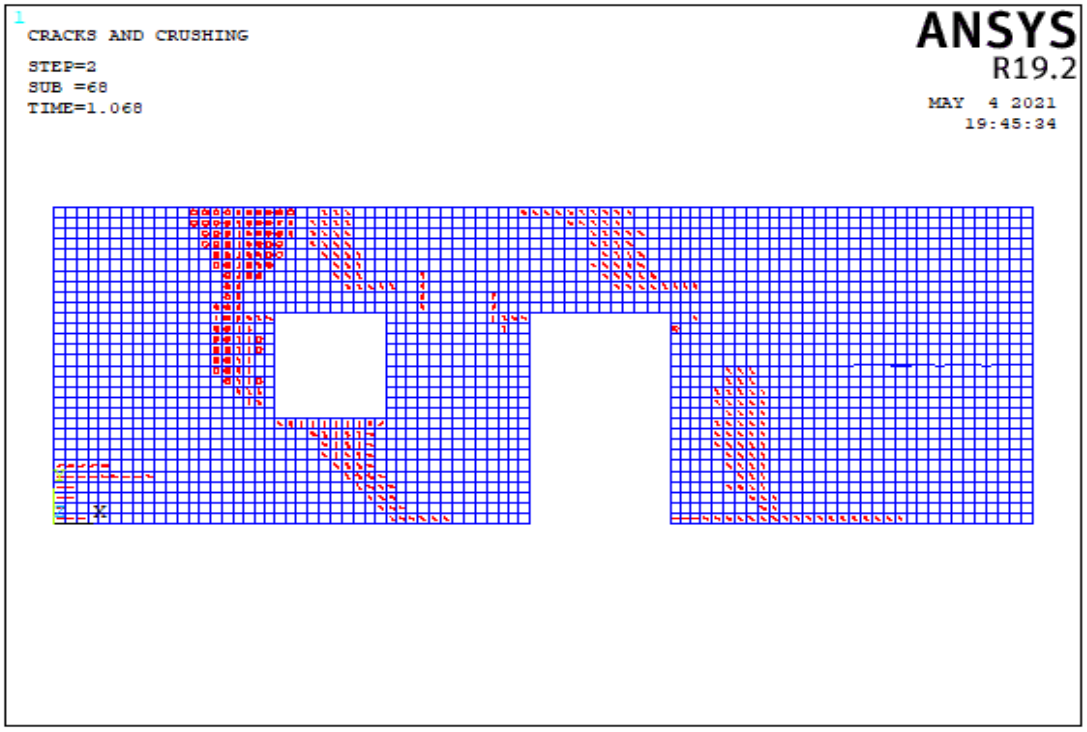

(a)

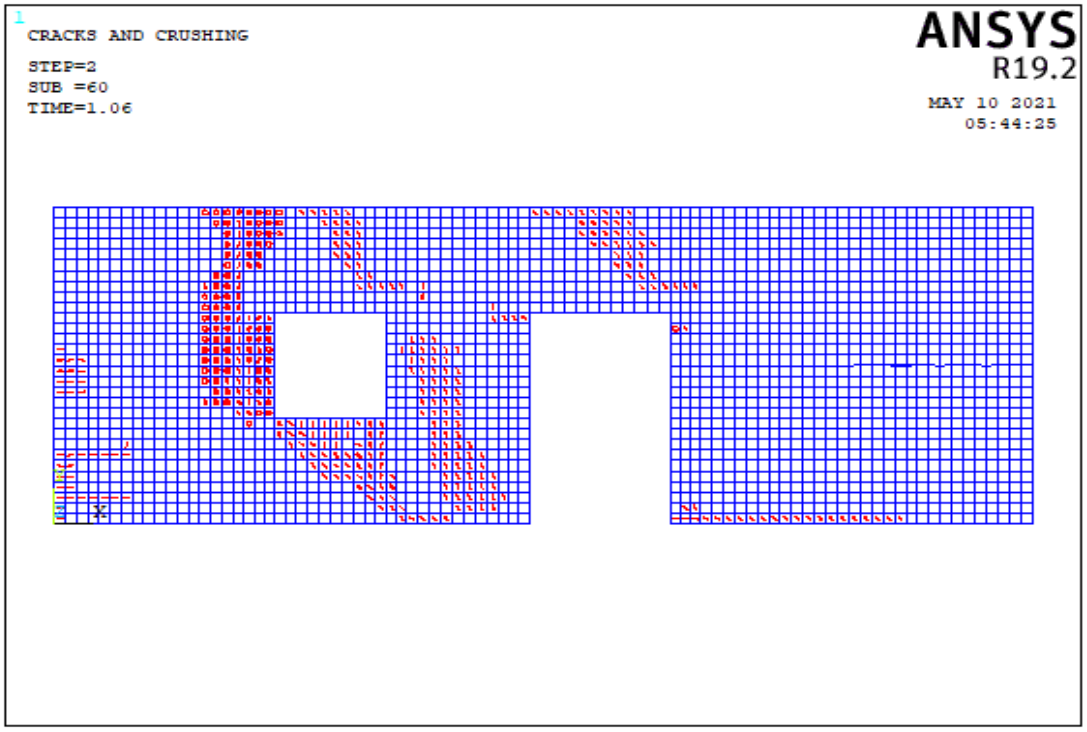

(b)

Figure 5.102. The Crack Pattern of Wall 12 Model 7 According to Compressive Strength Values of (a) 3 MPa, (b) 8 MPa

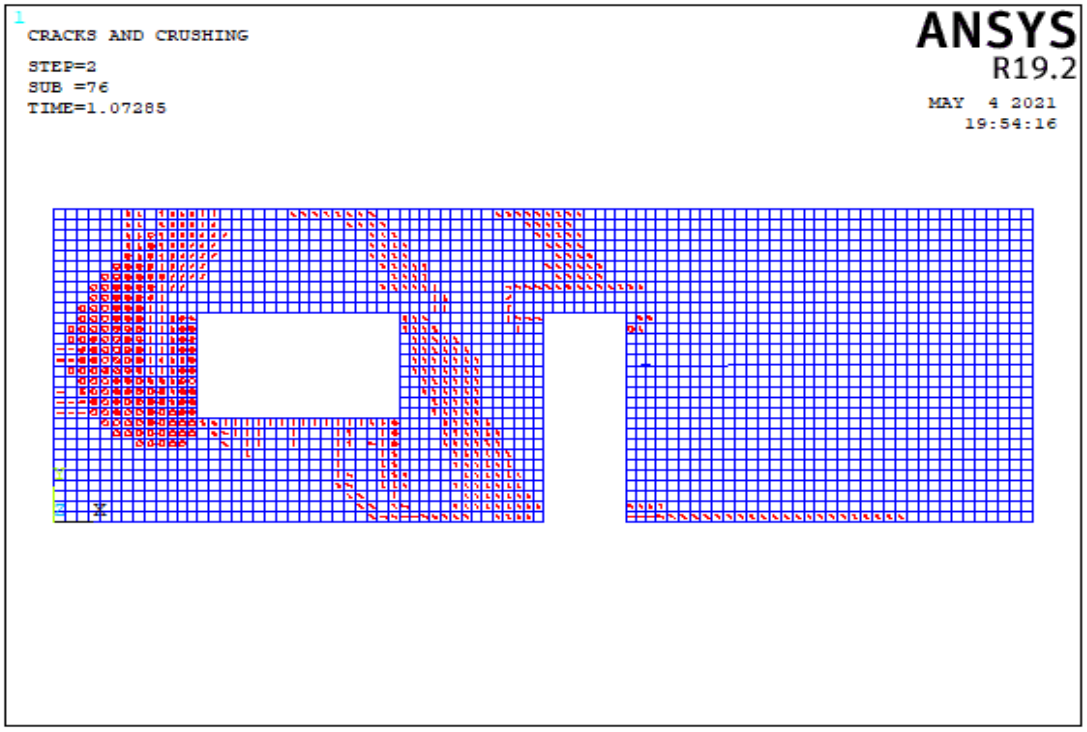

(a)

(b)

Figure 5.103. The Crack Pattern of Wall 12 Model 8 According to Compressive Strength Values of (a) 3 MPa, (b) 8 MPa

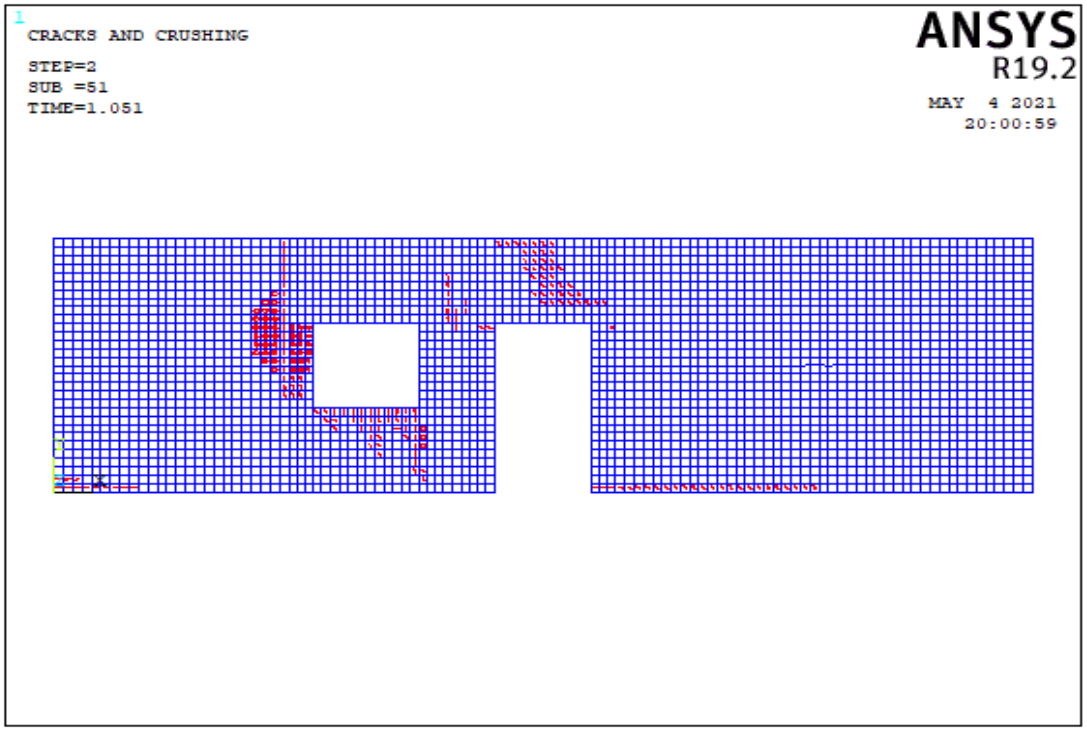

(a)

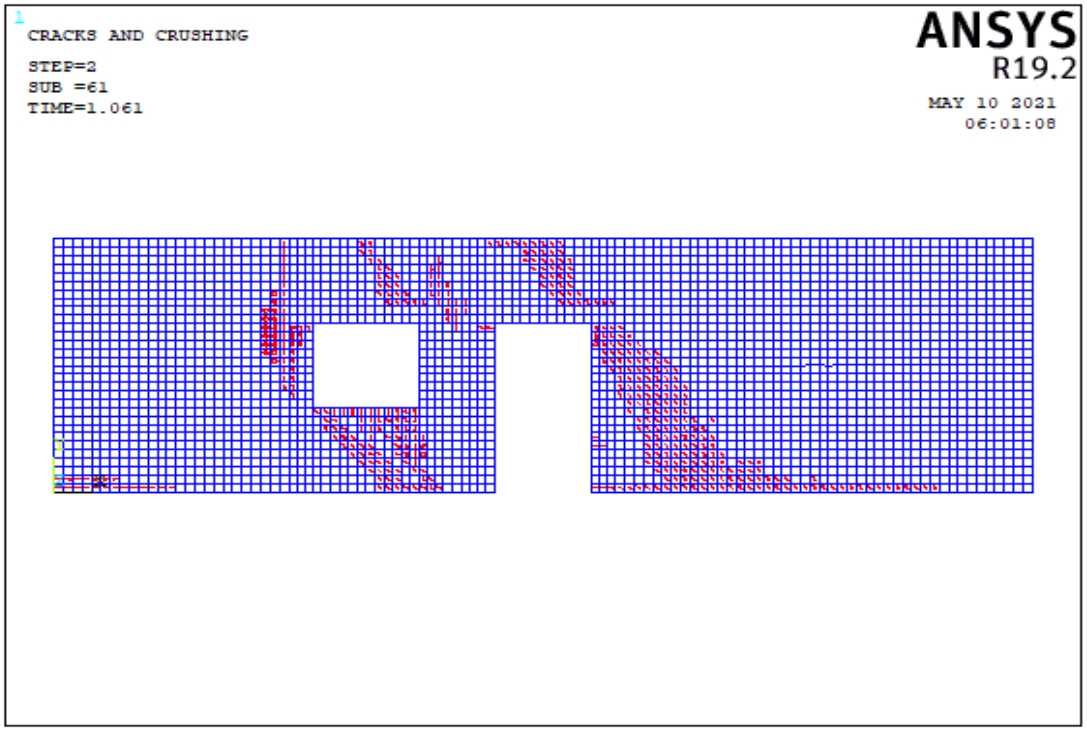

(b)

Figure 5.104. The Crack Pattern of Wall 12 Model 9 According to Compressive Strength Values of (a) 3 MPa, (b) 8 MPa

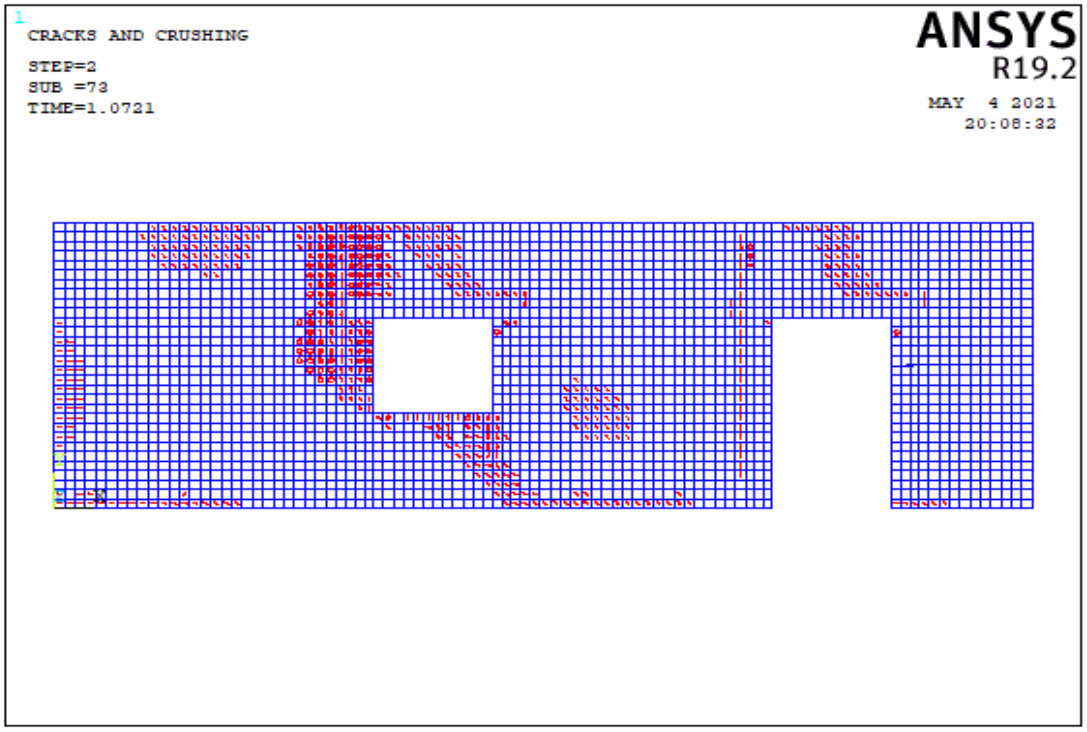

(a)

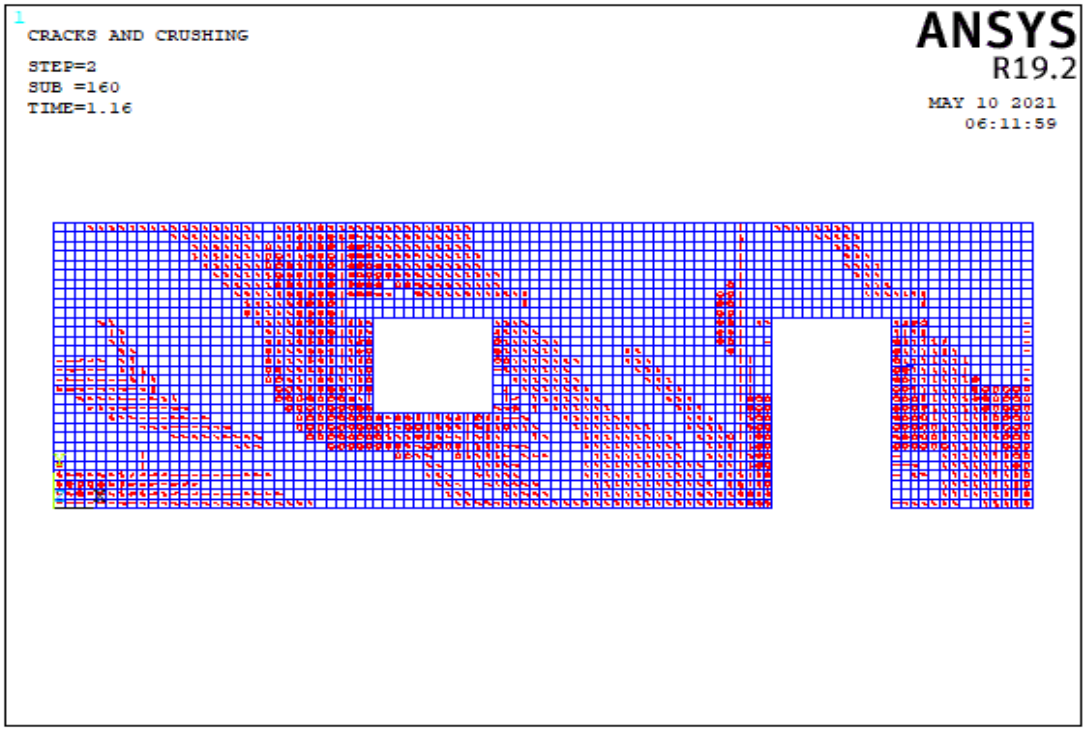

(b)

Figure 5.105. The Crack Pattern of Wall 12 Model 10 According to Compressive Strength Values of (a) 3 MPa, (b) 8 MPa

Table 5.14. Failure Patterns of Wall 12

Number of Model	Aspect ratio	fm=3 Mpa			fm=8 Mpa		
		Failure Pattern			Failure Pattern		
		Base Sliding	Rocking	Diagonal Tension	Base Sliding	Rocking	Diagonal Tension
Model 1	1.50	X			X		
	1.00	X			X		
	1.50	X			X		
Model 2	2.69		X			X	
	2.48						X
	0.98		X				X
Model 3	1.34		X			X	
	3.33					X	
	0.67	X					X
Model 4	2.37		X			X	
	2.73						
	0.96	X			X		
Model 5	2.37		X			X	
	2.73						
	0.96	X			X		
Model 6	3.70		X			X	
	2.08			X			
	1.39			X	X		
Model 7	1.61		X			X	
	2.50						
	0.98			X	X		
Model 8	2.45		X			X	
	2.45			X			X
	0.86	X					X
Model 9	1.09	X			X		
	3.80						
	0.64	X					X
Model 10	1.00	X					X
	1.14	X					X
	2.29	X				X	

In the Table A.12, all length of openings is less than 3 m for all models of wall 12 and total opening percentage of walls for all models is appropriate for TEC 2018. In model 1, 3, 7 and 9 for wall 12, the length of piers is more than 1.5 m. When model 6 is examined, the stiffness of wall is increased due to decreased aspect ratio. In model 1, the failure mechanism of piers is base sliding, but spandrels also have flexural and diagonal mechanisms. When models 3 and 9 are examined, the capacity of the corner pier increase as the aspect ratio of pier reduce. The shear is predominat in these corner piers. Table 5.14 shows that, the diagonal tension mechanism dominates in low aspect ratio of wall. On the other hand, the rocking mechanism is predominant in high aspect ratio of wall.

5.4.1.13 Failure Modes of Wall 13

In the wall 13 type, there are 10 different wall models. The impact of single door and two windows openings was studied in these models of wall 13. Table A.13 shows the lengths of the walls. As seen in Figure 5.3, each pier is designated from left to right. The crack patterns obtained from the analysis of wall models corresponding to 10 different wall models are described in this section.

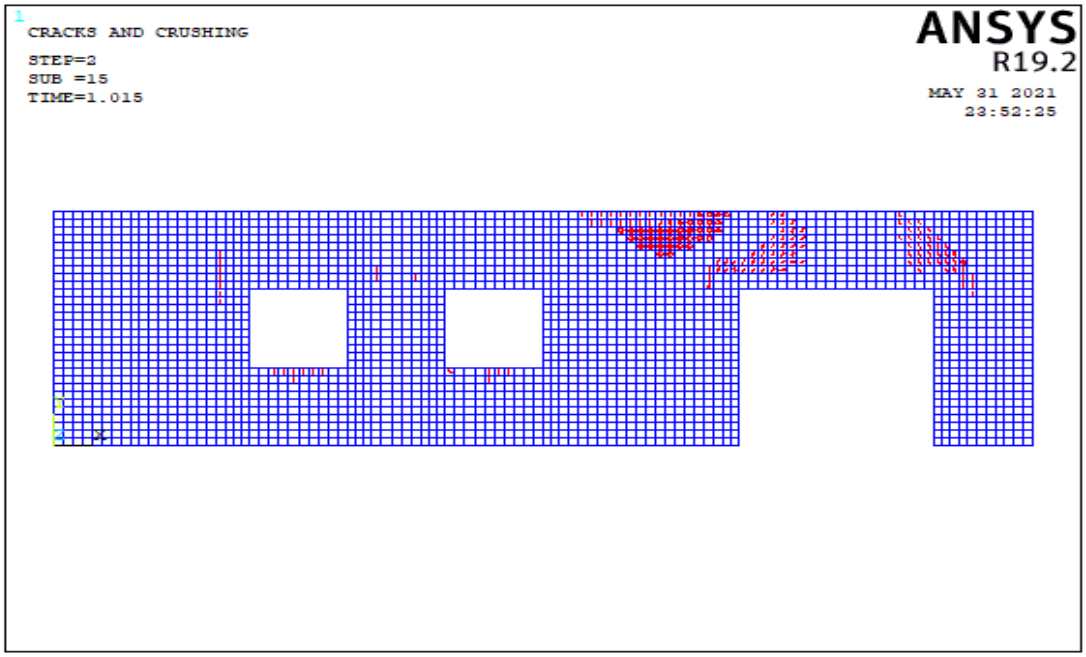

(a)

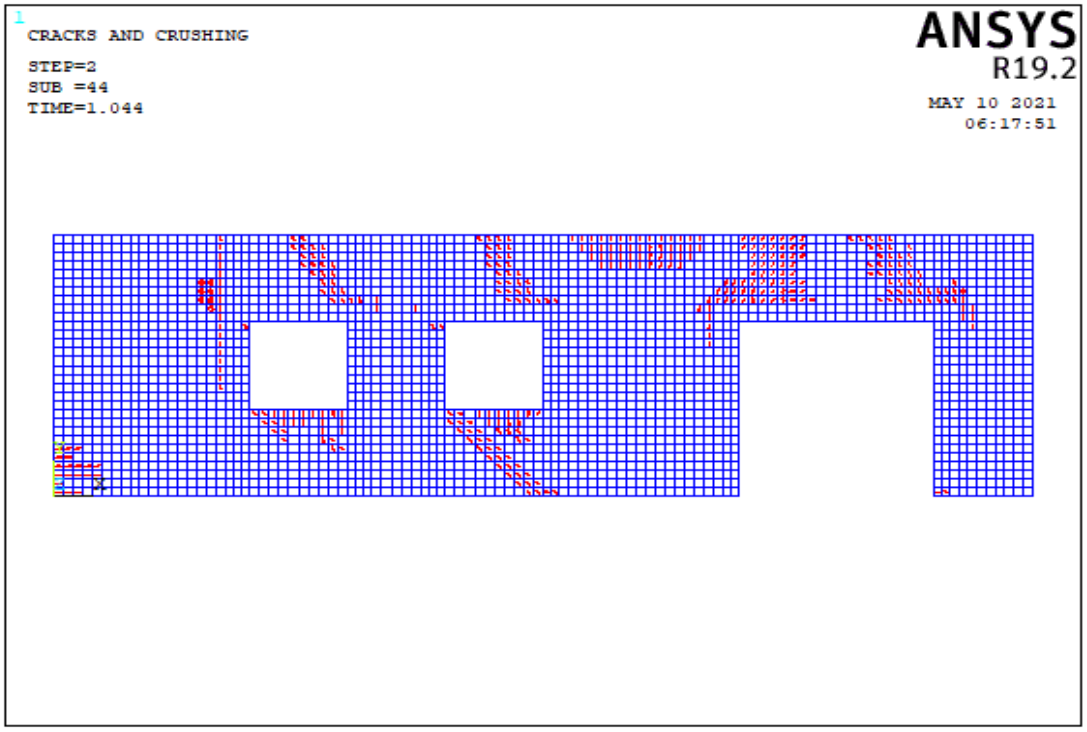

(b)

Figure 5.106. The Crack Pattern of Wall 13 Model 1 According to Compressive Strength Values of (a) 3 MPa, (b) 8 MPa

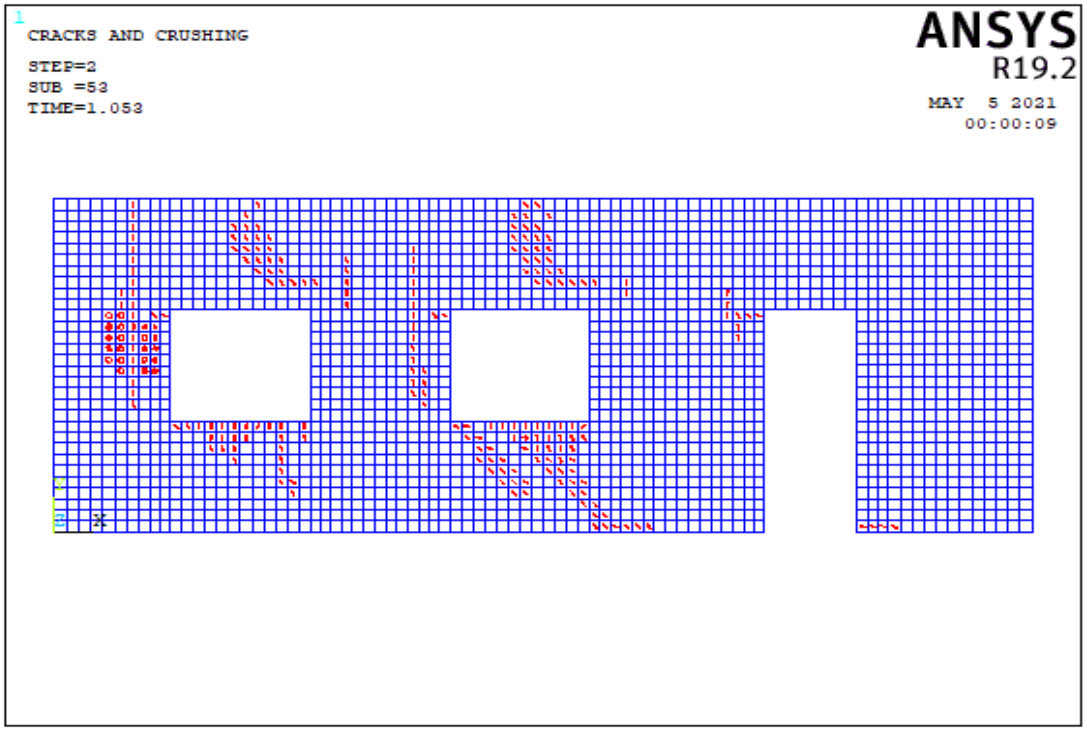

(a)

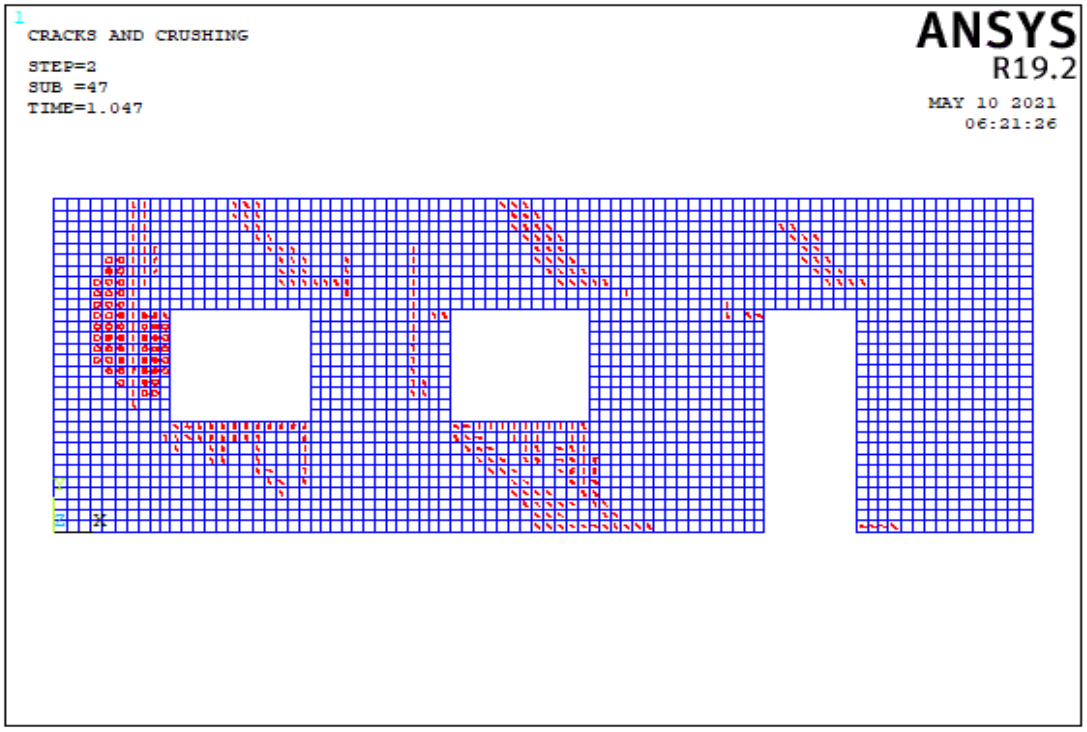

(b)

Figure 5.107. The Crack Pattern of Wall 13 Model 2 According to Compressive Strength Values of (a) 3 MPa, (b) 8 MPa

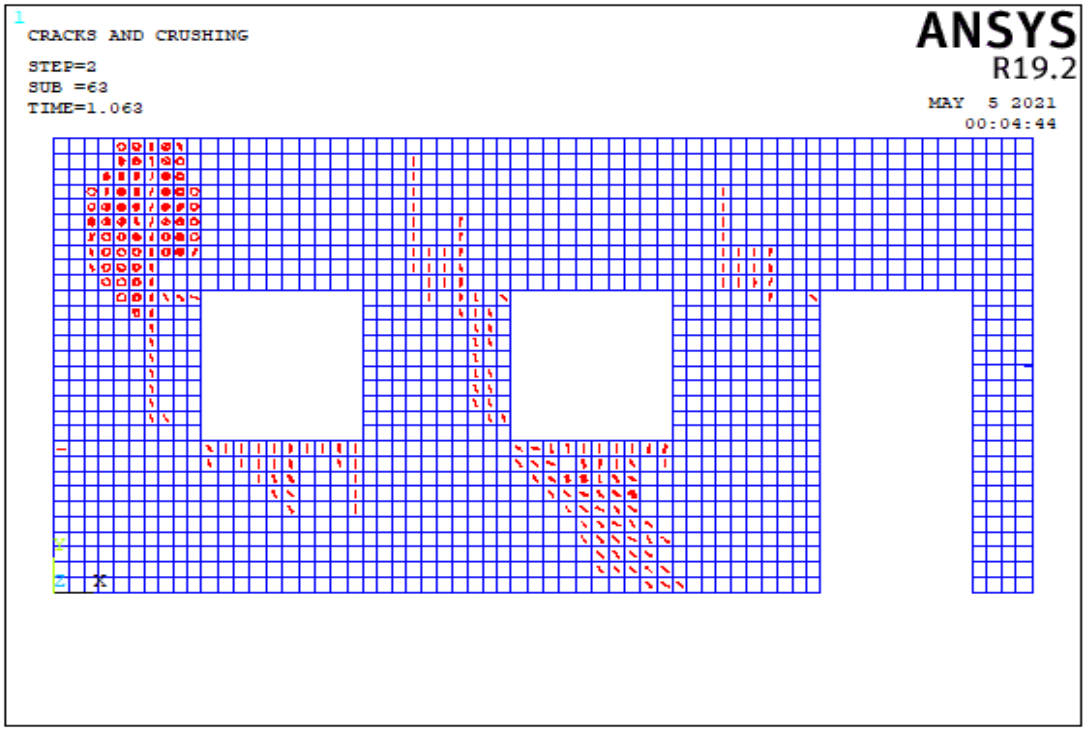

(a)

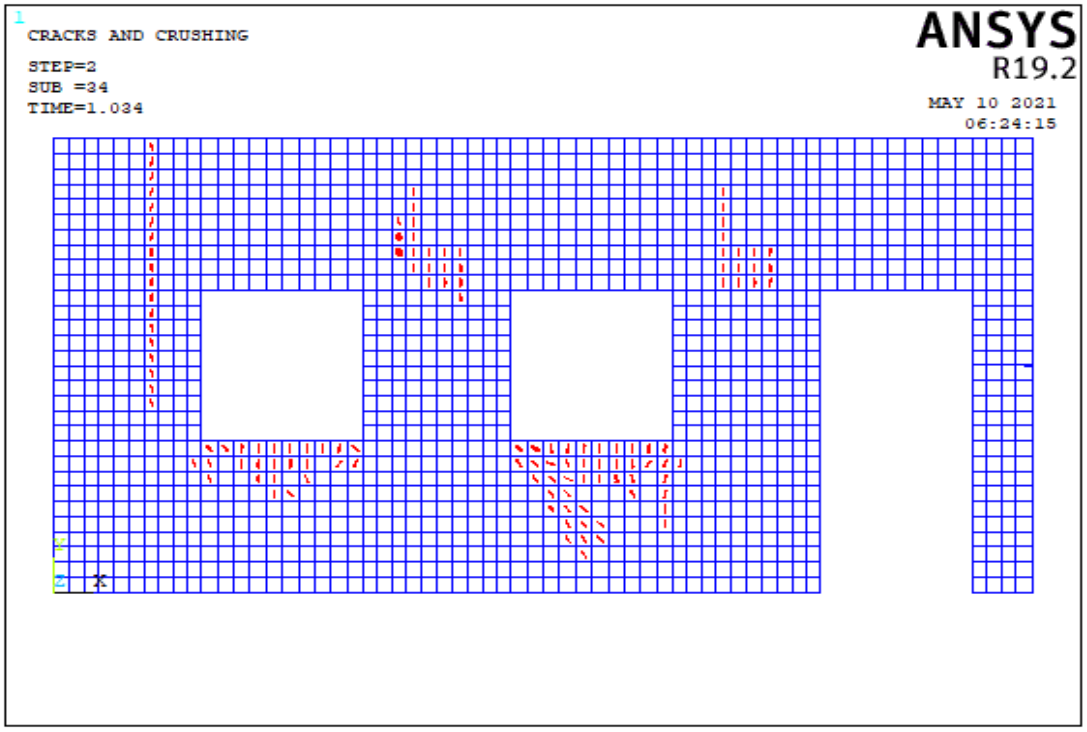

(b)

Figure 5.108. The Crack Pattern of Wall 13 Model 3 According to Compressive Strength Values of (a) 3 MPa, (b) 8 MPa

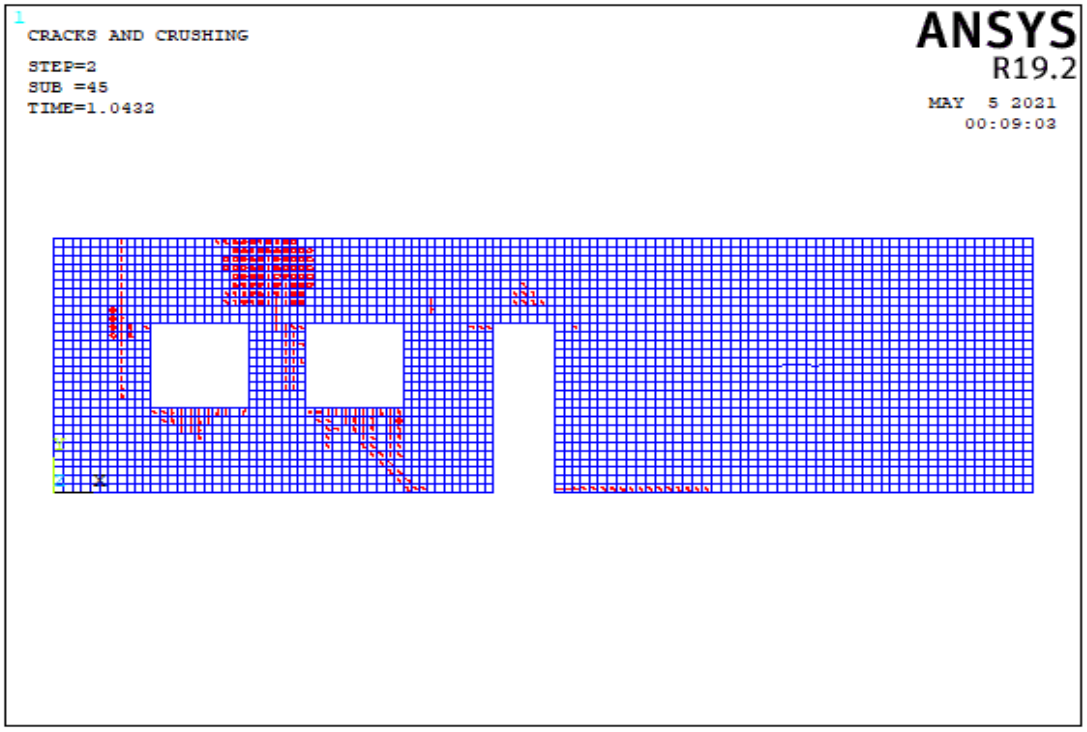

(a)

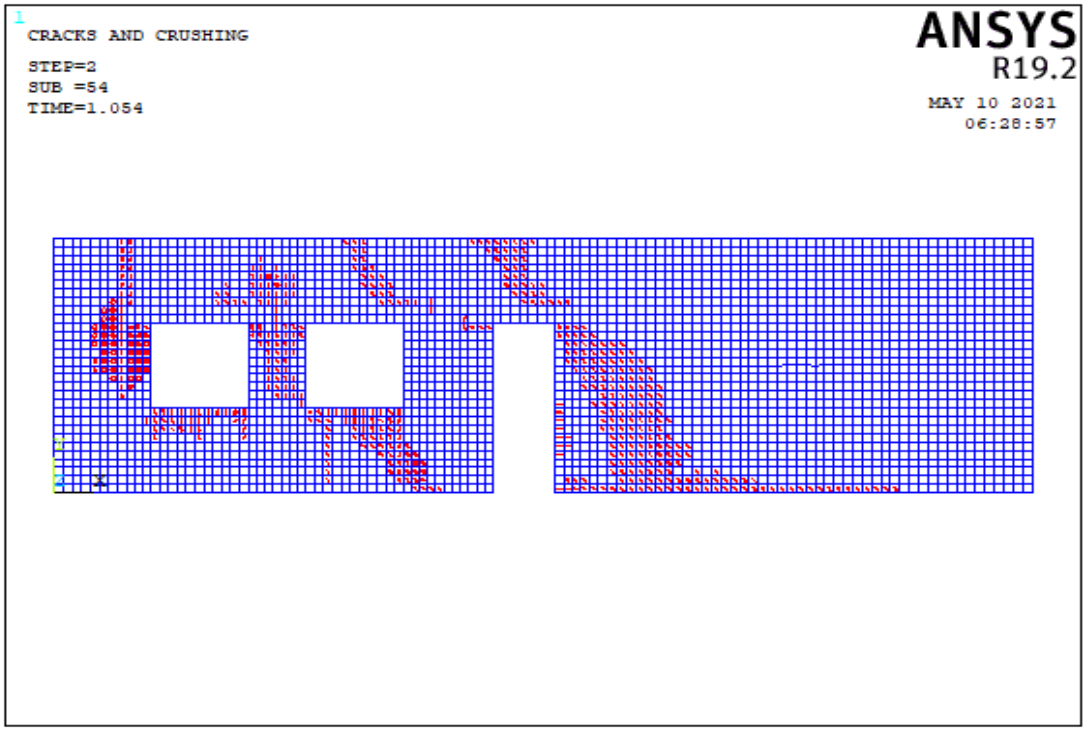

(b)

Figure 5.109. The Crack Pattern of Wall 13 Model 4 According to Compressive Strength Values of (a) 3 MPa, (b) 8 MPa

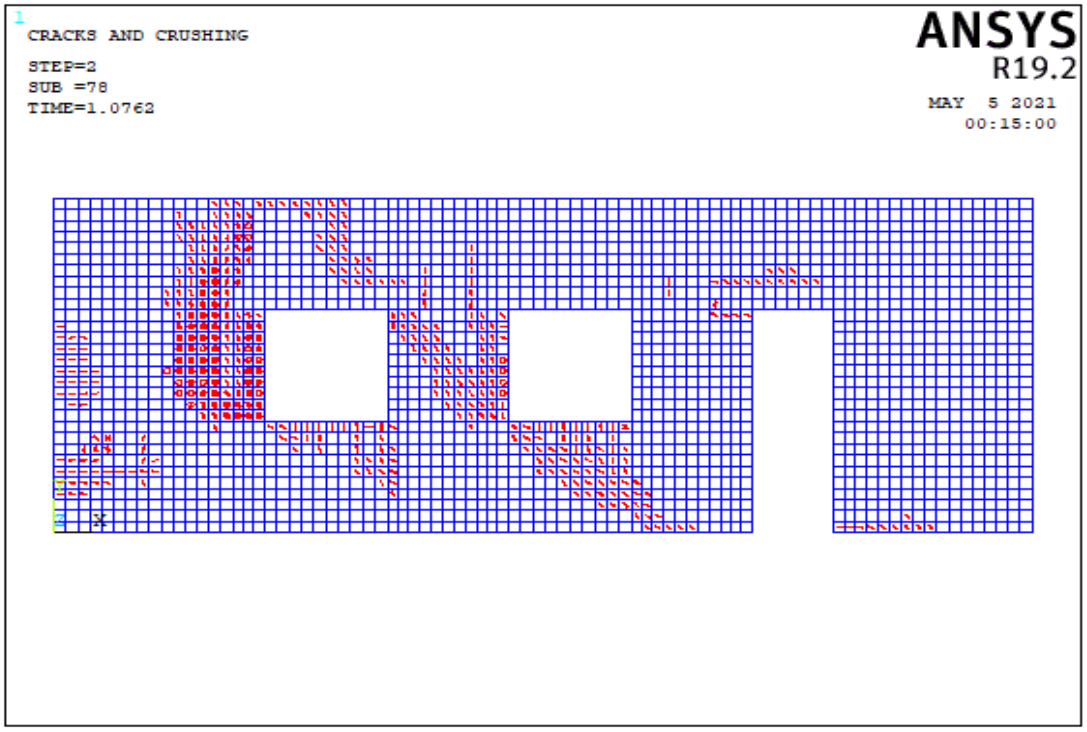

(a)

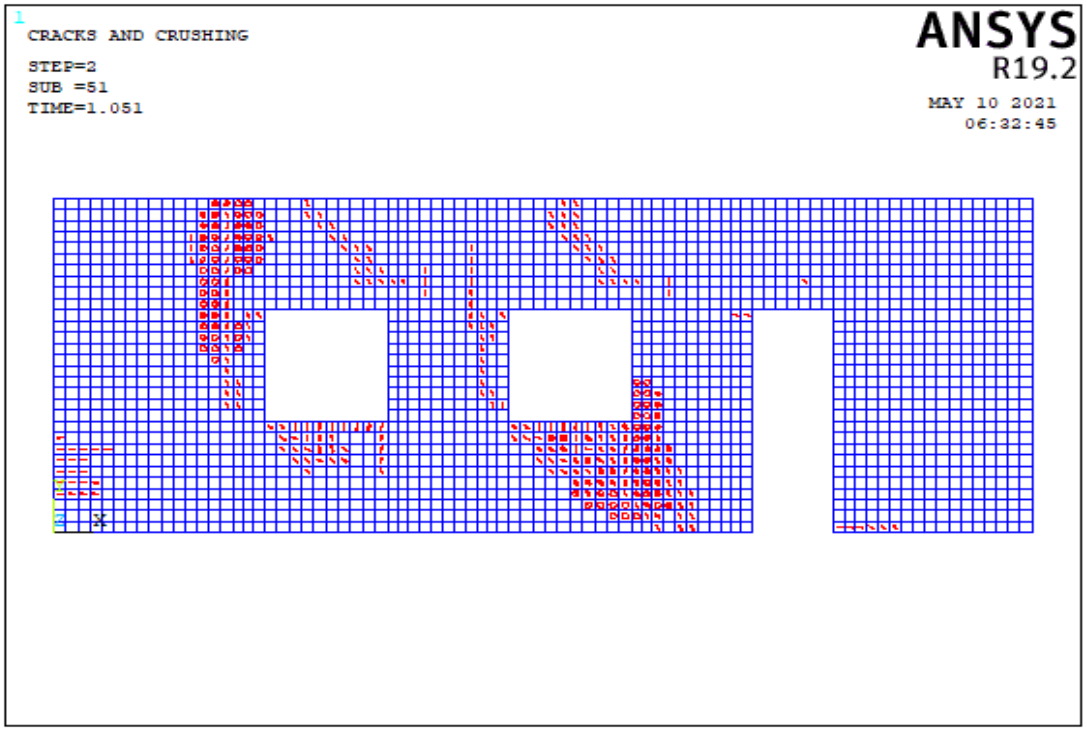

(b)

Figure 5.110. The Crack Pattern of Wall 13 Model 5 According to Compressive Strength Values of (a) 3 MPa, (b) 8 MPa

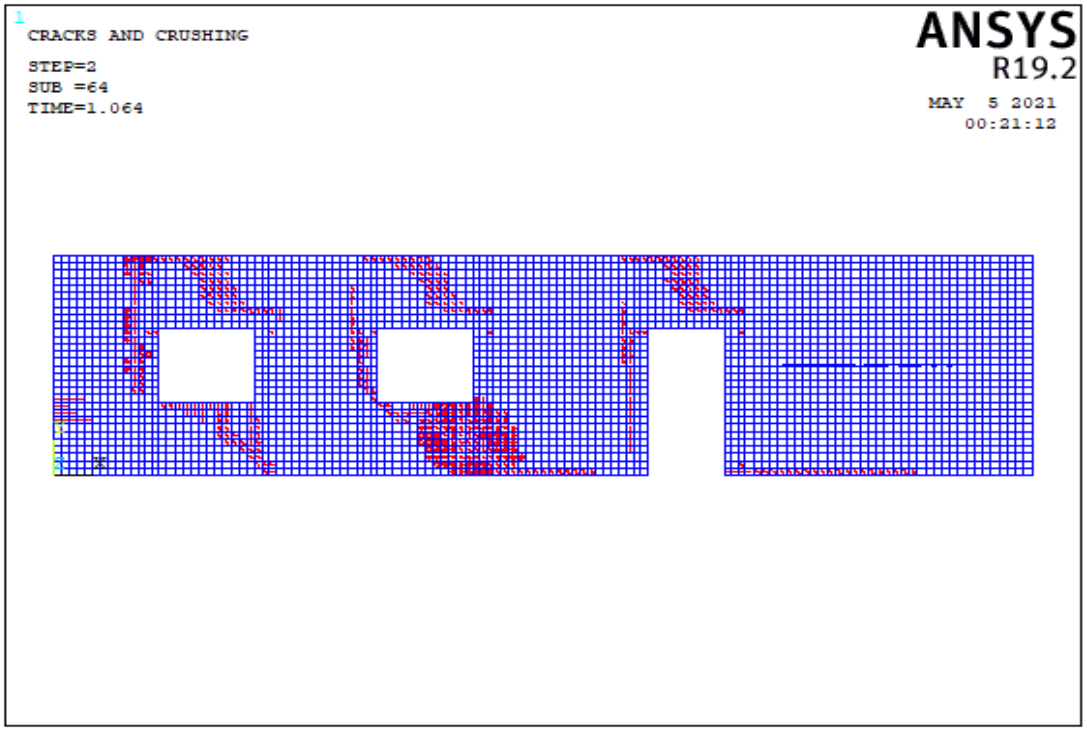

(a)

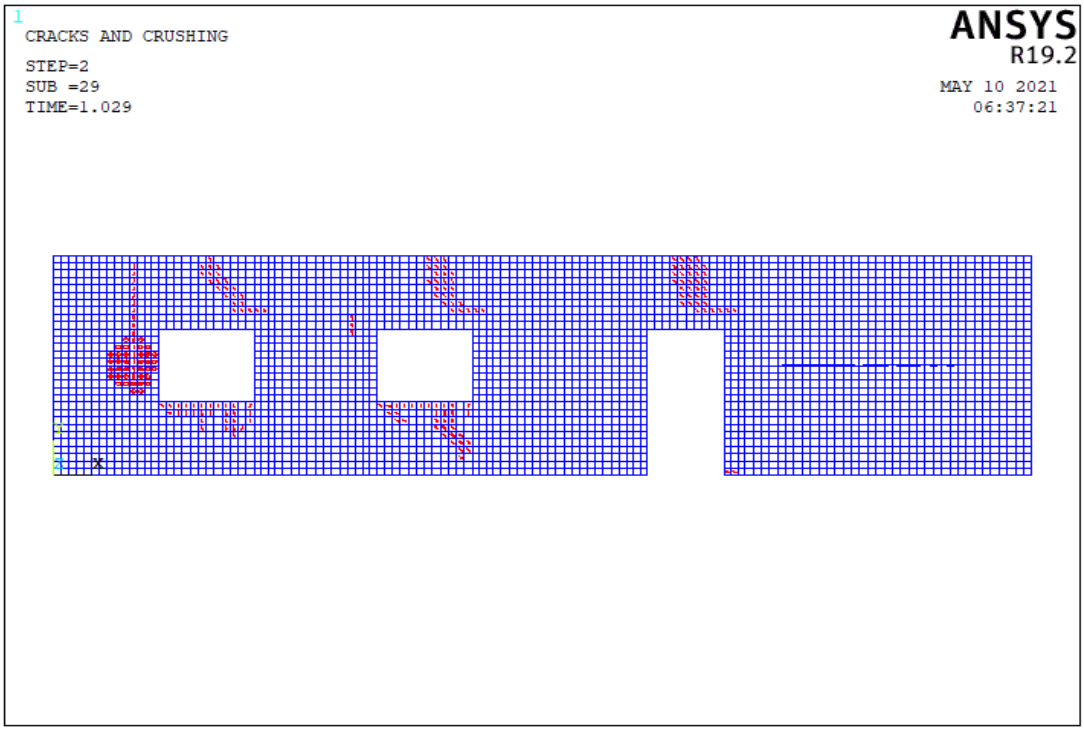

(b)

Figure 5.111. The Crack Pattern of Wall 13 Model 6 According to Compressive Strength Values of (a) 3 MPa, (b) 8 MPa

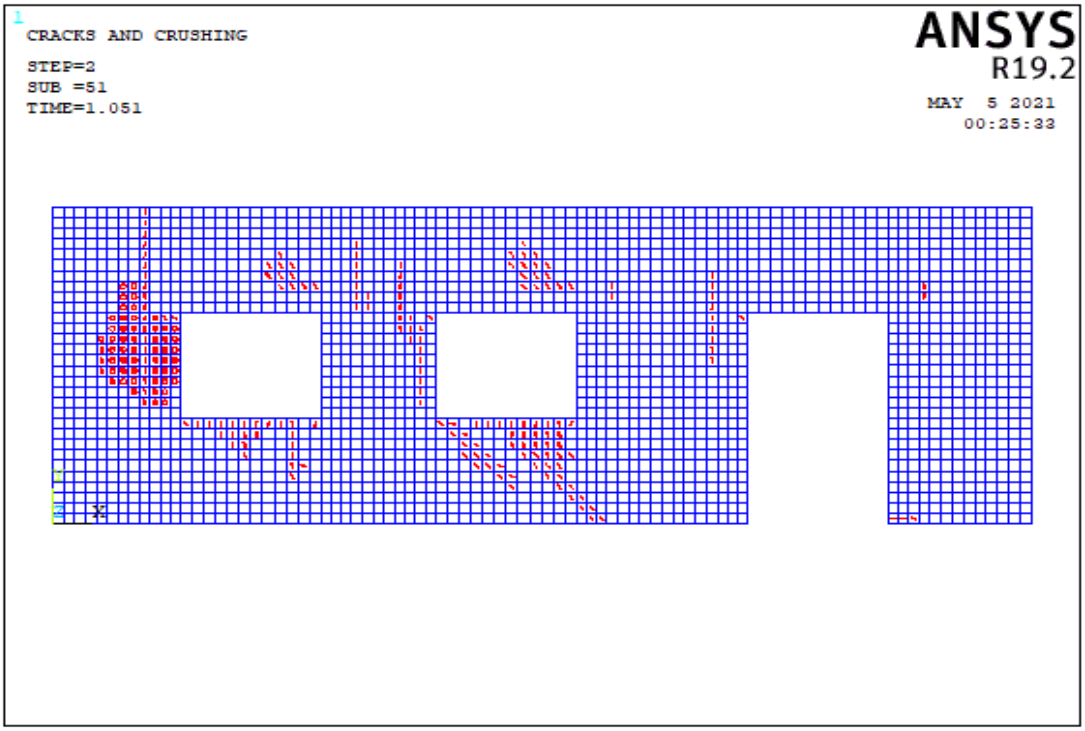

(a)

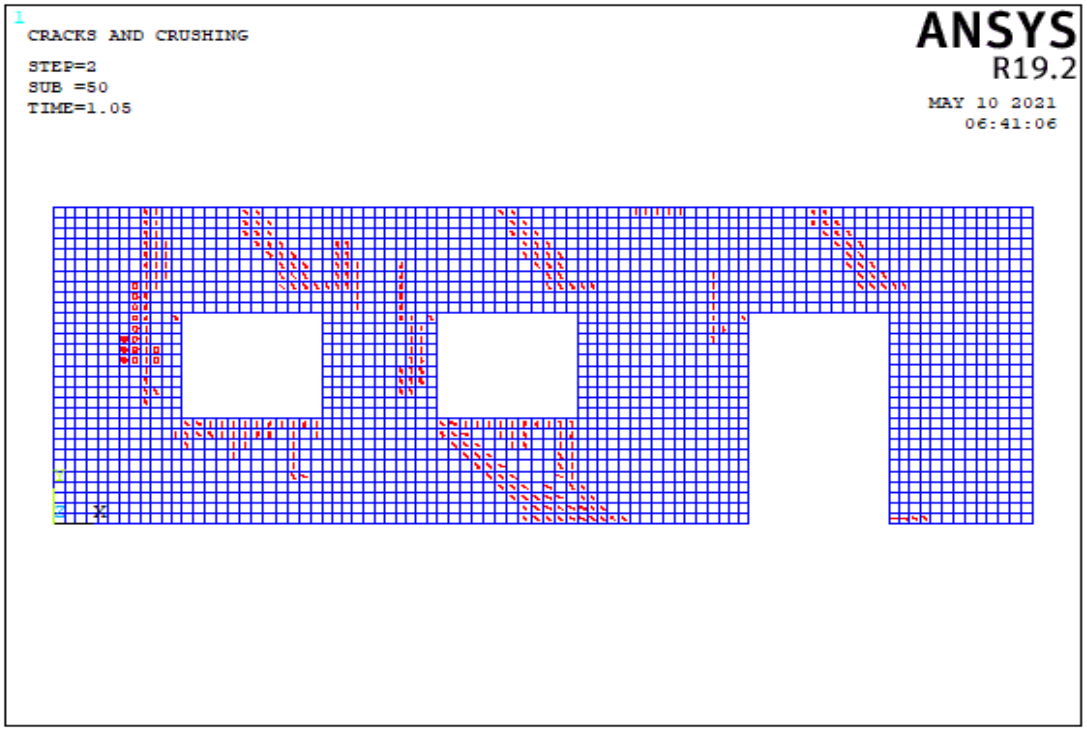

(b)

Figure 5.112. The Crack Pattern of Wall 13 Model 7 According to Compressive Strength Values of (a) 3 MPa, (b) 8 MPa

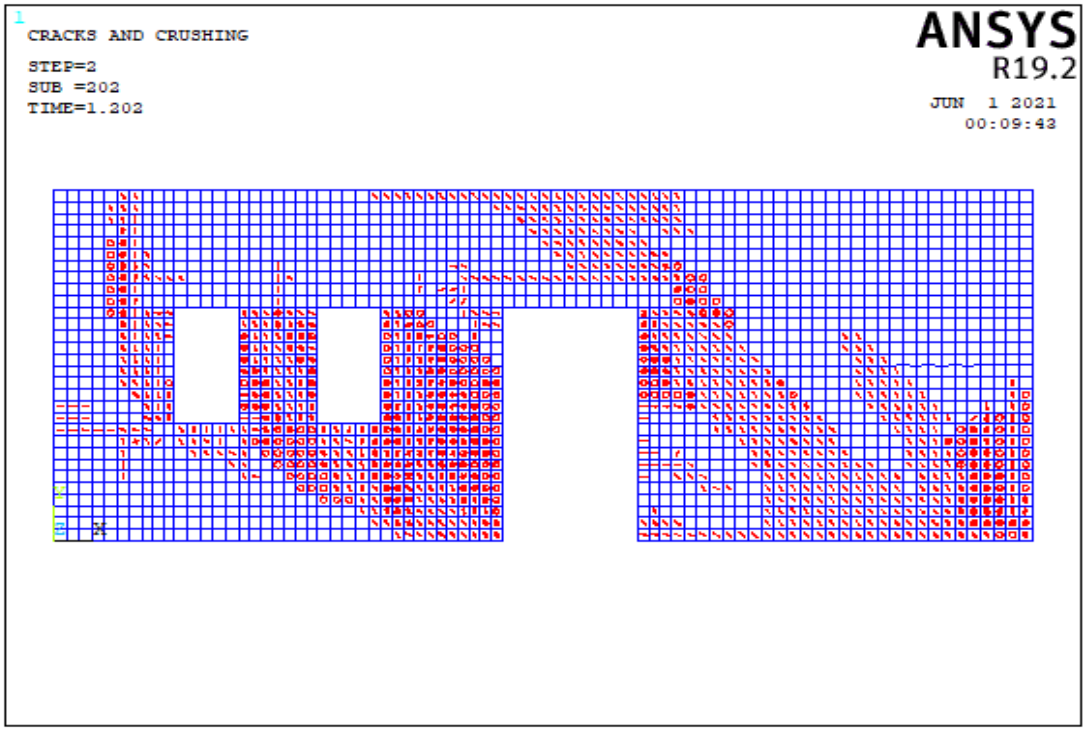

(a)

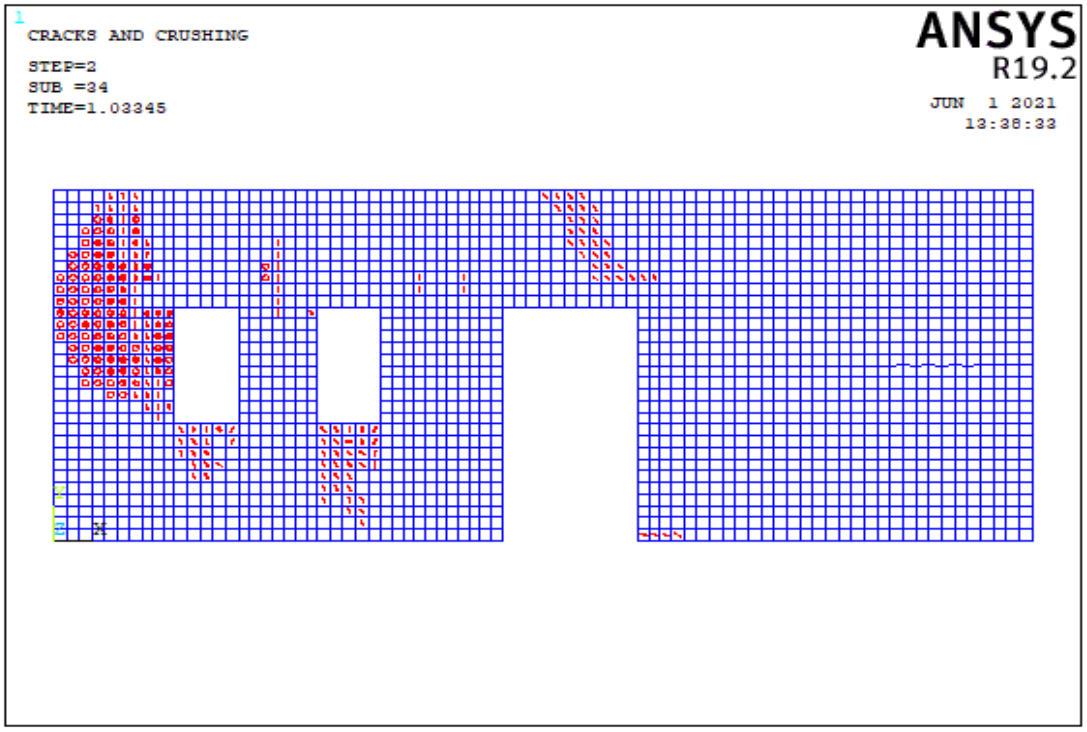

(b)

Figure 5.113. The Crack Pattern of Wall 13 Model 8 According to Compressive Strength Values of (a) 3 MPa, (b) 8 MPa

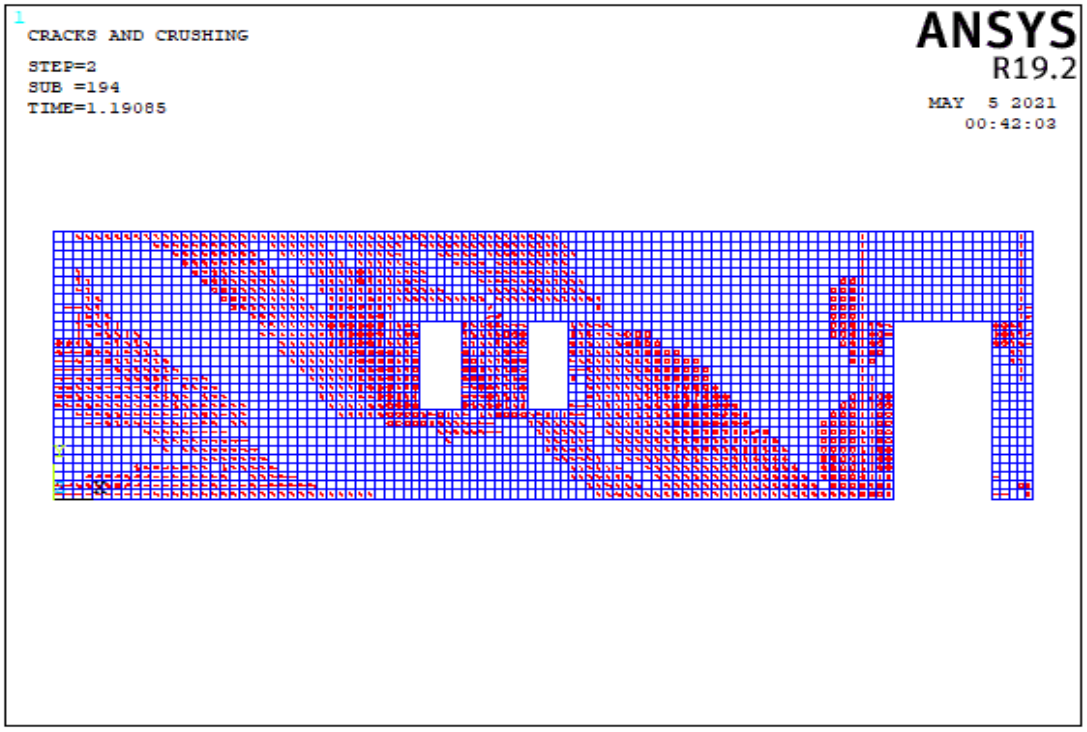

(a)

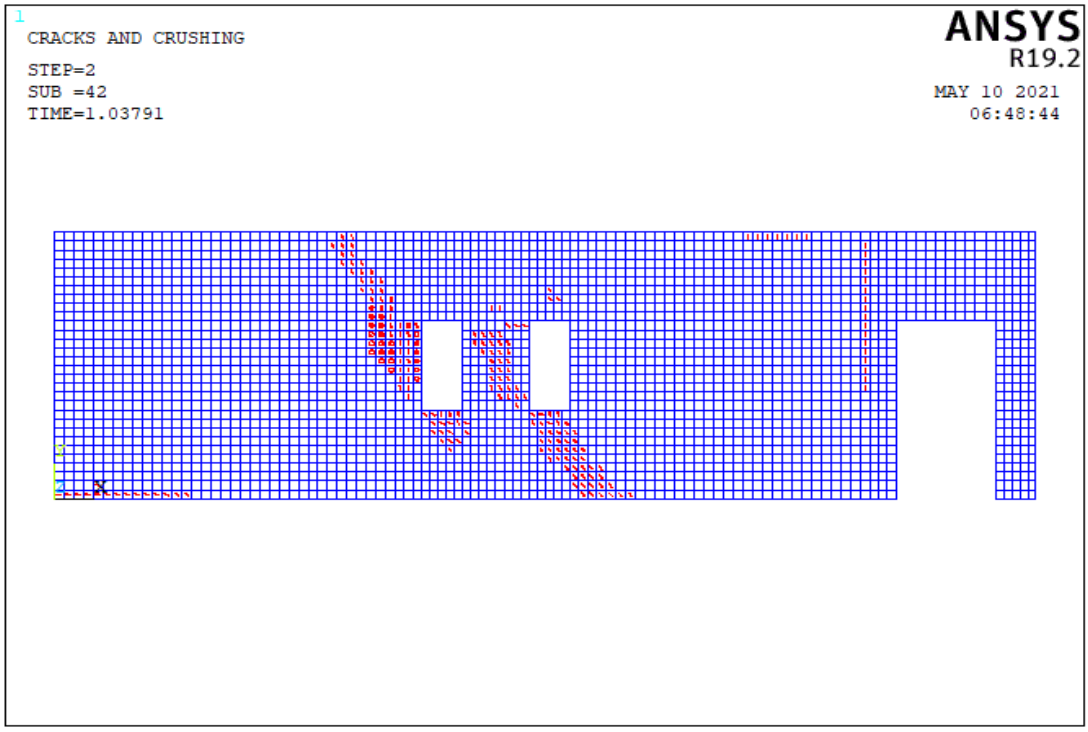

(b)

Figure 5.114. The Crack Pattern of Wall 13 Model 9 According to Compressive Strength Values of (a) 3 MPa, (b) 8 MPa

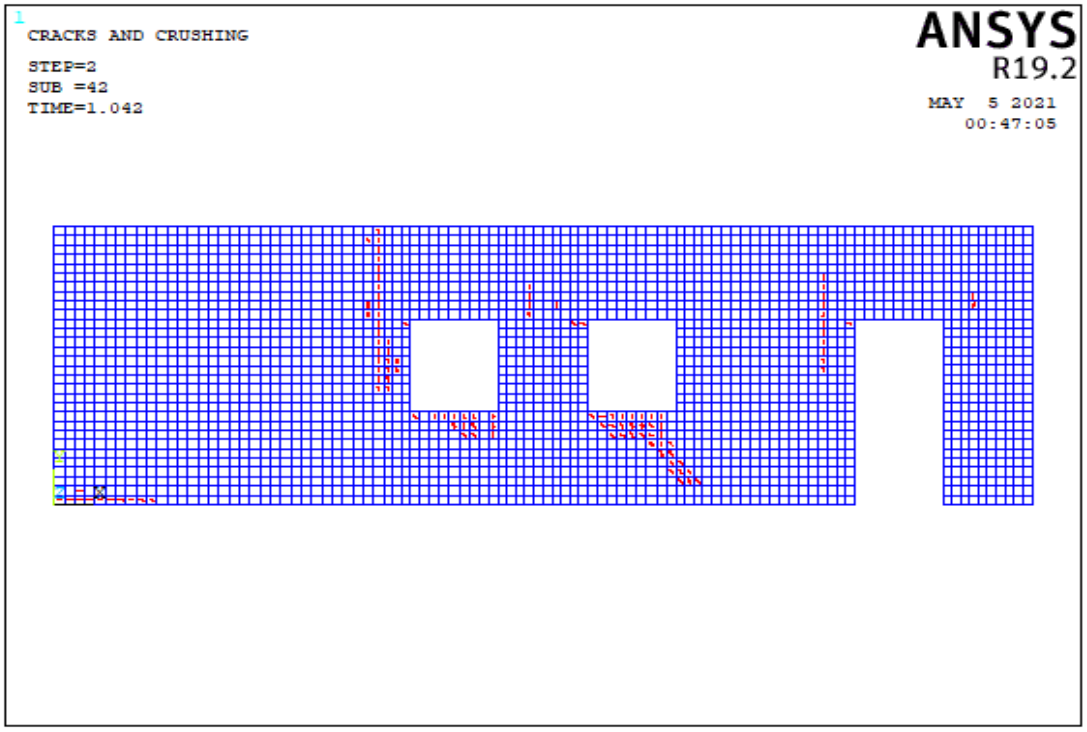

(a)

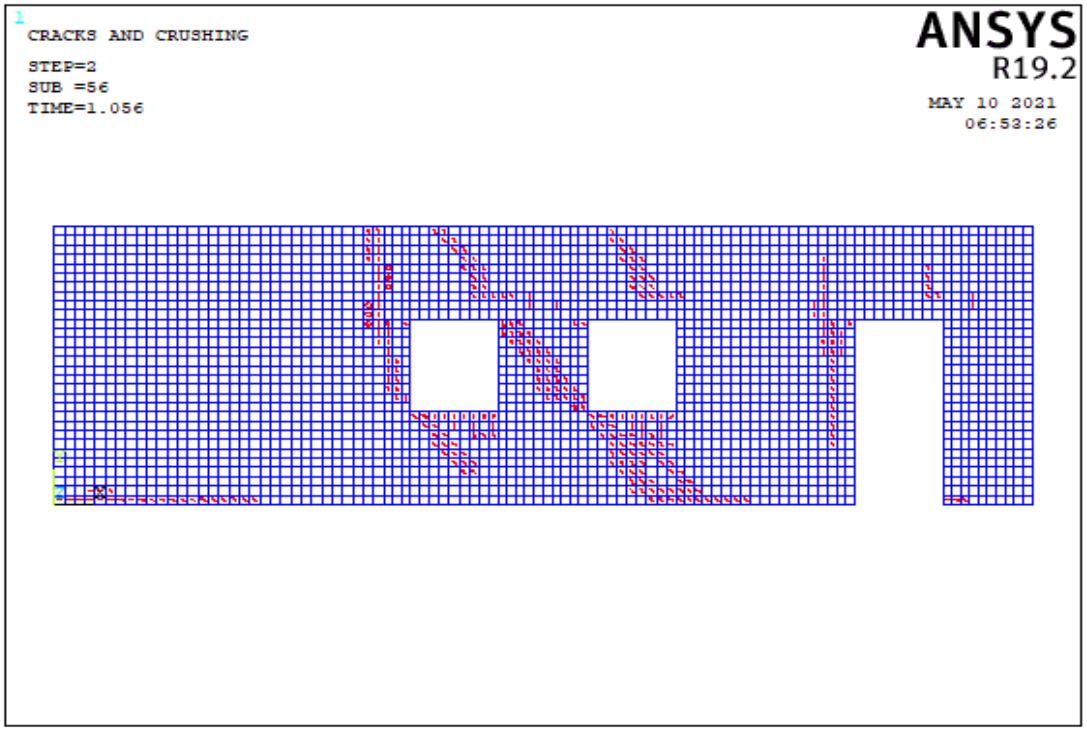

(b)

Figure 5.115. The Crack Pattern of Wall 13 Model 10 According to Compressive Strength Values of (a) 3 MPa, (b) 8 MPa

Table 5.15. Failure Patterns of Wall 13

Number of Model	Aspect ratio	fm=3 Mpa			fm=8 Mpa		
		Failure Pattern			Failure Pattern		
		Base Sliding	Rocking	Diagonal Tension	Base Sliding	Rocking	Diagonal Tension
Model 1	1.50					X	
	3.00						
	1.50						
	3.00						
Model 2	3.20		X			X	
	2.67			X			X
	2.13	X			X		
	2.13	X			X		
Model 3	3.45		X			X	
	3.45			X			
	3.45						
	8.57		X			X	
Model 4	2.96		X			X	
	5.00			X			X
	3.21						
	0.60	X			X		
Model 5	1.78		X			X	
	3.12			X			X
	3.12						
	1.90	X			X		
Model 6	2.35		X		X		
	2.01			X			
	1.41	X					
	0.80	X					
Model 7	2.80		X			X	
	3.13			X			X
	2.08						
	2.50						
Model 8	3.24		X			X	
	5.01			X			
	3.24			X			
	0.99			X			
Model 9	0.82			X			X
	4.50			X			X
	0.92			X			
	7.50		X			X	
Model 10	0.88	X			X		
	3.50			X			X
	1.75						
	3.50		X			X	

In the Table A.13, all length of openings is less than 3 m for all models of wall 13 and total opening percentage of walls for model 3 and 7 is not appropriate for TEC 2018. In only model 5 for wall 13, the length of corner piers is more than 1.5 m. In models 1, 2 and 6, the length of piers between the openings are more than 1 meter. In model 3, corner pier percentage is 6% and length of corner pier is 0,35 m, this insufficient length of piers cause local failure. The main reason for local collapses is that the size of opening is much or near the corners. Excessive aspect ratios of piers can cause local failures. Model 6 shows that as the aspect ratio of the piers decreases, the diagonal cracks occur and the strength of the wall increases. Table 5.15 shows that, the diagonal tension mechanism dominates in low aspect ratio of wall. On the other hand, the rocking mechanism is predominant in high aspect ratio of wall.

5.4.1.14 Failure Modes of Wall 14

In the wall 14 type, there are 11 different wall models. The impact of single door and three windows openings was studied in these models of wall 14. Table A.14 shows the lengths of the walls. As seen in Figure 5.3, each pier is designated from left to right. The crack patterns obtained from the analysis of wall models corresponding to 11 different wall models are described in this section.

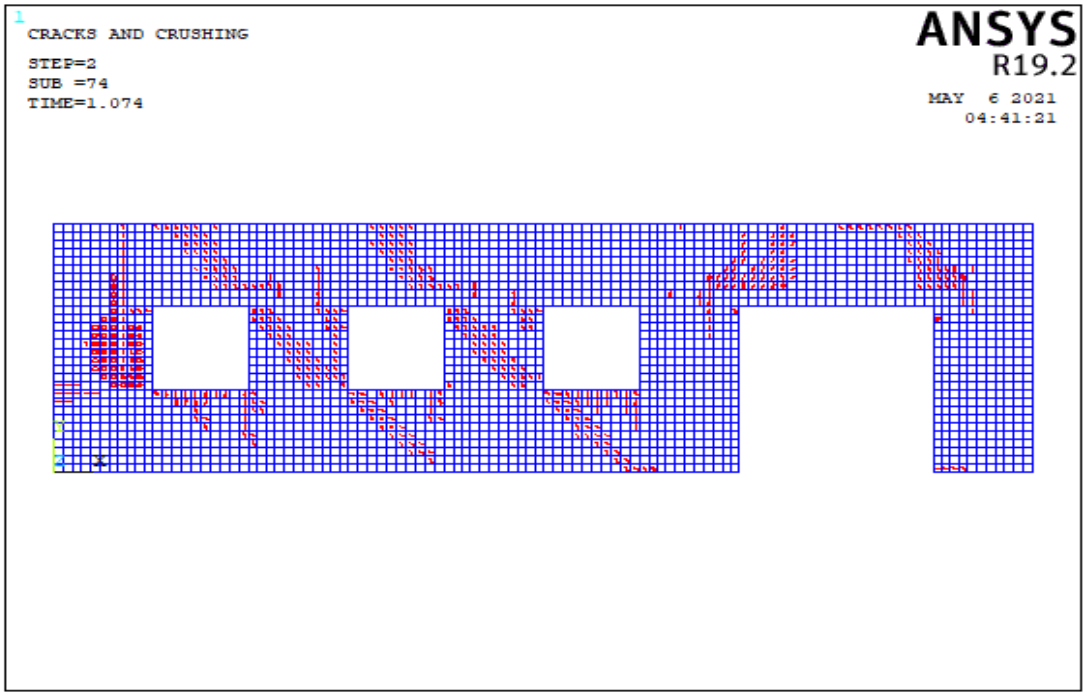

(a)

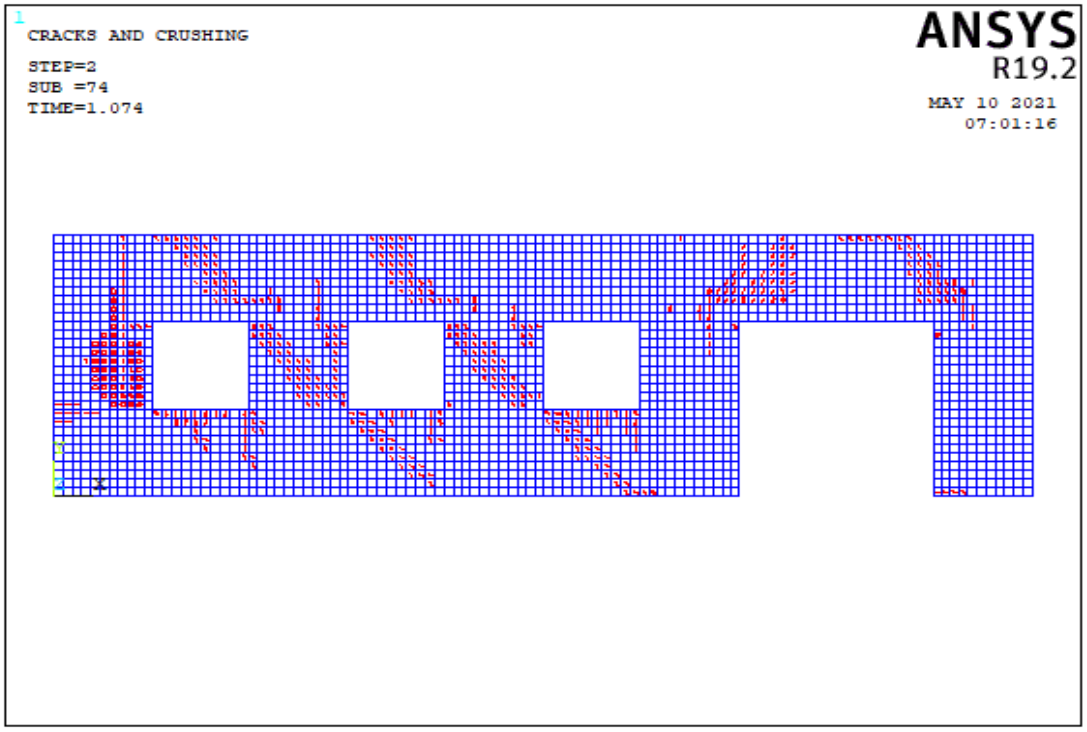

(b)

Figure 5.116. The Crack Pattern of Wall 14 Model 1 According to Compressive Strength Values of (a) 3 MPa, (b) 8 MPa

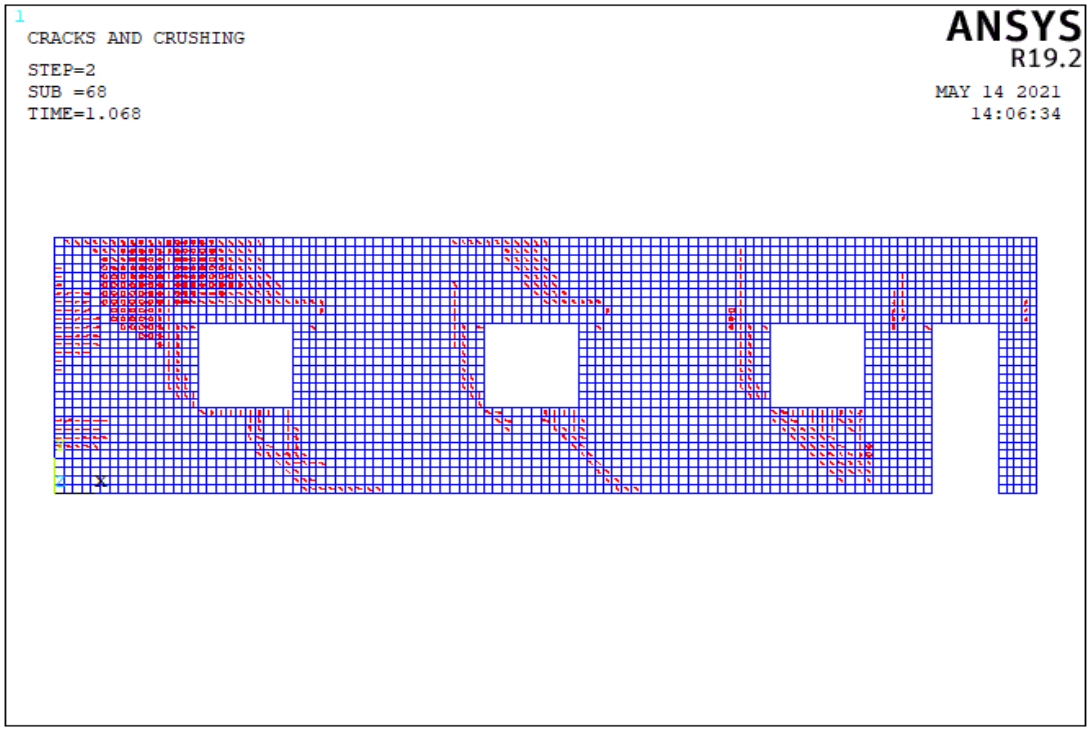

(a)

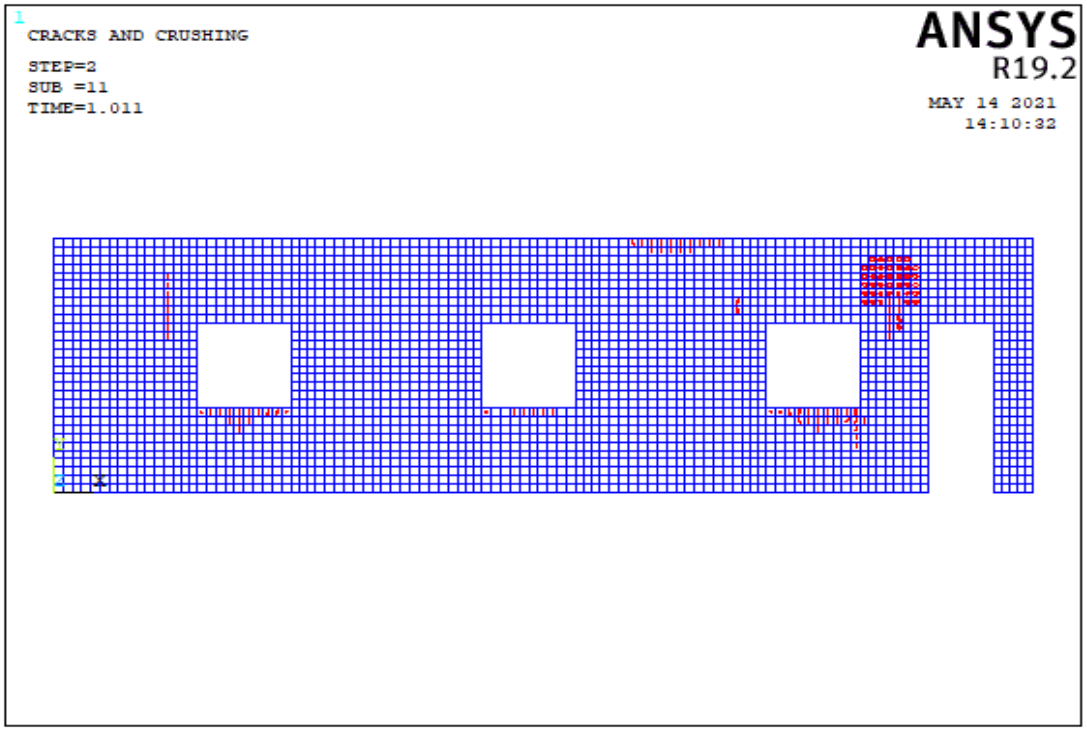

(b)

Figure 5.117. The Crack Pattern of Wall 14 Model 2 According to Compressive Strength Values of (a) 3 MPa, (b) 8 MPa

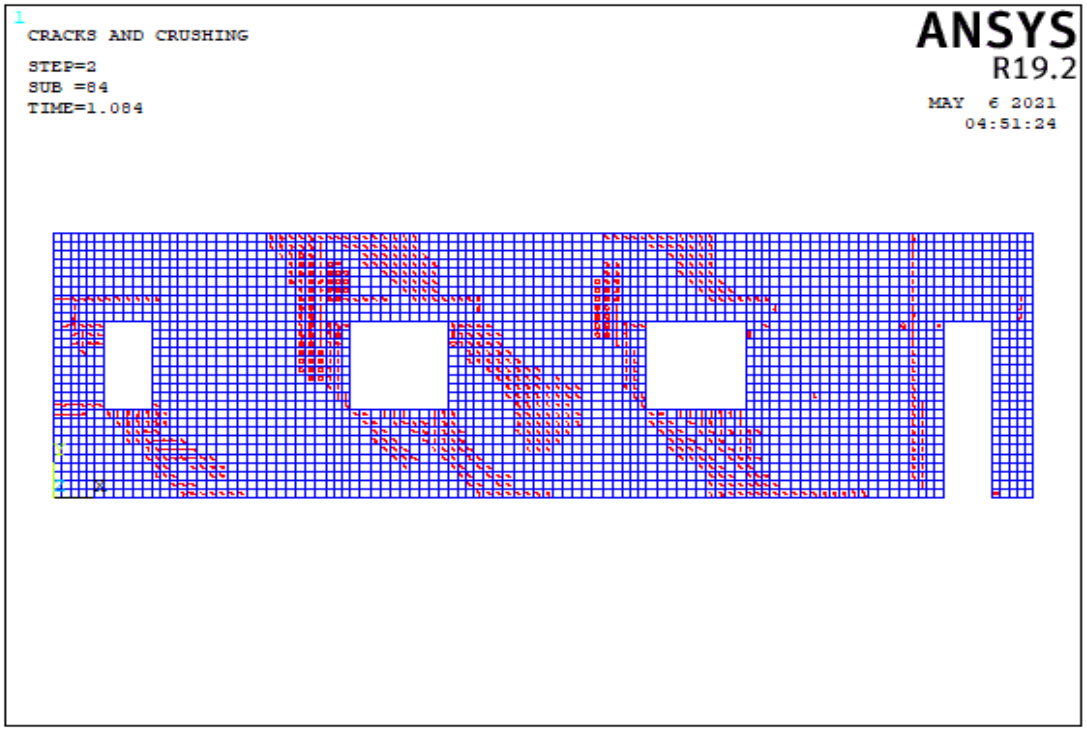

(a)

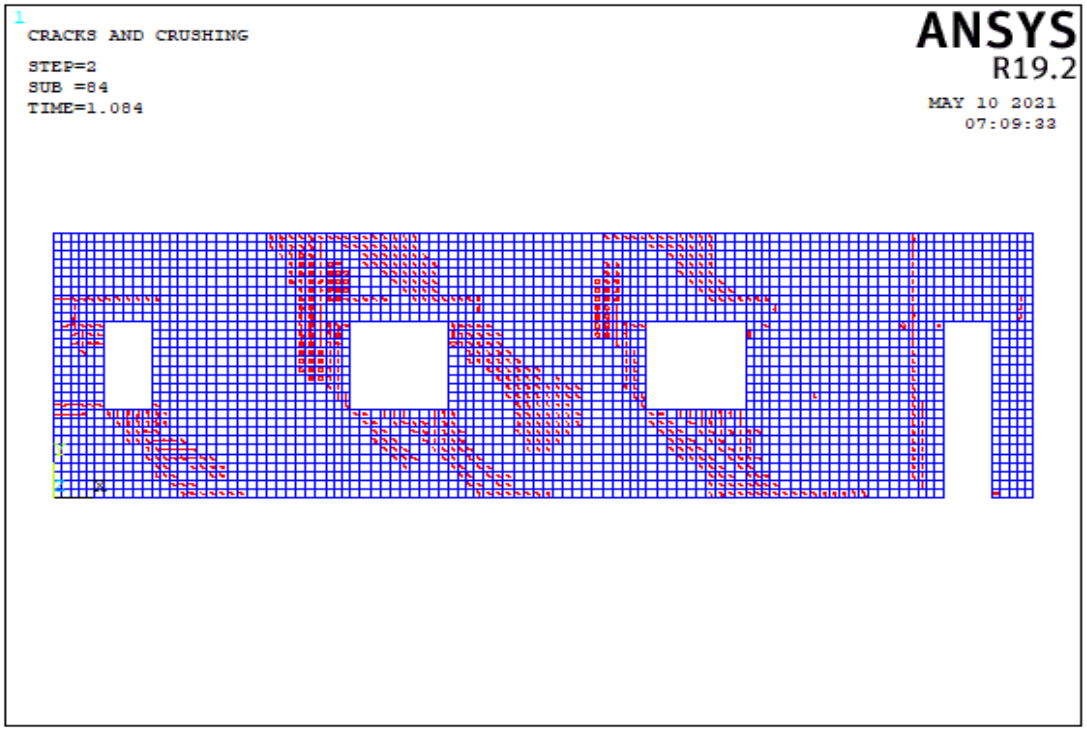

(b)

Figure 5.118. The Crack Pattern of Wall 14 Model 3 According to Compressive Strength Values of (a) 3 MPa, (b) 8 MPa

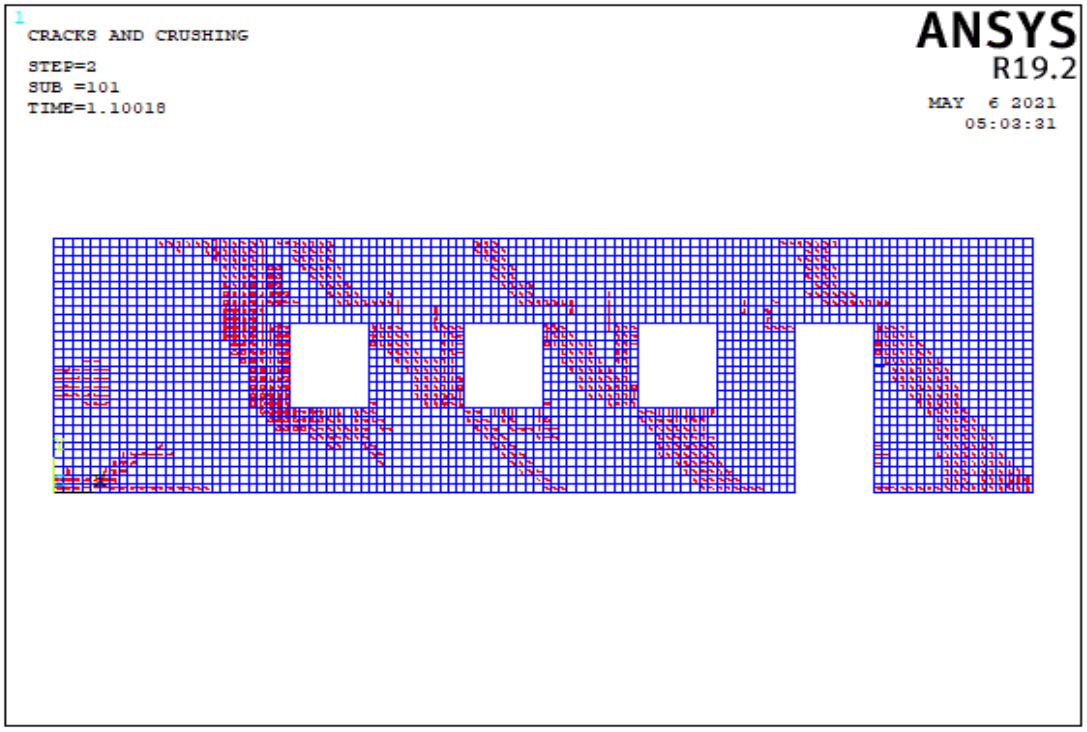

(a)

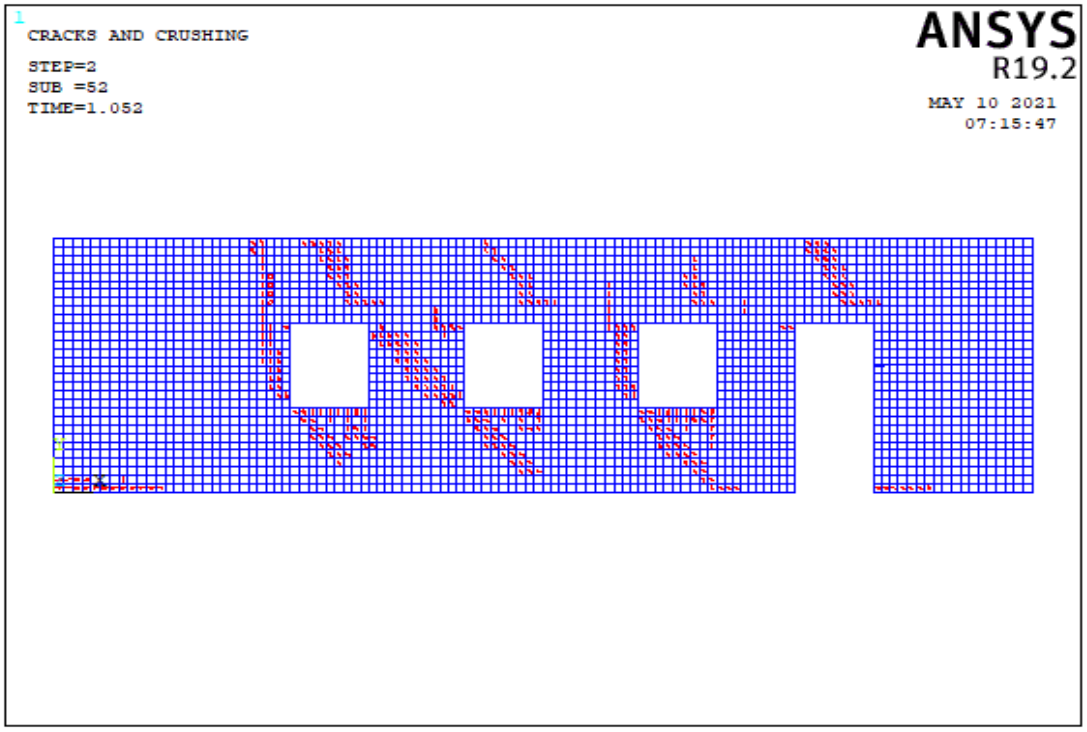

(b)

Figure 5.119. The Crack Pattern of Wall 14 Model 4 According to Compressive Strength Values of (a) 3 MPa, (b) 8 MPa

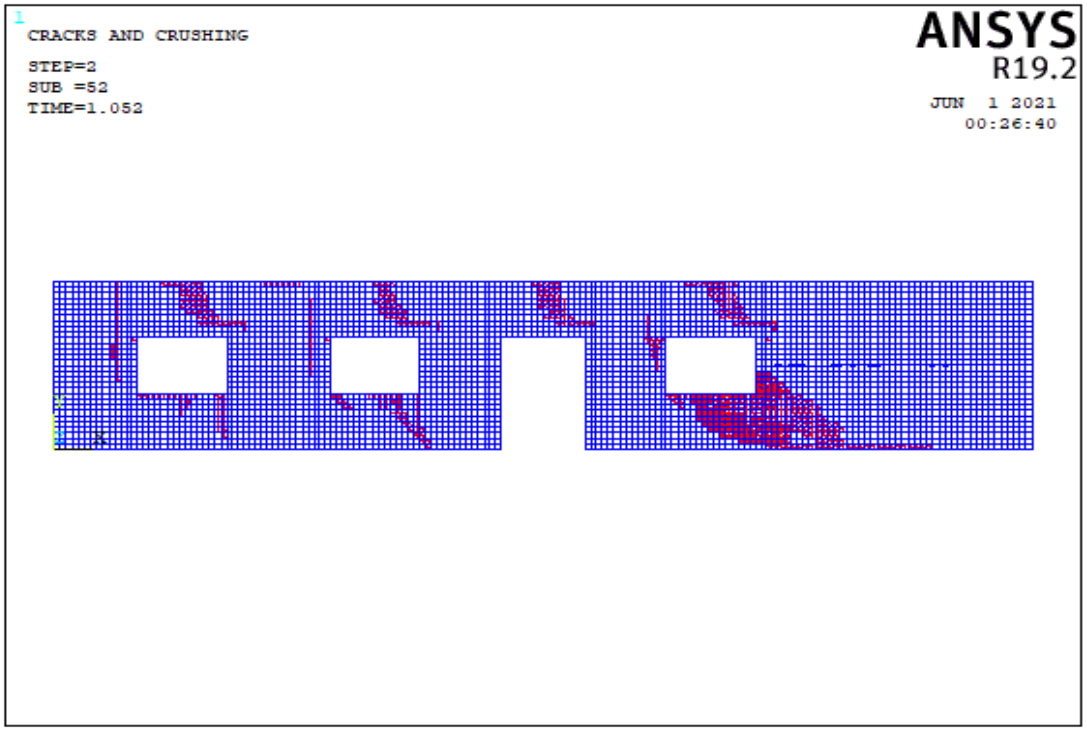

(a)

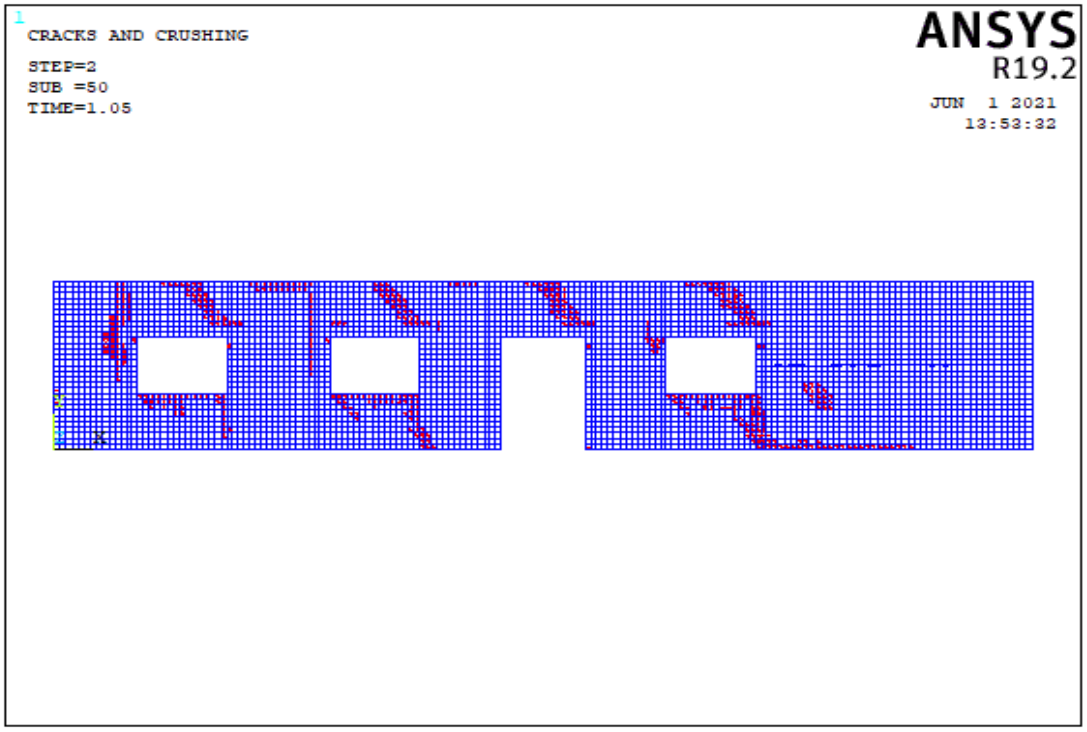

(b)

Figure 5.120. The Crack Pattern of Wall 14 Model 5 According to Compressive Strength Values of (a) 3 MPa, (b) 8 MPa

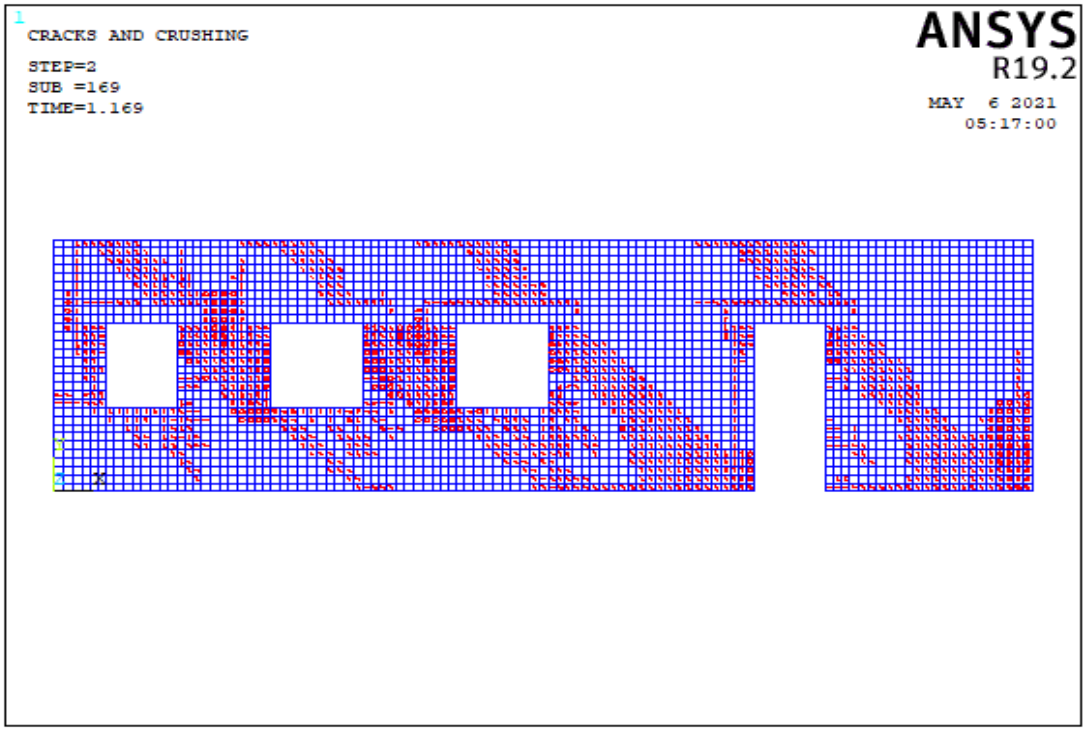

(a)

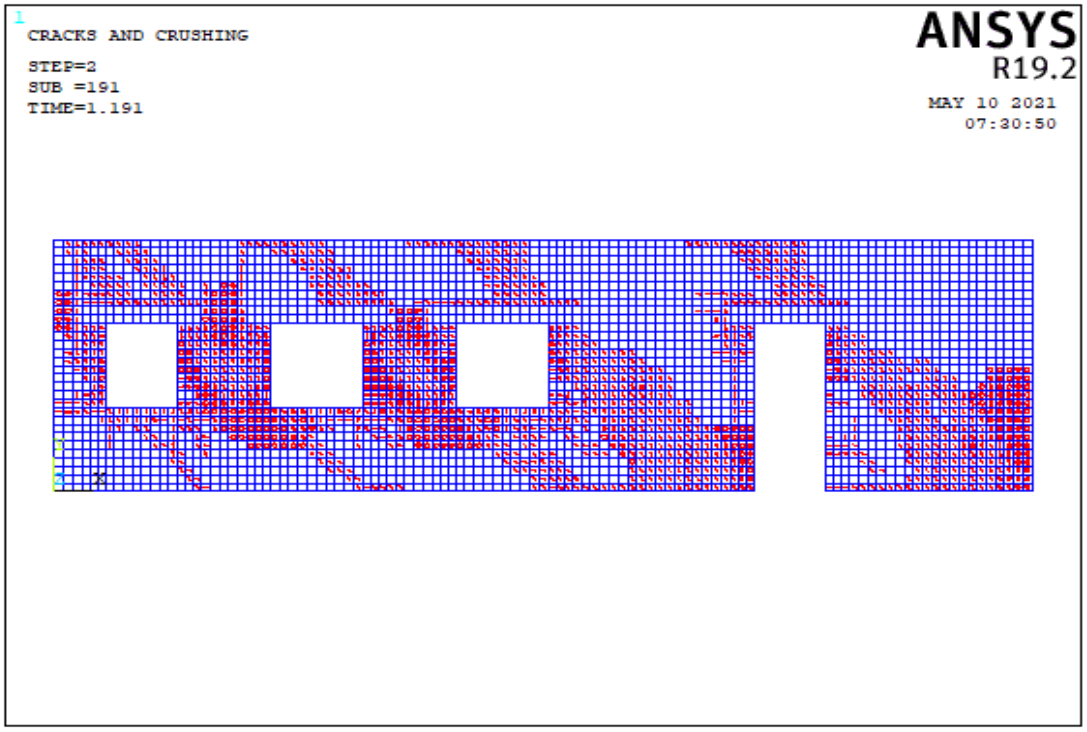

(b)

Figure 5.121. The Crack Pattern of Wall 14 Model 6 According to Compressive Strength Values of (a) 3 MPa, (b) 8 MPa

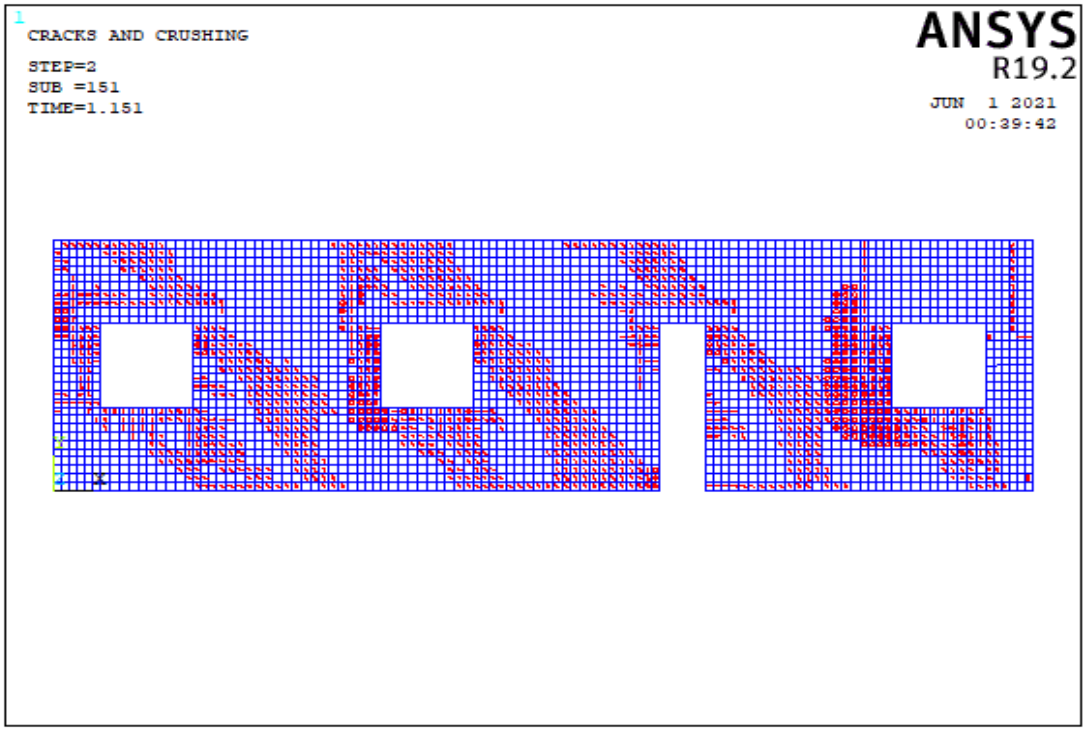

(a)

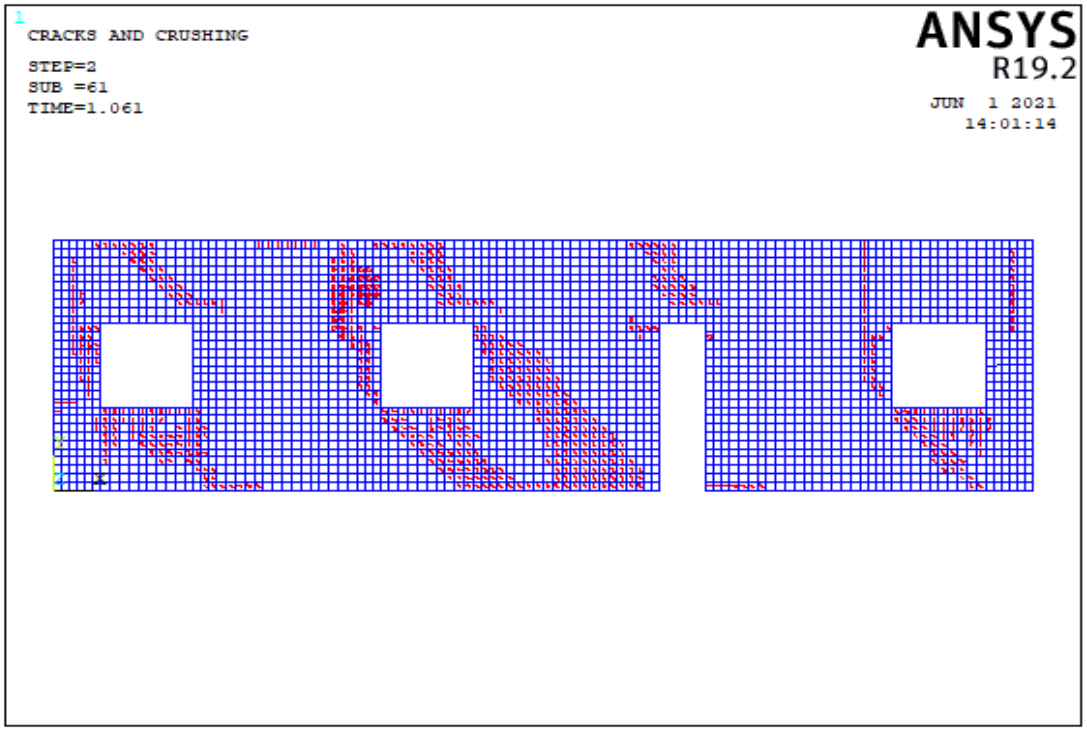

(b)

Figure 5.122. The Crack Pattern of Wall 14 Model 7 According to Compressive Strength Values of (a) 3 MPa, (b) 8 MPa

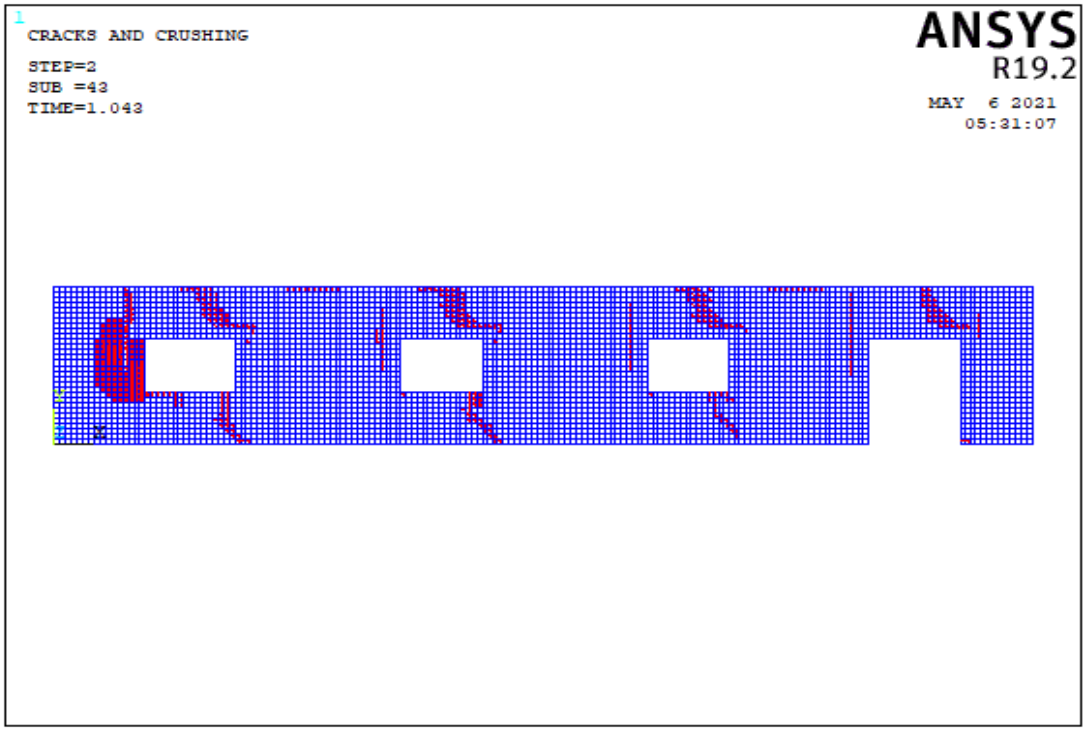

(a)

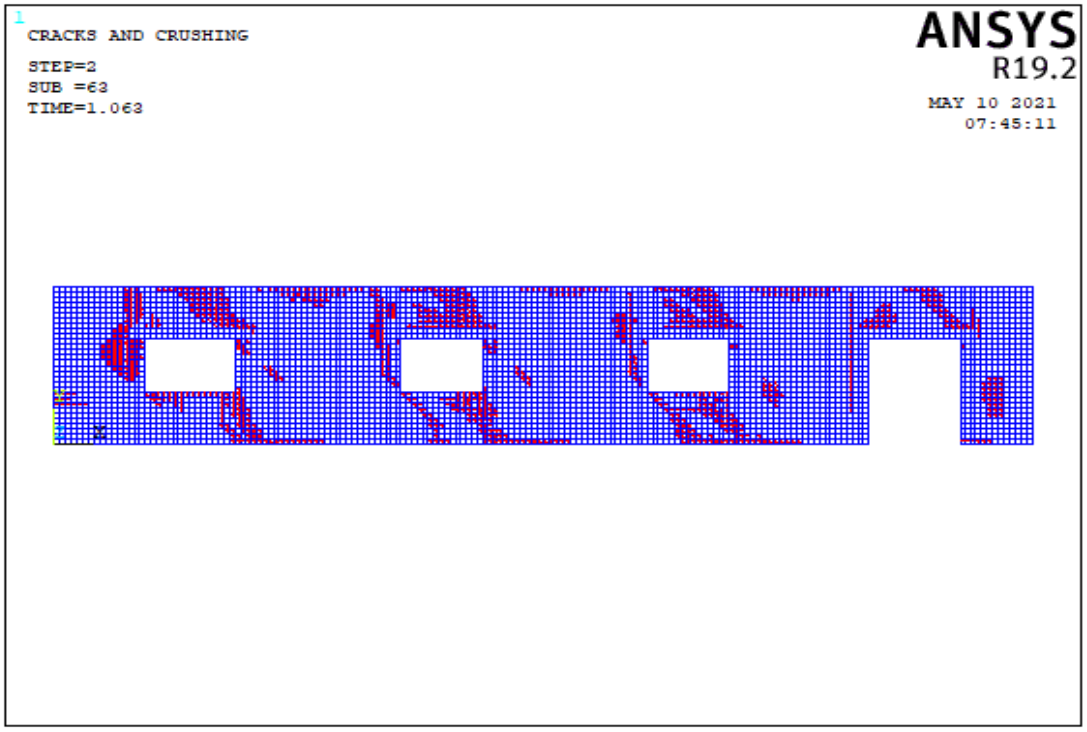

(b)

Figure 5.123. The Crack Pattern of Wall 14 Model 8 According to Compressive Strength Values of (a) 3 MPa, (b) 8 MPa

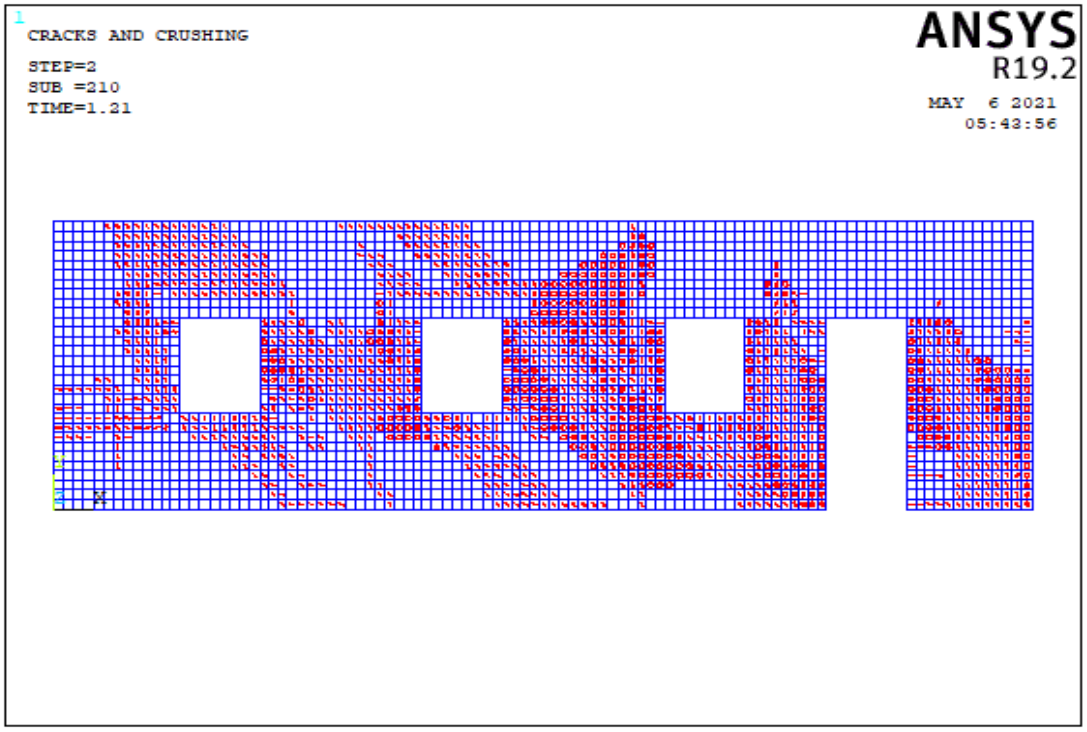

(a)

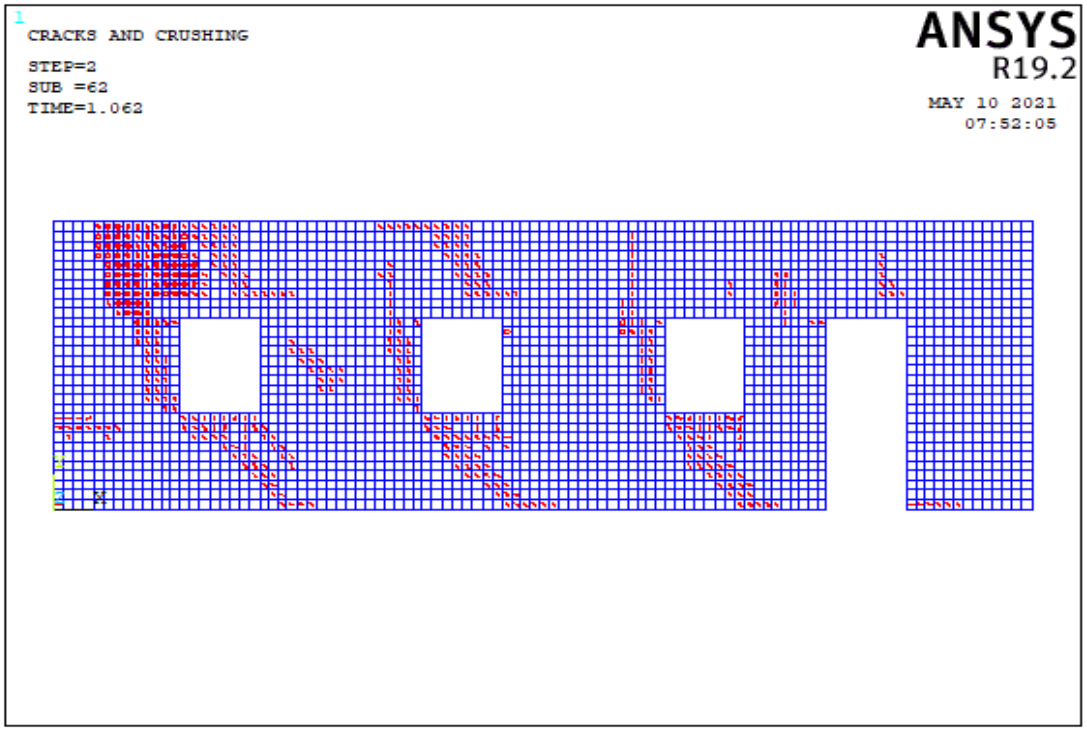

(b)

Figure 5.124. The Crack Pattern of Wall 14 Model 9 According to Compressive Strength Values of (a) 3 MPa, (b) 8 MPa

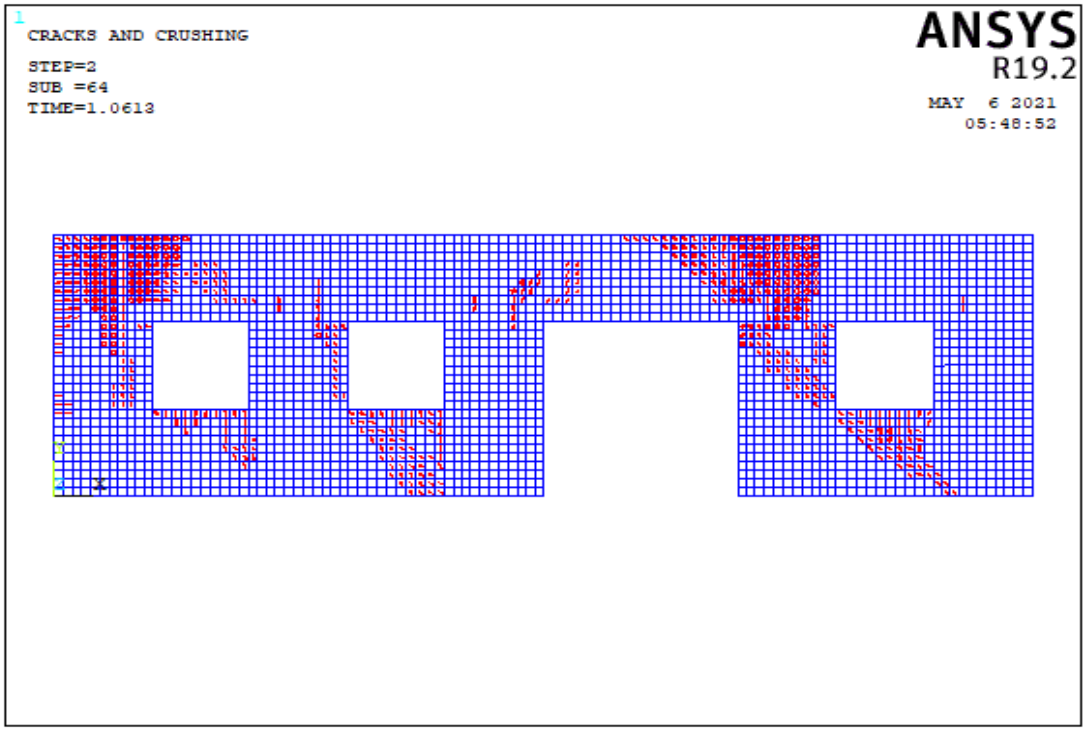

(a)

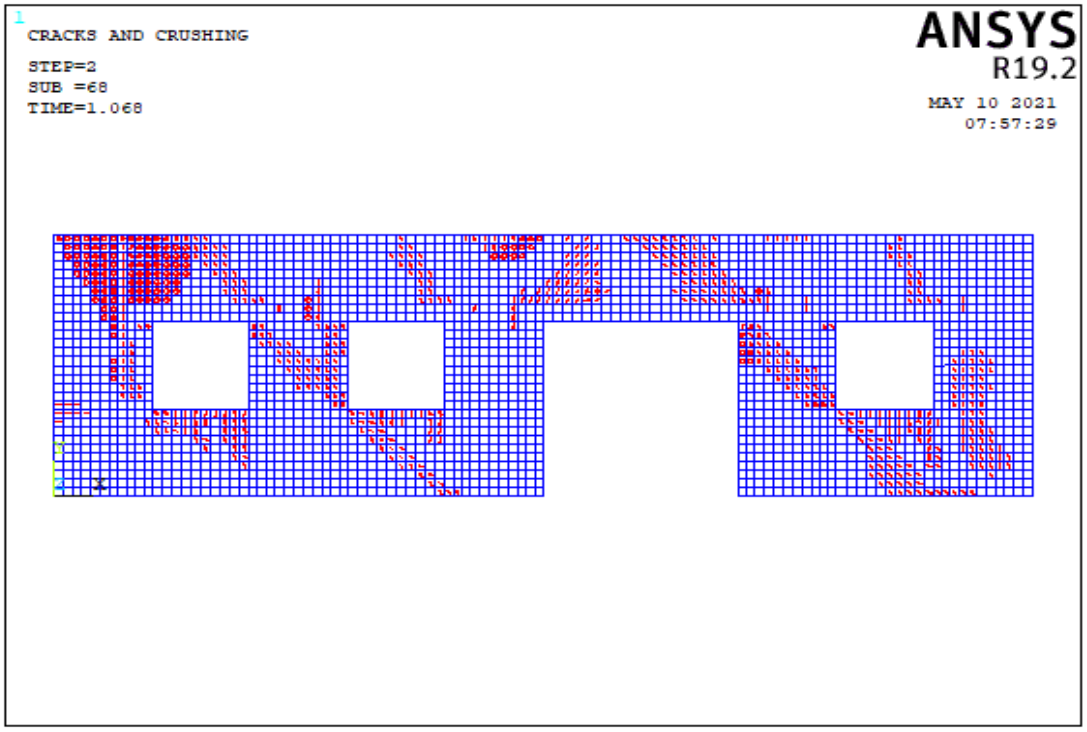

(b)

Figure 5.125. The Crack Pattern of Wall 14 Model 10 According to Compressive Strength Values of (a) 3 MPa, (b) 8 MPa

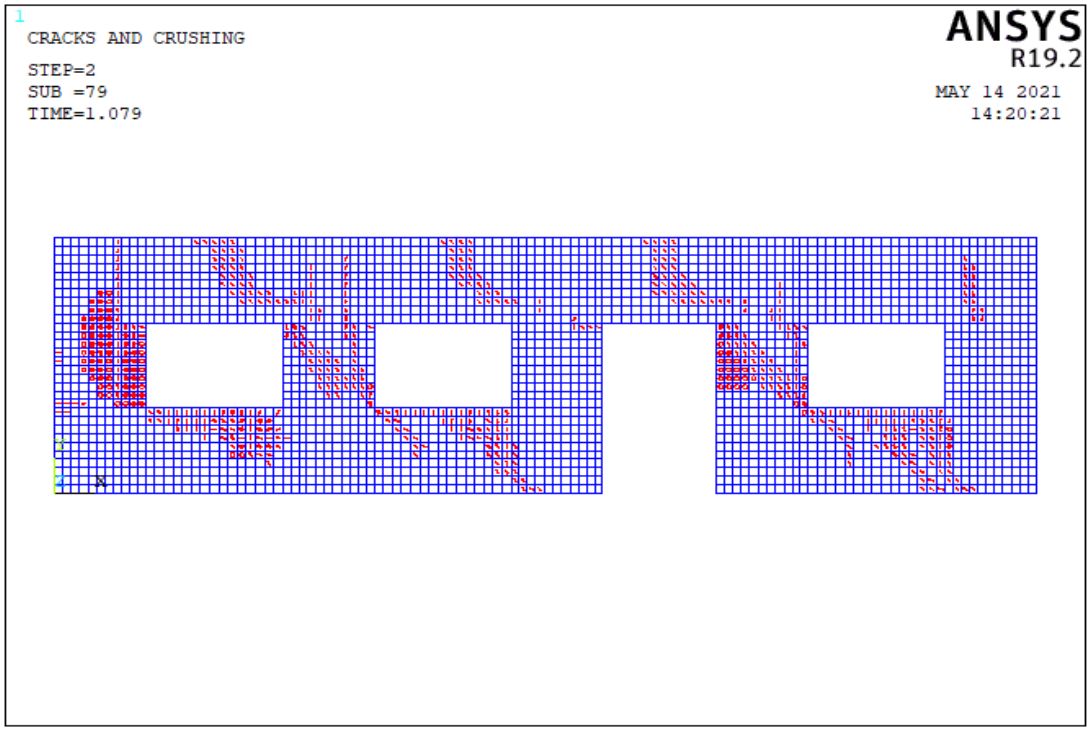

(a)

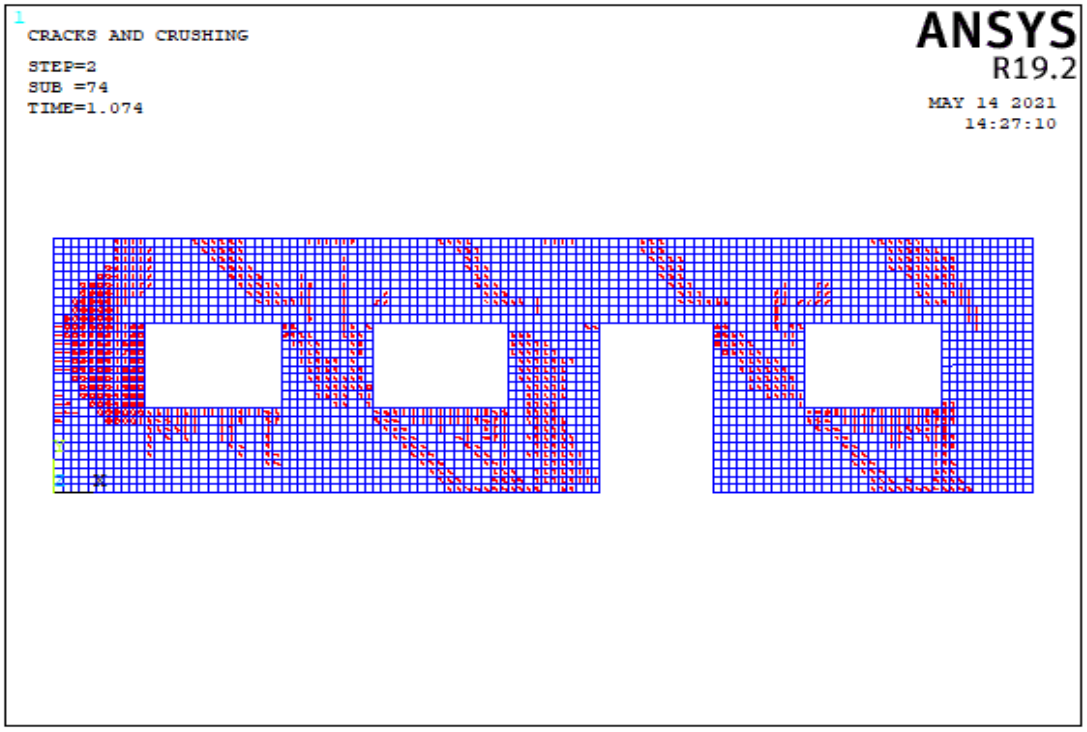

(b)

Figure 5.126. The Crack Pattern of Wall 14 Model 11 According to Compressive Strength Values of (a) 3 MPa, (b) 8 MPa

Table 5.16. Failure Patterns of Wall 14

Number of Model	Aspect ratio	fm=3 Mpa			fm=8 Mpa		
		Failure Pattern			Failure Pattern		
		Base	Rocki	Diagonal	Base	Rocki	Diagonal
Model 1	3.00		X			X	
	3.00			X			X
	3.00			X			X
	3.00						
	3.00						
Model 2	2.00		X				
	1.50	X					
	1.50						
	7.20						
	7.20						
Model 3	6.00		X			X	
	1.50			X			X
	1.50			X			X
	1.50	X			X		
	7.50		X			X	
Model 4	1.20	X			X		
	3.00			X		X	
	3.00			X		X	
	3.60						
	1.80			X	X		
Model 5	2.28		X			X	
	1.83						
	2.36						
	2.36						
	0.68			X	X		
Model 6	5.48		X			X	
	3.04			X			X
	3.04			X			X
	1.37			X			X
	1.37			X			X
Model 7	6.00		X			X	
	1.50			X			X
	1.50			X			X
	1.50			X			X
	6.00		X			X	
Model 8	1.95		X			X	
	1.06						
	1.06						
	1.26						
	2.45						
Model 9	2.57		X			X	
	1.99			X			X
	1.99			X			
	3.97			X			
	2.57			X	X		
Model 10	3.00		X			X	
	3.00						X
	3.00						
	3.00			X			X
	3.00		X			X	
Model 11	3.14		X			X	
	3.14			X			X
	3.14						X
	2.64			X			X
	3.14		X			X	

In the Table A.14, all length of openings is less than 3 m for all models of wall 14 and total opening percentage of load bearing walls for model 1, 10 and 11 is not appropriate for TEC 2018. In models 2, 4 and 11, the length of piers between the windows and doors are less than 1 meter. Models 5 and 8 shows that the larger piers increase the strength of the wall, although it reduces its stiffness. When models 4 and 6 are investigated, the increasing corner pier length affects the failure mechanism and increases the capacity of wall. In these figures, the change in the aspect ratios of the piers or location of openings change the failure modes and capacity of wall. The diagonal tension cracks appear in piers when the pier percentage or length of pier increase.

5.4.1.15 Failure Modes of Wall 15

In the wall 15 type, there are 10 different wall models. The impact of single door and four windows openings was studied in these models of wall 15. Table A.15 shows the lengths of the walls. As seen in Figure 5.3, each pier is designated from left to right. The crack patterns obtained from the analysis of wall models corresponding to 10 different wall models are described in this section.

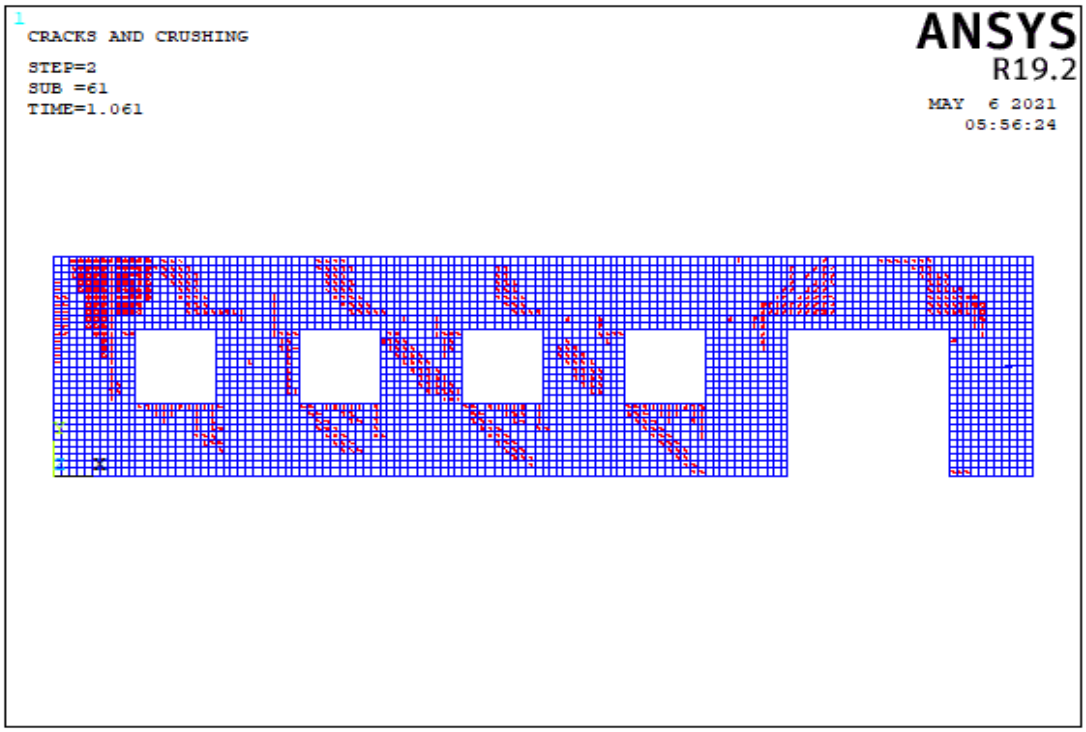

(a)

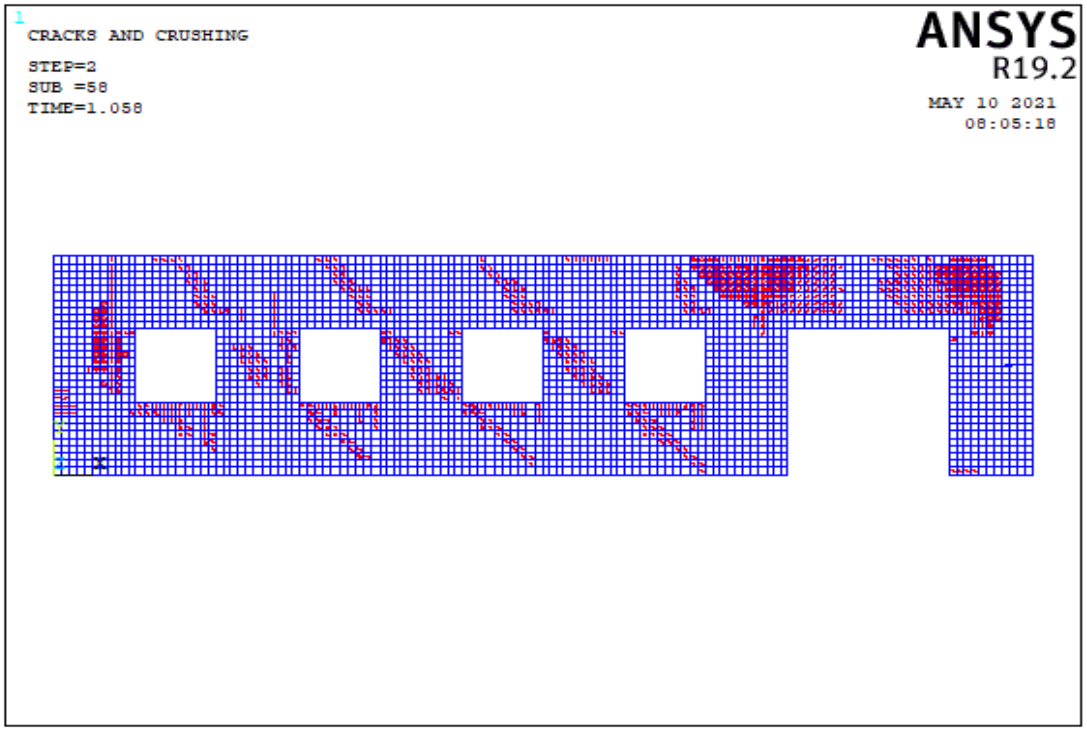

(b)

Figure 5.127. The Crack Pattern of Wall 15 Model 1 According to Compressive Strength Values of (a) 3 MPa, (b) 8 MPa

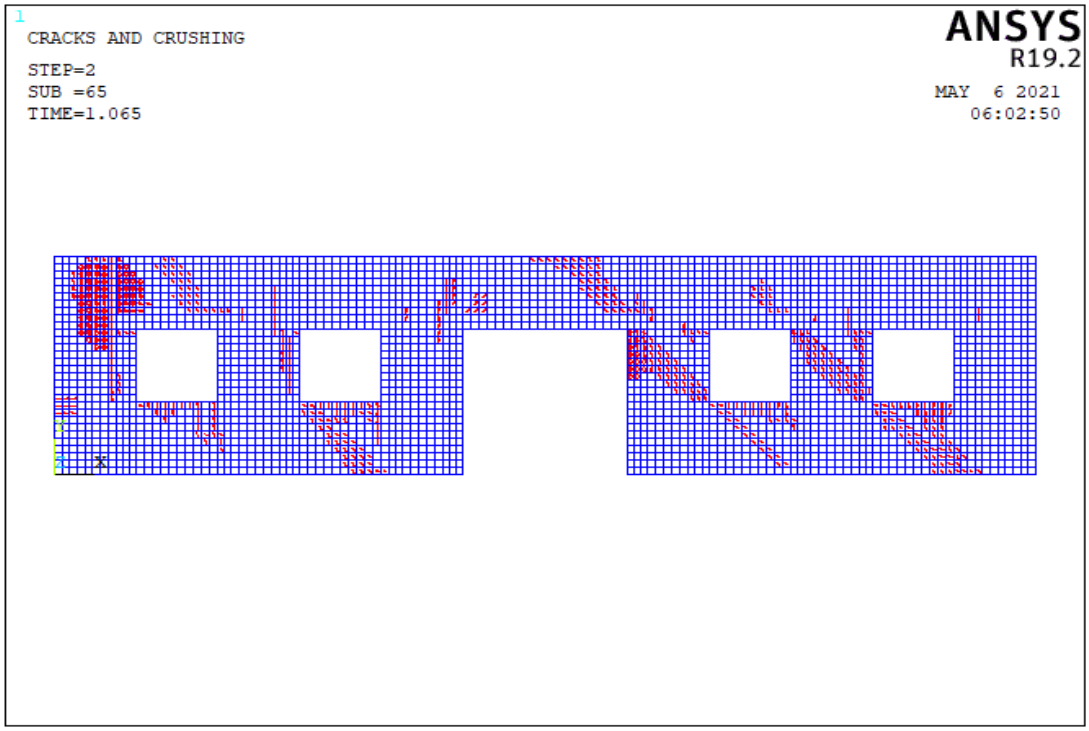

(a)

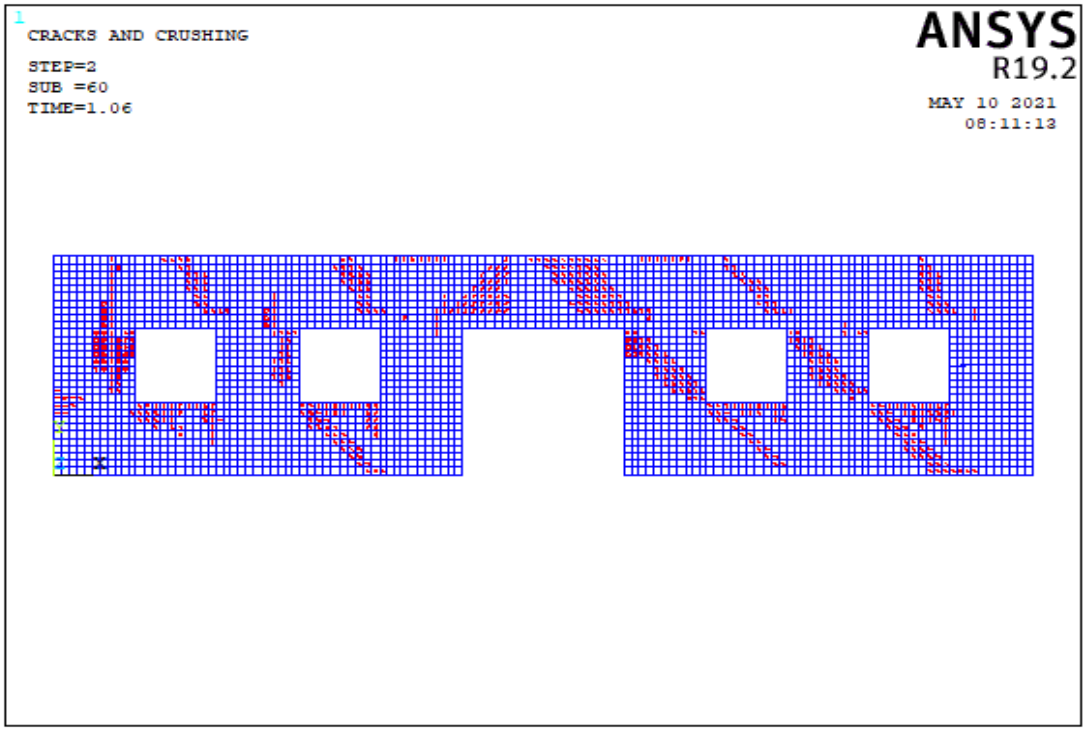

(b)

Figure 5.128. The Crack Pattern of Wall 15 Model 2 According to Compressive Strength Values of (a) 3 MPa, (b) 8 MPa

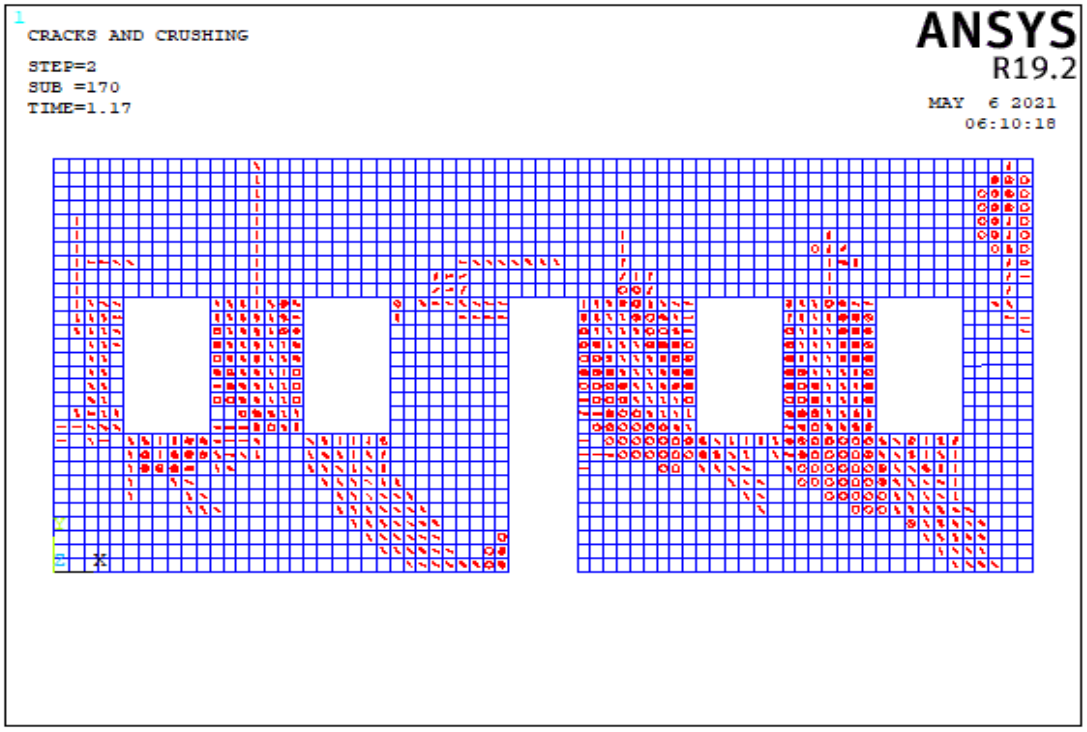

(a)

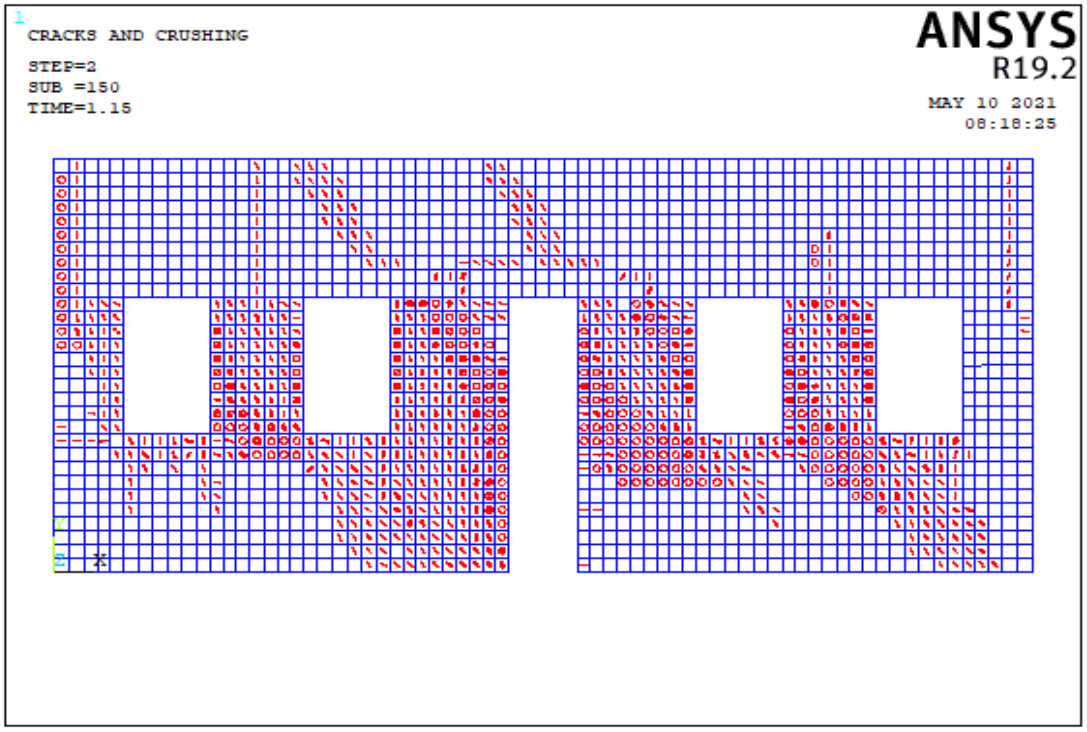

(b)

Figure 5.129. The Crack Pattern of Wall 15 Model 3 According to Compressive Strength Values of (a) 3 MPa, (b) 8 MPa

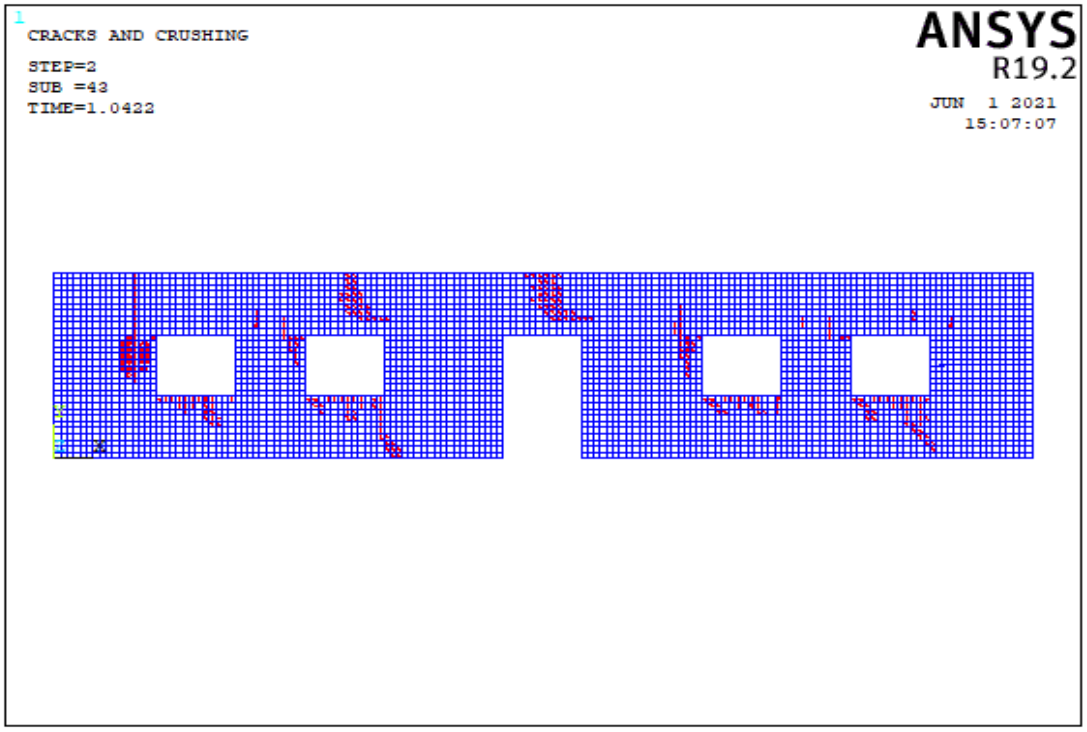

(a)

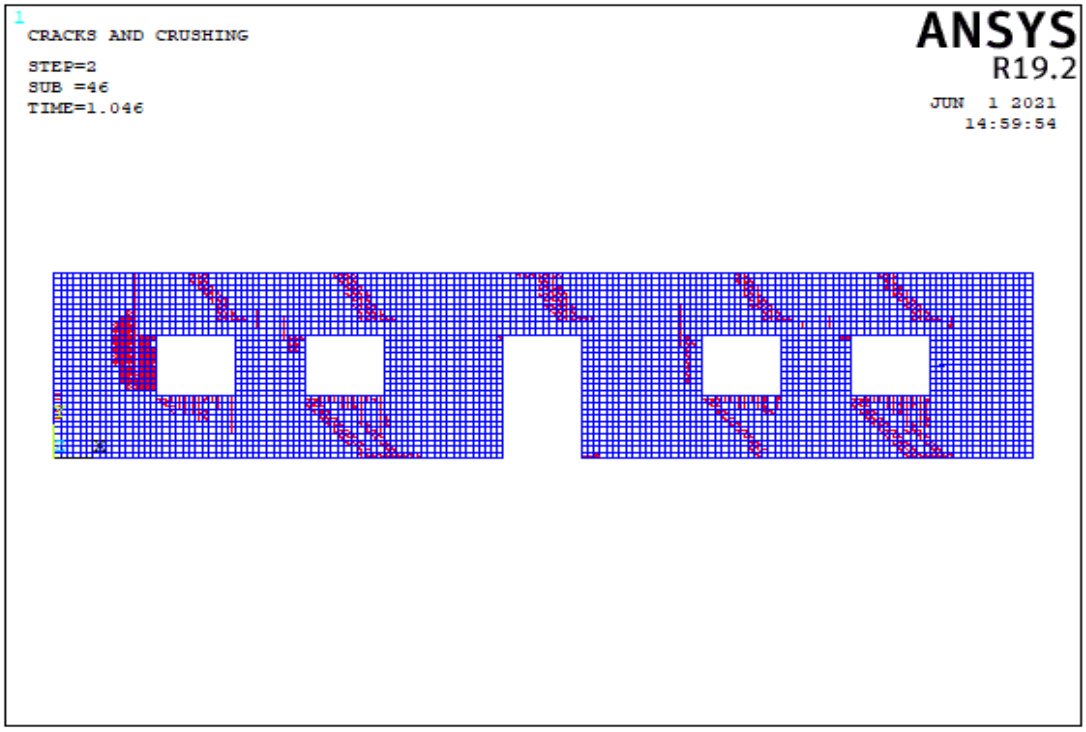

(b)

Figure 5.130. The Crack Pattern of Wall 15 Model 4 According to Compressive Strength Values of (a) 3 MPa, (b) 8 MPa

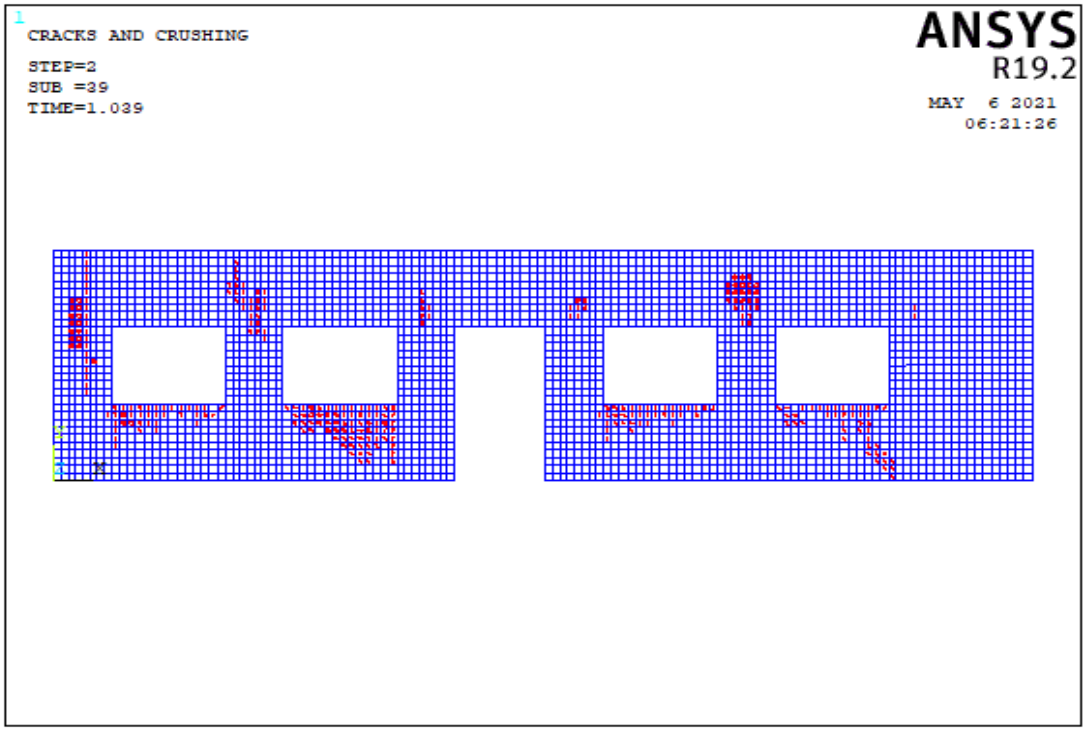

(a)

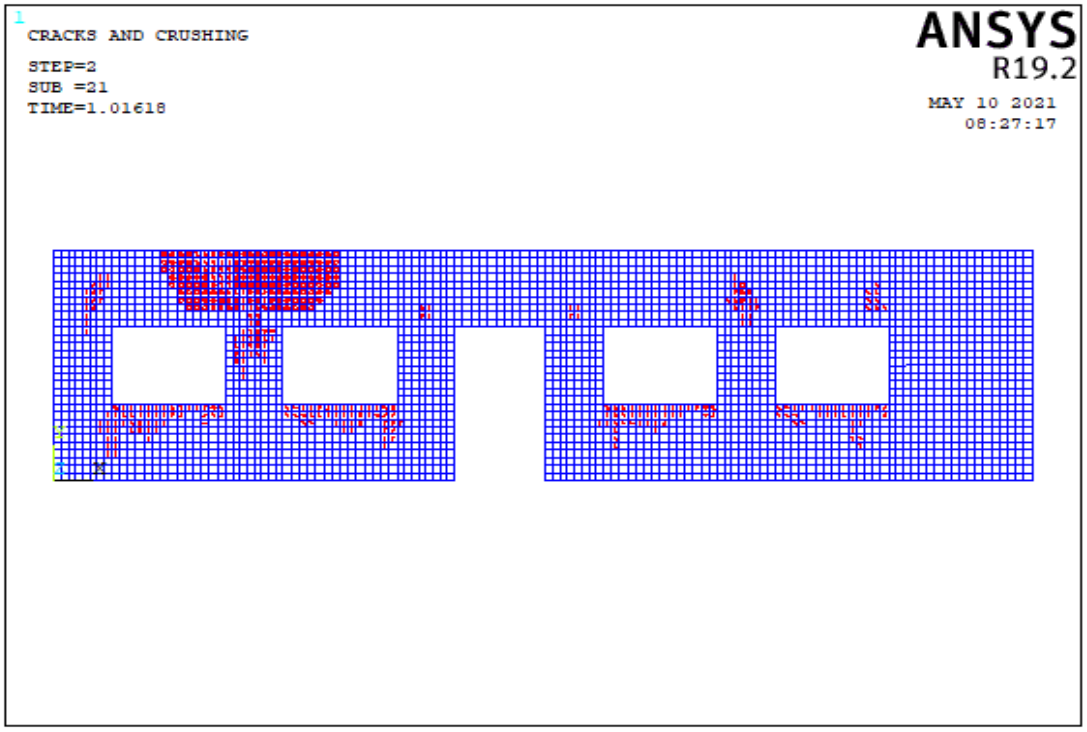

(b)

Figure 5.131. The Crack Pattern of Wall 15 Model 5 According to Compressive Strength Values of (a) 3 MPa, (b) 8 MPa

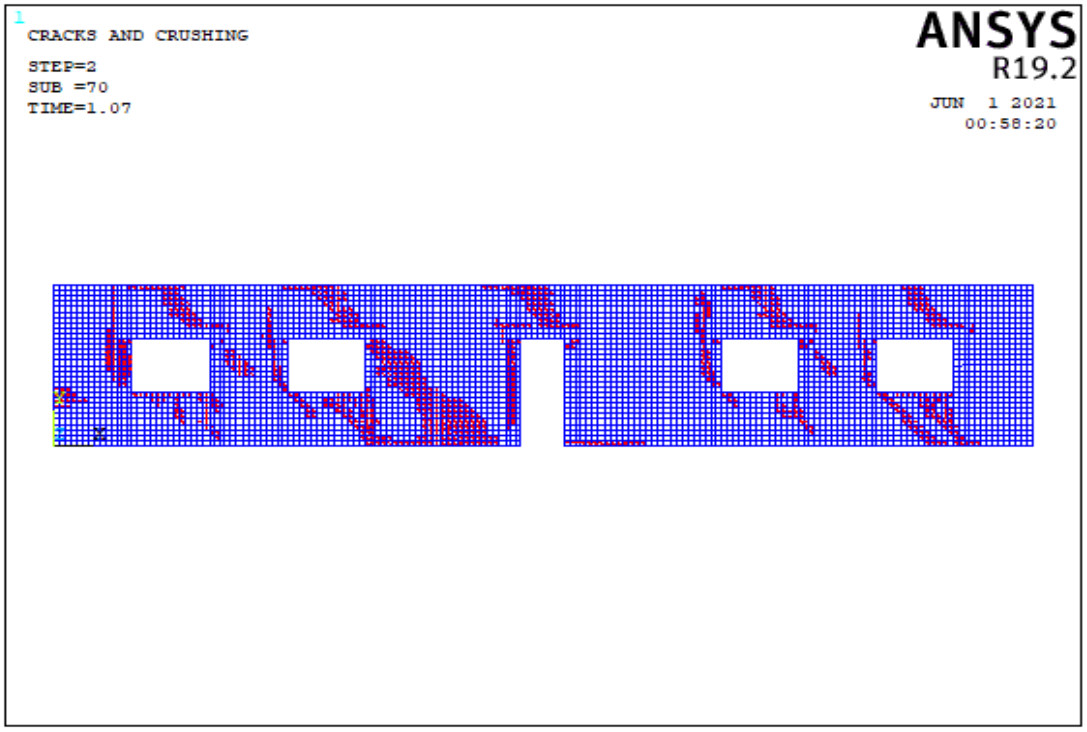

(a)

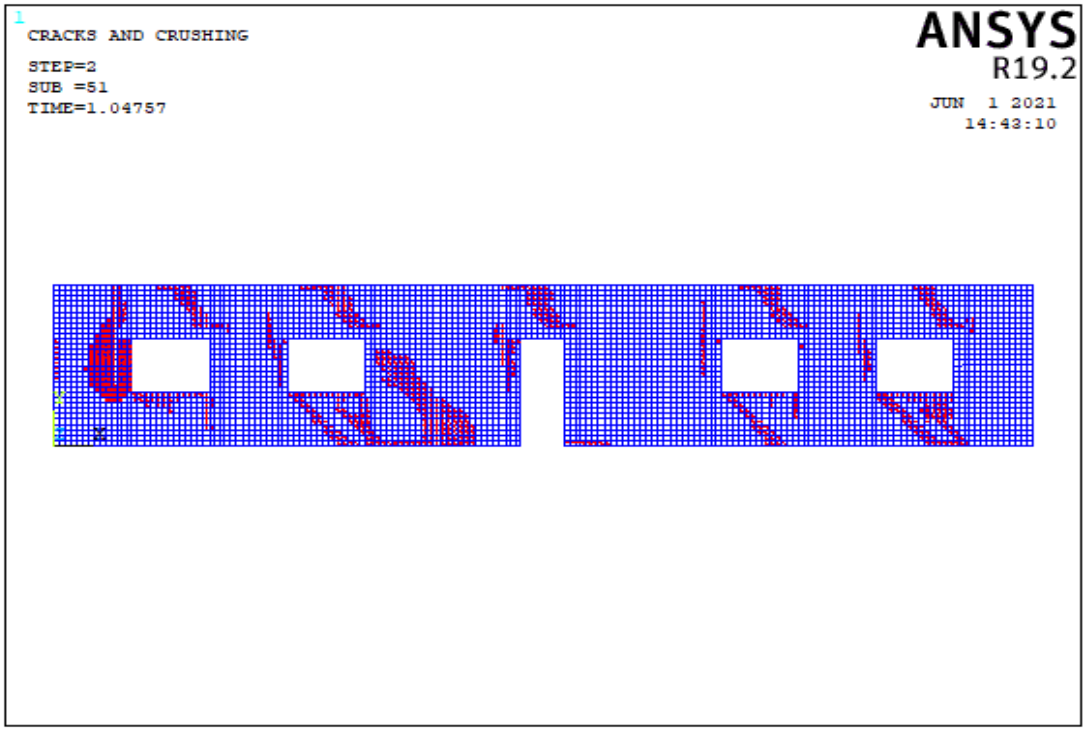

(b)

Figure 5.132. The Crack Pattern of Wall 15 Model 6 According to Compressive Strength Values of (a) 3 MPa, (b) 8 MPa

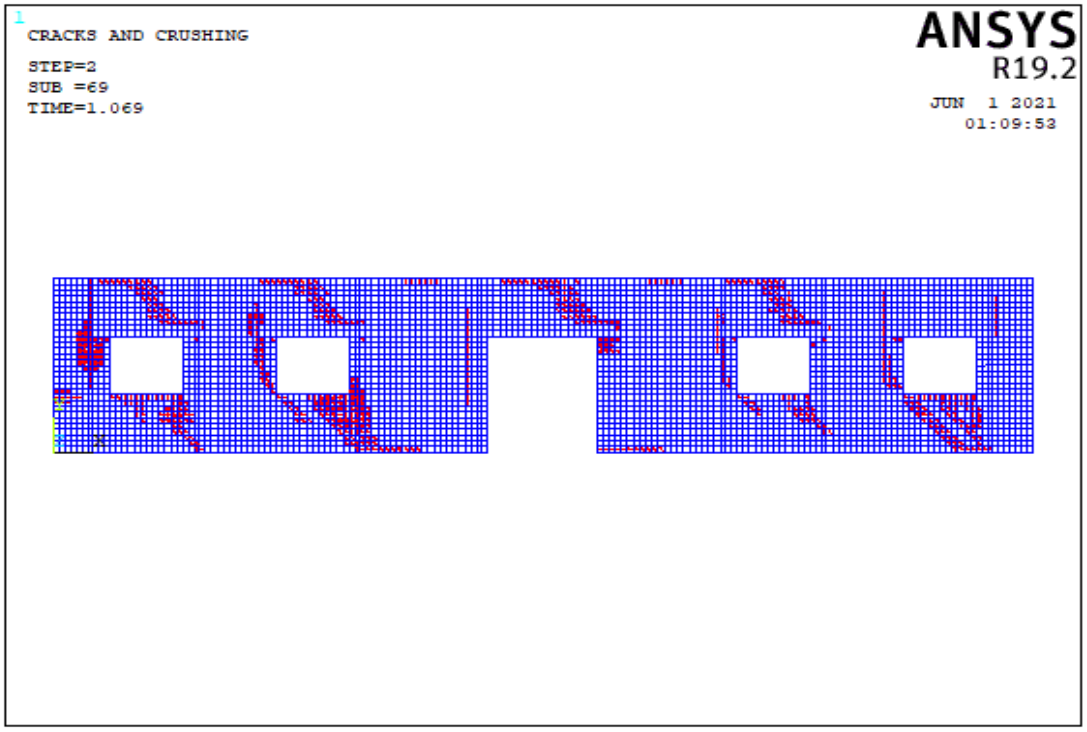

(a)

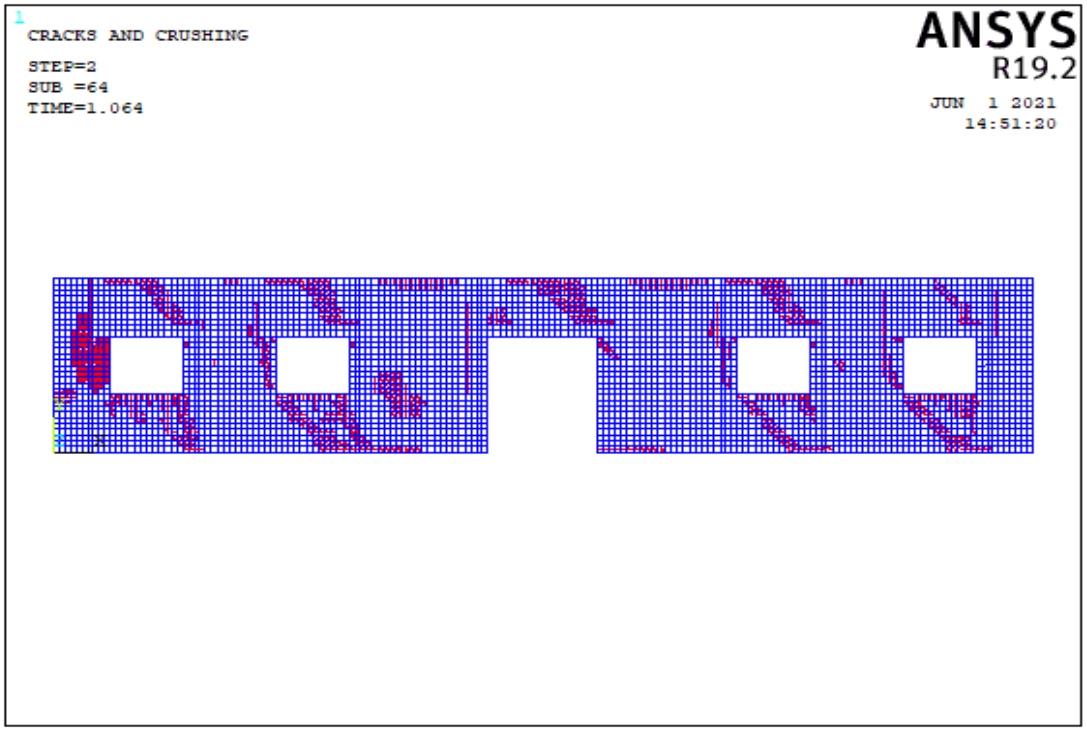

(b)

Figure 5.133. The Crack Pattern of Wall 15 Model 7 According to Compressive Strength Values of (a) 3 MPa, (b) 8 MPa

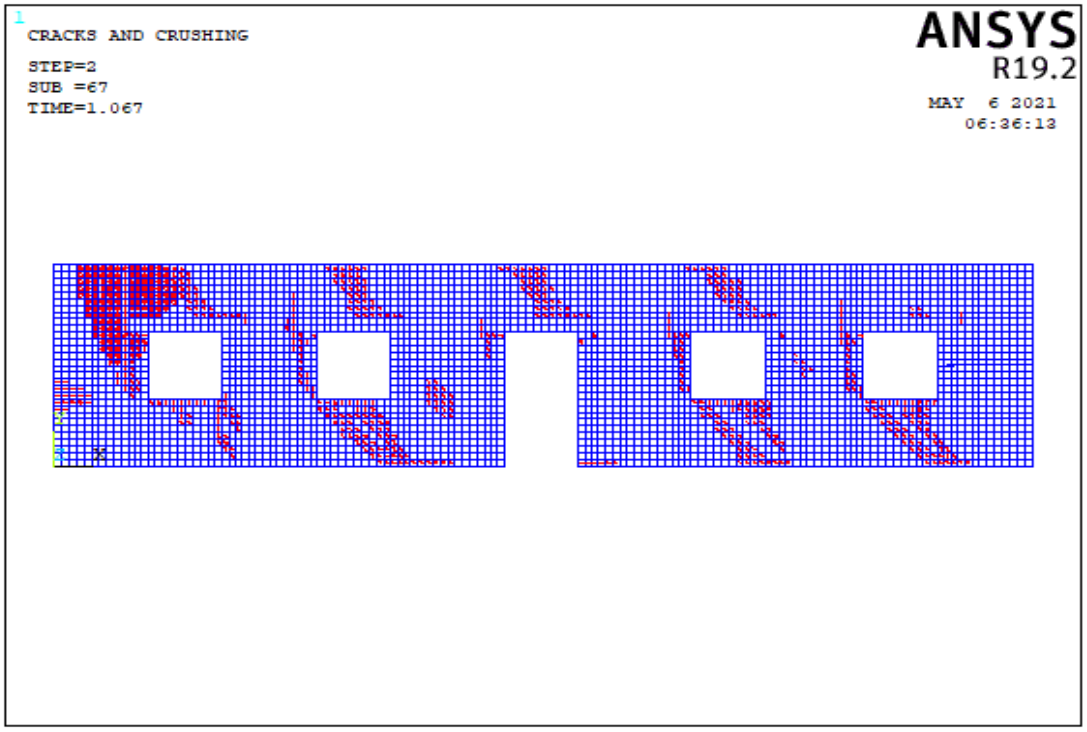

(a)

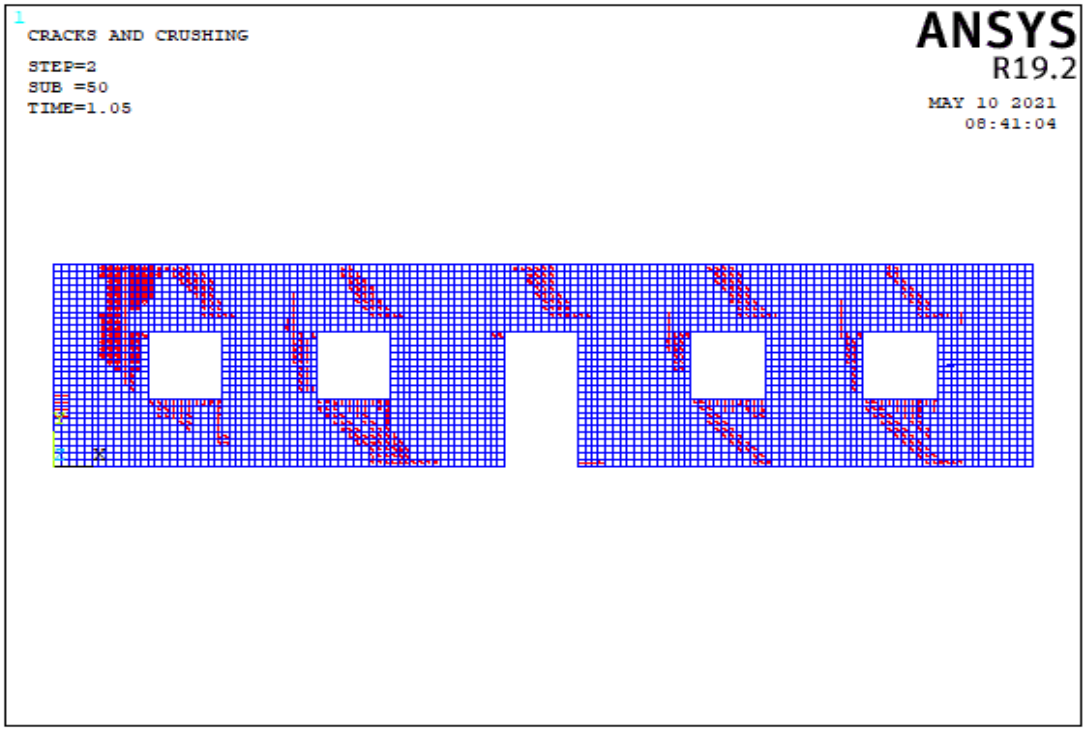

(b)

Figure 5.134. The Crack Pattern of Wall 15 Model 8 According to Compressive Strength Values of (a) 3 MPa, (b) 8 MPa

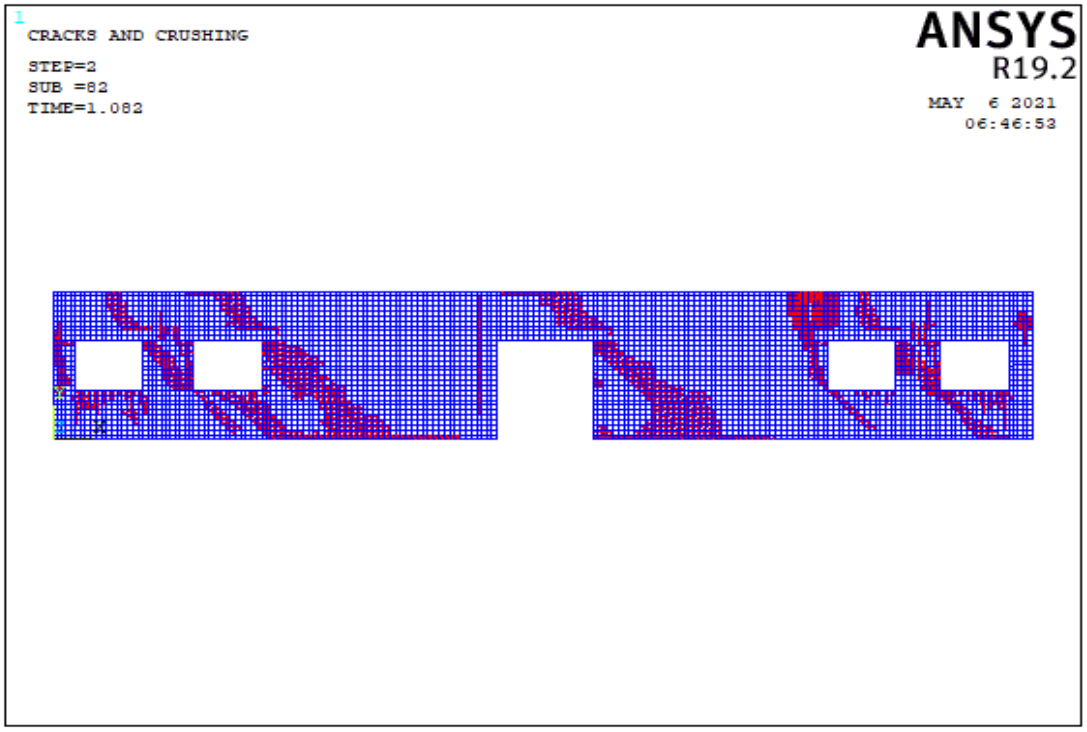

(a)

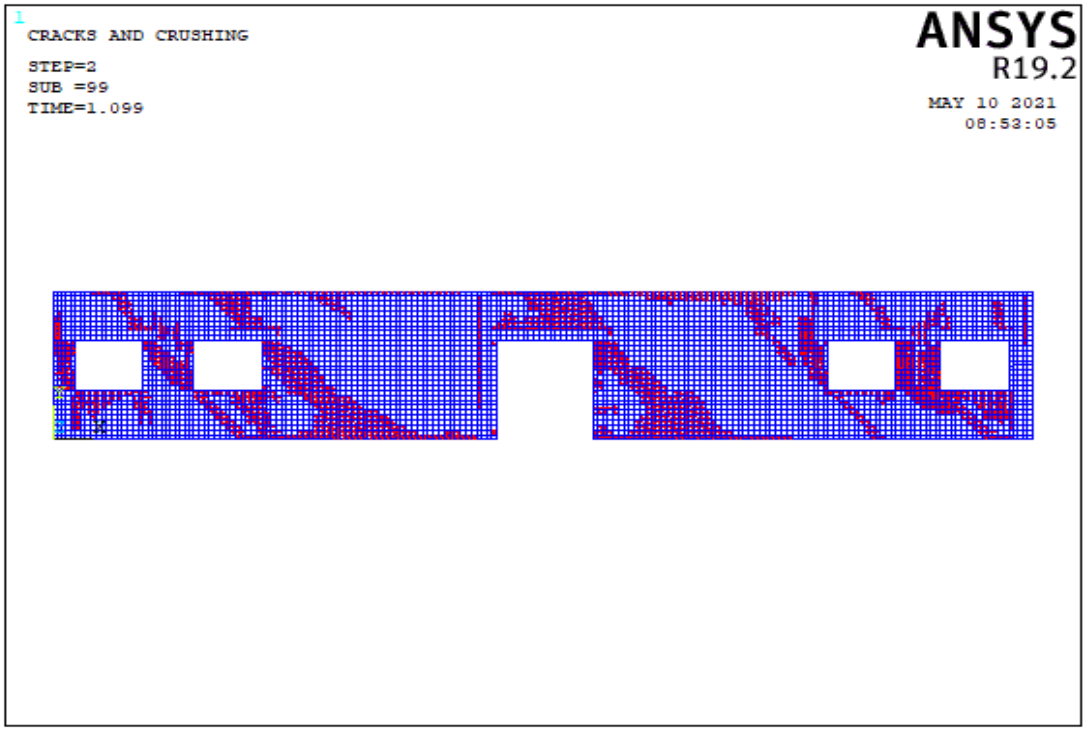

(b)

Figure 5.135. The Crack Pattern of Wall 15 Model 9 According to Compressive Strength Values of (a) 3 MPa, (b) 8 MPa

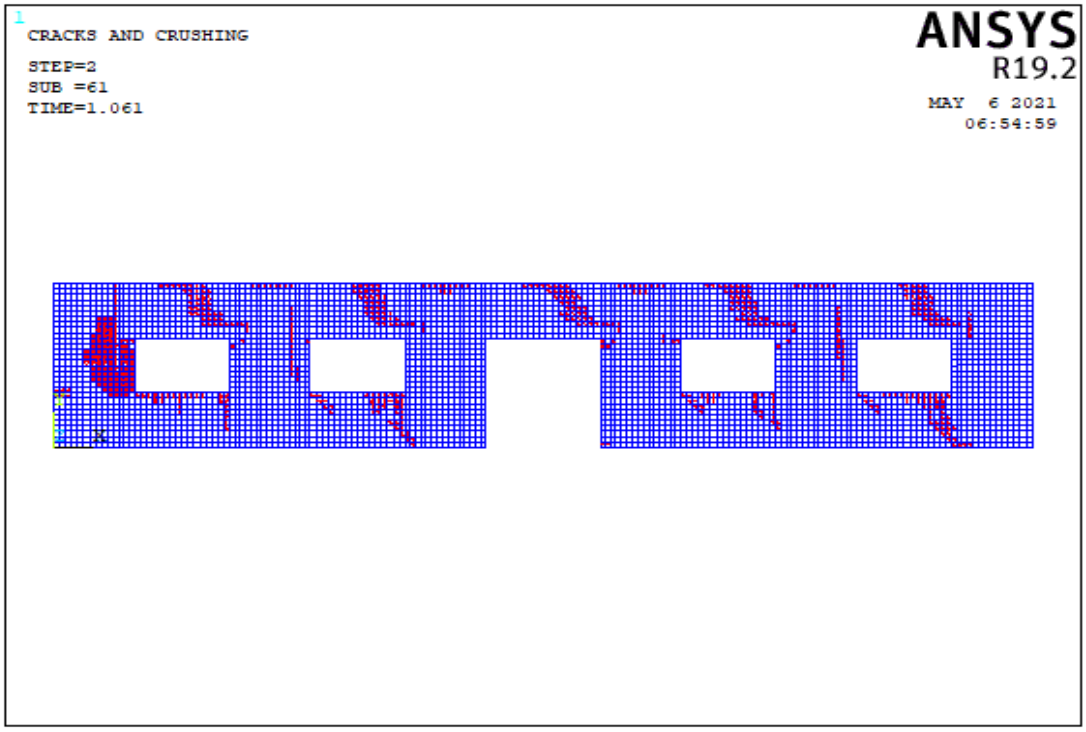

(a)

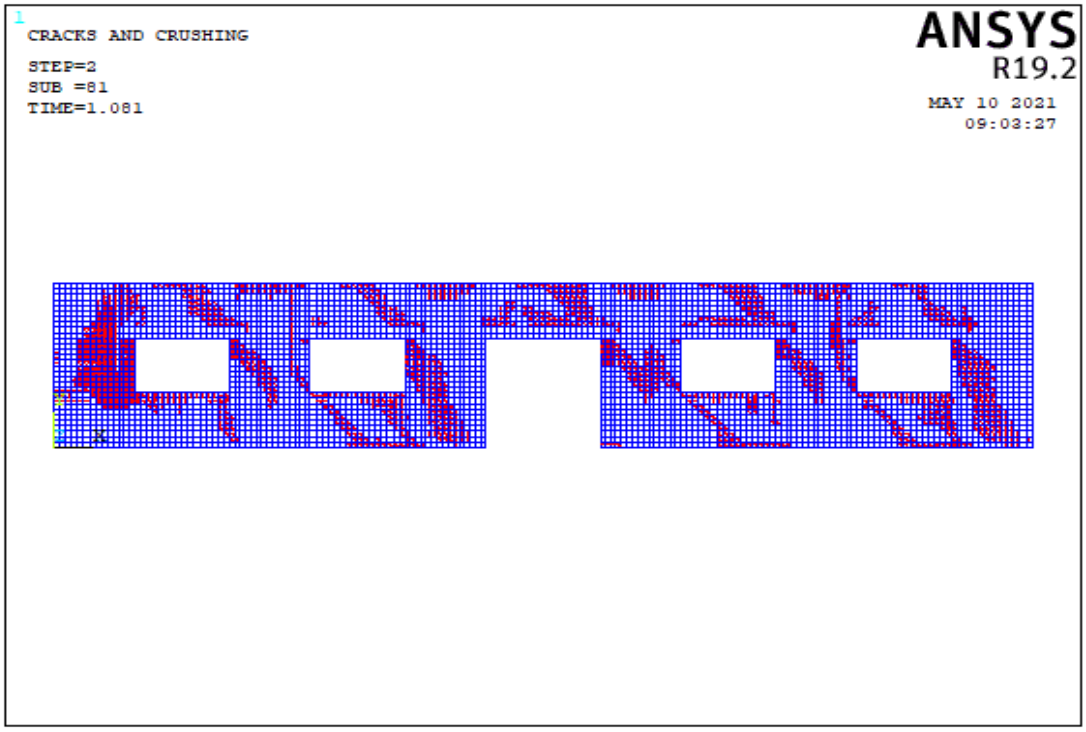

(b)

Figure 5.136. The Crack Pattern of Wall 15 Model 10 According to Compressive Strength Values of (a) 3 MPa, (b) 8 MPa

Table 5.17. Failure Patterns of Wall 15

Number of Model	Aspect ratio	fm=3 Mpa			fm=8 Mpa		
		Failure Pattern			Failure Pattern		
		Base Sliding	Rocking	Diagonal Tension	Base Sliding	Rocking	Diagonal Tension
Model 1	3.00		X			X	
	3.00			X			X
	3.00			X			X
	3.00			X			X
	3.00						
	3.00						
Model 2	3.00		X			X	
	3.00			X			X
	3.00						
	3.00			X			X
	3.00			X			X
	3.00						
Model 3	6.67		X			X	
	5.00			X			X
	3.92			X			X
	3.92			X			X
	5.00			X			X
	6.67		X			X	
Model 4	2.05		X			X	
	3.00						
	1.75						
	1.75						
	3.00						
	2.05						
Model 5	4.50		X			X	
	4.50						
	4.50						
	4.50						
	4.50						
	1.80						
Model 6	2.31		X			X	
	2.31			X			X
	1.15			X			X
	1.15	X			X		
	2.31			X			X
	2.31						
Model 7	3.50		X			X	
	2.10			X			X
	1.40			X			X
	1.40						
	2.10			X			X
	3.50						
Model 8	2.40		X			X	
	2.40			X			X
	2.00						
	2.00						
	2.31						
	2.40						
Model 9	7.89		X			X	
	3.31			X			X
	0.71			X			X
	0.71			X			X
	3.75			X			X
	7.14		X			X	
Model 10	2.29		X			X	
	2.29			X			X
	2.29						X
	2.29						X
	2.29						X
	2.29						X

In the Table A.15, all length of openings is less than 3 m for all models of wall 15 and total opening percentage of walls for model 6, 8 and 9 is appropriate for TEC 2018. In all models for wall 15, the length of all piers is less than 1.5 m. In models 3, 5 and 9, the piers between openings are less than 1 meter. This insufficient length of piers cause local failure. The main reason for local collapses is that the size of opening is much or near the corners. Excessive aspect ratios of piers can cause local failures. When walls 6 and 9 are examined, the length and percentage piers between door and window are increased and this case increase the stiffness and strength of wall. When models 1 and 2 are compared, only the location of the door has been changed, but there is no significant change in capacity. When comparing models 4 and 7, ductility of them is similar, but model 7 has more strength.

5.4.1.16 Failure Modes of Wall 16

In the wall 16 type, there are 5 different wall models. The impact of single door and five windows openings was studied in these models of wall 16. Table A.16 shows the lengths of the walls. As seen in Figure 5.3, each pier is designated from left to right. The crack patterns obtained from the analysis of wall models corresponding to 5 different wall models are described in this section.

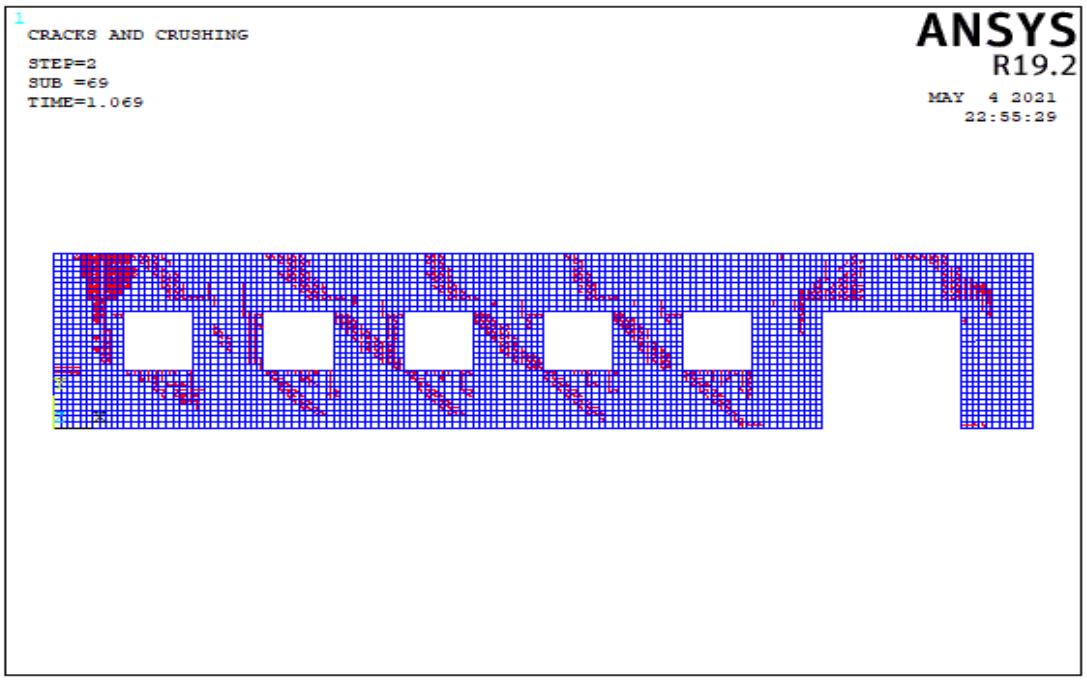

(a)

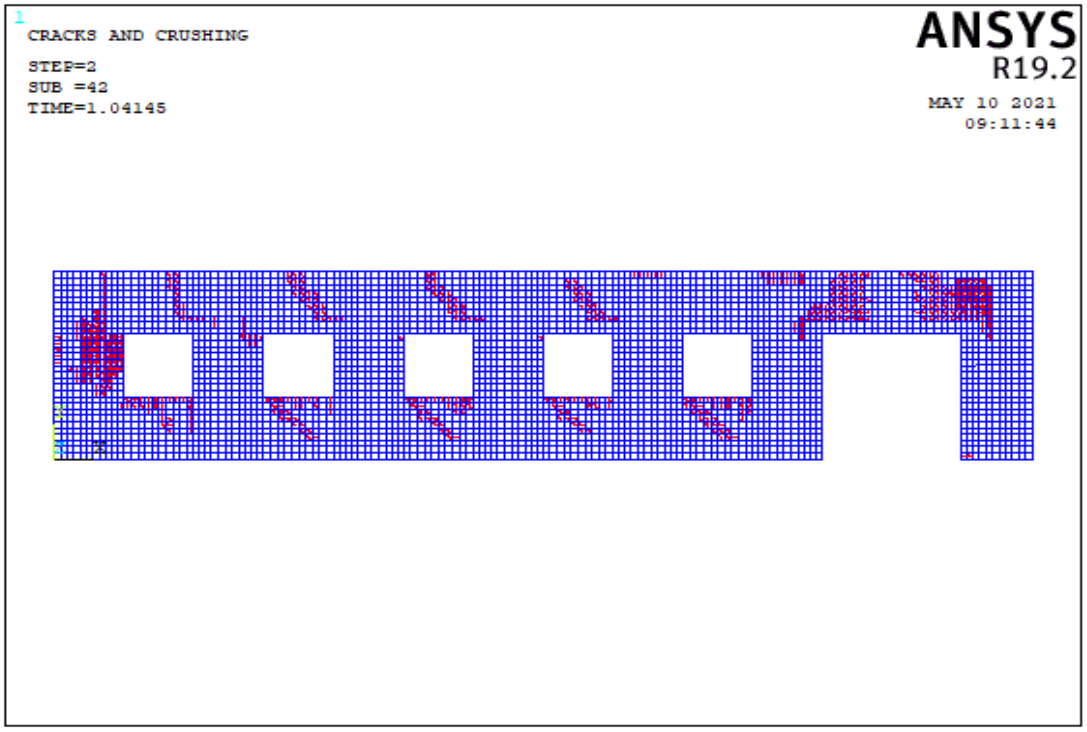

(b)

Figure 5.137. The Crack Pattern of Wall 16 Model 1 According to Compressive Strength Values of (a) 3 MPa, (b) 8 MPa

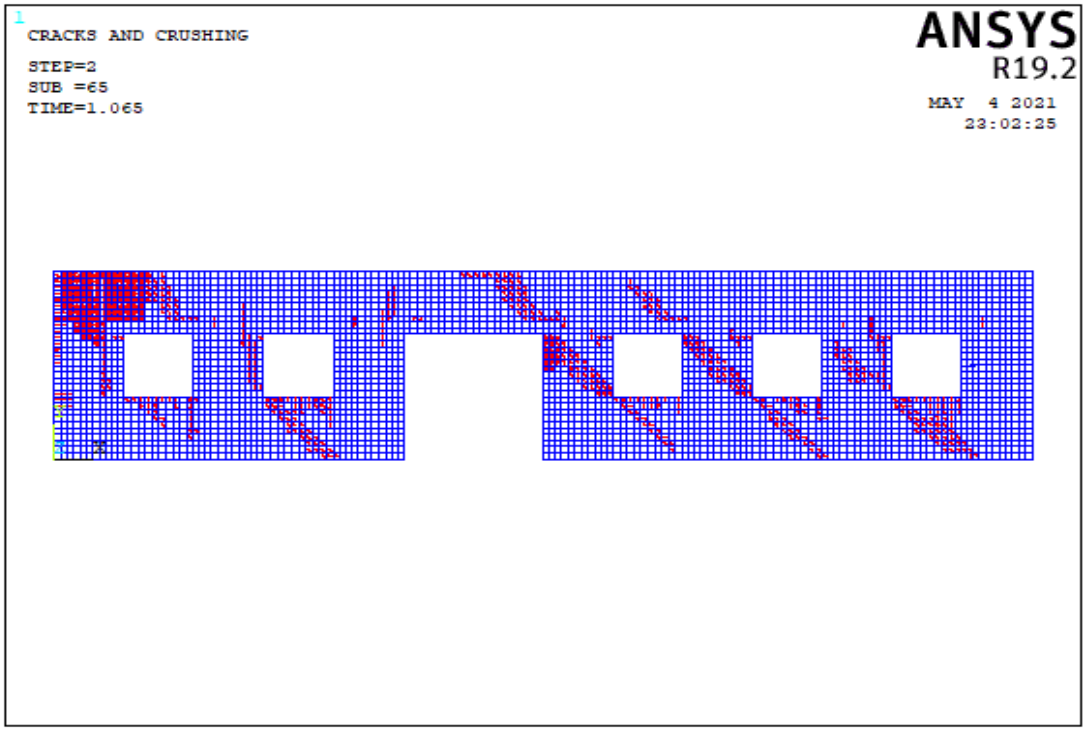

(a)

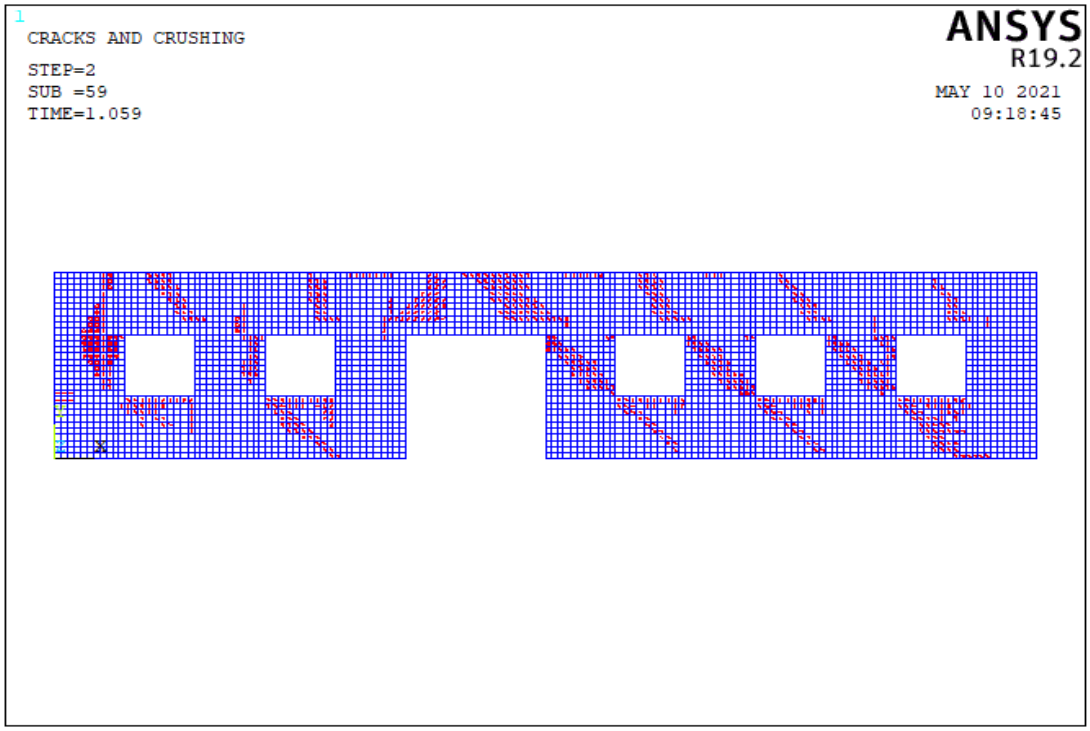

(b)

Figure 5.138. The Crack Pattern of Wall 16 Model 2 According to Compressive Strength Values of (a) 3 MPa, (b) 8 MPa

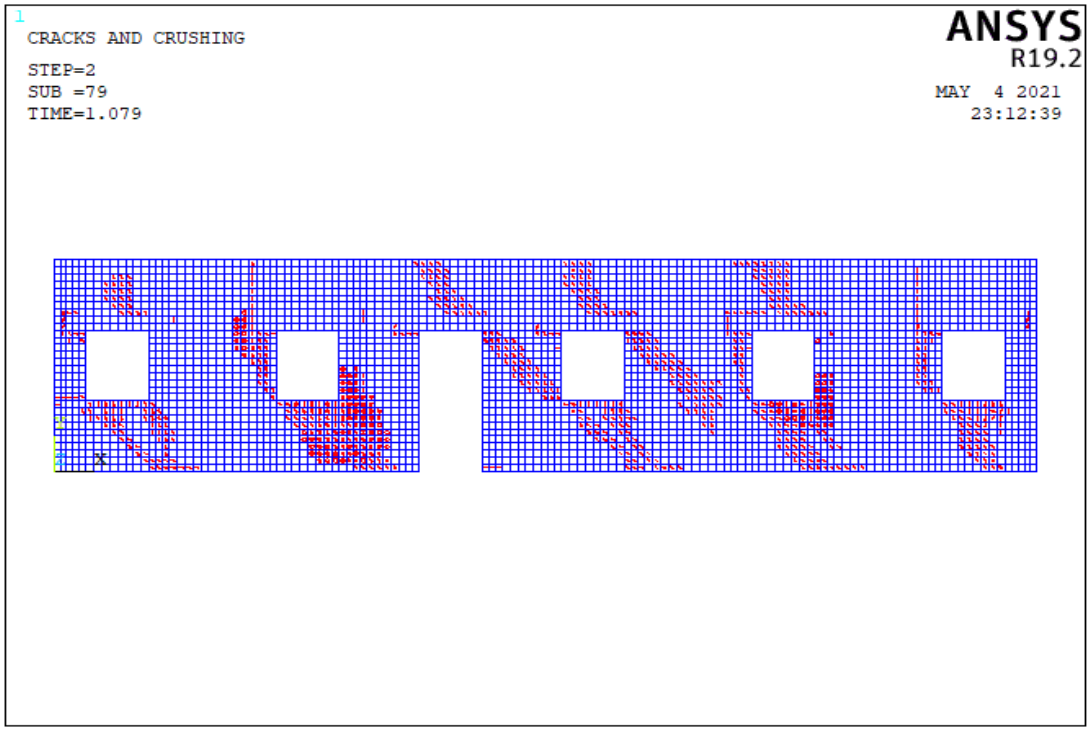

(a)

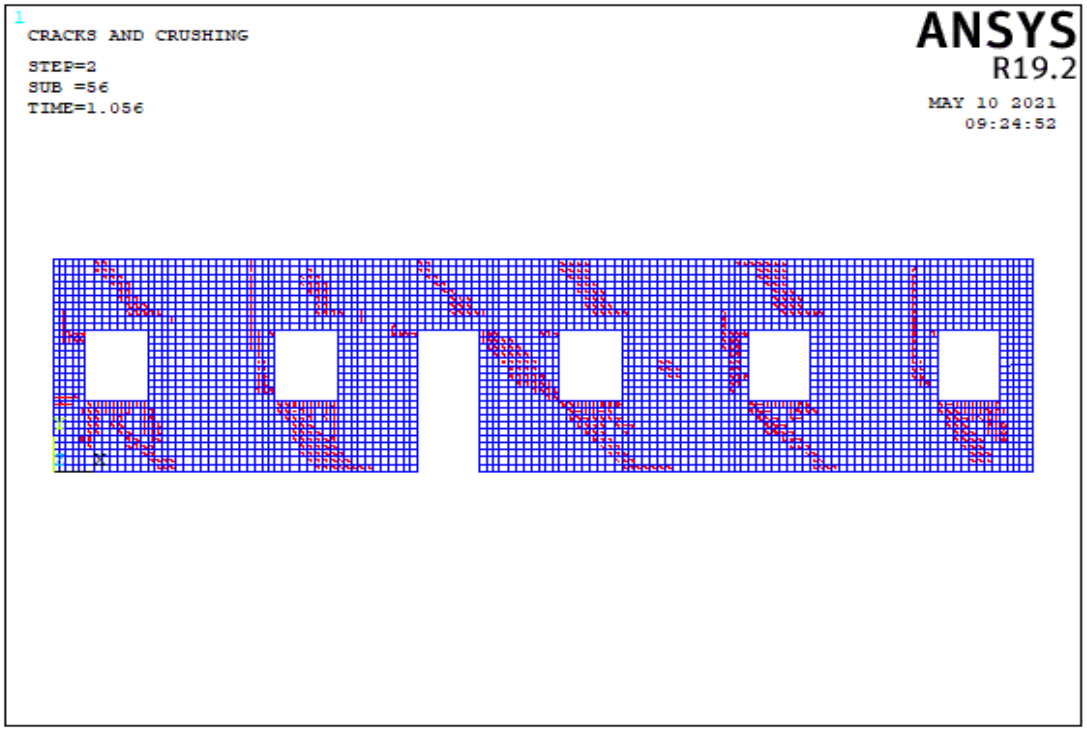

(b)

Figure 5.139. The Crack Pattern of Wall 16 Model 3 According to Compressive Strength Values of (a) 3 MPa, (b) 8 MPa

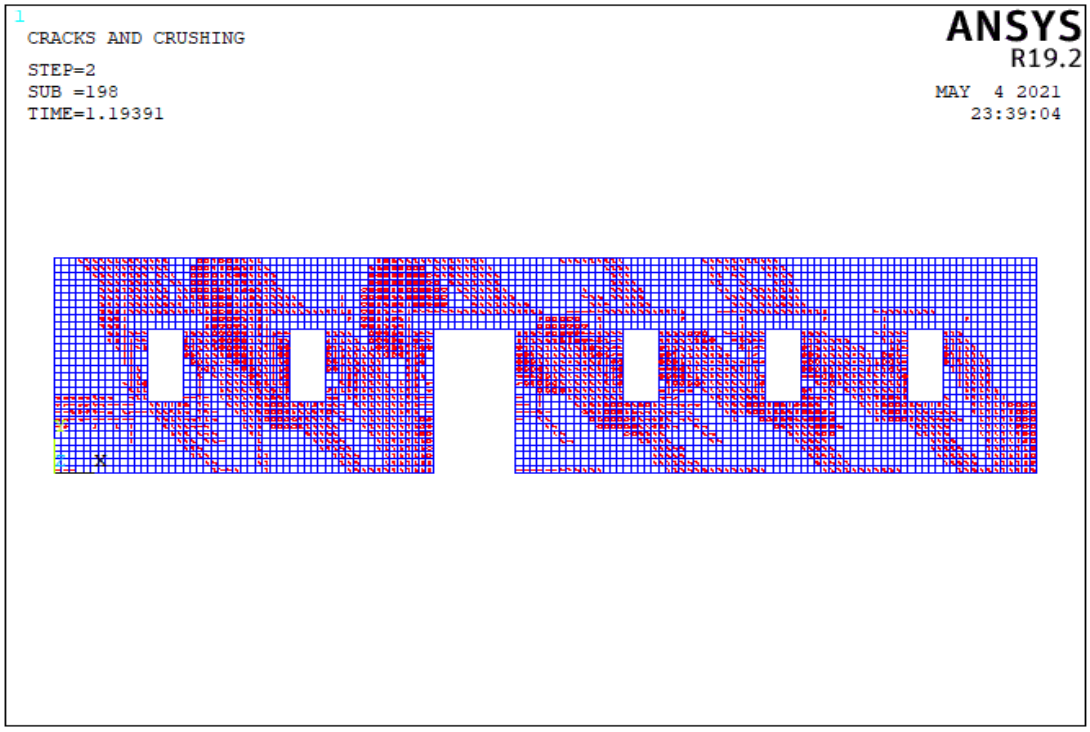

(a)

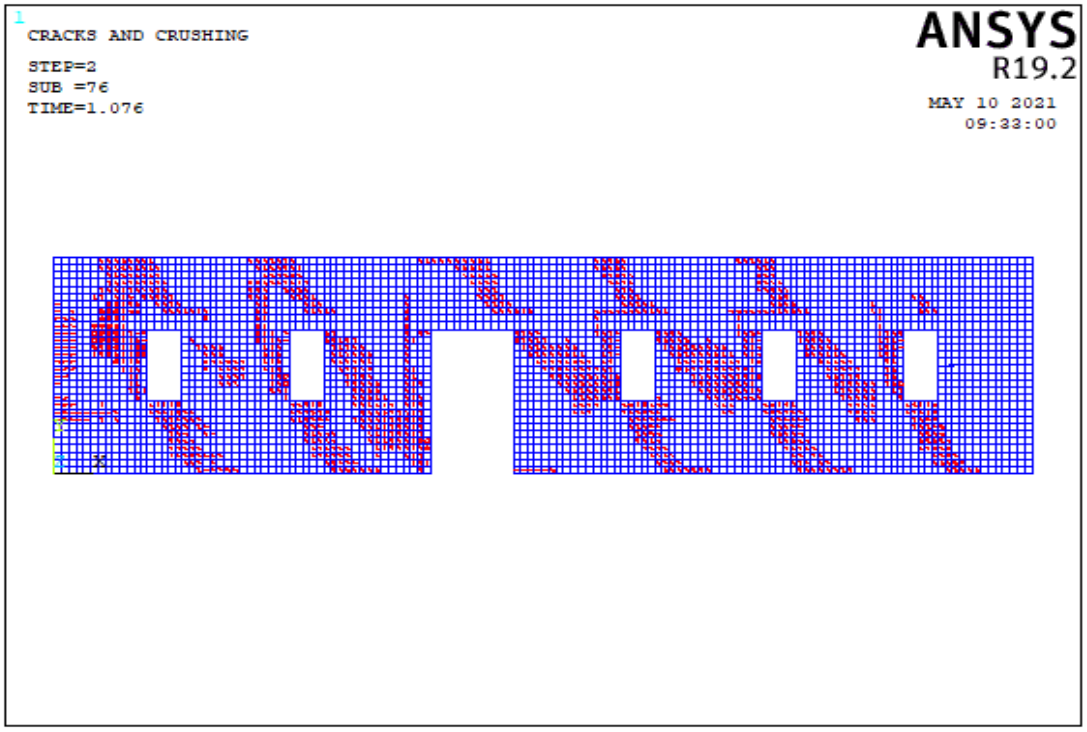

(b)

Figure 5.140. The Crack Pattern of Wall 16 Model 4 According to Compressive Strength Values of (a) 3 MPa, (b) 8 MPa

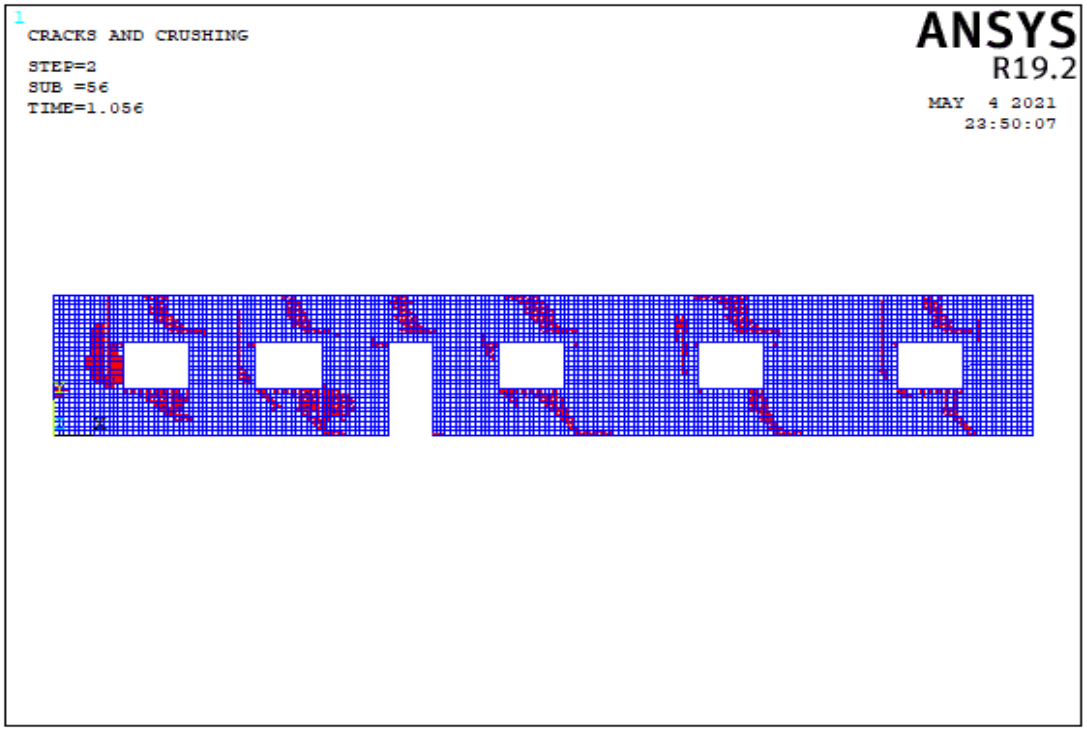

(a)

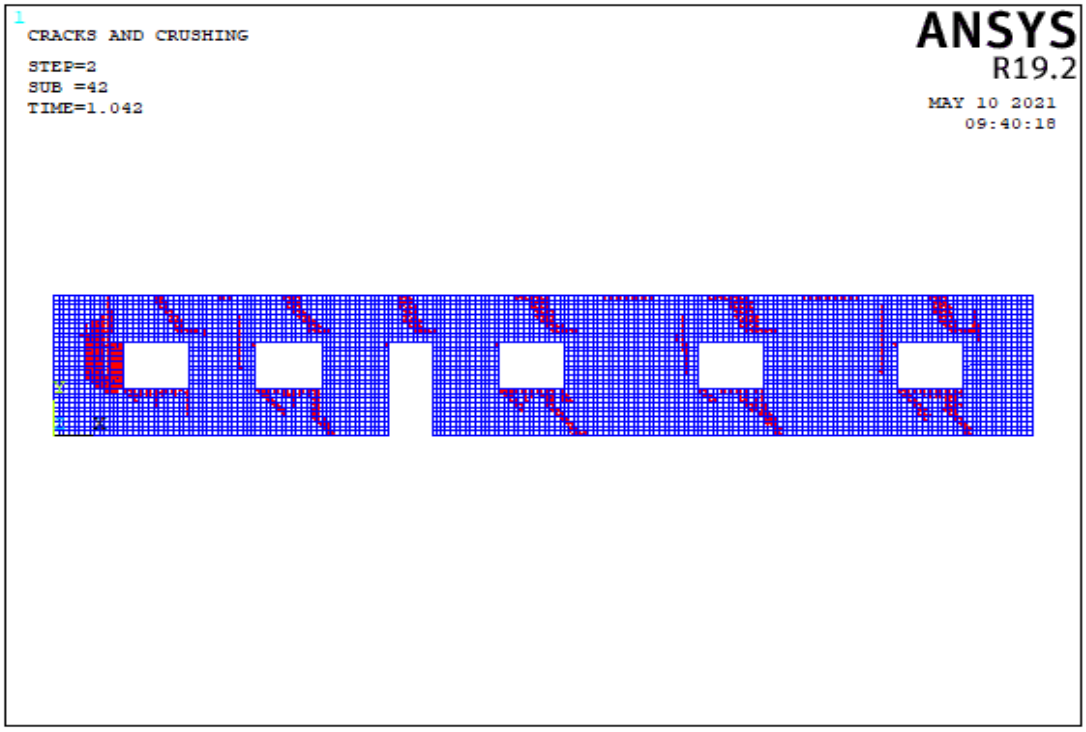

(b)

Figure 5.141. The Crack Pattern of Wall 16 Model 5 According to Compressive Strength Values of (a) 3 MPa, (b) 8 MPa

Table 5.18. Failure Patterns of Wall 16

Number of Model	Aspect ratio	fm=3 Mpa			fm=8 Mpa		
		Failure Pattern			Failure Pattern		
		Base Sliding	Rocking	Diagonal	Base Sliding	Rocking	Diagonal Tension
Model 1	3.00		X			X	
	3.00			X			
	3.00			X			
	3.00			X			
	3.00			X			
	3.00						
	3.00						
Model 2	3.00		X			X	
	3.00			X			X
	3.00						
	3.00			X			X
	3.00			X			X
	3.00			X			X
	3.00						
Model 3	7.50		X			X	
	1.88						
	3.00			X			X
	3.00			X			X
	1.88			X			X
	1.88						
	7.50		X			X	
Model 4	2.59			X			X
	2.26			X			X
	2.26			X			X
	2.26			X			X
	2.26			X			X
	2.26			X			X
	2.59			X			X
Model 5	2.28		X			X	
	2.36						
	2.36			X			X
	2.36						
	1.18						
	1.18						
	2.28						

In models 1 and 2, the wall lengths are similar. Only the location of the door is changed. The capacity curves of the walls are similar. Although the lengths of model 3 and 4 are the same, the capacity of model 4 is much higher due to reduced percentage of openings. Model 5 shows that low opening ratio and larger pier increase the strenth of wall. The change in the aspect ratios of the piers or location of openings change the failure modes and capacity of wall. In these figures, diagonal tension cracks appear in piers when the pier percentage or length of pier increase.

5.4.1.17 Failure Modes of Wall 17

In the wall 17 type, there are 3 different wall models. The impact of single door and six windows openings was studied in these models of wall 17. Table A.17 shows the lengths of the walls. As seen in Figure 5.3, each pier is designated from left to right. The crack patterns obtained from the analysis of wall models corresponding to 3 different wall models are described in this section.

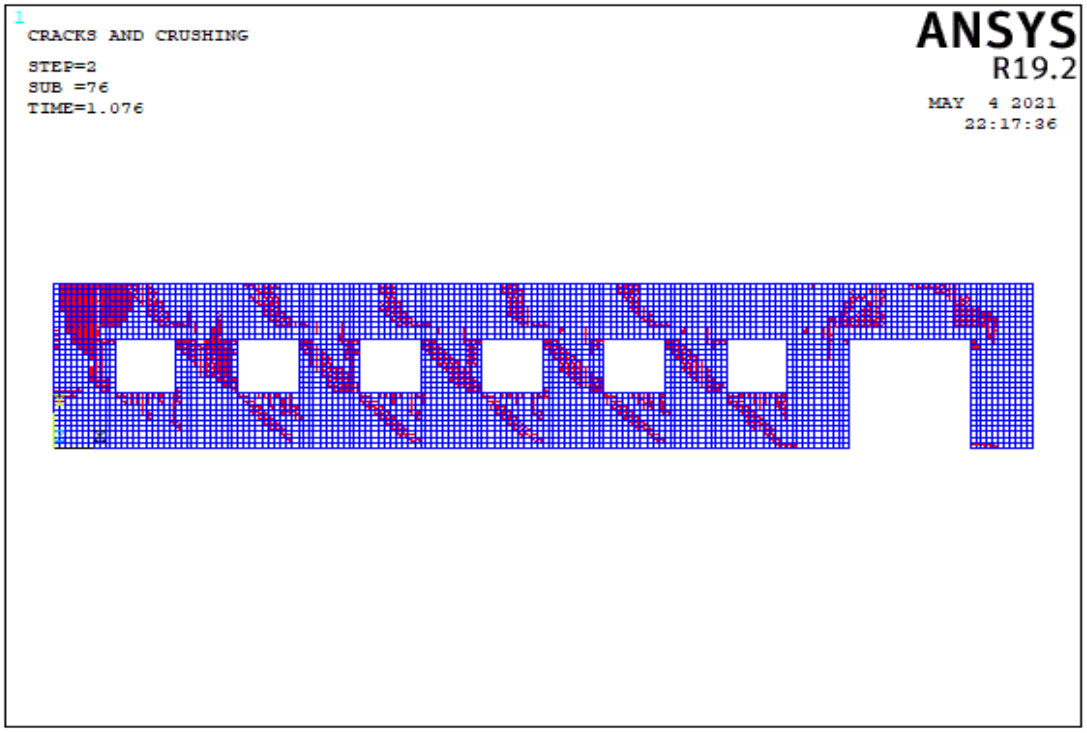

(a)

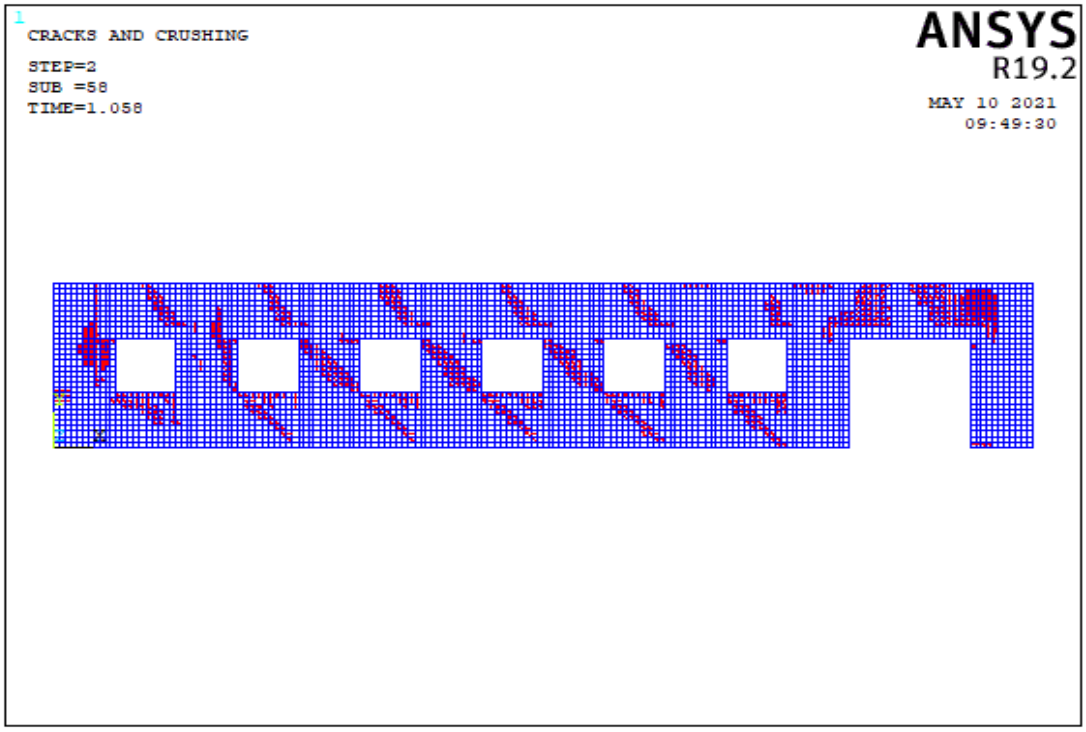

(b)

Figure 5.142. The Crack Pattern of Wall 17 Model 1 According to Compressive Strength Values of (a) 3 MPa, (b) 8 MPa

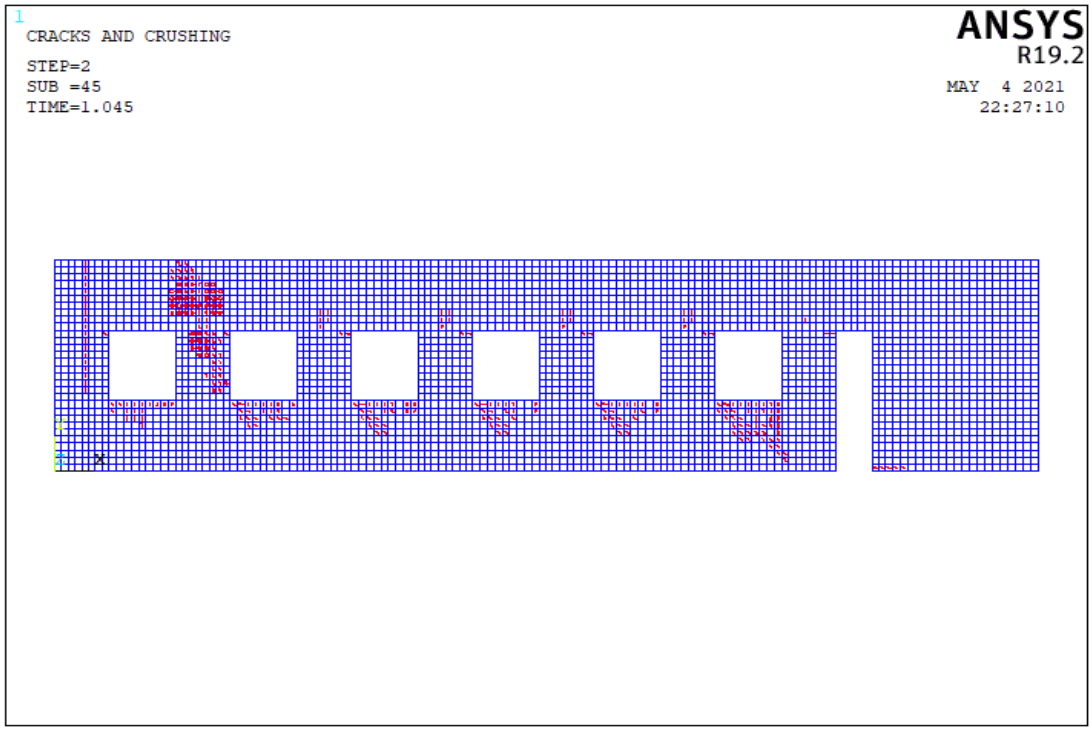

(a)

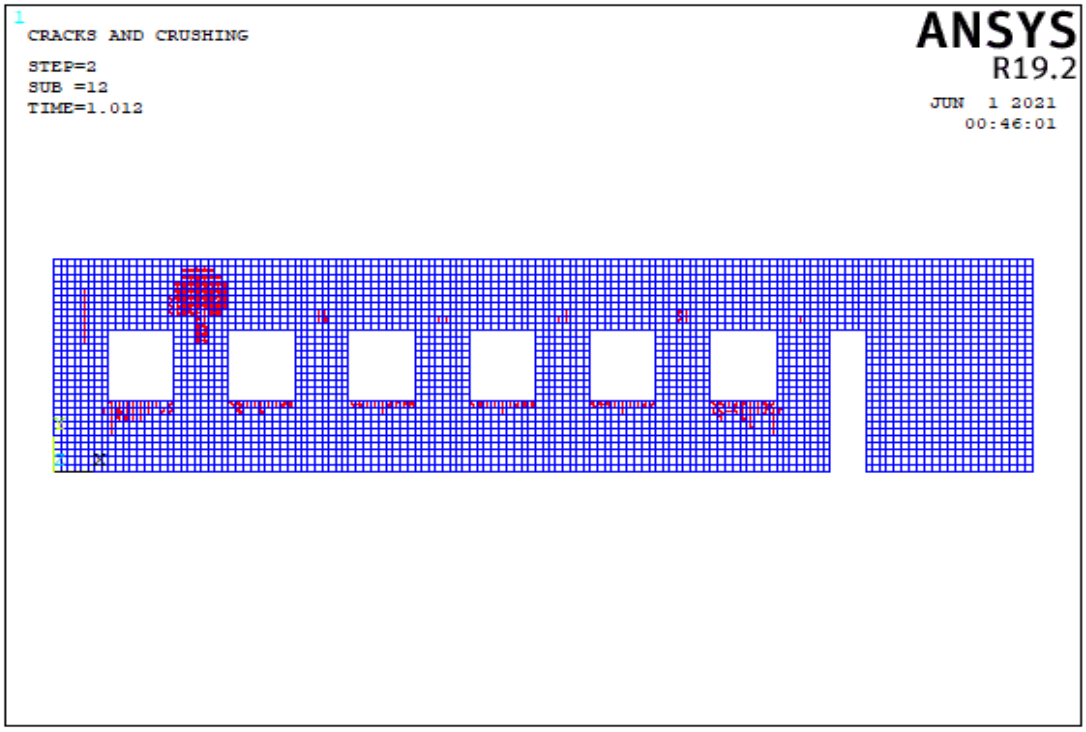

(b)

Figure 5.143. The Crack Pattern of Wall 17 Model 2 According to Compressive Strength Values of (a) 3 MPa, (b) 8 MPa

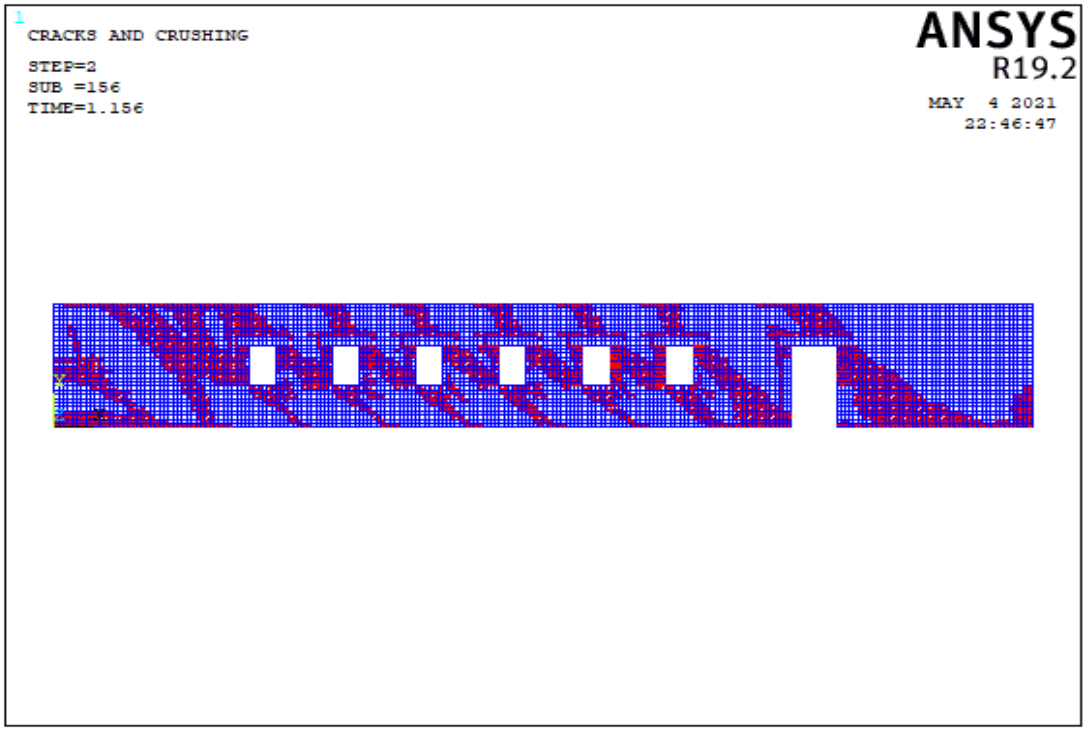

(a)

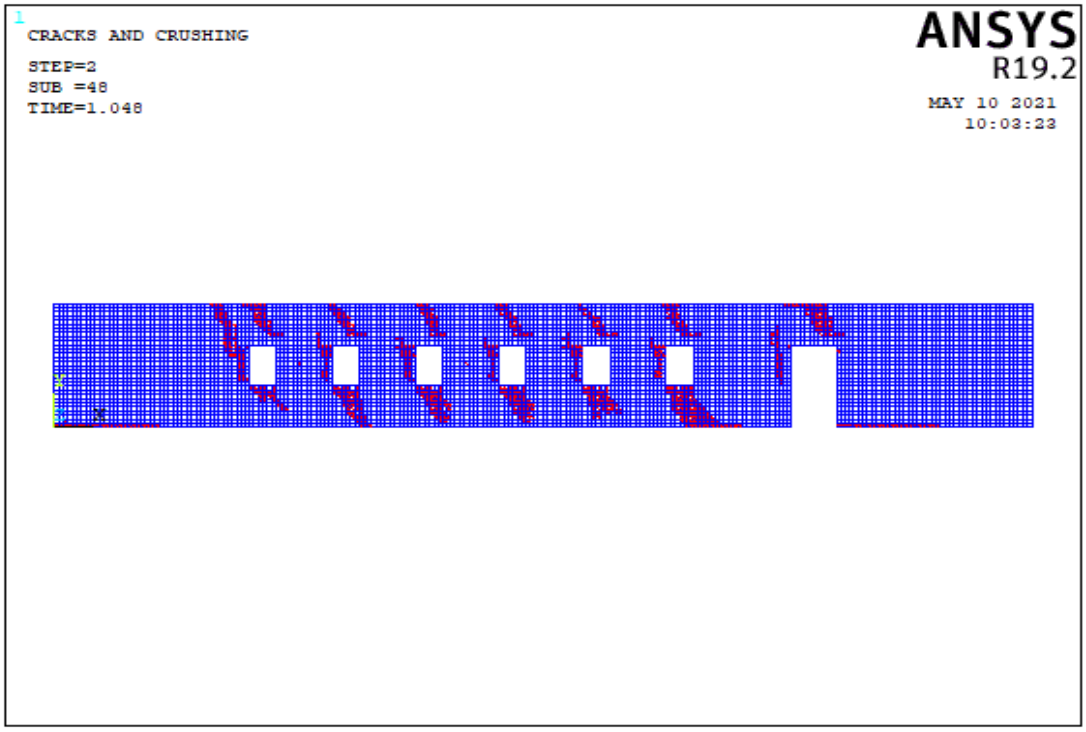

(b)

Figure 5.144. The Crack Pattern of Wall 17 Model 3 According to Compressive Strength Values of (a) 3 MPa, (b) 8 MPa

Table 5.19. Failure Patterns of Wall 17

Number of Model	Aspect ratio	fm=3 Mpa			fm=8 Mpa		
		Failure Pattern			Failure Pattern		
		Base Sliding	Rocking	Diagonal Tension	Base Sliding	Rocking	Diagonal Tension
Model 1	3.03		X			X	
	3.03			X			X
	3.03			X			X
	3.03			X			X
	3.03			X			X
	3.03			X			X
	3.03						
	3.03						
Model 2	4.40		X			X	
	4.40		X			X	
	4.40						
	4.40						
	4.40						
	4.40						
	4.40						
	1.43						
Model 3	0.71			X	X		
	2.50			X			X
	2.50			X			X
	2.50			X			X
	2.50			X			X
	2.50			X			X
	1.43			X			X
	0.71			X	X		

In the Table A.17, all length of openings are less than 3 m for all models of wall 17 and total opening percentage of wall in all models is appropriate for TEC 2018. In model 1 and 2 for wall 17, length of all the piers is less than 1.5 m. In model 2, the piers between windows and doors is less than 1 m and local failure is seen in this situation. Model 3 shows that the capacity of the wall improves as the percentage of the pier increases. The strength and stiffness of piers are improved by a reduced aspect ratio.

5.4.1.18 Failure Modes of Wall 18

In the wall 18 type, there are 3 different wall models. The impact of single door and eight windows openings was studied in these models of wall 18. Table A.18 shows the lengths of the walls. As seen in Figure 5.3, each pier is designated from left to right. The crack patterns obtained from the analysis of wall models corresponding to 3 different wall models are described in this section.

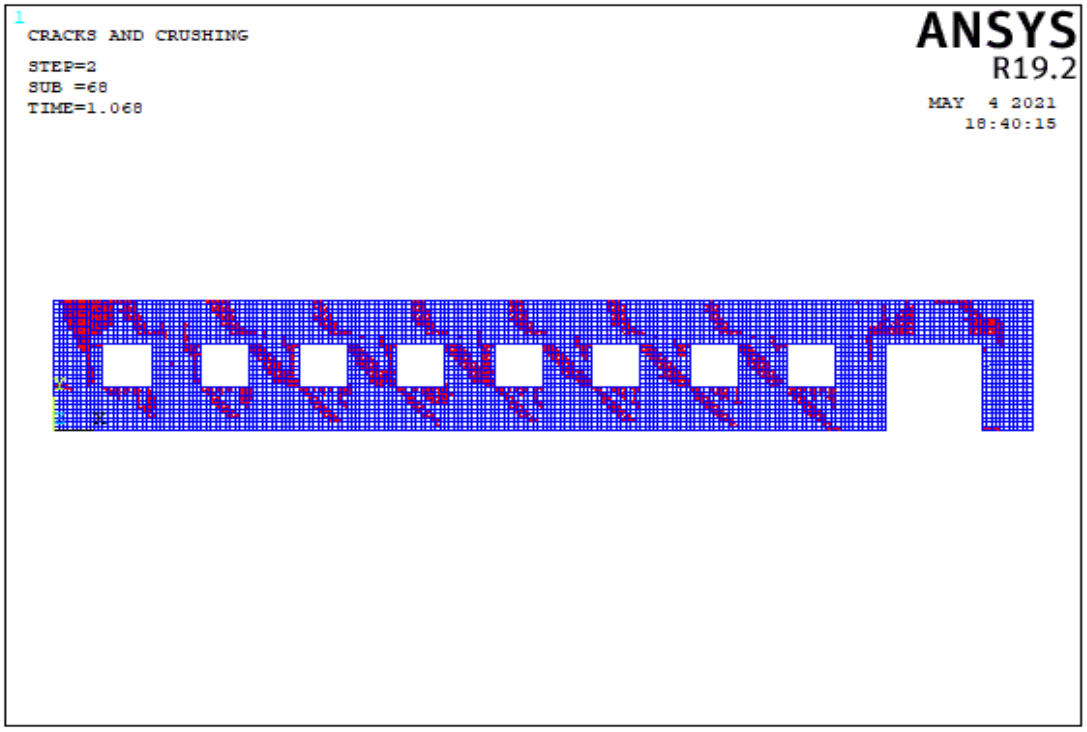

(a)

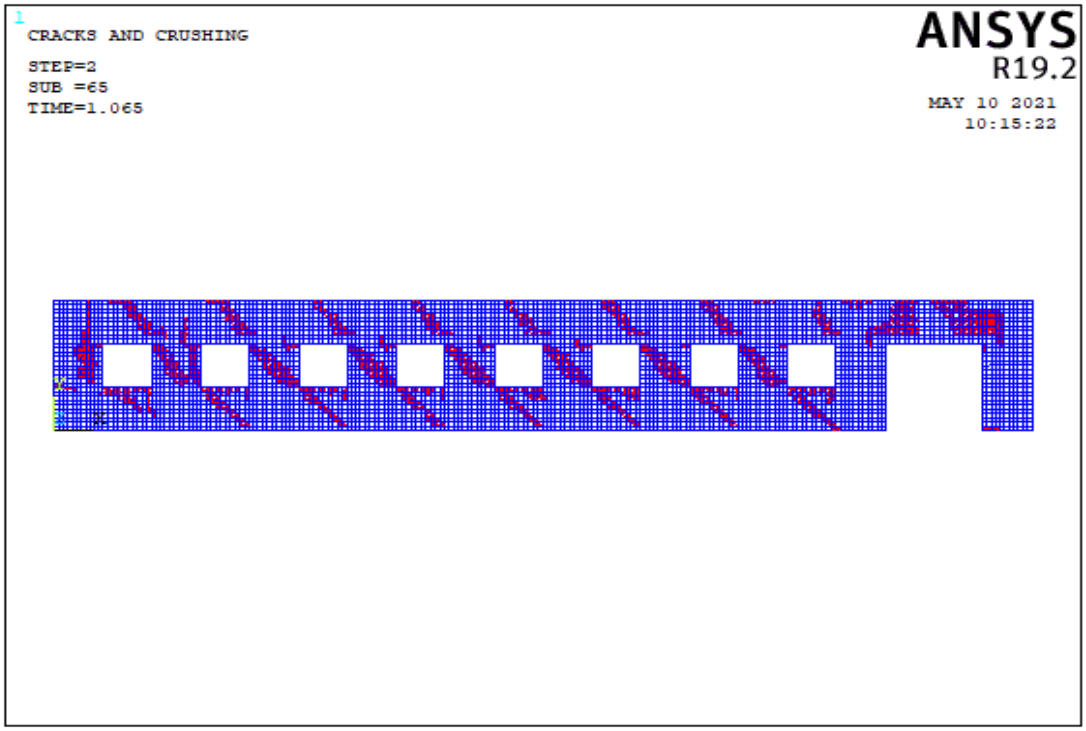

(b)

Figure 5.145. The Crack Pattern of Wall 18 Model 1 According to Compressive Strength Values of (a) 3 MPa, (b) 8 MPa

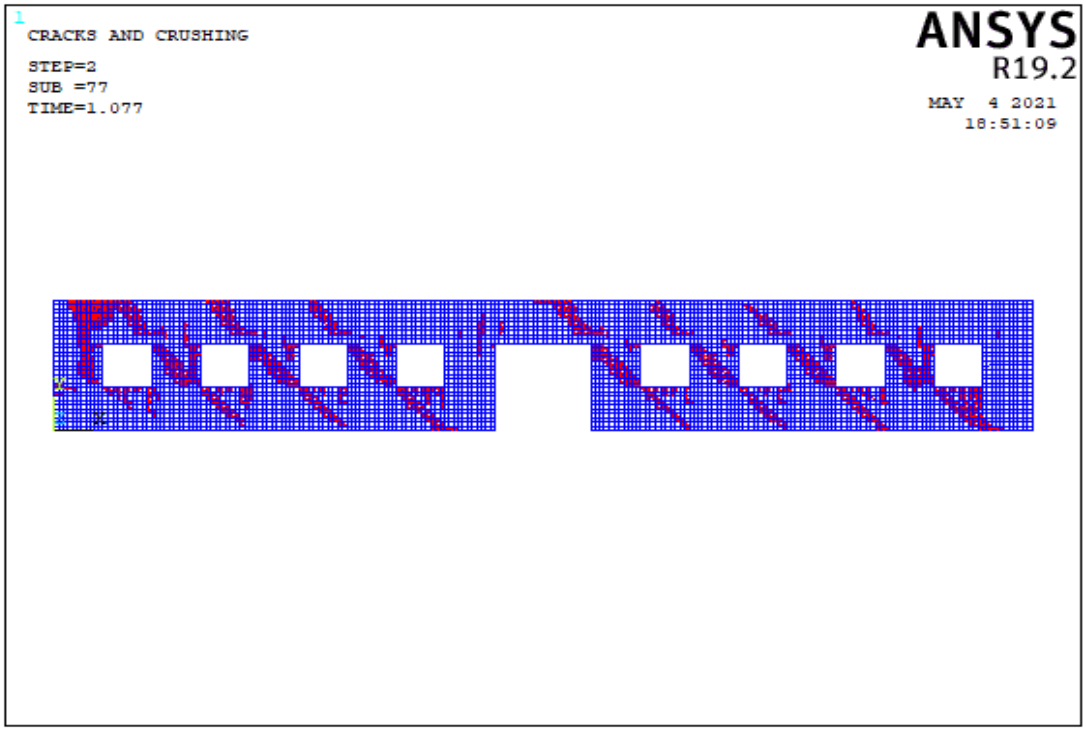

(a)

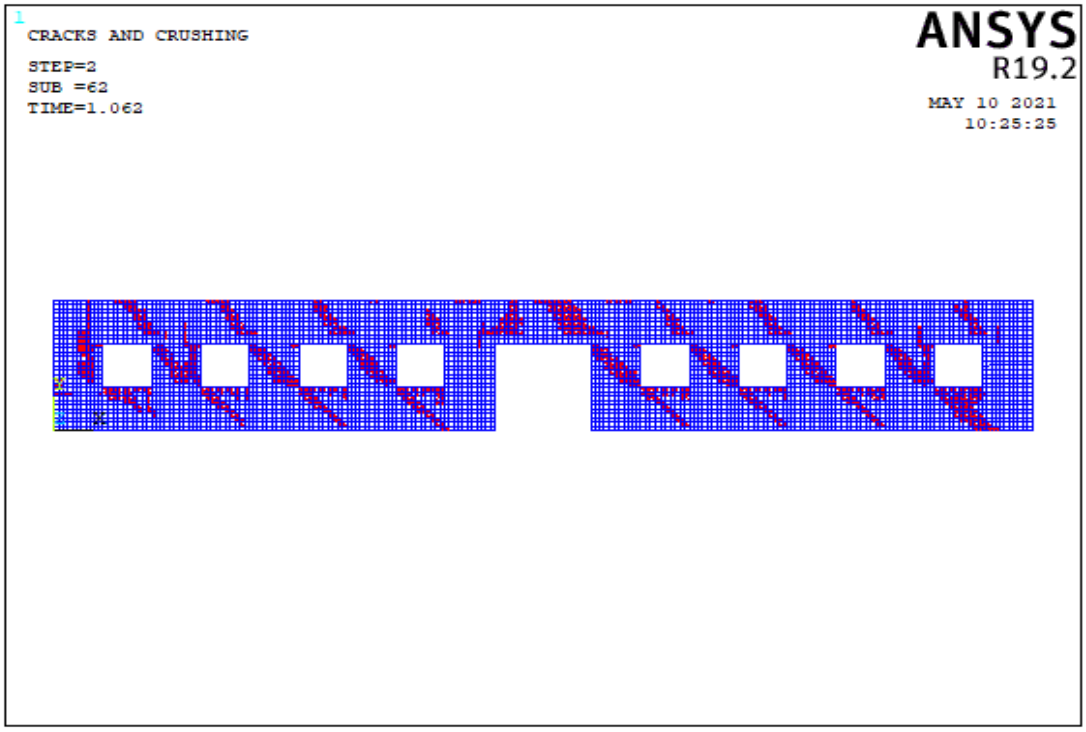

(b)

Figure 5.146. The Crack Pattern of Wall 18 Model 2 According to Compressive Strength Values of (a) 3 MPa, (b) 8 MPa

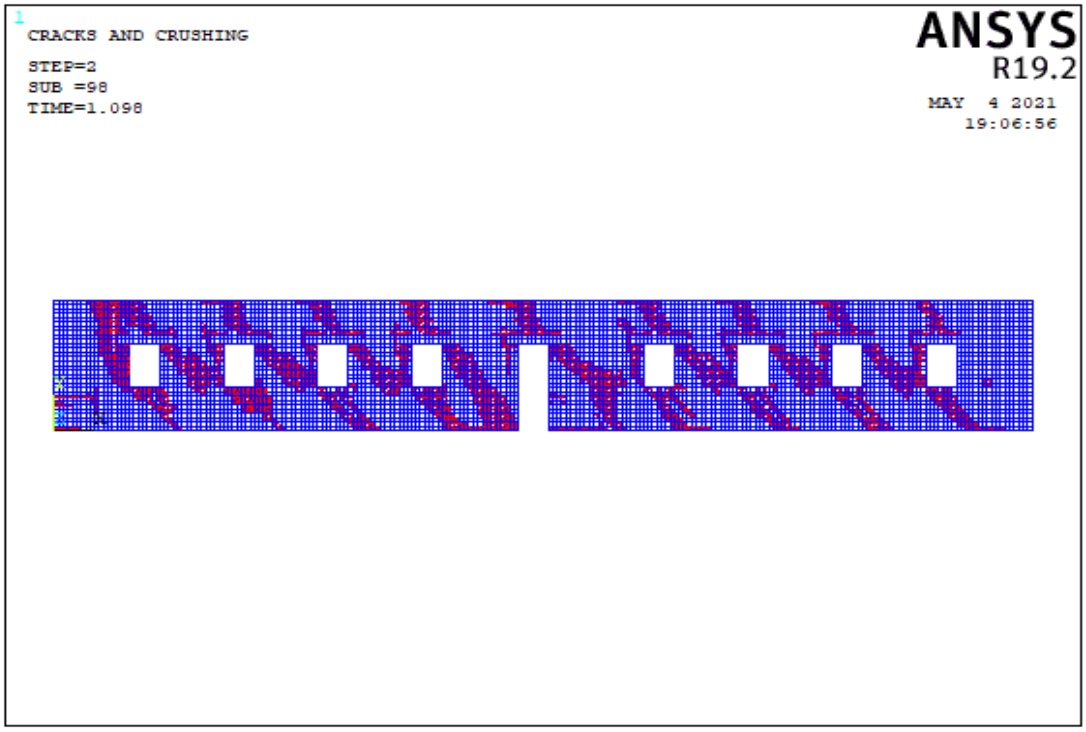

(a)

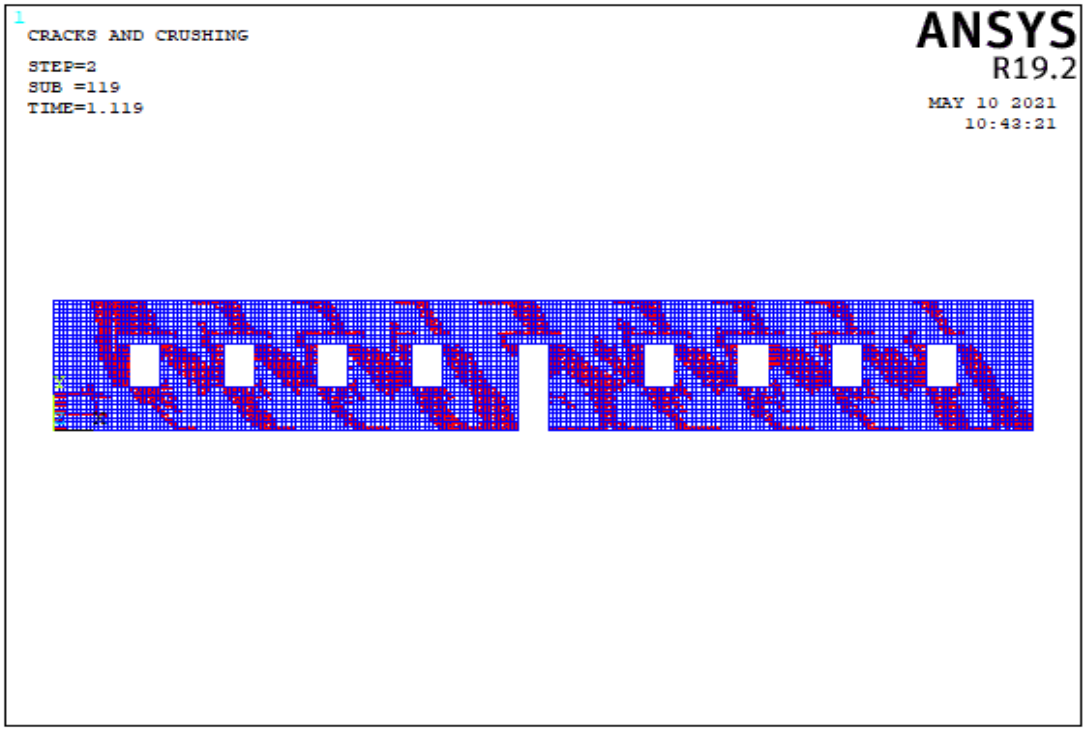

(b)

Figure 5.147. The Crack Pattern of Wall 18 Model 3 According to Compressive Strength Values of (a) 3 MPa, (b) 8 MPa

Table 5.20. Failure Patterns of Wall 18

Number of Model	Aspect ratio	fm=3 Mpa			fm=8 Mpa		
		Failure Pattern			Failure Pattern		
		Base Sliding	Rocking	Diagonal Tension	Base Sliding	Rocking	Diagonal Tension
Model 1	3.00		X			X	
	3.00			X			X
	3.00			X			X
	3.00			X			X
	3.00			X			X
	3.00			X			X
	3.00			X			X
	3.00			X			X
	3.00						
	3.00						
Model 2	3.00		X			X	
	3.00			X			X
	3.00			X			X
	3.00			X			X
	3.00			X			X
	3.00			X			X
	3.00			X			X
	3.00			X			X
	3.00			X			X
	3.00			X			X
Model 3	0.64			X			X
	0.77			X			X
	0.77			X			X
	0.77			X			X
	0.64			X			X
	0.52			X			X
	0.77			X			X
	0.77			X			X
	0.77			X			X
	0.64			X			X

In the Table A.18, all length of openings are less than 3 m for all models of wall 18 and total opening percentage of load bearing walls is appropriate for TEC 2018. In model 1 and 2 for wall 18, length of all the piers less than 1.5 m. In models 1 and 2, only the location of the door is changed. As the opening percentage of the model 3 is the lowest, its wall capacity increases significantly. Model 3 shows that the strength and stiffness of the wall increase when the percentage of the piers between the door and the window is 9% and its length is 1.94 m.

5.4.1.19 Failure Modes of Wall 19

In the wall 19 type, there are 3 different wall models. The impact of two door and four windows openings was studied in these models of wall 19. Table A.19 shows the lengths of the walls. As seen in Figure 5.3, each pier is designated from left to right. The crack patterns obtained from the analysis of wall models corresponding to 3 different wall models are described in this section.

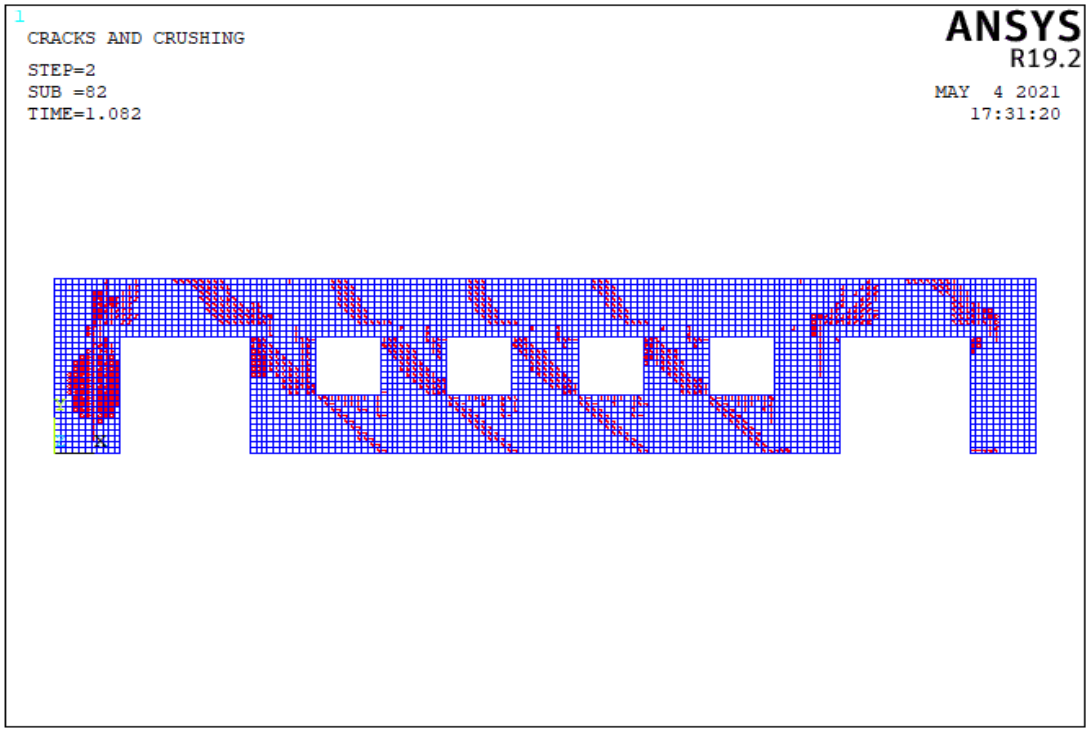

(a)

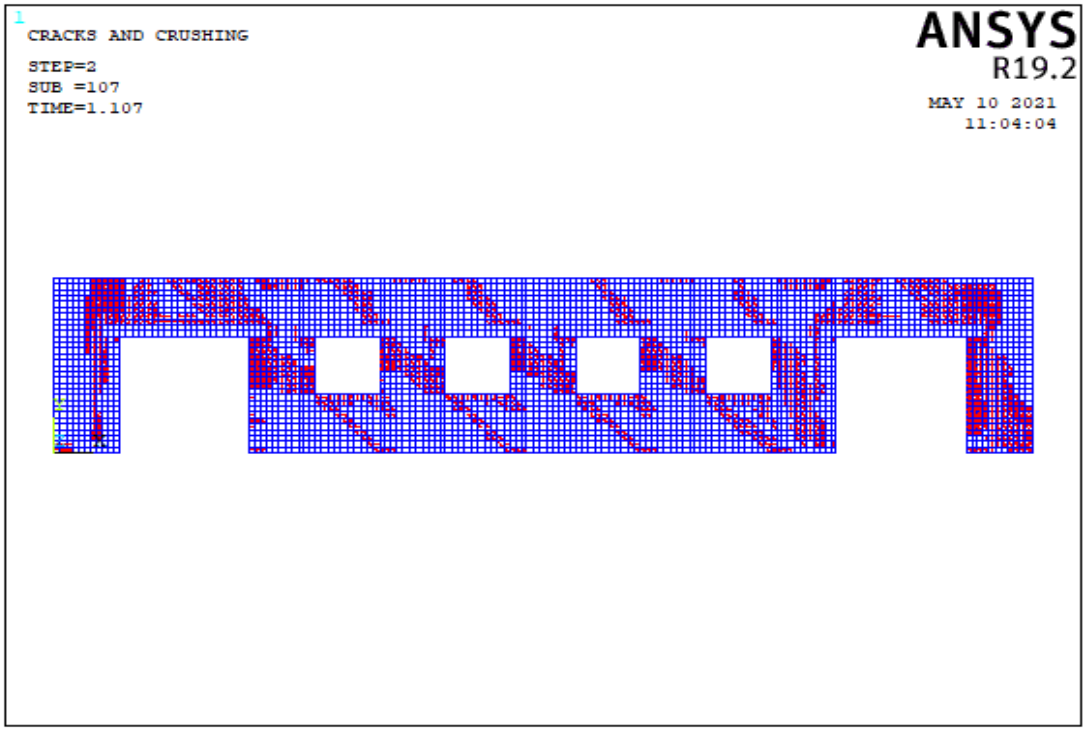

(b)

Figure 5.148. The Crack Pattern of Wall 19 Model 1 According to Compressive Strength Values of (a) 3 MPa, (b) 8 MPa

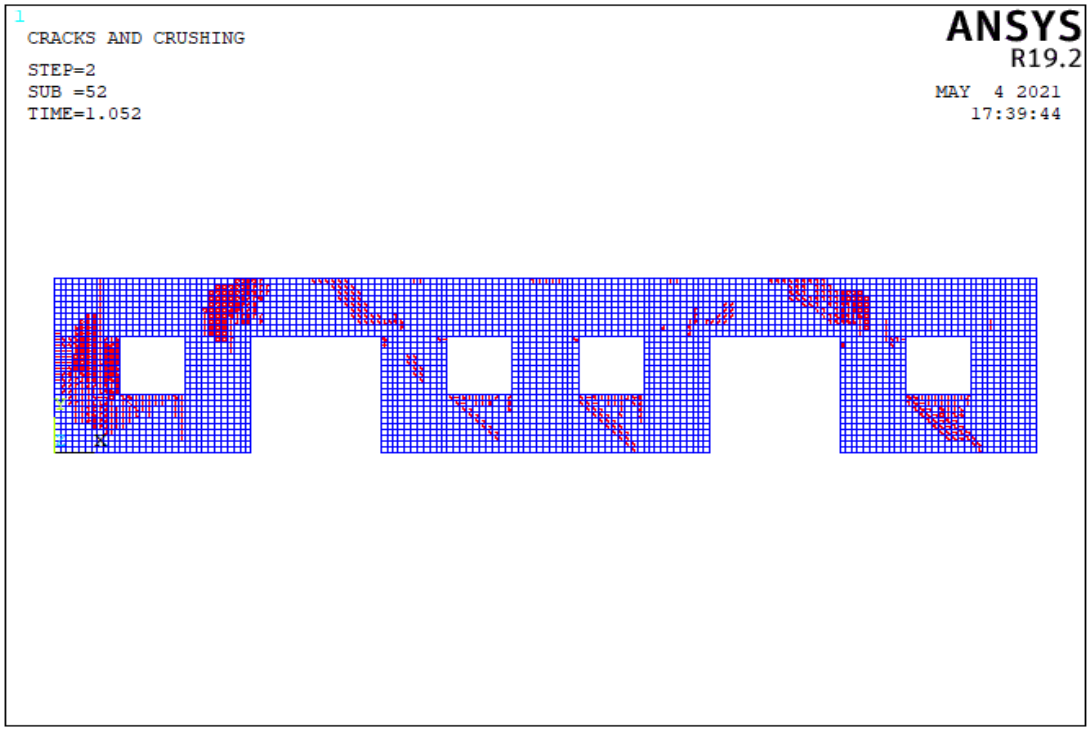

(a)

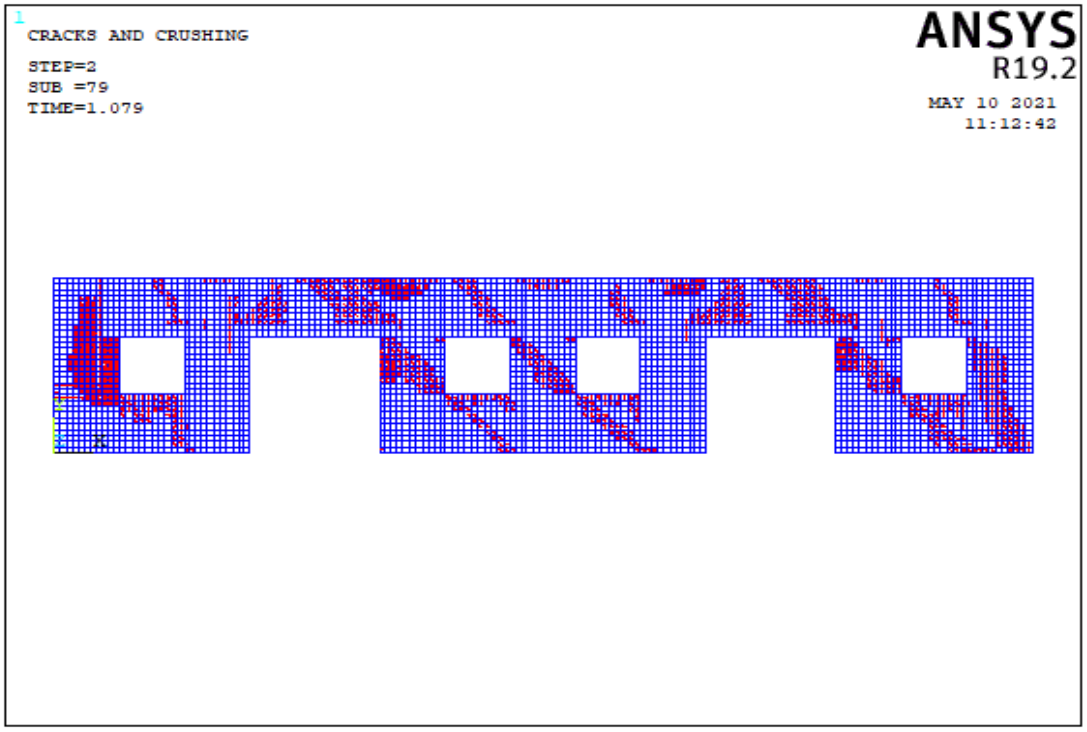

(b)

Figure 5.149. The Crack Pattern of Wall 19 Model 2 According to Compressive Strength Values of (a) 3 MPa, (b) 8 MPa

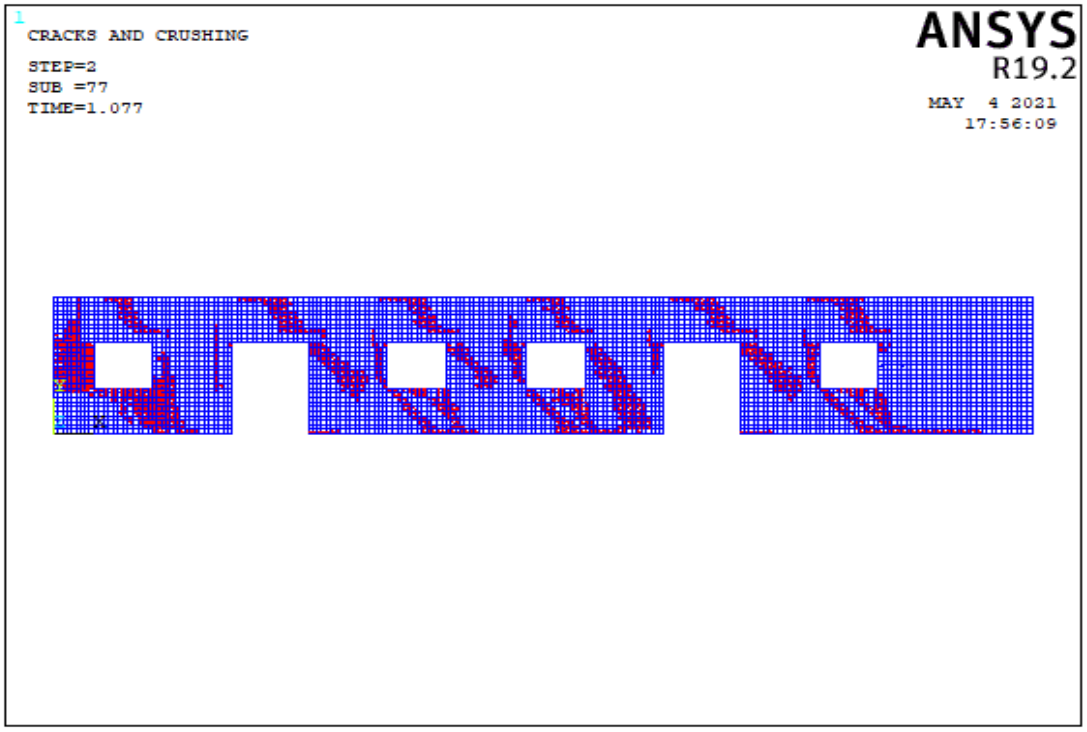

(a)

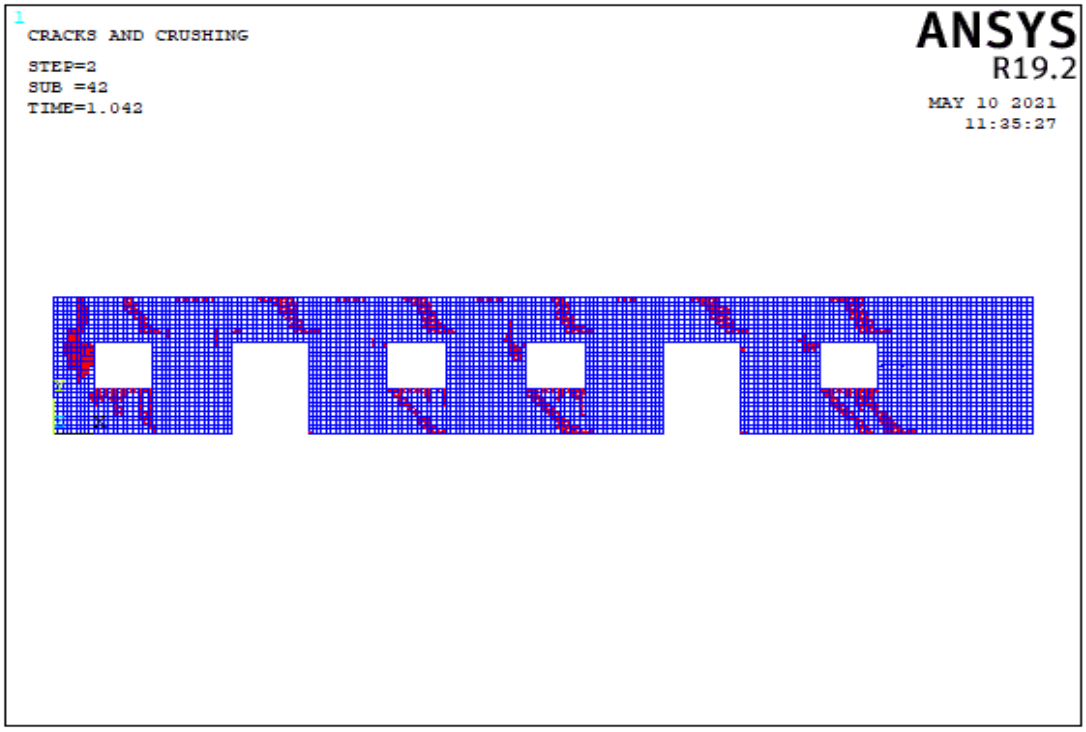

(b)

Figure 5.150. The Crack Pattern of Wall 19 Model 3 According to Compressive Strength Values of (a) 3 MPa, (b) 8 MPa

Table 5.21. Failure Patterns of Wall 19

Number of Model	Aspect ratio	fm=3 Mpa			fm=8 Mpa		
		Failure Pattern			Failure Pattern		
		Base Sliding	Rocking	Diagonal Tension	Base Sliding	Rocking	Diagonal Tension
Model 1	3.03		X			X	
	3.03			X			X
	3.03			X			X
	3.03			X			X
	3.03			X			X
	3.03						
	3.03		X			X	
Model 2	3.03		X			X	
	3.03			X			
	3.03			X			X
	3.03						X
	3.03						
	3.03						X
	3.03						X
Model 3	3.88		X		X		
	1.94			X			
	1.94			X			
	1.94			X			X
	1.94			X			
	1.94			X			
	1.00	X					

In models 1, 2 and 3, the wall lengths are almost the similar but wall capacity is the greatest in model 3 due to decreasing opening percentage. The less opening percentage increase the capacity of wall. In two door walls, the number of piers between windows increases, as the location of doors are closer to the corner, then this situation increases the capacity and the number of diagonal compression struts. There are local failures due to the length or percentage of the openings. The location of the openings is close to the corners, the failure patterns are changed. The aspect ratio of corner pier decrease in model 3 and the base sliding mechanism was observed, whereas the aspect ratio of corner pier increase in model 2, then the rocking mechanism was encountered and capacity of corner pier reduce in this situation.

5.4.1.20 Failure Modes of Wall 20

In the wall 20 type, there are 2 different wall models. The impact of two doors and six windows openings was studied in these models of wall 20. Table A.20 shows the lengths of the walls. As seen in Figure 5.3, each pier is designated from left to right. The crack patterns obtained from the analysis of wall models corresponding to 2 different wall models are described in this section.

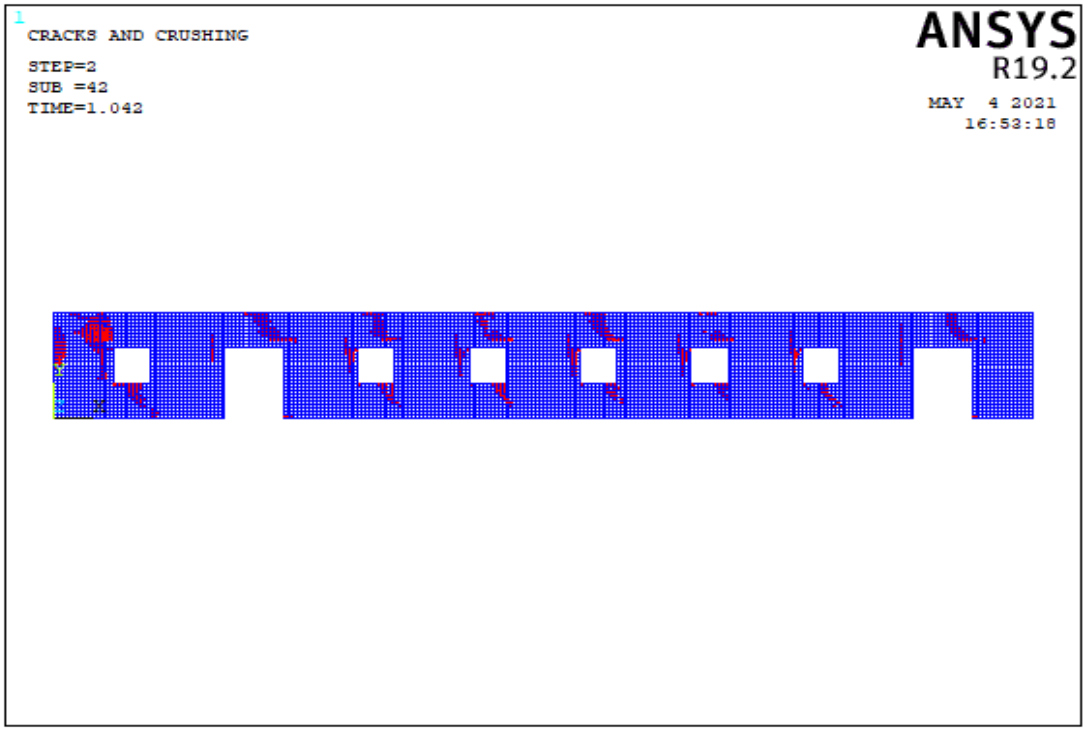

(a)

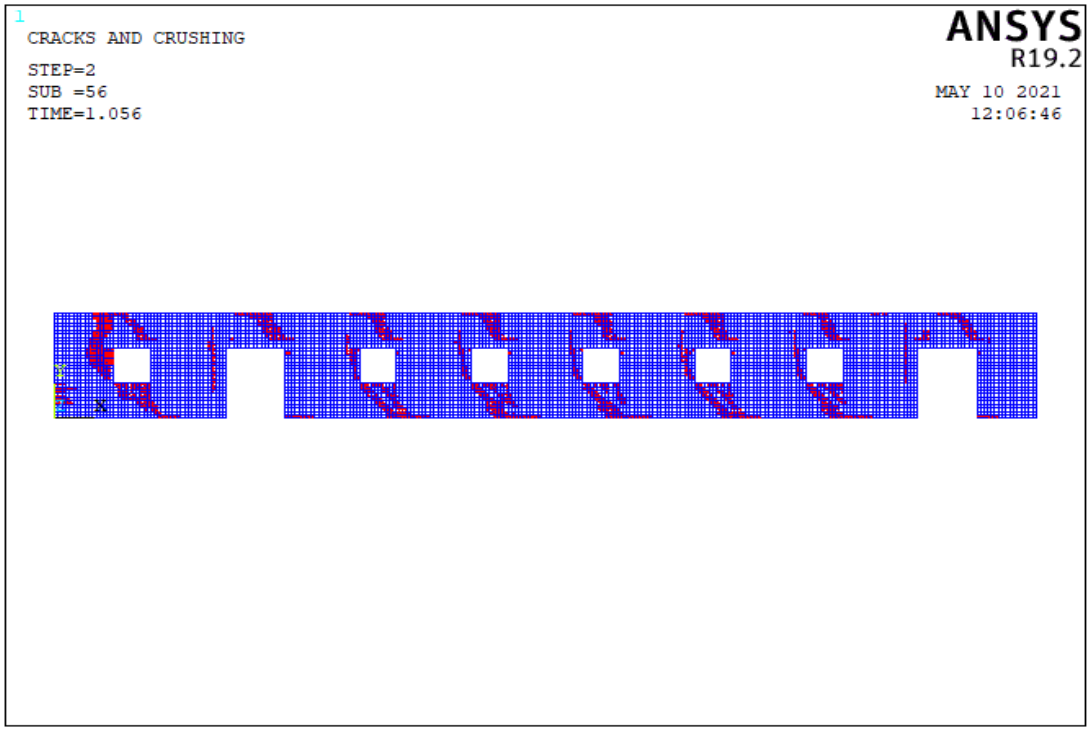

(b)

Figure 5.151. The Crack Pattern of Wall 20 Model 1 According to Compressive Strength Values of (a) 3 MPa, (b) 8 MPa

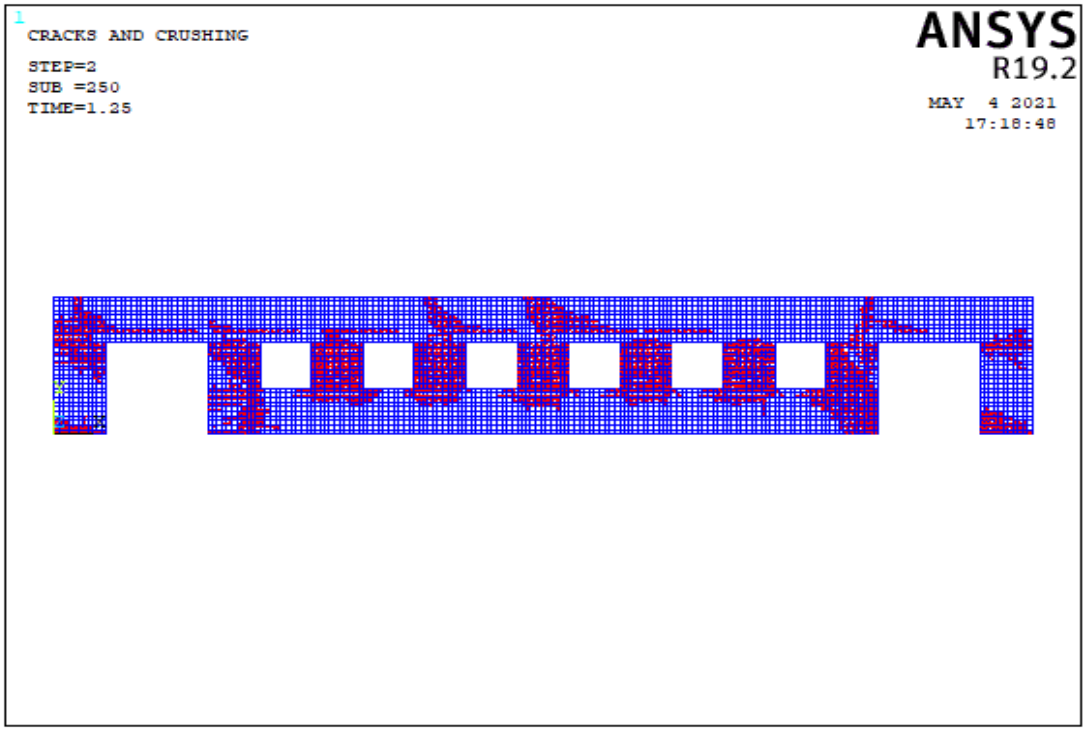

(a)

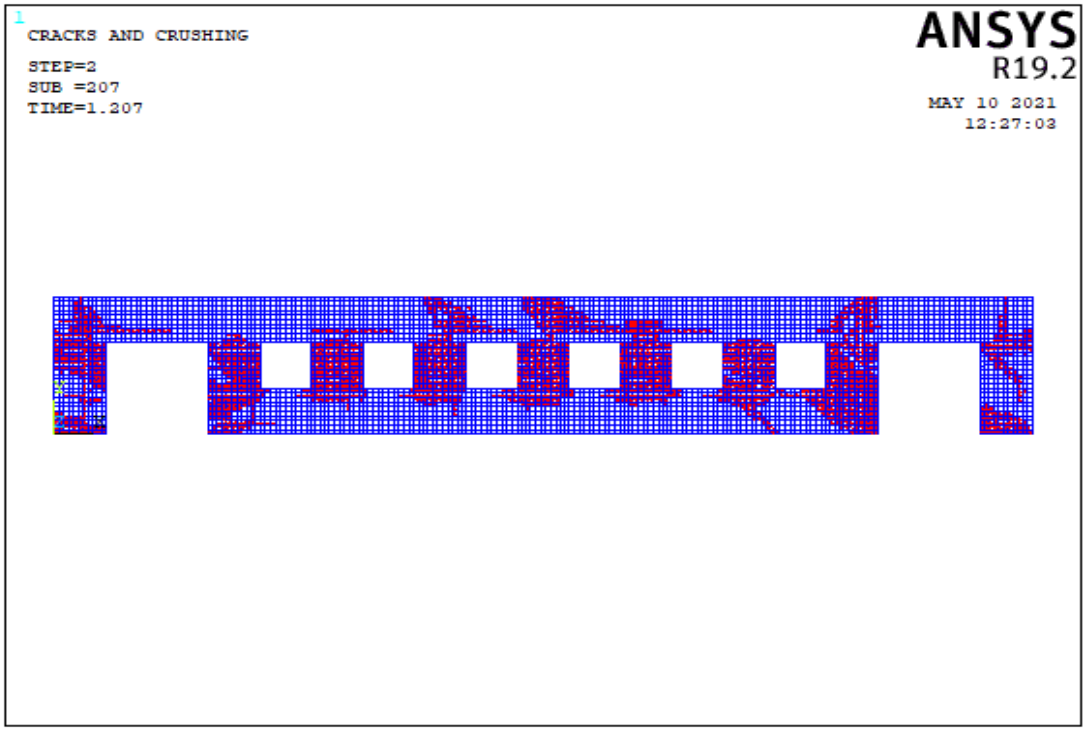

(b)

Figure 5.152. The Crack Pattern of Wall 20 Model 2 According to Compressive Strength Values of (a) 3 MPa, (b) 8 MPa

Table 5.22. Failure Patterns of Wall 20

Number of Model	Aspect ratio	fm=3 Mpa			fm=8 Mpa		
		Failure Pattern			Failure Pattern		
		Base Sliding	Rocking	Diagonal Tension	Base Sliding	Rocking	Diagonal Tension
Model 1	2			X			X
	1.6						
	1.6			X			X
	1.6			X			X
	1.6			X			X
	1.6			X			X
	1.6			X			X
	2						
Model 2	3.03		X			X	
	3.03			X			X
	3.03			X			X
	3.03			X			X
	3.03			X			X
	3.03			X			X
	3.03			X			X
	3.03		X			X	

Table 5.3 shows that, the piers between the openings have diagonal tension mechanism. There are also flexural cracks in the corner piers. In model 2 of wall 20, when the aspect ratio of the piers between the openings decrease, the strength of wall increase. As opening percentage increase , the in-plane capacity of wall reduce.

5.4.1.21 Failure Modes of Wall 21

In the wall 21 type, there is one wall model. The impact of two doors and seven windows openings was studied in this model of wall 21. Table A.21 shows the lengths of the wall. As seen in Figure 5.3, each pier is designated from left to right. The crack patterns obtained from the analysis of wall model corresponding to one wall model are described in this section.

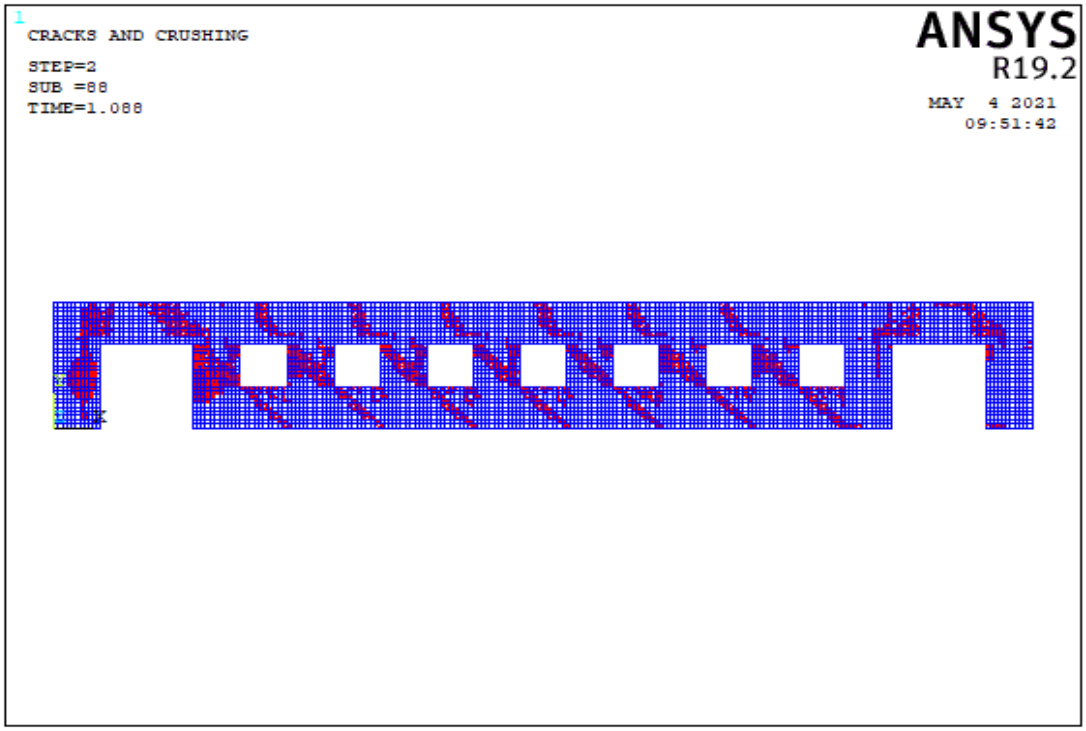

(a)

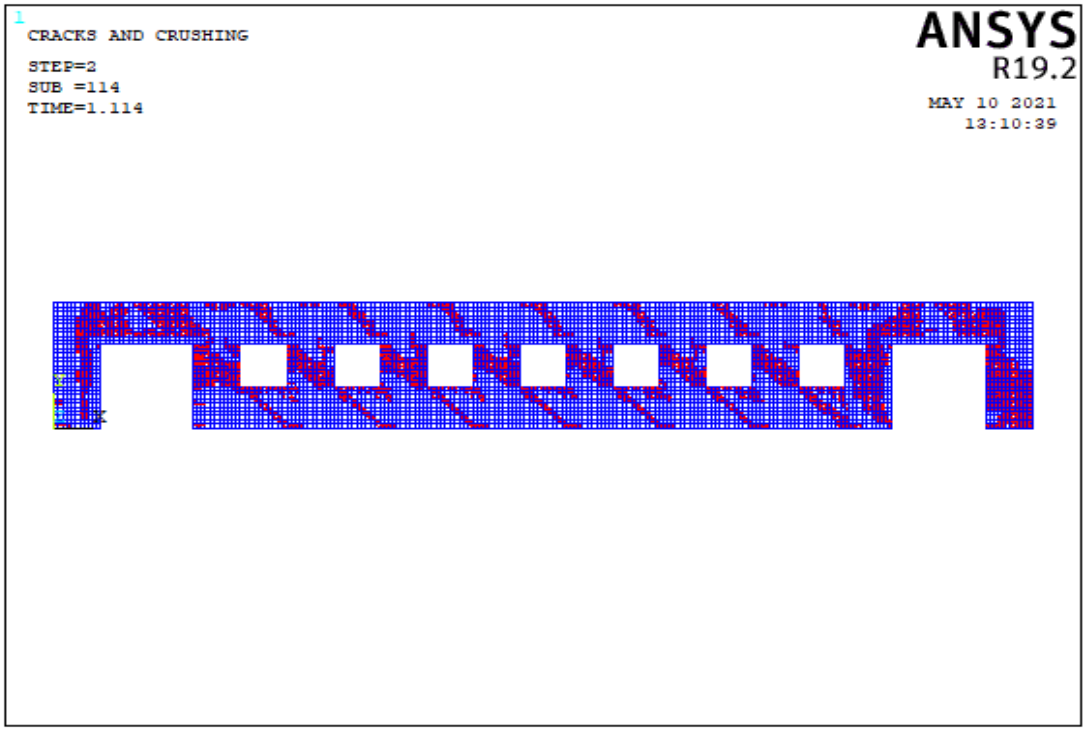

(b)

Figure 5.153. The Crack Pattern of Wall 21 Model 1 According to Compressive Strength Values of (a) 3 MPa, (b) 8 MPa

Table 5.23. Failure Patterns of Wall 21

Number of Model	Aspect ratio	fm=3 Mpa			fm=8 Mpa		
		Failure Pattern			Failure Pattern		
		Base Sliding	Rocking	Diagonal Tension	Base Sliding	Rocking	Diagonal Tension
Model 1	3.00		X			X	
	3.00			X			X
	3.00			X			X
	3.00			X			X
	3.00			X			X
	3.00			X			X
	3.00			X			X
	3.00		X			X	
	3.00		X			X	

In the Table A.21, all length of openings are less than 3 m for model 1 of wall 21. Total opening amount of load bearing walls is not appropriate for TEC 2018. In model 1, the length of corner pier is less than 1.5 meters. The length of pier between the door and window and the length of piers between windows is 1 meter. The Table 5.23 shows that there are diagonal tension struts in the piers between the openings and flexural cracks in the corner piers.

5.4.2 Capacity Curves for Different Masonry Walls with Opening

This section comprises the capacity curves for each models corresponding to 21 different wall types. Since the models have two different compressive strengths, two types of capacity curves are plotted for models. These all models are evaluated in comparison to each other.

5.4.2.1 Capacity Curves of Walls

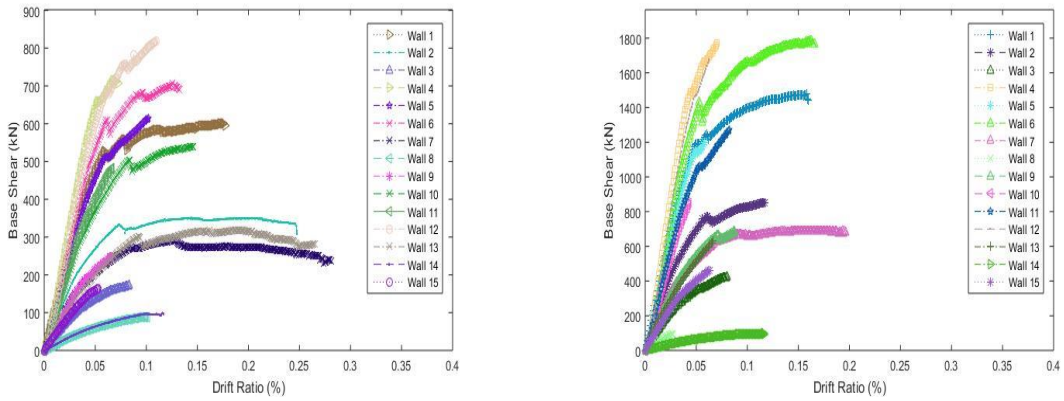

(a) (b)

Figure 5.154. Capacity Curves of Wall 1 According to Compressive Strength Values of (a) 3 MPa, (b) 8 MPa

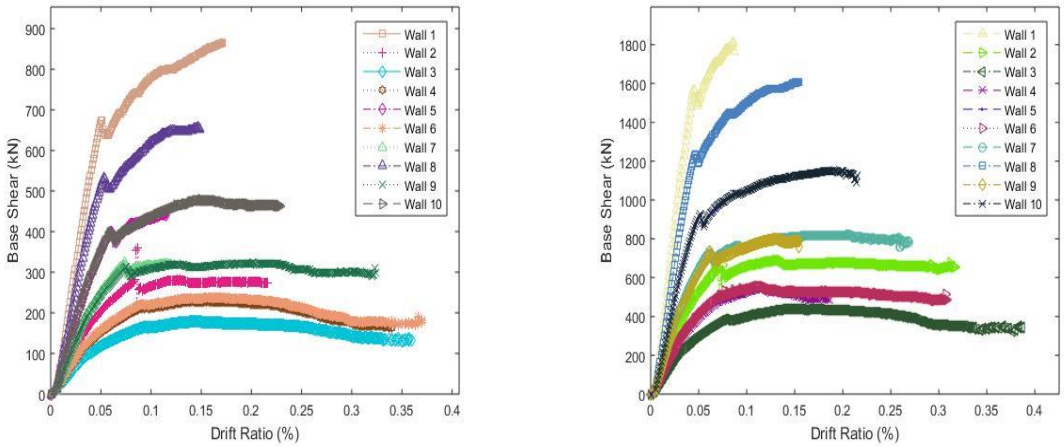

(a) (b)

Figure 5.155. Capacity Curves of Wall Model 2 According to Compressive Strength Values of (a) 3 MPa, (b) 8 MPa

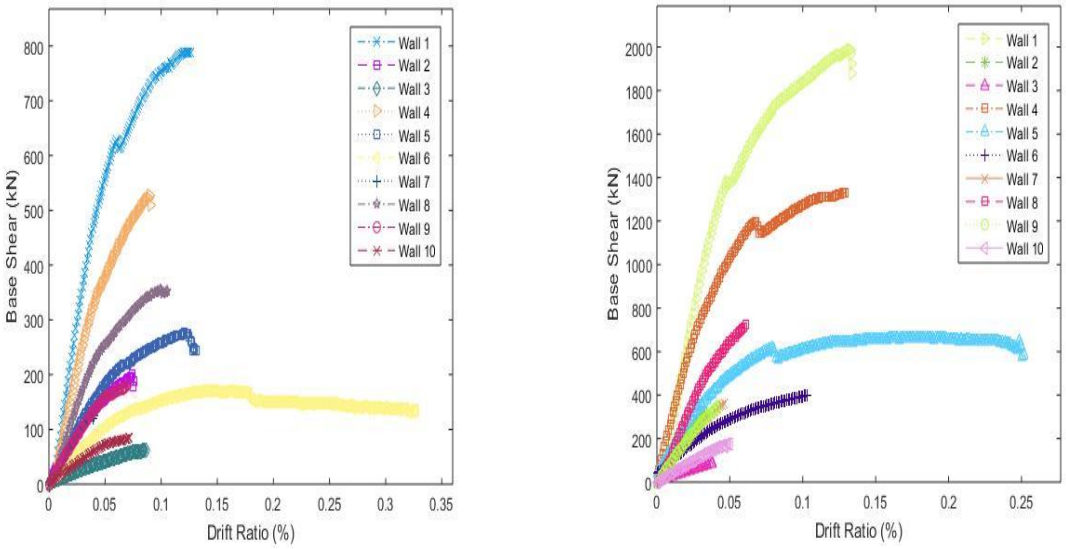

(a) (b)

Figure 5.156. Capacity Curves of Wall Model 3 According to Compressive Strength Values of (a) 3 MPa, (b) 8 MPa

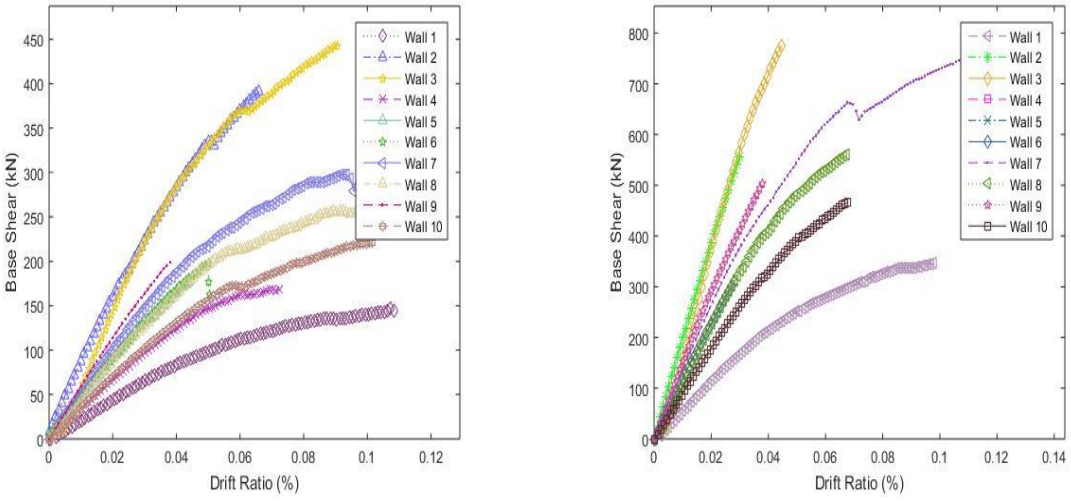

(a) (b)

Figure 5.156. Capacity Curves of Wall Model 4 According to Compressive Strength Values of (a) 3 MPa, (b) 8 MPa

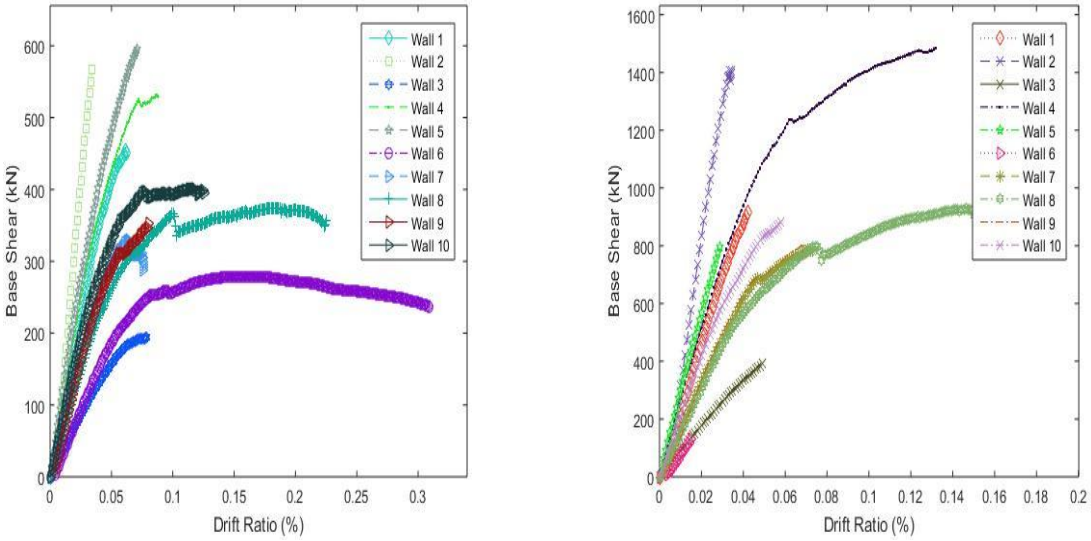

(a) (b)

Figure 5.157. Capacity Curves of Wall Model 5 According to Compressive Strength Values of (a) 3 MPa, (b) 8 MPa

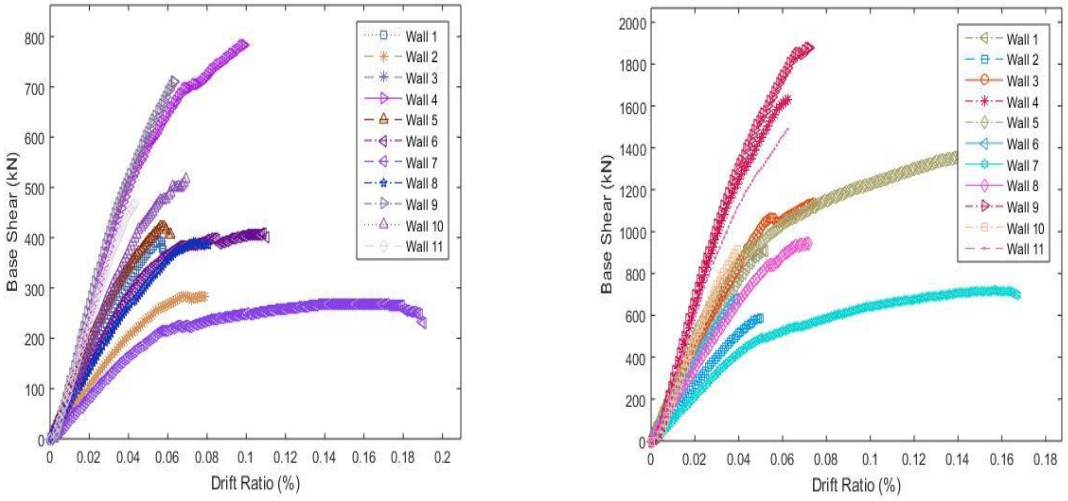

(a) (b)

Figure 5.158. Capacity Curves of Wall Model 6 According to Compressive Strength Values of (a) 3 MPa, (b) 8 MPa

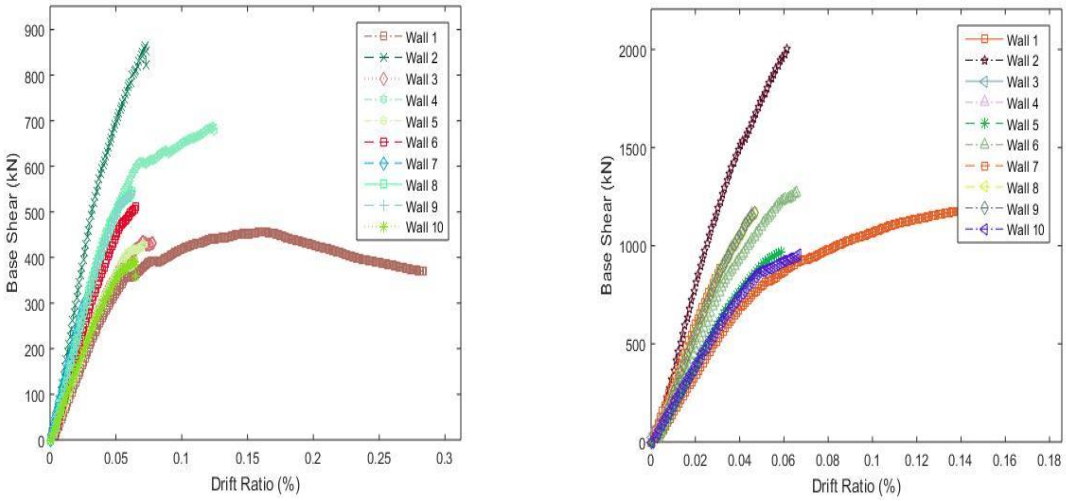

(a) (b)

Figure 5.159. Capacity Curves of Wall Model 7 According to Compressive Strength Values of (a) 3 MPa, (b) 8 MPa

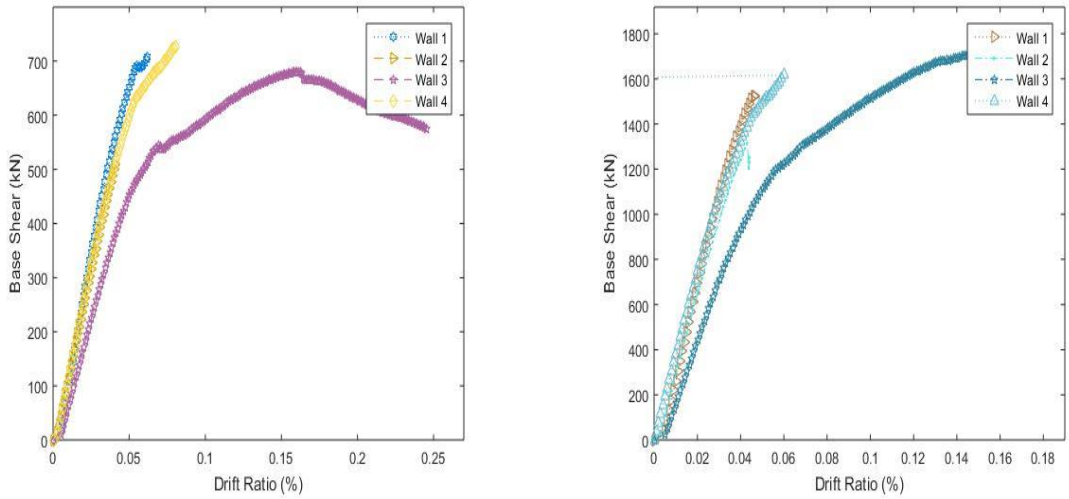

(a) (b)

Figure 5.160. Capacity Curves of Wall Model 8 According to Compressive Strength Values of (a) 3 MPa, (b) 8 MPa

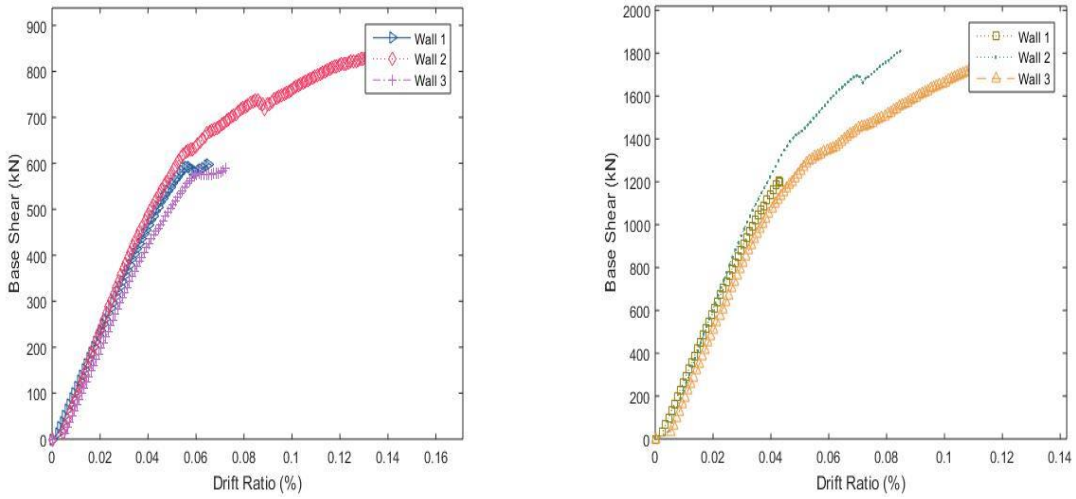

Figure 5.161. Capacity Curves of Wall Model 9 According to Compressive Strength Values of (a) 3 MPa, (b) 8 MPa

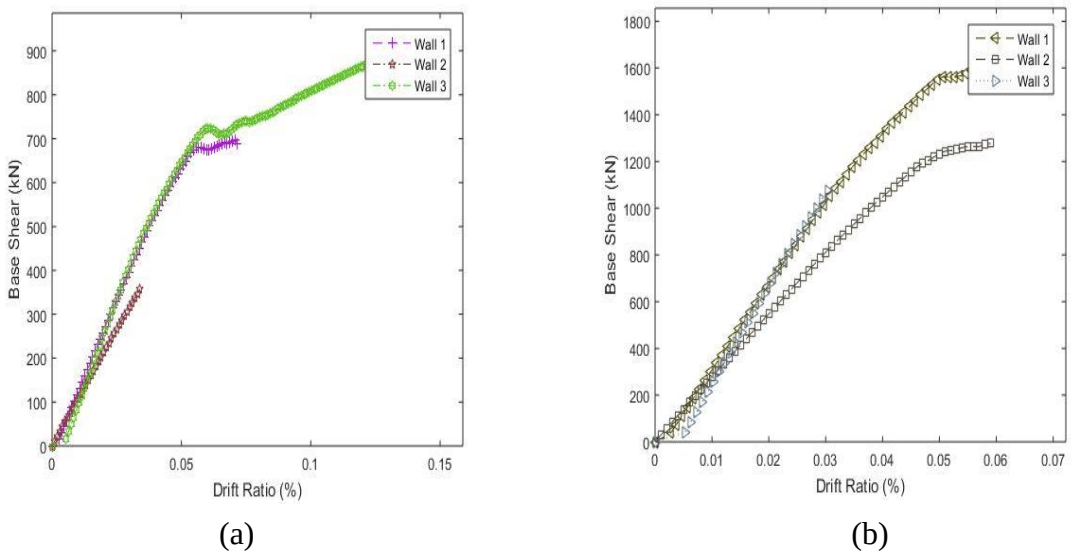

Figure 5.162. Capacity Curves of Wall Model 10 According to Compressive Strength Values of (a) 3 MPa, (b) 8 MPa

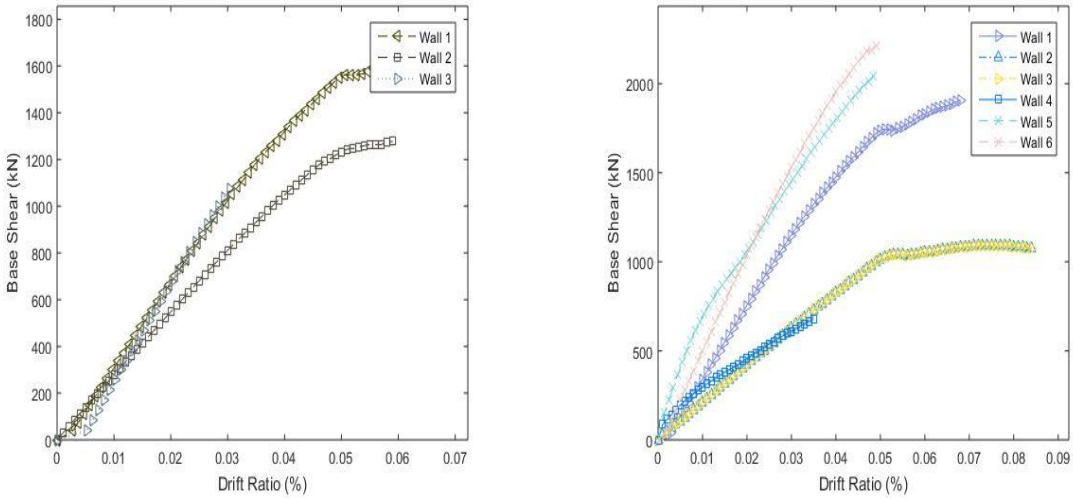

(a) (b)

Figure 5.163. Capacity Curves of Wall Model 11 According to Compressive Strength Values of (a) 3 MPa, (b) 8 MPa

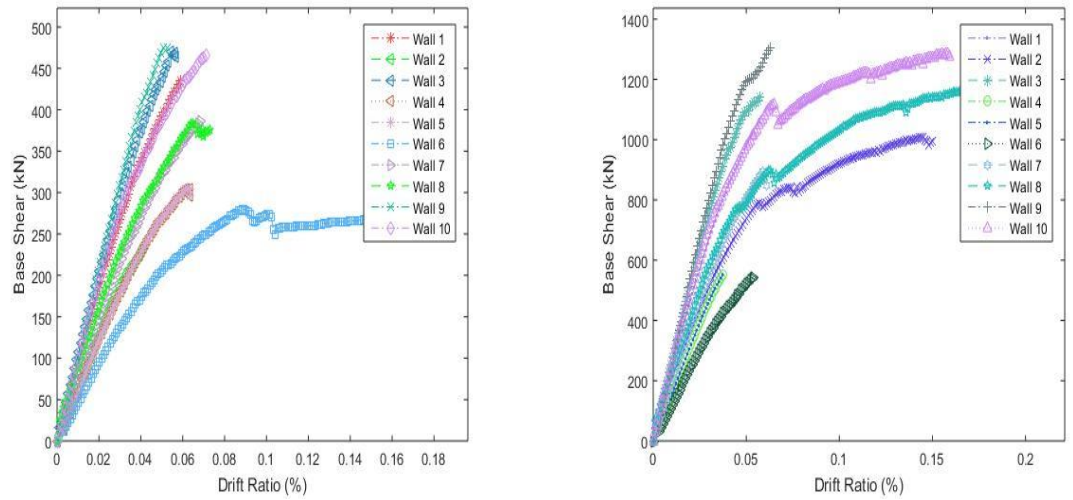

(a) (b)

Figure 5.163. Capacity Curves of Wall Model 12 According to Compressive Strength Values of (a) 3 MPa, (b) 8 MPa

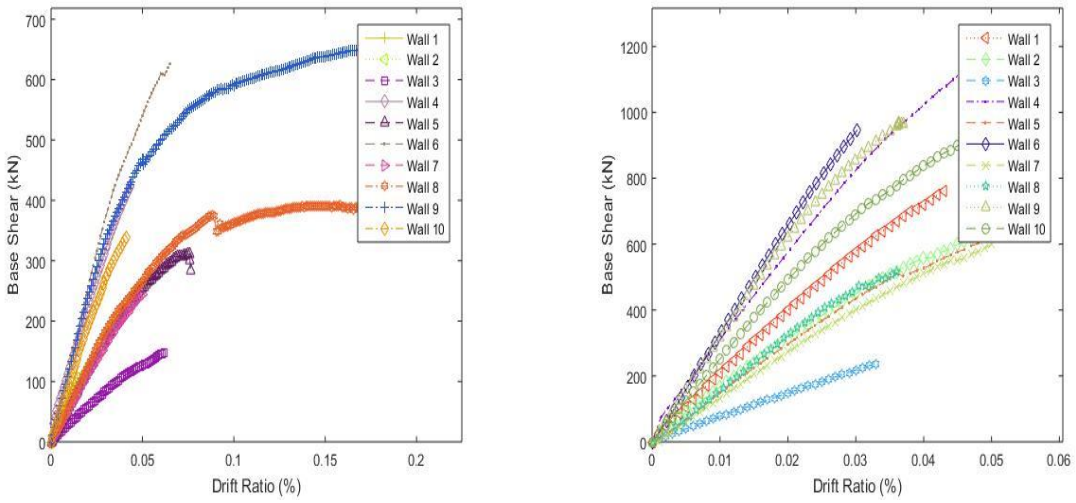

(a) (b)

Figure 5.164. Capacity Curves of Wall Model 13 According to Compressive Strength Values of (a) 3 MPa, (b) 8 MPa

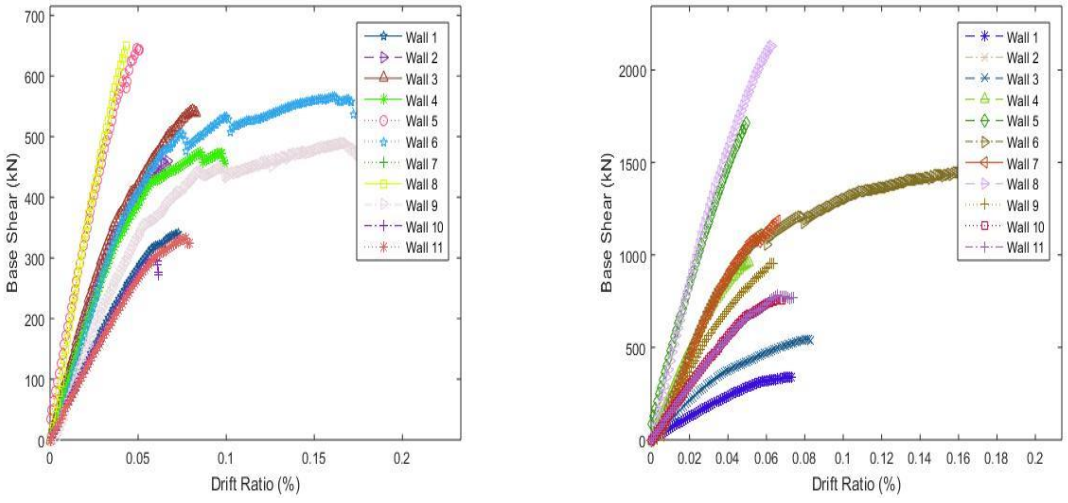

(a) (b)

Figure 5.165. Capacity Curves of Wall Model 14 According to Compressive Strength Values of (a) 3 MPa, (b) 8 MPa

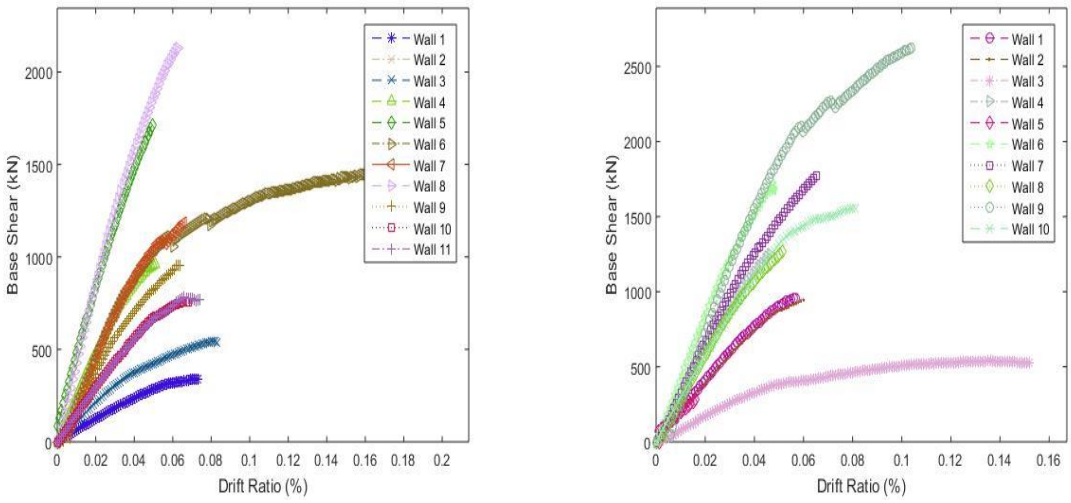

(a) (b)

Figure 5.166. Capacity Curves of Wall Model 15 According to Compressive Strength Values of (a) 3 MPa, (b) 8 MPa

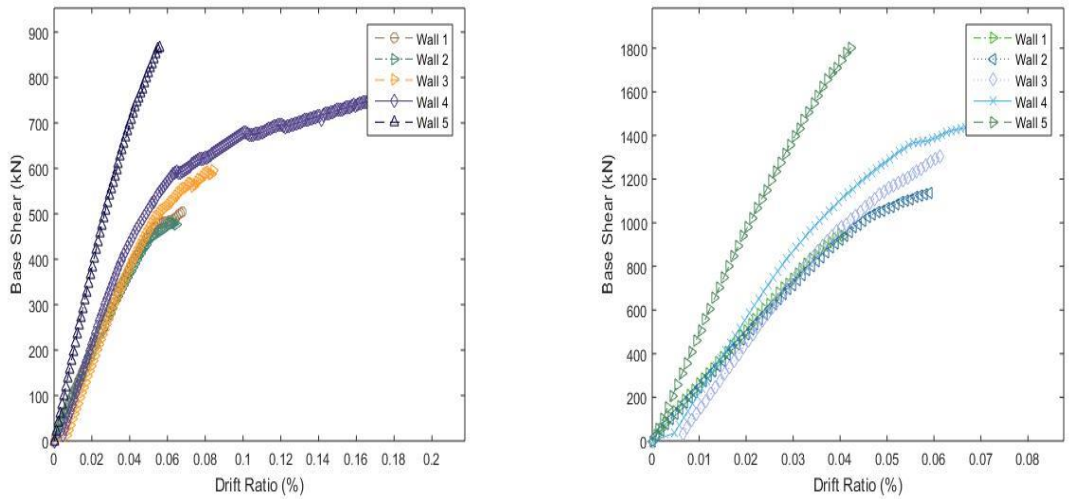

(a) (b)

Figure 5.167. Capacity Curves of Wall Model 16 According to Compressive Strength Values of (a) 3 MPa, (b) 8 MPa

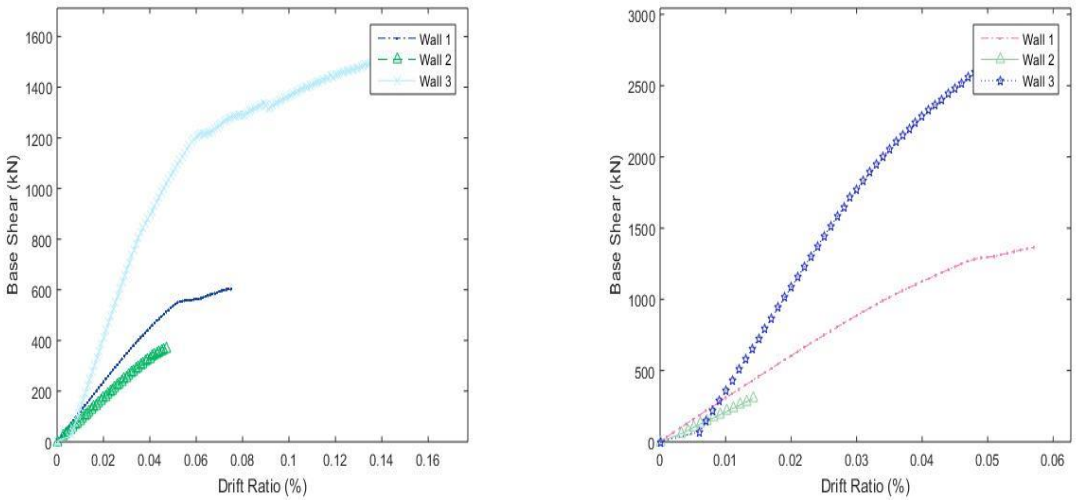

(a) (b)

Figure 5.168. Capacity Curves of Wall Model 17 According to Compressive Strength Values of (a) 3 MPa, (b) 8 MPa

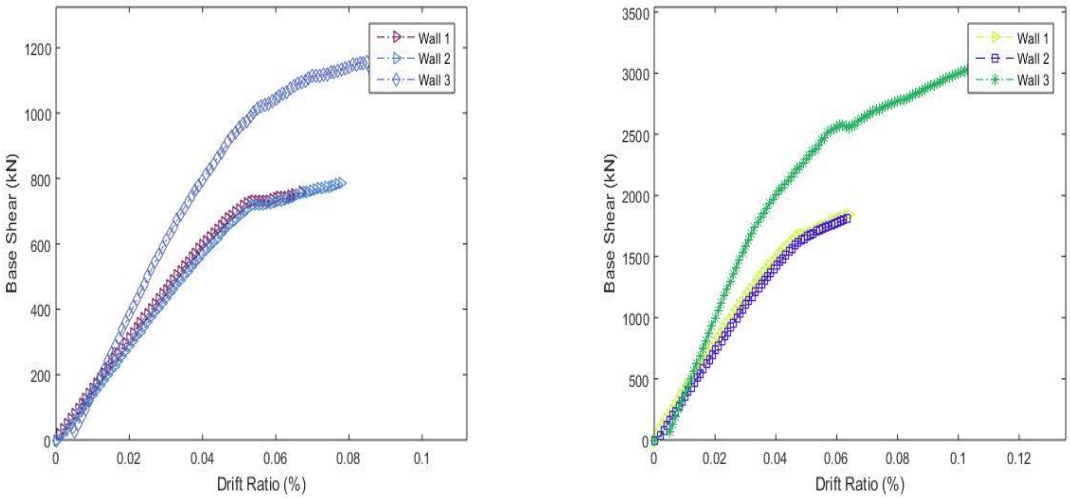

(a) (b)

Figure 5.169. Capacity Curves of Wall Model 18 According to Compressive Strength Values of (a) 3 MPa, (b) 8 MPa

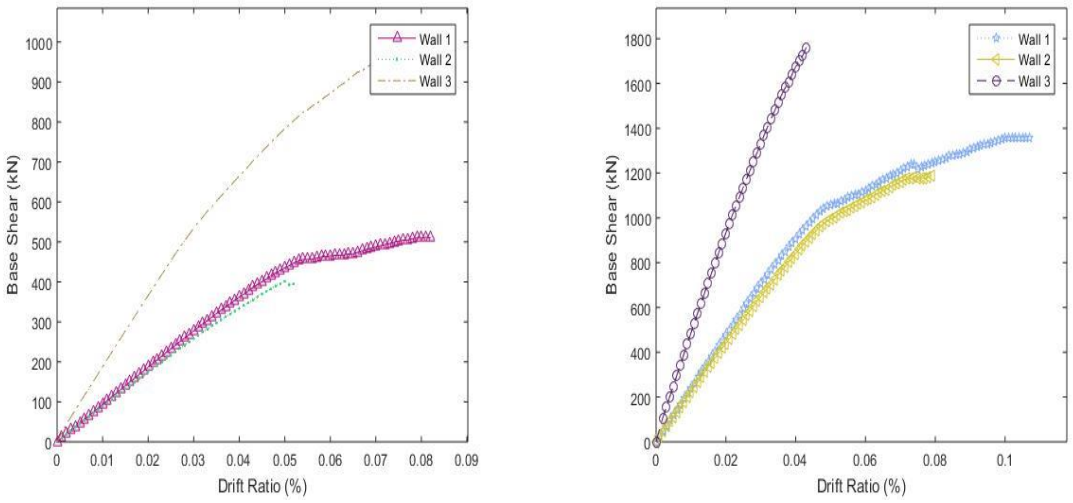

(a) (b)

Figure 5.170. Capacity Curves of Wall Model 19 According to Compressive Strength Values of (a) 3 MPa, (b) 8 MPa

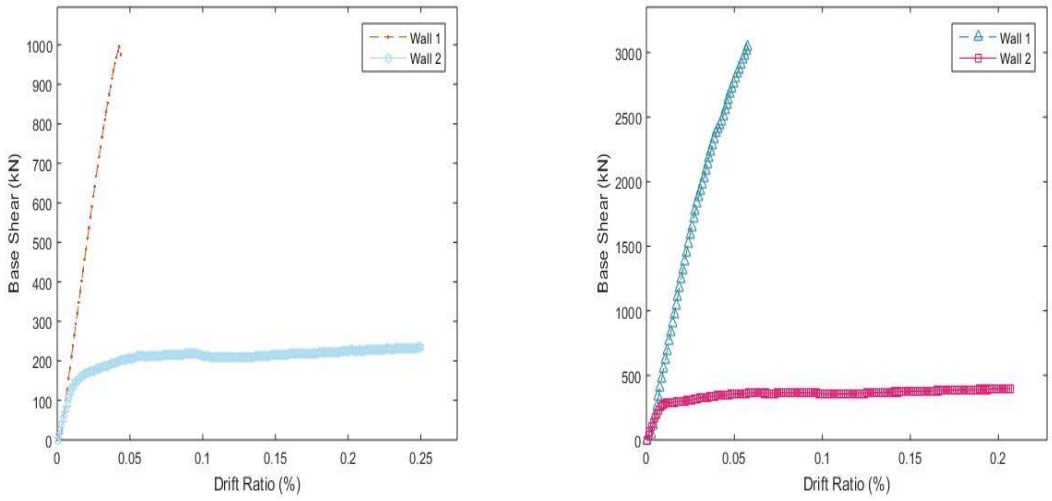

(a) (b)

Figure 5.171. Capacity Curves of Wall Model 20 According to Compressive Strength Values of (a) 3 MPa, (b) 8 MPa

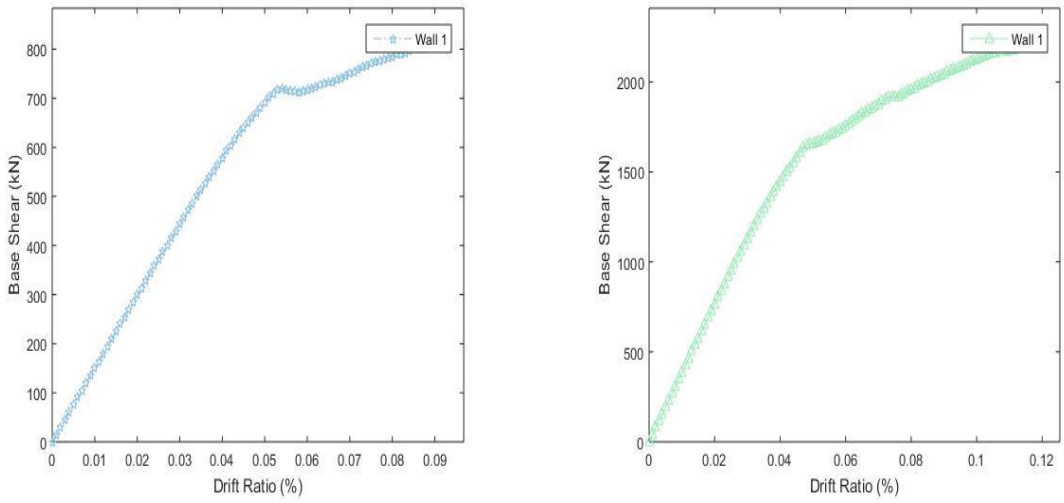

(a) (b)

Figure 5.172. Capacity Curves of Wall Model 21 According to Compressive Strength Values of (a) 3 MPa, (b) 8 MPa

Three key aspects were identified while evaluating the capacity variation on URM walls. These are size of opening, location of opening and compressive strength of walls. Since compressive strength of the masonry models are assumed to be 3 MPa and 8 MPa for each wall and two analyses for each wall have occurred. The pushover graphs show that the capacity of the wall increases as its overall area rises, but its ductility decreases. In all models, strength of piers increase, as the compressive strength of URM walls increase, although stiffness of piers is reduced.

The size and position of openings affect strength and stiffness of URM walls. The pushover curves for URM walls show that the crack pattern and failure mechanism of URM walls changes, as opening percentage increases. When opening percentage increases, rocking mechanism is predominant and the aspect ratio increase. On the other hand, shear is predominant and aspect ratio decrease, when opening percentage decrease. The capacity of wall is inversely proportional to the aspect ratio.

The opening position for pushover curves should be considered when evaluating the relationship between the percentage of openings and the wall capacity since it impacts the failure mechanism. Insufficient length of piers or large openings create local failure on the piers or spandrels. The in-plane capacity of URM walls decreases, as localized failure occurs.

6. SUMMARY AND CONCLUSIONS

6.1. Summary

In the first part of this study, the aims of the study and previous investigations are mentioned, then history of masonry structures, the properties of materials in masonry walls and the types of masonry walls were examined. The modeling techniques used in masonry walls for TEC2018 are mentioned. The macro model used in our study is explained. The design standards for masonry walls are mentioned and different specifications are compared. The failure modes in masonry walls are explained.

Then, the properties of Ansys and Solid65 elements used in URM wall are explained. The experimental studies and analytical models were compared. The comparison shows that lateral capacity curves are close to each other for all failure mechanisms.

In the last part, the loading and restriction of models and the mechanical properties of the material used in the models are mentioned in order to determine the in-plane behavior of URM walls with openings. Then, analytical models were analyzed. Lateral capacity curves are plotted. The length of openings and piers is evaluated based on the relationship between the location and percentage of openings and the wall capacity.

In this study, the impact of the openings on the in-plane capacity of URM was investigated. For this reason, the walls are modeled and analyzed with the finite element method. In TEC2018, the limits are given for length, sizes and capacities of openings such as windows and doors. As a result of the modeling and analysis, the compressive strength and length of the wall increase, its capacity increase. The capacity decrease, when the percentage of openings increase. An excessive size of openings change failure mechanism of walls and cause local failures.

6.2. Conclusions

In this study, the impact of the location and size of the openings on the in-plane capacity of URM was investigated therefore, the different numerical models are built which based on macro modeling technique. In TEC2018, specific restrictions on load-bearing walls were identified due to the detrimental effects of openings. These restrictions include the

length of the door or window, the length of the load-bearing wall, and the minimum distance between the window and the door. The effect of the size and location of the openings on the in-plane capacity of the URM walls is not adequately described in TEC2018. Therefore, the opening effect, different aspect ratio and compressive strength of piers on behavior of URM walls are researched using 21 different wall types. Since compressive strength of the masonry walls are assumed to be 3 MPa and 8 MPa for each wall, there are two analyses for each walls. A total of 334 modeling and analysis were carried out.

In all models, strength of piers increase, as the compressive strength of URM walls increase, although stiffness of piers reduce. As aspect ratio of piers change, piers have different failure mechanisms. The high aspect ratio cause slender walls moreover, flexural mechanism is predominant in these cases. The low aspect ratio cause diagonal tension mechanism and higher capacity of piers.

Insufficient length of piers or large openings create local failure on the piers or spandrels due to non-uniform distribution of loadings. When the doors percentage is greater than 13% and the doors length is greater than 2 m, local failure on spandrels occur. The localized failure of piers or spandrels emerge when the length of piers between windows are 1 meter. This failure result in reduced capacity of URM walls. When the pier percentage is greater than 11% and the pier length is greater than 1.5 m, the in-plane capacity of URM walls increase significantly.

The localized failure of piers become when the length of pier between window and door is less than 1.5 meter. When this pier percentage is greater than 13% and the pier length is greater than 2 m, the stiffness and strength of wall seriously increase. In multi-window walls, local failure is observed when the length of the corner pier is less than 1 meter and percentage of corner pier is less than 8%. The length of corner pier is greater than 1.5 m and percentage of corner pier is greater than 15% on walls with openings, then capacity of piers increase significantly. Because, aspect ratio replace the failure mechanism of pier and less aspect ratio cause more capacity on walls.

The location of openings plays important role on the in-plane capacity of URM. On the walls with opening such as windows and doors, the compression diagonal struts between

the windows increase, when the doors are located in the corner of the wall compared to when the doors are located in the middle of the wall. Then, the in-plane wall capacity is increased. When the openings are located on the left of the wall or the length of the corner pier on the right of the wall is greater than 3 meters and pier percentage is greater than 23%, in-plane capacity of the wall system reasonably increases. This is because, the strength and stiffness of piers are reduced when the openings are located along the diagonal struts.

6.3. Suggestions

The failure mechanisms and the seismic capacity of the wall are affected by the openings formed for various purposes. Therefore, size and location of openings must have restrictions. According to TEC 2018, the unsupported length, opening length and pier length for URM walls are given but, the effect of openings should be considered for walls with a length of more than 7.5 meters. The percentages of openings and piers should be limited to improve in-plane performance of URM walls. Otherwise, large openings for URM walls may cause local failure. When the doors percentage is greater than 13% and the doors length is greater than 2 m, local failure on spandrels occur. To reduce seismic damage, the door length should be less than 2 meters and the door percentage should be less than 13%. When the pier percentage between windows is greater than 11% and the pier length between windows is greater than 1.5 m, the in-plane capacity of URM walls increase significantly. When pier percentage between door and window is greater than 13% and the pier length is greater than 1.5 m, the stiffness and strength of wall seriously increase. The length of corner pier is greater than 1.5 m and percentage of corner pier is greater than 15% on walls with openings. Therefore, the percentages and lengths of piers and openings can be utilized together to decrease the impact of openings in URM walls.

7. REFERENCES

[1] L. Krstevska, L. Tashkov, G. Arun, F. Aköz, Evaluation of Seismic Behavior of Historical Monuments, SHH07 International Symposium on Studies on Historical Heritage Symposium Book, Antalya, p. 411-418, 2007.

[2] M. J . N. Priestley, Seismic Behaviour of Unreinforced Masonry Walls, Bulletin of the New Zealand Society for Earthquake Engineering, Vol. 18(2), p. 191-205, 1985.

[3] K. Chaimoon, M. M. Attard, Modeling of unreinforced masonry walls under shear and compression, Engineering Structures, Vol. 29(9), p. 2056–2068, 2007.

[4] D. P. Abrams, N. Shah, Cyclic Load Testing of Unreinforced Masonry Walls, Illinois Univ at Urbana Advanced Construction Technology Center, 1992.

[5] F. Parisi, N. Augenti, A. Prota, Implications of the spandrel type on the lateral behavior of unreinforced masonry walls, Earthquake Engineering & Structural Dynamics, Vol. 43(12), p. 1867-1887, 2014.

[6] G. Schwegler, Masonry Construction Strengthened with Fiber Composites in Seismically Endangered Zones, The 10th European Conference on Earthquake Engineering, Vienna, Austria. 1994.

[7] M. L. Albert, A. E. Elwi, J. J. R. Cheng, Strengthening of Unreinforced Masonry Walls Using FRPs, Journal of Composites for Construction, Vol. 5(2), p. 76–84, 2001.

[8] R. Bitar, G. Saad, E. Awwad, H. Khatib, M. Mabsout, Strengthening Unreinforced Masonry Walls Using Natural Hemp Fibers, Journal of Building Engineering.

[9] N. Ismail, J. M. Ingham, In-plane and Out-of-plane Testing of Unreinforced Masonry Walls Strengthened Using Polymer Textile Reinforced Mortar, Engineering Structures, p. 167-177, 2016.

[10] Y. Lin, D. Lawley, l. Wotherspoon, J. M. Ingham, Out-of-plane testing of unreinforced masonry walls strengthened using ECC shotcrete, Structures, Vol. 7, p. 33-42, 2016.

[11] A. Matsumura, Shear Strength of Reinforced Masonry Walls, Proc. 9th World Conf. on Earthquake Engineering, Tokyo, 1988, p. 121-126.

[12] M. H. Saghafi, S. Safakhah, A. Kheyroddin, M. Mohammadi, In-plane Shear Behavior of FRP Strengthened Masonry Walls, APCBEE Procedia, p. 264-268, 2014.

[13] F. Parisi, N. Augenti, Seismic Capacity of İrregular Unreinforced Masonry Walls with Openings, Earthquake Engineering & Structural Dynamics, Vol. 42(1), p. 101-121, 2013.

[14] Z. Liu, A. Crewe, Effects of Size and Position of Openings on in-Plane Capacity Of Unreinforced Masonry Walls, Bulletin of Earthquake Engineering, Vol. 18(10), 2020

[15] A. Ghobarah, K. E. M. Galal, Out-Of-Plane Strengthening of Unreinforced Masonry Walls With Openings, Journal Of Composites For Construction, Vol. 8(4), p. 298-305, 2004.

[16] F. Yáñez, M. Astroza, A. Holmberg , O. Ogaz, Behavior of Confined Masonry Shear Walls With Large Openings, 13th World Conference on Earthquake Engineering, 2004.

[17] C. Allen, M.J Masia, A.W. Page, M.C. Griffith, H. Derakhshan, N. Mojsilovic, Experimental Testing of Unreinforced Masonry Walls with Openings Subject to Cyclic In-Plane Shear, Brick and Block Masonry-Trends, Innovations and Challenges: Proceedings of the 16th International Brick and Block Masonry Conference, Italy, 2016.

[18] The History of Masonry Construction, https://contractorsinsurance.org/masonry-construction (Access date: 10.04.2020).

[19] History of Masonry, https://www.masoncontractors.org/history, (Access date: 15.04.2020).

[20] Masonry Construction: Advantages and Disadvantages, https://www.ny-engineers.com/blog/masonry-construction-advantages-and-disadvantages, (Access date: 17.04.2020).

[21] TEC2018, (Turkish Building Earthquake Code), Specifications for buildings to be built in seismic areas. Ministry of Public Works and Settlement, Ankara, Turkey, 2018

[22] B.C. Punmia, A.K. Jain, A.K. Jain, Basic Civil Engineering, Firewall Media, 2003

[23] M. Astroza,.O. Moroni, S. Brzev & J. Tanner, Seismic Performance of Engineered Masonry Buildings in the 2010 Maule Earthquake, Earthquake Spectra, Vol. 28(1), p.385-406, 2012.

[24] G. Arun, Yığma Kagir Yapı Davranışı, Yığma Yapıların Deprem Güvenliğinin Arttırılması Çalıştayı, 2005.

[25] A Detailed Study on Cavity Wall, https://www.structuralguide.com/cavity-walls (Access date: 10.04.2020)

[26] P.B. Lourenço, J. G. Rots, J. Blaauwendraad, Two Approaches for the Analysis of Masonry Structures: Micro and Macro-Modelling, HERON, Vol. 40(4), 1995.

[27] European Committee for Standardization (CEN) 2003b, “Eurocode 8: Design of structures for earthquake resistance”, Part 1, prEN 1998-1, Brussels, Belgium.

[28] International Code Council (2006), "International Building Code (IBC)", Whittier, California, USA.

[29] Masonry Standards Joint Committee (MSJC) (2005), "Building Code Requirements for Masonry Structures and Specification for Masonry Structures and Commentaries", American Concrete Institute, American Society of Civil Engineers, The Masonry Society, Boulder, Colorado.

[30] M. Tomaževič, Earthquake-resistant Design of Masonry Structures, Series on Innovation in Structures and Construction, 2000.

[31] G. Magenes, G.M. Calvi, In-Plane Seismic Response of Brick Masonry Walls, Earthquake Engineering & Structural Dynamics, Vol. 26(11), 1997.

[32] ANSYS 19.2, ANSYS Mechanical APDL Element Reference.

[33] P.B. Lourenço, Computational Strategies for Masonry Structures, Thesis Delft University of Technology, 1996.

[34] S. Franklin, Performance of Rehabilitated URM Shear Walls: Flexural Behavior of Piers, Master Thesis, University of Illinois, Illinois, 2001

[35] H. Tolunay, Investigations on the Characteristics of Brick Masonry Walls, Master's Thesis, 1966.

[36] European Committee for Standardization (CEN) 2003a, "Eurocode 6: Design of Masonry Structures", prEN 1996-1, Brussels, Belgium.

[37] FEMA 356. (2000). Prestandard and commentary for the seismic rehabilitation of buildings, Federal Emergency Management Agency, USA.

APPENDIX

APPENDIX A – Geometric Properties of Walls

Table A.1. Geometric Properties of All Models in Wall 1

Number of Models	Pier 1	Pier 2	Pier 1 Percentage	Pier 2 Percentage	Length of Door	Total Length	Opening Percentage
Model 1	6.00	2.00	60%	20%	2.00	10.00	13%
Model 2	4.94	0.30	80%	5%	0.92	6.15	10%
Model 3	2.26	1.50	52%	35%	0.56	4.33	9%
Model 4	1.67	8.03	15%	75%	1.08	10.78	7%
Model 5	2.47	5.45	28%	61%	1.00	8.93	7%
Model 6	6.12	3.06	62%	31%	0.73	9.92	5%
Model 7	4.14	0.30	76%	5%	1.03	5.47	13%
Model 8	1.43	1.00	48%	33%	0.57	3.00	13%
Model 9	2.42	2.42	41%	41%	1.10	5.93	12%
Model10	3.55	3.55	43%	43%	1.10	8.20	9%
Model 11	2.44	4.78	29%	57%	1.11	8.33	9%
Model 12	5.00	5.00	42%	42%	2.00	12.00	11%
Model 13	0.73	3.20	14%	60%	1.38	5.31	17%
Model 14	1.20	1.20	40%	40%	0.60	3.00	13%
Model 15	2.71	1.22	51%	23%	1.38	5.31	17%

Table A.2. Geometric Properties of All Models in Wall 2

Number of Models	Pier 1	Total Length
Model 1	10.00	10.00
Model 2	4.55	4.55
Model 3	3.41	3.41
Model 4	3.90	3.90
Model 5	6.38	6.38
Model 6	3.95	3.95
Model 7	5.17	5.17
Model 8	8.11	8.11
Model 9	5.08	5.08
Model 10	6.38	6.38

Table A.3. Geometric Properties of All Models in Wall 3

Number of Models	Pier 1	Pier 2	Pier 1 Percentage	Pier 2 Percentage	Length of Window	Total Length	Opening Percentage
Model 1	3.00	6.00	30%	60%	1.00	10.00	3
Model 2	0.87	2.46	20%	55%	1.12	4.45	8
Model 3	0.73	0.86	27%	33%	1.06	2.64	13
Model 4	3.49	3.49	45%	45%	0.75	7.73	3
Model 5	0.73	3.13	16%	69%	0.66	4.51	5
Model 6	0.60	2.04	17%	59%	0.84	3.48	8
Model 7	1.79	1.71	38%	36%	1.21	4.71	9
Model 8	2.94	2.29	48%	38%	0.84	6.07	5
Model 9	1.35	2.21	30%	50%	0.87	4.42	7
Model 10	1.80	0.56	59%	18%	0.68	3.04	7

Table A.4. Geometric Properties of All Models in Wall 4

Number of Models	Pier 1	Pier 2	Pier 3	Length of Windows	Total Length	Opening Percentage
Model 1	0.63	1.23	0.63	0.65	3.79	11%
Model 2	1.44	2.59	1.43	1.48	8.41	12%
Model 3	2.86	0.70	2.86	0.48	7.37	4%
Model 4	2.91	0.50	2.91	0.38	7.08	4%
Model 5	1.56	1.65	0.43	1.46	6.56	15%
Model 6	1.46	0.96	1.46	1.09	6.05	12%
Model 7	0.68	1.36	1.91	1.02	6.00	11%
Model 8	1.18	1.57	1.18	0.74	5.40	9%
Model 9	1.80	2.13	0.42	1.06	6.47	11%
Model 10	0.86	1.52	0.86	0.87	4.96	12%

Number of Models	Pier 1 Percentage	Pier 2 Percentage	Pier 3 Percentage
Model 1	17%	32%	17%
Model 2	17%	31%	17%
Model 3	39%	9%	39%
Model 4	43%	3%	43%
Model 5	24%	25%	7%
Model 6	24%	16%	24%
Model 7	11%	23%	32%
Model 8	22%	29%	22%
Model 9	28%	33%	7%
Model 10	17%	31%	17%

Table A.5. Geometric Properties of All Models in Wall 5

Number of Models	Pier 1	Pier 2	Pier 3	Pier 4	Length of Windows	Total Length	Opening Percentage
Model 1	2.40	0.6	0.6	1.81	1.00	8.41	12%
Model 2	2.01	3.75	3.75	2.01	0.85	14.07	6%
Model 3	0.82	1.16	0.52	0.59	1.07	6.31	17%
Model 4	2.88	1.44	1.44	0.96	1.44	11.05	13%
Model 5	2.21	1.80	2.61	0.70	1.50	11.81	13%
Model 6	0.35	1.50	0.94	0.35	1.20	6.74	18%
Model 7	2.40	0.6	0.6	1.81	1.50	9.91	15%
Model 8	0.58	0.60	0.60	3.03	0.63	6.70	9%
Model 9	1.99	0.94	0.94	1.99	0.38	6.97	5%
Model 10	3.95	0.60	0.60	0.75	0.94	8.71	11%

Number of Models	Pier 1 Percentage	Pier 2 Percentage	Pier 3 Percentage	Pier 4 Percentage
Model 1	31%	3%	3%	24%
Model 2	14%	27%	27%	14%
Model 3	13%	18%	8%	9%
Model 4	26%	13%	13%	9%
Model 5	19%	15%	22%	6%
Model 6	5%	22%	14%	5%
Model 7	26%	3%	3%	20%
Model 8	9%	9%	9%	45%
Model 9	28%	13%	13%	28%
Model 10	45%	7%	7%	9%

Table A.6. Geometric Properties of All Models in Wall 6

Number of Models	Pier 1	Pier 2	Pier 3	Pier 4	Pier 5	Length of Windows	Total Length	Opening Percentage
Model 1	1.50	1.00	1.00	1.00	1.50	1.00	10.00	13%
Model 2	0.80	1.00	0.70	1.00	0.80	0.87	7.78	15%
Model 3	1.83	0.91	0.91	0.91	1.83	1.46	12.24	16%
Model 4	2.63	1.32	1.32	1.32	2.63	0.95	13.02	10%
Model 5	2.97	1.03	1.03	1.03	0.65	0.65	9.31	9%
Model 6	1.17	1.00	1.00	1.00	1.17	1.17	10.01	16%
Model 7	0.52	0.84	0.84	0.84	0.52	0.86	6.98	16%
Model 8	0.72	1.09	1.09	1.09	0.72	1.44	10.48	18%
Model 9	1.50	2.17	2.73	2.17	0.55	1.09	13.48	11%
Model10	0.86	1.71	1.71	1.71	0.86	0.86	10.29	11%
Model11	1.50	2.26	0.70	2.26	1.50	1.50	1.03	11%

Number of Models	Pier 1 Percentage	Pier 2 Percentage	Pier 3 Percentage	Pier 4 Percentage	Pier 5 Percentage
Model 1	15%	10%	10%	10%	15%
Model 2	10%	13%	9%	13%	10%
Model 3	15%	7%	7%	7%	15%
Model 4	20%	10%	10%	10%	20%
Model 5	32%	11%	11%	11%	7%
Model 6	12%	10%	10%	10%	12%
Model 7	7%	12%	12%	12%	7%
Model 8	7%	10%	10%	10%	7%
Model 9	11%	16%	20%	16%	4%
Model10	8%	17%	17%	17%	8%
Model11	12%	18%	6%	18%	12%

Table A.7. Geometric Properties of All Models in Wall 7

Number of Models	Pier 1	Pier 2	Pier 3	Pier 4	Pier 5	Pier 6	Length of Window	Total Length	Opening Percentage
Model 1	0.50	1.00	1.00	1.00	1.00	0.50	1.00	10.00	17%
Model 2	1.70	1.70	1.70	1.70	1.70	1.70	1.09	15.69	12%
Model 3	0.84	0.84	0.84	1.26	0.84	0.84	1.34	12.17	18%
Model 4	1.26	1.26	1.26	1.26	1.26	1.26	1.09	12.99	14%
Model 5	0.73	1.10	1.10	1.10	1.10	0.73	0.80	9.88	14%
Model 6	0.86	1.29	1.29	1.29	1.29	0.86	0.86	11.15	13%
Model 7	1.10	1.28	1.28	1.28	1.28	1.10	1.28	13.73	16%
Model 8	1.57	0.70	0.70	2.86	0.70	1.57	0.71	11.67	10%
Model 9	1.57	0.70	0.70	2.86	0.70	1.57	0.71	11.67	10%
Model 10	0.93	0.93	0.93	0.93	0.93	0.93	0.99	10.52	16%

Number of Models	Pier 1 Percentage	Pier 2 Percentage	Pier 3 Percentage	Pier 4 Percentage	Pier 5 Percentage	Pier 6 Percentage
Model 1	5%	10%	10%	10%	10%	5%
Model 2	11%	11%	11%	11%	11%	11%
Model 3	7%	7%	7%	10%	7%	7%
Model 4	10%	10%	10%	10%	10%	10%
Model 5	7%	11%	11%	11%	11%	7%
Model 6	8%	12%	12%	12%	12%	8%
Model 7	8%	9%	9%	9%	9%	8%
Model 8	13%	6%	6%	24%	6%	13%
Model 9	13%	6%	6%	24%	6%	13%
Model 10	9%	9%	9%	9%	9%	9%

Table A.8. Geometric Properties of All Models in Wall 8

Number of Piers	Model 1	Model 2	Model 3	Model 4
Pier 1	3.09	2.00	0.45	1.16
Pier 2	0.70	1.00	1.14	0.93
Pier 3	0.70	1.00	1.14	0.93
Pier 4	1.76	1.00	1.14	2.91
Pier 5	0.70	1.00	1.14	0.93
Pier 6	0.70	1.00	1.14	0.93
Pier 7	3.09	2.00	0.45	1.16
Length of Windows	0.66	1	1	0.87
Total Length	14.71	15.00	12.59	14.17
Opening Percentage	10%	16%	19%	14%
Pier 1 Percentage	21%	13%	3%	8%
Pier 2 Percentage	5%	7%	9%	7%
Pier 3 Percentage	5%	7%	9%	7%
Pier 4 Percentage	12%	7%	9%	21%
Pier 5 Percentage	5%	7%	9%	7%
Pier 6 Percentage	5%	7%	9%	7%
Pier 7 Percentage	21%	13%	4%	8%

Table A.9. Geometric Properties of All Models in Wall 9

Number of Piers	Model 1	Model 2	Model 3
Pier 1	1	0.63	0.55
Pier 2	1	0.83	1.09
Pier 3	1	0.83	1.09
Pier 4	1	3.33	1.09
Pier 5	1	0.83	1.09
Pier 6	1	0.83	1.09
Pier 7	1	0.83	1.09
Pier 8	1	0.63	0.55
Length of Windows	1	0.83	0.82
Total Length	15.00	14.56	13.38
Opening Percentage	16%	13%	14%
Pier 1 Percentage	7%	4%	4%
Pier 2 Percentage	7%	6%	8%
Pier 3 Percentage	7%	6%	8%
Pier 4 Percentage	7%	23%	8%
Pier 5 Percentage	7%	6%	8%
Pier 6 Percentage	7%	6%	8%
Pier 7 Percentage	7%	6%	8%
Pier 8 Percentage	7%	4%	4%

Table A.10. Geometric Properties of All Models in Wall 10

Number of Piers	Model 1	Model 2	Model 3
Pier 1	1	0.99	0.93
Pier 2	1	0.70	1.16
Pier 3	1	0.70	1.16
Pier 4	1	0.70	1.16
Pier 5	1	1.23	1.16
Pier 6	1	0.70	1.16
Pier 7	1	0.70	1.16
Pier 8	1	0.70	1.16
Pier 9	1	0.99	0.93
Length of Windows	1	1.24	0.58
Total Length	17.00	17.32	14.64
Opening Percentage	16%	19%	11%
Pier 1 Percentage	6%	6%	6%
Pier 2 Percentage	6%	4%	8%
Pier 3 Percentage	6%	4%	8%
Pier 4 Percentage	6%	4%	8%
Pier 5 Percentage	6%	7%	8%
Pier 6 Percentage	6%	4%	8%
Pier 7 Percentage	6%	4%	8%
Pier 8 Percentage	6%	4%	8%
Pier 9 Percentage	6%	6%	6%

Table A.11. Geometric Properties of All Models in Wall 11

Number of Piers	Model 1	Model 2	Model 3	Model 4
Pier 1	1	0.46	0.46	1.03
Pier 2	1	0.60	0.60	0.35
Pier 3	1	0.60	0.60	0.35
Pier 4	1	0.60	0.60	0.35
Pier 5	1	0.92	0.92	1.40
Pier 6	1	0.60	0.60	0.35
Pier 7	1	0.60	0.60	0.35
Pier 8	1	0.60	0.60	0.35
Pier 9	1	0.60	0.60	0.35
Pier 10	1	0.46	0.46	1.03
Length of Windows	1	1.38	1.38	1.19
Total Length	19.00	18.46	18.46	16.64
Opening Percentage	16%	22%	22%	21%
Pier 1 Percentage	5%	2%	2%	6%
Pier 2 Percentage	5%	3%	3%	2%
Pier 3 Percentage	5%	3%	3%	2%
Pier 4 Percentage	5%	3%	3%	2%
Pier 5 Percentage	5%	5%	5%	8%
Pier 6 Percentage	5%	3%	3%	2%
Pier 7 Percentage	5%	3%	3%	2%
Pier 8 Percentage	5%	3%	3%	2%
Pier 9 Percentage	5%	3%	3%	2%
Pier 10 Percentage	5%	2%	2%	6%

Table A.12. Geometric Properties of All Models in Wall 12

Number of Models	Pier 1	Pier 2	Pier 3	Length of Doors	Length of Windows	Total Length	Opening Percentage
Model 1	2.00	3.00	2.00	2.00	1.00	10.00	17%
Model 2	1.12	1.21	3.06	1.08	1.35	7.81	15%
Model 3	2.24	0.90	4.48	0.96	1.28	9.85	11%
Model 4	1.27	1.10	3.13	0.57	0.63	6.69	9%
Model 5	1.27	1.10	3.13	0.57	0.63	6.69	9%
Model 6	0.81	1.44	2.16	0.66	0.71	5.78	12%
Model 7	1.86	1.20	3.06	1.20	0.96	8.28	14%
Model 8	1.22	1.22	3.49	0.71	1.74	8.39	13%
Model 9	2.75	0.79	4.69	1.04	1.13	10.40	10%
Model 10	3.00	2.63	1.31	1.13	1.13	9.20	12%

Number of Models	Pier 1 Percentage	Pier 2 Percentage	Pier 3 Percentage
Model 1	20%	30%	20%
Model 2	14%	15%	39%
Model 3	23%	9%	45%
Model 4	19%	16%	47%
Model 5	19%	16%	47%
Model 6	14%	25%	37%
Model 7	22%	14%	37%
Model 8	15%	15%	42%
Model 9	26%	8%	45%
Model 10	33%	29%	14%

Table A.13. Geometric Properties of All Models in Wall 13

Number of Models	Pier 1	Pier 2	Pier 3	Pier 4	Length of Door	Length of Window	Total Length	Opening Percentage
Model 1	2.00	1.00	2.00	1.00	2.00	1.00	10.00	20%
Model 2	0.94	1.12	1.41	1.41	0.75	1.13	7.89	16%
Model 3	0.87	0.87	0.87	0.35	0.90	0.96	5.78	21%
Model 4	1.01	0.60	0.93	5.00	0.67	1.03	10.28	11%
Model 5	1.69	0.96	0.96	1.58	0.66	0.99	7.83	14%
Model 6	1.28	1.49	2.13	3.75	0.94	1.17	11.93	12%
Model 7	1.07	0.96	1.44	1.20	1.20	1.20	8.27	19%
Model 8	0.93	0.60	0.93	3.03	1.05	0.49	7.51	14%
Model 9	3.66	0.67	3.26	0.40	1.00	0.42	9.83	10%
Model10	3.41	0.86	1.71	0.86	0.86	0.86	9.42	12%

Number of Models	Pier 1 Percentage	Pier 2 Percentage	Pier 3 Percentage	Pier 4 Percentage
Model 1	20%	10%	20%	10%
Model 2	12%	14%	18%	18%
Model 3	15%	15%	15%	6%
Model 4	10%	6%	9%	49%
Model 5	22%	12%	12%	20%
Model 6	11%	13%	18%	31%
Model 7	13%	12%	17%	15%
Model 8	12%	8%	12%	40%
Model 9	37%	7%	33%	4%
Model10	36%	9%	18%	9%

Table A.14. Geometric Properties of All Models in Wall 14

Number of Models	Pier 1	Pier 2	Pier 3	Pier 4	Pier 5	Length of Door	Length of Window	Total Length	Opening Percentage
Model 1	1.00	1.00	1.00	1.00	1.00	2.00	1.00	10.00	23%
Model 2	1.50	2.00	2.00	0.42	0.42	0.67	1.00	10.00	14%
Model 3	0.50	2.00	2.00	2.00	0.40	0.50	1.00	10.40	13%
Model 4	2.50	1.00	1.00	0.83	1.67	0.83	0.83	10.32	13%
Model 5	1.32	1.64	1.27	1.27	4.41	1.36	1.44	15.58	15%
Model 6	0.55	0.99	0.99	2.19	2.19	0.77	0.99	10.64	14%
Model 7	0.50	2.00	2.00	2.00	0.50	0.50	1.00	10.50	13%
Model 8	1.54	2.83	2.83	2.38	1.22	1.59	1.41	16.63	15%
Model 9	1.17	1.51	1.51	0.76	1.17	0.76	0.76	9.13	14%
Model 10	1.00	1.00	1.00	1.00	1.00	2.00	1.00	10.00	23%
Model 11	0.96	0.96	0.96	1.14	0.96	0.67	1.00	8.62	17%

Number of Models	Pier 1 Percentage	Pier 2 Percentage	Pier 3 Percentage	Pier 4 Percentage	Pier 5 Percentage
Model 1	10%	10%	10%	10%	10%
Model 2	15%	20%	20%	4%	4%
Model 3	5%	19%	19%	19%	4%
Model 4	24%	10%	10%	8%	16%
Model 5	8%	11%	8%	8%	28%
Model 6	5%	9%	9%	21%	21%
Model 7	5%	19%	19%	19%	5%
Model 8	9%	17%	17%	14%	7%
Model 9	13%	17%	17%	8%	13%
Model 10	10%	10%	10%	10%	10%
Model 11	11%	11%	11%	13%	11%

Table A.15. Geometric Properties of All Models in Wall 15

Number of Models	Pier 1	Pier 2	Pier 3	Pier 4	Pier 5	Pier 6	Lenght of Door	Length of Window	Total Length	Opening Percentage
Model 1	1.00	1.00	1.00	1.00	1.00	1.00	2.00	1.00	12.00	22%
Model 2	1.00	1.00	1.00	1.00	1.00	1.00	2.00	1.00	12.00	22%
Model 3	0.45	0.60	0.77	0.77	0.60	0.45	0.45	0.57	6.36	17%
Model 4	1.46	1.00	1.71	1.71	1.00	1.46	1.14	1.14	14.07	16%
Model 5	0.67	0.67	0.67	0.67	0.67	1.67	1.07	1.333	11.40	22%
Model 6	1.30	1.30	2.61	2.61	1.30	1.30	0.75	1.30	16.36	14%
Model 7	0.86	1.43	2.14	2.14	1.43	0.86	1.71	1.14	15.14	18%
Model 8	1.25	1.25	1.50	1.50	1.30	1.25	1.00	1.00	13.05	15%
Model 9	0.38	0.91	4.23	4.23	0.80	0.42	1.76	1.24	17.66	16%
Model10	1.31	1.31	1.31	1.31	1.31	1.31	1.88	1.56	15.96	21%

Number of Models	Pier 1 Percentage	Pier 2 Percentage	Pier 3 Percentage	Pier 4 Percentage	Pier 5 Percentage	Pier 6 Percentage
Model 1	8%	8%	8%	8%	8%	8%
Model 2	8%	8%	8%	8%	8%	8%
Model 3	7%	9%	12%	12%	9%	7%
Model 4	10%	7%	12%	12%	7%	10%
Model 5	6%	6%	6%	6%	6%	15%
Model 6	8%	8%	16%	16%	8%	8%
Model 7	6%	9%	14%	14%	9%	6%
Model 8	10%	10%	11%	11%	10%	10%
Model 9	2%	5%	24%	24%	5%	2%
Model10	8%	8%	8%	8%	8%	8%

Table A.16. Geometric Properties of All Models in Wall 16

Number of Piers	Model 1	Model 2	Model 3	Model 4	Model 5
Pier 1	1	1	0.40	1.16	1.32
Pier 2	1	1	1.60	1.33	1.27
Pier 3	1	1	1.00	1.33	1.27
Pier 4	1	1	1.00	1.33	1.27
Pier 5	1	1	1.60	1.33	2.54
Pier 6	1	1	1.60	1.33	2.54
Pier 7	1	1	0.40	1.16	1.32
Length of Windows	1	1	0.80	0.43	1.27
Length of Doors	2	2	0.80	1.03	0.84
Total Length	14	14	12.39	12.13	18.72
Opening Percentage	21%	21%	15%	12%	14%
Pier 1 Percentage	7%	7%	3%	10%	7%
Pier 2 Percentage	7%	7%	13%	11%	7%
Pier 3 Percentage	7%	7%	8%	11%	7%
Pier 4 Percentage	7%	7%	8%	11%	7%
Pier 5 Percentage	7%	7%	13%	11%	14%
Pier 6 Percentage	7%	7%	13%	11%	14%
Pier 7 Percentage	7%	7%	3%	10%	7%

Table A.17. Geometric Properties of All Models in Wall 17

Number of Piers	Model 1	Model 2	Model 3
Pier 1	1	0.68	4.23
Pier 2	1	0.68	1.20
Pier 3	1	0.68	1.20
Pier 4	1	0.68	1.20
Pier 5	1	0.68	1.20
Pier 6	1	0.68	1.20
Pier 7	1	0.68	2.10
Pier 8	1	2.10	4.23
Length of Windows	1	0.85	0.6
Length of Doors	2	0.46	1
Total Length	16	12.43	21.15
Opening Percentage	21%	16%	9%
Pier 1 Percentage	6%	5%	20%
Pier 2 Percentage	6%	5%	6%
Pier 3 Percentage	6%	5%	6%
Pier 4 Percentage	6%	5%	6%
Pier 5 Percentage	6%	5%	6%
Pier 6 Percentage	6%	5%	6%
Pier 7 Percentage	6%	5%	10%
Pier 8 Percentage	6%	17%	20%

Table A.18. Geometric Properties of All Models in Wall 18

Number of Piers	Model 1	Model 2	Model 3
Pier 1	1	1	1.55
Pier 2	1	1	1.29
Pier 3	1	1	1.29
Pier 4	1	1	1.29
Pier 5	1	1	1.94
Pier 6	1	1	1.94
Pier 7	1	1	1.29
Pier 8	1	1	1.29
Pier 9	1	1	1.29
Pier 10	1	1	1.55
Length of Windows	1	1	0.65
Length of Doors	2	2	0.65
Total Length	20	20	20.57
Opening Percentage	20%	20%	11%
Pier 1 Percentage	5%	5%	8%
Pier 2 Percentage	5%	5%	6%
Pier 3 Percentage	5%	5%	6%
Pier 4 Percentage	5%	5%	6%
Pier 5 Percentage	5%	5%	9%
Pier 6 Percentage	5%	5%	9%
Pier 7 Percentage	5%	5%	6%
Pier 8 Percentage	5%	5%	6%
Pier 9 Percentage	5%	5%	6%
Pier 10 Percentage	5%	5%	8%

Table A.19. Geometric Properties of All Models in Wall 19

Number of Piers	Model 1	Model 2	Model 3
Pier 1	1	1	0.77
Pier 2	1	1	1.55
Pier 3	1	1	1.55
Pier 4	1	1	1.55
Pier 5	1	1	1.55
Pier 6	1	1	1.55
Pier 7	1	1	3.00
Length of Windows	1	1	1
Length of Doors	2	2	1.5
Total Length	15	15	17.51
Opening Percentage	27%	27%	19%
Pier 1 Percentage	7%	7%	4%
Pier 2 Percentage	7%	7%	9%
Pier 3 Percentage	7%	7%	9%
Pier 4 Percentage	7%	7%	9%
Pier 5 Percentage	7%	7%	9%
Pier 6 Percentage	7%	7%	9%
Pier 7 Percentage	7%	7%	17%

Table A.20. Geometric Properties of All Models in Wall 20

Number of Piers	Model 1	Model 2
Pier 1	1.5	1
Pier 2	1.875	1
Pier 3	1.875	1
Pier 4	1.875	1
Pier 5	1.875	1
Pier 6	1.875	1
Pier 7	1.875	1
Pier 8	1.5	1
Length of Windows	0.94	1
Length of Doors	1.5	2
Total Length	22.89	18
Opening Percentage	17%	26%
Pier 1 Percentage	7%	6%
Pier 2 Percentage	8%	6%
Pier 3 Percentage	8%	6%
Pier 4 Percentage	8%	6%
Pier 5 Percentage	8%	6%
Pier 6 Percentage	8%	6%
Pier 7 Percentage	8%	6%
Pier 8 Percentage	7%	6%

Table A.21. Geometric Properties of All Models in Wall 21

Number of Piers	Model 1
Pier 1	1
Pier 2	1
Pier 3	1
Pier 4	1
Pier 5	1
Pier 6	1
Pier 7	1
Pier 8	1
Pier 9	1
Length of Windows	1
Length of Doors	2
Total Length	21
Opening Percentage	25%
Pier 1 Percentage	5%
Pier 2 Percentage	5%
Pier 3 Percentage	5%
Pier 4 Percentage	5%
Pier 5 Percentage	5%
Pier 6 Percentage	5%
Pier 7 Percentage	5%
Pier 8 Percentage	5%
Pier 9 Percentage	5%